Assessing The Erodibility of Cohesive Media in Southwestern Ontario With In-Situ Mini-JET Methodology

by

Caleb Jefferies

A thesis
presented to the University of Waterloo
in fulfillment of the
thesis requirement for the degree of
Master of Applied Science
in
Civil Engineering

Waterloo, Ontario, Canada, 2023

AUTHOR'S DECLARATION

I hereby declare that I am the sole author of this thesis. This is a true copy of the thesis, including any required final revisions, as accepted by my examiners.

I understand that my thesis may be made electronically available to the public.

Abstract

Despite research indicating that the resistance of cohesive sediments to fluvial erosion is related to the geologic media, regulators and industry in Southern Ontario do not typically consider the diversity in geologic landscapes when assessing the erosion potential of streams with cohesive boundaries. The development of the mini-Jet Erosion Test (JET) methodology has facilitated in-situ data collection of the resistance of cohesive media to erosion, however, it has not been widely applied in Ontario and there remain knowledge gaps in the interpretation of the test results. This research collected a mini-JET dataset of 245 in-situ tests spanning 13 sites and 10 distinct geologic units. To address the gradient of weathered material within JET scour holes, a method of test segmentation is proposed where each JET is separated into a segment representing a surficial (weathered) layer and an underlying (unweathered) layer. This method of analysis results in three output parameters per JET; the depth of the first segment, a critical shear stress (τ_c) and an erodibility coefficient (k_d). To estimate the τ_c and k_d parameters the JET dataset is analyzed using three methods of JET solution techniques (Scour Depth Method (SD), Blaisdell Method (BM), and Linear Regression Method (LR)) and the sensitivity of these solution techniques to JET duration and measurement frequency is assessed. It is demonstrated that BM is the most sensitive to test duration and LR is the most sensitive to measurement frequency. The estimation of τ_c is robust to JET duration and measurement frequency on a site scale, however, the estimation of k_d can be skewed on a site scale when JETs longer than 120 minutes are compared to tests shorter than 60 minutes.

Using the depth of the first segment as a surrogate for the presence of weathered material, subaerial tests are shown to have a higher presence of weathered material compared to submerged tests, and tests higher on banks have a greater presence of weathered material compared to tests lower on banks or along the streambed. No differences in the presence of weathered material are detected between geologic units.

SD and LR have close agreement on the estimates of τ_c imparting greater confidence in its representativeness, but they diverge substantially on estimates of k_d inserting uncertainty into the representativeness of that parameter. Halton Till is shown to have a statistically lower mean τ_c compared to the grouped results of all the geologic units investigated, however, the difference in

mean of 2.8 Pa may have limited implications given the range in τ_c at individual sites $(low\ \tau_C \leq mean\ \tau_C \leq high\ \tau_C)$.

Comparing tests from summer and early spring at the same site indicates that seasonal processes significantly increase the presence of the surficial weathered layer but do not influence the critical shear stress of the underlying unweathered material. The higher availability of readily erodible weathered material corresponding to seasonal freshet flows suggests that late winter/early spring may be responsible for an outsized amount of erosion in streams with cohesive boundaries, particularly in headwater systems with shorter, more frequent hydrographs. This suggests that regulators and industry should place higher importance on considering how modifications to watersheds alter the frequency of detrition and regeneration of the surficial weathered material. Future research should focus on relating the importance of weathering processes on fluvial erosion rates in cohesive soils to watershed size, land use, and stormwater management techniques.

Acknowledgements

Dedication

Dedicated to my parents, Ted and Judie Jefferies, who instilled in me the curiosity and tenacity required to complete this work.

"No man ever steps in the same river twice. For it's not the same river and he's not the same man"

Heraclitus

Table of Contents

List of Figures

List of Tables

xiii

List of Abbreviations

AM	Adaptive measurement
BM	Blaisdell Method
CT	Combined erosion types (Type 1 and Type 2) (i.e., tests without segmentation)
DCB	D'Aubigny Creek at Brantford
Erodibility parameters	τ_c and k_d
FC	Fletchers Creek at Mississauga
FL-FD	Full Length- Field Data Scenario
FL-NZ	Full Length- No Zero Erosion Points Data Scenario
GM	Gill method of test segmentation
GRL	Gainsborough Ravine at London
GT	Grindstone Creek Tributary at Waterdown
GTA	Greater Toronto Area
HC	Highland Creek at Scarborough
HRRM	High resolution Rapid Measurement
IDF	Intensity, Duration, Frequency (of channel flows)
JET	Jet Erosion Test
K-W	Kruskal-Wallis
LNC	Laurel Creek at University of Waterloo North Campus
LR	Linear Regression Method
MCE	Mimico Creek at Etobicoke
MNR	Maximum norm residual method of test segmentation
MPS	Multi Pressure Setting
NMB	Nith River at Millbank
NTL	Amulree Creek at Lisbon
RPR	Redundant Point Removal
SD	Scour Depth Method
SPS	Single Pressure Setting
ST5	Full Length- Standardized 5-minute readings Data Scenario
ST5R	Full Length- Standardized 5-minute readings with rapid readings Data Scenario
ST10	Full Length- Standardized 10-minute readings Data Scenario
ST10R	Full Length- Standardized 10-minute readings with rapid readings Data Scenario
TCH	Trout Creek at Harmony
T2	Type 2 erosion (i.e., tests with segmentation)
Type 1	Erosion of surficial weathered material
Type 2	Erosion of underlying representative material
VA	Visual assessment method of test segmentation
WCM	Whirl Creek at Mitchell
WCN	West Creek at New Market
100NZ	100 minute- No Zero Erosion Points Data Scenario
80NZ	80 minute- No Zero Erosion Points Data Scenario
60NZ	60 minute- No Zero Erosion Points Data Scenario
45NZ	45 minute- No Zero Erosion Points Data Scenario
30NZ	30 minute- No Zero Erosion Points Data Scenario

List of Symbols

a number of segments in the Gill method of segmentation (unitless)

b_j number of data points in the jth segment in the Gill method of segmentation (unitless)

C_d diffusion coefficient (unitless)

C_f coefficient of friction (unitless)

d_o diameter of the jet nozzle (L)

E depth erosion ($L\,T^{-1}$)

H height of nozzle from impinging wall (L)

H_p Distance that the jet potential core extends from jet nozzle (L)

k_d erodibility coefficient ($L^2\,M^{-1}\,T^1$)

k_{dBM} erodibility coefficient estimated from the Blaisdell method ($L^2\,M^{-1}\,T^1$)

k_{dLR} erodibility coefficient estimated from the Linear Regression method ($L^2\,M^{-1}\,T^1$)

k_{dSD} erodibility coefficient estimated from the Scour Depth method ($L^2\,M^{-1}\,T^1$)

$k_d{'}$ erodibility coefficient adjusted for mass-based excess shear stress model ($L^1\,T^1$)

M mass of eroded material (M T^{-1})

m empirical exponent in depth-based excess shear stress model (unitless)

n empirical exponent in mass-based excess shear stress model (unitless)

r radial distance from stagnation point of impinging jet (L)

R_G Ratio of sum of squares within subsegments and between subsegments in the Gill method of segmentation (unitless)

R^2 coefficient of determination (unitless)

SS_b sum of squares between sub-segments of the Gill method of segmentation ($L^2\,T^{-2}$)

SS_w sum of squares within sub-segment of the Gill method of segmentation ($L^2\,T^{-2}$)

U_o maximum velocity of fluid at the jet nozzle ($L\,T^{-1}$)

U velocity of fluid ($L\,T^{-1}$)

W_{max} maximum width of scour hole (L)

x_{ij} the ith point in the jth segment in the Gill method of segmentation (unitless)

X_j the mean of the jth segment in the Gill method of segmentation (unitless)

Z_{max} maximum measured depth of scour hole (L)

$\uparrow$ statistically significant increase in variable (unitless)

$\downarrow$ statistically significant decrease in variable (unitless)

$-$ no statistically significant change in variable (unitless)

Greek Symbols

ρ mass density of fluid (M L^{-3})

τ_c critical shear stress ($M\,L^{-1}T^{-2}$)

τ_{cBM} critical shear stress estimated from the Blaisdell method ($M\,L^{-1}T^{-2}$)

τ_{cSD} critical shear stress estimated from the Scour Depth method ($M\,L^{-1}T^{-2}$)

τ_{cLR} critical shear stress estimated from the Linear Regression method ($M\,L^{-1}T^{-2}$)

τ_o applied shear stress ($M\,L^{-1}T^{-2}$)

τ_{om} maximum applied shear stress ($M\,L^{-1}T^{-2}$)

$\Delta\mu_{\%change}$ The change resulting from test segmentation in mean change in erodibility parameter with test duration (%)

Chapter 1

Introduction

Watersheds impacted by land-use change are altered in their basic chemical, physical and biological processes. Hydrological and sedimentological imbalances can arise from anthropogenic changes resulting in excessive fluvial erosion of streambeds and banks leading to issues including bank retreat/land loss, degraded water quality, increased risk of infrastructure failure, altered channel morphology, downstream aggradation and loss of aquatic habitat (Osterkamp et al., 1998; Nelson and Booth, 2002; Shields et al., 2010; Briaud et al., 2001; Lawler, 1986; Simon and Klimetz, 2008; Simon, 1989; Simon, 1995). These issues can develop most rapidly in smaller order (Horton, 1945) urbanizing catchments, where extensive land use change has occurred within relatively short periods of time (Wolman, 1967; Meyer et al., 2005; Paul and Meyer, 2001; Walsh et al 2005; Nelson and Booth, 2002; Chin et al., 2013; Whitney et al., 2015).

Contemporaneous management of watersheds and watercourses often allows for prescribed alterations to discharge intensity, duration, and frequency (IDF) arising from land use change to limit the rates of channel degradation by specifying threshold limits related to sediment entrainment properties of channel bed and bank materials. However, erosion threshold criteria (in particular for cohesive media) vary greatly spatially, geologically, and temporally arising from the diversity in hydrophysiographic landscape settings (Lawler, 1986; Wynn et al., 2008; Simon et al., 2010; Mahalder et al., 2017). Stemming from this diversity and the relatively recent application of IDF erosion threshold criteria in managing watersheds, a dearth of erosion threshold information pertinent to cohesive media exists within Canada and internationally. This constrains the effectiveness of designers and decision-makers engaged in watershed management.

The unique glacial history of southern Ontario identifies at least 28 distinct cohesive geologic units situated in a 200 km radius of the Greater Toronto Area (GTA) (where significant land-use change has occurred over the past 100 years). Each of these cohesive deposits is associated with a distinct glacial epoch resulting in unique depositional environments, with varying grain size distributions, parent materials and consolidation histories (White, 1975; Cowan, 1976; Sharpe, 1990; Karrow and Easton, 2005; Karrow, 1987; Cowan, 1972; Sado and Vagners, 1975; Karrow, 1993; Karrow, 1977; Barnett et al, 1999; Karrow, 1967). These glacial deposits form the terrain through which many of Southern Ontario's streams have carved their channels and upon which cities and infrastructure have been constructed.

Despite the recent findings of Mahalder et al. (2017) that cohesive soils associated with unique physiographic regions possess distinct properties governing their erosion by fluvial forces, the cohesive materials composing the heterogeneous geology of southern Ontario are frequently considered alike and inadequately described when characterizing erosion during river engineering works. Thus, there is a necessity to collect representative data describing the erodibility of the various cohesive geologic units in southern Ontario and assess whether there is any quantifiable benefit to considering the unique erodibility parameters of those distinct geologic units as they relate to channel stability thresholds and subsequently rehabilitation strategies.

This research contribution investigates 10 of the 28 distinct cohesive geologic units identified in the 200 km radius around the GTA employing in-situ mini-Jet Erosion Test (JET) methodology. JETs have been demonstrated to be capable of characterizing erosion thresholds in cohesive sediments (Hanson and Simon, 2001; Simon et al., 2010; Al-Madhhachi et al., 2013a, Mahalder et al., 2022) and have also been applied in till media in Southern Ontario (Shugar et al., 2007; Khan and Kostachuck, 2011). Here, the mini-JET (adapted from the JET (Simon et al., 2010)) is employed to facilitate a more feasible field implementation of the methodology. The mini-JET has not yet been applied in Southern Ontario to the knowledge of the author which further provides an opportunity to evaluate the effectiveness of this device in field settings and its applicability in the aforementioned geologic units.

The specific objectives associated with this investigation are as follows:
- apply the mini-JET methodology across a variety of cohesive geologic units in southwestern Ontario to assess whether differences in erodibility parameters are greater between different geologic units compared to limiting tests to the same geologic unit,
- determine whether segmenting JET data is a feasible method of analysis to account for material heterogeneity and weathering encountered during in-situ applications of JET methodology,
- determine the uncertainty of three JET solution techniques (Blaisdell Method (BM), Scour depth Method (SD), Linear Regression Method (LR)) arising from the duration of the JET and frequency of scour depth measurements during the JET,
- provide context to the effects of seasonality on JET methodology in over-consolidated cohesive glacial deposits.

Chapter 2
Literature Review

The erosion of cohesive channel boundaries generally occurs through two primary processes: mass failure and fluvial/hydraulic erosion. Mass failure occurs along planes and is primarily governed by properties of the soil block including its weight, vegetative rooting stability, internal friction angle and the macroscale soil property of bulk shear strength (Osman and Thorne, 1988; Darby and Thorne, 1996; Millar and Quick, 1998; ASCE Task Committee, 1998). Fluvial erosion acts on a smaller scale which removes soil particles and aggregates through the shearing force of flowing water exceeding the microscale property of critical erosional strength (Sutarto et al., 2014; Zreik et al., 1998). These two erosion processes are inherently interlaced; fluvial erosion often acts as a precursor to the occurrence of mass failure through the steepening of bank slopes and toe undercutting resulting in unstable bank angles and cantilever banks (Rinaldi and Darby, 2008; Lawler et al, 1997; Sutarto et al., 2014; Pizzuto 2009). A third, often overlooked process of bank erosion is preparation (Lawler, 1997; Couper and Maddock, 2001). This process is a precursor to fluvial erosion and consists of the weakening of surficial materials making them available for entrainment at stresses lower than typical of the material and has been suggested to be a fundamental bank erosion process (Lawler, 1997; Couper and Maddock, 2001).

To reduce the risk of erosion to infrastructure and property, river engineering projects contemporaneously allow for prescribed alterations to the intensity, duration, and frequency (IDF) of channel flows to limit the rates of channel adjustment. These allowances are based on models at various scales (watershed to channel scale) which combine flow characteristics of the channel and sediment entrainment properties of the channel boundaries to assess the potential for exceedances of various thresholds such as shear stress, stream power and velocity (Langendoen et al., 2001). However, in cohesive sediments, a representative shear stress associated with incipient motion is complex and highly variable in space, time, and geology (Lawler, 1986; Hanson and Simon, 2001; Wynn et al., 2008; Mahalder et al., 2017).

Semi-alluvial streams in many regions of Southern Ontario consist of geologically diverse cohesive glacial deposits exposed within channel banks and streambeds. There exists a dearth of adequate information to characterize river channels carved within these geologic media in terms of resistance to erosion and as such they are subject to ongoing investigation. These systems have been highlighted as warranting further research efforts by others (Kamphuis and Hall, 1983; Kamphuis, 1990; Gaskin et al., 2003; Shugar et al., 2007; Khan and Kostachuk, 2011; Mier and Garcia, 2011; Pike et al., 2017, Bergman et al., 2022).

The preceding sections in this document will consist of a brief review of factors that govern cohesive soil's resistance to erosion, how the erosion of cohesive soil is typically modelled, and a review of the Jet Erosion Test (JET) Methodology.

2.1 Factors contributing to resistance to erosion in cohesive soil

The erosion of cohesive soils is complex and diverges from the generally established understanding of the processes that occur in non-cohesive material (Partheniades, 1965; Simon et al., 2010). The entrainment of non-cohesive materials largely occurs on a particle-by-particle basis and is predominantly governed by the balance of hydraulic shear and the resistive forces provided by the particle's mass and shape (Shields, 1936; Buffington and Montgomery 1997). However, cohesive sediments are composed of particles sufficiently small that additional electrostatic and electromagnetic resistive forces between individual particles must be included in the force balance at incipient motion (Partheniades, 1965; Le Bissonnais, 1996; Simon and Collison, 2001; Briaud et al; 2001; Briaud, 1999). The strength of these electromagnetic forces is influenced by a wide range of factors (Berlamont et al., 1993; Grabowski, 2011; Mahalder et al., 2017). These can be broadly categorized by the properties listed in *Table 1*. In the pursuit of the collection of representative data regarding the erosion of cohesive soils, it is necessary to be cognizant of how the factors listed in *Table 1* may influence the data being collected and any biases that they may introduce.

Table 1: Properties affecting resistance to erosion in cohesive soil.

Soil Property	Effect on erosion of cohesive soil
Clay Content	Increasing clay content can increase the number of particles small enough for van der Waals forces to act upon (Black et al., 1960; Grissinger, 1966; Briaud et al., 1999). Increasing the clay content has a greater corresponding increase in resistance to erosion when the existing clay content is low compared to when the clay content is already high (due to tradeoffs with bulk density) (Smerdon and Beasley, 1959; Julian and Torres, 2006; Bonelli et al., 2007; Lefebvre et al. 1985; Mitchener and Torfs, 1996; Panagiotopoulos et al., 1997; Grabowski et al., 2011).
Clay Mineralogy	The mineralogy of the clay fraction of the soil can influence the soil's resistance to erosion through the Cation Exchange Capacity (CEC), activity and plasticity (Smerdon and Beasley, 1959; Arulanandan et al., 1973; Mitchener and Torfs, 1996; Mehta and McAnally, 2008). Generally, clays with higher CEC and plasticity have higher resistance to erosion (Smerdon and Beasley, 1959; Gerbersdorf et al., 2007). However, depending on the water chemistry within the pores and of the eroding fluid, higher CEC can be associated with more swelling resulting in pore water pressure forcing clay particles apart and lowering interparticle attraction (Torfs, 1995; Grabowski, 2011; Khandia, 1974).
Pore Water Chemistry	The Sodium Adsorption Ratio (SAR), total salinity, pH and concentration of metals in the pore water of a soil can influence a cohesive soil's resistance to erosion (Partheniades and Paaswell, 1970; Paaswell, 1973; Arulanandan et al., 1973; Arulanandan et al., 1980; Kandiah, 1974; Raudkivi and Tan, 1984). Increasing total salinity and decreasing SAR in porewater both increase the soil's resistance to erosion by reducing the thickness of the electric double layer and increasing interparticle forces (Arulanandan et al., 1973; Raudkivi and Tan, 1984; Arulanandan et al., 1980). Khandia (1974) found clays with high CEC have erodibility which is more sensitive to the SAR of the porewater (with higher resistance to erosion at low SAR).
Eroding Water Chemistry	Generally, the critical shear stress of a cohesive soil increases as the total salinity of the eroding water increases (Parchure and Meta, 1985; Arulanandan, 1980; Raudkivi and Tan, 1984). Concentration gradients of salinity between the eroding fluid and the pore fluid can force water into the pores

	(increasing swelling and lowering resistance to erosion) or can cause ions to adsorb onto the clay surface (increasing resistance to erosion) (Arulanandan, 1975; Heinzen and Arulanandan, 1977). Similar adsorption can occur with metal ions in the water. (Partheniades, 1965). There have been indications that pH can also influence resistance to erosion, however, there is a lack of information on its relative importance in field settings (Khandia, 1974; Grabowski et al., 2011).
Soil Density	Generally, higher resistance to erosion and higher critical shear values are associated with higher bulk density (Laflen and Beasley, 1960; Jepsen et al., 1997; Lick and McNeil, 2001; Mitchener and Torfs, 1996; Berlamont et al, 1993; Kamphuis and Hall, 1983; Hanson, 1992; Hanson and Robinson, 1993; Hanson and Hunt, 2007; Khan and Kostachuk, 2011). This can be attributed to lower interparticle spacing and stronger interparticle bond strengths (Kamphuis and Hall, 1983). Consolidation of a soil to increase a cohesive soil's resistance to erosion depends on whether consolidation collapses the soil's natural structure, and whether the collapse of the clay structure increases or decreases interparticle bonds beyond the natural intact clay structure (Raudkivi and Tan, 1984; Kamphuis and Hall, 1983; Lefebvre et al., 1986).
Macroscopic Bulk Shear Strength	A positive relationship between macroscopic bulk shear measurements and a material's critical shear stress has often been reported with the hydraulic critical shear stress typically being several orders of magnitude lower than the macroscopic shear strength (Dunn, 1959; Kamphuis and Hall, 1983; Sutarto et al., 2014; Khan, 2006; Partheniades, 1965). The difference in magnitudes between macroscopic bulk shear and hydraulic critical shear stress is because the resistance to hydraulic erosion is dependent on the weakest bond between individual particles, whereas the resistance to macroscopic shearing is provided by an ensemble of bonds along the shearing face (Zreik et al., 1998).
Temperature	Generally, higher temperatures correspond to increased erodibility of cohesive soils and lower critical shear stresses (Christensen and Das,1973; Zreik et al, 1998; Khandia, 1974; Gularte et al., 1980; Grissinger, 1966). However, in relation to the sensitivity of cohesive material to other characteristics, temperature is not of primary importance in natural conditions (Raudkivi and Hutchison, 1974).
Biologic Influences	Interactions between sediment and biotic components of fluvial systems can have a wide range of influences on the material's resistance to erosion which can generally be categorized by bioturbation, biostabilization and biodestabilization (Black et al., 2002; Grabowski et al., 2011). Depending on the biologic process (e.g., development of biofilms, biodisturbance/biosuspension, burrowing, root network development) the cohesive sediment's resistance to erosion can be increased or decreased (Grabowski et al, 2011).
Pore Pressure	Simon and Collison (2001) demonstrated through lab experiments that pore water pressure within the channel boundary can build up during a hydrograph's rising limb and dissipate slowly during the falling limb resulting in an upward (toward the channel boundary) effective stress and increasing the likelihood of erosion and block separation. Midgley et al. (2013) observed elevated pore pressures corresponding to higher erosion rates using a trench injection system along a channel bank. Nouwakpo et al. (2010) and Nouwakpo and Huang (2012) investigated the influence of pore pressure on rill erosion and concluded that when upward hydraulic (seepage) forces were acting on the rill more erosion occurred and when downward hydraulic (drainage) forces were acting on the rill less erosion occurred. This was also experimentally demonstrated by Salem (2019).
Weathering of Materials	Material properties along channel boundaries are not temporally static due to weathering leading to the development of a softer, more erodible layer near the surface of the media (Wolman, 1959; Harrison, 1970; Davidson-Arnott, 1986; ASCE, 1998, Couper and Maddock, 2001 Yumoto et al., 2006). This corresponds with the preparatory process occurring as a precursor to fluvial erosion. These weathering processes (e.g., wetting-drying cycles, desiccation cracking, contact ice and frost formation, freeze-thaw cycles, abrasion) have the maximum influence on a surficial layer of material creating a gradient in material properties moving away from the channel boundary. This allows for the removal of surficial particles at shearing forces lower than the representative critical shear stress of the unweathered material (Gaskin, 2003; Davidson-Arnott, 1986, Davidson-Arnott and Langham, 2000; Khan 2006). The influence that weathering has on a media's resistance to erosion has been shown to vary seasonally (Wolman, 1959; Lawler, 1986; Couper and Maddock, 2001; Wynn et al., 2008).

2.2 Modelling erosion of cohesive soils

The excess shear stress model is frequently employed to represent erosion of cohesive sediment. This model relates the depth of erosion (E) which occurs to the shear stress that is applied by the eroding fluid

(τ_o) in excess of a critical shear stress (τ_C) threshold. At shear stresses below the critical shear stress, erosion is assumed not to occur. The erodibility coefficient (K_d) is an empirical coefficient that describes the rate at which the material erodes when the critical shear stress is exceeded. This model is expressed in terms of a depth of erosion (E) in *Equation 1* and in terms of the mass of material eroded (M) in *Equation 2*.

$$E = K_d * (\tau_o - \tau_c)^m \qquad (1)$$
$$M = K_d' * (\tau_o - \tau_c)^n \qquad (2)$$

The empirical exponents *m* and *n* are often assigned values of 1 resulting in the representation of erosion as a linear function of the excess shear imposed upon the material (Salem, 2019; Hanson and Simon, 2001). Various researchers have proposed different values of *m* and *n* to improve empirical fits of data or included that variable in the model-fitting process (Walder, 2015; Khanal et al. 2016b; Cossette, 2016; Wahl, 2021), however, the improved ability to fit empirical data is simply the result of an additional variable in the curve fitting exercise and the dimensionality of the exponents. While it can improve the fit of the modelled erosion to the observed erosion, it creates confusion when comparing materials due to the lack of relation of the exponents to any physical properties of the soils (Wahl, 2021; Salem, 2019).

There is considerable debate within the literature as to whether a critical shear stress parameter exists, and whether the excess shear stress model is an appropriate representation of erosion in cohesive sediment (Van Prooijen and Winterwerp, 2010; Debnath and Chaudhuri, 2010). Various alternatives to the excess shear stress model have been proposed including models based on stochastic representations of bed shear stress and bed strength, and models based on mechanistic and probabilistic functions. (Debnath and Chaudhuri, 2010; Salem, 2019; Wilson et al., 1993a).

One recently popularized model is the mechanistic and probabilistic function proposed by Wilson et al. (1993a) evaluated by Wilson et al. (1993b) and modified by Al-Madhhachi et al. (2013b). However, researchers have had varying levels of success in fitting experimental data to the model (Wahl, 2021; Al-Madhhachi et al., 2013b). The model, as proposed by Wilson (1993a) is based on the forces and moments involved in particle detachment, as well as the supposition that some minimal erosion continues to occur at stresses below the critical shear level. Al-Madhhachi et al. (2013b) expanded on this original model to include the effects of seepage on the particle detachment mechanism. Salem (2019) provided an in-depth review of the applicability of the mechanistic development of this model and concluded that "the complexities of the fundamental model proposed by Wilson are unnecessary and the model itself provides no real advantages over the simpler excess shear model."

2.3 Methods of measuring erosion in cohesive material

Regardless of how erosion in cohesive material is modelled, the success of the model depends on the quality of data informing its parameterization. Relying upon empirical relationships to assess a material's resistance to erosion increases the uncertainty in modelling erosion, so it is preferred to obtain direct measurements of a cohesive material's behaviour under specified erosive stresses and apply them to a theoretical framework (Briaud et al., 2001; Simon et al., 2010; Salem, 2019). The importance of obtaining accurate and representative measurements of erosion in cohesive material is demonstrated by the many techniques and equipment developed for this purpose. Methods of obtaining direct measurements of erosion of cohesive media include the Drill Hole Test (Rohan et al. 1986), Hole Erosion Test and Slot Erosion Test (Wan and Fell 2004; Wahl, 2010), Flow Pump Test (Reddi et al. 2000), Pinhole Test (Sherard et al. 1976), the Rotating Cylinder Apparatus (Moore and Masch, 1962; Chaphuis and Gatien, 1985; Lim and Khalili, 2009), the Erosionometer (Salem and Rennie., 2017), the Erosion Rate Meter (Salem, 2019), the Cohesive Strength Meter (Tolhurst et al, 1999; Tolhurst et al, 2000; Watts et al, 2003; Simon et al., 2010), Piston type flumes (McNeil et al., 1996; Briaud et al., 2001, Crowley et al., 2014; Mahalder et al., 2022; Sutarto et al., 2014) and the Jet Erosion Test (JET) (Hanson and Simon, 2001, Hanson and Cook, 2004).

The JET has been one of the most widely used methods of measuring erosion in cohesive soils since the 1990's due to its ability to be applied both in-situ and in laboratory settings, the straightforward operation of the test apparatus, and adaptations of the test apparatus to enhance practical field-use (Simon et al., 2010; Wahl, 2021). The ability to perform relatively quick and repeatable tests in-situ allows for the maintenance of the factors reviewed in Section 2.1, without having to recreate those conditions in a laboratory setting and eliminates the uncertainty associated with the replication of those conditions. For these reasons, the JET methodology was identified as the preferred method to collect representative data across many diverse sites within this investigation.

The JET (first employed by Dunn (1959)) involves the impingement of a submerged hydraulic jet onto cohesive soils to investigate their properties under erosive conditions. The test methodology was adapted to an in-situ device by Hanson et al. (1990) and has been applied extensively across the globe since its inception (Hanson and Simon, 2001; Clark and Wynn, 2007; Shugar et al, 2007; Thoman and Niezgoda., 2008; Simon et al, 2010; Khan and Kostachuck, 2011; Dutta and Karmakar, 2015; Haddadchi et al., 2017; Rose et al., 2018). The original device conceived for field implementation consisted of a circular jet nozzle diameter of 6.4 mm and a steel jet submergence tank 0.3 m in diameter (Hanson and Simon, 2001). As demonstrated in Clarke and Wynn (2007) and Charanko (2010), this apparatus was adapted for multi-

angle implementation to test steeply angled riverbanks by enclosing the top of the jet submergence tank. Along with being unwieldy to implement in remote areas, the test apparatus of this size required a large water intake to perform the test. To assist with practical field implementation, a modified smaller version of the device was developed (Figure 1) and has also been implemented extensively (Simon et al., 2010; Daly et al., 2015b; al-Madhhachi et al., 2013a; Mahalder et al., 2018), however, the concept and theory behind the test methodology remain the same as the Original JET device. The modified dimensions of the mini-jet apparatus include a 3.18 mm diameter nozzle, a 0.18 m diameter foundation ring, and a 0.1016 m submergence tank (Simon et al., 2010; Al-Madhhachi et al., 2013a).
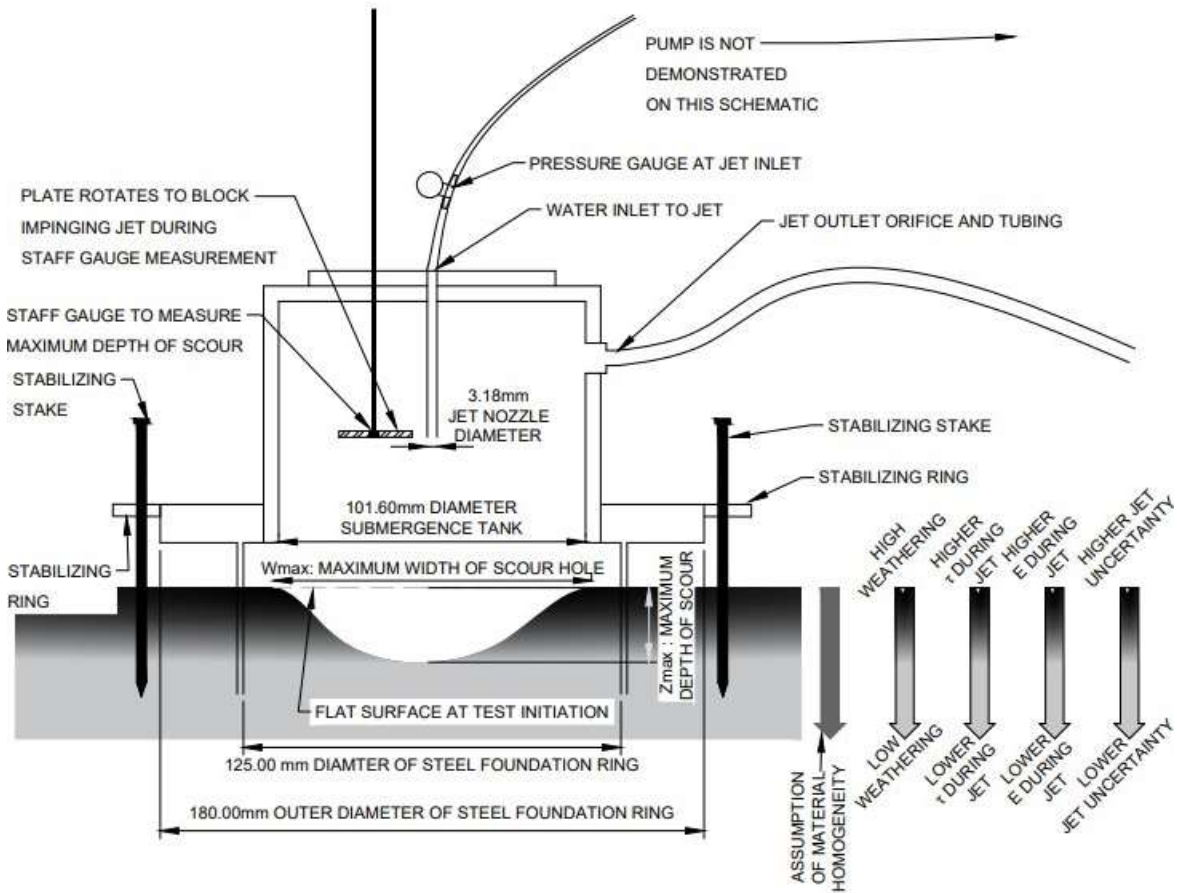
Figure 1: Mini-JET schematic

Operation of the JET consists of directing a vertical, submerged, circular hydraulic jet of water (at constant pressure) towards the sample material for fixed intervals. After taking an initial measurement of the distance of the jet nozzle from the material, the jet is allowed to impinge upon the surface for pre-defined time intervals. As the jet impinges upon the media, it is redirected radially along the test surface imposing a shear stress upon the material (Figure 2). At each designated time interval, the impingement of the jet is blocked and the depth of the scour hole that has developed up to that point (using the initial

depth measurement as a reference) is measured with a point gauge. The average applied shear stress is calculated for each interval based on the distance the jet travels before contacting the surface and the shear stress distribution of a vertical, submerged, circular hydraulic jet impinging upon a planar surface (Beltaos and Rajaratnam, 1974; Hanson et al., 1990; Hanson and Cook, 1997; Stein and Nett, 1997). As the duration of the test progresses and the depth of the scour hole increases, the distance that the jet must travel to contact the surface of the material also increases resulting in increased energy dissipation and a reduction in the amount of shear force imposed upon the material by the jet (Hanson et al., 1990). The calculated applied shear stress values are then coupled with the change in depth of the scour hole between measurements to construct an erosion rate versus applied shear stress curve.

2.4 Applied shear stress from impinging jets

The JET relies upon accurate determination of the shear stress imposed upon the test surface by the impinging, circular, vertical jet traveling through a uniform flow medium. Using air as the flow medium, Beltaos and Rajaratnam (1974) identified three regions of flow from a circular jet impinging upon a flat surface: the free jet region, the impingement region, and the wall jet region (*Figure 2*). Further, they measured static pressures and axial velocity distributions to develop *Equation 3* to predict the maximum wall shear stress within the impingement region of the jet flow when the jet is fully developed where τ_{om} is the maximum shear stress imposed upon the impinging wall, U_o is the uniform velocity of the fluid at the jet nozzle, d is the nozzle diameter, ρ is the mass density of the fluid and H is the height of the nozzle from the impinging wall.

$$\tau_{om} = 0.16\rho U_o^2 \left(\frac{d}{H}\right)^2 \qquad (3)$$

Rajaratnam and Beltaos (1977) defined the jet as fully developed when the impingement height is greater than the length of the jet potential core (H_p), which is the region of the jet where the fluid velocity (U) is equal to the fluid velocity at the nozzle (U_o). They calculated that jets were fully developed when the distance between the nozzle and the impingement surface is greater than 8.3 times the diameter of the nozzle.

Hanson et al. (1990) measured pressure and shear stress distributions under a circular, submerged, hydraulic jet impinging upon a flat surface using pressure transducers and hot-film probes. Generally, they noted similarities to the shear stress distributions observed from air jet studies but made the observations that the peak shear stress appeared to occur slightly closer to the stagnation point (*Figure 2*). Based upon their experimental results, they described the distribution of shear stress impinging upon the wall at various radial distances from the impingement point by *Equation 4* where τ_{om} is the maximum

shear stress imposed upon the impinging wall, τ_o is the applied shear stress at a radial distance (r) and H is the height of the nozzle from the impinging wall. The maximum shear stress imposed upon the impinging wall during their experiment is described by *Equation 5* where U_o is the uniform velocity of the fluid at the jet nozzle and ρ is the mass density of the fluid.

$$\frac{\tau_o}{\tau_{om}} = 66.5(\frac{r}{H})e^{-7.68\left(\frac{r}{H}\right)^{0.6}} \tag{4}$$

$$\tau_{om} = 0.56 \left(\frac{\rho U_o^2}{\left(\frac{H}{d}\right)^2}\right)^{0.74} \tag{5}$$

For fully developed jets and introducing a coefficient of friction (C_f), Hanson and Cook (1997) reduced the relationship for maximum applied bed shear stress to *Equation 6*. Where C_f is the friction coefficient and C_d is the diffusion coefficient. C_f and C_d are taken as 6.3 and 0.00416 respectively based on the experimental results of Hanson et al (1990).

$$\tau_{om} = C_f \rho \left(C_d U_o \frac{d}{H}\right)^2 \quad H > H_p \tag{6}$$
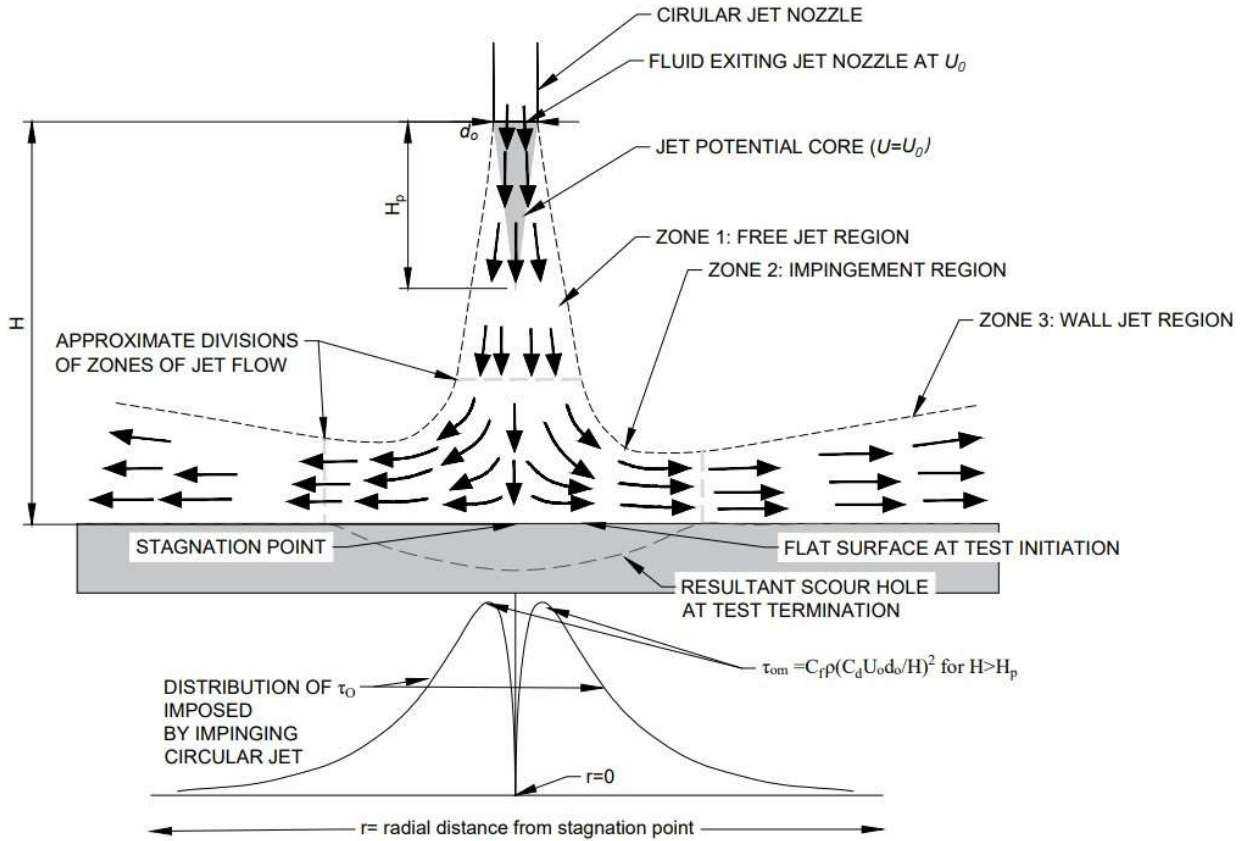
Figure 2: Submerged impinging circular hydraulic jet and resulting shear stress distribution. Adapted from Hanson et al. (1990), Beltaos and Rajaratnam (1974) and Khan (2006).

2.5 Sources of error in JETs

Considerable research effort has been conducted to advance the understanding of the hydrodynamics of the impinging jet during the test, and the degree to which assumptions made during the analysis of JET data influence test results (Mazurek et al., 2001; Rajaratnam and Mazurek, 2005; Amin and Mazurek, 2016; Cossette et al., 2012; Rajaratnam et al., 2010). Concerns raised in literature regarding the representativeness of JET results focus on the confinement within the JET apparatuses altering the calculation of imposed shear stresses, the assumption of the jet impinging upon a smooth and flat surface (relative to that of a natural geologic surface), the shape of the scour hole influencing local hydrodynamics and abrasion caused by larger grains (sand and gravels) when tests are performed in till materials (Karamigolbaghi et al., 2017; Khan and Kostachuck, 2011; Shugar et al., 2007; Mazurek et al., 2001; Weidner, 2012; Ghaneeizad et al., 2015). Understanding the limitations and potential errors arising during JET application is integral to formulating the methodology outlined in *Section 3* to minimize the influence of these limitations.

2.5.1 Confined environment

The prediction of the maximum shear stress imposed by a jet impinging upon a flat surface (*Equation 3*) developed by Beltaos and Rajaratnam (1974) includes the assumption that the jet impinges upon the test surface in an unconfined environment. Using Photo-Imaging Velocimetry (PIV), Ghaneeizad et al., (2015) measured actual shear stresses (τ_{om}) imposed upon the material in the original JET apparatus as much as 2.4 times higher than those predicted by jet impingement theory. However, in the development of *Equation 4* and *Equation 5*, Hanson et al. (1990) adjusted the semi-empirical equations developed by Beltaos and Rajaratnam (1974) to fit their experimental results of shear stress imposed by a submerged hydraulic jet measured by hot-film sensors. The semi-empirical relationship developed by Hanson et al. (1990) *(Equation 5)* implicitly includes the effect of confinement within their experimental test apparatus – which is a vital calibration parameter for the employment of *Equation 5*. Hanson and Cook (1997) furthered *Equation 4* and *Equation 5* in the development of *Equation 6* requiring uniformity in experimental conditions for comparison purposes between semi-empirical equations. These experiments employed a 13mm diameter submerged jet nozzle within a 0.61m diameter reservoir resulting in a reservoir diameter-to-jet diameter ratio of 46.9. The mini-JET apparatus has a reservoir diameter-to-jet diameter ratio of 37.8 with additional confinement of a sealed top to ensure the jet nozzle remains submerged during multi-angle tests. This additional confinement was not accounted for during the semi-empirical development of the maximum shear stress relationship by Hanson et al. (1990). Al-Madhhachi et al. (2013a) compared the results of a multi-angle Original JET apparatus and the mini-JET apparatus (both with sealed reservoir tops) and calculated lower critical shear stresses from the mini-JET device.

They attributed this discrepancy to the method of sample preparation; however, a secondary explanation was offered as the differences in ratios of the reservoirs to the jet nozzle diameters between the two devices. While maximum applied shear derived from Original JETs does not need to be corrected for confinement (based on the origin of the empirical results), there may need to be a correction applied to account for the greater confinement within the mini-JET device compared to the Original JET.

2.5.2 Smooth surface

The test conditions employed by Hanson et al. (1990) leading to the development of *Equation* 6 measured the shear stress imposed by the submerged hydraulic jet upon a relatively smooth plexiglass body. Rajaratnam and Mazurek (2005) demonstrated that the impingement of the jet upon a rough surface body can increase shear stresses imposed upon the surface by factors ranging between 2.5 – 5. In the application of JET methodology in field scenarios, the surface being tested is not smooth. It consists of undulations, pitting and general heterogeneities which are basic components of exposed surface bodies in natural environments. Further, the material roughness is constantly changing throughout the test, particularly in heterogeneous materials with wide ranges in grain size. These results may indicate that critical shear parameters estimated from JETs in field applications should be considered a lower bound on the actual critical shear.

2.5.3 Flat surface

The measured values of shear stress used to parameterize the semi-empirical relationship of shear stress imposed by the submerged hydraulic jet were originally measured on a flat surface by Hanson et al. (1990). While this is a reasonable representation of the test surface at test initiation, as a scour hole develops in practice, the surface will deviate from this flat surface assumption with greater deviation occurring in an ever-increasing deeper scour hole (i.e., conical depression). This has been identified to alter the flow regime of the impinging jet yielding a deviation of the imposed shear stress when the scour hole is narrow and deep, however, this deviation has been shown to have negligible effects in wider and shallower scour holes (Moore and Masch, 1962; Hollick, 1976; Mazurek et al., 2001; Weidner, 2012; Cossette, 2016; Ghaneeizad et al., 2015). In narrow and deep scour holes, the flow is observed to be strongly deflected causing a reverse flow thereby altering the dynamics of the jet impingement upon the surface and reducing its momentum by the entrainment of its own flow (Mazurek, 2001; Mercier et al., 2014). The development of narrow and deep scour holes has been suggested to be a criterion for test failure at aspect ratios greater than 2 (where $Aspect\ ratio = Z_{max}/W_{max}$ with Z_{max} and W_{max} representing the maximum depth of scour and maximum width of scour, respectively (*Figure 1*): JET analysis would not be considered applicable in those circumstances (Weidner, 2012). The threshold of

acceptable aspect ratios proposed by Weidner (2012) was derived from original JET datasets and did not consider how the smaller jet nozzle of the mini-JET may affect acceptable aspect ratios. Compared to the narrow and deep scour holes, the influence of shallow and wide scour holes is minimal (Mazurek et al., 2001; Mercier et al., 2014). There remains some uncertainty as to the magnitude of the influence of the flat surface assumption, however, it has been recommended that JET operators select pressure heads to aim for shallower scour holes during tests to limit the deviation from the flat surface assumption (Karamigolbaghi et al., 2017; Weidner, 2012).

2.5.4 Presence of stones and sand

Shugar et al. (2007) and Khan and Kostachuck (2011) both observed the influence of sands and gravels during the application of JET methodology upon tills in southern Ontario. Sands and gravels contained within the till material were observed to be released from the fine-grained matrix during the progression of the scour hole during the JET testing procedure which consequently altered the shear imposed upon the geologic media through the additional process of abrasion (Shugar et al, 2007; Khan and Kostachuck, 2011). Shugar et al. (2007) noted that particles that are unable to be evacuated from the hole by the jet must be removed manually from the scour hole by hand when the JET was paused for measurements, however, this is not always necessary during non-vertical tests on streambanks where the detached coarse particles are assisted out of the hole by the gravitational forces (Wahl, 2016). Shugar et al. (2007) postulated that sand and fine gravels would similarly be present during flood flows and that the abrasion that occurred during the JET may be more representative of erosion processes in a semi-alluvial system.

2.6 JET solution techniques

Perhaps the most confounding component of JETs is the wide variety of solution techniques that have been developed to characterize material tested with JETs and the different values of erodibility parameters (τ_C and K_d) they produce (Cossette et al., 2012; Wahl, 2021). This culminated in an investigation performed by Wahl (2021) where the results of nine different solution techniques were compared. Several of the solution techniques reviewed are listed in *Table 2* which are divided into four categories: experimental (only τ_C is estimated with no corresponding K_d), fitting to the linear excess shear stress model, energy-based models, and non-linear models.

Table 2: JET solution techniques

Technique	Category	Description
Visual Approximation	Experimental	Employed by Dunn (1959) and Cossette (2016), the flow rate through the JET device is incrementally increased until erosion is visually observed on the test surface.
Equilibrium Determination	Experimental	Employed by Mazurek (2010), Amin and Mazurek (2016) and Cossette (2016), the JET is conducted for a sufficient duration that the scour depth vs time plot approaches a horizontal asymptote corresponding to a critical shear stress. Cosette (2016) suggested that this technique overestimates critical shear stress, and Mazurek (2010) observed this technique to predict τ_c twice that of the Blaisdell Method.
Blaisdell Method (**BM**)	Linear Excess Shear Stress Model	This is the most historically prevalent JET solution technique and is described in detail by Hanson and Cook (2004). An equilibrium scour depth is estimated using a hyperbolic function developed by Blaisdell (1981) to predict a "practical equilibrium" of scour. Data collected during the JET is used to estimate the practical equilibrium scour depth, and in turn the shear stress at that depth is taken as the critical value. Then, K_d is converged upon by minimizing errors in a dimensionless time value between observed and predicted data sets. This technique has been demonstrated to underestimate the τ_c relative to other techniques but may be useful in providing conservative estimates of erodibility parameters for engineering projects (Cossette, 2016; Wahl, 2021).
Linear Regression Method (**LR**)	Linear Excess Shear Stress Model	Employed by Cossette (2016) and Wahl (2021), this technique estimates the erodibility parameters from a linear regression line through the measured erosion rates and applied shear stresses during a JET. The X-intercept of the regression represents τ_c and the slope represents k_d. This was the solution technique recommended by Wahl (2021) due to it obtaining the most consistent results in characterizing a material's erodibility characteristics. Both Cossette (2016) and Wahl (2021) observed that some standardization of test length is required so that the excess of data points in the low erosion rate tail of the test does not skew the linear regression.
Scour Depth Method (**SD**)	Linear Excess Shear Stress Model	Proposed by Daly et al. (2013), this technique simultaneously solves for τ_c and K_d in the excess shear stress model by minimizing the sum of the squares of error between predicted and observed scour depths using the Excel® Solver Function applying the Generalized Reduced Gradient (GRG) technique. This was compiled into a spreadsheet tool made available by the author. Wahl (2016) and Wahl (2021) observed that unrealistically large K_d values can be obtained and τ_c values are close to the stresses exhibited at the end of the test. They also observed that occasionally the resulting τ_c can occasionally be erroneously obtained as zero. This technique has been employed in many studies since its introduction and generally fits the measured test data stronger than BM (Khanal et al., 2016b; Mahalder et al., 2018; Daly et al., 2013; Daly et al. 2015a; Daly et al. 2015b; Wahl 2021).
Iterative Method	Linear Excess Shear Stress Model	Proposed by Simon et al. (2010), this technique has the same objectives of BM, but solves for τ_c (τ_c is constrained between 0 and the final applied shear stress) and K_d simultaneously to obtain a best fit. The Excel® GRG technique is provided an initial guess obtained from the BM, however, the results of this solution

		technique are sensitive to the initial guess (due to the polynomial nature of the results) adding an additional level of uncertainty into the analytic results.
Mass of Scoured Material	Energy-Based	JETs results were solved based upon the amount of energy required to achieve an observed mass of eroded soil rather than the shear stresses at certain depths (Moore and Masch, 1962; Hollick, 1976; Marot et al. 2011). This was advanced by Rose et al. (2018) who proposed a method of incorporating the mass of material eroded and the hydraulics of the impinging JET to determine the amount of energy required to remove the observed amount of material from the scour hole. Applying this method, Haddadchi et al. (2017) suggested that this solution technique can provide insight pertaining to the changing material bulk density with depth. Instead of arriving at a τ_C, this solution technique results in a soil resistance parameter J (J/kg).
Non-Linear Excess Shear Stress	Non-Linear Erosion Model	Wahl (2021) and Khanal et al. (2016b) calculated the τ_C and K_d by fitting the observed test results to the excess shear stress model without the assumption of unity on the exponent "m" in *Equation 1*. Similarly, Cossette (2016) allowed the m value to vary while applying the linear regression method by fitting a power function to the observed excess shear stress above the pre-determined τ_C. Wahl (2021) noted that while allowing the "m" value to vary can improve the curve fitting ability, the improvement cannot be tied to any material properties and no trends between tests or materials can be determined thus complicating material classification.
Wilson Model	Non-Linear Erosion Model	Al-Madhhachi et al. (2013b), Khanal et al. (2016b) and Wahl (2021) fit JET data to the Wilson Model (*Section 2.2*) using scour rates and scour depths as the parameters for model optimization. Wahl (2021) determined that the Wilson model did not perform as well as linear models when optimized for scour depth data. The lack of correlation between rate parameter and shear stress threshold parameter across tests complicated comparisons between tests and materials. Additionally, while the first two regions of the Wilson model can be adequately described with JET data, the final region is largely extrapolated with little to no definition in this region.
Exponential Linear Model	Non-Linear Erosion Model	An empirical model was proposed by Wahl (2021) which consisted of two regions: the initial region with accelerating scour rates as shear stress increases and a linear region for higher stresses. While this model demonstrated higher success in fitting observed data, similar to the Wilson model, the correlations between rate parameters and shear stress threshold parameters across tests were poor which diminishes the utility of the model and complicating the classification of soils into erodibility groups.

Wahl (2021) concluded that the Linear Regression Method (LR) (*Table 2*) is the most consistent solution technique for producing repeatable results and that fitting JET data to non-linear erosion models does not provide any statistical benefits over fitting JET data to the linear excess shear stress model. These conclusions are helpful guides in the selection of an appropriate JET solution technique. Given the different erodibility parameters that these techniques can produce, another consideration that must be accounted for is the standardization of solution technique when comparing a new dataset to historically compiled JET datasets. For instance, to compare JET results to those of Simon et al. (2010) a newly compiled dataset must employ the Blaisdell Method (BM) (*Table 2*) or the Iterative Method (*Table 2*). Based on the review of the various JET solution techniques in *Table 2*, this investigation employs LR, Scour Depth (SD) and BM.

2.7 Field Implementation of JET methodology

In-situ JET data acquisition has historically been employed following the methods outlined by Hanson and Cook (2004) with adaptations for the application of the mini-JET as outlined by Al-Madhhachi et al. (2013a). Minor adaptions and enhancements have been periodically employed to augment situational control such as the clearing of sloughed bank material and alluvial material from the test surface as per Khan and Kostachuk (2011), and the maintenance of ambient moisture content by avoiding tests on days with rainfall (Mahalder et al., 2018). However, both the frequency of scour depth measurements and the duration of tests have been quite varied and have consistently deviated from the recommended measurement frequency of 5-10 minutes for a set of 10-12 readings as outlined in Hanson and Cook (2004). Even such a specific recommendation leaves substantial room for variability in test durations, with tests consisting of 10 readings recorded at 5-minute intervals (50-minute duration) or 12 readings recorded at 10-minute intervals (120-minute duration). Field campaigns have employed various levels of standardization on measurement placement and test duration as summarized in *Table 3*.

Table 3*:* **Range of measurement frequency and test durations in JET studies.**

Study	Test Duration (min)	Measurement Frequency (min)
Clark and Wynn, 2007	45	5
Shugar et al., 2007	50-180	2
Khan and Kostachuck, 2011	12-165	2-10
Mahalder et al., 2018	46	0.5-2

The variability in test duration and measurement frequency in *Table 3* can lead to differences in the estimation of erodibility parameters (Cossette, 2016; Khanal et al., 2016a; Karamigolbaghi et al., 2017).

The most prominent departure from the original Hanson and Cook (2004) methodology was the proposal of stepped multi-pressure setting (MPS) tests by Mahalder et al. (2018) rather than applying a single pressure setting (SPS) throughout each JET. This results in a series of shorter JETs (12-20 minutes per pressure setting) being performed (maximum of five pressure increases) successively in the same location with a continuingly larger scour hole associated with each iterative pressure increase. This was proposed as a method to obtain depth-averaged samples to reduce the influence of heterogeneity of the material as the depth of scour progresses (arising from weathering processes).

2.8 Influence of material heterogeneity on JETs

Material close to the body surface in natural settings is exposed to weathering processes such as wetting/drying cycles, freeze/thaw cycles, frost weathering, cryo-fracturing, ice contact, abrasion, temperature fluctuations, thermal stress, and chemical weathering from water quality. These ambient processes have more muted effects deeper below the surface creating a layer of weaker material at the surface (Harrison 1970, Davidson-Arnott, 1986; Davidson-Arnott and Langham, 2000; Couper and Maddock, 2001). These weathering processes result in a near-surface gradient of changing material properties including bulk shear stress and moisture content (Khan, 2006). The ambient changes in material properties along this gradient are counter to the fundamental assumptions of a JET test; ergo the material is assumed to remain homogenous throughout the progression of the scour hole (Figure 1).

It should be noted that erodibility trends corresponding to the in-situ ambient weathering conditions as a function of depth from the surface are reciprocal with the applied shear imposed by the impinging JET. The maximum applied shear is experienced at the test body surface (the weakest material) when it is closest to the jet nozzle and the applied shear subsequently decreases with increasing depth where the most coherent matrix material is present (nearing termination of the test). This results in the weakest material being subject to the highest stresses. Since fluvial erosion is a surficial process and weathered material can represent outsized contributions to bank erosion (Wolman, 1959; Lawler, 1997; Couper and Maddock, 2001) the characterization of this layer cannot be ignored, however, the JET methodology is limited in the amount of relevant information it can collect regarding this layer. Many of these characteristics are shown in *Figure 1*.

Differences in critical shear stresses between the surficial layer of material and the underlying matrix were investigated by Khan (2006) using a paired-testing approach. Six JETs were performed on the weathered surface of a till material. Upon their completions, material was removed from the surrounding area of each of the six test locations such that new surfaces were exposed at the respective depths of the maximum scour (i.e. to place the JET test apparatus on a fresh matrix plane at the maximum scour depth

at each location). Six new tests were conducted commencing at the new planar surfaces. Results of the paired tests were analyzed using the BM (*Table 2*) and then differences between the surficial and underlying material were evaluated using the Mann-Whitney U test (Walpole et al., 2007) yielding no statistical difference between erodibility coefficients or critical shear stresses of the surficial and underlying materials. Khan (2006) noted that some disturbance of the material may have occurred during the removal of the surrounding surficial layer such that the JET could be placed on surface planes of the maximum scoured depths. It is also noted that the tests corresponding to the weakened surficial material may have been unduly influenced by the underlying unweathered material with the scour holes ranging from 1.16 cm to 7.99 cm in the upper layer, potentially extending to well within the underlying less weathered material. The expectation of weaker surficial layers (0-3cm thick) of material arising from weathering processes (wetting/drying cycles, frost cycles) also led Mahalder et al. (2018) to propose the Multi-Pressure setting test to obtain depth-averaged results of JETs.

The recognition of the heterogeneity of the material being tested during in-situ JET application led to the development of the test segmentation analytic methodology described in *Chapter 5*.

2.9 Surficial geology of Southwestern Ontario

The surficial geology throughout southwestern Ontario is generally associated with glacial processes corresponding to the Quaternary Period resulting in a complex distribution of glacially derived sediment including till (boulder clay) and glaciolacustrine deposits (Karrow, 1993; Barnett et al, 1999). Dreimanis and Schluchter (1985) defined till as *"a highly variable sediment that has been transported and deposited by or from glacier ice, with little or no sorting by water."* Throughout the late 20th century substantial effort was made to map the Quaternary geology of southwestern Ontario (White, 1975; Cowan, 1976; Sharpe, 1990; Karrow and Easton, 2005; Karrow, 1987; Cowan, 1972; Sado and Vagners, 1975; Karrow, 1993; Karrow, 1977; Barnett et al, 1999; Karrow, 1967). While there has recently been a shift away from some of the mapping techniques employed during these studies (Menzies and van der Meer, 2018), the geologic units identified during these mapping campaigns remain a common characteristic considered during site characterization in water resource engineering applications.

Chapter 3
Field Methodology

This section describes the equipment and methodology employed during the field data collection component of the investigation. The development of the applied methodologies incorporates information reviewed within *Chapter 2*.

3.1 Site selection

Based on anecdotal evidence of clay and fine-grained till exposures in streams in Southwestern Ontario, a list of potential study sites was compiled. These sites were screened based on the following three selection criteria:

- o a review of pertinent Ontario Geological Survey Quaternary Geology maps and reports such that sites included a broad range in consolidated sedimentary environments. Preference was given to tills of the region within a 150km radius of the University of Waterloo in consideration of land assemblages undergoing significant land use change and considering available economic resources,
- o Site conditions applicable to mini-jet methodology (e.g., if the depth of water over till exposure is conducive to testing),
- o Ease and safety of site access.

Each geologic media was determined through qualitative observations made in the field and the use of relevant geological reports and mapping. It should be noted that due to the variable nature of till materials, and the diverse geological history of southern Ontario, uncertainty can remain in till classification even when made by experienced geologists (Cowan, 1976; Dreimanis and Schluchter, 1985). Since no detailed material analysis (i.e., heavy mineral analysis, pebble lithology, carbonate analyses, percent calcite, percent dolomite) was performed as a part of this investigation, the material classifications were based on the field operators' best judgement in conjunction with Ontario Geological Survey Quaternary Geology maps. Detailed material descriptions and the geologic maps used in the material classification are provided in *Appendix A* with photos of the test material provided in *Appendix B*.

Table 4 lists the study sites subject to detailed investigation after the culling process as listed above and the corresponding geological unit in which mini-JETs were performed.
Figure **3** demonstrates the spatial distribution of the sites in Southern Ontario.

Table 4: Study sites

| Site (Site Abbreviation)	Geological Unit	Parent watershed	Geologic Report
Fletchers Creek at Mississauga (FC)	Halton Till	Credit River	Quaternary Geology of Brampton (Karrow and Easton, 2005)
Mimico Creek at Etobicoke (MCE)	Halton Till	Mimico Creek	Quaternary Geology of Brampton (Karrow and Easton, 2005)
Etobicoke Creek Tributary at Caledon (ETC)	Halton Till	Etobicoke Creek	Quaternary Geology of Brampton (Karrow and Easton, 2005)
Grindstone Creek Tributary at Waterdown (GT)	Halton Till	Grindstone Creek	Quaternary Geology of the Hamilton-Cambridge Area (Karrow, 1987)
Laurel Creek at University of Waterloo North Campus (LNC)	Maryhill Till	Grand River	Quaternary Geology of the Stratford-Conestogo Area (Karrow, 1993)
Nith River at Millbank (NMB)	Stirton Till	Grand River	Quaternary Geology of the Stratford-Conestogo Area (Karrow, 1993)
Amulree Creek at Lisbon (NTL)	Mornington Till	Grand River	Quaternary Geology of the Stratford-Conestogo Area (Karrow, 1993)
D'aubigny Creek at Brantford (DCB)	Haldimand Clay	Grand River	Pleistocene Geology of the Brantford Area (Cowan, 1972)
Gainsborough Ravine at London (GRL)	Dorchester Till	Thames River	Quaternary Geology of the Lucan Area (Sado and Vagners, 1975); Pike et al. (2017)
Trout Creek at Harmony (TCH)	Tavistock Till	Thames River	Quaternary Geology of the Stratford-Conestogo Area (Karrow, 1993)
Whirl Creek at Mitchell (WCM)	Wartburg Till	Thames River	Quaternary Geology of the St Mary's area (Karrow, 1977)
West Creek at New Market (WCN)	Schomberg Clay	Lake Simcoe	Quaternary Geology of the Newmarket Area (Barnett et al, 1999)
Highland Creek at Scarborough (HC)	Leaside Till	Highland Creek	Pleistocene Geology of the Scarboro Area (Karrow, 1967)
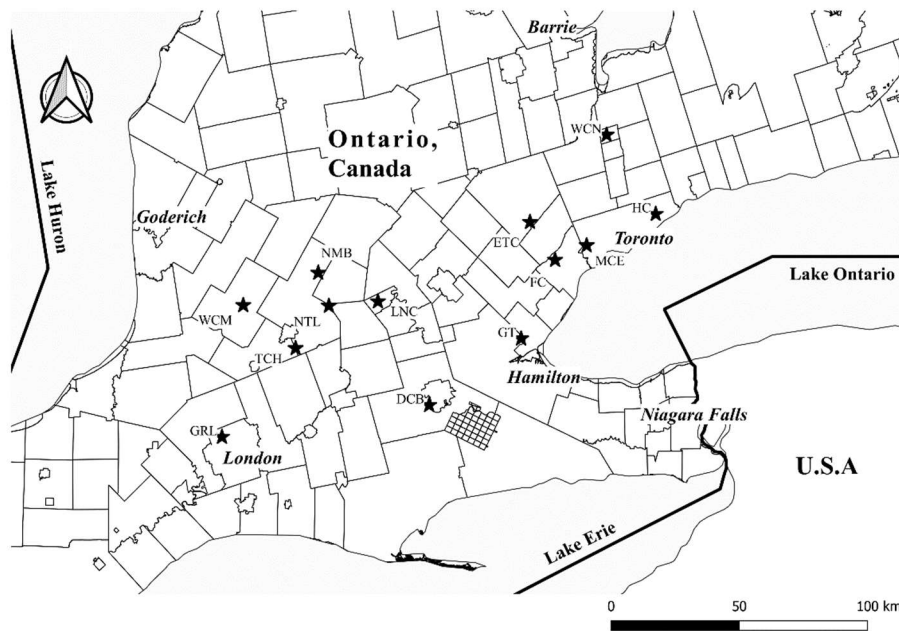
Figure 3: Study site locations

(contains information licensed under the Open Government License of Ontario). Note: Site names are referenced in Table 4.

3.1.1 Equipment

Due to the practicality in field application of the mini-JET methodology, and its ability to perform repeatable in-situ tests, it was selected as the preferred method to collect representative in-situ data spanning several test sites and geologic environments. The mini-jet apparatus used in this investigation was constructed to replicate the mini-JET employed by Simon et al. (2010), Daly et al. (2015), Al-Madhhachi et al. (2013a) and Mahalder et al. (2018). The device consists of a 125mm diameter steel foundation ring, a 101.6 mm diameter plexiglass submergence tank, a rotatable 3.175 mm jet nozzle, a deflector plate, and a point gauge (*Figure 1*). When the jet is not desired to impinge upon the test surface (at test set-up or during a discrete measurement), the jet nozzle is rotated to impinge upon the deflector plate preventing the flow from proceeding. At this orientation, the depth gauge is situated in the center of the test apparatus corresponding to the measuring point on the test surface. When the nozzle is rotated to the impinge setting, the jet aligns with the center of the test surface and is allowed to freely impinge upon the test material. When not being used, the staff gauge is retracted out of the reservoir such that it does not influence the hydrodynamics within the apparatus.
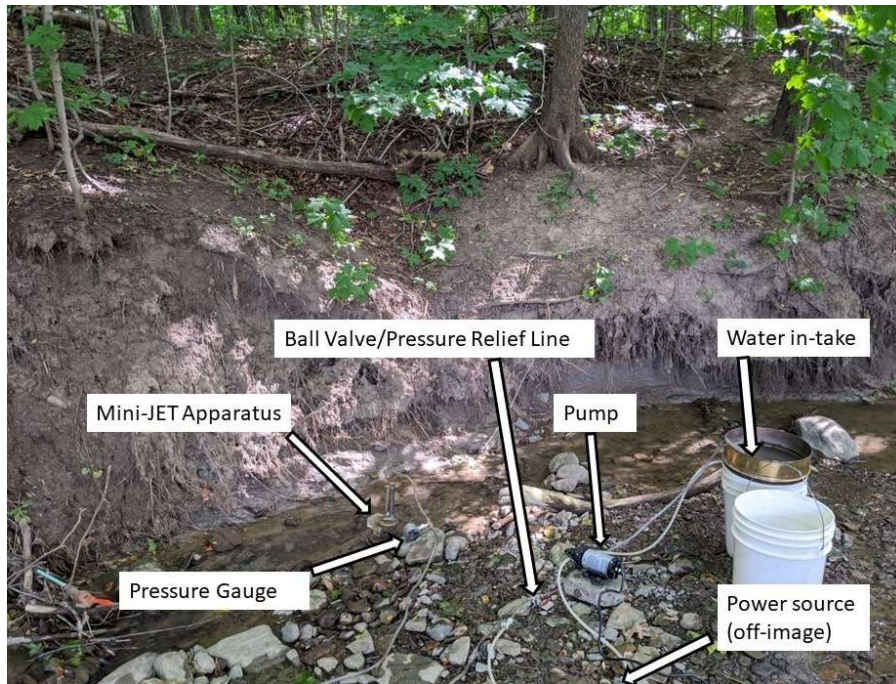

Photo 1: Example of field JET set-up.

Stream water was supplied to the test apparatus by an Aquatech 5800 demand-delivery pump connected to the mini-jet apparatus by 1/8″ vinyl tubing and powered by a Honda eu1000i gas-powered inverter. The use of in-situ stream water ensured its characteristics were representative of site conditions at the time of the test. The water was pumped through a t-joint with one branch proceeding to a digital pressure

gauge before flowing through the jet nozzle and the other branch acting as an overflow relief and controlling the pressure head with a ball valve. Pressure readings between 1.25 and 12 psi were able to be attained with pressures fluctuating +/- 0.1 psi at lower pressure settings and +/- 0.3 psi at higher pressure settings. Pressure readings were recorded upstream of one of two connecting tubes between the pressure gauge and the mini jet nozzle with lengths of 1.45 m and 0.5 m. The coefficient of discharge for both connecting tubes were calibrated using the procedures outlined in Al-Madhhachi et al. (2013a) to obtain corrected energy levels at the jet nozzle accounting for any head loss between the pressure gauge and nozzle (*Appendix C*).

3.1.2 Field JET data collection

Several researchers including Cossette (2016), Karamigolbaghi et al. (2017), Mahalder et al. (2018) and Wahl (2021) have noted there is a need to standardize JET data collection, including the test duration and measurement frequency. Wahl (2016) notes that there are ongoing efforts to create an updated ASTM Jet Erosion Test standard, however, at the time of data collection, analysis and reporting of the current research project, an updated ASTM for jet methodology had not been prepared. Peer-reviewed methodologies of in-situ JETs were compared (*Table 3*) to one another to determine variations between techniques and operators. These were then integrated with potential sources of error within the JET methodology (*Section 2.5*) to determine a procedure that optimized the quality of the data being collected by minimizing the influence of methodological limitations.

At each study site, an area of exposed cohesive material along the stream bed and streambank was chosen for tests to be performed. Care was taken to avoid disturbing the test surface, including not walking on the streambed at the desired testing location. To minimize the influences of ambient moisture content, tests were only performed on days without rainfall as per Mahalder et al. (2018) and Daly et al. (2015). Except for tests intentionally performed in the late winter/early spring (discussed further in Section 3.1.3), all tests were performed between June and October; (i.e. frost events and freeze-thaw cycles did not occur between field campaigns; outside of regulatory exclusion windows related to aquatic habitat and spawning). As per Mahalder et al. (2018) test surfaces were chosen such that the influence of debris, roots and vegetation and alluvial materials was minimized and clearing/modifying the test surface was avoided where possible. Large stones and pebbles which were visibly present in till materials were avoided to focus testing on the fine-grained matrix of the tills and reduce the potential for jet deflection by stones. Where it was unavoidable, debris, alluvium or small stones were gently plucked from the surface to minimize disruption of the surrounding material (similar to Khan and Kostachuk (2011)). As suggested in Hanson and Cook (2004), tests within the same vicinity were performed in an order such that the zone of

influence surrounding a test surface would not impact the succeeding tests (e.g., zone of saturation around the test instrument, water discharged from the apparatus). Often this consisted of staging tests in the same immediate vicinity such that tests at the bottom of the bank were performed before tests higher up a given bank.

Preparing and performing tests consisted of inserting the steel foundation ring (*Figure 1*) into the media surface by pressing on it evenly such that a seal formed between the bottom of the ring and the material being tested; similar to Mahalder et al. (2018). Some over-consolidated tills being investigated were quite stiff whereby the ring could not sufficiently penetrate the material. In these cases, a plastic insert was placed in the foundation ring and a folded hand towel was placed on top to cushion the impact of a mallet used to advance the ring into place. If fracturing or crumbling of the test surface occurred to an extent that it could potentially influence the test, the ring was removed, and the insertion process was restarted at another location. For tests on steep banks, two steel stakes were advanced through the stabilizing rings (*Figure 1*) on the edge of the steel foundation ring to ensure the test apparatus and foundation ring did not shift during the test. After the ring and steel stakes (if required) were in place, pictures of the test surface were taken before starting the test (if it was not obscured by overlying water).

The jet submergence tank was then inserted into the jet foundation ring with an O-ring creating a watertight seal between the two components. The outlet orifice was always positioned such that submergence of the jet nozzle occurred during tests performed on steep banks. Ensuring the JET instrument was turned to the "Measure" setting, where the jet nozzle was shielded by the deflector plate, the pump was turned on. The pressure was adjusted until the desired setting was attained. It was left to stabilize while the point gauge reading for the start of the test (Zero Point Gauge Reading – ZPG) was taken. As emphasized by Karamigolbaghi et al. (2017), the ZPG was checked against the minimum height of the nozzle required for a fully formed jet to occur before impingement; Beltaos and Rajaratnam (1977) defined this as occurring when $H > 8.3d$ where H is the height of the jet nozzle above the surface it is impinging upon, and d is the diameter of the jet orifice. This is a refinement of the 6 to 35 nozzle diameters suggested to be used as a guideline for a suitable ZPG by Hanson and Cook (2004). The instrument used in this investigation had a jet nozzle diameter of 3.175 mm resulting in a minimum nozzle height of 26.35 mm for a fully formed jet to develop prior to impingement.

Pressure settings were chosen based on the experience of the operator to aim for a moderately shallow scour hole (~1-2 cm) to minimize deviations from the assumption of jet impingement upon a flat surface. Here, Single Pressure Setting (SPS) tests were chosen instead of the MPS methodology proposed by Mahalder et al. (2018) to be run for four reasons:

- MPS implicitly causes larger scour holes which increase the likelihood of obstructions and influences being introduced in till materials (impeding stones in the till, sand lenses, fine gravels contributing to abrasion),
- The larger scour holes resulting from MPS tests result in greater deviations of the flat surface assumption in the estimation of applied shear stresses (Karamigolbaghi et al. 2017; Weidner, 2012),
- In general, running one test at a constant pressure allows for the duration of the test to be maximized rather than running shorter tests at various pressure settings. Maximizing test durations is also a recommendation of Karamigolbaghi et al. (2017) and Cosette (2016). The longer test duration also offers the opportunity to investigate the uncertainty of JETs caused by changing test durations,
- Depth averaging of MPS results yields an average of the weathered surficial material and the underlying material, which is not a true representation of either of the materials. The resulting parameters represent a material that is more resistant to erosion than the surficial material (which is responsible for governing when erosion truly initiates), yet weaker than the underlying material governing erosion upon removal of the surficial layer. Thus, the average parameters derived from MPS are not representative of either process.

In the instance of subaerial tests, the test surface was saturated for 5 minutes before allowing impingement to occur by pumping water through the instrument while it was left on the measurement setting (i.e., no impingement). This was done to standardize how long subaerial samples were submerged before the beginning of the test and to allow for the pump to achieve a stable pressure head prior to initiating the test.

At test initiation, the jet nozzle was rotated to "Impinge" (the jet being applied to the geologic body of interest) at the same time as a stopwatch started to record time. At each measurement interval a pressure reading was obtained, the jet nozzle was turned to "Measure" (the jet being applied to the metal deflection plate (*Figure 1*) to temporarily cease advancement in the geologic media) and the stopwatch was paused. The staff gauge was gently lowered until it reached the test surface, and the corresponding gage height was recorded. At each measurement interval (pursuant to field conditions) the status of the test surface and the Measuring Point (where the staff gauge intersected the test surface) was observed through the top of the plexiglass of the JET reservoir. In some instances, particularly early in the test, this required waiting for turbid water in the JET reservoir to be replaced with clear water being pumped in. This visual assessment ensured the representativeness and the quality of the data as the test progressed and assisted in the early visual detection of potential obstructions impeding the impingement of the jet and preventing scour hole progression (i.e., large stones or pebbles).

Most field implementations of JETs have a higher temporal resolution of measurements than originally recommended by Hanson and Cook (2004). Recognizing the gradient of weathered material with increasing depth (Wolman, 1959; Gaskin, 2003; Davidson-Arnott and Langham, 2000; Mahalder et al.,

2018) and gradients in bulk density and moisture content observed by Khan (2006), the applied measurement frequency was highest in the early stages of each test with decreasing measurement frequency as each test progressed. Here, the schedule of measurements during JETs was divided into two segments; The High-Resolution Rapid Measurement (HRRM) portion occurred from 0-5 min, and an Adaptive Measurement (AM) portion occurred after the HRRM which extended until the termination of each test. The typical distribution in measurement intervals is listed in *Table 5*, however, a key component of the AM portion is that the measurement intervals were adjusted to accurately describe scour hole progression. For instance, if an increase in erosion or turbidity was noted while conducting a particular test, then additional measurements were recorded as needed.

Table 5: Typical test measurement schedule.

	Measurement	Measurement Interval (Δt) (min)	Cumulative Time (T) (min)
High Resolution Rapid Measurements (HRRM)	0 (ZPG)	0	0
	1-4	0.25	$0 < T \leq 1$
	5-6	0.5	$1 < T \leq 2$
	7-9	1	$2 < T \leq 5$
Adaptive Measurements (AM)	10-11	2	$5 < T \leq 9$
	12-13	2.5	$9 < T \leq 14$
	14-15	5	$14 < T \leq 24$
	16	6	$24 < T \leq 30$
	17-19	10	$30 < T \leq 60$
	20-21	15	$60 < T \leq 90$
	22-23	20	$90 < T \leq 130$

Test durations were typically conducted over a 120–140-minute period. Tests were terminated early or extended if obstructions or substantial deviations from expected conditions occurred or it was deemed appropriate by the operator, respectively. Throughout each test, detailed field notes and the presence of potentially influencing factors (*Table 6*) were recorded for quality control of each test. The presence or absence of the quality assurance (QA) factors listed in *Table 6* was taken into consideration when assigning a field grade of the representativeness of the test. Based upon the operator's qualitative assessment of the testing procedure, considering the QA factors, a field grade of good, moderate, or poor was assigned to the quality of each test. Test results identified as poor were excluded from any subsequent analysis; results from moderate tests were either included or excluded based on a desktop review of the test results. Tests identified as good were included in all analyses where applicable.

Table 6: Influencing Factors Considered During Field Grading of Tests

Quality Assurance Identification Number	Culling Factor	Expected influence on resistance to erosion	Description
QA1	Armoring by coarse pebbles	↑	Coarser particles fall into scour hole and are not displaced out of the hole by the JET. Particles can impede access of the gauge to the bottom of the scour hole resulting in shallower scour hole depths than what is representative.
QA2	Accumulation of sands/fine gravels	↓	Sands and fine gravels are entrained by the jet flow causing abrasion and increasing the forces applied to the test surface beyond that of the impinging hydraulic jet.
QA3	Obstructions impeding jet impingement	↑	Roots or stones which don't allow the jet to directly impinge on the body surface causing increased energy dissipation before encountering the test surface. If located directly at the measuring point, a non-erodible feature directly affects the development of scour hole.
QA4	Fracturing during ring insertion	↓	Fracturing during advancement of the foundation ring exaggerates pre-existing planes of weakness within the material facilitating increased erosion by the impinging jet.
QA5	Crumbling during ring insertion	↑	The removal of weathered material at the test surface prior to obtaining a ZPG results in more resistant material being exposed at shallower scour depths.
QA6	Block separation during test	↑↓	Blocks of material being eroded by the material creates discontinuities in the scour depth versus time dataset with its influence on prediction of erodibility parameters unclear and dependent on individual circumstances.
QA7	Narrow scour hole	↑↓	This would likely increase the apparent resistance to erosion of the material due to the deflection of the jet flow and reduction of jet energy impinging upon the material, however, this remains inconclusive based on the current state of research (Mazurek, 2001; Weidner, 2012).
QA8	Maximum scour not at measuring point	↑	When the deepest point of a scour hole does not occur at the measuring point it increases the apparent resistance to erosion of the material since lower levels of resistance exist within the test domain than what is captured at the measurement point. However, the test is still representative of a point sample at the specific measurement point and this phenomenon is attributed to material heterogeneity.
QA9	Critical Shear Stress of Material not exceeded	↑↓	When the JET causes insufficient scour within the test material the material cannot be characterized based on erodibility parameters. These instances do provide a lower bound on what the critical shear stress
QA10	Insufficient Test Duration	↑↓	When the test has to be abandoned due to equipment malfunction before sufficient data has been collected to inform JET analysis the material cannot be characterized

Where ↑ indicates an expected increase in the resistance to erosion, ↓ symbol indicates an expected decrease in the resistance to erosion, and ↑↓ indicates a potential increase or decrease in resistance to erosion.

After each test was completed, the jet submergence tank was gently removed from the foundation ring without contacting or disturbing the test surface. As recommended by Weidner (2012), Cossette (2016) and Rose et al. (2018), the aspect ratio of the resultant scour hole was measured based on the maximum width of the hole and the measurement perpendicular to that axis. Pictures of the resulting scour hole and test surface were acquired where feasible (*Appendix B*).

3.1.3 Seasonal Influences

In August and September of 2020, 21 tests were performed at Gainsborough Ravine (GRL) and in March and April of 2021, 11 tests were performed at the same site to assess the influence of seasonality on JET results. The tests performed in the spring of 2021 were concentrated on subaerial material with 10 out of the 11 tests performed on subaerially exposed portions of the bank and one test performed on the bed of the creek. The late winter and early spring conditions coincide with a seasonal peak in weathering processes acting on cohesive sediment (coinciding with the spring freshet). This primarily occurs as a peak in the frequency of freeze-thaw cycles coinciding with increased saturation levels, moisture content and pore water pressure from snow melt. Seasonal processes are responsible for the preparation of weakened material and erosion at this time of the year can be responsible for outsized proportions of erosion in a system (Wolman, 1959; Harrison, 1970; Lawler, 1986; Couper and Maddock, 2001; Wynn et al., 2008). A comparison between the summer and spring tests allows for an evaluation of how seasonal weathering processes in the early spring alter the characteristics of weathered material along the surfaces of bank material compared to the summer.

Chapter 4
Results of Field Campaign

This section presents the results of the field campaign (2019-2021) including empirical and qualitative comments regarding the suitability and representativeness of JET methodology at the study sites.

4.1 Field campaign summary

During the field campaign, 231 tests were performed during the summer data collection period and 11 tests were performed in the spring data collection period. *Table 7* lists the number of tests that were conducted per site and tests removed through the quality assurance culling procedure as per *Table 6*. More detailed qualitative assessments of JETs performed at each site are summarized in *Appendix A*.

Table 7: Quality assurance culling of JETs by test site

Test site (See Figure 3 and Table 4	Number of tests (Total/Summer/Spring)	Field Grade			Tests excluded from analysis (QA cull - *Table 6)*	Number of representative tests
		Good	Moderate	Poor		
FC	24/24/0	23	1	0	1 (QA3)	23
MCE	14/14/0	14	0	0	0	14
ETC	9/9/0	6	2	1	1 (QA4); 1 (QA9)	7
GT	15/15/0	13	2	0	2 (QA1)	13
LNC	19/19/0	16	2	1	1 (QA3)	18
NMB	20/20/0	15	1	4	1 (QA10); 3 (QA6)	16
NTL	22/22/0	21	1	0	1 (QA3)	21
DCB	14/14/0	11	2	1	1 (QA4)	13
GRL	32/21/11	29	2	1	1 (QA1); 1 (QA9); 1 (QA10)	29
TCH	24/24/0	20	3	1	1 (QA7)	23
WCM	16/16/0	9	6	1	1 (QA6)	15
WCN	9/9/0	9	0	0	0	9
HC	24/24/0	19	4	1	1 (QA1) 1 (QA3); 1 (QA4)	21
Total	242//231/11	205	26	11	20	222 (Total) 213 (summer) 9 (Spring)

Histograms of test durations, the maximum measured scour depths and the zero-point gage readings from the JETs completed during the field campaign are displayed in *Figure 4*. Test durations centre about the 120-minute duration (*Figure 4a*), maximum scour along the centreline of the impinging jet (*Figure 4b*) is skewed towards shallower scour depths and all zero-point gage readings exceed the $8.3d_o$ minimum requirement (*Figure 4c*) for a fully formed jet to develop prior to impingement, ensuring that *Equation 6* is applicable during the analysis of the JET results (*Section 2.4* and *Section 3.1.2* - i.e., the jet nozzle is at a sufficient height above the test surface at test initiation such that the test surface does not encroach upon the jet potential core as per Rajaratnam and Beltaos (1977), Karamigolbaghi et al., (2017)).
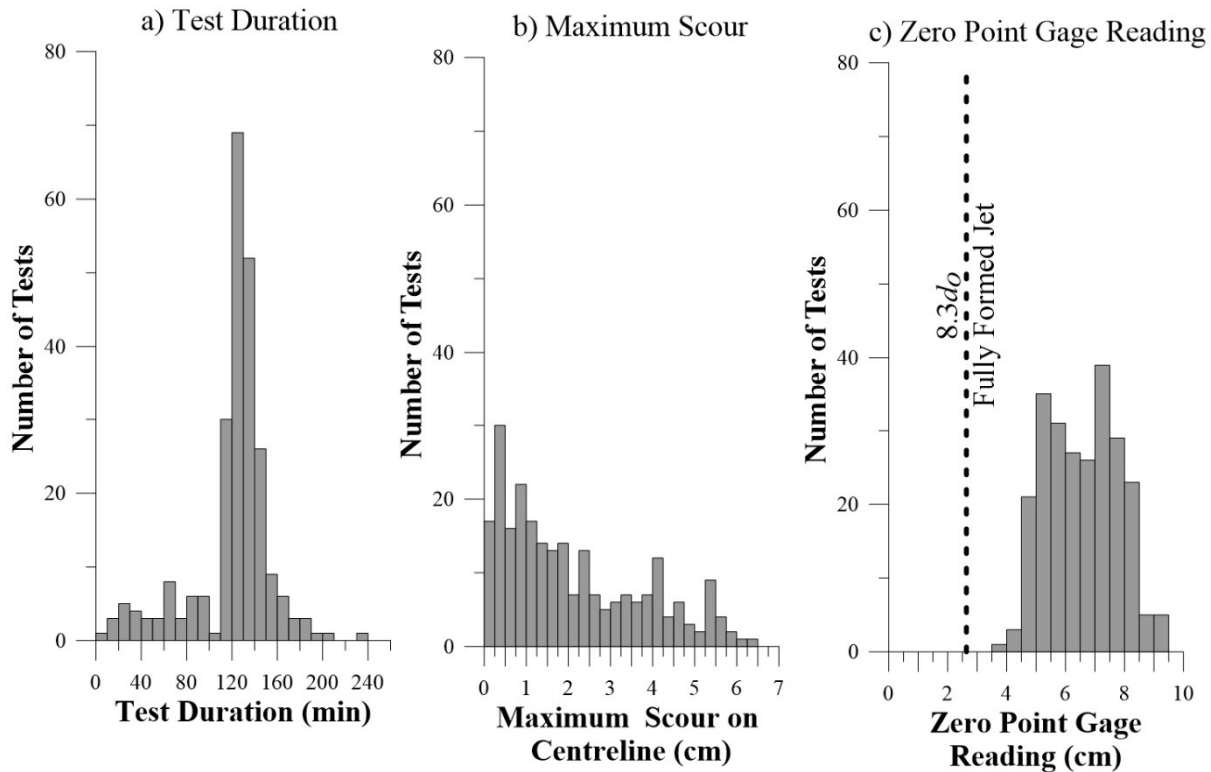
Figure 4: Histograms of a) Test duration, b) Maximum scour on centreline of the impinging jet and c) Zero-point gage readings

4.2 Suitability of JET methodology at study sites

The JET was able to adequately perform in the materials tested in this investigation with some limitations. Wartburg Till (WCM) at Whirl Creek in Mitchell, Ontario (Figure 3) was noted to be an especially challenging material to apply the JET methodology within. This material was observed to be friable and prone to block separation with fractures often forming during the insertion of the foundation ring. Further, the pressure heads at this location were often observed to be either too low to initiate scour or initiated block separation and entrapment at the point of impingement (*Figure 5a*). Another instance in which JET

application was observed to have limited applicability is along banks of laminated clays where the progression of the scour hole is parallel to the bedding layers. This induces a greater degree of block separation with the jet impinging directly upon pre-existing planes of weakness. This was not observed to be an issue in tills which typically have a massive texture rather than laminated.

Similar to other investigations applying JETs within till (Khan and Kostachuk, 2011; Shugar et al., 2007), abrasion was observed to occur relatively frequently during testing (*Figure 5b* and *Figure 5c*). The frequency at which it occurred was dependent upon the material being tested, with more clayey tills (e.g. Maryhill Till, Stirton Till) being less influenced by abrasion of sands and fine gravels, whereas tills with more variable grain size were more frequently subjected to abrasion during the JETs. How much the abrasion alters the erodibility parameters estimated from JET methodology is expected to be related to the pressure at which the tests were conducted. Tests at higher pressure settings impart higher velocities to the mobilized particles which subsequently impart higher forces upon the test surface. Further, the change in the jet nozzle to jet reservoir ratio between the original jet and mini-jet is expected to slightly amplify abrasion within the mini-jet apparatus compared to the original JET employed by Khan and Kostachuk (2011) and Shugar et al. (2007). However, no differences were observed when comparing erodibility parameters estimated from Original JET data (Khan, 2006) and Mini-JET results (this investigation) at Fletchers Creek (*Appendix G)*. While not the only factor, the presence of abrasion could potentially contribute to the lack of plateauing in the scour depth versus time data sets observed in some tests (*Appendix I)*. This would be a result of the applied shear stress (and driving force behind scour progression) deviating from the jet hydraulics (τ_o decreases as the distance between the jet nozzle and test material increases) toward the abrasive forces controlled by the impact velocities and angles of the particles.

Shugar et al. (2007) noted that abrasion during JETs may be more representative of natural conditions during flood events which would mobilize particles within a channel resulting in suspended and saltating loads contacting stream banks and stream beds. Further, Kamphuis (1990) observed that the erosion of consolidated cohesive soil is largely described by the transport properties of non-cohesive particles overlying the cohesive soil and Pike et al. (2017) observed that the transport of gravel particles overlying cohesive till significantly reduces the critical shear stress of the cohesive material. This indicates that the characterization of cohesive material's resistance to erosion cannot neglect interactions with non-cohesive material. This also indicates that while abrasion during JETs may deviate from the theory deriving the imposed shear stress (which assumes clear water impinging upon the test surface), the inclusion of abrasion within the test circumstances may increase the representativeness of the JET results to real erosive events. At the very least, the occurrence of abrasion would increase the shear stress being imposed

relative to the theoretical clear water conditions and subsequently add a factor of safety embedded into the JET results which may be useful from an engineering perspective with respect to prescribing critical hydraulic shear thresholds. However, this point of discussion is constrained by the fact that abrasion is altering the forces applied to the material and not the properties of the material itself (which the erodibility parameters resulting from a JET are intended to describe).

Figure 5: Factors influencing the representativeness of JET. a) fracturing and block separation at Whirl Creek, b) sands causing abrasion during test at MCE, c) sands retrieved from scour hole at FC, d) Maximum scour not aligning with measuring point at NTL.

In tills with variable grain sizes, it was occasionally observed that larger particles are unable to be ejected in the suspension of the jet effluent, accumulate within the jet reservoir and potentially settle within the scour hole. This can cause armouring of the scour hole, preventing the jet from impinging directly upon the test surface which may influence the depth of scour that is read from the point gage. Shugar et al. (2007) and Khan (2006) noted that when performing tests in tills they removed material trapped in the scour hole by hand during measurement periods when the test was paused. However, this is not practical with the enclosed top of the multi-angle mini-jet apparatus. This was observed to potentially bias results in some tests along bed materials at low pressures where the jet did not have enough energy to displace larger grains from the scour hole. However, this problem was negligible during tests on angled banks where gravitational forces assisted material out of the scour hole similar to what was observed by Wahl (2016). Further, due to the smaller jet nozzle and subsequently smaller scour holes that develop from

31

mini-JETs compared to original JETs, the frequency of encountering grains large enough to be trapped in the scour hole is reduced.

In some instances, it was observed that the deepest part of the scour hole did not align with the centreline axis of the jet and subsequently did not align with the measurement point axis of the staff gauge (*Figure 5d*). This is evidence that there is variability in erosion resistance even within the small domain of the JET apparatus – in this instance more erosion occurs at a location with lower applied shear stress than the centre of the impinging jet. This material heterogeneity is unavoidable and not limited to JET methodology. Flume tests also note that certain parts of samples will erode at different shear stresses than others (Partheniades, 1965; Pike, 2014; Kamphuis, 1990). This highlights the fact that the JET is a point sample at the direct location of jet impingement and as a result, it is inappropriate to take an individual test as representative of site conditions. As recommended by Daly et al (2015a) a minimum of 3-5 tests per layer of material being investigated can provide an order of magnitude estimate of the erodibility parameters.

Aspect ratios of the resulting scour holes were measured for each test, however, they were not used as a criterion in the determination of the quality of the JET data. A recommended minimum aspect ratio ($\frac{Z_{max}}{W_{max}}$ in *Figure 1*) of 2 was proposed by Weidner (2012), however, this was based on the results of tests using the original JET apparatus and is not reflective of the mini-JET. No similar investigation has been performed using the smaller nozzle size of the mini-JET. Applying the minimum acceptable aspect ratio of 2 to the results of this investigation is unreasonably stringent, and filtered out tests which were observed to be representative and aligned with similarly situated tests. This is consistent with the conceptual premise that the minimum acceptable aspect ratio must be related in some manner to the jet nozzle diameter rather than being independent of it (as in the case of the threshold proposed by Weidner (2012)). With the mini-JET nozzle being smaller than the Original JET, it is reasonable to estimate that the minimum acceptable aspect ratio for mini-JET tests is lower than the value of 2 determined for Original JETs. Investigation into a minimum acceptable aspect ratio which relates an acceptable aspect ratio to the jet nozzle diameter is an area that should be subject to further research.

Chapter 5
Analytic Methodology

This section details the methods employed in this research to analyze the data presented in *Chapter 4* and ensure that the analysis provides results that are representative of site conditions. First, an alternative method to the Multi Pressure Setting (MPS) tests proposed by Mahalder et al. (2018) to account for material heterogeneity is proposed in the form of test segmentation (*Section 5.1*) as outlined in *Figure 6*. This results in each JET being separated into two regions based on depth. The first region represents the weathered surficial material (Type 1), and the second represents the unweathered underlying material (Type 2).
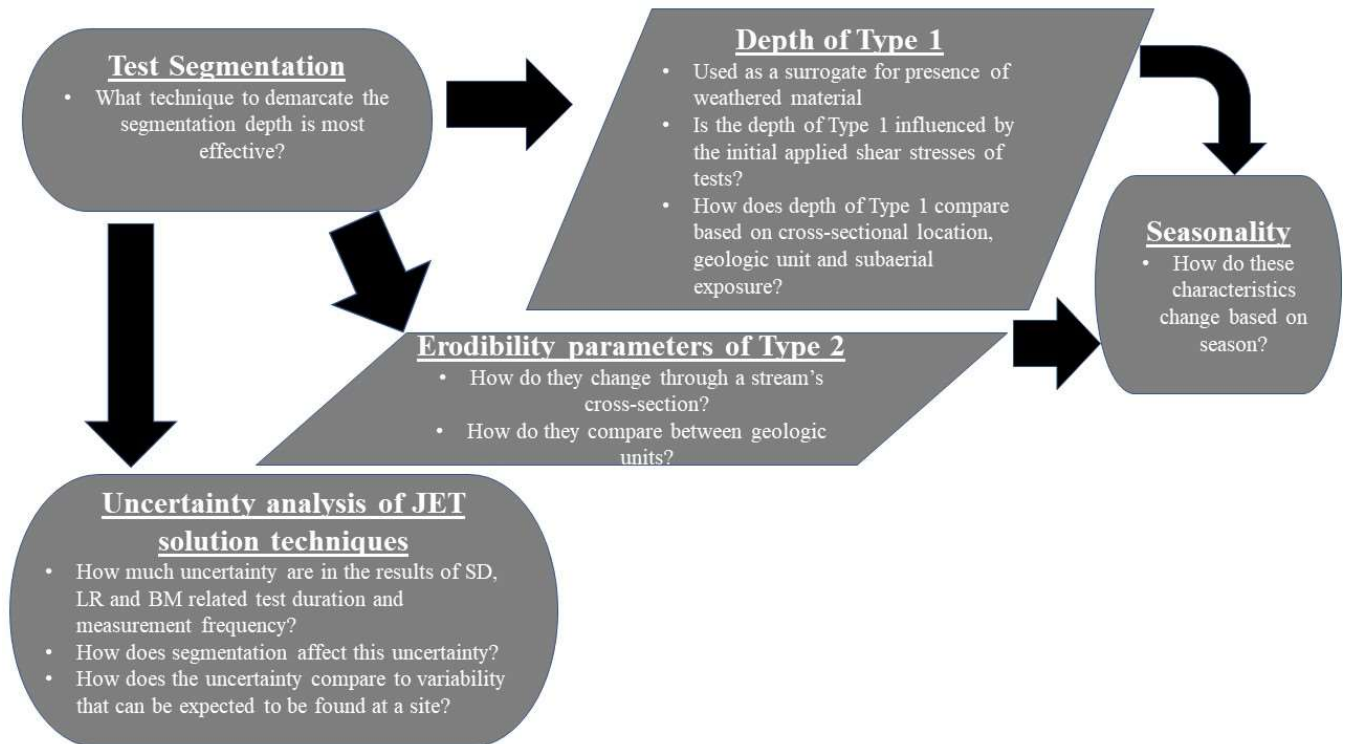
Figure 6: Outline of analysis workflow.

Next, an uncertainty analysis of three JET solution techniques (LR, SD and BM) was performed to assess how much influence the duration of a JET and the frequency of measurements taken during a JET have on the estimated erodibility parameters (*Section 5.2*). The differing solution techniques have been noted to affect the reliability of JET results by Cossette (2016) and Karamigolbaghi (2017) amongst others. This uncertainty analysis is performed by resampling JETs under various timed measurement intervals and cumulative time scenarios (*Table 8*). To assess whether the uncertainty associated with the JET solution

techniques is a result of material heterogeneity within JETs. The uncertainty analysis is performed with and without test segmentation being applied.

Then, the results of JETs within Halton Till (measured at 4 sites) are taken as an example of potential intra-geologic unit variability of erodibility parameters and compared to erodibility parameters estimated across all (13) sites irrespective of geologic unit (*Section 5.3*). Further, analyses are performed to ascertain how estimates of erodibility parameters change throughout a stream's cross-section (i.e., channel bed vs. channel bank sampling stations as shown in *Figure 10* and discussed in *Section 5.3*).

Next, the depth of the Type 1 region for each JET (determined during test segmentation) is used as a surrogate for the presence of weathered material at each test location (*Section 5.4*). Similar to the Type 2 erodibility parameters, this value is compared between Halton Till and all geologic units, compared throughout a stream's cross-section, and compared between submerged and subaerial tests.

Lastly, to assess the influence of seasonal processes on cohesive material's resistance to erosion, the depth of the Type 1 region and the Type 2 erodibility parameters are compared between JETs performed in the summer and the early spring at Gainsborough Ravine (see *Section 3.1.3*).

5.1 Test segmentation

To account for material heterogeneity in the direction of scour progression (see *Figure 1* and *Figure 7*), and the elevated uncertainty at the initiation of JETs (arising from subjecting the most weathered material to the highest stresses and the sudden application of applied shear stress), an analytic methodology is employed that segments the JET into two regions; Type 1 – a region of elevated uncertainty and, Type 2 – a region of higher confidence that the assumption of material homogeneity required to analyze the JET data holds true. This terminology is adapted from the classifications of Mehta and Partheniades (1982) for Type I erosion (the erosion rate exponentially decays with time) and Type II erosion (the erosion rate is constant with time) which Khan (2006) employed to classify which type of erosion was dominant in JETs. The test segmentation methodology is conceptually demonstrated in *Figure 7*.

34
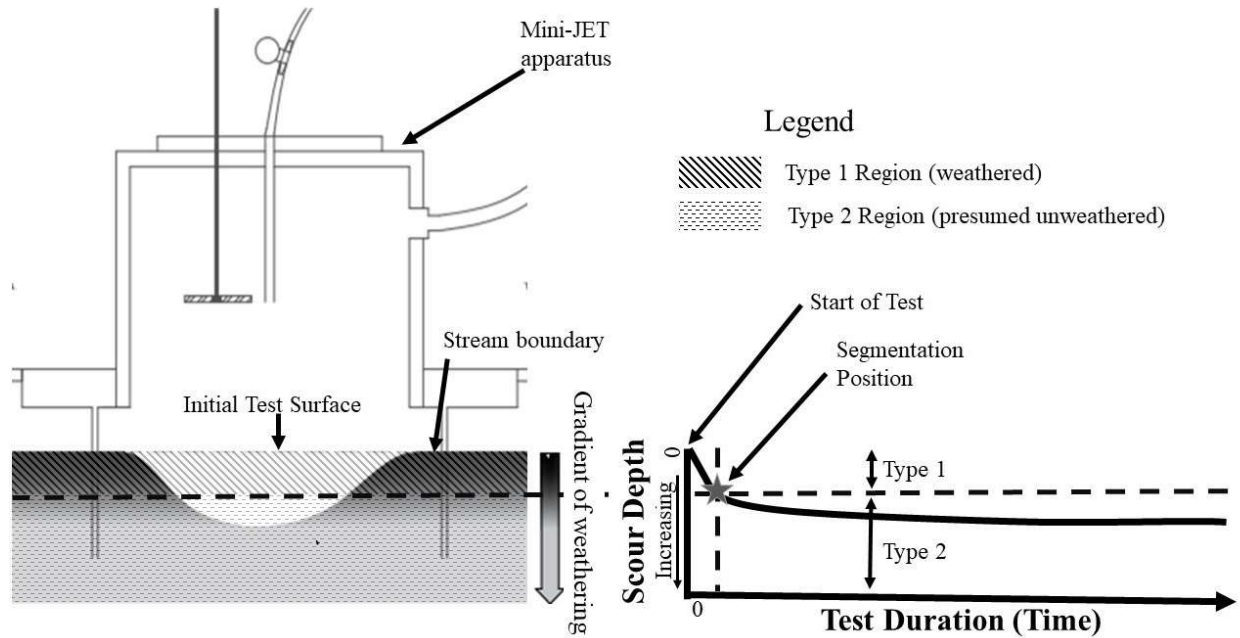
Figure 7: Conceptualization of test segmentation.

Segmenting the tests in this manner accounts for material heterogeneity within the profile of the resulting scour hole and methodological limitations of the JET. This is hypothesized to:

- Improve the representativeness of the resulting erodibility parameters,
- Reduce the uncertainty of the erodibility parameter estimates from JET duration and measurement frequency,
- Facilitate the use of the depth of the first segment as a surrogate for the prevalence of weathered material at a site.

The segmentation of JETs is proposed as an alternative method to MPS (Mahalder et al., 2018) to account for material heterogeneity within JET scour holes. MPS was precluded from use in this investigation due to its limitations summarized in *Section 3.1.3.*

The measurement scheme (adaptive time stepping) employed during JET data collection offers sufficient temporal resolution to capture the relatively elevated rates of erosion arising from surface weathering processes at the beginning of each test versus those of the relatively non-weathered matrix below in the later cumulative time of each test. Here, we demarcate a depth below the initial test surface (referred to as the segmentation depth) through the techniques listed below that separate the erosion rates observed in the weathered region (Type 1) and those below in the relatively non-weathered region (Type 2). The three techniques of demarking the segmentation depth are:

35

- visual inspection of an inflection point in the erosion rate trend analysis as a function of progressing cumulative test duration (Figure 8),
- the point of the maximum norm of residual error between the scour depth predicted by the Scour Depth Method (SD) and the measured scour depth (Figure 8),
- and an iterative analysis of variance technique developed by Gill (1970) and applied to the erosion rates of each JET (Figure 8).

The first technique of segmentation depth demarcation is a Visual Assessment (VA) of each JET to evaluate the progression of the scour depth versus time plot and discern where discontinuities or notable inflection points occur (demonstrated in *Figure 8)*. The segmentation depth identified is then compared with notations made during the field test to ensure it aligns with qualitative observations regarding the progression of the test. The use of block separation as identifiers of Type 1 was limited to the first 30 minutes of the test. This cumulative time duration threshold is in recognition that block separation has an increased frequency of occurrence in the early stages of tests, however, it is generally accepted that block separation continues to occur within Type II erosion as it progresses along planes of weakness and discontinuities (Lefebvre et al., 1986; Kamphuis and Hall, 1983; Amos et al., 1992; Mazurek, 2001).

The second technique of demarking the segmentation depth (Maximum Norm of the Residual - MNR) involves comparing observed scour depth results to the predicted scour depths estimated by SD (*Figure 8*). By minimizing the sum of the norm of the residuals at each scour depth measurement between the predicted and observed scour depths, the modelled scour depth progression resulting from SD methodology represents the closest attainable approximation of *Equation 2* with an *m* value of 1 (the linear excess shear stress model) to the observed dataset (Daly et al., 2013). The superior curve-fitting abilities of SD compared to BM are demonstrated in *Appendix I*. Where the SD predicted scour depth and the observed scour depth demonstrate maximum divergence can be considered as the point where the linear excess shear stress model (*Equation 1* with *m* = 1) has the maximum deviation from test observations. This technique of demarking the segmentation depth defines the position in the cumulative time series with the Maximum Norm of the Residual between the scour depths modeled by SD and the observed depths as the segmentation depth (demonstrated in *Figure 8*).

The third technique of demarking the segmentation depth (TG) is an iterative analysis of variance of the measured sequential erosion rates throughout each JET based on the Gill Method (Gill,1970; Davis, 1986). This technique can be repeatedly applied to sequential cumulative time dataset segments and divided into as many time segments as desired. Here, a binary model is applied to the JET data. First, the dataset is divided into one short segment (with a minimum of two data points) and one long segment. The sum of squares within each sub-segment (SS_W) is then calculated as:

36

$$SS_w = \frac{\sum_{j=1}^{a} \sum_{i=1}^{b_j} (x_{ij} - X_j)^2}{\sum_{j=1}^{a} n_j - a} \tag{7}$$

where a is the number of segments (for this research $a \leq 2$), b_j is the number of data points in the jth segment, x_{ij} is the ith point in the jth segment, X_j is the mean of the jth segment. The sum of squares between segments (SS_b) is then calculated using *Equation 8*:

$$SS_b = \frac{\sum_{j=1}^{a} (X_j - X)^2}{a - 1} \tag{8}$$

where X is the overall mean of the sequence over the entire test duration (combined Type 1 and Type 2 regions):

$$X = \frac{\sum_{j=1}^{a} \sum_{i=1}^{b_j} x_{ij}}{\sum_{j=1}^{a} b_j} \tag{9}$$

The transition point between segments is trialed in all possible depth locations with SS_w and SS_b calculated for each possible segmentation depth. For each possible segmentation depth, the ratio R_G is calculated as:

$$R_G = \frac{SS_b - SS_w}{SS_b}. \tag{10}$$

The measurement point with the maximum value of R_G, as illustrated in *Figure 8,* is identified as the segmentation depth, delineating the transition between the Type 1 and Type 2 regions.

The results of these three methods of segmentation depth demarcation will be compared to determine a representative segmentation depth for each JET. Due to the small sample size collected during the spring season tests, the comparison of test segmentation techniques is restricted to the tests collected during the summer season to avoid any undue influence from seasonality in this assessment.
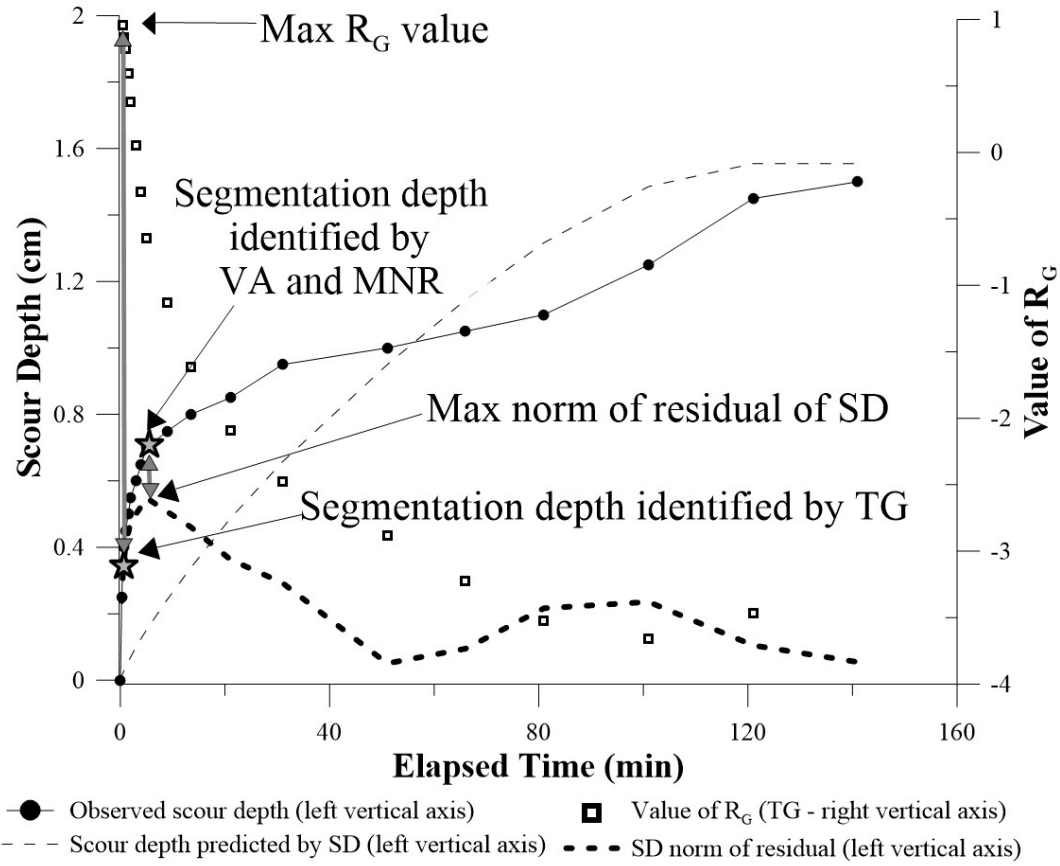
Figure 8: Demonstration of segmentation depth demarcation techniques VA, MNR and TG.

5.2 Resampling methodology for uncertainty analysis

JET data will be analyzed using three solution techniques listed in *Table 2*; the Blaisdell Method (BM) proposed by Hanson and Cook (2004), the Scour Depth Method (SD) proposed by Daly et al. (2013) and the linear regression of applied stresses and erosion rates (LR) described by Wahl (2021). This results in three pairs of erodibility parameters (k_d and τ_c) characterizing the material; ($\tau_{c_{BM}}$ and $k_{d_{BM}}$), ($\tau_{c_{SD}}$ and $k_{d_{SD}}$), ($\tau_{c_{LR}}$ and $k_{d_{LR}}$) where the subscripts BM, SD and LR represent the three solution techniques listed in *Table 2* respectively.

Several researchers including Cosette (2016), Karamigolbaghi et al. (2017), Khanal et al. (2016a) and Mahalder et al. (2018) have observed that uncertainty can be introduced into the erodibility parameters estimated from JETs by altering the duration of the JET and frequency of scour depth measurements during the JET. To compare the uncertainty of the three solution techniques (i.e. SD, BM, LR) caused by test duration and measurement frequency, each JET's data will be resampled to allow for the same JET to

38

be analyzed using the BM, SD and LR methods with 11 different Data Scenarios (*Table 8*). Data Scenarios 2 – 7 are used to compare how estimates of the erodibility parameters change with test duration. Data Scenarios 1, 2 and 8 – 11 are used to compare how estimates of erodibility parameters change with measurement frequency. Further, these resampling strategies will be repeated with and without test segmentation being applied to JETs to determine how the uncertainty of the solution techniques is altered by test segmentation (Figure 9). The results of this analysis will:

- Facilitate comparisons between solution techniques to assess their uncertainty arising from test duration and measurement frequency,
- Facilitate assessment if test duration and/or measurement frequency require standardization when comparing JETs,
- Determine if the Type 1 region at the beginning of a JET contributes to uncertainty in the estimation of erodibility parameters.

The various Data Scenarios considered in this uncertainty analysis are listed in *Table 8*.

All Data Scenarios except Data Scenario 1 (only considered without segmentation) were analyzed with BM, SD, and LR with and without test segmentation being applied resulting in each JET dataset being analyzed for a total of 63 different combinations of Data Scenarios and solution techniques.

Table 8: Data input scenarios for uncertainty analysis of JET solution techniques

Data Scenario ID	Data Scenario	Description	Applied to tests without segmentation (CT)	Applied to tests with segmentation (T2)
1	Full Length–Field Data (FLFD)	The raw data sequence from field records. This includes measurements which do not indicate that any incremental erosion occurred.	Yes	No
2	Full Length–No Zero Erosion Points (FLNZ)	This scenario removes redundant measurements which do not describe any erosion occurring since the previous measurement. This removes measurements which do not add any descriptive value of the scour depth progression	Yes	Yes
3	100 min-No Zero Erosion Points (100NZ):	This input scenario truncates the #2 scenario at a test length of 100 minutes. If no field measurement occurred at the 100-minute mark, a measurement was linearly interpolated. Also, a minimum terminal measuring interval of 5 minutes was maintained during the resampling process as recommended by Khanal (2016a). In the instance that the interpolated interval was less than the required 5 minutes, the time and incremental scour depth was added to the penultimate measurement. All other measurements remain unchanged from the #2 scenario.	Yes	Yes
4	80 min-No Zero Erosion Points (80NZ):	Input Scenario is similar to # 3 but truncated at 80 minutes.	Yes	Yes
5	60 min-No Zero Erosion Points (60NZ)	Input Scenario is similar to # 3 but truncated at 60 minutes.	Yes	Yes
6	45 min-No Zero Erosion Points (45NZ).	Input Scenario is similar to # 3 but truncated at 45 minutes.	Yes	Yes
7	30 min-No Zero Erosion Points (30NZ)	Input Scenario is similar to # 3 but truncated at 30 minutes.	Yes	Yes
8	Full length – Standardized 5 min Readings (ST5)	This scenario utilizes the #2 as a baseline and adjusts the timing of the measurements such that one measurement occurs every 5 minutes. Linear interpolation of measurements on either side of the desired 5-minute intervals were performed. Since test durations did not always fall on a multiple of 5-minute intervals, the terminal measurement interval was adjusted to reflect the proper test duration while still maintaining a minimum of a 5-minute terminal time as per Khanal (2016a). This results in a terminal measurement interval between 5 and 10 minutes.	Yes	Yes
9	Full length – Standardized 10 min Readings (ST10)	This input scenario is similar to #8, here with measurements occurring and/or extrapolated explicitly to 10-minute intervals rather than 5-minute intervals. This results in a terminal measurement interval between 5 and 15 minutes.	Yes	Yes
10	Full length – Standardized 5 min +Rapid Readings (ST5R)	This input scenario is similar to # 8, however, it incorporates measurements on 1-minute intervals for the first 5 minutes before switching to subsequent measurements at 5-minute intervals.	Yes	Yes
11	Full length – Standardized 10 min +Rapid Readings (ST10R)	This input scenario is similar to the # 9; however, it incorporates measurements at 1-minute intervals for the first 5 minutes, a subsequent 5-minute interval followed by 10-minute interval observations.	Yes	Yes

To differentiate between Data Scenarios with and without test segmentation being applied, the prefix CT (combined Type 1 and Type 2 segments) will be applied to Data Scenarios without segmentation, and T2 (Type 2 erosion) will be applied to Data Scenarios with segmentation. The Data Scenarios evaluated to assess the uncertainty related to test duration are summarized in *Figure 9a* and the Data Scenarios evaluated to assess uncertainty related to measurement frequency are summarized in *Figure 9b*.
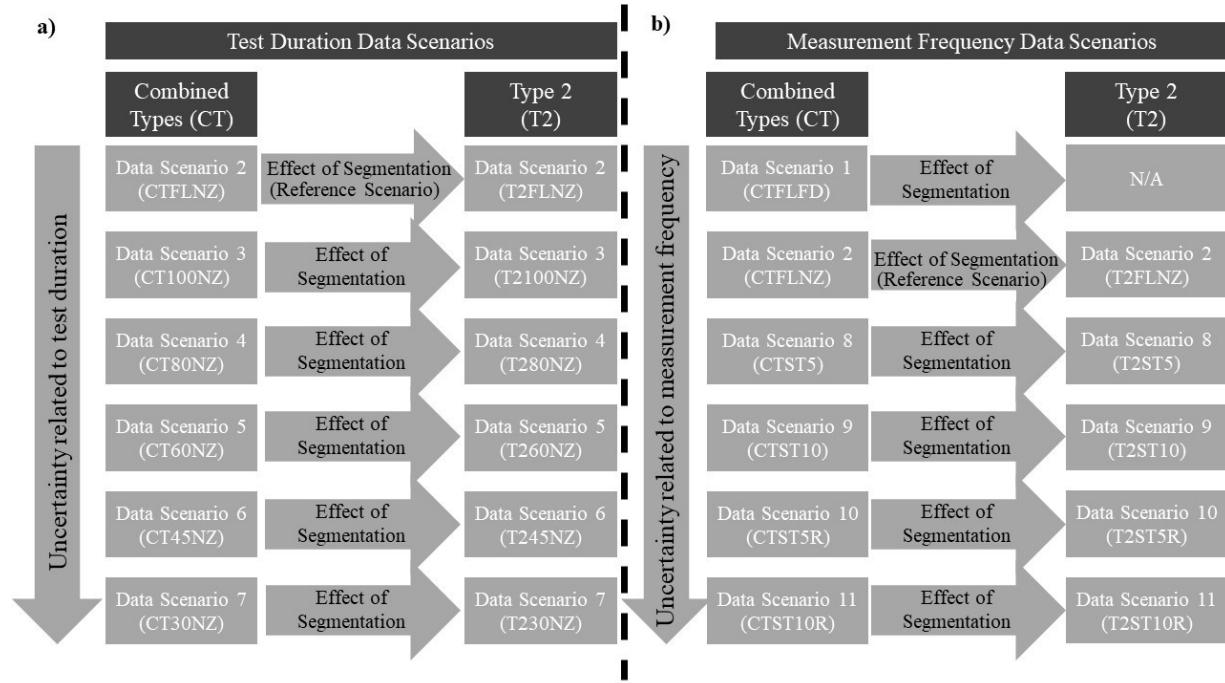
Figure 9: Data Scenarios used to assess uncertainty of JET analysis to a) test duration and segmentation and, b) measurement frequency and segmentation

The uncertainty of erodibility parameters (k_d and τ_c) as a function of test duration are evaluated by calculating the percent change in erodibility parameters for the given data scenarios relative to Data Scenario 2 (FLNZ). An example of comparing k_d estimated from BM for Data Scenario 3 (CTNZ100) to the erodibility parameter estimated from Data Scenario 2 (CTFLNZ) is provided in the expression below.

$$\%Change\ K_{dBM}\ for\ CTFLNZ\ to\ CT100NZ = \frac{K_{dBM-CT100NZ} - K_{dBM-CTFLN}}{K_{dBM-CTFLNZ}} \times 100 \qquad (11)$$

Where $K_{dBM-CTFLNZ}$ is the erodibility coefficient estimated by BM from Data Scenario 2 without segmentation (CTFLNZ) and $K_{dBM-CT100NZ}$ is the erodibility coefficient estimated by BM from Data Scenario 3 without segmentation (CT100NZ).

To assess if segmenting the JETs (i.e., isolating the Type 2 region) reduces the uncertainty related to test duration, the changes in erodibility parameters resulting from the same Data Scenario evaluation were compared with and without segmentation (e.g., the results of *Equation 11* and *Equation 12*). T2 comparisons were standardized to the erodibility parameters derived from Data Scenario 2 (T2FLNZ) as demonstrated below using the same comparison presented in *Equation 11*:

$$\%Change\ K_{dBM}\ for\ T2FLNZ\ to\ T2100NZ\ = \frac{K_{dBM-T2100N}\ -K_{dBM-T2FLNZ}}{K_{dBM-T2FLNZ}} \times 100 \qquad (12)$$

where $K_{dBM-T2FLNZ}$ is the erodibility coefficient estimated by BM from Data Scenario 2 (T2FLNZ) with segmentation and $K_{dBM-T2100N}$ is the erodibility coefficient estimated by BM from Data Scenario 3 (T2100NZ) with segmentation.

The uncertainty of erodibility parameters caused by measurement frequency (*Figure 9b*) was assessed through six comparisons outlined below:

a) The change between Data Scenarios 1 (FLFD) and 2 (FLNZ) offers insight into how the presence of redundant points influences the solution techniques,
b) The change between Data Scenarios 2 (FLNZ) and 8 (ST5) offers insight into how shifting the measurement scheme to the lower limit of measurement intervals recommended by Hanson and Cook (2004) influences the solution techniques,
c) Comparison between Data Scenarios 8 (ST5) and 9 (ST10) offers insight into how decreasing the measurement frequency (to the upper limit of measurement intervals recommended by Hanson and Cook (2004)) can influence the solution techniques,
d) Comparison of Data Scenarios 8 (ST5) and 10 (ST5R) examines how more measurements at the beginning of a test may influence the results of the three solution techniques evaluated. Historically, the measurement schemes recommended by Hanson and Cook (2004) did not incorporate a rapid measurement component,
e) Comparison between Data Scenarios 9 (ST10) and 11(ST10R) offers insight into how increasing the measurement frequency at the beginning of the test and maintaining less frequent measurements later in each test influence the erodibility parameter estimated from the solution techniques,
f) The change between Data Scenario 10 (ST5R) and 11 (ST10R) offers insight into how the influence of rapid measurements on erodibility parameter estimation changes with less frequent measurements later in the test.

To maintain consistency in these comparisons, all changes in the erodibility parameters were expressed as a percent of the Data Scenario 2 (FLNZ) erodibility parameter; regardless of whether it is directly

involved in the comparison being made. For example, the change in K_{dBM} (without segmentation) between Data Scenario 10 (ST5R) and Data Scenario 11 (ST10R) was calculated by the expression below.

$$\%Change\ K_{dBM}\ for\ CTST5R\ to\ CTST10R = \frac{K_{dBM-CTST5R} - K_{dBM-CTST10}}{K_{dBM-CTFLN}} \times 100 \qquad (13)$$

where $K_{dBM-CTST5R}$ is the erodibility coefficient estimated by BM from Data Scenario 10 (CTST5R) without test segmentation, $K_{dBM-CTST10}$ is the erodibility coefficient estimated by BM from Data Scenario 11 (CTST10R) without test segmentation and $K_{dBM-CTFLNZ}$ is the erodibility coefficient estimated by BM from Data Scenario 2 (CTFLNZ) without test segmentation.

5.2.1 Culling of JET dataset for uncertainty analysis

To ensure that the uncertainty analysis of the solution techniques to JET duration and measurement frequency is not biased by analytic anomalies of the three solution techniques, or by the inclusion of JETs whose representativeness may change with the various Data Scenarios, four screening criteria were applied to the summer JET dataset (n = 213) before performing the uncertainty analysis of the solution techniques to test duration and measurement frequency:

1. $JET\ Duration_{Postsegmentation} > 100$min ,
2. $Maximum\ Depth\ of\ Scour_{Postsegmentation} \geq 0.15cm$,
3. $Number\ of\ Measurements\ in\ Data\ Scenario\ 4\ (T230NZ) \geq 4$
   $to\ ensure\ sufficient\ data\ for\ the\ solution\ techniques$,
4. $No\ occurrence\ of\ SD\ Failure\ (i.e.,\ incorrect\ prediction\ of\ \tau_{cSD} = 0\ (Wahl,\ 2016)\ )\ or\ LR$
   $Failure\ (i.e.\ negative\ \tau_{cLR}\ or\ negative\ K_{dLR}).\ (Discussed\ in\ detail\ in\ Appendix\ H).$

Data Scenario 4 as described in *Table 8* represents the data scenario with the least number of measurements and as such ensuring that a sufficient number of measurements are present in this data scenario will ensure all other data scenarios contain sufficient measurement points to inform the solution techniques. The screening results are summarized below in *Table 9* with a resultant population of 90 tests.

Table 9: Population Screening for uncertainty analysis

Total summer tests performed	Field QA/QC assessment screening	Screening criteria 1	Screening criteria 2	Screening criteria 3	Screening criteria 4
231	213	186	177	163	90

5.3 Type 2 Erodibility Parameters

For all JETs that exceeded 60 min in duration and achieved greater than 0.15 mm of erosion in the Type 2 region, the erodibility parameters were estimated from the BM, SD and LR solution techniques. These erodibility parameters were then statistically evaluated to compare inter-geologic unit and intra-geologic unit variability in erodibility parameters. The population of tests from Halton Till spanning 4 study sites was taken as a sample pool of potential variability of erodibility parameters within a geologic unit whereas the population of tests from all sites (inclusive of Halton Till) was used to represent how erodibility parameters vary between geologic units. The inclusion of Halton Till within the second population represents a population where no distinction of geologic units has been considered. Comparison of these two populations will indicate whether identifying the geologic unit exposed at a stream boundary can result in the estimation of stronger representativeness of erodibility parameters compared to simply identifying the bank geology as a hard clay (or till) (i.e., with no distinction of the geologic unit). Erodibility parameters were further compared based on where tests were conducted within a stream's cross-section (e.g., streambed, first bank tier, middle bank tier or upper bank tier) as demonstrated in *Figure 10*.
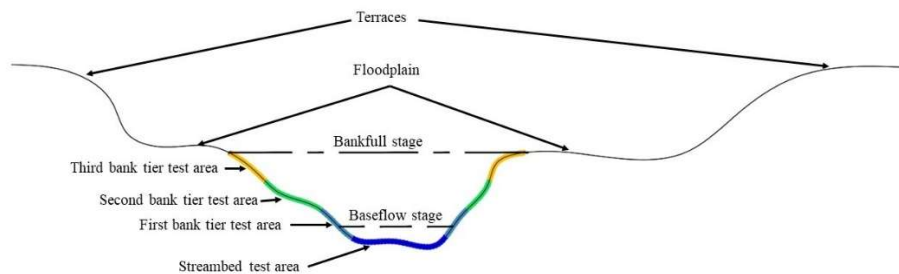
Figure 10: Stream cross-section test areas

5.4 Depth of Type 1 region

Material identified in the Type 1 region of tests and isolated from their respective Type 2 regions were considered representative of where the media is associated with higher degrees of exposure to weathering processes (*Figure 1*). As previously discussed (*Section 2.8* and *Section 5.1)*, the higher uncertainty within the Type 1 region is not solely attributable to material weathering, however, it is expected to be a major contributing factor. The portion of the test identified as the Type 1 region is not of sufficient duration to be analyzed to estimate erodibility parameters (τ_c and K_d) through the solution techniques developed for JETs (e.g., BM, SD and LR). However, the depth of the Type 1 region will be used as a surrogate to investigate the extent of weathering at each test location. To ensure that this surrogate metric is not directly influenced by varying field pressures at which individual tests are performed, the depths of the first segment will be compared against the shear stress applied at the time of test initiation to assess whether greater depths of the Type 1 region can be attributed to greater applied shear forces.

The depths of the Type 1 region in each test will then be compared between the inter-geologic and intra-geologic populations to assess whether the geology of a site influences how much weathered material is observed. Further, comparisons are performed between submerged and subaerial tests, and based on where the tests were situated within a stream's cross-section (*Figure 10*) to determine whether those characteristics affect the amount of weathered material at the stream boundary.

Chapter 6

Results

This section presents the results of the data analysis (*Chapter 5*). The results of test segmentation (*Section 6.1*) are followed by the uncertainty analysis with respect to test duration (*Section 6.2.1*) and measurement frequency (*Section 6.2.2*). Subsequently, an analysis of the Type 2 erodibility parameters is presented in *Section 6.3*, followed by the results of the depth of Type 1 analysis (*Section 6.4*), and finally, a comparison of the seasonality of JET results is presented in *Section 6.5*.

6.1 Test Segmentation

213 summer tests that passed the field quality assessment criteria were segmented using the three segmentation techniques introduced in *Section 5.1*: Visual Assessment (VA), Maximum Norm Residual (MNR) and the Gill Technique (TG). The resulting segmentation depths determined by the three techniques are demonstrated in *Figure 11*. Results show (*Figure 11*a) a skewed distribution towards a shallower segmentation depth with the TG technique exhibiting the greatest frequency in the first bin.

For cases where there was no agreement in segmentation depth between the three techniques, a manual differentiation process was performed whereby segmentation depths were compared based on their position in the cumulative time-scour depth plot (*Figure 8*) and the most appropriate segmentation depth was taken as the deterministic segmentation depth for each test (listed in *Table 10*). As an example, the segmentation depth identified by VA and MNR in *Figure 8* was taken as the deterministic segmentation depth because of the evident underestimation by TG. These deterministic segmentation depths (illustrated in *Figure 11b*) were carried forward in the succeeding analyses (*Section 6.2* and *Section 6.4*).

a) Comparison of Results of Segmentation Techniques

b) Deterministic Segmentation Depth
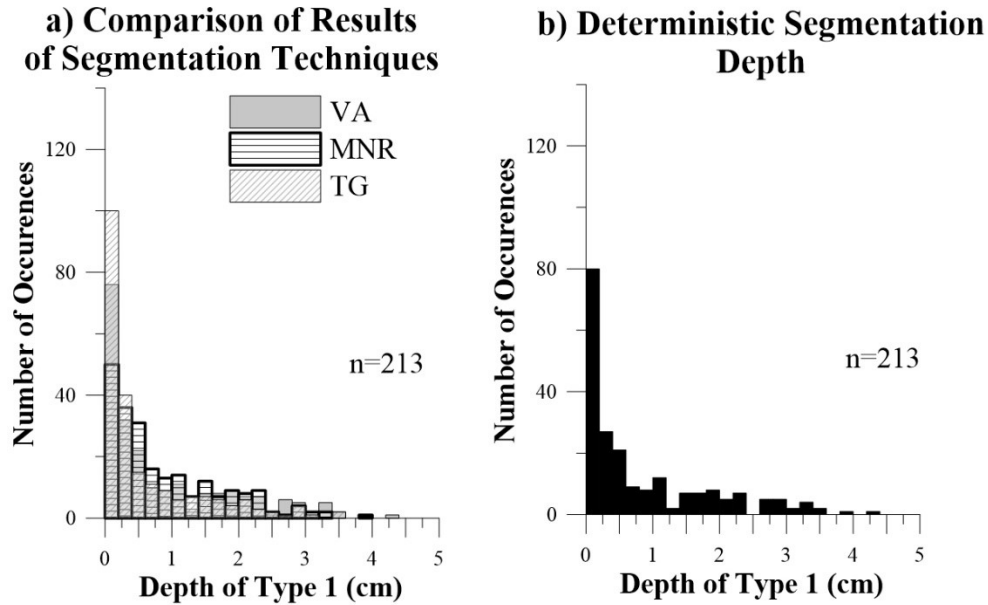
Figure 11: a) comparison of the results of the VA, MNR and TG segmentation techniques, b) the deterministic segmentation depth confirmed by manual comparison of segmentation technique results for each test.

Table 10: Segmentation techniques resulting in deterministic segmentation depth after manual differentiation.

Segmentation technique applied to achieve deterministic segmentation depth	Number of deterministic segmentation depths
VA and MNR and GM (all agree)	30 (14.1%)
VA and MNR	58 (27.2%)
VA and GM	39 (18.3%)
MNR and GM	2 (0.9%)
Solely VA	70 (32.9%)
Solely GM	12 (5.6%)
Solely MNR	2 (0.9%)

TG and MNR techniques both incorporate objectivity into the segmentation process; however, their limitations reduce their efficacy and applicability as outlined below. The most evident limitation of the TG technique contributing to the high frequency of shallow depth delineations (i.e., the first bin in *Figure 11a*) is when the iterative analysis of variance comparison (implicit within the solution technique) is

47

skewed by the presence of elevated erosion rates in the first measurement. While these high erosion rates are physically observed and representative of the test conditions, several results are outliers in the erosion rate dataset which skew the calculated variances in erosion rates of the segmented populations. This causes relatively elevated erosion rate measurements later in each JET or smaller secondary block separations occurring within each JET to be closer in magnitude to the later stage Type 2 erosion than those exceedingly high initial erosion rates. The TG technique further requires a minimum of two erosion rate data points to parameterize its process (i.e., *Equation 7* and *Equation 8* in *Section 5.1)*. Based on the measurement scheme used during data collection, this results in a minimum duration of the first segment of 0.5 minutes.

The most notable limitation of MNR is its inability to adequately describe block separation. MNR often incorrectly identifies the data point immediately before block separation as the segmentation depth (*Figure 12a*). The inclusion of late-stage block separation events is a secondary limitation of the technique. While VA was constrained to only include block separation in the first 30 minutes, this constraint was not applied to MNR to maintain objectivity in the metric used in the technique.
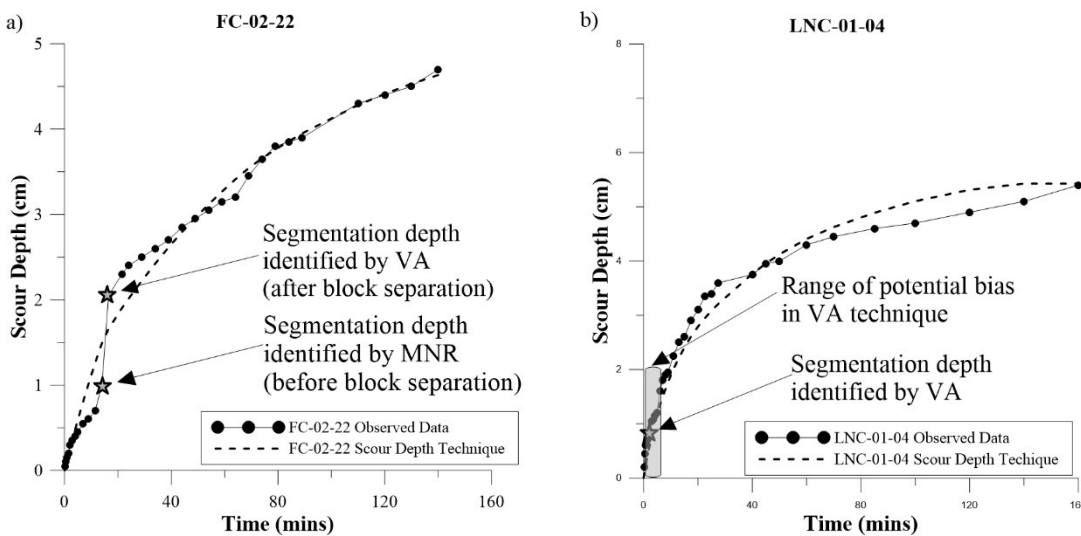
Figure 12: Limitations of segmentation techniques. a) incorrect identification of block separation by MNR.. b)potential range of bias in VA with no distinct inflection point

The most evident limitation of the VA technique is the subjective nature of test interpretation and potential bias that can be introduced when there is no clear inflection point in the erosion rates of the test

48

(Figure 12b). When the same analyst is segmenting the tests, any biases remain consistent reducing the influence on the compiled dataset. However, disparities in the subjective interpretation may become more apparent and have a greater influence when comparing data sets that are segmented by different analysts. When applying the VA technique, the review of field notes for notable changes in turbidity, changes in scour hole shape and instances of block separation during the JET can assist with the interpretation of the test progression and accurately include block separation in the Type 1 region (*Figure 12a*).

While it is logistically challenging, the comparison of the results of these segmentation techniques would benefit from a high-resolution characterization of material properties (e.g., moisture content, bulk density) along a depth profile near the JET location, similar to Khan (2006) and Khan and Kostachuck (2011). As demonstrated in *Figure 13*, the vast majority of segmentation depths were identified to be shallower than 1 cm, which is the depth of the first data point of the material characteristics measured by Khan (2006) and Khan and Kostachuck (2011). Increasing the spatial resolution of the properties measured by Khan (2006) closer to the surface may provide information on whether the results of the segmentation techniques correlate with gradients in material properties expected to relate to material weathering. This would also be useful to assess the remaining gradient in material properties in the Type 2 region after segmentation occurs.
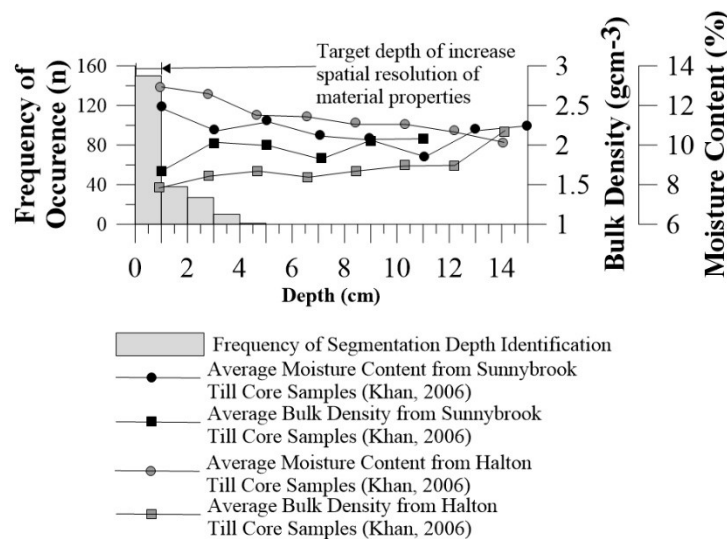
Figure 13: Relation of segmentation depths to average moisture content and bulk density profiles measured by Khan (2006) (Adapted from Khan (2006)).

49

From the application of the three segmentation techniques across all eligible JETs, it was determined that the VA technique was the most consistent and provided the most representative segmentation depth. The limitations of the more objective methods (MNR and TG) impede their ability to be relied upon consistently, however, they offer a complementary segmentation depth that can be manually compared to the VA method to ensure an appropriate segmentation depth is chosen.

6.2 Uncertainty analysis of erodibility parameters

6.2.1 Uncertainty of erodibility parameters caused by test duration.

Results of applying the solution techniques (BM, LR, and SD) to Data Scenarios 2-7 (*Table 8)* for the JETs are shown in *Figure 14* with and without test segmentation demonstrating how the erodibility parameters estimated from the various solution techniques change with test duration. It should be noted that due to the greater magnitude in K_{dSD} values (compared to K_{dBM} and K_{dLR} values), they are plotted on a separate axis on the right-hand side of *Figure 14* (shaded in grey).

τ_c estimates of all three solution techniques remain relatively consistent compared to the changes demonstrated in the K_d estimates. As the test duration decreases, both τ_c and K_d values generally increase for all solution techniques. These trends are statistically significant at a confidence level of p = 0.1 for both τ_c and K_d by comparing sequentially longer test durations using the Wilcoxon Signed Rank Test for paired samples (Walpole et al., 2007). This validates the observations made by Cossette (2016) regarding the sensitivity in erodibility parameters estimated by BM to test duration and expands on this to include SD and LR. The physical basis of this uncertainty in field data sets is attributed to a greater proportion of shorter tests coinciding with higher applied shear stresses, higher erosion rates and weaker surficial weathered material.

These results will be used to inform the succeeding analyses quantifying how segmentation affects the uncertainty of erodibility parameters arising from test duration (Section 6.2.1.1), how the uncertainty related to test duration compares between solution techniques (Section 6.2.1.2) and, how uncertainty arising from test duration affects the characterization of material on a site scale (Section 6.2.1.3).
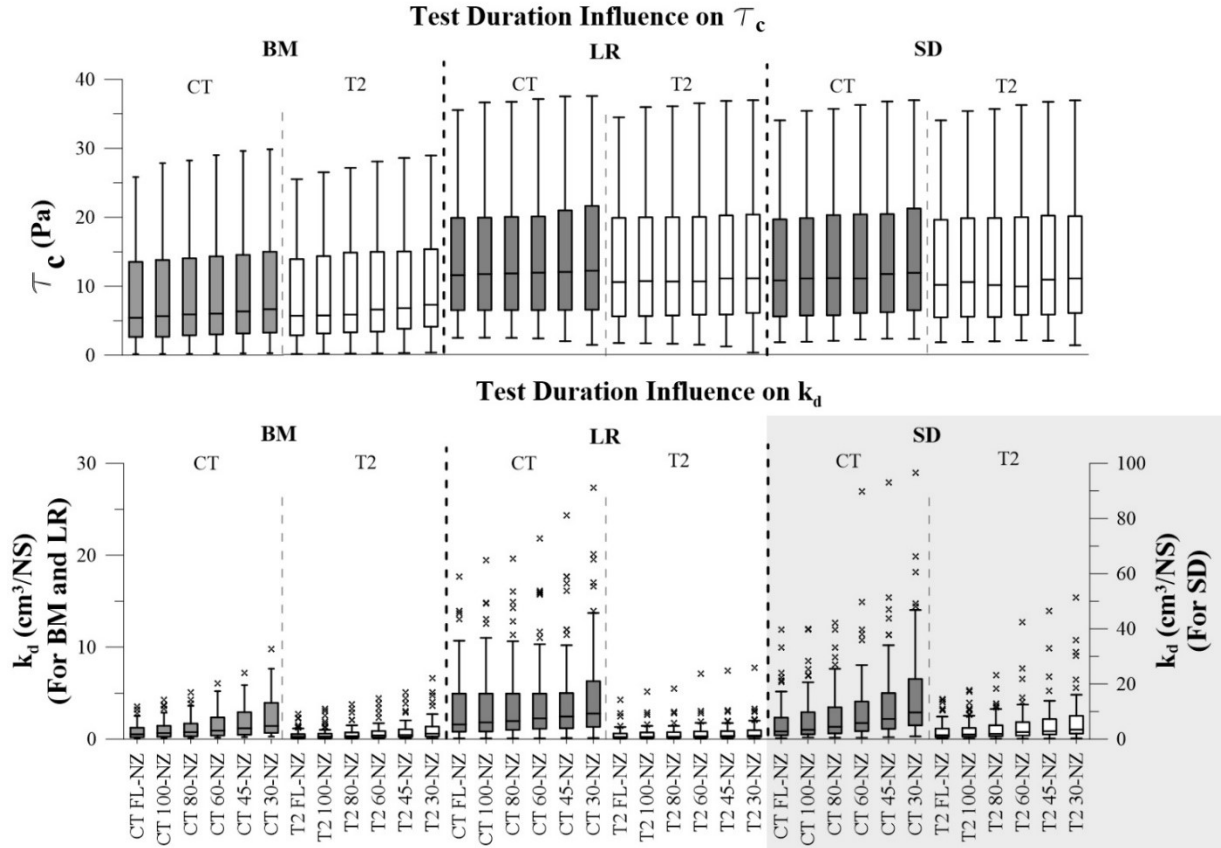
Figure 14: Distributions of erodibility parameters estimated by BM, SD and LR solution techniques for different test durations.

(Where grey box and whiskers are evaluations without segmentation and white box and whiskers are results with segmentation. Tests within the CT subregions of the figure indicate tests without segmentation and tests within the T2 subregions indicate tests with segmentation.)

6.2.1.1 Effect of segmentation on uncertainty resulting from test duration

Segmentation of the JETs causes a slight decrease in the estimated τ_c and a visible reduction in K_d for the three solution techniques (*Figure 14*). Both trends are confirmed through the Wilcoxon Signed Rank Test (Walpole et al., 2007) with a confidence level of p = 0.1 for paired samples by comparing erodibility parameters estimated with and without test segmentation for the same test durations.

Percent changes (e.g., *Equation 11* and *Equation 12* with and without segmentation respectively as explained in *Section 5.2*) of erodibility parameters at each test duration are illustrated in *Figure 15*. The differing percentage scales on the τ_c and K_d ordinate axis highlight that K_d is more sensitive to changes

in test duration than τ_c. For both K_d and τ_c, as test durations are truncated, the changes to the erodibility parameters become larger; regardless of whether segmentation has been applied.
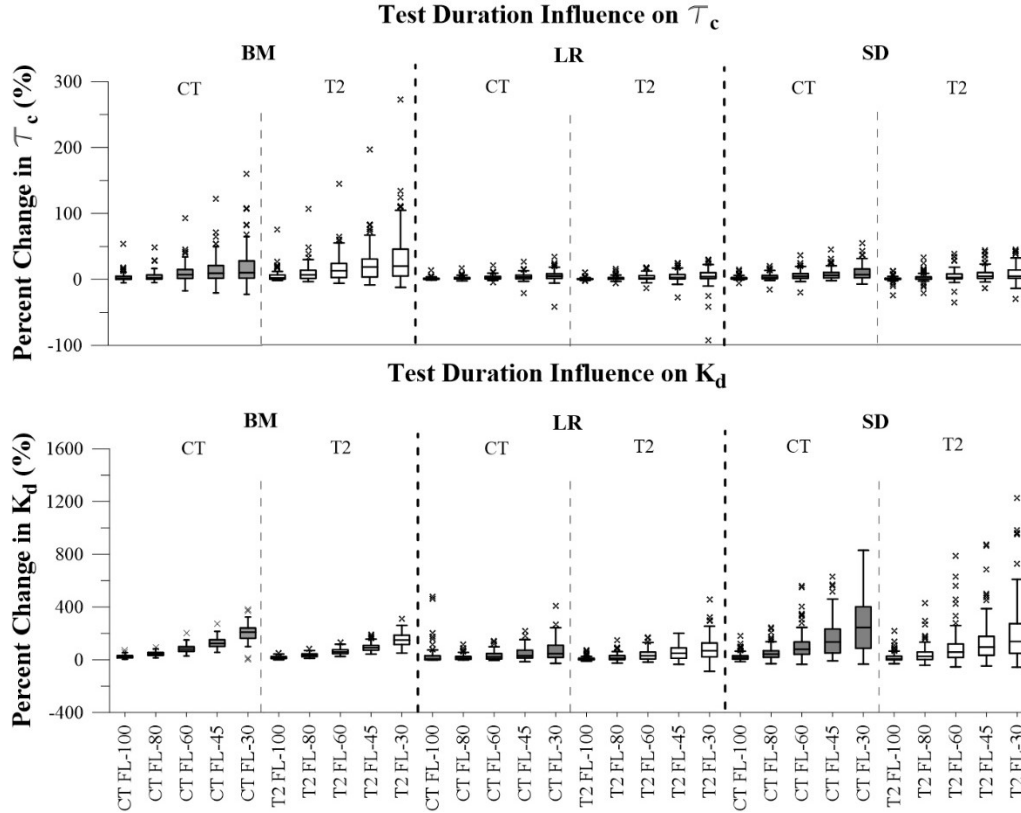
Figure 15: Percent changes in erodibility parameters with reduction in test duration.

(Where grey box and whiskers are evaluations without segmentation and white box and whiskers are results with segmentation. Tests within the CT subregions of the figure indicate tests without segmentation and tests within the T2 subregions indicate tests with segmentation.)

Paired t-tests were employed to assess if segmentation causes a statistically significant change in the uncertainty of the erodibility parameters resulting from test duration. Here, for each reduction in test duration, the ratios:

$$\frac{\left|\% \, change \, k_{d_{without \, segmentation}}\right|}{\left|\% change \, k_{d_{with \, segmentation}}\right|}, \text{ and } \frac{\left|\% \, chang \, \tau_{c_{without \, segmentation}}\right|}{\left|\% chang \, \tau_{c_{with \, segmentation}}\right|}$$

were compared. Where ratios were greater than 1.0, applying the segmentation strategy reduced the parameter uncertainty to changes in test duration. Absolute values ensure that the uncertainty is based

solely on the magnitude of the change and not the directionality of the change. The results of the two-tailed paired t-tests at a p = 0.05 confidence level are listed in *Table 11*.

Table 11: Effect of segmentation on the uncertainty of erodibility parameters resulting from test duration.

	τ_{cBM}	τ_{cSD}	τ_{cLR}	K_{dBM}	K_{dSD}	K_{dLR}
FL to 100	↑	-	-	↓	-	-
FL to 80	↑	-	-	↓	-	-
FL to 60	↑	-	-	↓	-	↑
FL to 45	↑	-	-	↓	-	↑
FL to 30	↑	-	-	↓	↓	↑

Note: upward and downward arrows indicate increases and decreases in parameter uncertainty to test duration respectively with segmentation. The symbol "-" represents no statistically significant change at the p = 0.05 confidence level.

Results listed in Table 11 demonstrate that BM is the only solution technique that is consistently influenced by segmentation based on the percent changes in erodibility parameters. The uncertainty of τ_{cBM} increases with segmentation, whereas K_{dBM} decreases in uncertainty with segmentation.

The percent changes as calculated by *Equation 11* (without segmentation) *and Equation 12* (with segmentation) are referenced against values from Data Scenario 2 for CT and T2 respectively. This does not consider the notable reduction in K_d values that occurs when segmentation is applied (*Figure 14*). This is further highlighted in *Table 12* where the mean values of the erodibility parameters from Data Scenario 2 (FLNZ) are listed with (T2) and without (CT) segmentation. Since K_d values against which the percent changes are standardized in *Equation 12* have notably decreased, a change of a smaller magnitude can represent a larger percent of the Data Scenario 2 value.

Table 12: Mean erodibility parameters of Data Scenario 2 with and without test segmentation.

	τ_{cBM}	τ_{cSD}	τ_{cLR}	K_{dBM}	K_{dSD}	K_{dLR}
Mean CTFLNZ Value	8.5	13.1	14.0	0.80	5.91	3.22
Mean T2FLNZ Value	8.5	12.9	13.1	0.43	2.70	0.46
Percent Change	**0%**	**-1.5%**	**-6.4%**	**-46%**	**-54%**	**-86%**

To investigate the role that the change in Data Scenario 2 values has in the comparison, the analysis is repeated after altering *Equation 12* to *Equation 14* below in which the reference population in the T2 calculation is adjusted to Data Scenario 2 without segmentation (CTFLNZ). This facilitates an assessment of how the magnitude of change in erodibility parameter is altered with segmentation.

$$\%Change\ K_{dBM}\ T2FLNZ\ to\ T2100NZ = \frac{K_{dBM-T2100N} - K_{dBM-T2FLNZ}}{K_{dBM-CTFLNZ}} \times 100 \qquad (14)$$

Repeating the paired t-test analysis on the percent changes calculated with a consistent reference population produces the results listed in *Table 13*. It is clear that there is a statistically significant reduction in the magnitude-based uncertainty of K_d predicted by all solution techniques with segmentation. The increase in uncertainty in τ_{cBM} remains evident as previously noted.

Table 13: **Effect of segmentation on magnitude-based (consistent reference population) change in erodibility parameter with test duration.**

	τ_{cBM}	τ_{cSD}	τ_{cLR}	K_{dBM}	K_{dSD}	K_{dLR}
FLNZ to 100NZ	↑	-	-	↓	↓	↓
FLNZ to 80NZ	↑	-	-	↓	↓	↓
FLNZ to 60NZ	↑	-	-	↓	↓	↓
FLNZ to 45NZ	↑	↓	-	↓	↓	↓
FLNZ to 30NZ	↑	-	-	↓	↓	↓

Note: upward and downward arrows indicate increases and decreases in parameter uncertainty to test duration respectively with segmentation. The symbol "-" represents no statistically significant change at the p = 0.05 confidence level.

These results indicate that the uncertainty of τ_{cBM} is worsened with segmentation on percentage change and magnitude change basis, however, τ_{cLR} and τ_{cSD} are quite robust to test duration and are largely unaffected by test segmentation.

K_d uncertainty related to test duration is notably reduced with test segmentation on a magnitude of change basis. Tests with segmentation also demonstrate more physically realistic values of K_d, particularly for LR and SD solution techniques, which estimate high K_d values without segmentation. This is attributed to segmentation removing the portion of the test with the highest applied shear stresses, highest erosion rates and weakest material causing lower estimated K_d values for all solution techniques. However, segmentation does not reduce uncertainty related to test duration in the estimation of K_{dSD} or K_{dLR} on a percent change basis. Even though the Type 1 region is removed from the analysis, the non-linear behaviour of the linear excess shear stress equation (*Equation 1*; *m = 1*) in the Type 2 region where some weathering may persist cannot entirely be accounted for in the analysis.

6.2.1.2 Comparison of solution technique uncertainty resulting from test duration

Paired t-tests were used to compare the percent change of erodibility parameters (*Figure 16*) between data scenarios (*Table 8*) for the three solution techniques. The results of the t-tests (p=0.05) are presented below in Table 14 and Table 15.
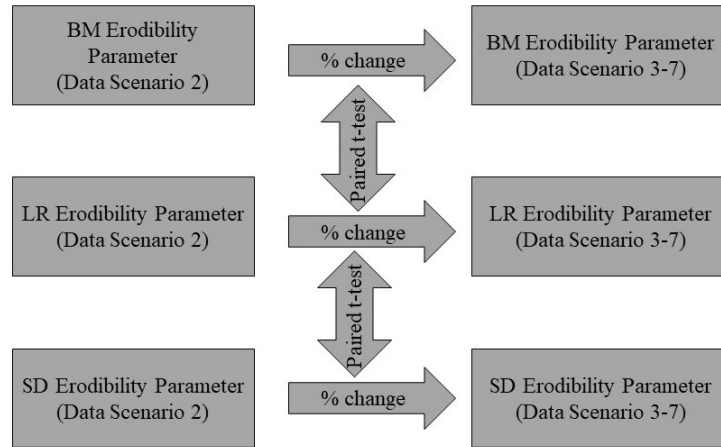
Figure 16: Comparison of solution technique uncertainty related to test duration.

Table 14: T-test results demonstrating the solution technique with less certainty related to test duration in the estimation of critical shear stresses.

	Without Segmentation (CT)			With Segmentation (T2)		
	τ_{cBM} compared to τ_{cLR}	τ_{cBM} compared to τ_{cSD}	τ_{cSD} compared to τ_{cLR}	τ_{cBM} compared to τ_{cLR}	τ_{cBM} compared to τ_{cSD}	τ_{cSD} compared to τ_{cLR}
FL to 100	τ_{cBM}	τ_{cBM}	τ_{cSD}	τ_{cBM}	τ_{cBM}	τ_{cSD}
FL to 80	τ_{cBM}	τ_{cBM}	τ_{cSD}	τ_{cBM}	τ_{cBM}	τ_{cSD}
FL to 60	τ_{cBM}	τ_{cBM}	τ_{cSD}	τ_{cBM}	τ_{cBM}	τ_{cSD}
FL to 45	τ_{cBM}	τ_{cBM}	τ_{cSD}	τ_{cBM}	τ_{cBM}	τ_{cSD}
FL to 30	τ_{cBM}	τ_{cBM}	τ_{cSD}	τ_{cBM}	τ_{cBM}	-

Note: the erodibility parameter listed in each cell is the one with greater changes in the data scenario comparison at a confidence level of p=0.05.

If there is not a statistically significant difference in the changes in erodibility parameter it is denoted with '-'.

Table 15: T-test results demonstrating the solution techniques with less certainty related to test duration in the estimation of the erodibility coefficient.

	Without Segmentation (CT)			With Segmentation (T2)		
	K_{dBM} compared to K_{dLR}	K_{dBM} compared to K_{dSD}	K_{dSD} compared to K_{dLR}	K_{dBM} compared to K_{dLR}	K_{dBM} compared to K_{dSD}	K_{dSD} compared to K_{dLR}
FL to 100	K_{dBM}	-	K_{dSD}	K_{dBM}	K_{dSD}	K_{dSD}
FL to 80	K_{dBM}	K_{dSD}	K_{dSD}	K_{dBM}	K_{dSD}	K_{dSD}
FL to 60	K_{dBM}	K_{dSD}	K_{dSD}	K_{dBM}	K_{dSD}	K_{dSD}
FL to 45	K_{dBM}	K_{dSD}	K_{dSD}	K_{dBM}	K_{dSD}	K_{dSD}
FL to 30	K_{dBM}	K_{dSD}	K_{dSD}	K_{dBM}	K_{dSD}	K_{dSD}

Note: the erodibility parameter listed in each cell is the one with greater changes in the data scenario comparison at a confidence level of p=0.05. If there is not a statistically significant difference in the changes in erodibility parameter it is denoted with '-'.

A consistent ranking of the certainty of the solution techniques is evident with and without segmentation and is summarized in *Table 16*. These results indicate that the choice of solution technique may factor considerably in affecting the uncertainty of the estimated erodibility parameters (in particular K_d) arising from the duration of a JET. An important corollary to this observation relates to the evaluation and comparison of historically compiled JET datasets. Several JET studies were performed and published before alternative solution techniques to BM (e.g., Shugar et al., 2007; Khan and Kostachuck, 2011; Clark and Wynn, 2007) or before LR was recommended to be used by Wahl (2022) (e.g., Simon et al., 2010). Even if historically compiled data sets employ a consistent solution technique (BM), their results may diverge from one another due to differing test durations. If LR is applied more consistently moving forward as recommended by Wahl (2021), then comparisons between JET datasets will be more robust to differences in JET durations than when BM was the standard solution technique applied to JETs.

Table 16: Ranking of solution technique certainty to test duration.

	τ_c certainty from Test Duration	K_d certainty from Test Duration
LR	Most	Most
SD	Intermediate	Least
BM	Least	Intermediate

6.2.1.3 Test Duration effect on site characterization

The 90-test population employed in the uncertainty analysis spans 13 sites and 10 geological units causing the variance of the population to be larger than the variance at an individual site. To investigate how the duration of a JET can influence how a site is characterized while considering the expected variability at a site scale, Kruskal-Wallis (K-W) tests (Walpole et al., 2007) were performed on the erodibility parameters derived from the data scenarios at the two sites with the largest sample pool subpopulation: TCH (n=14) and NTL (n=12). The results presented in *Table 17* indicate that in some instances, test segmentation can reduce the test duration required to maintain a consistent site characterization based on K_{dBM} and K_{dSD}, but it can increase the test duration required to maintain a consistent site characterization based on K_{dLR}. Bolded cells indicate instances in which a reduction in test duration resulted in significantly different populations of respective erodibility parameters. Values listed in parentheses indicate conditions where changes in test durations on erodibility parameters become statistically significant at the p = 0.05 confidence level.

Table 17: Test duration influence on site characterization.

	TCH (n=14)		NTL (n=12)	
	CT	*T2*	*CT*	*T2*
τ_{cBM} K-W Significance	No	No	No	No
K_{dBM} K-W Significance	**Yes (60)**	**Yes (60)**	**Yes (60)**	**Yes (45)**
τ_{cSD} K-W Significance	No	No	No	No
K_{dSD} K-W Significance	**Yes (60)**	**Yes (30)**	**Yes (60)**	**Yes (60)**
τ_{cLR} K-W Significance	No	No	No	No
K_{dLR} K-W Significance	No	No	No	**Yes (45)**

Results listed in *Table 17* further show that the effects of changing test durations on the estimation of τ_c is minimal at the site scale. This indicates that the change in estimated τ_c (regardless of the solution technique) arising from repeating a test at the same site is likely greater than the variability arising from truncating the test duration to as low as 30 minutes.

K_d is more sensitive to the duration of a given JET and changing the durations of JETs at a site can alter how a site is characterized based on K_d. This observation generally begins to be significant at a

confidence level of $p = 0.05$ when test durations are 60 minutes or shorter but is dependent on the solution technique employed and whether segmentation occurs. The characterization of a site based on K_{dLR} does not change with test duration without segmentation. However, K_{dSD} and K_{dBM} are more sensitive to test duration with and without segmentation. Findings here suggest that when comparing results between tests with different test durations, tests with shorter durations (t< 60 minutes.) may introduce a bias in the estimated erodibility parameters compared to longer tests (i.e., t ~ 120 minutes in duration).

Results presented here help assess the resilience of conclusions of other investigations employing JETs. Shugar et al. (2007) performed JETs with durations ranging from ($50 \, mins. \leq t \leq 180 \, mins.$) and reported ranges in critical shear stress of 6 orders of magnitude applying the BM method. Khan (2006) performed tests ranging in duration from ($12 \, mins. \leq t \leq 165 \, mins.$) and reported ranges in τ_c estimates of up to 63 Pa at an individual site. Despite the range in test durations in these studies, their estimates of critical shear stress are likely not unduly influenced by this factor. Further, the robustness of τ_c estimates to test duration indicates that the results of Clark and Wynn (2007) comparing τ_c estimated from JETs to various empirical estimates of τ_c (Smerdon and Beasley, 1961; Julian and Torres, 2006) were not influenced by the relatively short JET durations (45 minutes) employed in their investigation.

Results of Clark and Wynn (2007) where K_{dBM} estimated from JETs (45-minute durations) were compared to K_d derived from empirical relationships (e.g., Osman and Thorne, 1988; Hanson and Simon, 2001) may be skewed by the short JET durations. They reported K_d estimates that were higher than those predicted by empirical relationships, however, if the tests were conducted for longer durations, K_d estimates would have tended towards lower values trending towards the empirical methods examined. As an example, and to help visualize the unintentional bias in the Clark and Wynn (2007) investigation, the erodibility parameters estimated from BM (the solution technique employed in Clark and Wynn (2007)) from the current study are plotted based on full test durations and test durations truncated to 45 minutes (*Figure 17)*. The shift in the dataset demonstrates how test durations of JETs may influence and confound broader analyses based on JET results.
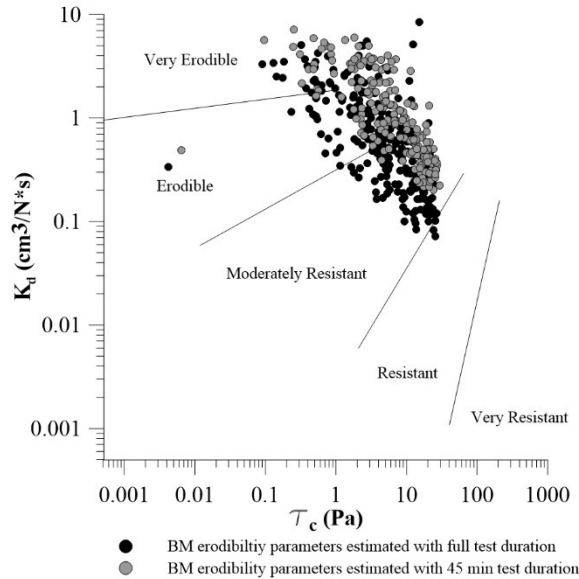
Figure 17: Effect of restricting test duration to 45 minutes on BM erodibility parameters employing the classification system of Hanson and Simon (2001).

6.2.2 Uncertainty from measurement frequency

The erodibility parameters from Data Scenarios 1, 2 and 8-11 from *Table 8* are summarized in *Figure 18* with and without segmentation. τ_{cLR} and τ_{cSD} remain relatively constant with respect to the changes in measurement frequency. τ_{cBM} is more sensitive with a greater decrease when no early time, rapid measurements are incorporated into the data scenarios. K_d shows more variability in the CT Data Scenarios compared to the T2 Data Scenarios and the data scenarios with more measurements early in the test show higher estimated K_d values.
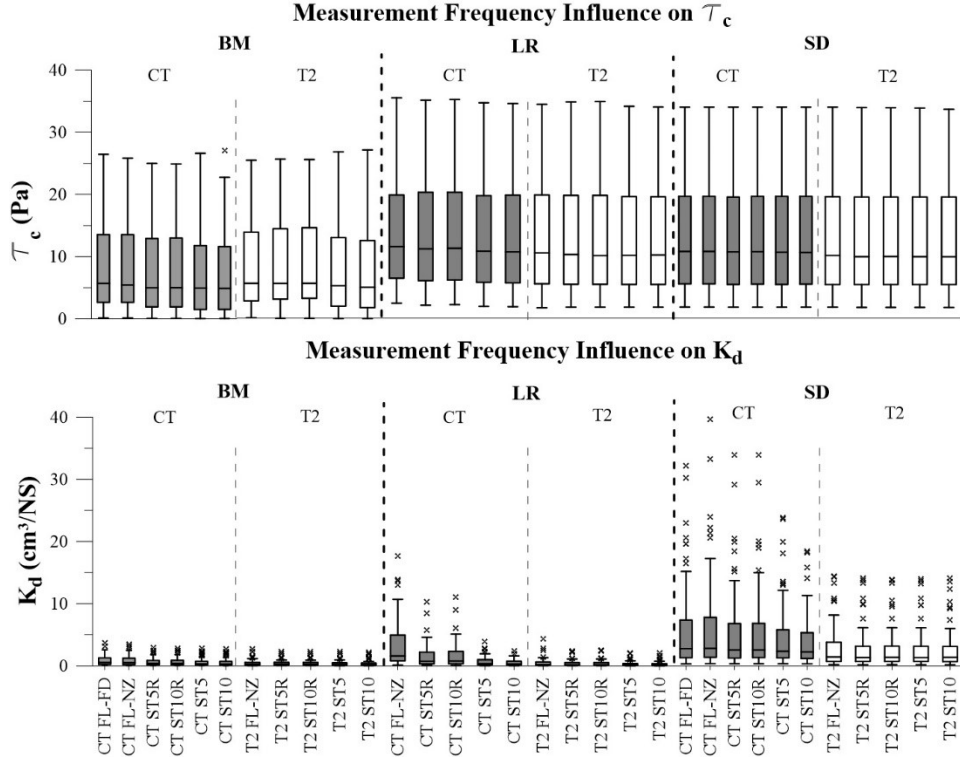
Figure 18: Distributions of erodibility parameters with changes in measurement frequency

(Where grey box and whiskers are evaluations without segmentation and white box and whiskers are results with segmentation. Tests within the CT subregions of the figure indicate tests without segmentation and tests within the T2 subregions indicate tests with segmentation.)

The six comparison scenarios discussed in *Section 5.2* are displayed in *Figure* 19 to demonstrate how changes to the measurement frequency influence the estimated erodibility parameters. In *Figure* 19, the comparison between Data Scenario 1 and Data Scenario 2 is labelled as RPR (Redundant Point Removal) to highlight that the comparison scenario was not applied to LR, and not made with the T2 dataset.
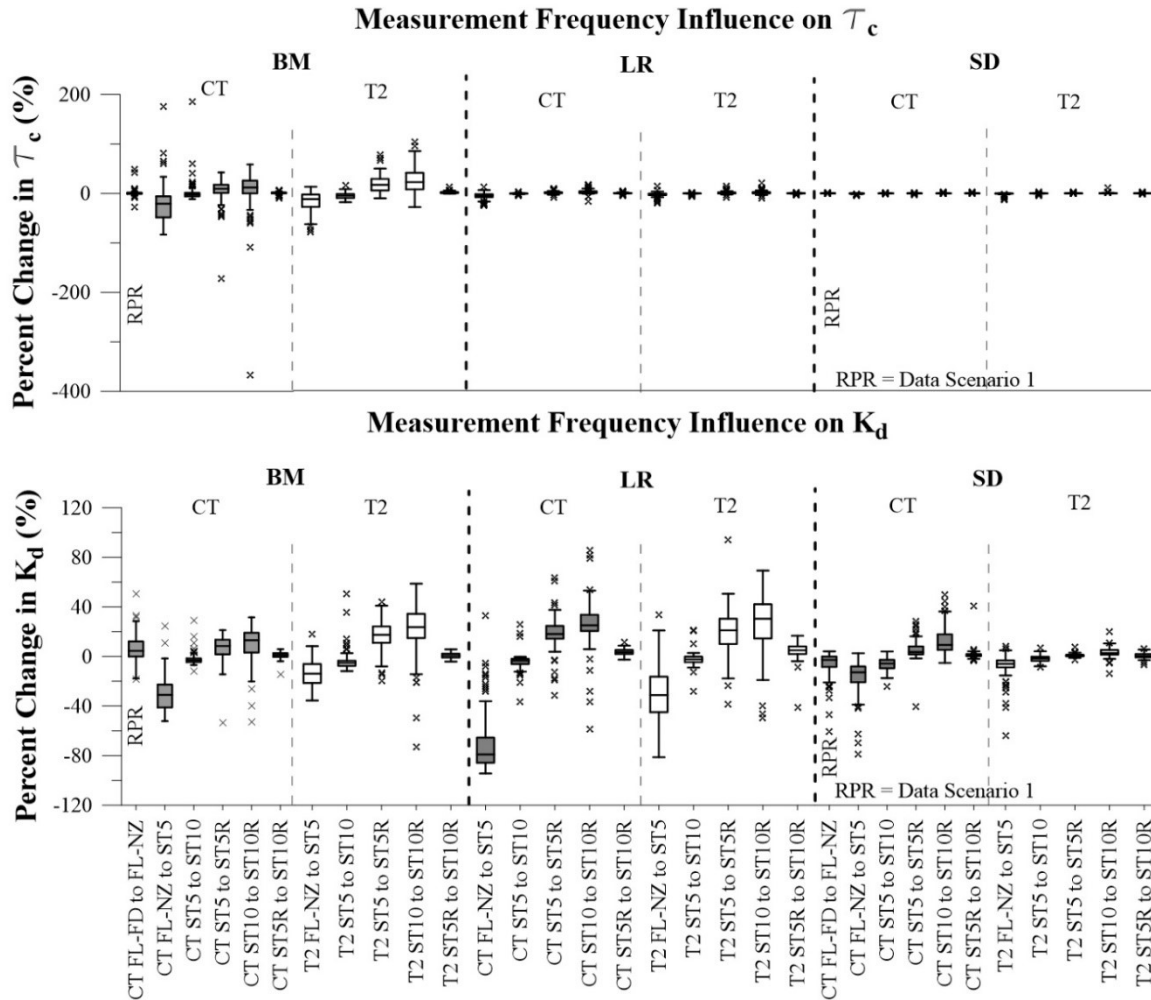
Figure 19*: Percent changes in erodibility parameters with changes in measurement frequency.

(Where grey box and whiskers are evaluations without segmentation and white box and whiskers are results with segmentation. Tests within the CT subregions of the figure indicate tests without segmentation and tests within the T2 subregions indicate tests with segmentation.)

T-tests were performed to assess whether the change in data scenarios resulted in statistically significant changes in mean erodibility parameters (i.e., $\mu_{\%change} \neq 0$) at a confidence level of p = 0.1. *Table 18* and *Table 19* summarize the results of this analysis. To contextualize significant changes, the mean changes in the erodibility parameter are emphasized with parentheses.

Table 18: T-test results of changing measurement frequency on critical shear stress estimation

comparison	τ_{cBM} Without seg.	With seg.	τ_{cSD} Without seg.	With seg.	τ_{cLR} Without seg.	With seg.
FL FD to FL NZ	-	N/A	↑ (0.1%)	N/A	N/A	N/A
FL NZ to ST5	↓ (-21%)	↓ (-17%)	↓ (-0.5%)	↓ (-1%)	↓ (-6%)	↓ (-2%)
ST5 to ST10	-	↓ (-5%)	-	↓ (-0.2%)	↓ (-0.6%)	↓ (-0.3%)
ST5 to ST5R	↑ (7%)	↑ (20%)	-	↑ (0.2%)	↑ (2%)	↑ (2%)
ST10 to ST10R	-	↑ (27%)	↑ (0.2%)	↑ (0.5%)	↑ (3%)	↑ (2%)
ST5R to ST10R	↑ (0.9%)	↑ (2%)	↑ (0.2%)	↑ (0.2%)	↑ (0.7%)	↑ (0.1%)

Where ↑ and ↓ represents statistically significant increases and decreases respectively in the mean erodibility parameter and, – represents no significant change at a confidence level of p= 0.1. The value in parentheses is the mean change in erodibility parameter between Data Scenarios and is provided for significant results.

Table 19: T-test results of changing measurement frequency on erodibility coefficient estimation

comparison	K_{dBM} Without seg.	With seg.	K_{dSD} Without seg.	With seg.	K_{dLR} Without seg.	With seg.
FL FD to FL NZ	↑ (6%)	N/A	↓ (-7%)	N/A	N/A	N/A
FL NZ to ST5	↓ (-30%)	↓ (-13%)	↓ (-16%)	↓ (-8%)	↓ (-69%)	↓ (-30%)
ST5 to ST10	↓ (-2%)	↓ (-4%)	↓ (-6%)	↓ (-2%)	↓ (-4%)	↓ (-2%)
ST5 to ST5R	↑ (7%)	↑ (17%)	↑ (5%)	↑ (0.9%)	↑ (19%)	↑ (19%)
ST10 to ST10R	↑ (10%)	↑ (21%)	↑ (13%)	↑ (3%)	↑ (27%)	↑ (26%)
ST5R to ST10R	↑ (1%)	↑ (0.7%)	↑ (1%)	↑ (0.6%)	↑ (4%)	↑ (5%)

Where ↑ and ↓ represents statistically significant increase or decrease respectively in the mean erodibility parameter and, – represents no significant change at a confidence level of p=0.1. The value in parentheses is the mean change in erodibility parameter between Data Scenarios and is provided for significant results.

These results indicate that τ_{cSD} and τ_{cLR} are quite robust to changing measurement frequencies (statistically significant changes, but nominal magnitude changes), whereas τ_{cBM} generally predicts higher values for data scenarios with a greater emphasis on earlier measurements. Further, the removal of

redundant measurement points (FL FD to FL NZ) does not substantially change the estimation of τ_{cBM} or τ_{cSD}; however, it can alter the estimated K_{dBM} and K_{dSD}.

In general, data scenarios with a greater emphasis placed on measurements earlier in tests display higher K_d estimates for all three solution techniques. This is caused by increasing or decreasing the representation of the rapid erosion portion of the test. While not changing the amount of erosion that occurs, data scenarios with longer measurement intervals early in tests force the same amount of erosion to be recorded over longer time intervals thus reducing the apparent rate of erosion. For example, if no measurement is taken for 10 minutes, the elevated erosion that occurred prior to initial measurements will be averaged over a 10-minute duration. Once the scour begins to progress at a more gradual rate, the temporal resolution of the measurements becomes less important as demonstrated in the comparison of ST5R and ST10R in *Table 18* and *Table 19*.

6.2.2.1 Effect of test segmentation on uncertainty from measurement frequency

To investigate how test segmentation changes the uncertainty of LR, BM and SD related to measurement frequency, paired t-tests were performed on CT and T2 datasets to evaluate the percent change in erodibility parameters between data scenarios (i.e., results of *Equation 13* in *Section 5.2*). During the comparison, the absolute values determined from *Equation 13* are applied to the same data scenarios with and without segmentation. In the cases of statistically significant results at the p=0.05 confidence level, the value of *Equation 15* is provided in parentheses to emphasize the results.

$$\Delta\mu_{\%change} = |\mu_{\%change\ presegmentation}| - |\mu_{\%change\ postsegmentation}| \qquad (15)$$

Table 20 demonstrates that segmenting the tests has mixed results on the uncertainty of the solution techniques to measurement frequency depending on the comparison scenario and erodibility parameter considered.

The comparison that was most influenced by segmentation is when comparing FLNZ to ST5. In this comparison, segmentation reduces the uncertainty of all erodibility parameter estimates to the measurement frequency except τ_{cSD} which saw a negligible increase in uncertainty. This agrees with the expected outcomes. Since the portion of the test with the most rapid erosion is removed during segmentation, implementing rapid measurements with segmentation will not capture the same reduction of erosion rates early in the test as it does without segmentation.

63

Table 20: Effect of segmentation on uncertainty of erodibility parameters related to measurement frequency.

	τ_{cBM}	τ_{cSD}	τ_{cLR}	K_{dBM}	K_{dSD}	K_{dLR}
FL-NZ to ST5	↓ (-14.43%)	↑ (0.55%)	↓ (-3.07%)	↓ (-16.78%)	↓ (-8.4%)	↓(-38.02%)
ST5 to ST10	-	↑ (0.19%)	↓ (-.076%)	↑ (2.85%)	↓(-4.02%)	↓(-1.72%)
ST5 to ST5R	-	-	-	↑ (8.71%)	↓ (-5.23%)	-
ST10 to ST10R	-	↑ (0.35%)	↓ (-1.09)	↑(11.55%)	↓(-9.28%)	-
ST5R to ST10R	-	↑ (0.16%)	↓(-0.47%)	-	-	↑(2.45%)

Where ↑ and ↓ indicate a statistically significant increase or decrease respectively in parameter uncertainty with segmentation, and, - represents no statistically significant change in uncertainty from measurement frequency at the 95% confidence level.

In all other scenarios evaluated, the effect of segmentation on the estimates of τ_c are negligible. τ_{cSD} and τ_{cLR} identified statistically significant but trivial (based on the mean percentage change) increases in uncertainty. τ_{cBM} experiences a noteworthy reduction in uncertainty after segmentation for the FLNZ to ST5 comparison but resulted in no statistically significant changes at the 95% confidence level for any of the other scenarios evaluated.

While K_{dBM} demonstrates a notable decrease in uncertainty with segmentation from the FLNZ to ST5 scenario, the uncertainty for three of the other scenarios considered increased (*Table 20*). K_{dSD} is the only parameter to display consistent (4/5 scenarios) reductions in uncertainty to measurement frequency with segmentation of the tests. K_{dLR} experiences a significant reduction (-38.02%) in uncertainty with segmentation in the FLNZ to ST5 scenario, however, the other scenarios demonstrate mixed results.

6.2.2.2 Solution Technique Comparison of Measurement Frequency Uncertainty

Paired t-tests were used to compare the percent change (*Figure 20*) of erodibility parameters between data scenarios (*Table 8*) for the three solution techniques. The results of the t-tests (p=0.1) are presented in *Table 21* and *Table 22*.

BM Erodibility Parameter (Data Scenario 2) — % change → BM Erodibility Parameter (Data Scenario 8-11)

Paired t-test

LR Erodibility Parameter (Data Scenario 2) — % change → LR Erodibility Parameter (Data Scenario 8-11)

Paired t-test

SD Erodibility Parameter (Data Scenario 2) — % change → SD Erodibility Parameter (Data Scenario 8-11)
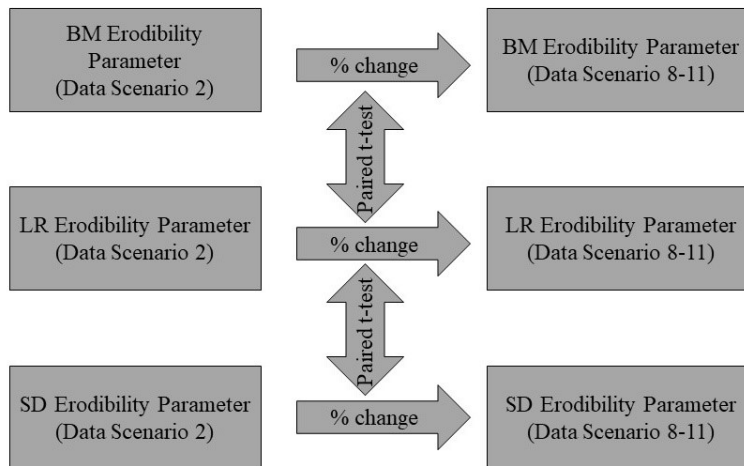
Figure 20: Comparison of solution technique certainty related to measurement frequency.

Table 21:T-test results demonstrating the solution techniques with less certainty related to measurement frequency in the estimation of critical shear stress.

	Without Segmentation (CT)			With Segmentation (T2)		
	τ_{cBM} compared to τ_{cLR}	τ_{cBM} compared to τ_{cSD}	τ_{cSD} compared tτ_{cLR}o	τ_{cBM} compared to τ_{cLR}	τ_{cBM} compared to τ_{cSD}	τ_{cSD} compared to τ_{cLR}
FL-NZ to ST5	τ_{cBM}	τ_{cBM}	τ_{cLR}	τ_{cBM}	τ_{cBM}	τ_{cLR}
ST5 to ST10	τ_{cBM}	τ_{cBM}	τ_{cLR}	τ_{cBM}	-	τ_{cLR}
ST5 to ST5R	τ_{cBM}	τ_{cBM}	τ_{cLR}	τ_{cBM}	τ_{cBM}	τ_{cLR}
ST10 to ST10R	τ_{cBM}	τ_{cBM}	τ_{cLR}	τ_{cBM}	-	τ_{cLR}
ST5R to ST10R	τ_{cBM}	τ_{cBM}	τ_{cLR}	τ_{cBM}	τ_{cBM}	-

Note: the erodibility parameter listed in each cell is the one with greater changes in the data scenario comparison at a confidence level of p=0.05.

If there is not a statistically significant difference in the changes in erodibility parameter it is denoted with '-'.

Table 22: T-test results demonstrating the solution techniques with less certainty related to measurement frequency in the estimation of the erodibility coefficients.

	Without Segmentation (CT)			With Segmentation (T2)		
	K_{dBM} compared to K_{dLR}	K_{dBM} compared to K_{dSD}	K_{dSD} compared to K_{dLR}	K_{dBM} compared to K_{dLR}	K_{dBM} compared to K_{dSD}	K_{dSD} compared to K_{dLR}
FL-NZ to ST5	K_{dLR}	K_{dBM}	K_{dLR}	K_{dLR}	K_{dBM}	K_{dLR}
ST5 to ST10	K_{dLR}	K_{dSD}	K_{dSD}	K_{dBM}	K_{dBM}	-
ST5 to ST5R	K_{dLR}	-	K_{dLR}	-	K_{dBM}	K_{dLR}
ST10 to ST10R	K_{dLR}	-	K_{dLR}	K_{dLR}	K_{dBM}	K_{dLR}
ST5R to ST10R	K_{dLR}	-	K_{dLR}	K_{dLR}	-	K_{dLR}

Note: the erodibility parameter listed in each cell is the one with greater changes in the data scenario comparison at a confidence level of p=0.05.

If there is not a statistically significant difference in the changes in erodibility parameter it is denoted with '-'.

A consistent trend was observed in the ranking of certainty of the three-solution technique estimates of τ_c. A less consistent trend was observed in the ranking of solution technique certainty related to measurement frequency in K_d. These rankings are summarized in Table 23.

Table 23: Ranking of solution technique certainty from measurement frequency.

	τ_c certainty related to Measurement Frequency	K_d certainty related to Measurement Frequency
LR	Intermediate	Least
SD	Most	Inconclusive
BM	Least	Inconclusive

Without segmentation, there is no consistent ranking between K_{dSD} and K_{dBM} as to which one is more certain with respect to the influence of measurement frequency. However, with segmentation, K_{dSD} is more certain than K_{dBM}. Since this trend was not consistent with and without segmentation, it was listed as inconclusive. These results suggest that if LR is implemented as the preferred solution technique as recommended by Wahl (2021), then best efforts should be undertaken to standardize the measurement frequency of JETs (where feasible) to limit the influence of uncertainty of K_{dLR} related to measurement frequency.

6.2.2.3 Effect of measurement frequency on site characterization

The 90-test population employed in the uncertainty analysis spatially spans 13 sites and 10 geological units causing the variance of the population to be larger than the variance at an individual site. To investigate how the measurement frequency during a JET can influence erodibility parameter characterization on a site scale, Kruskal-Wallis (K-W) tests (Walpole et al., 2007) were conducted for the erodibility parameters derived from LR, SD and BM techniques for the measurement frequency data scenarios for the two sites with the largest sample pool subpopulation: TCH (n=14) and NTL (n=12). The results are listed in *Table 24.*

Evaluation of measurement frequency scenarios identified no impact on the characterization of a site based on τ_{cBM}, K_{dBM}, τ_{cSD}, K_{dSD}, or τ_{cLR}, indicating that the changes to erodibility parameters introduced by altering the measurement frequency generally do not exceed the expected levels of site-scale variability. Namely, the range in erodibility parameters resulting from repeated tests at the same site outweighs variability arising from altering measurement frequency during a series of tests at a given site.

Table 24: Measurement frequency influence on site characterization.

	TCH (n=14)		NTL (n=12)	
	CT	*T2*	*CT*	*T2*
τ_{cBM} K-W Significance	No	No	No	No
K_{dBM} K-W Significance	No	No	No	No
τ_{cSD} K-W Significance	No	No	No	No
K_{dSD} K-W Significance	No	No	No	No
τ_{cLR} K-W Significance	No	No	No	No
K_{dLR} K-W Significance	**Yes (ST5, ST10)**	No	**Yes (ST5R, ST5, ST10, ST10R)**	No

Bolded cells indicate instances where statistically distinct populations arose at the same site by changing the measurement frequency, and the Data Scenarios in parentheses are identified being statistically different than FL-NZ at a confidence level of p=0.1.

K_{dLR}, however, demonstrates some uncertainty related to measurement frequency with the CTST5 and CTST10 Data Scenarios being statistically different from CTFL-NZ at the TCH site (*Table 24)* and CTST5R, CTST5, CTST10 and CTST10R being statistically different from CT FL-NZ at the NTL site. With segmentation, uncertainty is reduced such that none of the populations are significantly different

from CTFL-NZ at the confidence level p = 0.1. This demonstrates that segmentation can provide a benefit in reducing the uncertainty related to measurement frequency when characterizing K_{dLR} at the site scale.

The results presented here also help to emphasize the level of importance of the recommended initial JET measurement time intervals of 30 seconds (Khanal et al., 2016). It was further observed that maintaining a sufficiently short measurement time interval ($0.25 min \leq \Delta t \leq 1 \ min$) at the beginning of JETs helps define the progression of the scour hole early in the test and is useful for segmenting the JET data. The segmentation of JET test analysis is recommended to reduce the influence of measurement frequency to a level that will not alter how a site is characterized based on K_{dLR}.

6.3 Erodibility parameters of the Type 2 region of tests

6.3.1 Geologic comparison

JETs within the Halton Till (n=56) were compared to tests undertaken in other geologic units (inclusive of Halton Till, n=199) to evaluate an example of intra-geologic unit variability in erodibility parameters. Comparative populations excluded tests collected during the spring season, were restricted to tests passing the QA/QC review, were limited to test durations longer than 60 minutes and, excluded tests which were observed not to exceed τ_c. The erodibility parameters estimated using LR, BM and SD are displayed in *Figure 21* with and without segmentation. In instances of SD failure (τ_{cSD} erroneously estimated as 0 similar to Wahl (2016)) or LR failure (τ_{cLR} or K_{dLR} estimated with negative values), the tests were corrected using Correction Method 2 (see *Appendix H*).

The population of Halton Till tests was compared to the population of All Sites using a two-tailed t-test assuming unequal variances with a confidence level of p=0.05 (Walpole et al., 2007). Regardless of whether the JETs are segmented, all solution techniques estimate a statistically different mean τ_c for Halton Till compared to the All Sites population (*Figure 21*). *Figure 21* illustrates a lower mean τ_c within the Halton Till population. Levene's tests further demonstrate that the Halton Till has a lower variance of estimated τ_c for all solution techniques regardless if segmentation is applied or not. Results here support the edict that *apriori* classification of the geologic unit of study can help bound estimates of τ_c. This supports the conclusions made by Mahalder et al. (2017) who demonstrated that soils from different physiographic regions, or in this case different geologic units, can demonstrate unique clusters of their respective erodibility parameters.

68

There was no significant difference in predicted K_d values when applying any of the three solution techniques between the Halton Till and All Sites populations at the confidence level of p=0.1 with or without segmentation. This suggests that the values obtained are largely attributable to site-specific factors beyond the geologic unit.
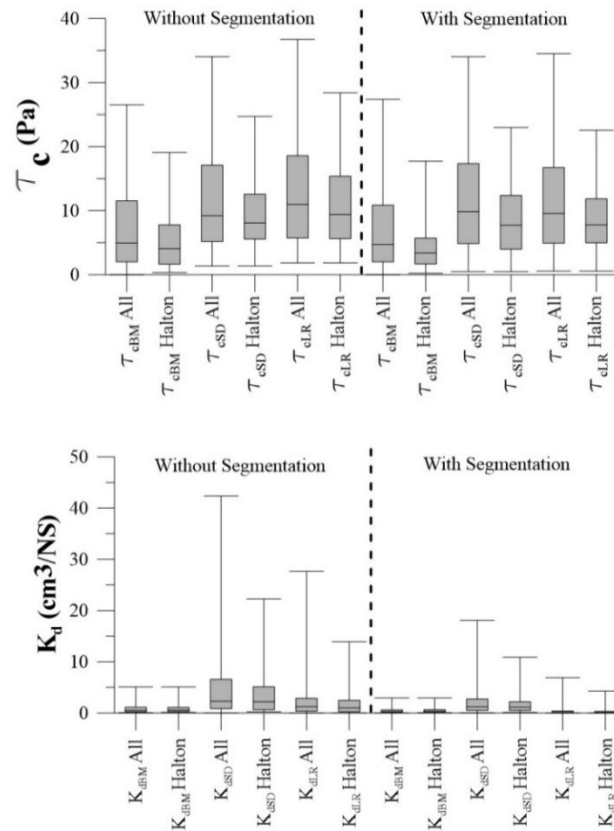
Figure 21: Comparison of erodibility parameters across All Sites versus sites within Halton Till.

Corresponding to empirical observations that media more resistant to erosion also erode at slower rates, several researchers have fit power regressions through the results of JET data relating K_d to τ_c (Hanson and Simon, 2001; Simon 2010; Wahl 2022). The regression of the data collected in this investigation for each of the three solution techniques with and without segmentation for each JET is displayed in *Figure 22* following a similar approach to the aforementioned investigations. The regression analysis of the All Sites population was compared to the regression analysis of the Halton Till population with results listed in *Table 25*.

Table 25: Regression results of K_d-τ_c relationships.

	Without Segmentation		With Segmentation	
	All sites	Halton Till	All Sites	Halton Till
BM	$K_{dBM} = 1.077 * \tau_{cBM}^{-0.533}$ $R^2 = 0.505$	$K_{dBM} = 1.088 * \tau_{cBM}^{-0.572}$ $R^2 = 0.534$	$K_{dBM} = 0.636 * \tau_{cBM}^{-0.586}$ $R^2 = 0.518$	$K_{dBM} = 0.599 * \tau_{cBM}^{-0.545}$ $R^2 = 0.449$
SD	$K_{dSD} = 17.960 * \tau_{cSD}^{-0.933}$ $R^2 = 0.250$	$K_{dSD} = 24.714 * \tau_{cSD}^{-1.213}$ $R^2 = 0.399$	$K_{dSD} = 6.285 * \tau_{cSD}^{-0.772}$ $R^2 = 0.276$	$K_{dSD} = 1.881 * \tau_{cSD}^{-0.311}$ $R^2 = 0.063$
LR	$K_{dLR} = 9.603 * \tau_{cLR}^{-0.927}$ $R^2 = 0.183$	$K_{dLR} = 7.643 * \tau_{cLR}^{-1.006}$ $R^2 = 0.140$	$K_{dLR} = 1.125 * \tau_{cLR}^{-0.878}$ $R^2 = 0.252$	$K_{dLR} = 0.703 * \tau_{cLR}^{-0.785}$ $R^2 = 0.214$

The relationship between K_d and τ_c is the strongest when the Blaisdell method is used to analyze the JET data. This is counter to the observation made by Wahl (2021) where the LR method exhibited the strongest relationship between K_d and τ_c with an R^2 value of 0.79 compared to an R^2 of 0.55 for BM. The investigation of Wahl (2021) focused on remolded samples which were prepared and tested in a laboratory setting, whereas this investigation focused on tests performed in-situ where sample heterogeneity may further impact testing results. Further, the stronger relationship between K_d and τ_c from BM in the current study is attributed to the technique employing a two-step sequence of analysis where τ_{cBM} is estimated individually and then applied to the estimation of K_{dBM}. As a result, a spurious relationship exists between the two erodibility parameters. This likely contributes to the relatively consistent R^2 values for BM regressions between the current investigation (0.45<R^2<0.53) and Wahl (2021) (R^2 <0.55). The SD and LR techniques solve for τ_c and K_d simultaneously resulting in these solution techniques obtaining lower R^2 values of their power regression fits. Overall, the low goodness of fit values does not support employing power function relationships to correlate τ_c-K_d .

The only scenario in which the "Halton Till" and "All Sites" sample populations were significantly different in regression analysis from one another was SD with segmentation. However, in this instance, the R^2 value of the fit through the Halton Till data was exceptionally low (R^2=0.063) thereby inadequately describing the two distinct populations.
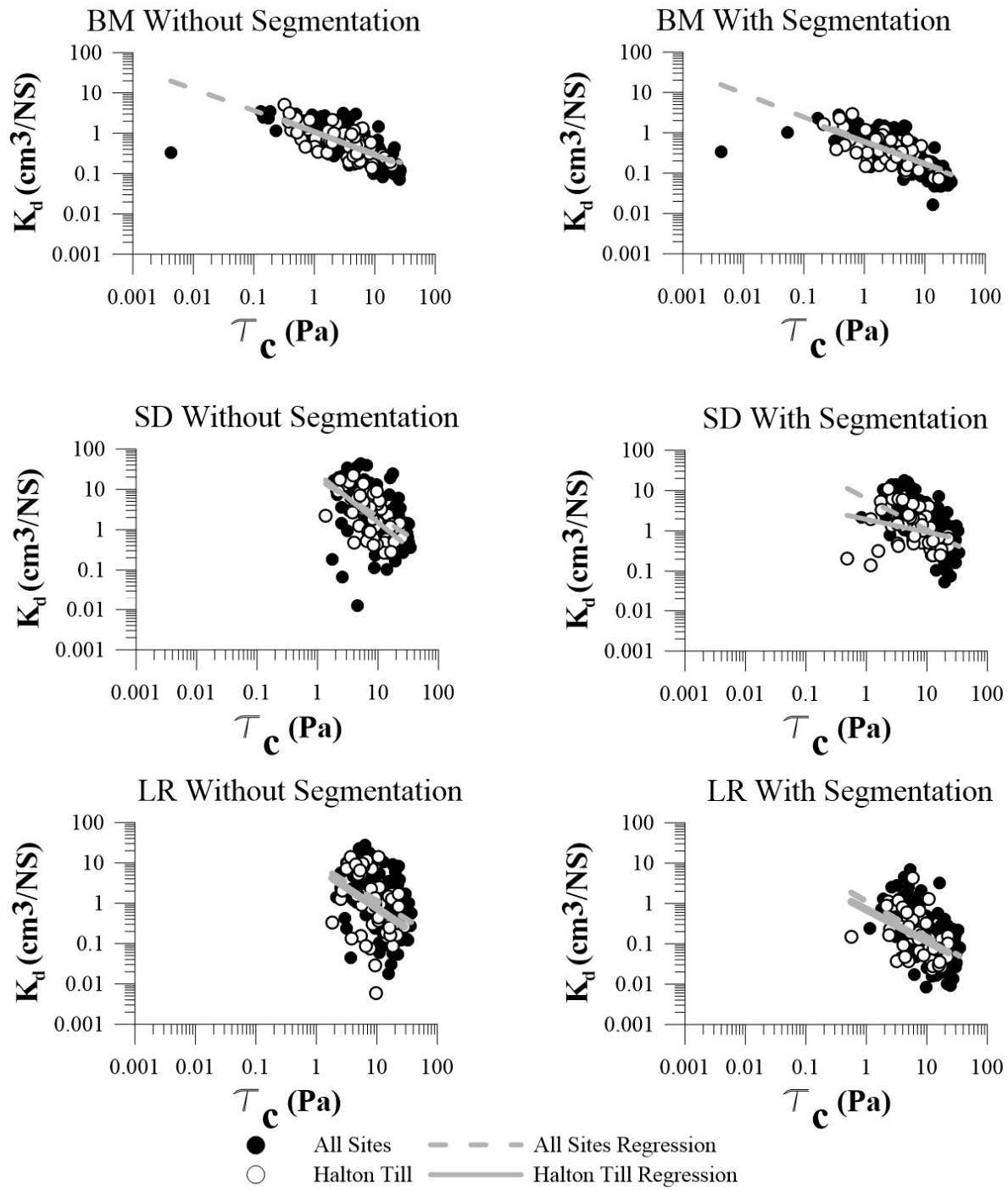
Figure 22: τ_c vs K_d regressions of tests spanning All sites and tests within Halton Till

71

Results here indicate that any relationship between K_d and τ_c is not unique to a given geologic unit and thus cannot be refined by taking into consideration which geologic unit a site falls within. Further, deriving the τ_c-K_d relationship for an isolated geologic unit does not improve the representativeness or applicability of the relationship (i.e., the fit of the data). This suggests that the substantial scatter within the τ_c-K_d relationship obtained in this investigation and others (Simon et al., 2010) is not a result of the inclusion of classed geologic units. Trends in erodibility parameters specific to geologic units must be more nuanced than simply relating K_d to τ_c and include other parameters as suggested by Mahalder et al. (2017).

6.3.2 At-A-Station cross-section sample location comparison based upon Type 2 erodibility parameters

The Type 2 regions of the tests (i.e., JETs with segmentation) can be grouped based on their location within a stream's cross-section (*Figure 10* in *Section 5.3*). *Figure 23* demonstrates how the Type 2 erodibility parameters predicted by SD and LR change based on the test location within the stream cross-section for the 199 tests spanning all the study sites. BM was excluded from this analysis due to its poor ability to fit observed data (*Appendix I*). It should be highlighted that comparisons to the third bank tier may be restricted by the relatively small sample sizes of the population (n=10).

Kruskall-Wallis tests with follow-up pairwise Mann-Whitney Tests revealed similar trends between the cross-section location of tests for both SD or LR techniques. At the confidence level p=0.1, the median τ_c is significantly different for the second bank tier compared with the other three cross-section locations and it is observed within *Figure 23a* that the second bank tier plot has a higher median τ_c compared to the other populations. The stream bed, first bank tier and third bank tier are unable to reject the Kruskall Wallis null hypothesis of all samples originating from the same distribution of τ_c. While these results do not necessarily agree with the increasing τ_c corresponding to lower portions of a stream bank observed by Sutarto (2015) (regions of higher in-situ moisture content), it does lend credence to the finding that different sections of a streambank should be characterized individually and not by a set of erodibility parameters averaged across the face of a given bank.
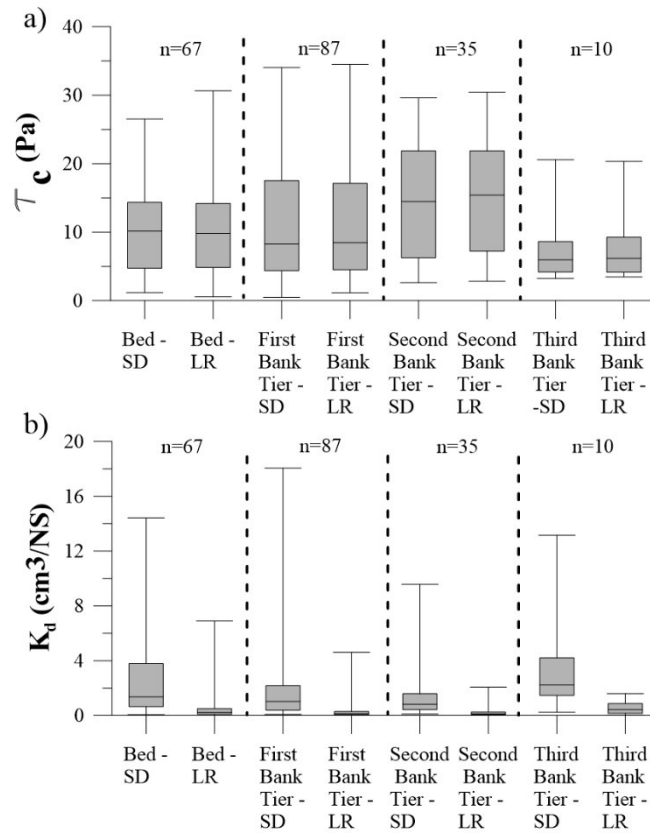
Figure 23: Erodibility parameters of Type 2 region based on cross section placement.

Where the extents of the whiskers represent the maximum and minimum of the populations.

K_d demonstrates different trends related to the cross-section locations than τ_c. A Kruskall-Wallis Test with follow-up pairwise Mann-Whitney Tests indicates that the populations of K_d fall into two unique groups (for both SD and LR techniques). The median K_d of the streambed and the third bank tier do not have significantly different medians from one another at the confidence level p=0.1 but are significantly different from the median K_d of the first and second bank tiers, which have statistically similar medians between themselves.

6.4 Type 1 Region comparison

To assess how the presence of weathered material changes based on test characteristics (i.e., test material submergence, geologic unit, location in the stream's cross-section) the depths of the Type 1 regions were compared between various populations. This analysis includes all the JETs performed, except for those

assigned a poor field grade or deemed inadmissible based on a desktop review of the data. Tests that were performed for an insufficient duration to estimate erodibility parameters for the Type 2 region of the test were included here if there was a distinguishable transition from Type 1 to Type 2 erosion. This results in a total of 224 tests spanning both summer and spring data collection periods.
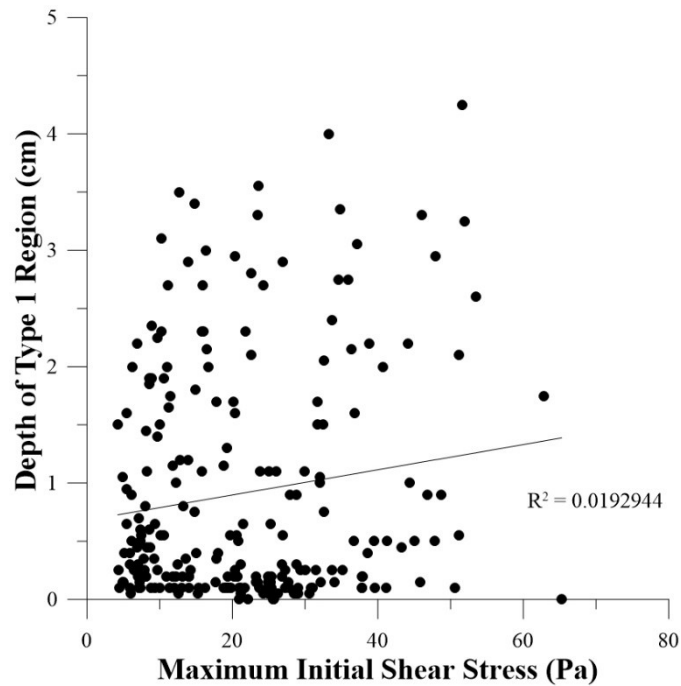
Figure 24: Relationship between maximum initial shear stress and depth of Type 1 region

To investigate the potential influence of the shear stresses applied at test initiation on determining the depths of the first segment (Type 1 Region), these two parameters were plotted against each other and are shown in *Figure 24*. Recognizing that higher applied shear stress exists at the beginning of a given test, rapid erosion in the early time steps of a test may result and subsequently the depth of the Type 1 Region may be overestimated when higher stresses are applied. *Figure 24* demonstrates that this is not true and there is a negligible relationship between the depth of the Type 1 region and initial applied shear stress ($R^2 = 0.019$). This indicates that the selection of an appropriate pressure head based on the operator's field assessment of the material properties (e.g., higher initial shear stresses applied to material assessed to be more resistant to erosion) does not unduly influence the depth of Type 1 material identified at a test location.

74

The absence of a relationship between initial shear stress and the depth of the Type 1 region (i.e., the depth of weathered material) indicates that other factors external to the initial applied shear stress dominate the determination of the depth of the first segment. It can still be argued that if a test was conducted at the same location at a higher pressure then a greater depth of Type 1 would be classified compared to a lower pressure setting. This is recognized as a limitation in the methodology and is best managed through operator experience in selecting reasonable pressure heads for the testing material

Figure 25 demonstrates the differences in the depth of the Type 1 region in submerged tests and subaerial tests, in Halton Till and the other geological units investigated, and in different test locations within the stream cross-section. It should be highlighted that the number of tests in each box and whisker depicted in the figure are not equal.

The subaerial mean is confirmed to be higher than the submerged mean at the confidence level $p=0.05$ through a t-test for samples of unequal variances. Levene Tests ($p=0.05$) confirm that the variance in depth of Type 1 in the subaerial tests is greater than in submerged tests. These results agree with the work of Wynn et al. (2008) on the impact of subaerial processes on resistance to erosion. Subaerial tests are likely exposed to more wetting-drying cycles than submerged tests, especially since the submerged tests in this investigation were collected at low flows during the summer data collection period and are likely submerged year-round. Some submerged tests that display relatively high depths of the Type 1 region which could be attributed to other weathering processes specific to submerged material (i.e. gravel saltation as per Pike et al., 2017), or could be an indication of a material's previous exposure to subaerial processes. Alluvial transport of non-cohesive particles on top of cohesive media is expected to be a notable weathering process in semi-alluvial streams in Southern Ontario contributing to the weakened surficial layer along submerged streambeds (Pike et al., 2017; Kamphuis, 1990). These findings also agree with qualitative observations made during the current investigation of sediment-starved or heavily armoured streams where alluvial transport is expected to be lower corresponding to sites with more resistant cohesive material along channel beds.

Comparison of Depth of Type 1 Region
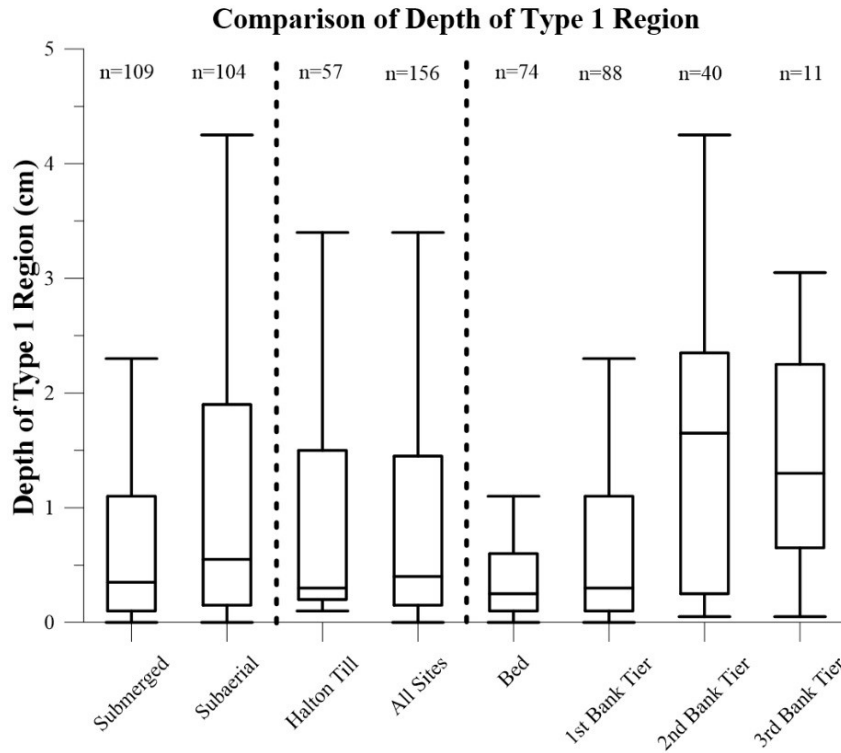
Figure 25: Comparison of depths of Type 1 between submerged and subaerial tests

Where the extents of the whiskers represent the maximum and minimum of the populations.

The division of tests by their location within a stream's cross-section (*Figure 25*) provides interesting results, with the caveat that the population of tests representing the 3rd bank tier has a relatively small population compared to the other cross-section locations. Visually, it is apparent that as one progresses up a bank, the depth of the Type 1 region increases. A Kruskal-Wallis Test (p=0.05) with follow-up pairwise Mann-Whitney tests reveal that the bed and 1st bank tier do not have significantly different medians, but they have significantly lower medians compared to the 2nd and 3rd bank tier. This may be interpreted as the tests higher up on banks are exposed to more impactful weathering processes (e.g. desiccation) compared to tests lower in a stream's cross-section. However, this could also be an indication that the locations higher up in a stream's cross section are less likely to have recently received flows capable of removing the surficial layer resulting in a longer cumulative time interval to accumulate a deeper layer of weathered material from persistent weathering processes.

6.5 Seasonal influences on JET results

During the spring data collection at GRL, some of the limitations of the JET methodology were more pronounced compared to the summer data collection field campaigns. Namely, in the spring the presence of a layer of weathered material was consistent and at certain locations exceeded the depth of the steel JET foundation ring. The weak and soft properties of the media at that particular time of year would not create a seal with the JET foundation ring which in turn would not ensure submergence of the jet nozzle. This introduced a bias in the test location selection process where some of the locations with more weathered material present would be avoided to ensure a successful test. Additionally, at GRL there are several overhanging banks where bank slumping and cantilever bank failure were observed. These locations were avoided due to the difficulties in determining whether these locations were representative of the typical gradient of weathering expected to be found on a streambank and the inability to deploy the jet apparatus at the required angles. Both criteria would bias the test locations to have less of a presence of weathered material than may be representative.

The depth of the Type 1 region for the tests collected in the summer of 2020 and the spring of 2021 at Gainsborough Ravine are presented in *Figure 26a*. The samples collected during the summer of 2020 have a smaller median and smaller variance in depths of the first region compared to the samples collected during the spring of 2021. This is confirmed for the median of the samples through the significant results of a Mann-Whitney test at the confidence level p=0.05 and through a Levene's test to confirm significantly different variances at the confidence level p=0.05. This agrees with observations made by Wolman (1959), Lawler (1986), Lawler (1997), Couper and Maddock (2001) and Wynn et al. (2008) of streambanks being more susceptible to erosion in the winter and early spring months and is largely attributed to increases in moisture content, frost action and freeze-thaw cycles resulting in the preparation of a layer of material for removal during subsequent rises in stage.

 When investigating the erodibility parameters of the second test segment (Type 2 region), the stark contrast between the populations as observed in the spring Type 1 region is no longer apparent. *Figure 26b* displays the results of the analysis by LR and SD solution techniques. Comparing the populations using Mann-Whitney tests, there were no significant differences in the populations of τ_{cSD}, τ_{cLR}, or K_{dSD} between early spring and summer tests. K_{dLR}, however, exhibits a higher value in the spring (median of $0.137 \frac{cm^3}{NS}$) compared to the summer (median of $0.040 \frac{cm^3}{NS}$) between the spring and summer populations.

These results preliminarily show that the influence of seasonality on a material's τ_c is constrained to a surficial layer, however, the influence of seasonality on the underlying material's K_d may slightly increase the underlying material's susceptibility to erosion once the critical shear stress is exceeded. This suggests that seasonal increases in erosion rates are governed by, and largely restricted to, the presence of a layer of weathered material more susceptible to detrition than the underlying material. This builds on the conclusion regarding seasonal variation in resistance to erosion made by Wynn et al. (2008) by separating the different responses of the surficial and underlying material rather than considering them a single sample population.
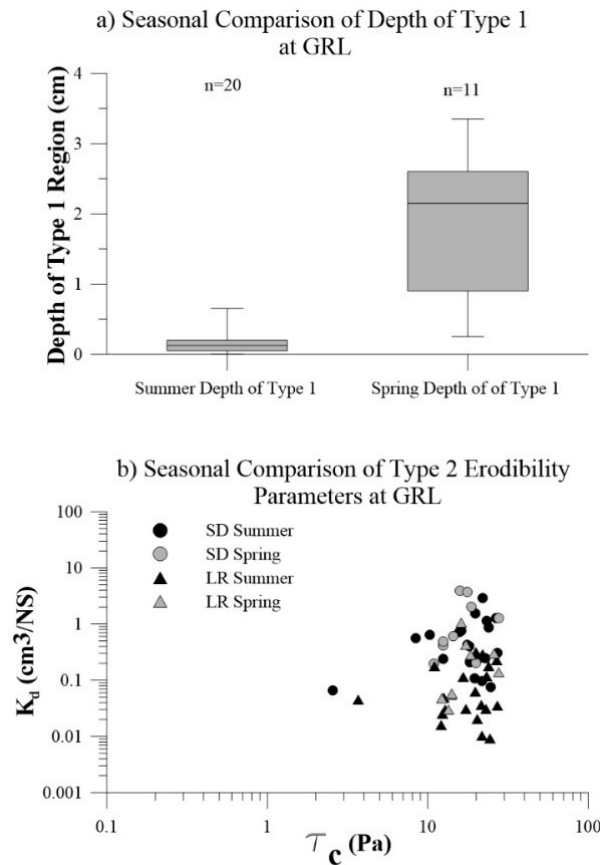
Figure 26: a) Comparison of depth of Type 1 between summer and spring tests from GRL and b) Type 2 erodibility parameters between summer and spring tests from GRL.

78

Chapter 7

Discussion

7.1 Application of mini-JET methodology

Over a three-year field campaign, the JET methodology was successfully employed at 13 watercourses spanning 10 different geologic units. Despite nuances that required field adaptation at several sites (as is common in most field programs) 242 JETs were conducted. After applying the QA/QC protocol, 208 tests spanning two seasons were available for detailed analysis. Several details were identified during the field-testing program which were important procedures methodologically to achieve successful tests which should be considered in future testing campaigns.

The most notable limitation of the mini-JET methodology observed was the bias that is incorporated in selecting a location to perform any given test. When selecting a test surface, areas that are more likely to prevent a successful test (surfaces with fractures, visible presence of stones, greater rooting density) were avoided. This inherent selection criteria tends to bias the selection of test surfaces towards more homogenous areas which are not as likely to erode due to reduced weathering of the media. This selection bias skews the results of any given test towards more resistant surfaces and away from locations more prone to erosion.

This bias was observed to be more prevalent in spring sampling versus summer sampling periods. At GRL it was observed that there was a consistent layer of weathered material which often exceeded the depth of the steel JET foundation ring. The weak and soft properties of this media could not create a seal with the JET foundation ring which in turn could not ensure submergence of the jet nozzle. It is important to note that this selection bias likely affects all test methodologies to some extent when evaluating in-situ conditions - in particular when specimens are extracted and transported to laboratories.

Overall, the JET proved to be an effective method for an individual to collect large quantities of site-specific data pertaining to erosion thresholds in cohesive material. It should be highlighted that to properly assess and apply the results of a JET investigation, they should be interpreted by people intimately familiar with the processes governing erosion in cohesive soils, the limitations of JET methodology, and those who have a high degree of familiarity with the site conditions from which data are collected.

7.2 Uncertainty of erodibility parameters derived from JETs.

The uncertainty of the JET solution techniques related to measurement frequency and test duration on the estimation of τ_c is minimal with and without segmentation. The minimal uncertainty in τ_c that does exist related to measurement frequency and test duration is superseded by the site scale variability in the parameter and does not influence how a site is characterized. Further, there is a high degree of similitude between τ_{cSD} and τ_{cLR} as demonstrated in *Figure 21* or *Figure 23* in Section 6.3: This is further highlighted in *Figure 27a*.
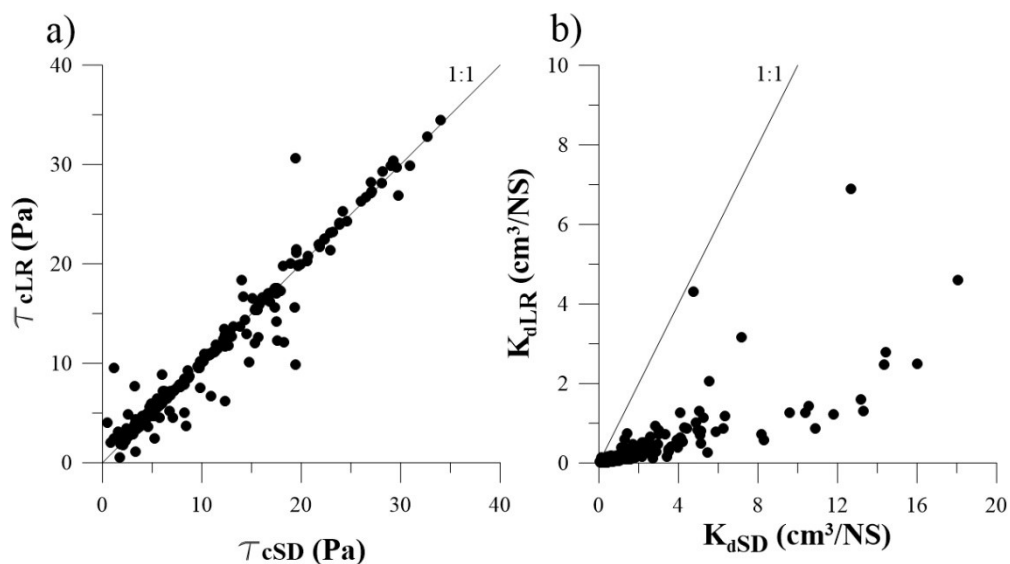
Figure 27: Comparison of SD and LR erodibility parameters

Having two separate and distinct JET solution techniques converge upon similar τ_c estimates lends a higher degree of confidence in their representativeness and reduces uncertainty related to the selection of an appropriate solution technique. It is worth noting that τ_{cSD} and τ_{cLR} are both consistently higher than τ_{cBM} which has previously been noted by Cossette (2016) to underpredict critical shear stresses.

Estimates of K_d, however, demonstrate greater uncertainty with respect to test duration, measurement frequency and the solution technique applied. For all solution techniques, JETs with shorter durations estimate higher K_d values and JETs with an increased early measurement frequency estimate higher K_d values. Test segmentation reduces the uncertainty related to measurement frequency such that the

characterization of a site is not impacted by changing the frequency of scour depth measurements during the JET.

While test segmentation reduces the uncertainty of K_d related to test duration based on the magnitude of change in the parameter, the uncertainty in K_d remains largely unchanged on a percentage change basis. Even with segmentation, the characterization of a site based on K_d can still be affected when JETs are shorter than 60 minutes in duration.

To reduce uncertainty in K_d estimates derived from JETs, it is recommended that measurement time schedules include a rapid measurement component at the beginning of tests to properly describe the rapid scour development. Tests should also be conducted for a minimum of 60 minutes (similar to a sampling regimen outlined in Table 5). Uncertainty of K_d related to the selection of solution technique remains high compared with no correlation between K_{dSD} and K_{dLR} (*Figure 27b*). Further tests are required to better assess which solution technique provides better estimates of K_d.

7.3 Type 2 Region erodibility parameters

The mean τ_c within the Halton Till population is found to be lower relative to the All Sites population, however, this requires contextualization. Despite the statistically significant difference in means, the actual difference ranges between $2.3 \leq \Delta\tau_C \leq 2.8$ Pa (depending on whether SD or LR is considered). This difference in the mean τ_c between Halton Till and the All Sites population is nominal relative to the range in τ_c values obtained at any given individual site (*Figure 28*). The wide range in τ_c at individual sites also reinforces the importance of considering the full range of erodibility parameters at a site rather than only the mean values. Especially since erosion will preferentially occur where macro-scale conditions are more conducive to erosion (lower τ_C and higher K_d).

The ranges in erodibility parameters for the geologic units investigated here are presented *in Table 26* and *Table 27*. In addition to the bias in the macro-scale spatial test locations of JETs at a given site, is important to note that these summarized values pertain to the Type 2 region and as a result do not incorporate the role of surficial weathered material in initiating erosion. For these reasons, the lower range in critical shear stress will likely tend closer to zero than what is reflected in the summarized values. It is recommended that when characterizing erosion of cohesive stream boundaries it is approached from the vantage point of *how much erosion will occur* rather than *will erosion occur*.
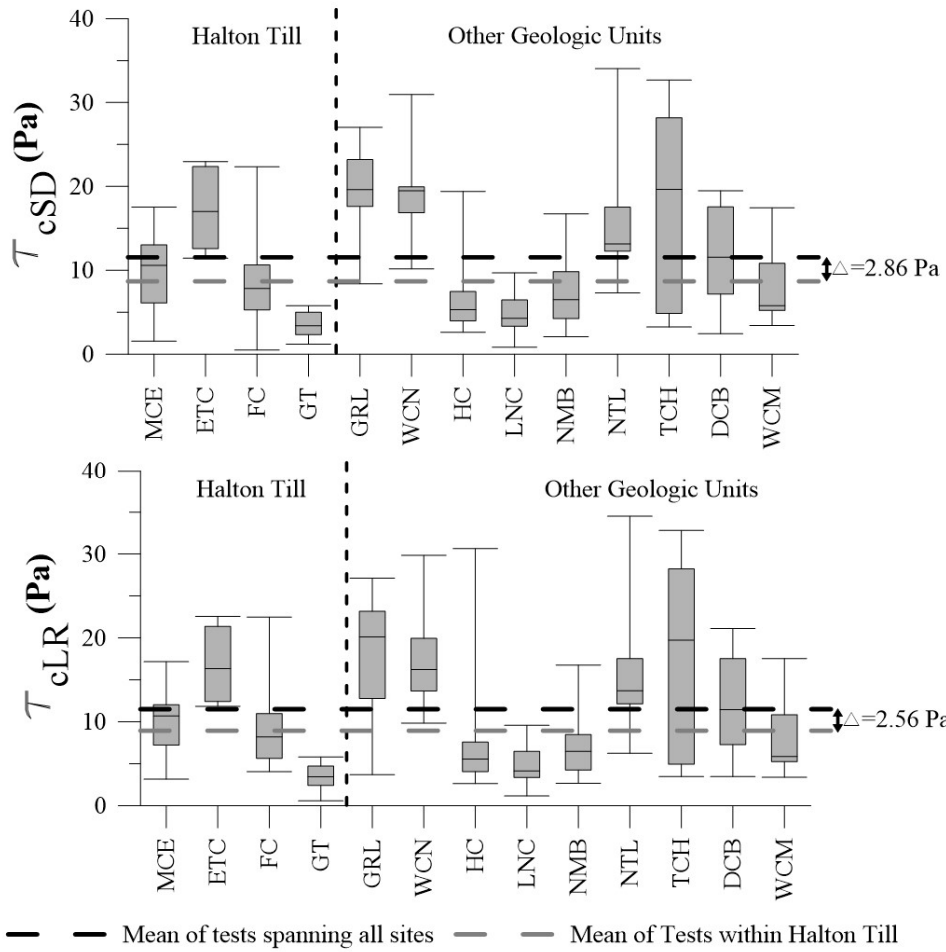
Figure 28: Comparing differences in mean of critical shear stress between Halton Till and All Sites to ranges at individual sites.

Table 26: Critical shear stress ranges for geologic units

	τ_{cLR} (Pa) min*<mean<max	τ_{cSD} (Pa) min*<mean<max	τ_{cBM} (Pa) min*<mean<max
Halton Till (n=56)	0.56<8.95<22.56	0.48<8.67<22.9	0.21<4.34<17.71
Schomberg Clay (n=9)	9.84<18.16<29.84	10.16<19.77<30.95	3.20<12.81<27.34
Dorchester Till (n=20)	3.68<18.60<27.11	8.39<19.32<27.05	0.01<11.61<21.66
Stirton Till (n=16)	2.66<6.77<16.75	2.08<7.29<16.72	0.47<3.87<11.08
Leaside Till (n=19)	2.62<8.20<30.63	2.60<7.52<19.40	0.74<5.26<18.22
Mornington Till (n=21)	6.23<15.74<34.50	7.29<15.99<34.04	1.89<9.76<24.07
Tavistock Till (n=20)	3.47<18.20<32.81	3.23<17.97<32.67	0.43<10.73<25.52
Maryhill Till (n=18)	1.14<4.67<9.57	0.82<4.66<9.68	0.05<2.54<8.47
Wartburg Till (n=9)	3.37<8.38<17.53	3.40<8.34<17.45	0.79<7.13<14.46
Haldimand Clay (n=11)	3.45<12.42<21.11	2.42<12.04<19.48	0.32<7.24<13.16

*The minimum τ_c values summarized in this table are overestimates based on bias within JET location selection and the exclusion of the Type 1 region in the JET analysis.

While the mean K_d of the tests spanning All Sites versus the ones constrained to Halton Till were not found to be dissimilar, this may be related to the relatively heterogeneous material (Halton Till) that was used to assess intra-unit characteristics in this investigation. Compared to lacustrine deposited materials observed at other sites, it is reasonable to expect tills to have higher levels of heterogeneity in grain size distribution, clay content and sorting processes potentially resulting in greater intra-geologic unit variability of the erodibility parameter. The estimated K_d values are summarized by geologic unit in *Table 27* to facilitate comparison and discussion with future research projects, however, due to the uncertainty remaining in the accuracy of the parameters estimated from JETs (e.g., *Figure 27b*) the values should be employed with caution in practice.

Table 27: Erodibility coefficient ranges for geologic units

	K_{dLR} (cm^3/NS) min*<mean<max	K_{dSD} (cm^3/NS) min*<mean<max	K_{dBM} (cm^3/NS) min*<mean<max
Halton Till (n=56)	0.02<0.33<4.30	0.14<1.78<10.88	0.07<0.49<2.92
Schomberg Clay (n=9)	0.01<0.13<0.40	0.24<0.95<1.59	0.06<0.15<0.31
Dorchester Till (n=20)	0.01<0.09<0.31	0.08<0.65<2.89	0.02<0.13<0.34
Stirton Till (n=16)	0.025<0.66<4.60	0.25<3.47<18.06	0.06<0.55<1.51
Leaside Till (n=19)	0.02<0.59<2.48	0.054<3.68<14.35	0.05<0.61<1.39
Mornington Till (n=21)	0.017<0.15<0.89	0.28<1.07<4.31	0.05<0.18<0.37
Tavistock Till (n=20)	0.013<0.23<1.60	0.16<1.79<13.15	0.05<0.35<1.58
Maryhill Till (n=18)	0.08<0.75<2.49	0.93<5.24<16.01	0.26<0.97<2.75
Wartburg Till (n=9)	0.13<1.65<6.90	0.83<5.71<12.67	0.08<0.78<1.70
Haldimand Clay (n=11)	0.03<0.26<0.83	0.25<1.44<3.34	0.10<0.36<0.86

*The minimum K_d values summarized in this table are overestimates based on bias within JET location selection and the exclusion of the Type 1 region in the JET analysis.

Concerning cross-sectional variation in erodibility parameters, the results of this investigation indicate that the second bank tier is the location within the stream's cross-section which demonstrates the highest τ_c. While this is a different location within the stream's cross-section than what Sutarto et al. (2015) found to have the highest critical shear stress, it does suggest that how erodibility parameters vary within a stream's cross-section is likely site-specific and can change based on geologic, hydrologic properties and climatologic (weathering processes) properties of the site. This reinforces the importance of site-specific data pertaining to erosion thresholds of cohesive sediment. Further, it is important to highlight that bank erosion does not occur solely as a function of the resistance to erosion of the bank material. There are also variations in the hydraulic shear, level of vegetation and level of weathering throughout a stream cross-section that will also contribute to the overall bank behaviour under erosive events.

7.4 Test segmentation and depth of Type 1 region

Removal of thin surface layers at stresses below the critical shear stresses thresholds of underlying media have previously been reported (Kamphuis, 1990; Lefebvre, 1985) with the importance of this observation identifying "*the critical tractive force does not appear sufficient to describe the erodibility of natural intact clay. The rate of erosion, prior to critical condition, has to be considered*" (Lefebvre, 1985). Lawler (1986), Couper and Maddock (2001), Gaskin et al. (2003) and Davidson-Arnott and Langham (2000) expanded upon this edict to relate the erosion prior to critical condition to weathering processes reducing the material's resistance to erosion.

Given the importance of this surficial layer in potentially governing the rates of erosion in cohesive materials, characterization of the surficial zone can be of obvious importance in executing JET tests and developing datasets. However, the progression of JETs from high to low applied shear stresses coupled with the soil profiles which commonly contain the weakest (and most erosion-prone) media at the surface, limits the amount of useful information that is attainable pertaining to this layer. This is an important advantage in applying the segmentation offered in the current research on JET data sets. The segmentation technique applied to JET data sets is simple, intuitive and offers an improvement upon the assumption of homogeneity within the soil profile and an alternative method of analyzing JET data which incorporates media heterogeneity. It is noteworthy that Mahalder et al. (2018) offered a solution technique (MPS) to evaluate weathering, however, this technique results in depth-averaged erodibility parameters that are not necessarily representative of either the surficial layer or the underlying material. Further MPS is not considered feasible to employ in materials with variable grain sizes where obstructions are likely to be encountered in the larger scour holes associated with the method. Test segmentation also offers some reduction in erodibility parameter uncertainty with respect to test duration and measurement frequency, however, some uncertainty with respect to test duration persists. These improvements offered by test segmentation offer an alternative to overcoming gradients in material properties (Khan, 2007; Mahalder et al.,2018; Gaskin et al., 2003; Couper and Maddock, 2001) throughout a JET scour hole.

7.5 Seasonal influence in erosion of cohesive material

Similar to the results of Wynn et al. (2008), there is a significant change in material properties governing resistance to erosion of cohesive media in the spring data collection period compared to the summer.

However, the results obtained in this research indicate that the differences are largely constrained to the surficial layer consisting of weathered material and the seasonal differences in material properties generally do not propagate below this layer. The occurrence of this surficial weakened, weathered layer in the springtime corresponds to elevated flows during the spring-time freshet which subsequently impose higher shear stresses upon the bank material and increases the likelihood of material being entrained (Wynn et al., 2008; Lawler, 1985; Couper and Maddock, 2001). Depending on the weathering processes producing the weaker upper layer and the hydrologic regime of the stream, several cycles of material weathering and detrition (i.e., complete cycles of Stage 1 to Stage 4 in *Figure 29)* may occur in an individual season. This can then lead to mass failures along over-steepened banks completing the cycle of preparation, fluvial erosion and mass erosion in stream systems composed of cohesive material suggested by Maddock and Couper (2001), Sutarto et al. (2014), Rinaldi and Darby (2008) and Pizzuto (2009).
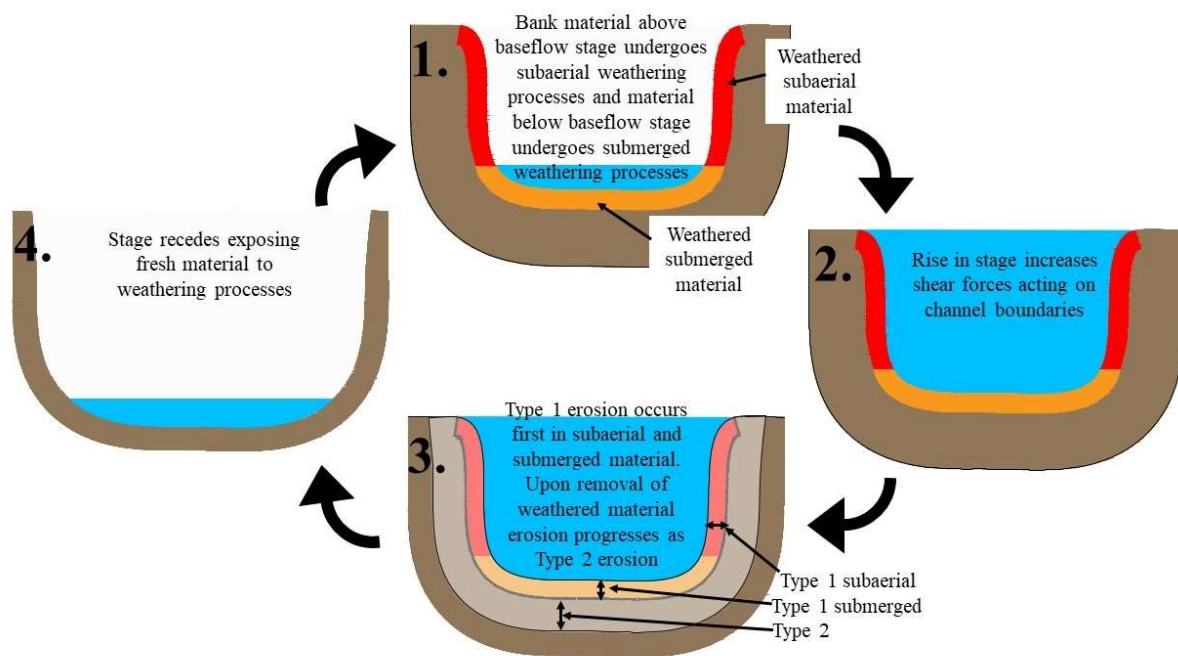
Figure 29: **Cycle and stages of weathering governing erosion rates**

This also indicates that the erodibility parameters of the Type 2 Region or underlying material are not necessarily the properties that control the progression of erosion at a particular site. As demonstrated in Stage 3 of *Figure 29*, the erodibility parameters will control erosion rates once the Type 1 region has been

removed, however, a non-trivial component of erosion within the system is how frequently and how quickly the Type 1 Region is replenished (moving from Stage 4 to Stage 1).

7.6 Frequency of weathering and detrition cycle of cohesive media

While the weathering processes acting upon the surface of cohesive materials are largely climatologically driven, watershed characteristics will govern the frequency at which the cycle within *Figure 29* is completed. In scenarios in which the cycle is completed more frequently, the weathering and detrition cycle will play a larger role in bank erosion.

Smaller watersheds have shorter hydrographs compared to larger watersheds which result in a quicker cycle of rising and falling stages and a more frequent re-exposure of subaerial bank material than in a larger watershed. As demonstrated in *Figure 30,* the urbanization of a smaller watershed (lacking any stormwater management controls in place) exacerbates the shorter hydrograph cycles and reoccurrence of subaerial weathering processes. Conversely, in larger watersheds with longer duration hydrographs, there is more natural attenuation of flows as flood waves diffuse moving through the stream network. This results in a lower likelihood of individual hydrographs completing full cycles of stage rises and declines, in particular during the freshet period corresponding to the maximum weathering processes. This reduced frequency of the weathering and detrition cycle elicits diminished importance of the weathering-detrition cycle and higher importance on the Type 2 erodibility parameters.

In the case of GRL, the catchment is a small (~2 km^2) highly urbanized watershed with no stormwater management facilities to attenuate flows. These characteristics have exacerbated the frequency of the cycle in *Figure 29,* particularly in the early spring season when near diurnal increases in stage from snowmelt runoff are at a peak. This hydromodication can alter the frequency and magnitudes of the driving forces responsible for erosion at the time of year when the resisting forces are the weakest. The small size and high level of urbanization within GRL represent a maximum of the importance that the weathering and detrition cycle may play on the erosion rates of a system.
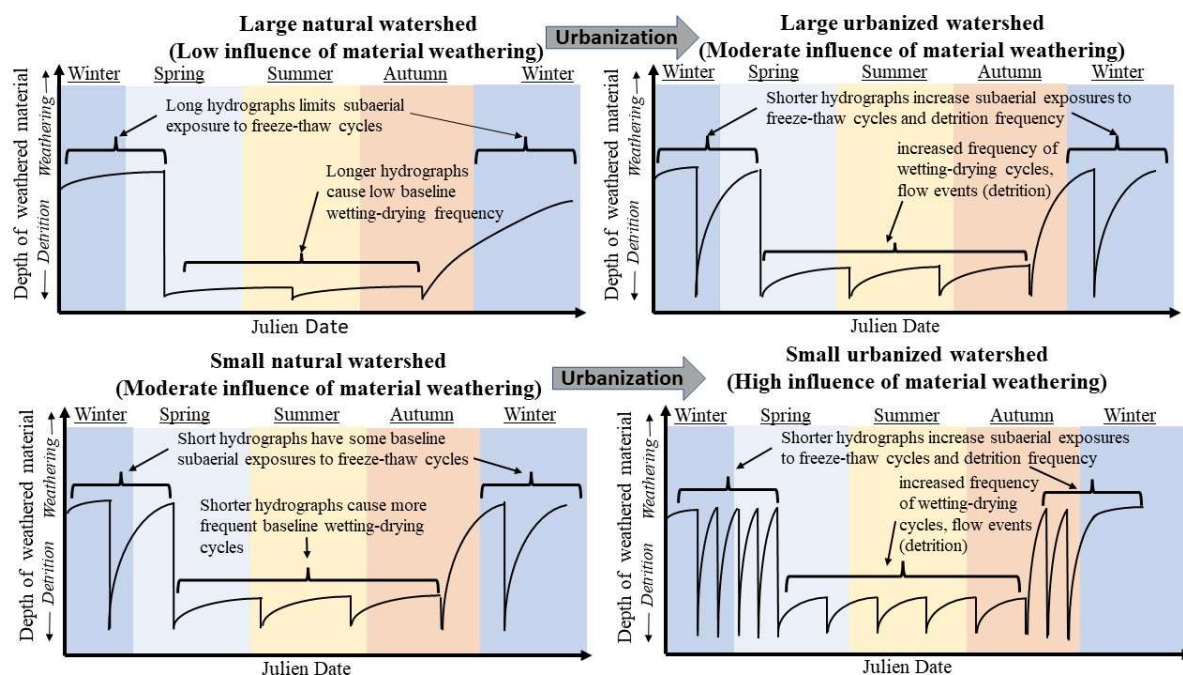
Figure 30: Influence of watershed size on the importance of weathering processes.

Further, in watersheds where traditional stormwater management techniques are applied, the objective is to attenuate the elevated runoff from urbanized watersheds, however, they do not eliminate the excess runoff. Rain events that occurred pre-hydromodifcation which would not have exceeded depressional storage or infiltration capacity and in turn would not result in an associated increase in streamflows are now redirected to a storage basin and emitted as streamflows in the post-hydromodification scenario. This results in an increase in stage and completion of the weathering-detrition cycle in the post-hydromodifcation scenario where none existed in the pre-hydromodifcation scenario. To contextualize this, Annable et al. (2011) observed bankfull flows to occur as often as 18 times a year in urban streams. A similar increase in frequency in flows below bankfull would further amplify the weathering-detrition cycle acting on the lower bank tiers, and may also act to increase material weathering through changes to the wetting and drying cycle. Once these disturbances occur in the weathering cycle, they will propagate through time with the development of feedback loops (e.g., steeper and taller banks creating more surface area for subaerial processes to act upon, wider channels and lower baseflows resulting in lower water levels and more subaerial exposures) as the river system adapts to its new systemic parameters and attempts to establish a new quasi-equilibrium.

Chapter 8

Conclusions

242 mini-JETs were performed spanning 13 study sites and 10 distinct geologic units in Southern Ontario to characterize differences in resistance to fluvial erosion between geologic units. While some limitations may arise when materials are excessively stony, laminated, or friable it was concluded that the mini-JET methodology can adequately collect representative data to inform the erodibility parameters of the excess shear stress model. To overcome potential limitations of JET methodology related to material heterogeneity along the depth profile of the JET scour holes, each test was divided into two segments: one representing the surficial weathered layer (Type 1) and one representing the underlying unweathered material (Type 2). Further, an uncertainty analysis was completed to ascertain how test duration and frequency of measurements during the JET affect the erodibility parameters estimated from Blaisdell, Scour Depth and Linear Regression solution techniques.

Based on the results of this investigation, the following is concluded:

- Running mini-JETS for shorter durations increases the critical shear stress and erodibility parameters estimated from the mini-JET regardless of which solution technique is used, however, this does not change how a site is characterized unless a test is run for durations shorter than 60 minutes. The erodibility parameters estimated using the Linear Regression Method are the least sensitive to changing test durations of the solution techniques considered,

- A higher frequency of scour depth measurements early in tests increases the erodibility coefficient that is estimated from all solution techniques, however, the measurement frequency later in tests has a negligible influence on the erodibility parameters estimated with test segmentation. The Linear Regression solution technique produces the erodibility parameters that are the most sensitive to the frequency of measurements, however, this generally has no impact on material characterization on a site scale if the JET is segmented during analysis,

- Incorporating test segmentation into JET analysis allows for the consideration of material weathering through the surrogate attribute of the depth of the Type 1 region and the results in the Type 2 region more closely align with the assumption of material homogeneity inherent in JET analysis. Segmenting JET data should be considered as an alternative method of JET analysis in future investigations due to the more realistic representation of material heterogeneity and the

ability to obtain important information pertinent to the surficial layer ultimately governing fluvial erosion,

- Using the depth of the Type 1 region as a surrogate for the presence of weathered material, it was demonstrated that subaerial tests have a higher mean and higher variance in the depth of weathered material. Further, there is a greater presence of weathered material in the upper two-thirds of streambanks compared to the bottom third of streambanks or streambeds. The tests performed during the summer months conclude there are no differences in the presence of weathered material between geologic units indicating that material weathering is the result of site-specific processes and is not governed by which geologic unit the weathering processes act upon,

- Halton Till has a lower mean critical shear stress, but similar erodibility coefficient compared to the suite of other geologic units investigated. This agrees with previous research, which indicates that the geologic unit composing a stream boundary can alter how erosion will manifest. However, the relatively small difference (2.8Pa) in mean critical shear stress arising from the difference in geology is too small to leverage for engineering purposes when considered in conjunction with the range of values at individual sites (maximum observed range of 29.4 Pa) and the seasonal variability in the weathered surficial layer,

- Different locations within a stream's cross-section display different properties of resistance to erosion, however, they are likely site-specific and based on the geologic, hydrologic and climatologic properties of the site. This is an important factor to consider when modelling how erosion will progress suggesting that different regions should be considered unique and provided distinct parameters and that these parameters should be informed by site-specific tests,

- Results from this investigation indicate that an enhanced layer of weathered material exists on the surface of cohesive material in the early spring which is more susceptible to detrition. This aligns with observations made by others regarding temporal changes to erosion resistance in cohesive materials in other geographic regions. Critically, this investigation indicates that the weaker material readily available for detrition is constrained to a surficial layer whereas the underlying material has not been significantly altered by the weathering processes and maintains similar erodibility parameters in the spring as it does in the summer,

- The importance of the weathering-detrition cycle of surficial material along cohesive stream boundaries is likely related to watershed characteristics such as size and land use.

While this investigation indicated a difference in mean critical shear stress between geologic units the magnitude of the difference compared to site-scale variability will limit the applicability of this finding. Further, the importance of seasonal variations in surficial material characteristics indicates that in some instances a more pertinent consideration is how material properties change in relation to different weathering processes rather than their characterization by a single pair of mean erodibility parameters. This suggests that simply describing a cohesive material by a threshold characteristic (as is typical in watershed management in Ontario) will underestimate the erosion that will occur in the system due to the neglect of weathering. This underestimation will be more profound in smaller sub-watersheds where the weathering of material is expected to play a larger role in governing the erosion of cohesive materials than the erodibility parameters of the underlying material. Due to temporal fluctuations in the prominence of the surficial weathered material it is highlighted that the resistance to erosion of cohesive material should be characterized during the season and conditions (including antecedent factors) at which it would be expected to undergo detrition. In the context of convective storm-dominated systems of Southern Ontario combined with seasonal freshet events, the weathering processes prevalent in early spring coupled with elevated flows resulting from a melting snowpack indicate that a cohesive material's resistance to erosion should be characterized during the seasonal interception of these factors.

Chapter 9

Recommendations for Future Research

It is recommended that future research investigate the linkage between watershed hydrology (size, land use and hydrograph characteristics) and the importance of weathering processes on erosion rates in cohesive river systems. It would be beneficial to extend this investigation to a comparison of how current and potential future industry standard stormwater management techniques alter the weathering-detrition cycle of cohesive material in early spring months. This may have specific implications on the recommendation of stormwater management techniques applied in watersheds with cohesive stream boundaries and on the prioritization of the retrofitting of historically urbanized watersheds with stormwater management controls to reduce the impacts of systemic degradation.

References

Al-Madhhachi, AT, GJ Hanson, GA Fox, AK Tyagi, R Bulut, 2013a. *Measuring soil erodibility using a laboratory "mini" JET*, Trans. ASABE, Vol. 56(3), pp. 901–910.

Al-Madhhachi, AT, GJ Hanson, GA Fox, AK Tyagi, R Bulut, 2013b, *Deriving parameters of a fundamental detachment model for cohesive soils from flume and jet erosion tests*. Trans. ASABE, Vol. 56(2), pp. 489–504.

Annable, WK, VG Lounder, CC Watson, 2011, *Estimating Channel-Forming Discharge in Urban Watercourses,* River Research and Applications, Vol 27, pp. 738-753. DOI: 10.1002/rra.1391

Amin, MR, K Mazurek, 2016, *Assessment of Equilibrium Scour by a Submerged Circular Turbulent Impinging Jet in Cohesive Soils,* In B. Crookston & B. Tullis (Eds.), Hydraulic Structures and Water System Management. 6th IAHR International Symposium on Hydraulic Structures, Portland, Oregon, 27-30 June (pp. 467-476). doi:10.15142/T3350628160853 (ISBN 978-1-884575-75-4).

Amos, CL, GR Daborn, HA Christian, A Atkinson, A Robertson, 1992, *In situ erosion measurements on fine-grained sediments from the Bay of Fundy,* Marine Geology, Vol. 108 (2), pp. 175-196.

Arulanandan, K, A Sargunam, P Loganathan, RB Krone, 1973, *Application of Chemical and Electrical Parameters to Prediction of Erodibility,* Highway Research Board Special Report

Arulanandan, K, *Fundamental Aspects of Erosion of Cohesive Soils,* Journal of the Hydraulics Division, Vol. 101(5). DOI: https://doi.org/10.1061/JYCEAJ.0004366

Arulanandan, K, E Gillogley, R Tully, 1980, *Development of a quantitative method to predict critical shear stress and rate of erosion of natural undisturbed cohesive soils*, USACE, Waterways Experiment Station Technical Report, GL-80-5, Vicksburg, MS.

ASCE Task Committee on Hydraulics, Bank Mechanics, and Modeling Of River Width Adjustment, 1998, *River Width Adjustment. I: Processes and Mechanisms¸* Journal of Hydraulic Engineering, Vol. 124(9), pp. 881-902. DOI: 10.1061/(ASCE)0733-9429(1998)124:9(881)

Ashmore, P, M Church, 2001, *Bulletin 555: The Impact of Climate Change on Rivers and River Processes in Canada*, Geological Survey of Canada.

Christensen, RW, BM Das, 1973, *Hydraulic Erosion of Remolded Cohesive Soils,* Highway Research Board Special Report.

Barnett, PJ, JEP Dodge, MK McCrae, A Stuart, 1999. *Quaternary geology, Newmarket area, Ontario*, Ontario Geological Survey, Map 2562, scale 1:50 000.

Beltaos, S, N, Rajaratnam, 1974, *Impinging Circular Turbulent Jets*, Journal of the Hvdraulics Division, ASCE, Vol. 100**(**HY10), pp. 1313-1328.

Bergman. N, MJ Van De Wiel, SR Hicock, 2022, *Sedimentary characteristics and morphologic change of till-bedded semi-alluvial streams: Medway Creek, Southern Ontario, Canada*, Geomorphology, Vol. 399. DOI: https://doi.org/10.1016/j.geomorph.2021.108061

Berlamont, J, M Ockenden, E Toorman, J Winterwerp, 1993, *The characterisation of cohesive sediment properties,* Coastal Engineering, Vol. 21 (1-3), pp.105-128. DOI: 10.1016/0378-3839(93)90047-C.

Black, KS, TJ Tolhurst, DM Paterson, SE Hagerthey, 2002, *Working with natural cohesive sediments*, Journal of Hydraulic Engineering, ASCE, Vol. 128 (1), pp. 2-8.

Black, W, JGV De Jongh, JTG Overbeek, MJ Sparnaay, 1960, *Measurements of retarded Van Der Waals' forces*, Transactions of the Faraday Society, Vol. 56, pp. 1597-1608. DOI: https://doi.org/10.1039/TF9605601597

Blaisdell, FW, GG, Hebaus, CL Anderson, 1981, *Ultimate dimensions of local scour,* Journal of the Hvdraulics Division, ASCE, Vol. 107 (HY3), pp. 327–337.

Bonelli, S, D Marot, F Ternat, N Benahmed, 2007, *Criteria of erosion for cohesive soils. Assessment of the risk of internal erosion of water retaining structures: dams, dykes and levees,* Symposium of the European Working Group of ICOLD, Friesing, Germany, pp.45-59.

Briaud, JL, FCK Ting, HC Chen, R Gudavalli, S Perugu, G Wei, 1999, *SRICOS: Prediction of Scour Rate in Cohesive Soils at Bridge Piers*, Journal of Geotechnical and Geoenvironmental Engineering, Vol. 125 (4), pp. 237-246. DOI: 10.1061/(ASCE)1090-0241(1999)125:4(237)

Briaud, JL, FCK Ting, HC Chen, Y Cao, SW Han, KW Kwak, 2001, *Erosion Function Apparatus for Scour Rate Predictions,* Journal of Geotechnical and Geoenvironmental Engineering, Vol. 127(2), pp. 105-113. DOI: 10.1061/(ASCE)1090-0241(2001)127:2(105)

Buffington, JM, DR Montgomery, 1997, *A systemic analysis of eight decades of incipient motion studies with special reference to gravel-bedded rivers,* Water Resources Research, Vol. 33 (8), pp. 1993-2029. DOI: https://doi.org/10.1029/96WR03190

Charonko CM, 2010, *Evaluation of an in situ measurement technique for streambank critical shear stress and soil erodibility*, Thesis in fulfillment of the requirements of a Masters of Science, Virginia Tech University, Blacksburg, VA.

Chaphuis, RP, T Gatien, 1985, *An improved rotating cylinder technique for quantitative measurements of the scour resistance of clays*, Canadian Geotechnical Journal, Vol. 23 (1), pp. 83-87. DOI: https://doi.org/10.1139/t86-01

Chin, A, AP O'Dowd, KJ Gregory, 2013, *Chapter 9.39 - Urbanization and River Channels,* In Treatise on Geomorphology, John F Shroder, Elsevier Academic Press, pp. 809-827. DOI: 10.1016/B978-0-12-374739-6.00266-9

Christensen, RW, BM Das, 1973, *Hydraulic Erosion of Remolded Cohesive Soils,* Highway Research Board Special Report.

Clark, LA, T Wynn, 2007, *Methods for determining streambank critical shear stress and soil erodibility: Implications for erosion rate predictions*, Trans. ASABE, Vol. 50(1), pp. 95–106.

Cossette, D, KA Mazurek, CD Rennie, 2012,. *Critical shear stress from varied method of analysis of a submerged circular turbulent impinging jet test for determining erosion resistance of cohesive soils*, In Proceedings of the. 6th International Conference on Scour and Erosion, August 27-August 31, 2012.

Cossette, D, 2016, *Erodibility and Scour by a vertical submerged circular turbulent impinging jet in cohesive soils,* Thesis in fulfillment of the requirements of a Masters of Science in Civil and Geological Engineering, University of Saskatchewan, Saskatoon, Saskatchewan

Cowan, W.R, 1972, *Pleistocene geology of the Brantford Area, southern Ontario,* Ontario Dept. Mines and Northern Affairs, IMR 37, 66p. Accompanied by Maps 2240 and 2241, scale 1 inch to 1 mile.

Cowan, WR, 1976, *Quaternary Geology of the Orangeville Area, Southern Ontario,* Ontario Div. of Mines, GR141, 98p. Accompanied by Maps 2326, 2327 and 2328, scale 1:50,000.

Crowley, RW, C Robeck, RJ Thieke, 2014, *Computational Modeling of Bed Material Shear Stresses in Piston-Type Erosion Rate Testing Devices,* Journal of Hydraulic Engineering, Vol. 140 (1), pp. 24-34. DOI: 10.1061/(ASCE)HY.1943-7900.0000797

Couper, PR, IP Maddock, *Subaerial River Bank Erosion Processes and Their Interaction With Other Bank Erosion Mechanisms on The River Arrow, Warwickshire, UK*, Earth Surface Processes and Landforms, Vol. 26, pp. 631-656. DOI: https://doi.org/10.1002/esp.212

Daly, ER., GA Fox, AT Al-Madhhachi, RB Miller, 2013, *A scour depth approach for deriving erodibility parameters from jet erosion tests*, Trans. ASABE, Vol. 56(6), pp. 1343–1351.

Daly, ER, GA Fox, HK Enlow, DE Storm, SL Hunt, 2015a, *Site-scale Variability of Streambank Fluvial Erodibility Parameters as Measured with a Jet Erosion Test,* Journal of Hydrol. Process., Vol. 29, pp. 5451–5464, doi:10.1002/hyp.10547.

Daly, ER, GA Fox, A-ST Al-Madhhachi, DE Storm, 2015b, *Variability of fluvial erodibility parameters for streambanks on a watershed scale*, Geomorphology, Vol. 231, pp. 281-291, doi: 10.1016/j.geomorph.2014.12.016.

Darby, SE, CR Thorne, 1996, *Development and Testing of Riverbank-Stability Analysis*, Journal of Hydraulic Engineering, Vol. 122(8), pp. 443-454. DOI: 10.1061/(ASCE)0733-9429(1996)122:8(443)

Davidson-Arnott, RGD, 1986, *Rates of Erosion of Till in the Nearshore Zone,* Earth Surface Processes and Landforms, Vol. 11, pp. 53-58.

Davidson-Arnott, RGD, DRJ Langham, 2000, *The effects of softening on nearshore erosion of a cohesive shoreline*, International Journal of Marine Geology, Vol 166, pp. 145-162.

Davis, JC, 1986, *Statistics and Data Analysis in Geology Second Edition,* Toronto, John Wiley & Sons.

Debnath, K, S Chaudhuri, 2010, *Cohesive Sediment Erosion Threshold: A Review,* ISH Journal of Hyraulic Engineering, Vol. 16 (1), pp. 36-56. DOI: 10.1080/09715010.2010.10514987

Dreimanis, A, Schluchter, C, 1985, *Field Criteria for the Recognition of Till or Tillite,* Paleogeography, Paleoclimatology, Paleoecology, Vol. 51(1-4), pp.7-14.

Dunn, SI, 1959, *Tractive Resistance of Cohesive Channels*, Journal of the Soil Mechanics and Foundations Division, Vol. 85 (3), pp.287-310. DOI: https://doi.org/10.1061/JSFEAQ.0000195

Dutta, S, T Karmakar, 2015, *Erosion Processes in Composite Riverbanks: Experiments and Modelling,* International Journal of Research in Engineering and Technology, Vol 4 (11), pp. 85-92.

Gaskin, SJ, J Pieterse, A Al Shafie, S Lepage, 2003, *Erosion of undisturbed clay samples from the banks of the St Lawrence River*, Canadian Journal of Civil Engineering, Vol. 30, pp.583-595. DOI: 10.1139/l03-008

Gerbersdorf, SU, T Jancke, B Westrick, 2007, *Sediment Properties for Assessing the Erosion Risk of Contaminated Riverine Sites: a comprehensive approach to evaluate sediment properties and their covariance patterns over depth in relation to erosion resistance – First investigations in natural sediments at three contaminated reservoirs,* Journal of soils and sediments, Vol. 7, pp. 25-35. DOI: 10.1065/jss2006.11.190

Ghaneeizad, SM, JF Atkinson, SJ Bennett, 2015, *Effect of flow confinement on the hydrodynamics of circular impinging jets: implications for erosion assessment*. Environ. Fluid Mech., Vol. 15, pp. 1–25.

Gill, D, 1970, *Application of a statistical zonation method to reservoir evaluation and digitized-log analysis*, Bulletin of the American Association of Petroleum Geologists, 54(5), pp. 719-729.

Grabowski, RC, IG Droppo, G Wharton, 2011, *Erodibility of cohesive sediment: the importance of sediment properties*, Earth Science Reviews Vol. 105 (3-4), pp. 101-120.

Grissinger, EH, 1966, *Resistance of Selected Clay Systems to Erosion by Water*, Water Resources Research, Vol. 2 (1), pp. 131-138. DOI: 10.1029/WR002i001p00131

Gularte, RC, WE Kelly, VA Nacci, 1980, *Erosion of Cohesive Sediments as a Rate Process*, Ocean Engineering, Vol. 7 (4), pp. 539-551. DOI: 10.1016/0029-8018(80)90051-7

Haddadchi, A, CW Rose, JM Olley, AP Brooks, J McMahon, T Pietsch, 2017, *An alternative method for interpreting JET erosion test (JET) data: Part 2. Application*, Earth Surface Processes and Landforms, Vol. 43, pp. 743-754. DOI: 10.1002/esp.4270

Hanson, GJ, KM Robinson, DM Temple, 1990, *Pressure and Stress Distributions Due to a Submerged Impinging Jet,* In Proceedings of Hydraulic Engineering National Conference, San Diegom California, USA, July 30-August 3, 1990

Hanson, GJ, 1992, *Erosion Resistance of Compacted Soils,* Transportation Research Record, Vol. 1369, pp.26-30.

Hanson, GJ, KM Robinson, 1993, *The Influence of Soil Moisture and Compaction on Spillway Erosion,* Transactions of the American Society of Agricultural Engineering, Vol. 36 (5) pp. 1349-1352. DOI: 10.13031/2013.28469

Hanson, GJ, KR Cook, 1997, *Development of Excess Shear Stress Parameters For Circular Jet Testing,* In Proceedings of ASAE Annual Meeting, Minneapolis, Minnesota, August 10-August 14, 1997.

Hanson, GJ, A Simon, 2001, *Erodibility of cohesive streambeds in the loess area of the midwestern USA*, Hydrol. Process., vol. 15, pp. 23–38.

Hanson, GJ, KR Cook, 2004, *Apparatus, Test Procedures and Analytical Methods to Measure Soil Erodibility In-Situ,* Applied Engineering in Agriculture, Vol. 20 (4), pp. 455-462. DOI: 10.13031/2013.16492

Hanson, GJ, SL Hunt, 2007, *Lessons Learned Using Laboratory JET Method to Measure Soil Erodibility of Compacted Soils*, Applied Engineering in Agriculture, Vol. 23 (3), pp. 305-312. DOI: 10.13031/2013.22686

Harrison, SS, 1970, *Note on the Importance of Frost Weathering in the Disintegration and Erosion of Till in East-Central Wisconsin.* GSA Bulletin 81(11), pp. 3407-3409. DOI: https://doi.org/10.1130/0016-7606(1970)81(3407:NOTIOF)2.0.CO;2

Heinzen, RT, K Arulanandan, 1977, *Factors Influencing Dispersive Clays and Methods of Identification*, Dispersive Clays, Related Piping, and Erosion in Geotechnical Projects, ASTM STP 623, JL Sherard and RS Decker, Eds., American Society for Testing and Materials, pp. 202-217.

Hollick, M, 1976, *Towards a Routine Test for the Assessment of the Critical Tractive Forces of Cohesive Soils,* Transactions of the American Society of Agricultural Engineers, Vol. 19 (6), pp. 1076-1081. DOI: 10.13031/2013.36179

Horton RE, 1945, *Erosional Development of Streams and Their Drainage Basins; Hydrophysical Approach to Quantitative Morphology*, Geological Society of America Bulletin 56 (3): 275-370. DOI: https://doi-org.proxy.lib.uwaterloo.ca/10.1130/0016-7606(1945)56(275:EDOSAT)2.0.CO;2

Jepsen, R, J Roberts, W Lick, 1997, *Effects of Bulk Density on Sediment Erosion Rates*, Water, Air and Soil Pollution, Vol. 99, pp. 21-31. DOI:https://doi.org/10.1007/BF02406841

Julian, JP, R Torres, 2006, *Hydraulic erosion of cohesive riverbanks*, Geomorphology, Vol. 76, pp. 193–206

Kamphuis, JW, KR Hall, 1983, *Cohesive Material Erosion by Unidirectional Current*, Journal of Hydraulic Engineering, Vol. 109(1), pp 49-61.

Kamphuis, JW, 1990, *Influence of sand or gravel on the erosion of cohesive sediment*, Journal of Hydraulic Research, Vol. 28(1), pp. 43-53. DOI: 10.1080/00221689009499146

Karamigolbaghi, M, SM Ghaneeizad, JF Atkinson, SJ Bennett, RR Wells, 2017, *Critical assessment of jet erosion test methodologies for cohesive soil and sediment*, Geomorphology, Vol. 295, pp.529-536.

Karrow, PF, 1967, *Pleistocene Geology of the Scarboro Area*, Ontario Geological Survey Report 46, 108p. Accompanied by 2 maps and 2 charts.

Karrow, PF, 1977, *Quaternary geology of the St Marys area, southern Ontario,* Ontario Division of Mines, Geological Report 148, 59p.

Karrow, PF, 1987, *Quaternary Geology of the Hamilton-Cambridge Area, Southern Ontario,* Ontario Geological Survey Report 255, 94p. Accompanied by Maps 2508 and 2509, scale 1:50 000 and 4 charts

Karrow, PF, 1993, *Quaternary geology, Stratford-Conestogo area*, Ontario Geological Survey, Report 283. 104p.

Karrow, PF, J Easton, 2005, *Quaternary geology of the Brampton area*, Ontario Geological Survey, Map 2223, scale 1:50 000.

Khan, I, 2006, *Determining the Erodibility of Cohesive Glacial Till Bed Sediments in the Toronto Region*, Thesis in fulfillment of the requirements of a Masters of Science, University of Guelph, Guelph, Ontario.

Khan, I, R, Kostaschuk, 2011, *Erodibility of cohesive glacial till bed sediments in urban stream channel systems*. Canadian Journal of Civil Engineering, Vol. 38, pp. 1363-1372. DOI: 10.1139/l11-099

Khanal, A, GA Fox, AT Al-Madhhachi, 2016a, *Variability of Erodibility Parameters from Laboratory mini Jet Erosion Tests,* J. Hydrol. Eng., Vol. 21(10), doi:10.1061/(ASCE)HE.1943-5548.0001404.

Khanal, A, KR Klavon, GA Fox, ER Daly, 2016b, *Comparison of Linear and Nonlinear Models for cohesive Sediment Detachment: Rill Erosion, Hole Erosion Test and Streambank Erosion Studies*. Journal of Hydraulic Engineering, Vol. 142(9), DOI: 10.1061/(ASCE)HY.1943-7900.0001147

Khandia, A, 1974, *Fundamental Aspects of Surface Erosion of Cohesive Soils*, Dissertation in fulfillment of the requirements of a Doctor of Philosophy in Civil Engineering, University of California, Davis, California.

Laflen, JM, RP Beasley, 1960, *Effects of Compaction on Critical Tractive Forces in Cohesive Soils*, University of Missouri, College of Agriculture, Agricultural Experiment Station Research Bulletin 749

Langendoen, EJ A Simon, RE Thomas, 2001, *CONCEPTS – A Process-Based Modeling Tool to Evaluate Stream Corridor Restoration Designs*, In the Proceedings of the 2001 Wetlands Engineering and River Restoration Conference, Reno, Nevada, August 27-August 31.

Lawler, DM, 1986, *River bank erosion and the influence of frost: a statistical examination,* Trans. Inst. Br. Geogr., Vol. 11(2), pp. 227-242. DOI: 10.2307/622008

Lawler, DM, J Couperthwaite, J Bull, NM Harris, 1997, *Bank erosion events and processes in the Upper Severn basin,* Hydrology and Earth System Sciences, Vol. 1(3), pp. 523-534. DOI: 10.5194/hess-1-523-1997

Lefebvre, G, K Rohan, S Douville, 1985, *Erosivity of natural intact structured clay: Evaluation*, Canadian Geotechnical Journal, Vol. 22 (4), pp. 508-517. DOI:https://doi.org/10.1139/t85-071

Lefebvre, G, K Rohan, JP Milette, 1986, *Erosivity of intact clay: influence of the natural structure*, Canadian Geotechnical Journal, Vol. 23 (4), pp. 427-434. DOI:https://doi.org/10.1139/t86-072

Le Bissonnais, Y, 1996, *Aggregate stability and assessment of soil crustability and erodibility: I. Theory and methodology*, European Journal of Soil Science, Vol. 47(4), pp. 425-437. DOI:10.1111/j.1365-2389.1996.tb01843.x

Lick, W, J McNeil, 2001, *Effects of sediment bulk properties on erosion rates,* The Science of the Total Environment, Vol. 266(1-3), pp. 41-48. DOI: 10.1016/s0048-9697(00)00747-6

Lim, SS, N Khalili, 2009, *An Improved Rotating Cylinder Test Design for Laboratory Measurement of Erosion in Clayey Soil*, Geotechnical Testing Journal, Vol 32 (3), pp. 1-7. DOI: 10.1520/GTJ101448https://doi.org/10.1111/ejss.4_12311

Mahalder, B, JS Schwartz, AM Palomino, J Zirkle, 2017, *Relationships between physical-geochemical soil properties and erodibility of streambanks among different physiographic provinces of Tennessee, USA,* Earth Surf. Process. Landf., Vol. 43, pp. 401-416, doi:10.1002/esp.4252.

Mahalder, B, JS Schwartz, AM Palomino, J Zirkle, 2018, *Estimating Erodibility Parameters for Streambanks with Cohesive Soils Using Mini JET Test Device: A Comparison of Field and Computational Methods*, Water, Vol. 10 (3), pp. 1-20. DOI: 10.3390/w10030304

Mahalder, B, JS Schwartz, TM Wynn-Thompson, AM Palomino, J Zirkle, 2022, *Comparison of Erodibility Parameters for Cohesive Streambank Soils between In Situ Jet Test Device and Laboratory*

Conduit Flume, Journal of Hydraulic Engineering, Vol. 148 (1), pp.1-14. DOI: 10.1061/(ASCE)HY.1943-7900.0001938.

Marot, M, PL Regazzoni, T Wahl, 2011, *Energy based method for providing soil surface erodibility rankings*, Journal of Geotechnical and Geoenvironmental Engineering, American Society of Civil Engineers, Vol. 137(12), pp 1290-1294.

Mazurek, KA, 2001, *Scour of Clay by Jets,* A Thesis submitted in fulfillment of a Doctor of Philosophy in Water Resources Engineering, University of Alberta, Edmonton, Alberta.

Mazurek, KA, N Rajaratnam, D Sego, 2001, *Scour of Cohesive Soil by Submerged Circular Turbulent Impinging Jets*, J. Hydraul. Eng., ASCE, Vol. 127 (7), pp. 598-606. DOI: 10.1061/(ASCE)0733-9429(2001)127:7(598)

Mazurek, KA, 2010, *Erodibility of a cohesive soil using a submerged circular turbulent impinging jet test,* In 2nd Joint Federal Interagency Conference, Las Vegas, Nevada, June 27–July 1 2010, p. 10.

McNeil, J, C Taylor, W Lick, 1996, *Measurement of Erosion of Undisturbed Bottom Sediments with Depth,* Journal of Hydraulic Engineering, Vol. 122 (6), pp. 316-324. DOI: https://doi.org/10.1061/(ASCE)0733-9429(1996)122:6(316)

Mehta, AJ, E Partheniades, 1982, *Resuspension of Deposited Cohesive Sediment Beds,* In the 18th Conference of Coastal Engineering, New York, New York, 1569-1588.

Mehta, A, W McAnally, 2008, *Fine Grained Sediment Transport*, In M, Garcia *Sediment Engineering: Processes, Measurements, Modeling and Practice*(Volume 110 of ASCE Manuals and Reports on Engineering Practice), pp. 253-306). DOI: 10.1061/9780784408148.ch04

Mercier, F, S Bonelli, P Pinettes, F Anselmet, 2014, *Comparison of Computational Fluid Dynamic Simulations with Experimental Jet Erosion Test Results,* Journal of Hydraulic Engineering, Vol. 140(5). DOI:10.1061/(ASCE)HY.1943-7900.0000829

Menzies, J, JM van der Meer, 2018, *Chapter 1: Introduction*, in book: *Past Glacial Environments*, Elsevier Ltd. DOI: 10.1016/B978-0-08-100524-8.00027-0.

Meyer, JL, MJ Paul, TW Keith, 2005, *Stream ecosystem function in urbanizing landscapes,* Journal of the North American Benthological Society, Vol. 24 (3), pp. 602-612. DOI: 10.1899/04-021.1

Midgley, TL, GA Fox, GV Wilson, DM Heeren, EJ Langendoen, A Simon, 2013, *Seepage-Induced Streambank Erosion and Instability: In Situ Constant-Head Experiments,* Journal of Hydrologic Engineering, Vol. 18(10), pp. 1200-1210.

Mier, JM, MH Garcia, 2011, *Erosion of glacial till from the St. Clair River (Great Lakes Basin)*, Journal of Great Lakes Research, Vol. 37, pp. 399-410.

Millar, RG, MC Quick, 1998, *Stable Width and Depth of Gravel-Bed Rivers with Cohesive Banks*, Vol. 124(10), pp. 1005-1013. DOI: 10.1061/(ASCE)0733-9429(1998)124:10(1005)

Mitchener, H, H Torfs, 1996, *Erosion of mud/sand mixtures*, Coastal Engineering, Vol. 29(1-2), pp.1-25. DOI: https://doi.org/10.1016/S0378-3839(96)00002-6

Moore, WL, FD Masch, 1962, *Experiments on the Scour Resistance of Cohesive Sediments,* Journal of Geophyiscal Research, Vol. 67 (4), pp. 1437-1446. DOI: https://doi.org/10.1029/JZ067i004p01437

Nouwakpo, SK, C Huang, L Bowling, P Owens, 2010, *Impact of Vertical Hydraulic Gradient on Rill Erodibility and Critical Shear Stress*, Soil Science Society of America Journal, Vol. 74 (6), pp. 1914-1921. DOI: https://doi.org/10.2136/sssaj2009.0096

Nouwakpo, SK, C Huang, 2012, *The Role of Subsurface Hydrology in Soil Erosion and Channel Network Development on a* Laboratory Hillslope, Soil Science Society of America Journal, Vol 76, pp. 1197-1211. DOI: https://doi.org/10.2136/sssaj2012.0013

Nelson, E, D Booth, 2002, *Sediment Sources in an Urbanizing, Mixed Land-Use Watershed*, Journal of Hydrology, Vol. 264(1-4), pp. 51-68. DOI: 10.1016/S0022-1694(02)00059-8.

Osman, AK, CR Thorne, 1988, *Riverbank Stability Analysis. I: Theory,* Journal of Hydraulic Engineering, Vol. 114 (2), pp. 134-150. DOI: 10.1061/(ASCE)0733-9429(1988)114:2(134).

Osterkamp, WR, P Heilman, LJ Lane, 1998, *Economic considerations of a continental sediment-monitoring program, International Journal of Sediment Research,* Vol. 13(4), pp. 12-24.

Paaswell, RE, 1973, *Causes and Mechanisms of Cohesive Soil Erosion: The State of the Art,* Highway Research Board Special Report (135).

Panagiotopoulos, G, G Voulgaris, MB Collins, 1997, *The influence of clay on the threshold of movement of fine sandy beds*, Coastal Engineering, Vol. 32 (1), pp. 19-43. DOI: https://doi.org/10.1016/S0378-3839(97)00013-6

Parchure, TM, AJ Mehta, 1985, *Erosion of soft cohesive sediment deposits*, Journal of Hydraulic Engineering, Vol. 111 (10), pp. 1308-1326. DOI: https://doi.org/10.1061/(ASCE)0733-9429(1985)111:10(1308)

Partheniades, E, 1965, *Erosion and deposition of cohesive soils*, J. Hyd. Div. ASCE, Vol. 91(1), pp.105-139.

Partheniades, E, R Paaswell, 1970, *Erodibility of channels with cohesive boundary,* Journal of the Hydraulics Division, Vol. 97 (12), pp. 755-771. DOI: 10.1061/JYCEAJ.0009505

Paul, MJ, JL Meyer, 2001, *Streams in the Urban Landscape,* Annual Review of Ecology and Systematics, Vol. 32, pp.333-365. DOI:https://doi.org/10.1146/annurev.ecolsys.32.081501.114040

Pike, L, SJ Gaskin, P Ashmore, 2017, *Flume tests on fluvial erosion mechanisms in till-bed channels,* Earth Surface Processes and Landforms, Vol. 43, pp. 259-170. DOI: 10.1002/esp.4240

Pizzuto, J, 2009, *An empirical model of event scale cohesive bank and profile evolution*, Earth Surface Processes and Landforms, Vol. 34(9), pp. 1234-1244. DOI: 10.1002/esp

Rajaratnam, N, S Beltaos, 1977, *Erosion by impinging circular turbulent Jets,* Journal of Hydraulic Engineering, Vol. 103 (10), pp. 1191-1205. DOI: https://doi.org/10.1061/JYCEAJ.0004852

Rajaratnam, N, KA Mazurek, 2005, *Impingement of circular turbulent jets on rough boundaries*, Journal of Hydraulic Research, Vol. 43(6), pp. 689-695. DOI: 10.1080/00221680509500388

Rajartanam, N, DZ Zhu, SP Rai, 2010, *Turbulence measurements in the impinging region of a circular jet*. Canadian Journal of Civil Engineering, Vol. 37(5), pp. 782-785. Doi: 10.1139/L10-014

Raudkivi, AJ, DL Hutchison, 1974, *Erosion of Kaolinite by flowing water*, Proceedings of the Royal Society of London Series A, Mathematical and Physical Sciences, Vol. 337 (1611), pp. 537-554. DOI: https://doi.org/10.1098/rspa.1974.0066

Raudkivi, AJ, SK Tan, 1984, *Erosion of Cohesive Soils*, Journal of Hydraulic Research, Vol. 22(4), pp. 217-233. DOI: https://doi.org/10.1080/00221688409499380

Reddi, LN, IM Lee, MVS Bonala, 2000, *Comparison of Internal and Surface Erosion Using Flow Pump Tests on a Sand-Kaolinite Mixture*, Geotechnical Testing Journal, Vol. 23(1), pp. 116-122. DOI: 10.1520/GTJ11129J

Rinaldi, M, SE Darby, 2008, *Modelling river-bank-erosion processes and mass failure mechanisms: progress towards fully coupled simulations.* Gravel-Bed Rivers VI: From Process Understanding to River Restoration, Developments in Earth surface Processes, Vol. 11, pp. 213-239. DOI: 10.1016/S0928-2025(07)11126-3

Rohan, K, G Lefebvre, S Douville, JP Milette, 1986, *A New Technique to Evaluate Erosivity of Cohesive Material*, Geotechnical Testing Journal, Vol. 9 (2), pp. 87-92. DOI: 10.1520/GTJ11034J

Rose, CW, JM Olley, A Haddadchi, AP Brooks, J McMahon, 2018, *An alternative method for interpreting jet erosion test (JET) data: part 1. Theory*, Earth Surface Processes and Landforms, Vol. 43, pp735-742. DOI: 10.1002/esp.4269.

Sado, EV, UJ Vagners, 1975, *Quaternary Geology of the Lucan Area, Southern Ontario*. Ontario Div. Mines, Prelim. Map P.1048. Geol. Ser., scale 1:50,000. Geology 1971,1972.

Salem, H, CD Rennie, 2017, *Practical Determination of Critical Shear Stress in Cohesive Soils*. Journal of Hydraulic Engineering, Vol. 143(10). DOI: 10.1061/(ASCE)HY.1943-7900.0001363

Salem, H, 2019, *A practical approach to the erodibility of cohesive soils*, Dissertation in fulfillment of the requirements of a Doctor of Philosophy in Civil Engineering, University of Ottawa, Ottawa, Ontario.

Sharpe, DR, 1990, *Quaternary geology of the Durham area,* Ontario Geological Survey, Open File Report 5596, llOp.

Sherard, JL, LP Dunnigan, RS Decker, EF Steele, 1976, *Pinhole Test for Identifying Dispersive Soils,* Journal of Geotechnical Engineering, Vol. 102 (1), pp.69-85.

Shields, A, 1936, *Anwendung der Aehnlichkeitsmechanik und der Turbulenzforschung auf die Geschiebebewegung*, Mitt. Preuss. Versuchsanst. Wasserbau Schiffbau, 26, 26, 1936. (English translation by WP Ott and JC van Uchelen, Vol. (36) pp., U.S. Dep. of Agric. SoilConser. Serv. Coop. Lab., Calif., Inst. of Technol., Pasadena, 1936.)

Shields, FD, RE Lizotte, SS Knight, CM Cooper, D Wilcox, 2010, *The stream channel incision syndrome and water quality,* Ecological Engineering, Vol. 36 (1), pp. 78-90. DOI: 10.1016/j.ecoleng.2009.09.014

Shugar, D, R Kostaschuk, P Ashmore, JR Desloges, L Burge, 2007, *In situ jet testing of the erosional resistance of cohesive streambeds*, Canadian Journal of Civil Engineering, Vol. 34(9), pp. 1192–1195. doi:10.1139/l07-024.

Simon, A, 1989, *A Model of Channel Response in Disturbed Alluvial Channels,* Earth Surface Processes and Landforms, Vol. 14(11-26), pp. 11-26. DOI: 10.1002/esp.3290140103

Simon, A, 1995, *Adjustment and Recovery of Unstable Alluvial Channels: Identification and Approaches for Engineering Management*, Earth Surface Processes and Landforms, Vol. 20, pp. 611-628

Simon, A, JC Collison, (2001), *Pore-water Pressure effects on detachment of cohesive streambeds: seepage forces and matric suction*, Earth Surface Processes and Landforms, Vol. 26, pp. 1421-1442. DOI: https://doi.org/10.1002/esp.287

Simon, A, L Klimetz, 2008, *Relative magnitudes and sources of sediment in benchmark watersheds of the Conservation Effects Assessment Project,* Journal of Soil and Water Conservation, Vol. 63(6). Pp. 504-522. DOI: 10.2489/jswc.63.6.504.

Simon, A, RE Thomas, L Klimetz, 2010, *Comparison and Experiences with Field Techniques to Measure Critical Shear Stress and Erodibility of Cohesive Deposits*, In Proceedings of the 2nd Joint Federal Interagency Conference on Sedimentation and Hydrologic Modeling, Las Vegas, NV, USA, 27 June–1 July 2010.

Smerdon, ET, RP Beasley, 1959, *The Tractive Force Theory Applied to Stability of Open Channels in Cohesive Soils,* University of Missouri, College of Agriculture, Agricultural Experiment Station Research Bulletin 715

Stein, O.R, PY Julien, CV Alonso, 1993, *Mechanics of jet scour downstream of a headcut*, Journal of Hydraulic Research, Vol. 31(6), pp. 723-738. DOI: 10.1080/00221689309498814.3.

Stein, OR, NN Nett, 1997, *Impinging Jet Calibration of Excess Shear Sediment Detachment Parameters*. Trans. ASABE, Vol. 40(6), pp. 1573-1580. DOI: 10.13031/2013.21421

Sutarto, T, AN Papanicolaou, CG Wilson, EJ Langendoen, 2014, *Stability Analysis of Semicohesive Streambanks with CONCEPTS: Coupling Field and Laboratory Investigations to Quantify the Onset of Fluvial Erosion and Mass Failure*, Journal of Hydraulic Engineering, Vol. 140(9):04014041. DOI: 10.1061/(ASCE)HY.1943-7900.0000899

Thoman, RW, SL Niezgoda, 2008, *Determining Erodibility, Critical Shear Stress, and Allowable Discharge Estimates for Cohesive Channels: Case Study in the Powder River Basin of Wyoming*, Journal of Hydraulic Engineering, Vol 134 (12), pp. 1677-1687. DOI: https://doi.org/10.1061/(ASCE)0733-9429(2008)134:12(1677)

Tolhurst, TJ, KS Black, SA Shayler, S Mather, I Black, K Baker, DM Paterson, 1999, *Measuring the in situ erosion shear stress of intertidal sediments with the Cohesive Strength Meter (CSM)*, Estuarine, Coastal and Shelf Science, Vol. 49 (2), pp. 281-294. DOI: https://doi.org/10.1006/ecss.1999.0512

Tolhurst, TJ, KS Black, DM Paterson, HJ Mitchener, GR Termaat, SA Shayler, 2000, *A comparison and measurement standardisation of four in situ devices for determining the erosion shear stress of intertidal sediments*, Continental Shelf Research, Vol. 20(10-11), pp. 1397-1418. DOI: https://doi.org/10.1016/S0278-4343(00)00029-7

Torfs, H, 1995, *Erosion of Mud/Sand Mixtures,* Thesis submitted in fulfillment of Doctor of Philosophy in Applied Sciences, Katholieke Universiteit Leuven, Leuven, Belgium.

Van Prooijen, BC, JC Winterwerp, 2010, *A stochastic formulation for erosion of cohesive sediments*, Journal of Geophysical Research, Vol. 115, C01005. DOI: 10.1029/2008JC005189.

Wahl, TL, 2010, *A Comparison of The Hole Erosion Test and Jet Erosion Test,* Joint Federal Interagency Conference on Sedimentation and Hydrologic Modelling, June 27th-July 1st, 2010. Las Vegas, NV.

Wahl, TL, 2016, *The Submerged Jet Erosion Test: Past-Present-Future,* Presented at the USSD International Symposium on the Mechanics of Internal Erosion for Dams and Levees Salt Lake City, UT – August 8-10, 2016

Wahl, TL, 2021, *Methods for Analyzing Submerged Jet Erosion Test Data to Model Scour of Cohesive soils*. Trans. ASABE, Vol 64(3), pp. 785-799.

Walder, JS, 2015, *Dimensionless Erosion Laws for Cohesive Sediment,* Journal of Hydraulic Engineering, Vol 142(2), pp. 1-13. DOI: https://doi.org/10.1061/(ASCE)HY.1943-7900.0001068

Walsh, CJ, AH Roy, JW Feminalla, PD Cottingham, PM Groffman, RP Morgan II, 2005, *The urban stream syndrome: current knowledge and the search for a cure*, Journal of the North American Benthological Society, Vol. 24 (3) pp. 706-723. DOI: 10.1899/0887-3593(2005)024\(0706:TUSSCK\)2.0.CO;2

Walpole, RE, RH Myers, SL Myers, K Ye, 2007, *Probability & Statistics for Engineers & Scientists. 9th Edition*, Pearson Education Inc.

Wan, CF, R Fell, 2004, *Investigation of Rate of Erosion of Soils in Embankment Dams*, Journal of Geotechnical and Geoenvironmental Engineering, Vol. 130 (4), pp. 373-380. DOI: 10.1061/(ASCE)1090-0241(2004)130:4(373)

Watts, CW, TJ Tolhurst, KS Black, AP Whitmore, 2003, *In situ measurement of erosion shear stress and geotechnical shear strength of the intertidal sediments of the experimental managed realignment scheme at Tollesbury, Essex, UK,* Estuarine, Coastal and Shelf Science, Vol. 58 (3), pp. 611-620. DOI: https://doi.org/10.1016/S0272-7714(03)00139-2

Weidner, KL, 2012, *Evaluation of the Jet Test Method for determining the erosional properties of cohesive soils; A numerical approach,* Thesis submitted in fulfillment of a Master of Science in Civil Engineering, Virginia Polytechnic Institute and State University, Blacksburg, Virginia.

White, OL, 1975, *Quaternary Geology of the Bolton Area, Southern Ontario*, Ontario Div. of Mines, GR 117, 119p. Accompanied by Maps 2275 and 2276, scale l inch to l mile.

Whitney, JW, PA Glancy, SE Buckingham, AC Ehrenberg, 2015, *Effects of rapid urbanization on streamflow, erosion and sedimentation in a desert stream in the American southwest,* Anthropocene, Vol. 10, pp. 29-45. DOI: https://doi.org/10.1016/j.ancene.2015.09.002

Wilson, BN, 1993a, *Development of a Fundamentally Based Detachment Model,* Transactions of the American Society of Agricultural and Biological Engineers, Vol. 36 (4), pp. 1105-1114. DOI: 10.13031/2013.28441

Wilson, BN, 1993b, *Evaluation of a Fundamentally Based Detachment Model,* Transactions of the American Society of Agricultural and Biological Engineers, Vol. 36 (4), pp. 115-1122. DOI: 10.13031/2013.28442

Wolmanm, MG, 1959, *Factors Influencing Erosion of a Cohesive River Bank,* American Journal of Science, Vol. 257 (3), pp. 204-216. DOI: https://doi.org/10.2475/ajs.257.3.204

Wolman, MG, 1967, *A cycle of sedimentation and erosion in urban river channels,* Geografiska Annaler, Vol. 49 (2), pp. 385-395. DOI: 10.2307/520904

Wynn, TM, MB Henderson, DH Vaughan, 2008, *Changes in streambank erodibility and critical shear stress due to subaerial processes along a headwater stream, southwestern Virginia, USA*, Geomorphology, Vol. 97 (3-4), pp. 260-273. DOI: https://doi.org/10.1016/j.geomorph.2007.08.010

Yumoto, M, T Ogata, N Matsuoka, E Matsumoto, 2006, *Riverbank Freeze-thaw Erosion Along a Small Mountain Stream, Nikko Volcanic Area, Central Japan*, Permafrost and Periglacial Processes, Vol. 17, pp. 325-339. DOI: 10.1002/ppp.569

Zreik, DA, BG Krishnappan, JT Germaine, OS Madsen, CC Ladd, 1998, *Erosional and Mechanical Strengths of Deposited Cohesive Sediments,* Journal of Hydraulic Engineering, Vol. 124(11), pp. 1076-1085. DOI: 10.1061/(ASCE)0733-9429(1998)124:11(1076)

Appendix A: Study Sites and Site Photos
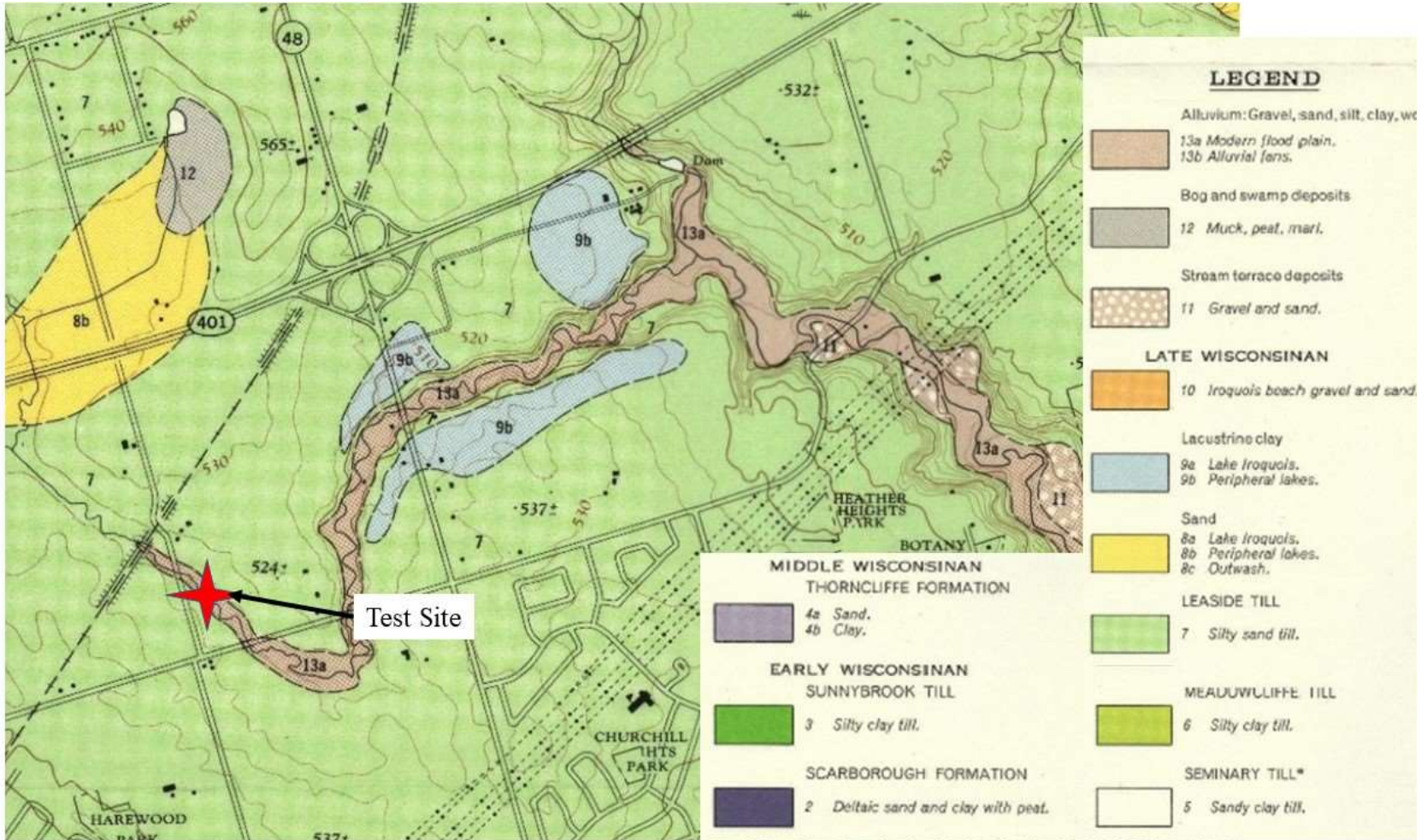
HC Site Geological Mapping. Map adapted from Karrow (1967).
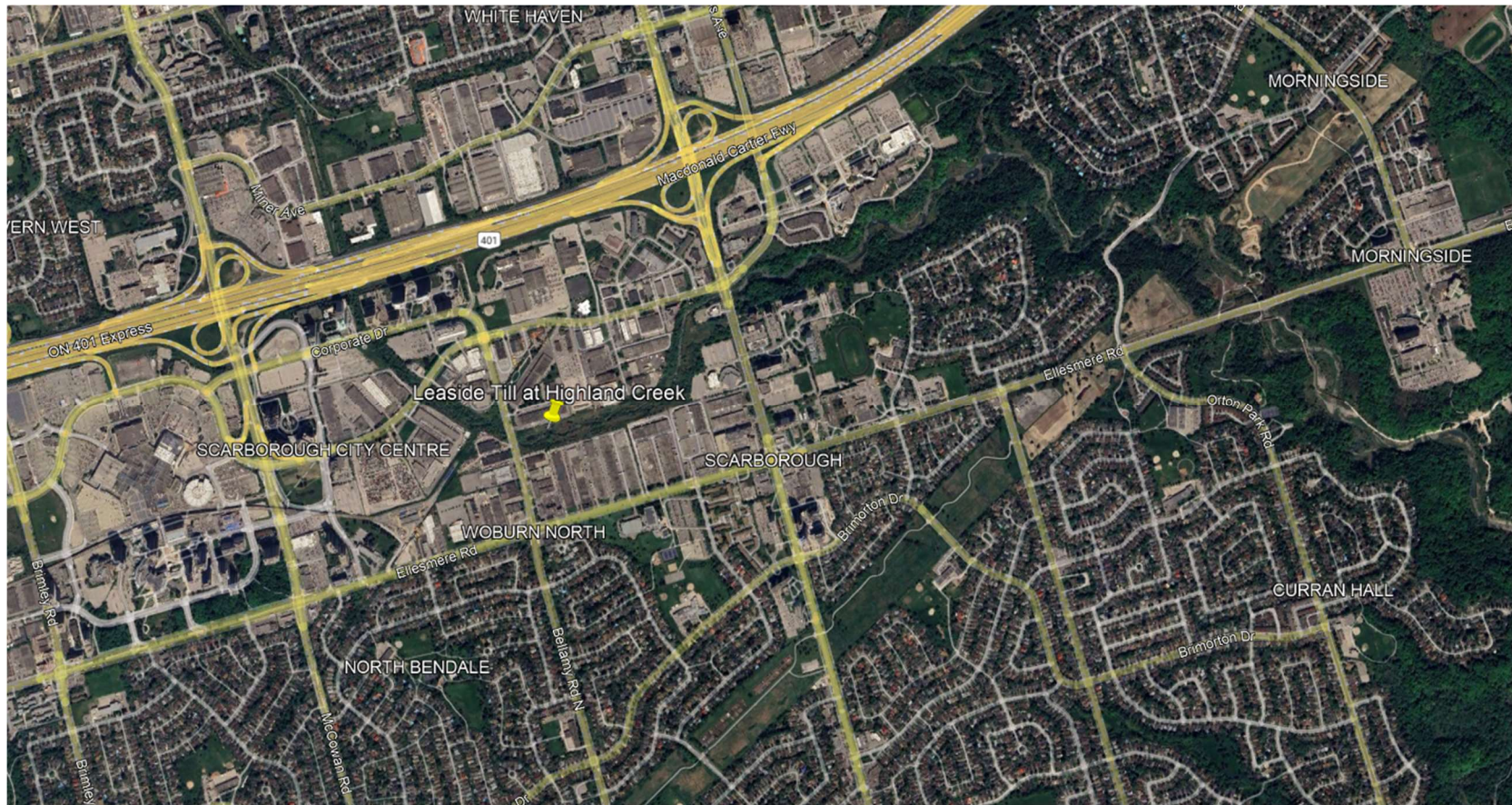
HC Site Location
Image retrieved from Google Earth Pro©
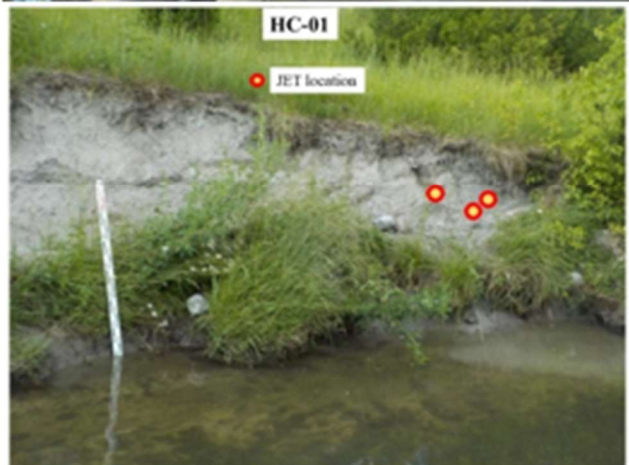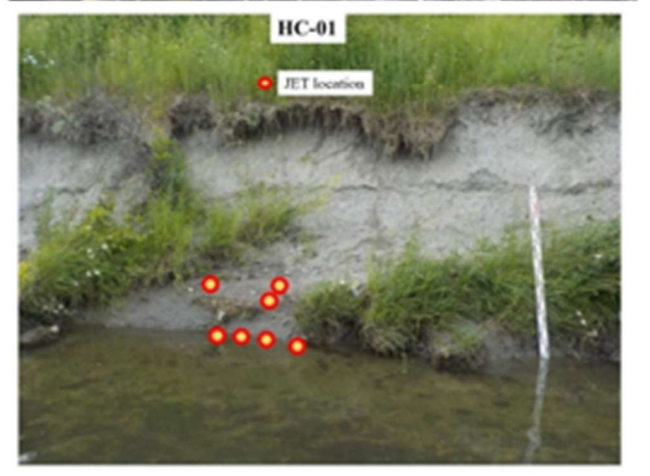
HC Qualitative Comments:

The material present at HC is a light grey silty-clay till with some sand and gravels present. The material is exposed along the bed and on banks with erosion scarring. The submerged material along the bed is stiff and hard (insertion of foundation ring was difficult) with material along the bank toe and middle of the bank notably softer. Material in the upper third of the bank displayed desiccation cracking. At HC one test received a poor field grade and four tests received a moderate field grade. The test with the poor field grade was excessively influenced by the presence of vegetative roots resulting in an inadmissible test. Two tests with the moderate grade did not cause sufficient erosion to characterize the material. While these tests were unsuccessful in the characterization of the material's erodibility parameters, they still provide important information regarding a threshold at which the material does not erode. One test was influenced by the armoring of the bottom of the scour hole. After reviewing the data collected during this test it was deemed inadmissible. The last test with a moderate field grade was influenced by a stone impeding the impinging jet, limiting the usable test duration to 30 minutes.
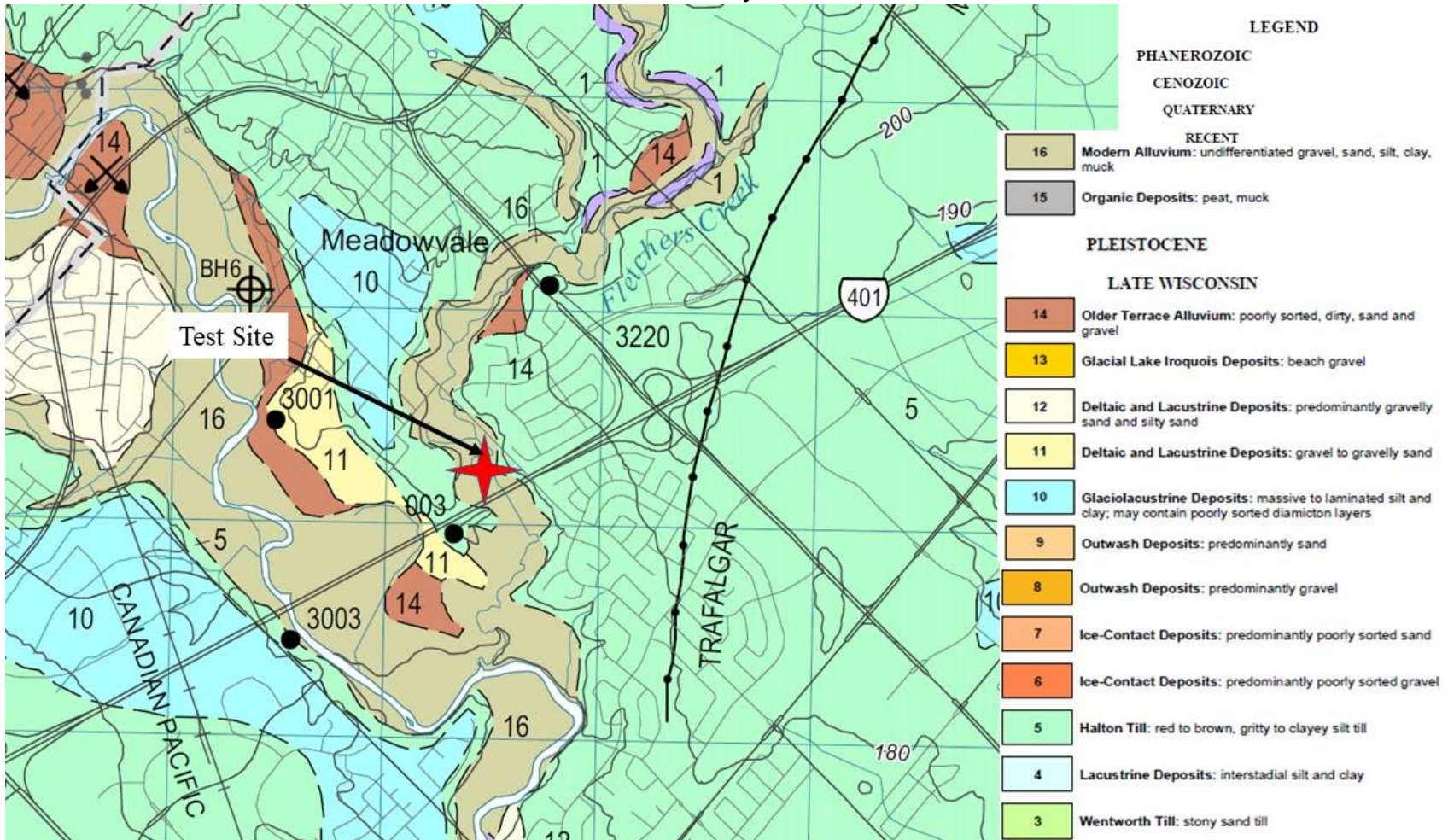
FC Site Geological Mapping. Map adapted from Karrow and Easton (2005).
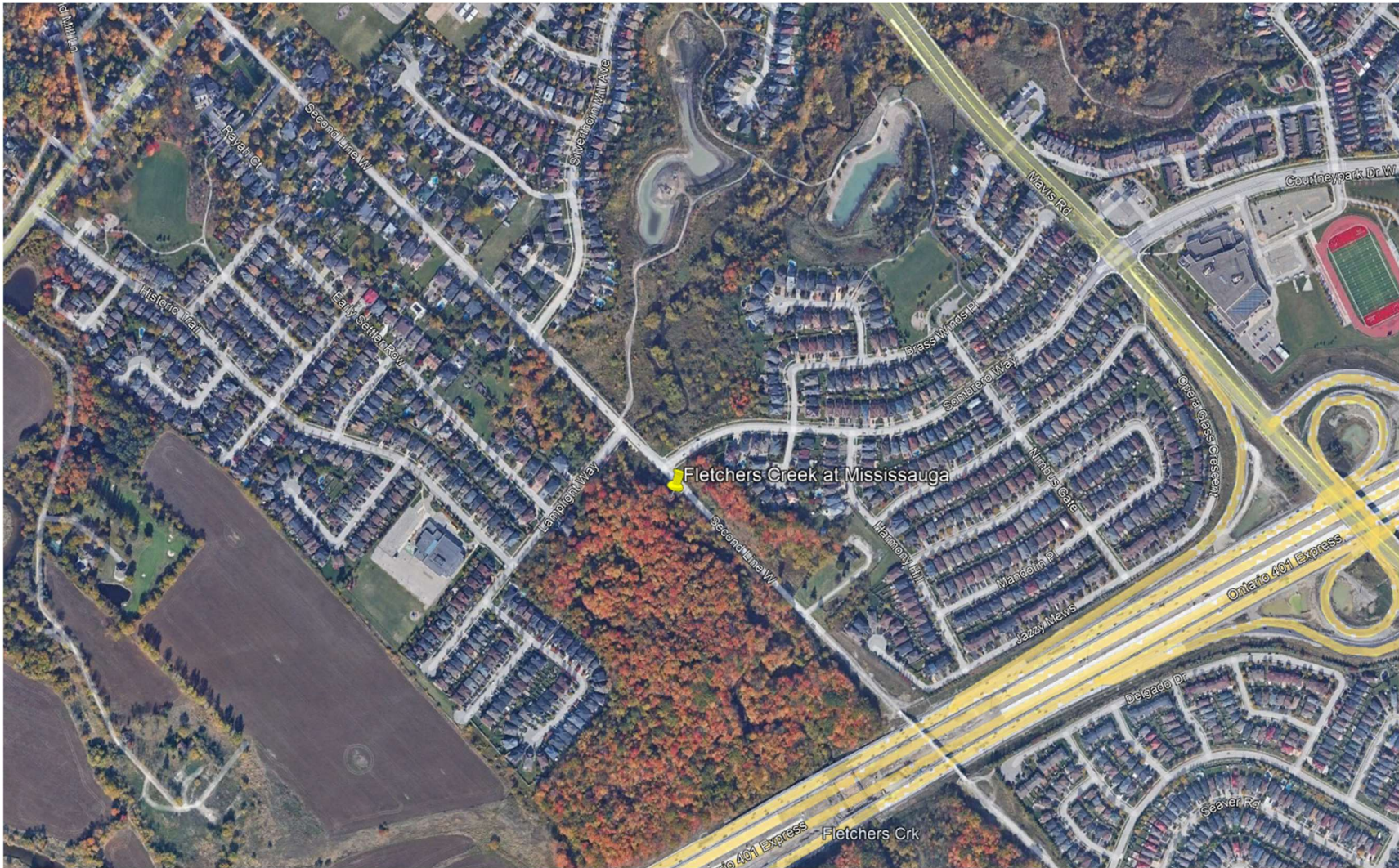
FC Site Location
Image retrieved from Google Earth Pro©

FC Qualitative Comments:

The material located at FC is a grey silty-clay till with some sand and small gravels present. At the study site the material is predominantly exposed along bank toes, however, there are patches exposed along portions of the bed where the alluvial cover is thin. One test at FC was assigned a moderate grade based on the influence of a stone present at the point of jet impingement. Upon inspection of the data, the test was deemed unusable. The remaining tests at FC were assigned a good field grade with minor instances of fine gravels present in the scour hole and minor instances of vegetative roots along edges of scour holes.
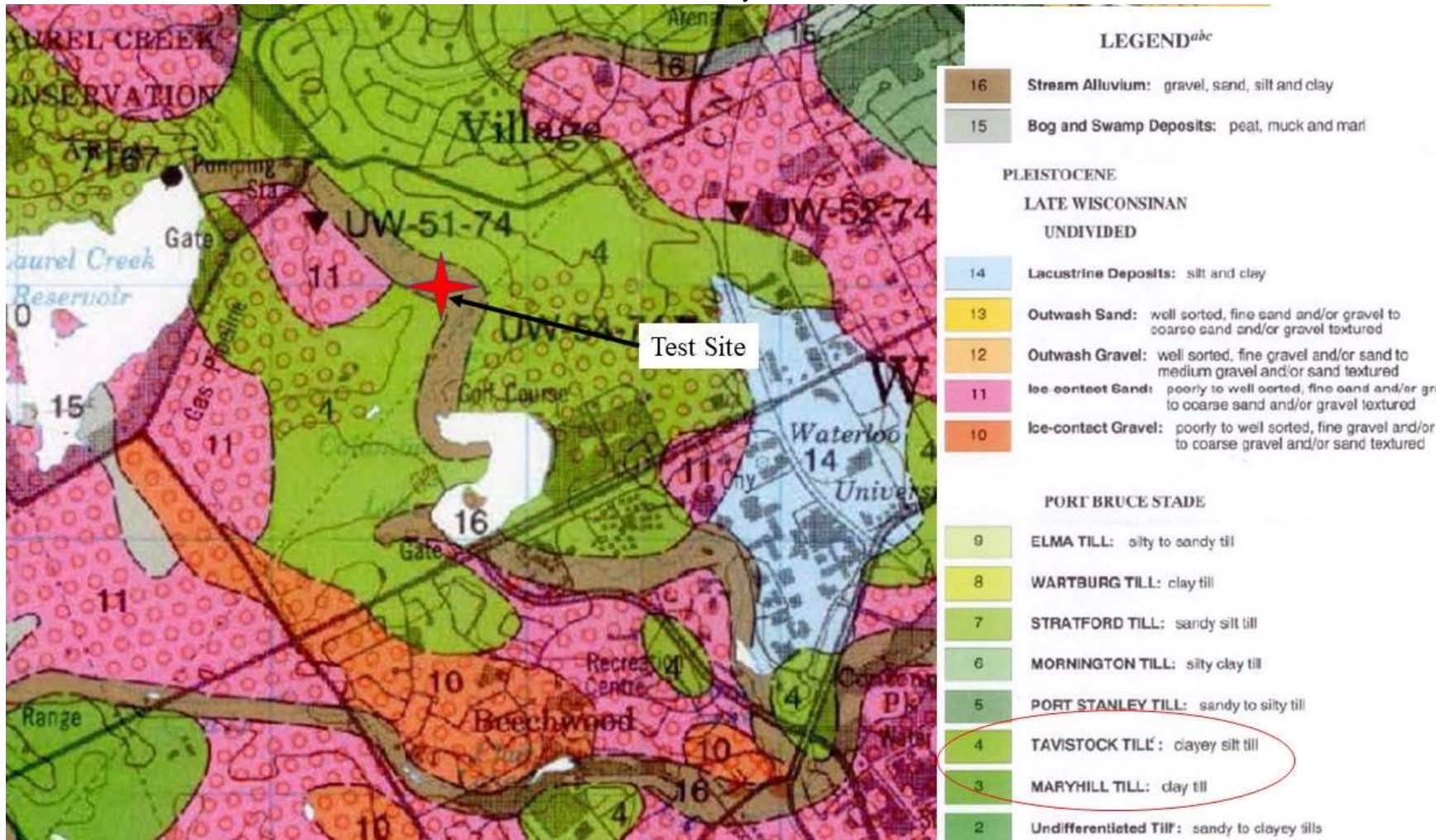
LNC Site Geological Mapping. Map adapted from Karrow (1993).
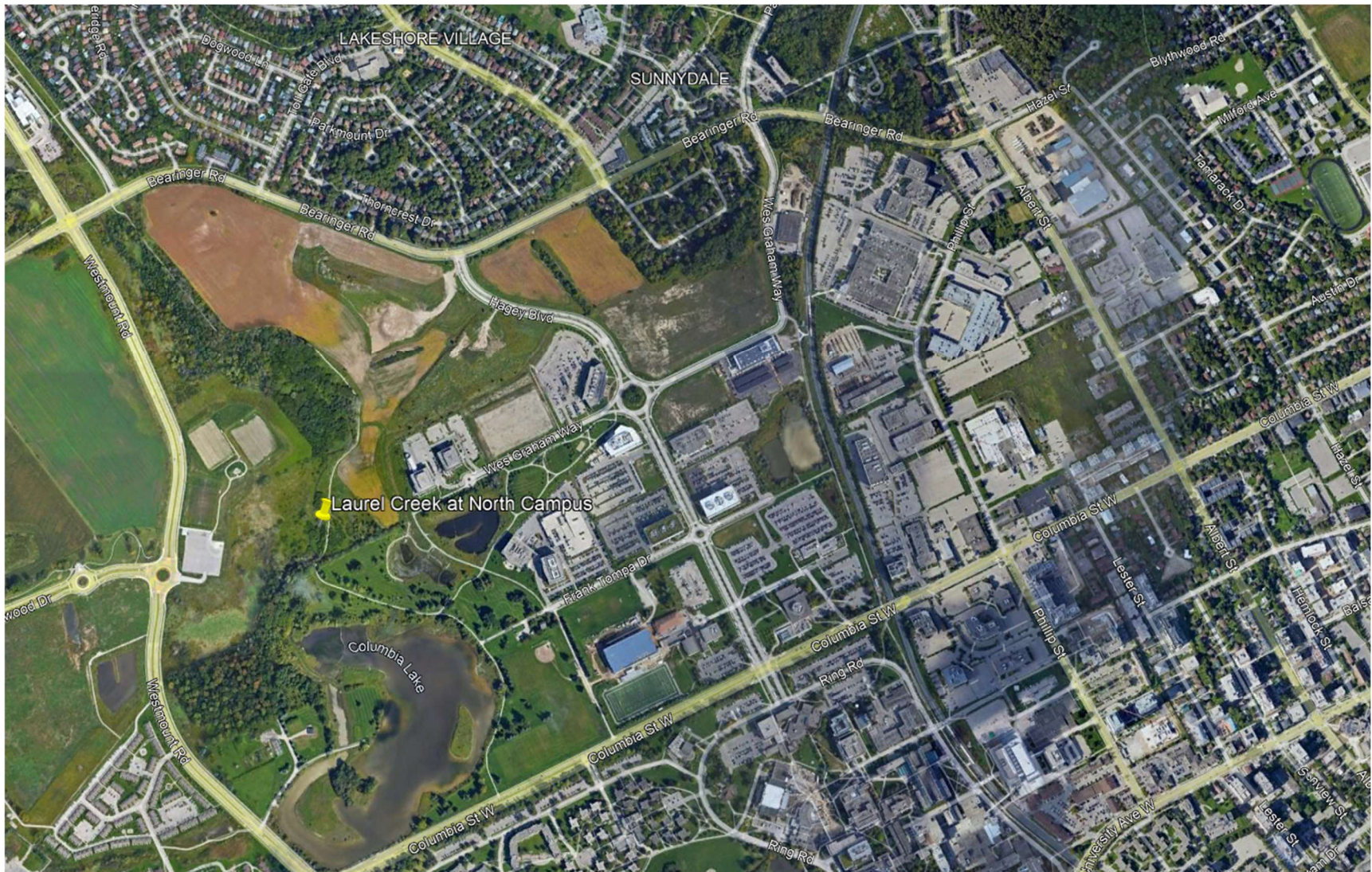
LNC Site Location
Image retrieved from Google Earth Pro©

LNC Qualitative Comments:

The material at LNC was a light brown clayey till with few stones present. The material was predominantly present along bank toes and a few sections of the bed. The material along the bed sometimes presented with a fragile pockmarked surface. It was challenging to capture the pockmarked material's characteristics with the mini-JET since it easily fractured during ring insertion. At LNC, two tests were assigned field grades of moderate. Both moderate grades were a result of vegetative presence along the periphery of the scour holes. One was deemed to be admissible, however, the other was excessively influenced by the presence of vegetative roots and was deemed inadmissible.
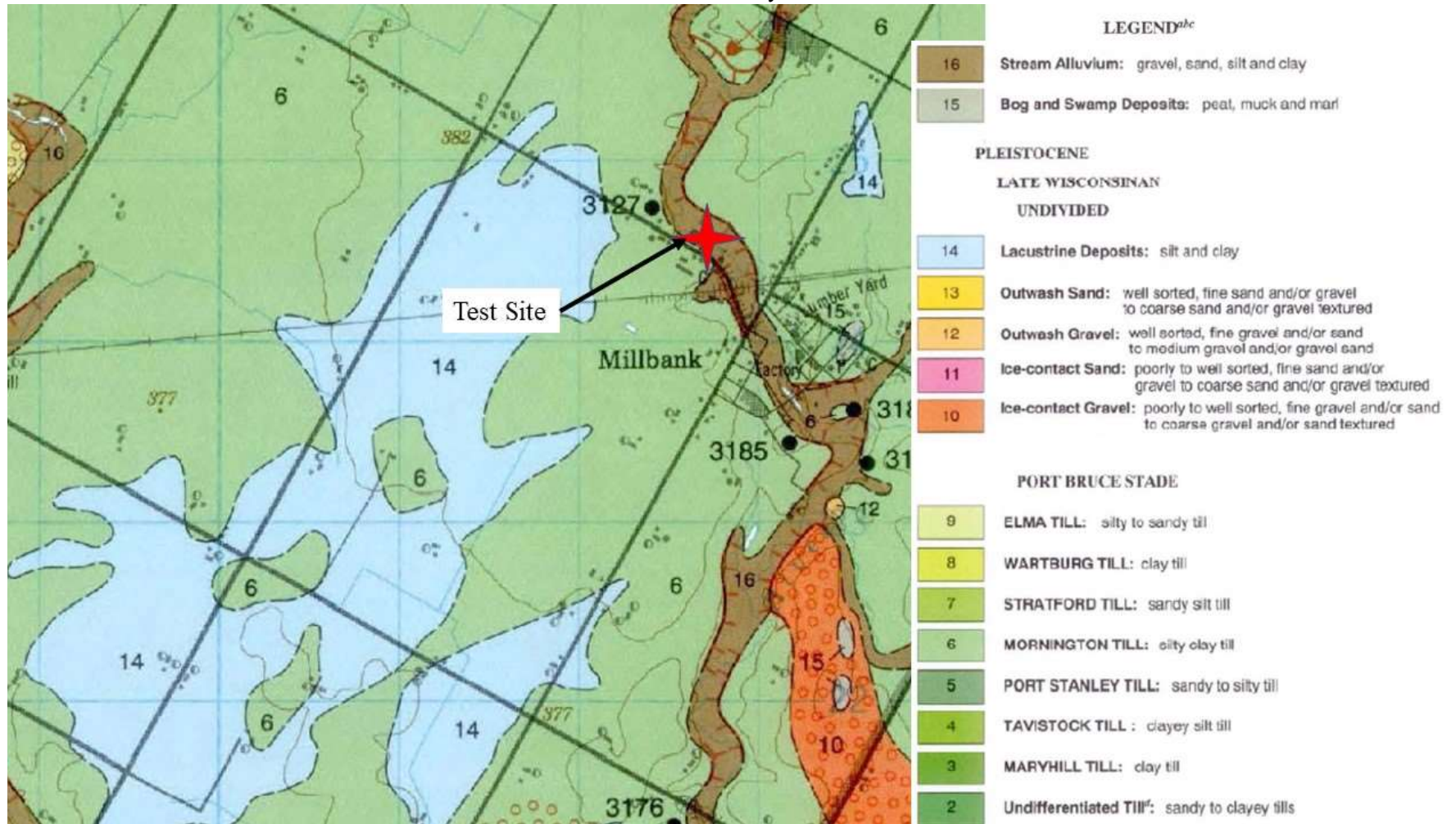
NMB Site Geological Mapping. Map adapted from Karrow (1993).
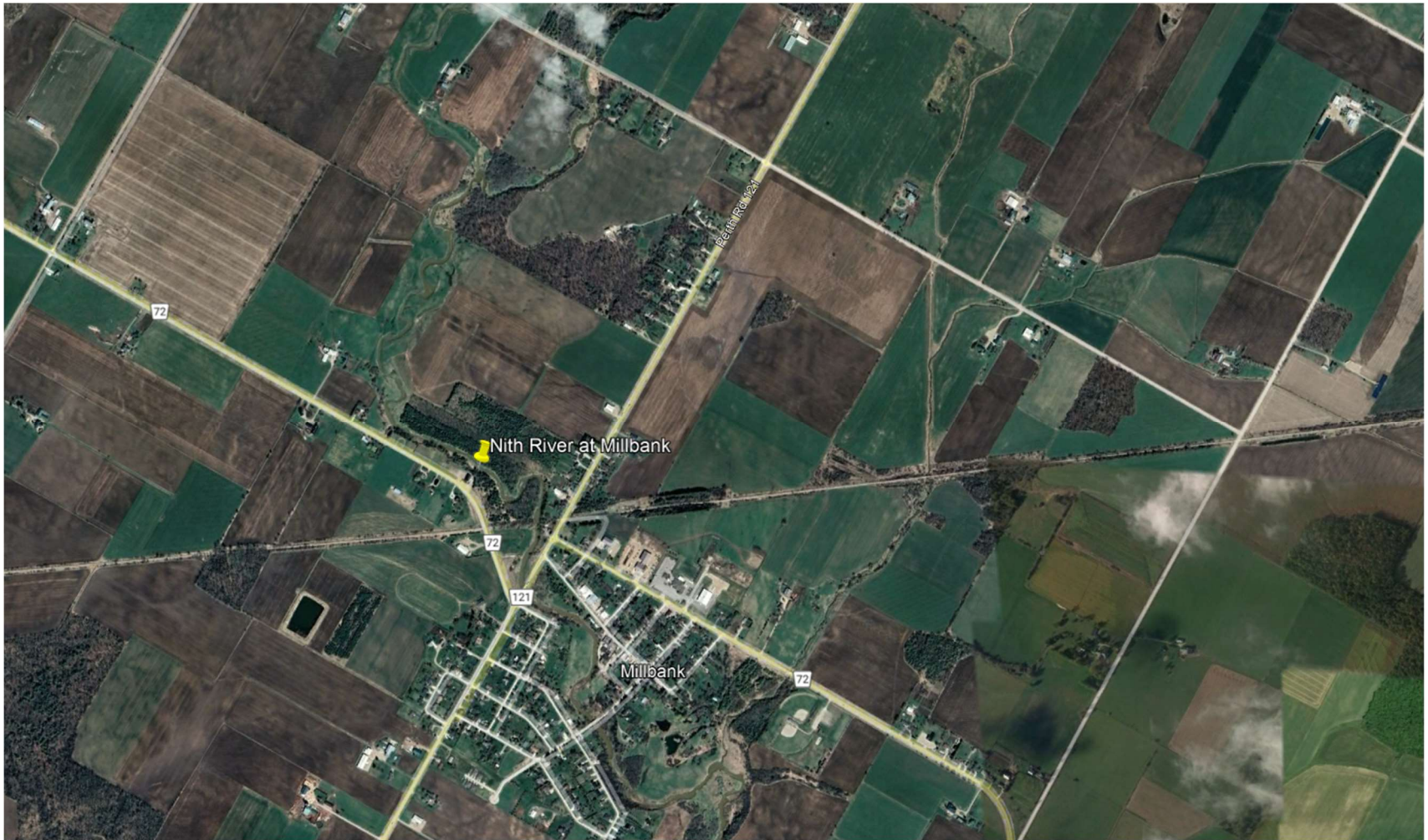
NMB Site Location
Image retrieved from Google Earth Pro©

NMB Qualitative Comments:

At NMB, the material is light grey with a high clay content. The subaerially exposed material has a slightly darker tone than the submerged material. The material had a blocky appearance and was prone to block separation, but no laminated layers were observed. The material was exposed along bank toes, sections of the bed and along cutbanks. At NMB, one test was assigned a moderate field grade and four tests were assigned poor field grades. The test that was assigned a moderate field grade had borderline amounts of scour to sufficiently characterize the material but was deemed sufficient after considering the data. Three of the four tests with poor field grades were excessively influenced by block separation and the subsequent impediment of the jet impinging upon the bottom of the scour hole. These tests were inadmissible. The last test with a poor field grade was subject to shifting of the foundation ring during the test such that the point of impingement changed. This test was also unusable.
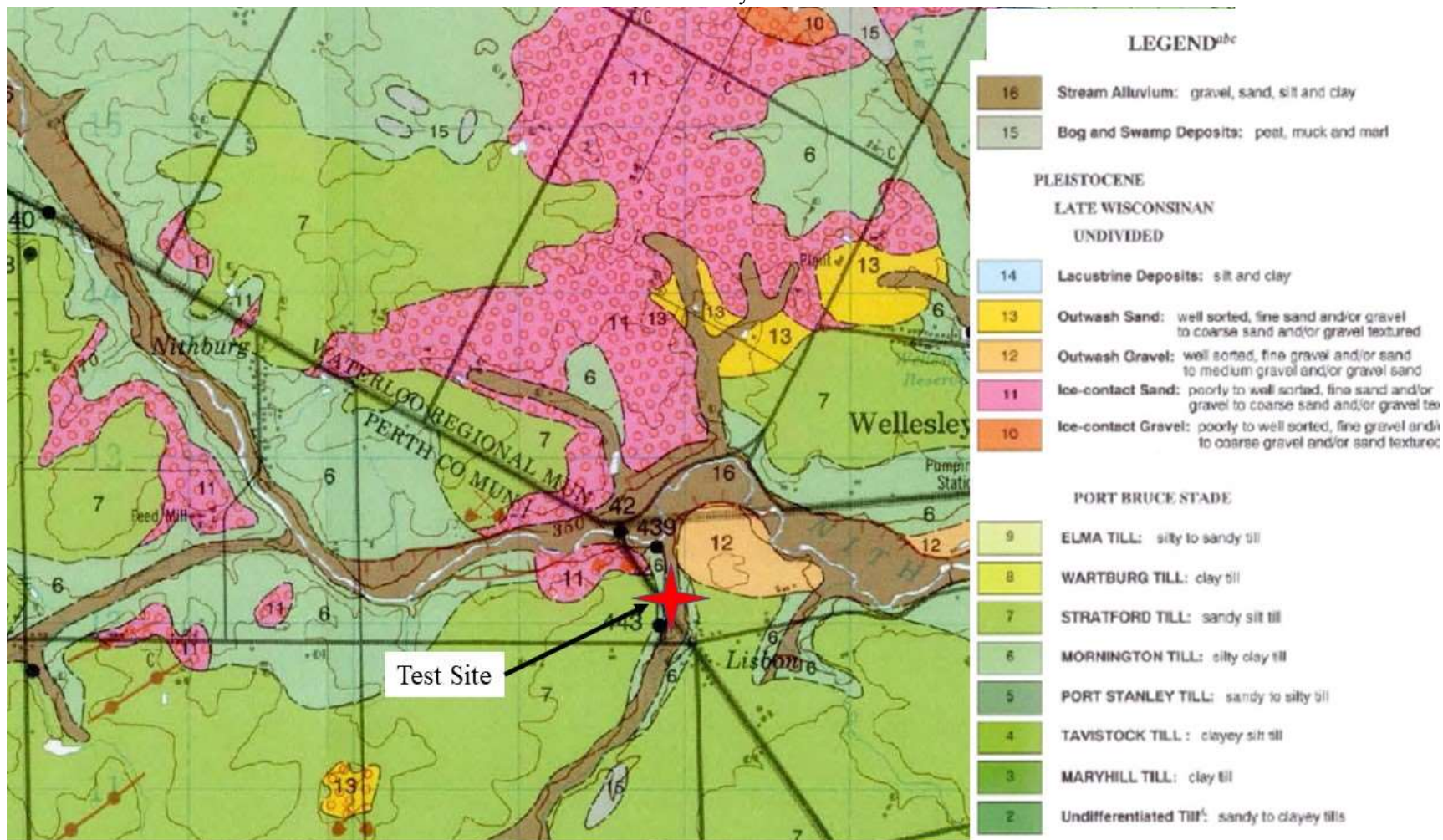
NTL Site Geological Mapping. Map adapted from Karrow (1993).

NTL Site Location
Image retrieved from Google Earth Pro©
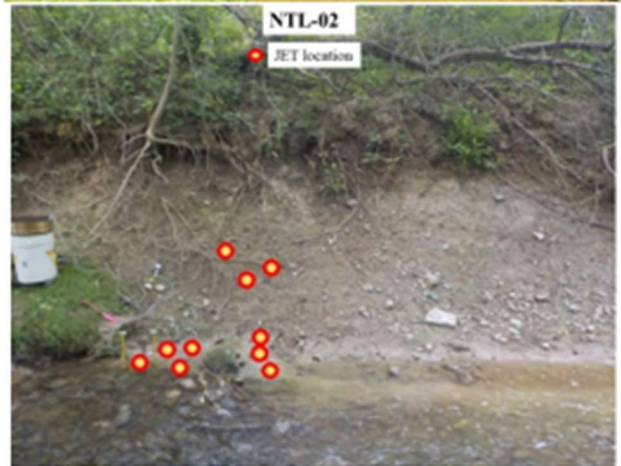
NTL Qualitative Comments:

The material present at NTL is a light brown clayey material with a small presence of stones and fine gravels. The subaerial bank material was observed to be slightly darker than the submerged material. Some block separation was observed during the mini-JETs. At NTL, one test was assigned a moderate grade due to the presence of a stone impeding jet impingement at the 30-minute mark of the test. The data collected prior to this observation was reviewed and deemed valid, however, after the notation of the presence of the stone the test results were discarded resulting in a shortened test duration. The remaining tests were assigned good field grades with observations including some instances of the maximum scour occurring slightly off-centre from the measuring point, and minor notations of potential abrasion.

LEGEND

PLEISTOCENE
LATE WISCONSINAN

14	Alluvial fan gravel
13	Beach gravel
12	Lacustrine and outwash sand
11	Lake deposits: stratified to varved clay, silt, and fine sand
10	Halton Till: clay or silt till
9	Outcrop complex: bouldery till and bedrock ridges
8	Ice-contact sand: kames and eskers
7	Outwash gravel
6	Ice-contact gravel: kames and eskers
5	Wentworth Till: stony, sandy, silt till
4	Port Stanley Till*: silt to sandy silt till
3	Maryhill Till*: clayey silt till
2	Catfish Creek Till*: stony, sandy, silt till

GT Site Geological Mapping. Map adapted from Karrow (1987).

GT Site Location
Image retrieved from Google Earth Pro©

GT Qualitative Comments:

The material located at the tributary to Grindstone Creek had a light brown colour and a slightly higher presence of fine gravels compared to the other sites identified as Halton Till. It was also observed to be softer with a notable ease of insertion of the foundation ring into the material. At GT, 2 of the tests were assigned a moderate field grade. They were both influenced by the presence of fine gravels causing excessive abrasion and armoring the bottom of the scour hole. Upon review of the field data, they were deemed inadmissible and unusable. Abrasion was noted in some of the other tests at this site, however, they were deemed not to excessively influence the results of the test. Tests performed on the sloped banks avoided the armoring of the scour hole through the assistance of gravitational forces removing particles from the hole.

TCH Site Geological Mapping. Map adapted from Karrow (1993).

TCH Site Location
Image retrieved from Google Earth Pro©
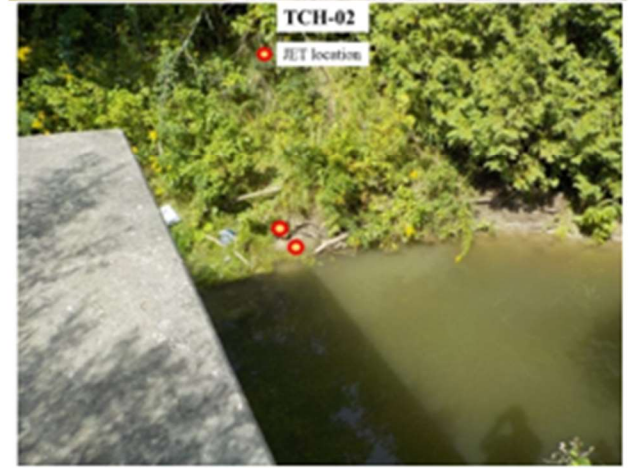
TCH Qualitative Comments:

The material present at TCH is a brown/dark grey fine-grained till with some occurrences of stones. Submerged material had a slightly lighter hue of grey compared to subaerial material. Desiccation cracking was observed along portions of the material within the upper regions of the bank. At TCH three tests were assigned field grades of moderate and one test was assigned a field grade of poor. The moderate field grades were assigned due to the shortened test durations (19-45 minutes) caused by the maximum scour being reached relatively early in the test. The test with the poor rating was influenced by a "narrow and deep" scour hole and stones influencing the impingement of the jet resulting in an inadmissible test.
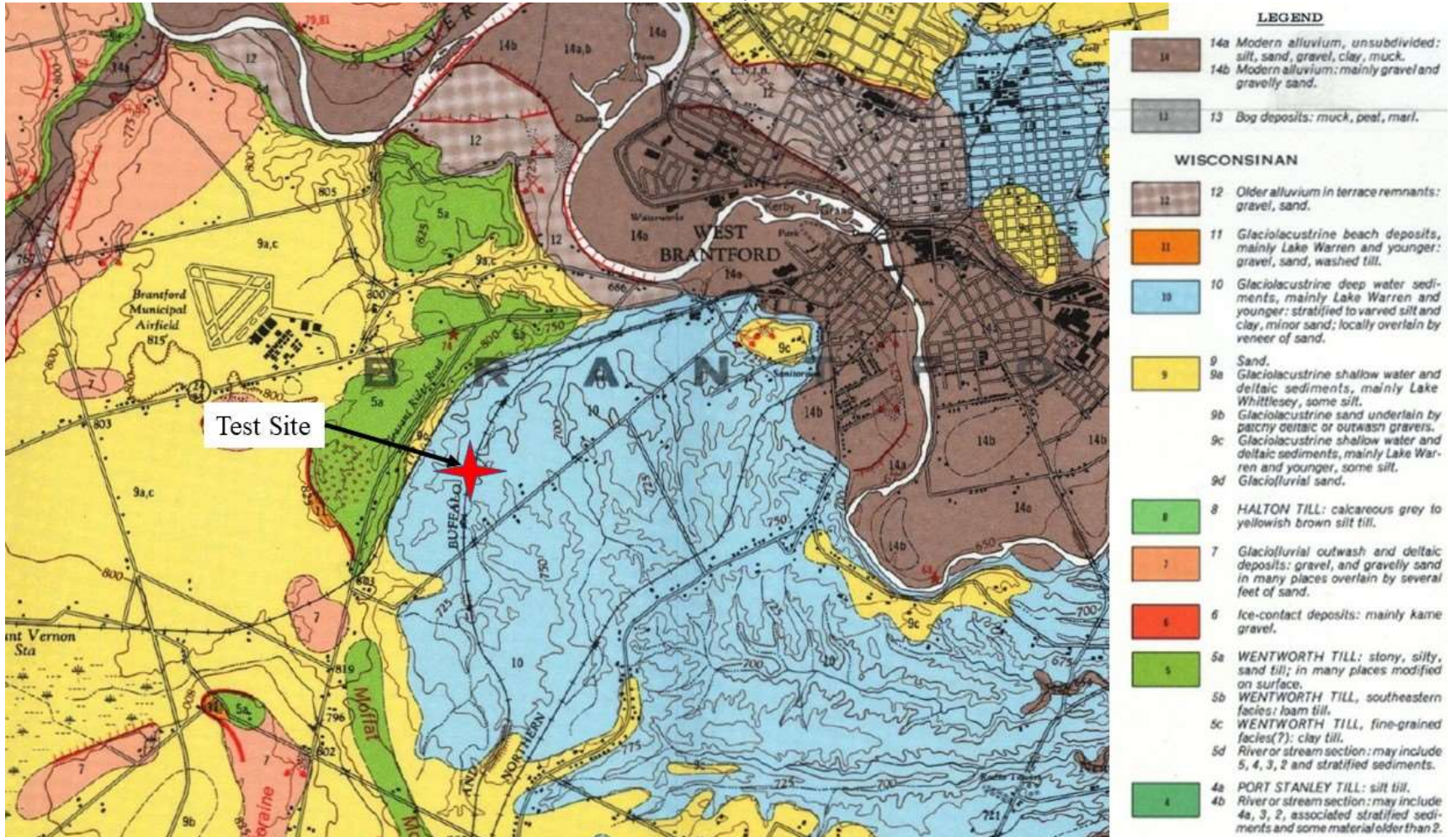
DCB Site Geological Mapping. Map adapted from Cowan (1972).
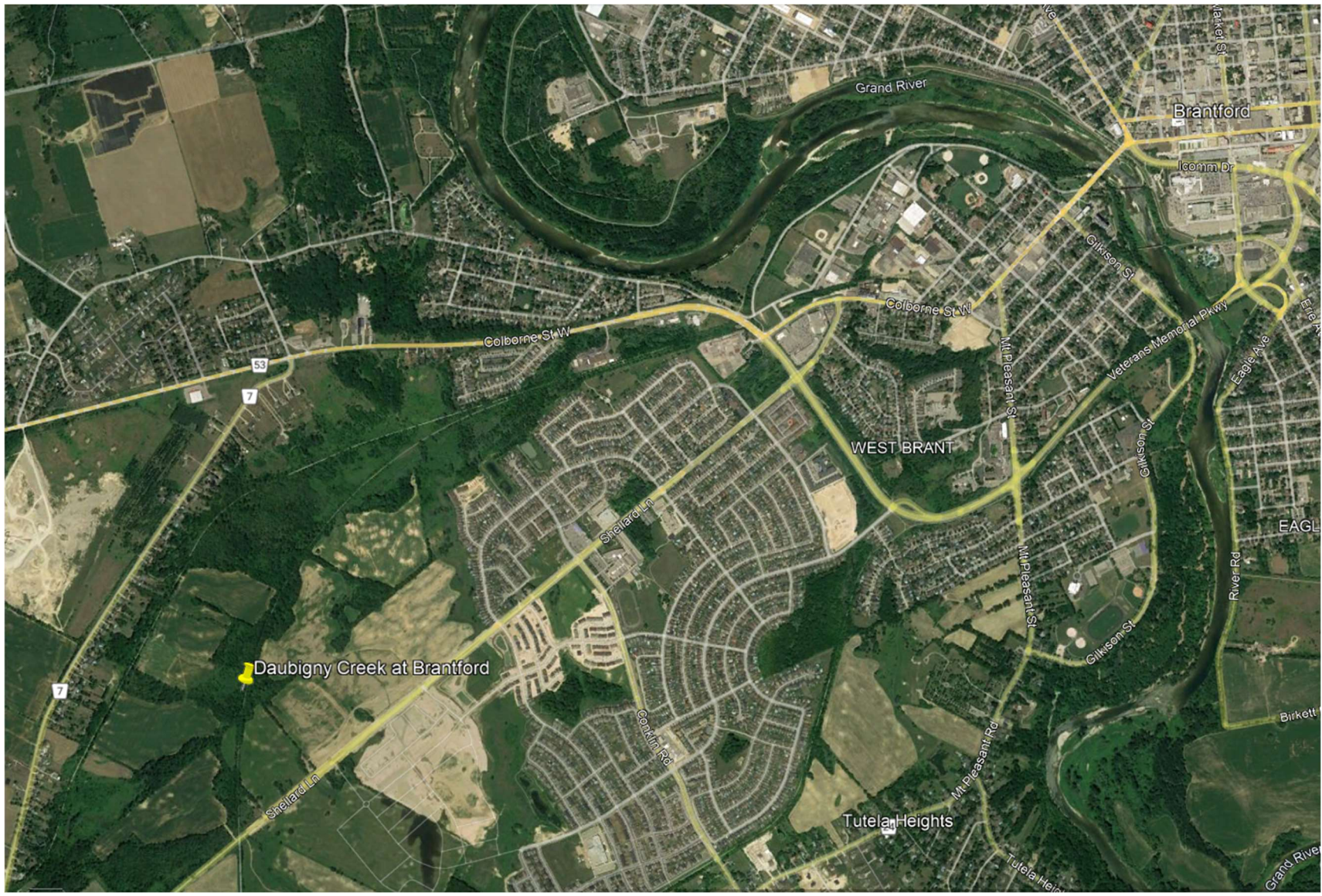
DCB Site Location
Image retrieved from Google Earth Pro©

134
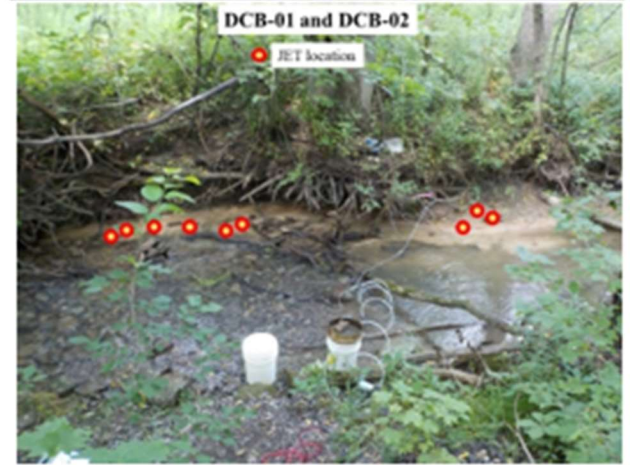
DCB Qualitative Comments:

The material located at DCB is a light brown clay with laminated layers. The material was observed to be prone to fracturing and block separation with the fracturing of the subaerial material predominantly occurring along planes between laminated layers. Occurrences of a pockmarked surface was observed at several locations as well as larger fractures running along the streambed. At DCB, two tests received moderate field grades and one test received a poor field grade. One of the tests with a moderate field grade did not cause sufficient scour to characterize the erosion of the material. While this test was unsuccessful in the characterization of the material's erodibility parameters, it still provides important information regarding a threshold at which the material does not erode. The other test with a moderate grade had a shortened duration (27 minutes) due to equipment malfunction. The data up until that point is valid, however, the test has a shortened duration. During the poor field grade test, the material was excessively influenced by the staff gauge at the measurement point such that the readings were not representative of the scour caused by jet impingement.

135
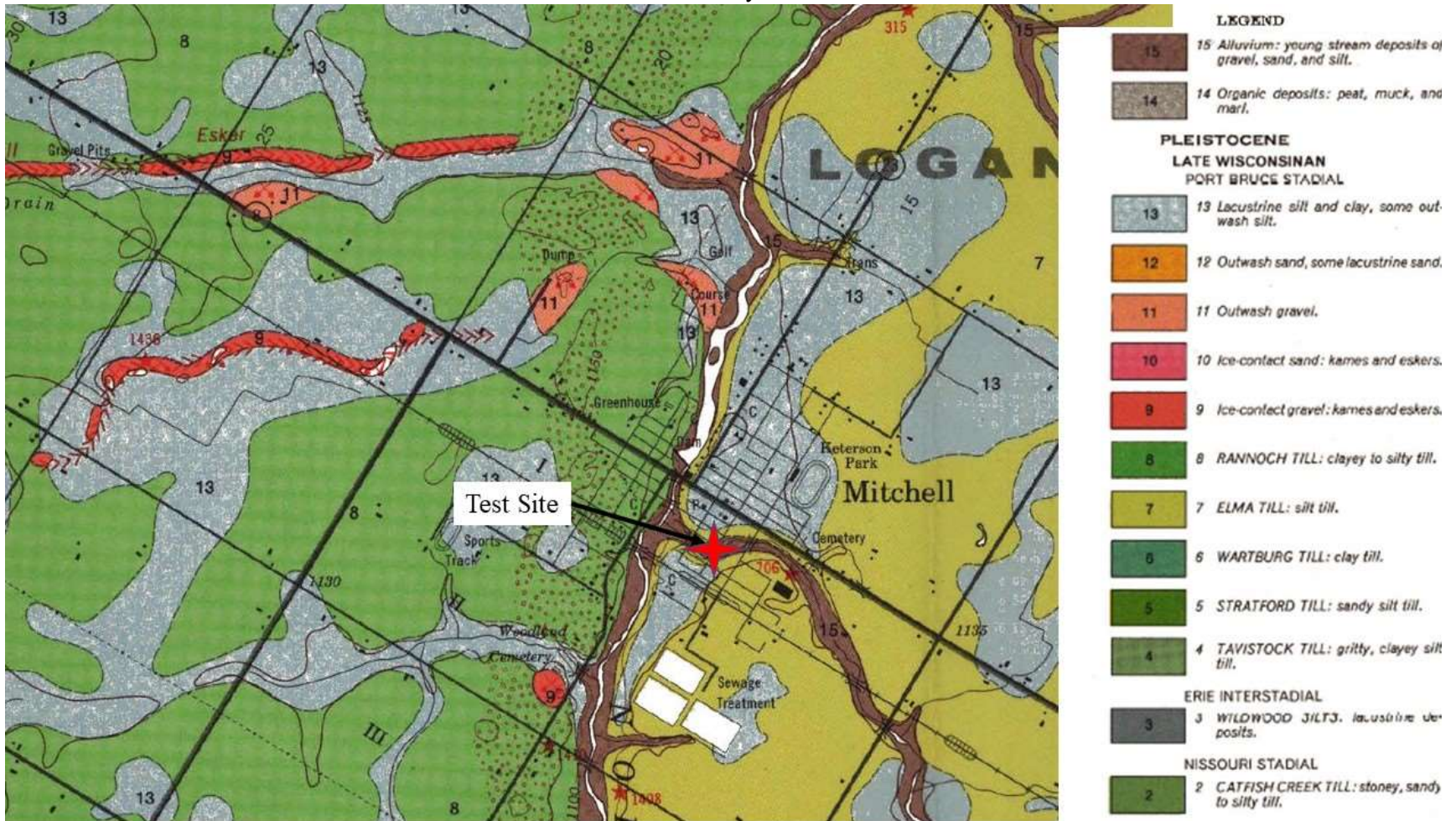
WCM Site Geological Mapping. Map adapted from Karrow (1977).
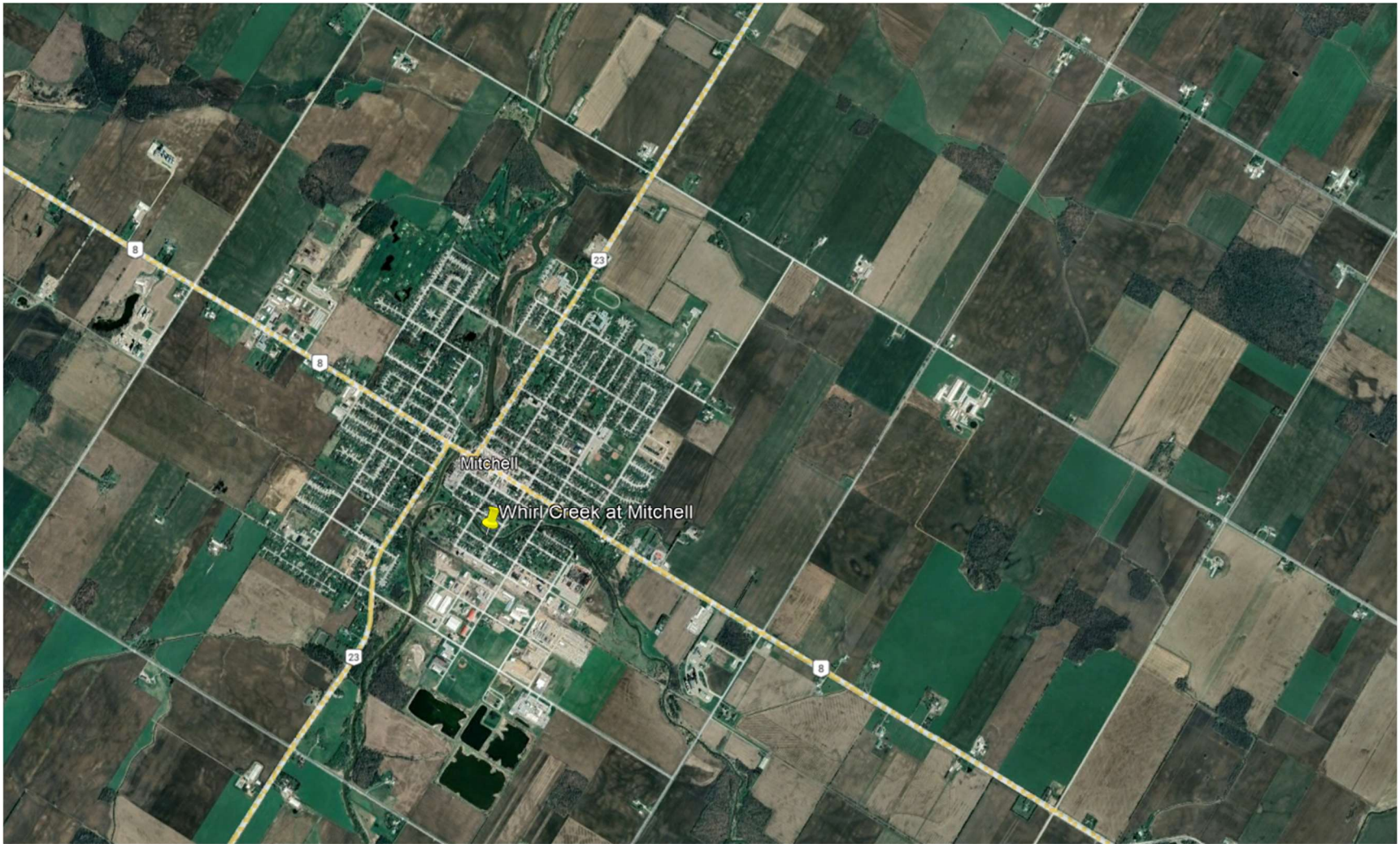
WCM Site Location
Image retrieved from Google Earth Pro©

WCM Qualitative Comments:

The material at WCM is a friable fine grained till prone to block separation, with submerged material being greyer in colour and subaerial material being more light brown. The material was prone to fracturing upon the insertion of the foundation ring, and prone to block separation during the mini-JET. At WCM 1 of the tests received field grade of poor, 6 tests received field grades of moderate and 9 received field grades of good. All of the tests with grades of moderate were influenced by block separation. These tests had usable results prior to the separation occurring, but due to the trapping of blocks within the scour holes did not collect usable data after the separation occurred. These block separations were a result of the friable nature of the material and were noted to be a challenge when performing JETs at this site.
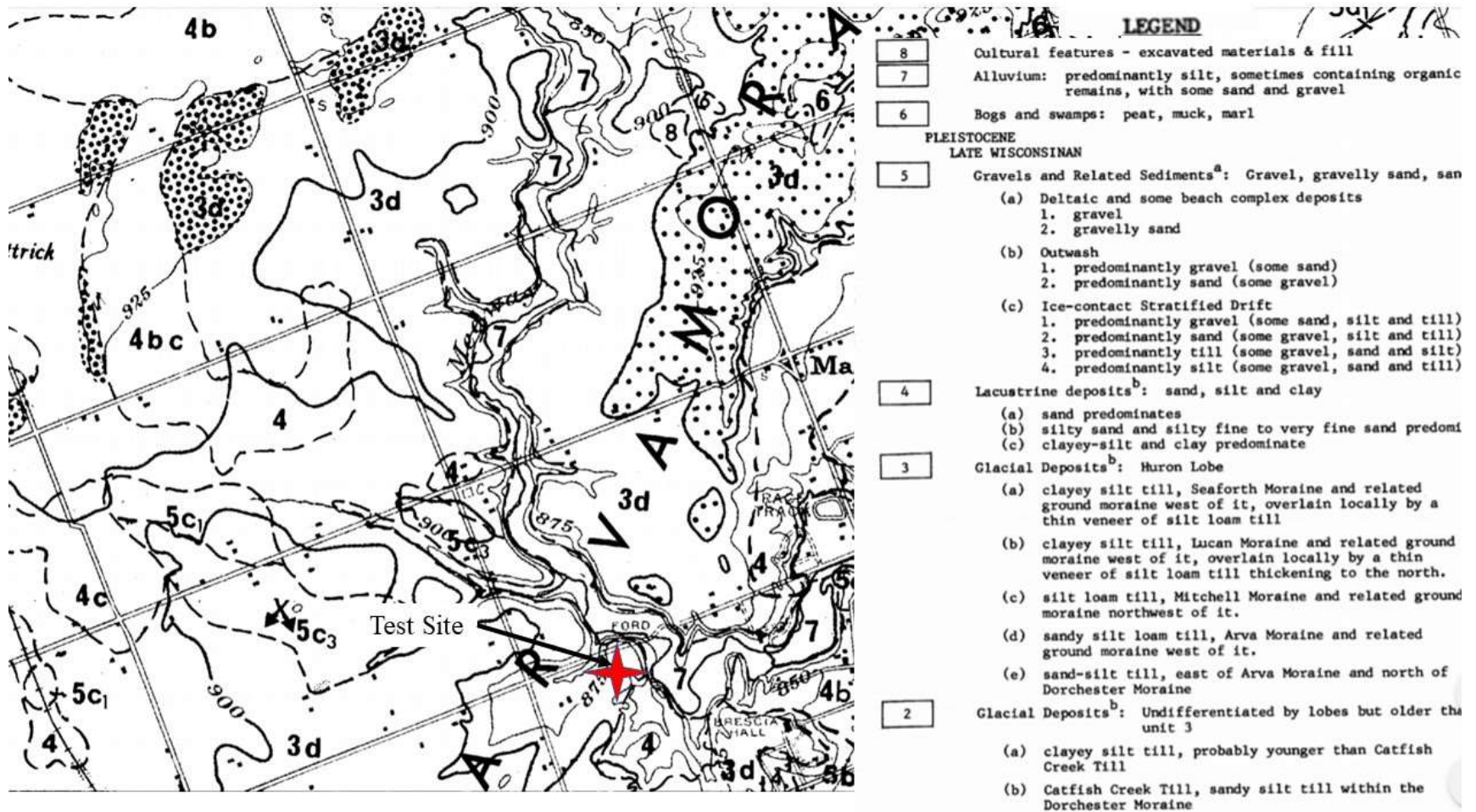
GRL Site Geological Mapping. Map adapted from Sado and Vagners (1975).
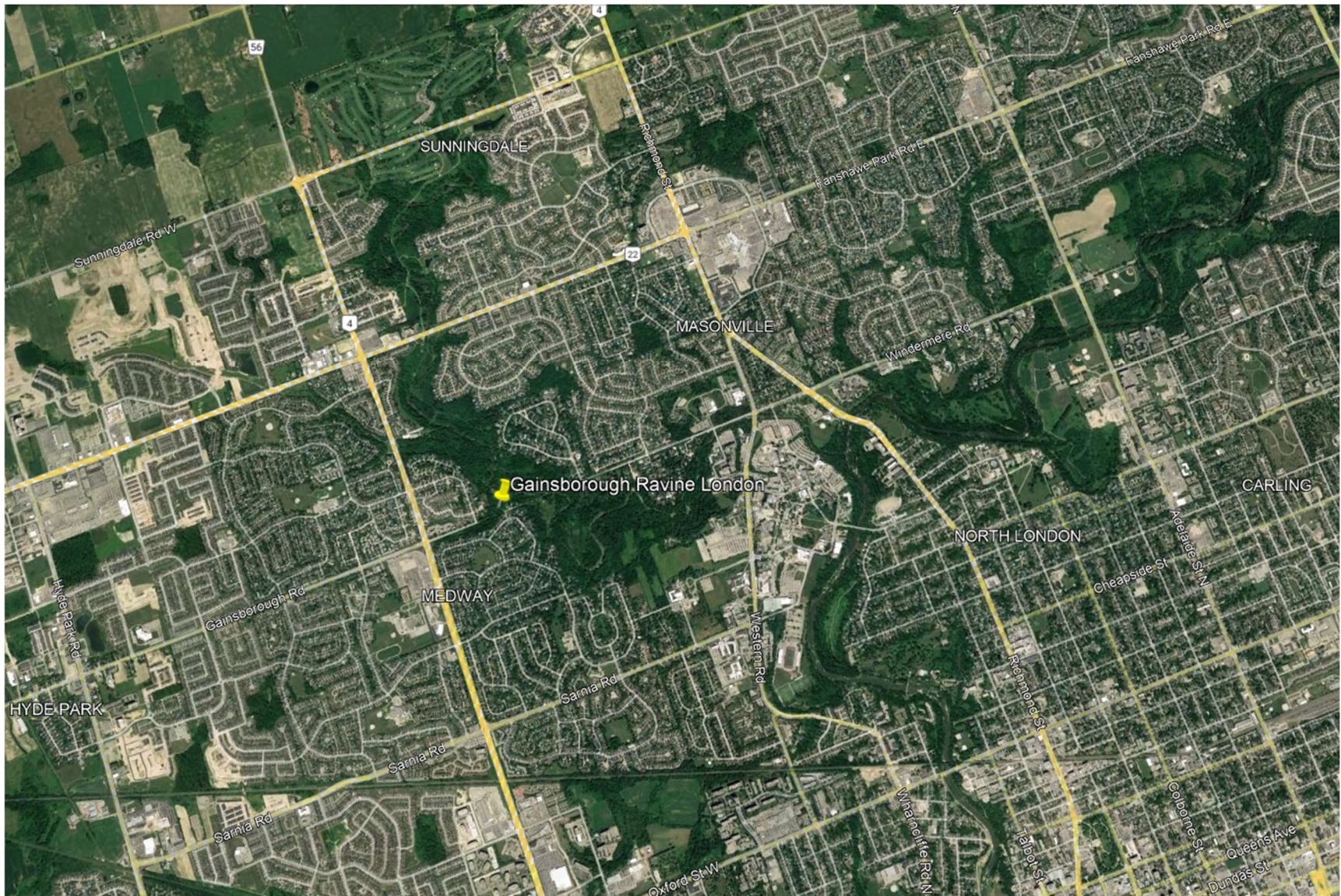
GRL Site Location
Image retrieved from Google Earth Pro©
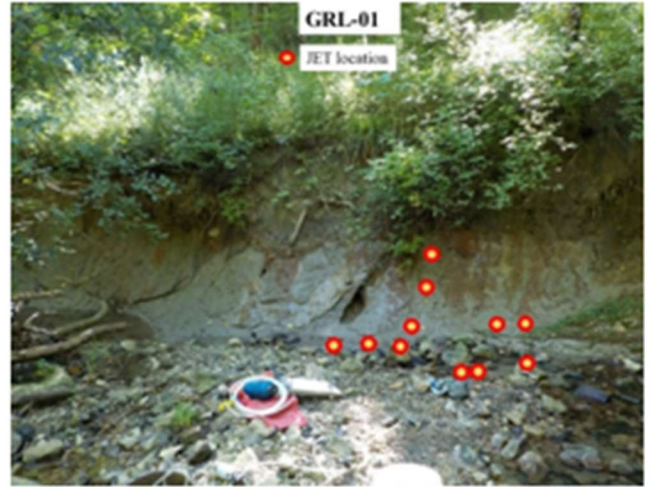
GRL Qualitative Comments:

The material at GRL was observed to be a stiff grey, till with some sands and stones present. The material was frequently exposed along the banks and in patches of the bed with active widening and degradation occurring at the site. GRL tests were mostly assigned a field grade of good. One test assigned a field grade of moderate did not exceed the critical shear of the material with insufficient scour being achieved to characterize the material. While this test was unsuccessful in the characterization of the material's erodibility parameters, it still provides important information regarding a threshold at which the material does not erode. The other test with a moderate grade had a shorter test duration due to the maximum scour depth being reached at 35 minutes. The test with a poor grade ended after 9 minutes due to blocks separated during the test falling into the scour hole and obstructing the progression of the test. The first 9 minutes of the test was uninfluenced by the blocks. Some of the other tests assigned a good field grade were observed to experience small amounts of abrasion by sands and fine gravels, but it was not expected to substantially influence the test results.

LEGEND

16	**Modern Alluvium:** undifferentiated gravel, sand, silt, clay, muck
15	**Organic Deposits:** peat, muck

PLEISTOCENE

LATE WISCONSIN

14	**Older Terrace Alluvium:** poorly sorted, dirty, sand and gravel
13	**Glacial Lake Iroquois Deposits:** beach gravel
12	**Deltaic and Lacustrine Deposits:** predominantly gravelly sand and silty sand
11	**Deltaic and Lacustrine Deposits:** gravel to gravelly sand
10	**Glaciolacustrine Deposits:** massive to laminated silt and clay; may contain poorly sorted diamicton layers
9	**Outwash Deposits:** predominantly sand
8	**Outwash Deposits:** predominantly gravel
7	**Ice-Contact Deposits:** predominantly poorly sorted sand
6	**Ice-Contact Deposits:** predominantly poorly sorted grave
5	**Halton Till:** red to brown, gritty to clayey silt till
4	**Lacustrine Deposits:** interstadial silt and clay
3	**Wentworth Till:** stony sand till

ETC Site Geological Mapping. Map adapted from Karrow and Easton (2005).

ETC Site Location
Image retrieved from Google Earth Pro©

ETC Qualitative Comments:

The material located at ETC displayed characteristics similar to MCE and FC, however, the material was observed to be notably stiffer. The material was exposed along banks and sections of the bed. Here one test was assigned a poor field grade, two tests were assigned moderate field grades and 6 tests were assigned good field grades. During the poor field grade test, the material was excessively influenced by the staff gauge at the measurement point such that the readings were not representative of the scour caused by jet impingement. One of the moderately graded tests did not exceed the critical shear stress of the material. While this test was unsuccessful in the characterization of the material, it still provides important information regarding a threshold at which the material does not erode. The second test with a moderate grade had the foundation ring undermined during the test resulting in the jet nozzle no longer being submerged. The beginning portion of this test remains useable but has a shortened test duration. Sands and fine gravels were observed to potentially contribute to abrasion during some tests.
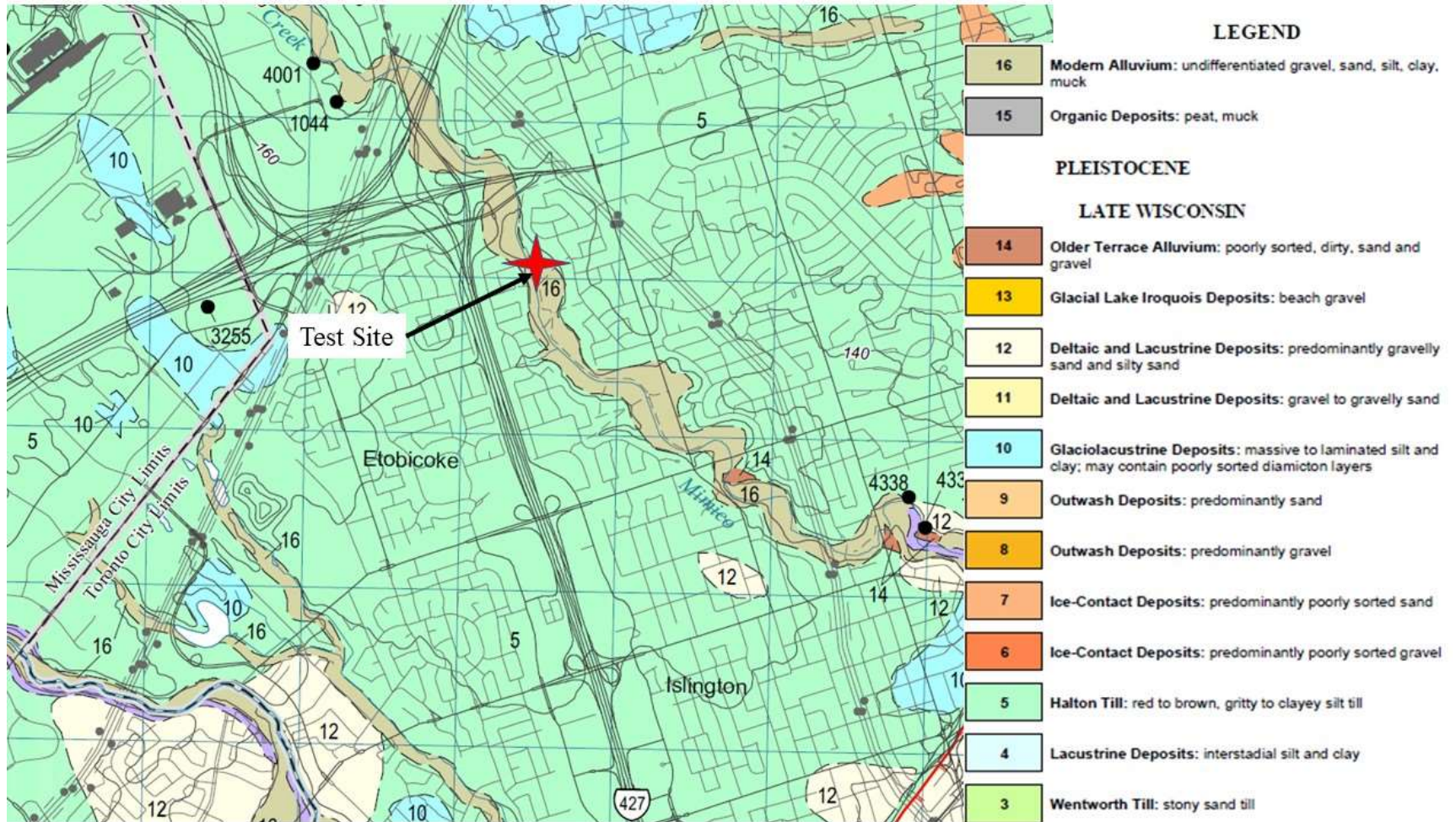
MCE Site Geological Mapping. Map adapted from Karrow and Easton (2005).
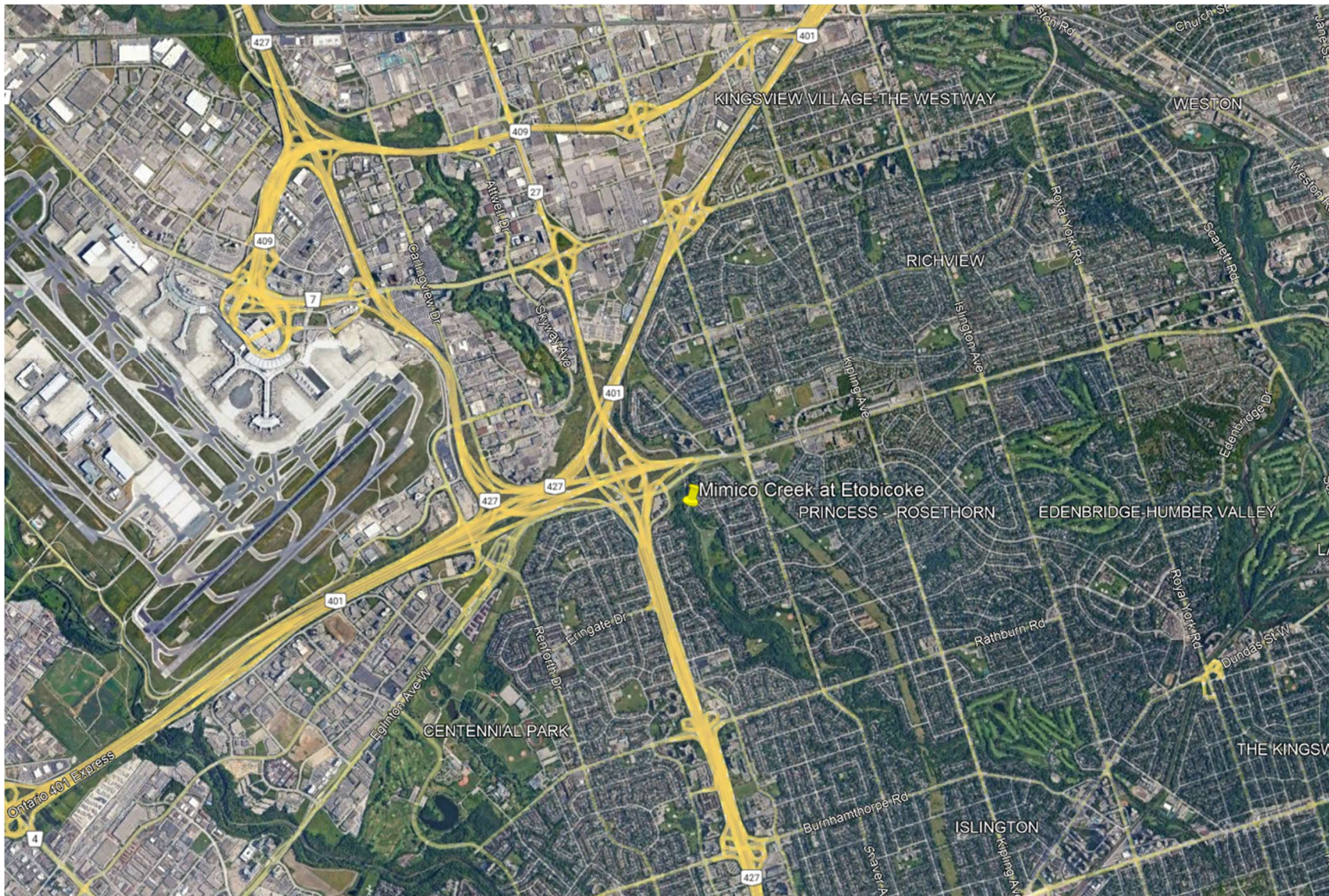
MCE Site Location
Image retrieved from Google Earth Pro©
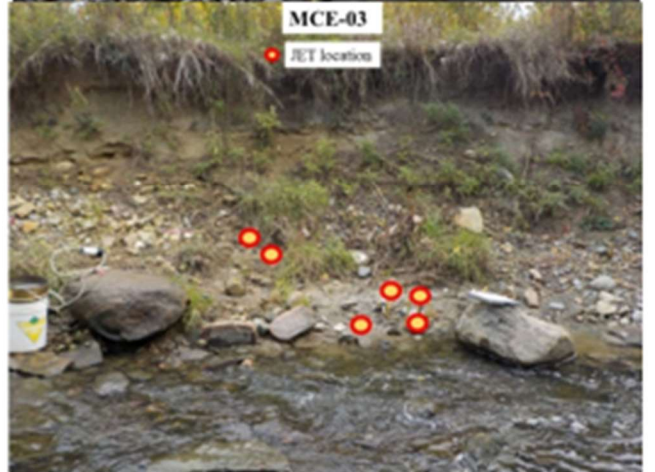
MCE Qualitative Comments:

The material located at MCE displayed similar characteristics to FC (i.e. texture, colour, presence of stones) to FC. It was also exposed along bank toes, along the bed in areas of thin alluvial cover and at higher bank heights along some areas of erosion scarring. All tests at MCE were assigned a field grade of good, however, several tests included observations of sands and gravels potentially contributing to abrasion during the tests. Further, some instances were observed where the maximum point of scour did not align with the measuring point. Based on observations made during the tests, these occurrences were not sufficient to discard the test results.

LEGEND

17	Glaciolacustrine Deposits: gravel and sand in raised (abandoned) shoreline deposits
16	Glaciolacustrine Deposits: sand, minor silt; massive to laminated, nearshore or deltaic bottomset or distal fan deposits
15	Glaciolacustrine Deposits: silt and clay; massive to laminated or rhythmically bedded, basin deposits
14	Glaciodeltaic and Glaciolacustrine Deposits: thick rhythmically bedded sand; including silt, clay and rare flowtills deposited in ice-marginal deltas or subaqueous fa
13	Glaciofluvial Outwash and Glaciodeltaic Deposits: sand and gravel, frequently overlain by several decimetres of sa 13a Deposited as topset beds in an ice-marginal delta 13b Deposited as topset beds in a distal glacier-fed delta
12	Ice-Contact Stratified Deposits: unsubdivided sand and gravel; including minor silt, clay and flowtills; deposited in moraines, eskers, kames, subaqueous fans 12a Sand and gravel 12b Mainly sand
11	Ice-Contact Stratified Deposits: silt, very fine sand and clay; minor gravel, sand and flowtills deposited in ice-supported supraglacial or marginal lake.
10	Ice-Contact Deposits: bedded, massive sandy-silt to clayey-silt, moderate to low clast content (flowtill and subglacial Halton Till); minor gravel, sand, silt and clay deposited along the terminus of a glacier.
9	Till: massive, silt to clayey-silt matrix, high in matrix carbonate content, commonly clast poor; can contain high deformed glaciolacustine sediments (map units 6 and 7 below) (Kettlyby Till)
8	Till: massive, silt to clayey-silt matrix, high in matrix carbonate content, commonly clast poor (Halton Till)
7	Glaciolacustrine Deposits: sand, minor silt; massive to laminated, nearshore or deltaic bottomset or distal fan deposits
6	Glaciolacustrine Deposits: silt and clay; massive to laminated or rhythmically bedded, basin deposits

5	Till: massive, silty sand to sandy-silt matrix, moderate to high matrix carbonate content, clast content moderate to high (includes Newmarket and northern tills)
4	Glaciolacustrine Deposits: sand, minor silt; massive to laminated, nearshore or deltaic bottomset or distal fan deposits
3	Glaciolacustrine Deposits: silt and clay; massive to laminated or rhythmically bedded, basin deposits
2	Glaciofluvial and Ice-Contact Stratified Deposits: sand and gravel; minor silt, clay and flowtills
1	Till: clayey-silt to silty-clay matrix, high in matrix carbonate content, commonly clast poor

WCN Site Geological Mapping. Map adapted from Barnett et al. (2005).

WCN Site Location
Image retrieved from Google Earth Pro©

WCN Qualitative Comments:

The material at WCN is a stiff light brown clay. The material was predominantly exposed along bank toes, portions of the bed and cut banks. At WCN all tests received good field grades. Some of the tests had minimal amounts of scour with the stresses applied during the test being close to the critical shear stress of the material, however, sufficient erosion occurred to characterize the material.

Appendix B: Test Photos

DCB-01-01	
Surface Pre-Test	Surface Post-Test

DCB-01-02	
Surface Pre-Test	Surface Post-Test
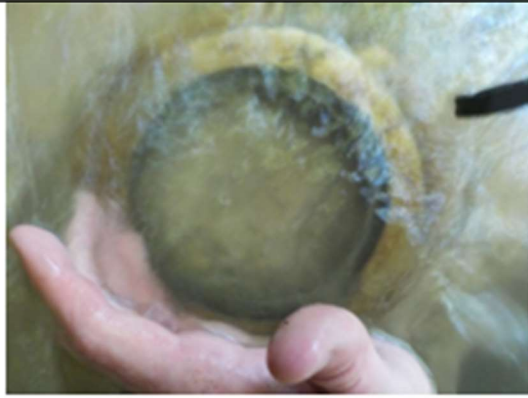
DCB-01-03	
Surface Pre-Test	Surface Post-Test

DCB-01-04	
Surface Pre-Test	Surface Post-Test
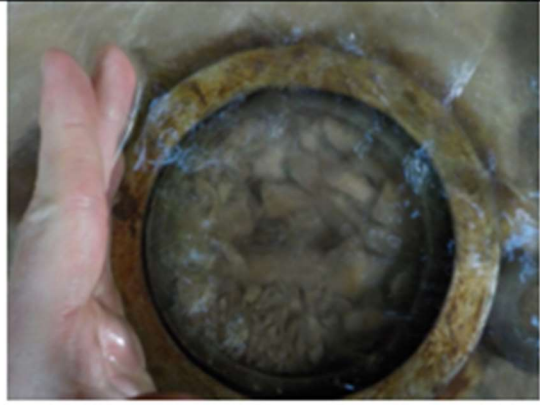
DCB-01-05	
Surface Pre-Test	Surface Post-Test
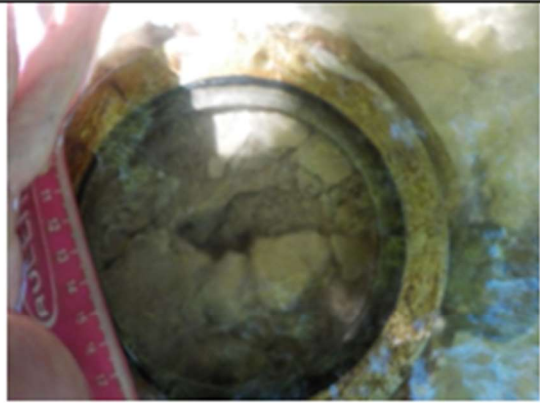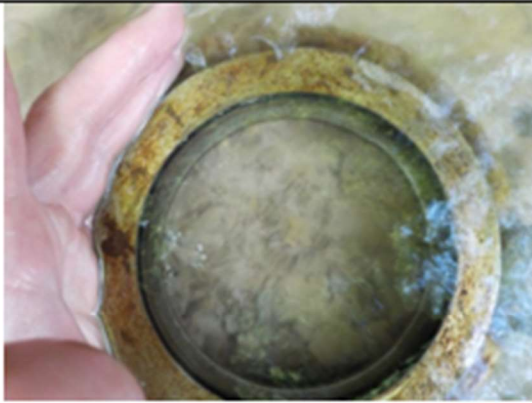
DCB-01-06	
Surface Pre-Test	Surface Post-Test

155
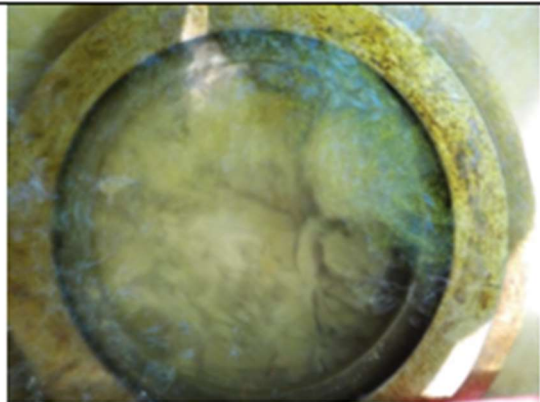
DCB-02-11	
Surface Pre-Test	Surface Post-Test

DCB-02-12	
Surface Pre-Test	Surface Post-Test

DCB-02-13	
Surface Pre-Test	Surface Post-Test

DCB-02-14

Surface Pre-Test	Surface Post-Test

DCB-02-21

Surface Pre-Test	Surface Post-Test

DCB-02-22

Surface Pre-Test	Surface Post-Test

DCB-03-01	
Surface Pre-Test	Surface Post-Test
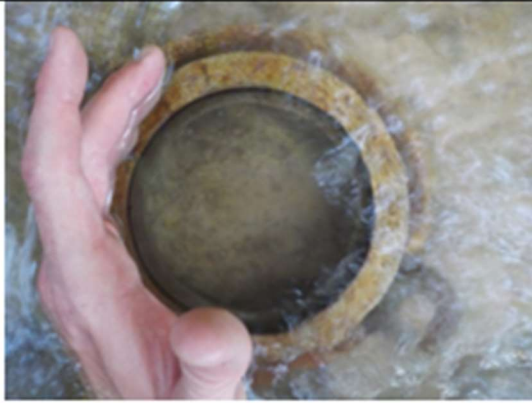
DCB-03-02	
Surface Pre-Test	Surface Post-Test
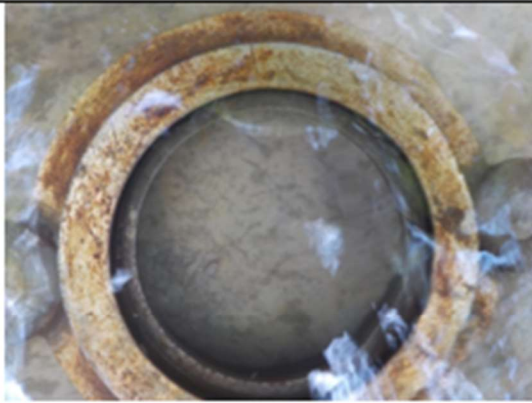
ETC-01-01	
Surface Pre-Test	Surface Post-Test

N/A

ETC-01-02	
Surface Pre-Test	Surface Post-Test

ETC-01-03	
Surface Pre-Test	Surface Post-Test

ETC-01-11	
Surface Pre-Test	Surface Post-Test

ETC-01-12	
Surface Pre-Test	Surface Post-Test

ETC-01-13	
Surface Pre-Test	Surface Post-Test
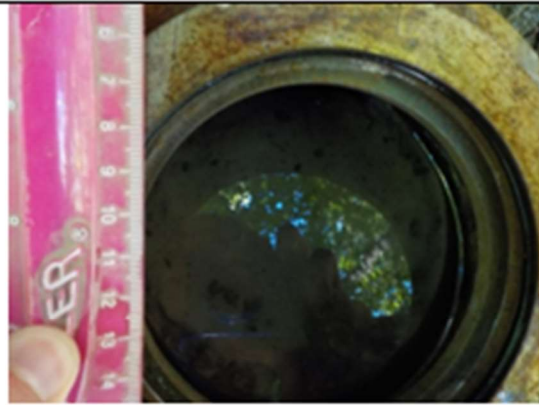
ETC-02-01	
Surface Pre-Test	Surface Post-Test

160

ETC-02-11	
Surface Pre-Test	Surface Post-Test

ETC-02-12	
Surface Pre-Test	Surface Post-Test

FC-01-01	
Surface Pre-Test	Surface Post-Test
N/A	

FC-01-02	
Surface Pre-Test	Surface Post-Test
N/A	

FC-01-03	
Surface Pre-Test	Surface Post-Test
N/A	

FC-01-11	
Surface Pre-Test	Surface Post-Test
N/A	

162

FC-01-12	
Surface Pre-Test	Surface Post-Test
N/A	
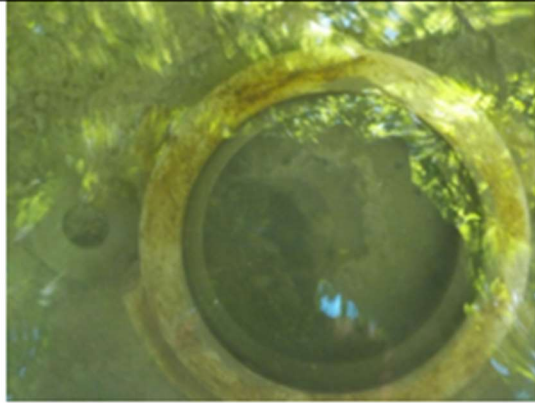
FC-01-13	
Surface Pre-Test	Surface Post-Test
N/A	

FC-02-11	
Surface Pre-Test	Surface Post-Test
N/A	

FC-02-12	
Surface Pre-Test	Surface Post-Test
N/A	

FC-02-13	
Surface Pre-Test	Surface Post-Test
N/A	

FC-02-21	
Surface Pre-Test	Surface Post-Test
N/A	

FC-02-22	
Surface Pre-Test	Surface Post-Test
N/A	

FC-02-23	
Surface Pre-Test	Surface Post-Test
N/A	

FC-02-24	
Surface Pre-Test	Surface Post-Test
N/A	

FC-02-25	
Surface Pre-Test	Surface Post-Test
N/A	

FC-02-26	
Surface Pre-Test	Surface Post-Test
N/A	

FC-03-01	
Surface Pre-Test	Surface Post-Test
N/A	

FC-03-02	
Surface Pre-Test	Surface Post-Test
N/A	

FC-03-03	
Surface Pre-Test	Surface Post-Test
N/A	N/A

FC-03-11	
Surface Pre-Test	Surface Post-Test
N/A	

FC-03-12	
Surface Pre-Test	Surface Post-Test
N/A	

FC-03-13	
Surface Pre-Test	Surface Post-Test
N/A	

FC-03-21	
Surface Pre-Test	Surface Post-Test
N/A	

FC-03-22	
Surface Pre-Test	Surface Post-Test
N/A	

FC-03-23	
Surface Pre-Test	Surface Post-Test
N/A	

GRL-01-01	
Surface Pre-Test	Surface Post-Test
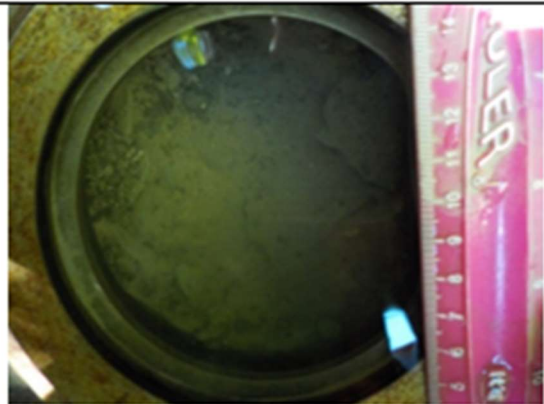
GRL-01-02	
Surface Pre-Test	Surface Post-Test

GRL-01-03	
Surface Pre-Test	Surface Post-Test
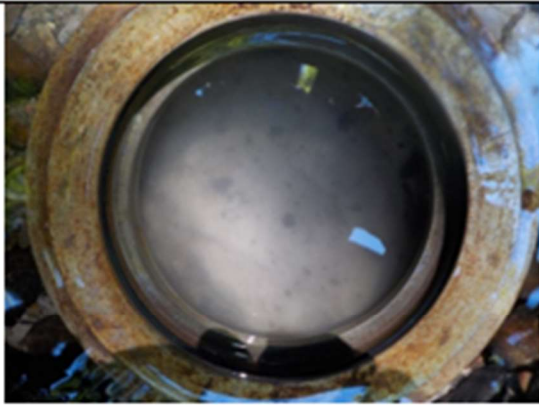
GRL-01-04	
Surface Pre-Test	Surface Post-Test

GRL-01-05	
Surface Pre-Test	Surface Post-Test

GRL-01-06	
Surface Pre-Test	Surface Post-Test

GRL-01-11	
Surface Pre-Test	Surface Post-Test

GRL-01-12	
Surface Pre-Test	Surface Post-Test

GRL-01-13	
Surface Pre-Test	Surface Post-Test

GRL-01-21	
Surface Pre-Test	Surface Post-Test

GRL-01-31	
Surface Pre-Test	Surface Post-Test

GRL-02-11	
Surface Pre-Test	Surface Post-Test

GRL-02-21	
Surface Pre-Test	Surface Post-Test

GRL-02-31	
Surface Pre-Test	Surface Post-Test

GRL-03-11	
Surface Pre-Test	Surface Post-Test

GRL-03-21	
Surface Pre-Test	Surface Post-Test

GRL-03-22	
Surface Pre-Test	Surface Post-Test
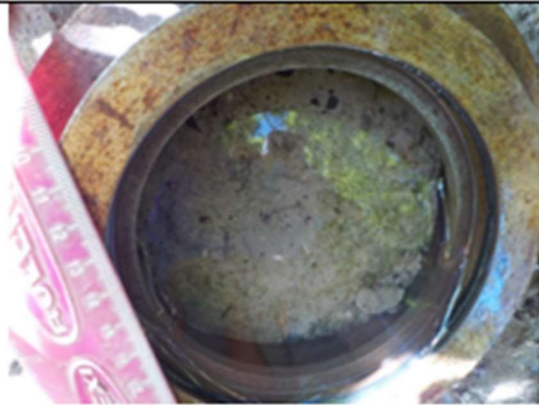
GRL-04-01	
Surface Pre-Test	Surface Post-Test
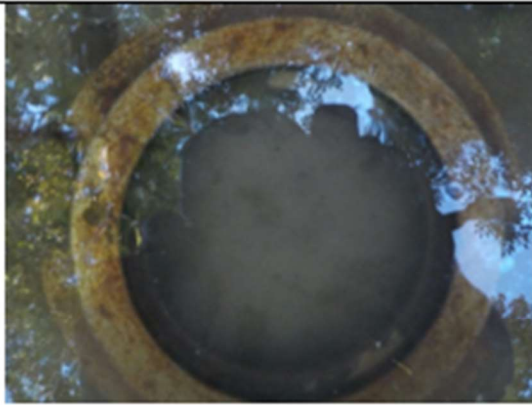
GRL-04-02	
Surface Pre-Test	Surface Post-Test

GRL-05-11	
Surface Pre-Test	Surface Post-Test

GRL-05-12	
Surface Pre-Test	Surface Post-Test

GRL21-01-01	
Surface Pre-Test	Surface Post-Test

GRL21-01-11	
Surface Pre-Test	Surface Post-Test

GRL21-01-12	
Surface Pre-Test	Surface Post-Test

GRL21-01-21	
Surface Pre-Test	Surface Post-Test

GRL21-01-22	
Surface Pre-Test	Surface Post-Test

GRL21-01-23	
Surface Pre-Test	Surface Post-Test

GRL21-01-24	
Surface Pre-Test	Surface Post-Test

GRL21-01-25	
Surface Pre-Test	Surface Post-Test

GRL21-01-26	
Surface Pre-Test	Surface Post-Test

GRL21-01-31	
Surface Pre-Test	Surface Post-Test

GRL21-01-32	
Surface Pre-Test	Surface Post-Test
N/A	

GT-01-04	
Surface Pre-Test	Surface Post-Test

GT-01-05	
Surface Pre-Test	Surface Post-Test
N/A	

GT-01-06	
Surface Pre-Test	Surface Post-Test
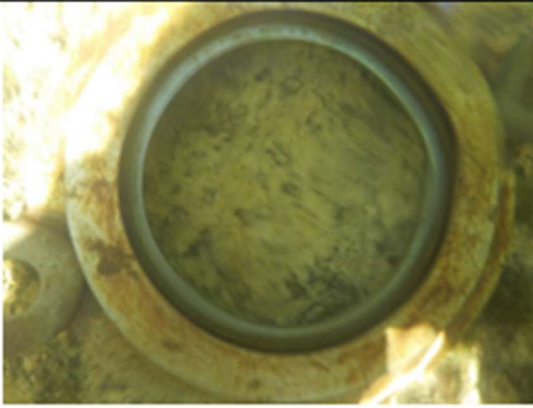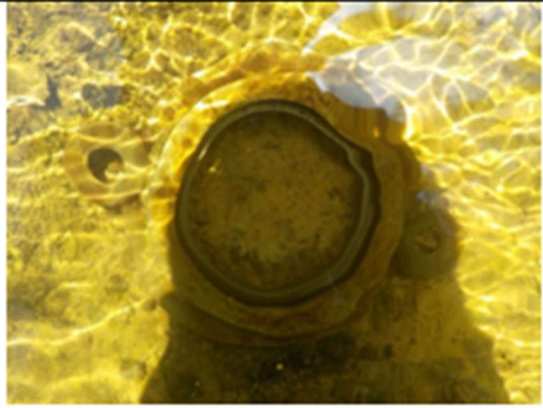
GT-01-07	
Surface Pre-Test	Surface Post-Test
N/A	

GT-01-08	
Surface Pre-Test	Surface Post-Test
N/A	

GT-01-09	
Surface Pre-Test	Surface Post-Test
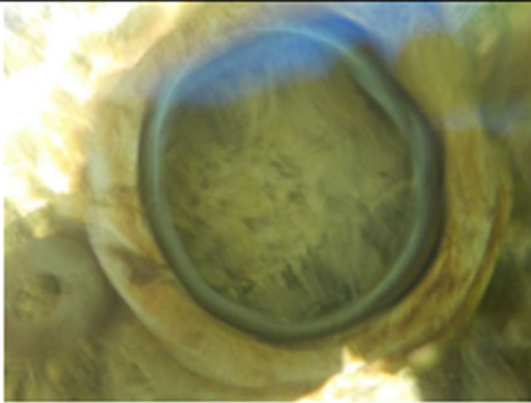
GT-01-010	
Surface Pre-Test	Surface Post-Test
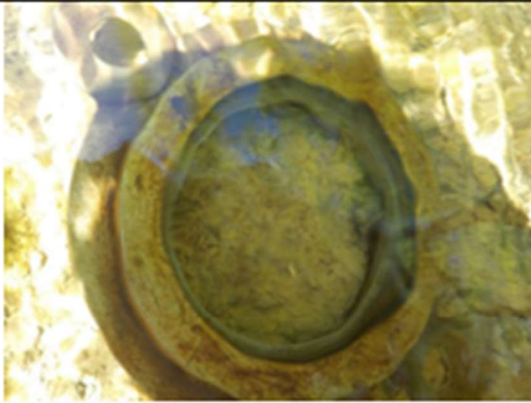
GT-01-011	
Surface Pre-Test	Surface Post-Test

GT-01-012	
Surface Pre-Test	Surface Post-Test
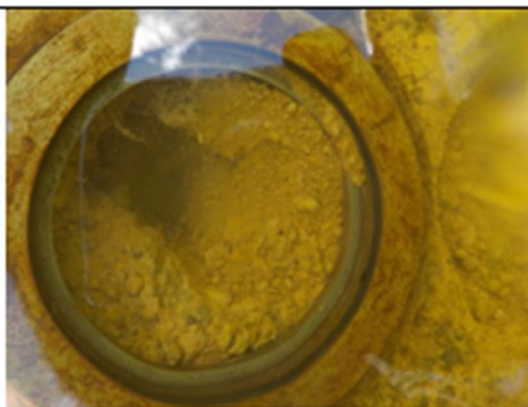
GT-01-013	
Surface Pre-Test	Surface Post-Test

GT-01-11	
Surface Pre-Test	Surface Post-Test

N/A
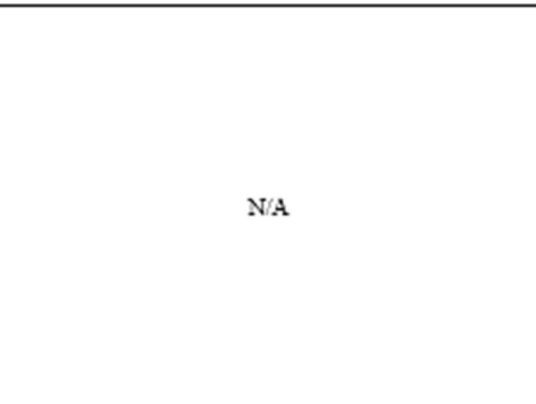
GT-01-12	
Surface Pre-Test	Surface Post-Test
N/A	

GT-01-13	
Surface Pre-Test	Surface Post-Test
N/A	

GT-01-15	
Surface Pre-Test	Surface Post-Test
N/A	

GT-01-16	
Surface Pre-Test	Surface Post-Test
N/A	

HC-01-11	
Surface Pre-Test	Surface Post-Test
N/A	
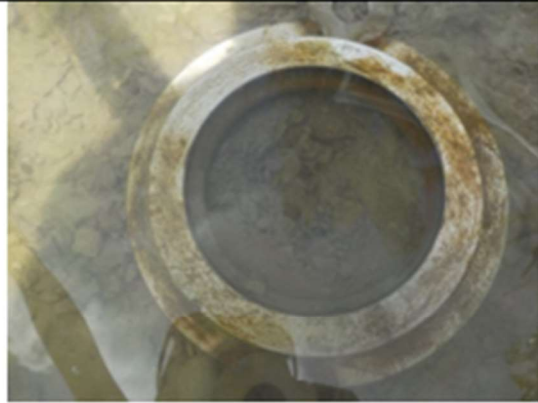
HC-01-12	
Surface Pre-Test	Surface Post-Test
N/A	

HC-01-13	
Surface Pre-Test	Surface Post-Test
N/A	

HC-01-14	
Surface Pre-Test	Surface Post-Test
N/A	

HC-01-21	
Surface Pre-Test	Surface Post-Test
N/A	

HC-01-22	
Surface Pre-Test	Surface Post-Test
N/A	

HC-01-23	
Surface Pre-Test	Surface Post-Test
N/A	

HC-01-31	
Surface Pre-Test	Surface Post-Test
N/A	

HC-01-32	
Surface Pre-Test	Surface Post-Test
N/A	

HC-01-33	
Surface Pre-Test	Surface Post-Test
N/A	

HC-02-01	
Surface Pre-Test	Surface Post-Test
N/A	
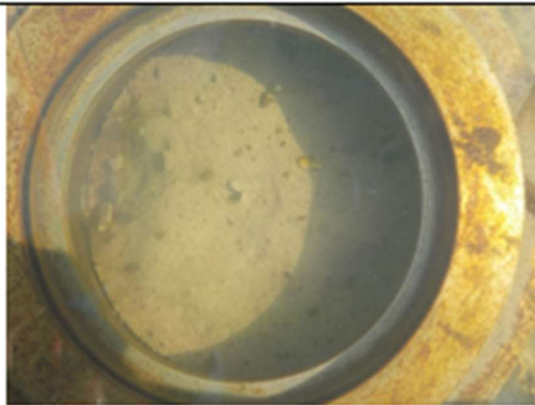
HC-02-02	
Surface Pre-Test	Surface Post-Test
N/A	

HC-02-03	
Surface Pre-Test	Surface Post-Test
N/A	

HC-02-11	
Surface Pre-Test	Surface Post-Test
N/A	

HC-02-12	
Surface Pre-Test	Surface Post-Test
N/A	

HC-02-13	
Surface Pre-Test	Surface Post-Test
N/A	

HC-02-21	
Surface Pre-Test	Surface Post-Test
N/A	

HC-02-22	
Surface Pre-Test	Surface Post-Test
N/A	

HC-03-01	
Surface Pre-Test	Surface Post-Test
N/A	

HC-03-02	
Surface Pre-Test	Surface Post-Test
N/A	

HC-03-03	
Surface Pre-Test	Surface Post-Test
N/A	
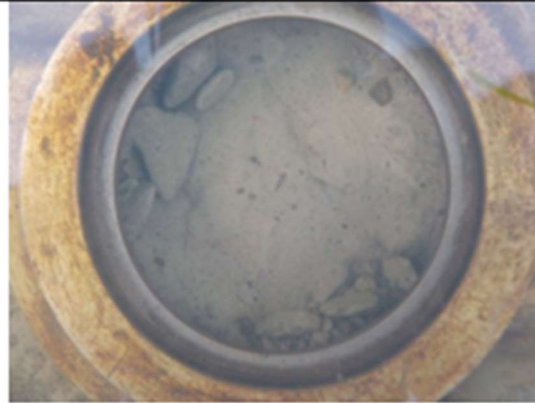
HC-03-11	
Surface Pre-Test	Surface Post-Test
N/A	

HC-03-12	
Surface Pre-Test	Surface Post-Test
N/A	

HC-03-13	
Surface Pre-Test	Surface Post-Test
N/A	

LNC-01-01	
Surface Pre-Test	Surface Post-Test
N/A	

LNC-01-02	
Surface Pre-Test	Surface Post-Test
N/A	

LNC-01-03	
Surface Pre-Test	Surface Post-Test
N/A	

LNC-01-04	
Surface Pre-Test	Surface Post-Test
N/A	

LNC-01-05	
Surface Pre-Test	Surface Post-Test
N/A	

LNC-01-07	
Surface Pre-Test	Surface Post-Test
N/A	

LNC-01-08	
Surface Pre-Test	Surface Post-Test

LNC-01-28	
Surface Pre-Test	Surface Post-Test
N/A	

LNC-01-29	
Surface Pre-Test	Surface Post-Test
N/A	

LNC-01-210	
Surface Pre-Test	Surface Post-Test
N/A	

LNC-02-02	
Surface Pre-Test	Surface Post-Test
N/A	

LNC-02-04	
Surface Pre-Test	Surface Post-Test
N/A	

LNC-02-05	
Surface Pre-Test	Surface Post-Test
N/A	

LNC-03-21	
Surface Pre-Test	Surface Post-Test
N/A	

LNC-03-31	
Surface Pre-Test	Surface Post-Test
N/A	

LNC-04-01	
Surface Pre-Test	Surface Post-Test
N/A	

LNC-04-02	
Surface Pre-Test	Surface Post-Test
N/A	

LNC-04-03	
Surface Pre-Test	Surface Post-Test
N/A	

LNC-04-04	
Surface Pre-Test	Surface Post-Test
N/A	
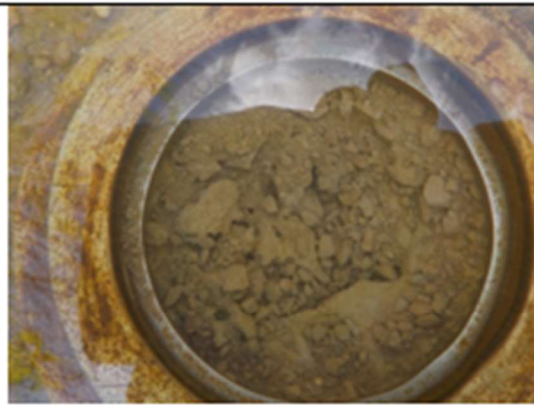
MCE-01-01	
Surface Pre-Test	Surface Post-Test

MCE-01-02	
Surface Pre-Test	Surface Post-Test

MCE-01-03	
Surface Pre-Test	Surface Post-Test
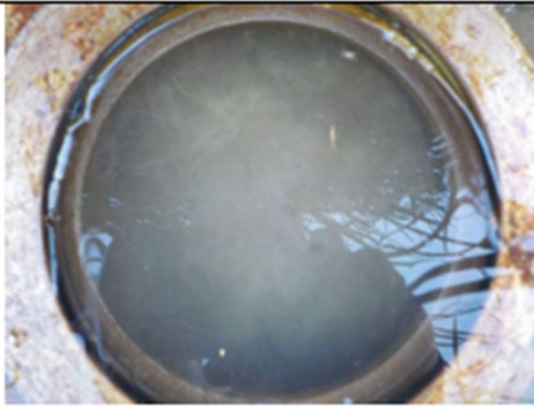
MCE-01-11	
Surface Pre-Test	Surface Post-Test

MCE-01-12	
Surface Pre-Test	Surface Post-Test

MCE-02-01	
Surface Pre-Test	Surface Post-Test

MCE-02-11	
Surface Pre-Test	Surface Post-Test

MCE-02-12	
Surface Pre-Test	Surface Post-Test

MCE-03-11	
Surface Pre-Test	Surface Post-Test

MCE-03-12	
Surface Pre-Test	Surface Post-Test

MCE-03-13	
Surface Pre-Test	Surface Post-Test

MCE-03-14	
Surface Pre-Test	Surface Post-Test
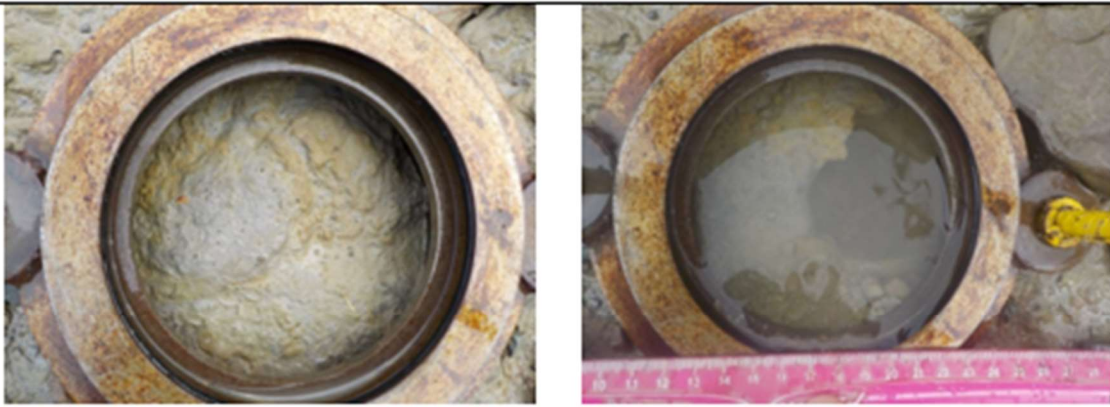
MCE-03-21	
Surface Pre-Test	Surface Post-Test

203

MCE-03-22	
Surface Pre-Test	Surface Post-Test

NMB-01-01	
Surface Pre-Test	Surface Post-Test
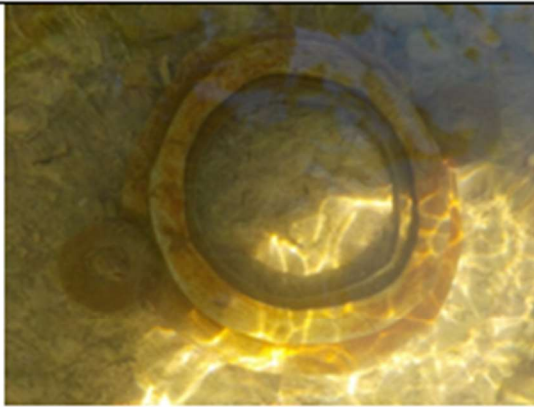
NMB-01-02	
Surface Pre-Test	Surface Post-Test

204

NMB-01-03	
Surface Pre-Test	Surface Post-Test
N/A	

NMB-01-04	
Surface Pre-Test	Surface Post-Test
N/A	

NMB-01-11	
Surface Pre-Test	Surface Post-Test
N/A	

NMB-01-12	
Surface Pre-Test	Surface Post-Test
N/A	

NMB-01-13	
Surface Pre-Test	Surface Post-Test

NMB-01-14	
Surface Pre-Test	Surface Post-Test

NMB-02-01	
Surface Pre-Test	Surface Post-Test
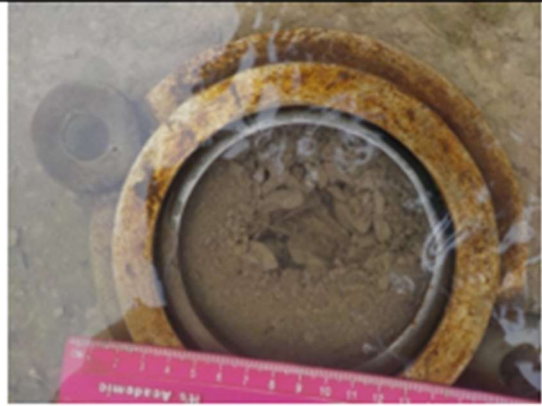
NMB-02-02	
Surface Pre-Test	Surface Post-Test
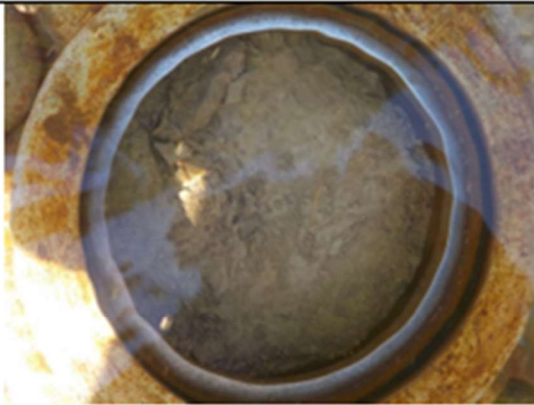
NMB-02-11	
Surface Pre-Test	Surface Post-Test

NMB-02-13	
Surface Pre-Test	Surface Post-Test

NMB-02-14	
Surface Pre-Test	Surface Post-Test

NMB-02-15	
Surface Pre-Test	Surface Post-Test

N/A

NMB-03-11	
Surface Pre-Test	Surface Post-Test

NMB-03-12	
Surface Pre-Test	Surface Post-Test

NMB-03-13	
Surface Pre-Test	Surface Post-Test

NMB-04-11	
Surface Pre-Test	Surface Post-Test

NMB-04-12	
Surface Pre-Test	Surface Post-Test

NMB-04-13	
Surface Pre-Test	Surface Post-Test

NTL-01-01	
Surface Pre-Test	Surface Post-Test
N/A	

NTL-01-02	
Surface Pre-Test	Surface Post-Test

NTL-01-03	
Surface Pre-Test	Surface Post-Test
N/A	
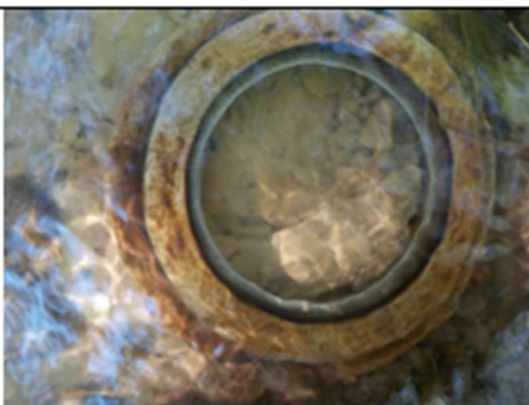
NTL-01-04	
Surface Pre-Test	Surface Post-Test
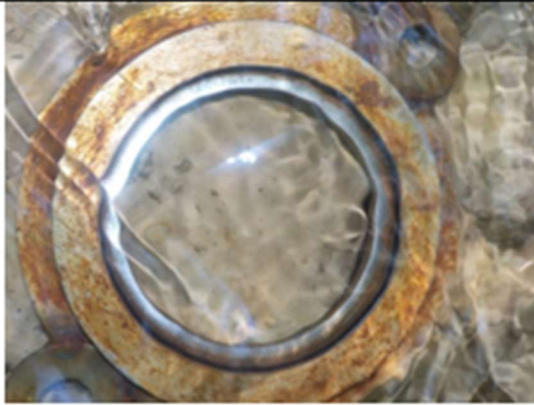
NTL-01-05	
Surface Pre-Test	Surface Post-Test
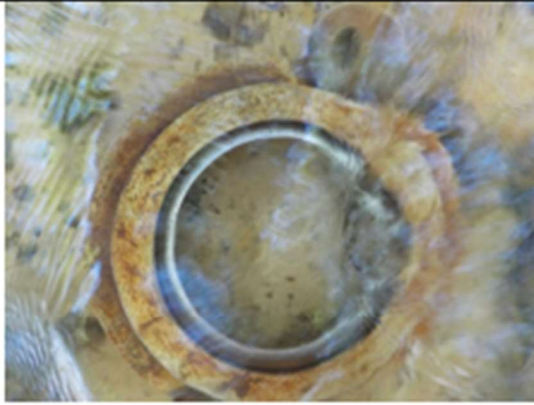
NTL-01-06	
Surface Pre-Test	Surface Post-Test

NTL-01-07	
Surface Pre-Test	Surface Post-Test
N/A	

NTL-01-11	
Surface Pre-Test	Surface Post-Test

NTL-01-12	
Surface Pre-Test	Surface Post-Test

NTL-01-13

Surface Pre-Test	Surface Post-Test

NTL-01-14

Surface Pre-Test	Surface Post-Test

NTL-01-15

Surface Pre-Test	Surface Post-Test

NTL-02-01	
Surface Pre-Test	Surface Post-Test

NTL-02-02	
Surface Pre-Test	Surface Post-Test

NTL-02-03	
Surface Pre-Test	Surface Post-Test

NTL-02-11	
Surface Pre-Test	Surface Post-Test

NTL-02-12	
Surface Pre-Test	Surface Post-Test

N/A

NTL-02-13	
Surface Pre-Test	Surface Post-Test

NTL-02-14	
Surface Pre-Test	Surface Post-Test

NTL-02-21	
Surface Pre-Test	Surface Post-Test

NTL-02-22	
Surface Pre-Test	Surface Post-Test

NTL-02-23	
Surface Pre-Test	Surface Post-Test

TCH-01-01	
Surface Pre-Test	Surface Post-Test

TCH-01-02	
Surface Pre-Test	Surface Post-Test

218
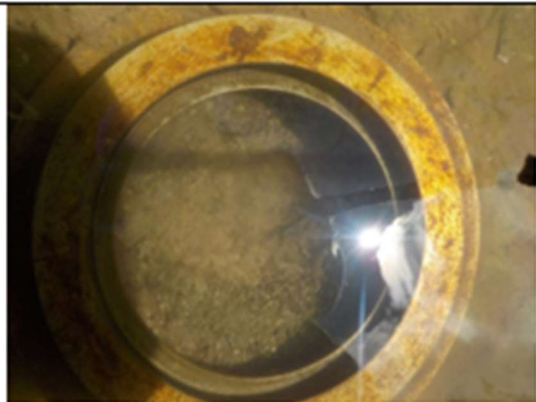
TCH-01-11	
Surface Pre-Test	Surface Post-Test

TCH-01-12	
Surface Pre-Test	Surface Post-Test

TCH-01-13	
Surface Pre-Test	Surface Post-Test

TCH-01-14	
Surface Pre-Test	Surface Post-Test

TCH-01-15	
Surface Pre-Test	Surface Post-Test

TCH-01-16	
Surface Pre-Test	Surface Post-Test

220

TCH-01-17	
Surface Pre-Test	Surface Post-Test

TCH-01-18	
Surface Pre-Test	Surface Post-Test

TCH-01-21	
Surface Pre-Test	Surface Post-Test

221

TCH-01-22	
Surface Pre-Test	Surface Post-Test

TCH-01-23	
Surface Pre-Test	Surface Post-Test

TCH-01-24	
Surface Pre-Test	Surface Post-Test

TCH-01-25	
Surface Pre-Test	Surface Post-Test

TCH-01-26	
Surface Pre-Test	Surface Post-Test

TCH-01-27	
Surface Pre-Test	Surface Post-Test

TCH-01-31	
Surface Pre-Test	Surface Post-Test

TCH-01-32	
Surface Pre-Test	Surface Post-Test

TCH-01-33	
Surface Pre-Test	Surface Post-Test

224

TCH-01-34	
Surface Pre-Test	Surface Post-Test

TCH-01-35	
Surface Pre-Test	Surface Post-Test

TCH-02-11	
Surface Pre-Test	Surface Post-Test

TCH-02-12	
Surface Pre-Test	Surface Post-Test

WCN-01-01	
Surface Pre-Test	Surface Post-Test

WCN-01-02	
Surface Pre-Test	Surface Post-Test
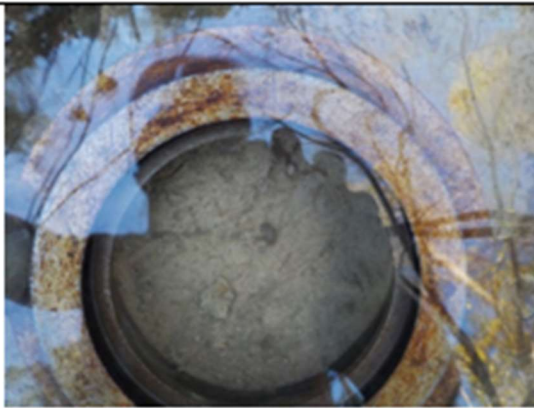
WCN-01-03	
Surface Pre-Test	Surface Post-Test

WCN-01-11	
Surface Pre-Test	Surface Post-Test

WCN-01-12	
Surface Pre-Test	Surface Post-Test

WCN-01-13	
Surface Pre-Test	Surface Post-Test

WCN-02-21	
Surface Pre-Test	Surface Post-Test

WCN-02-22	
Surface Pre-Test	Surface Post-Test

WCN-02-23	
Surface Pre-Test	Surface Post-Test

WCM-01-01	
Surface Pre-Test	Surface Post-Test

WCM-01-02	
Surface Pre-Test	Surface Post-Test
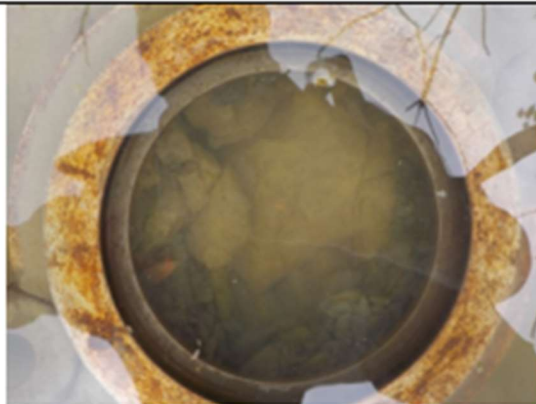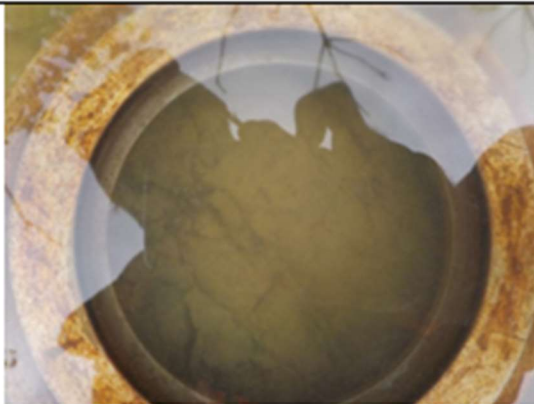
WCM-01-03

Surface Pre-Test	Surface Post-Test
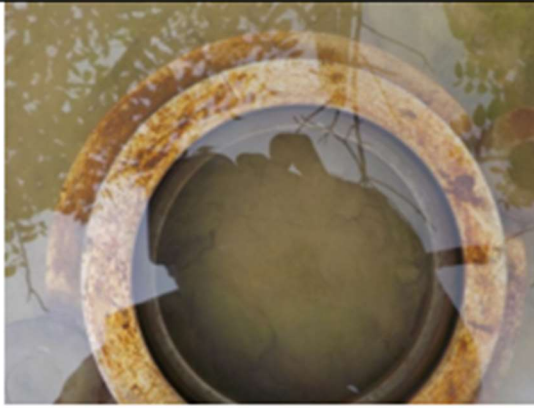
WCM-01-11

Surface Pre-Test	Surface Post-Test
	N/A

WCM-01-12

Surface Pre-Test	Surface Post-Test

WCM-01-13	
Surface Pre-Test	Surface Post-Test

WCM-01-14	
Surface Pre-Test	Surface Post-Test

WCM-01-21	
Surface Pre-Test	Surface Post-Test

WCM-01-22	
Surface Pre-Test	Surface Post-Test

WCM-01-23	
Surface Pre-Test	Surface Post-Test

WCM-01-24	
Surface Pre-Test	Surface Post-Test

WCM-01-25	
Surface Pre-Test	Surface Post-Test

WCM-02-01	
Surface Pre-Test	Surface Post-Test

WCM-02-02	
Surface Pre-Test	Surface Post-Test

WCM-02-03	
Surface Pre-Test	Surface Post-Test
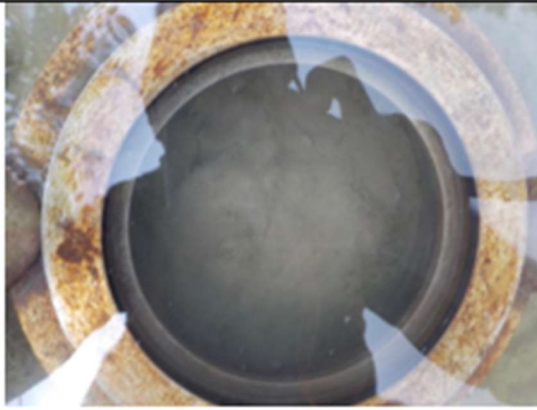
WCM-02-04	
Surface Pre-Test	Surface Post-Test

Appendix C: Coefficient of Discharge Calibration

To account for head-losses between the position of the pressure gauge and the jet nozzle (see Figure 1), Coefficient of Discharge (Cd) calibrations were performed for two tubing connections used in the field (0.5 m and 1.45 m) following the methodology outlined by Al-Madhhachi et al. (2013a). The discharge from the outlet of the JET apparatus was measured using a graduated cylinder over the typical range in field applied pressures. Calculated and measured discharge rates for identical pressure heads (over the range of field applied pressures) were collected and plotted and goodness of fit calculations were performed for both tubing setups yielding a $C_d = 0.96$ and $C_d = 0.73$ for the 0.5 m and 1.45 m tubbing connection respectively.
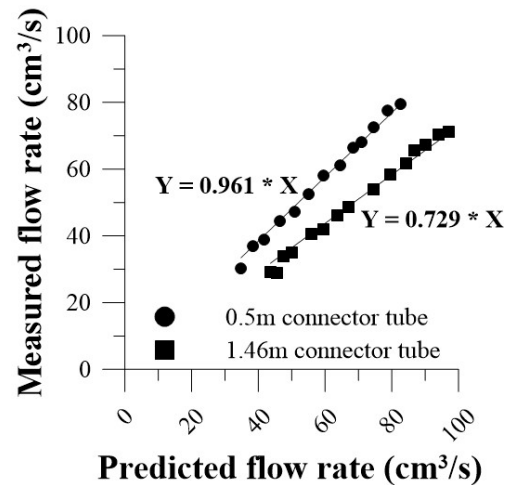
Figure C1: Coefficient pf Discharge Calibration Results

Table C1: Cd Calibration for 0.5m tubing 2020-10-13

Pressure	Head	V	T1	T2	T3	T4	T5	Avg	Q Measured	Q Predicted
(psi)	(cm)	(L)	(Sec)	(sec)	(sec)	(Sec)	(sec)	(sec)	(cm3/s)	(cm3/s)
1.40	98.53	0.50	16.20	16.50	17.00	16.70	16.30	16.54	30.23	34.81
1.70	119.64	0.50	13.75	13.40	13.40	13.60	13.80	13.59	36.79	38.36
2.00	140.75	0.50	13.00	12.80	12.80	12.90		12.88	38.83	41.61
2.50	175.94	0.50	11.50	10.70	11.30	11.20	11.50	11.24	44.48	46.52
3.00	211.13	0.50	10.50	10.80	10.30	10.50	10.70	10.56	47.35	50.96
3.50	246.32	0.50	9.30	9.50	9.60	9.70	9.40	9.50	52.63	55.04
4.10	288.55	0.50	8.70	8.70	8.60	8.40	8.70	8.62	58.00	59.57
4.80	337.81	0.50	8.30	8.00	8.30	8.10	8.20	8.18	61.12	64.46
5.40	380.04	0.50	7.70	7.70	7.50	7.20	7.60	7.54	66.31	68.37
5.80	408.19	0.50	7.30	7.30	7.40	7.50	7.20	7.34	68.12	70.85
6.40	450.42	0.50	6.70	6.80	7.10	7.00	6.80	6.88	72.67	74.43
7.15	503.20	0.50	6.30	6.40	6.50	6.50	6.50	6.44	77.64	78.67
7.90	555.98	0.50	6.40	6.30	6.30	6.30	6.20	6.30	79.37	82.69

Table C2: Cd Calibration for 1.46m tubing 2020-10-20

Pressure (psi)	Head (cm)	V (L)	T1 (Sec)	T2 (sec)	T3 (sec)	T4 (Sec)	T5 (sec)	Avg (sec)	Q Measured (cm3/s)	Q Predicted (cm3/s)
2.40	154.83	0.50	17.20	17.30	17.10	17.20	17.10	17.18	29.10	43.64
2.60	168.91	0.50	17.50	17.30	17.00	17.40	17.60	17.36	28.80	45.58
2.80	182.98	0.50	14.80	14.80	14.60	15.00	14.90	14.82	33.74	47.44
3.10	204.09	0.50	14.30	14.20	14.10	14.40	14.40	14.28	35.01	50.10
3.80	253.36	0.50	12.20	12.50	12.20	12.50	12.30	12.34	40.52	55.82
4.30	288.55	0.50	11.80	11.80	12.00	12.00	11.90	11.90	42.02	59.57
4.90	330.77	0.50	11.00	10.80	10.90	10.80	10.80	10.86	46.04	63.78
5.40	365.96	0.50	10.40	10.20	10.00	10.50	10.30	10.28	48.64	67.09
6.60	450.42	0.50	9.30	9.30	9.30	9.20	9.20	9.26	54.00	74.43
7.50	513.76	0.50	8.60	8.50	8.60	8.50	8.60	8.56	58.41	79.49
8.40	577.10	0.50	8.30	8.30	8.00	8.00	7.90	8.10	61.73	84.25
8.90	612.28	0.50	7.50	7.80	7.80	7.50	7.50	7.62	65.62	86.78
9.60	661.55	0.50	7.40	7.40	7.60	7.30	7.50	7.44	67.20	90.20
10.40	717.85	0.50	7.00	7.10	7.10	7.20	7.20	7.12	70.22	93.96
11.10	767.11	0.50	7.00	6.90	7.10	7.10	7.00	7.02	71.23	97.13

Appendix D: JET Qualitative Observations (field notes)

Test	Test Duration (min)	ZPG (mm)	Max Scour on CL (cm)	Final Shear Stress (Pa)	Fracturing at Ring Insertion	Jet Impingement Issues	Armoring By Pebbles	Vegetation Impacts	Submerged /Subaerial	Scour hole Length (cm)	scour hole Width (cm)	Notes - Field Rating	Final Rating
MCE-01-01	190	74	4.2	12.23	No	No	No	No	Submerged	11.5	11.5	Good test - some abrasion - some sand/pebbles present	Good Test
MCE-01-02	200	63	2.9	13.79	No	No	No	No	Submerged	8	5	Good test - minimal abrasion (less sand/pebbles than MCE-01-01)	Good Test
MCE-01-03	155	76	1.85	13.67	No	No	No	No	Submerged	9	8	Good Test minimal sand/gravel present	Good Test
MCE-02-01	190	77.5	1.75	10	No	No	No	No	Submerged	8	7	Good Test - some sand/gravel present	Good Test
MCE-01-11	145	74.5	2.2	7.75	No	No	No	No	Submerged	8.5	7.5	Good Test- minimal sand/gravel present	Good Test
MCE-01-12	135	74.5	0.3	17.67	no	no	no	no	subaerial	N/A	N/A	Good Test - some roots present on test surface but no impact	Good Test
MCE-02-11	90	62	5.3	9.3	no	no	no	no	subaerial	10.5	8.5	Good test -influenced by abrasion - sand and gravel present by mp was clear	Good Test
MCE-02-12	140	61	5.7	6.48	no	no	no	no	subaerial	9	7.5	Good test - influenced by abrasion - sand and gravel present but mp was clear	Good Test
MCE-03-11	80	74	1.5	14.2	No	No	No	No	Subaerial	10	9	Good test (ring was undermined at 80 mins so test stopped) - some small roots present but no impact. Small hole off centre of MP	Good Test
MCE-03-12	170	62.5	5.35	8.36	No	No	No	No	Subaerial	6.5	6	Good Test - maybe narrow scour hole - jet deflection?	Good Test
MCE-03-13	135	63	1.5	18.32	Slight fracture off centre of MP did influence test	No	No	No	Subaerial	7	6	Good test - not representative of max scour	Good Test
MCE-03-14	140	59.5	2.7	18.73	No	No	No	Small roots present on edge of hole - maybe impacted shape of scour hole but not MP?	Subaerial	7.5	6	Good test- scour limited to one side of test surface	Good Test

ID												Comment	Rating
MCE-03-21	240	57	5.4	8.87	No	No	No	No	Subaerial	11	10.5	Good Test - some minimal abrasion - some sand present but no pebbles/gravels	Good Test
MCE-03-22	135	73	4	7.01	No	No	No	No	Subaerial	11	11	Good test - potentially influenced by abrasion - sand present, some larger stones, MP was clear for test duration	Good Test
GRL-01-01	140	93.5	0.9	10.91	No	No	No	No	Submerged	10	9.5	Good test - some evidence of smaller block erosion at edges. Small amount of sand present	Good Test
GRL-01-02	120	90	1.1	16.44	No	No	No	No	Submerged	N/A	N/A	Good test - small amount of sand present	Good Test
GRL-01-03	100	87.5	0.05	12.34	No	No	No	No	submerged	N/A	N/A	Moderate Test- Tc not exceeded	Poor/Not used
GRL-01-04	120	77.5	0.35	26.53	No	No	No	No	Submerged	N/A	N/A	Good test -s some block separation at edges of surface	Good Test
GRL-01-05	170	83.5	1.25	19.35	No	No	No	No	Submerged	5	4	Good test -small amount of sand present	Good Test
GRL-01-06	105	85	1.25	18.98	No	No	No	No	Submerged	N/A	N/A	Good test - stopped at 105 because of rain	Good Test
GRL-04-01	145	66.5	2.3	20.94	No	No	No	No	Submerged	7.5	7	Good Test -softer than most spots but harder than 05 and 03-11	Good Test
GR-04-02	170	60.5	3.15	19.81	No	No	No	No	Submerged	8.5	7	Good Test -softer than most spots but harder than 05 and 03-11 - last half hour of test removed due to stone causing impingement issues noted at 180 min	Good Test
GRL-01-11	210	71.5	2.4	19.67	No	No	No	No	subaerial	6	5.5	Good Test - small amount of sand	Good Test
GRL-01-12	160	77	0.45	27.49	No	No	No	No	Subaerial	N/A	N/A	Good Test	Good Test
GRL-01-13	150	78.5	0.85	21.88	No	No	No	No	Subaerial	N/A	N/A	Good test - small amount of sand	Good Test
GRL-05-11	180	51	6.5	12.62	No	No	No	No	Subaerial	7	4.5	Good Test - influenced by abrasion -softer material (like 03-11)- sand and small pebbles present	Good Test

GRL-05-12	180	77	0.3	26.54	No	No	No	No	Subaerial	N/A	N/A	Good Test	Good Test
GRL-01-21	70	82.5	0.35	23.25	No	No	No	No	Subaerial	5	5	Good test - ended at 70 due to potential future impact of stone (no impact during test)	Good Test
GRL-02-11	150	78.5	0.55	23.77	No	No	No	No	Subaerial	4	4	Good Test -small amount of sand	Good Test
GRL-02-21	125	83	0.2	23.8	No	No	No	No	Subaerial	7.5	6	Good Test - some block separation at edges of test surface	Good Test
GRL-03-11	150	58	4.25	17.02	No	No	No	No	Subaerial	11	9	Good test -material was softer than other bank tests -some sand/small pebbles	Good Test
GRL-03-21	130	84	0.3	21.88	No	No	No	No	Subaerial	4	3	Good Test	Good Test
GRL-03-22	145	74	0.6	26.54	No	No	No	No	Subaerial	3.5	3	Good Test - some surficial algae, no impact	Good Test
GRL-01-31	155	83	1.1	19.7	No	No	No	No	Subaerial	10.5	6	Good test - scour hole like a line across test surface	Good Test
GRL-02-31	140	75	1.3	22.2	No	No	No	No	Subaerial	9.5	9	Good Test	Good Test
ETC-01-01	125	83.5	0.3	12.2	No	No	No	No	Submerged	N/A	N/A	Poor Test - No scour actually occurred (caused by staff gauge depression) Tc not exceeded	Poor (not usable)
ETC-01-02	125	72	0.2	26.36	No	No	No	No	Submerged	N/A	N/A	Moderate Test right at TC	Tc Not exceeded
ETC-01-03	145	91	0.85	16.94	Some existing "plate" like faults were present but not worsened during ring insertion	No	No	No	Submerged	8	7	Good Test - material was slightly softer than ETC-01-01 and ETC-01-02	Good Test
ETC-02-01	190	81	2.6	14.28	No	No	No	No	Submerged	8	8	Good test - some sand/gravels present	Good Test
ETC-01-11	145	81	0.45	22.36	No	No	No	No	Subaerial	N/A	N/A	Good test	Good Test
ETC-01-12	19	82.5	0.2	22.89	No	No	No	No	Subaerial	N/A	N/A	Moderate Test - Short - ring undermined and nozzle was no longer submerged	Type 1 Only

242

ID														
ETC-01-13	255	92	1.85	13.56	No	No	No	No		Subaerial	8	7	Good test - some potential abrasion - some sand/pebbles present	Good Test
ETC-02-11	65	66	1.55	24.77	No	Test stopped prior to stone impacting impingement	No	No		Subaerial	7	6	Good test -stopped at 65 min due to encountering a stone	Good Test
ETC-02-12	150	73	1.9	19.8	No	No	No	No		Subaerial	8.5	8	Good Test	Good Test
WCN-01-01	125	70	2.05	10.63	No	No	No	some present, may have impacted shape of scour hole? Not MP though	Submerged	9.5	9	Good Test - scour hole was slightly deeper (2-3mm) closer to the roots than MP	Good Test
WCN-01-02	140	86	0.3	19.56	No	No	No	No		Submerged	N/A	N/A	Good Test - small stone just off centre of MP did not impact test at all	Good Test
WCN-01-03	135	81	1.5	18.54	One small block separated right at edge of test surface. Had no impact	No	No	No		Submerged	9	8	Good test - max scour was 1-2 cm deeper than MP	Good Test
WCN-01-11	125	72	3.3	14.92	No	No	No	Some minor roots but no impact		Subaerial	9	7	Good Test - measurements from 85 min to 105 min were removed due to block trapped in hole	Good Test
WCN-01-12	115	48	0.5	30.99	Some pre-existing minor cracks were not worsened at all during ring insertion	No	No	No		Subaerial	N/A	N/A	Good Test - not much erosion	Good Test
WCN-01-13	130	83	0.75	21	No	No	No	No		Subaerial	N/A	N/A	Good Test	Good Test
WCN-02-21	120	73	2.7	16.88	No	No	No	No		Subaerial	11.5	10	Good Test - lots of block erosion early in test	Good Test

243

WCN-02-22	120	60	0.25	29.62	No	No	No	Some roots present - influenced minor erosion off centre of MP but did not influence MP	Subaerial	N/A	N/A	Good test -right at Tc not much scour -one small block separated off centre of MP	Good Test
WCN-02-23	120	69	2.5	19.82	No	No	No	some small roots present but did not have any influence	Subaerial	8.5	8	Good Test	Good Test
FC-01-01	120	62	4.2	5.65	No	No	No	No	Submerged	4.5	4	Good Test	Good Test
FC-01-02	130	63	1	11.46	No	No	No	No	Submerged	4	3.5	Good Test	Good Test
FC-01-03	120	67	0.65	11.31	No	No	No	No	Submerged	3	3	Good Test	Good Test
FC-03-01	122	52.5	5.3	8.23	No	No	some pebbles/sand removed during test	some roots present on one side of hole	Submerged	9	7	Good Test- armouring stones removed during test but continued after without incident. Veg impact was slight on one side portion of test (16mins-32 mins was removed)	Good Test
FC-03-02	119	72	0.7	9.79	No	No	No	No	Submerged	3.5	2.5	Good Test One stone entrenched on one side of scour hole but did not impact test	Good Test
FC-03-03	94	78	0.5	10.64	No	No	No	No	Submerged	3.5	3	Good Test -ended early due to rain/lightning	Good Test
FC-01-11	123	46	1.55	5.65	No	No	No	No	submerged	4	2.5	Good Test	Good Test
FC-01-12	141	65.5	1.5	4.71	No	No	Pebbles present but did not impede test (on edge of hole)	No	submerged	8	6	Good Test Peripheries of scour hole had small gravels but did not influence test or impingement	Good Test
FC-01-13	124	47	1.1	9.08	No	Stone impeding test	No	No	submerged	N/A	N/A	Moderate test: Jet impingement impacted by stone present in scour hole	Poor/Unusable
FC-02-11	129	72	0.95	5.52	No	No	No	No	Submerged	5	4.5	Good Test	Good Test

FC-02-12	134	71	1.05	7.36	No	No	Pebbles removed during test (deemed not to have impacted test)	No	Submerged	7	6	Good Test- Small pebble was removed mid test but test was continued after without impacting the tests	Good Test
FC-02-13	119	55	2.5	9.54	No	No	No	No	Submerged	6	4	Good Test stone present on side of scour hole but did not impact test, just shape of scour hole	Good Test
FC-03-11	145	78	0.95	7.98	No	No	No	No	Submerged	5.5	4	Good Test - 2 small stones in hole but did not impact test	Good Test
FC-03-12	149	65.5	1.4	9.67	No	No	No	No	Submerged	8	7	Good Test - no impingement issues, veg impacts or armouring	Good Test
FC-03-13	127.5	70	1.65	8.16	No	No	stones present outside of hole	No	Submerged	6.5	6	Good Test - small amount of pebbles/sand present outside of hole (abrasion?)	Good Test
FC-02-21	149	65	3.25	9.64	No	No	No	No	Subaerial	8.5	7.5	Good Test - small amount of sand present	Good Test
FC-02-22	140	53	4.7	9.16	No	No	Some pebbles getting tossed - negligible influence on MP	No	subaerial	9.5	6.5	Good Test maybe abrasion	Good Test
FC-02-23	124	58.5	0.55	22.37	No	No	No	No	Subaerial	4	3.5	Good Test	Good Test
FC-02-24	124	57.5	1.4	17.92	No	No	No	No	subaerial	9	7	Good Test	Good Test
FC-02-25	124	53.5	2.25	15.86	No	No	No	No	Subaerial	9	6	Good Test - no impingement issues, veg impacts or armouring	Good Test
FC-02-26	119	58	2.5	13.3	No	No	No	No	Subaerial	9	7	Good Test	Good Test
FC-03-21	135	55.5	2.95	7.61	No	No	small amount of sand present	No	subaerial	6.5	5	Good Test - One stone on side of scour hole did not impact test	Good Test
FC-03-22	90	52	5.4	4.89	No	No	No	roots all around and crossing hole	Subaerial	10	9	Good Test - roots may have impacted test, veg impacts all around	Good Test

245

												scour hole and crossing the hole	
FC-03-23	119	58	1.45	7.55	No	No	No	No	Subaerial	8	5.5	Good Test - no impingement issues, veg impacts or armouring	Good Test
HC-02-01	135	77	0.2	22.51	No	No	No	No	Submerged	N/A	N/A	Moderate Test - Tc Not exceeded	Tc Not exceeded
HC-02-02	135	81.5	0.15	20.39	No	No	No	No	Submerged	N/A	N/A	Moderate Test - Tc Not exceeded	Tc Not exceeded
HC-02-03	155	57	1.1	30.38	No	No	No	No	Submerged	6.5	5.5	Good Test	Good Test
HC-03-01	150	75	0.25	15.26	No	No	No	No	Submerged	N/A	N/A	Good Test	Good Test
HC-03-02	134	82	0.45	18.78	No	No	No	No	Submerged	5	3.5	Good Test	Good Test
HC-03-03	168	74	0.8	20.89	No	No	No	No	Submerged	6	5	Good Test	Good Test
HC-01-11	137	67	2.1	3.15	No	No	some pebbles on bottom of hole	No	submerged	8	9	Moderate Test - Particles were accumulating at the bottom of scour hole	Poor Test - Not Useable
HC-01-12	143	76	2.1	2.6	No	No	No	No	Submerged	7	5.5	Good Test - clean scour hole, some particles on edge of scour hole	Good Test
HC-01-13	124	70	0.85	3.97	No	No	No	No	Submerged	6	4.5	Good Test - No armouring	Good Test
HC-01-14	124	91	0.4	6.77	No	No	No	No	Submerged	5	3	Good Test - No Armouring	Good Test
HC-02-11	149	61	2.5	7.43	slight - should not have influenced test	No	some stones around peripheries of hole	No	Submerged	11	10	Good Test - particle accumulation outside of scour hole	Good Test
HC-02-12	30	58	2.9	7.26	No	Yes -after 30 mins	No	No	Submerged	10	10	Moderate Test - first 30 mins useable- test encountered stone after that	Type 1 Only
HC-02-13	121	70	3	5.5	No	No	no-some sand present	No	Submerged	8	10	Good Test - maybe some abrasion?	Good Test
HC-03-11	124	59	4.2	5.39	No	No	small amount of sand	No	submerged	12	12	Good Test - No armouring but sand present in scour hole - maybe abrasion?	Good Test

							present, no armouring						
HC-03-12	126	58	5.3	4.46	No	No	some small pebbles present - minimal impact	No	Submerged	11	8	Good Test - small pebbles present but no armouring	Good Test
HC-03-13	126	62	4.8	3.53	No	No	small amount of sand present	No	Submerged	8.5	9	Good Test - No armouring but sand present in scour hole - maybe abrasion?	Good Test
HC-01-21_IP	65	52.5	0.9	5.65	No	No	No	roots may have influenced shape	Subaerial	8	7	Good Test - Roots present but were not thought to have influenced test results	Good Test
HC-01-22	120	53.5	3.5	5.46	No	No	No	roots may have influenced shape	Subaerial	7	5	Good Test - Roots present on sides of scour hole, but not on bottom of hole. They were not thought to have influenced results. Sand present (abrasion?)	Good Test
HC-01-23	125	43.5	4.65	5.28	No	No	No	Roots present	Subaerial	8	6.5	Good Test-roots present/crossing hole	Good Test
HC-02-21	129	56	5.8	2.35	No	No	No	roots impacted shape	Subaerial	6	4	Poor Test- Roots present on edges of scour hole and impacted shape, but bottom of scour hole was clear	Poor Test - Not Useable
HC-02-22	124	49	4.95	3.14	No	No	some stones present	roots impacted shape	Subaerial	5.5	4.5	Good Test - small amount of Stones/pebbles present on bottom of scour hole relatively minor impact on MP	Good Test
HC-01-31	129	51.5	2.55	5.15	No	No	No	No	Subaerial	10	8.5	Good Test	Good Test
HC-01-32	129	50	1.7	6.8	No	No	No	No	Subaerial	10	8	good Test	Good Test
HC-01-33	120	57.5	0.65	7.45	Yes	No	No	No	Subaerial	N/A	N/A	Good Test fracturing occurred during hammering of reservoir	Good Test
LNC-01-01_IP	83	61	1.85	4.83	No	No	No	No	Submerged	N/A	N/A	Good Test- scour hole collapsed after running the test at secondary pressure, but initial	Good Test

													pressure test was not impacted
LNC-01-03	158	48	4.15	3.82	no	no	some sand/pebbles present, impact on MP negligible	no	Submerged	6.5	7	Good Test	Good Test
LNC-01-04	160	50	5.4	1.98	No	No	small amount of sand present	minor root presence on one side of scour hole	Submerged	6.5	5.5	Good Test	Good Test
LNC-01-05	147	50	5.7	1.87	No	No	No	root presence on one side of scour hole	submerged	7.25	5	Moderate Test - vegetative influence?	Poor Test - Not Useable
LNC-01-07	138	49	5.3	2.06	No	No	small presence of sand and till pebbles	minor root presence on one side of scour hole	subaerial	6.5	5	scour hole was squarish, and some armouring may have occurred	Good Test
LNC-01-08	116	70.5	0.75	3.51	No	No	No	No	submerged	4	3	Good test	Good Test
LNC-01-28	135	54.5	1.65	4.85	No	No	some small pebbles- negligible influence	No	submerged	8	7.5	Good test	Good Test
LNC-01-29	119	51	0.9	6.79	No	No	some small pebbles present - minimal impact	root presence on one side of scour hole	submerged	5	5	Moderate Test maybe some slight veg impacts on edge of scour hole	Good Test
LNC-01-210	119	55.5	1.05	5.61	No	No	No	minor root presence on one side of scour hole	submerged	5.5	4.5	Good test	Good Test
LNC-02-02_IP	130	48	3.1	3.92	No	No	No	minor vegetation presence	subaerial - right at WL	N/A	N/A	Good Test	Good Test
LNC-02-04	122	63	2	3.55	No	No	No	No	Submerged right at WL	5	4	Good Test	Good Test
LNC-02-05_IP	153	44	4.2	4.13	No	No	No	No	submerged	N/A	N/A	Good Test	Good Test
LNC-03-21	145	51	3.8	7.72	No	No	No	some roots on edge of hole did not impede test	subaerial	5.5	4.5	Good Test	Good Test
LNC-03-31	151	57	2.5	9.08	No	No	No	No	Subaerial	9	7	Good Test	Good Test
LNC-04-01	155	67.5	1.5	4.52	No	No	on periphery of hole but no	No	Submerged	5	4	good test	Good Test

ID													
							impediment to MP						
LNC-04-02	135	69	1.7	4.63	No	No	cleaned scour hole at min 35	No	Submerged	6	5.5	Good test – some block separation	Good Test
LNC-04-03	125	58	0.35	9.69	No	No	one side of hole was covered in blocks. Did not impede MP	No	submerged	7	5	good test	Good Test
lnc-04-04	125	71	1.6	6.46	No	No	some blocks present but not impeding MP - some fell into hole upon removal of JET	No	Submerged	8	6	Good test (pockmarked material fractured during hammering in, test performed on fresh material)	Good Test
GT-01-04	85	53.5	6.25	2.18	No	No	No	Yes roots most likely influenced scour hole shape	submerged	8	8	Good Test - Sand pocket - Lower Tc? More abrasion	Good Test
GT-01-05	140	72	0.8	5.73	No	No	No	No	submerged	5	4.5	Good test	Good Test
GT-01-06	125	73	0.7	5.73	No	No	No	No	Submerged	4	3.5	Good Test	Good Test
GT-01-07	130	64	3.4	3.82	No	pebble armouring	Yes pebbles and sand	No	Submerged	8	7	Moderate Test - stony pebbles armouring hole	Poor Test - Not Useable
GT-01-08	165	69	4.3	2.24	No	pebble armouring	Yes pebbles and sand	No	Submerged	5.5	5	Moderate Test - stony pebbles armouring hole and causing abrasion	Poor Test - Not Useable
GT-01-09	130	67	3.5	2.7	No	no	some pebbles and sand	roots on one side of hole impacted shape	submerged	7	6	Good Test - minimal stony pebbles armouring and causing abrasion. Some vegetative impacts	Good Test
GT-01-010	140	63.5	4.05	2.71	No	No	small presence of pebbles	No	Submerged	6.5	5	Good Test	Good Test
GT-01-011	125	61.5	1.7	3.37	No	No	No	No	Submerged	9	0.5	Good Test - small pebbles fell into hole upon apparatus removal but were not obscuring mp during test	Good Test

ID														
GT-01-012	140	61.5	3.55	2.21	No	No	No	some roots potentially influenced shape	Submerged	8	6	Good Test -some pebbles helped out by slant of test (maybe abrasion)	Good Test
GT-01-013	125	50.5	4.4	2.326	No	No	No	some roots (influenced shape)	submerged	7	4	Good Test	Good Test
GT-01-11	145	41	3.65	5.7	No	No	No- some on "lip" of scour hole	some root presence on edge of scour hole	Submerged	4.5	4.5	good test - some surfical algae was gently removed prior to test	Good Test
GT-01-12	140	48	4.55	3.91	No	No	Material cleaned out partway through	no	submerged	N/A	N/A	Good test (cleaned out scour hole- but end of test was good) - Ended up being good upon data review	Good Test
GT-01-13	140	54	2.7	4.47	No	No	No	some surficial roots around perimeter of hole	submerged	9	8	good test - some surficial algae gently removed prior to test	Good Test
GT-01-15	140	64.5	1.8	3.95	No	No	No	No	Submerged	4.5	4	Good test	Good Test
GT-01-16	120	67.5	0.55	5.04	No	No	No	No	Submerged	5.5	4	Good test	Good Test
NMB-01-01	130	55	4.55	6.53	No	No	No	some roots on edge of hole did not impede test	Submerged	8	8	Good Test	Good Test
NMB-01-02	122.5	58	3.5	3.39	No	Block removed at 11.5 min	No	No	Submerged	8	8	Good Test - blocks were removed and test continued	Good Test
NBM-01-03	140	66	2.8	2.9	No	Blocks removed at 55 min	No	No	Submerged	9	8	Good Test - blocks were removed and test continued	Good Test
NMB-01-04	130	72.5	1.85	3.1	No	No	No	No	submerged	8	7.5	Good Test	Good Test
NMB-01-11	50	71	1	3.72	No	Yes -after 30 mins	No	No	submerged	N/A	N/A	Poor Test - testing a block that had fallen in not the bulk material	Poor Test - Not Useable
NMB-01-12	125	74	0.2	4.23	No	No	No	minor root presence - no impact	submerged	8.5	8	Moderate Test - more resistant material at measuring point (block separation at periphery of test surface) - maybe not enough erosion?	Good Test
NMB-01-13	125	72	0.15	4.52	No	Yes	No	No	Submerged	9	6	Poor Test - maybe good for demonstrating Tc of block- jet was	Poor Test - Not Useable

250

impinging on "ledge" after hole clean

												Poor Test - block erosion kept occurring (3 times)	Poor Test - Not Useable
NMB-01-14					No	Yes	No	No	submerged	7	6	Poor Test - block erosion kept occurring (3 times)	Poor Test - Not Useable
NMB-02-01	125	68	2.15	10.37	No	No	No	minor root presence, no impact	submerged	6	5	Good test	Good Test
NMB-02-02	130	78.5	1.25	3.84	No	No	No	No	Submerged	7	7	Good Test	Good Test
NMB-02-11	125	89	0.9	7.12	No	No	No	No	Submerged	8	7	Good Test	Good Test
NMB-02-13	125	70	2.6	7.42	minor fracturing right by ring - did not impact test	No	No	No	Submerged	8	8	Good Test - some blocks fell into hole upon removal of apparatus, but MP was clear the whole time	Good Test
NMB-02-14	145	72.5	1.35	8.92	minor fracturing right by ring - did not impact test	No	No	NO	Submerged	10	8	Good Test	Good Test
NMB-02-15									subaerial			JET fell out of bank - not useable	Poor Test - Not Useable
NMB-03-11	145	62.5	0.95	6.13	No	No	No	minor root presence - no impact	subaerial	9	5	Good Test	Good Test
NMB-03-12	145	54.5	1.85	7.79	No	No	No	minor root presence - no impact	subaerial	8	4.5	Good Test	Good Test
NMB-03-13	145	57	1.7	7.59	No	No	No	minor root presence - no impact	subaerial	7	5	Good Test - some blocks fell into hole upon removal of apparatus but MP was clear the whole time	Good Test
NMB-04-11	140	65	0.4	12.49	No	No	No	minor root presence - no impact	subaerial	8	7	Good Test	Good Test
NMB-04-12	140	59.5	0.55	17.08	No	No	No	minor root presence - no impact	subaerial	7.5	7	Good Test	Good Test
NMB-04-13	135	50	3.4	15.95	No	No	No	minor root presence - no impact	subaerial	7	6.5	Good Test - some blocks fell into hole upon removal of apparatus byt MP was clear the whole time	Good Test

251

NTL-01-01	135	92.5	0.35	7.29	No	No	No	No	Submerged	8	6	Good Test	Good Test
NTL-01-02	135	79.5	0.8	8.78	No	No	No	No	Submerged	6	5	Good Test	Good Test
NTL-01-03	135	83	0.25	14.37	No	No	No	No	Submerged	N/A	N/A	Good Test	Good Test
NTL-01-04	135	80.5	0.3	17.52	Slight fracture at edge of test surface	No	No	No	Submerged	N/A	N/A	Good Test (had to remove some blocks at 19 min but continued)	Good Test
NTL-01-05	135	80	0.4	17.57	No	No	No	No	Submerged	4	2	Good Test	Good Test
NTL-01-06	130	81	1.2	14.55	No	No	No	No	Submerged	8	7	Not representative of max scour (flow path went underneath ring)	Good Test
NTL-01-07	130	73.5	0.45	20.68	No	No	No	No	Submerged	N/A	N/A	Good test	Good Test
NTL-01-11	130	78	1.6	14.52	No	No	No	No	Subaerial (right at water line)	9	8	Good Test	Good Test
NTL-01-12	24	68	0.9	21.02	No	No	No	No	Subaerial(right at water line)	7	6	Moderate Test - Encountered stone at 30 mins (30-50 mins was not used)	Type 1 Only
NTL-01-13	130	60	4.55	11.2	No	No	No	Yes, roots had a minor impact on shape/progression of scour hole	Subaerial (right at water line)	9	8	good test - maximum scour not captured in early parts of test but it was at later parts after block separation	Good Test
NTL-01-14	130	65.5	0.3	26.04	No	No	No	No	Subaerial	N/A	N/A	Good Test some blocks separated upon removal of JET but not present during test	Good Test
NTL-01-15	140	72	2.45	13.25	No	No	No	No	Subaerial	10	7	Good test	Good Test
NTL-02-01	130	79.5	0.85	16.17	No	No	No	No	Submerged	7	6	Good test	Good Test
NTL-02-02	130	70.5	3.25	11.75	No	No	No	No	Submerged	7.5	5.5	Good Test	Good Test
NTL-02-03	120	77.5	1.8	13.66	No	No	No	No	Submerged	10	8	Not a flat surface for a portion of test - max scour was off centre	Good Test
NTL-02-11	130	75	2.5	12.46	No	No	No	No	Subaerial (right at waterline)	8.5	7.5	Good Test	Good Test

NTL-02-12	130	69	0.3	24.16	No	No	No	No	Subaerial	N/A	N/A	Good Test	Good Test
NTL-02-13	140	55	0.55	34.04	No	No	No	No	Subaerial	7	4.5	Good Test - max scour (~2-3mm deeper) occurred off centre of MP	Good Test
NTL-02-14	135	60.5	0.75	26.95	No	No	No	No	Subaerial	7	6	Good Test	
NTL-02-21	140	61	4.2	16.81	Some preexisting desiccation cracks were not worsened during ring insertion	No	No	No	Subaerial	10	9	Good Test	Good Test
NTL-02-22	125	63	5.15	13.93	No	no	No	No	Subaerial	11	11	Good Test	Good Test
NTL-02-23	130	52.5	5.35	12.66	No	No	No	No	Subaerial	11	10	Good Test- small amount of pebbles present (minor abrasion?)	Good Test
TCH-01-01	135	80	2.55	4.94	No	stone removed at 30 mins	No	No	Submerged	10.5	8.5	Good Test	Good Test
TCH-01-02	145	74	1.55	5.03	No	No	No	No	Submerged	7	6	Good Test	Good Test
TCH-01-11	135	58.5	0.35	15.74	No	No	No	No	Subaerial	10	7	Good Test	Good Test
TCH-01-12	135	52	1.1	28.08	minor fracturing right by ring - did not impact test	No	No	minor root presence, no impact	Subaerial	6	5.5	Good Test	Good Test
TCH-01-13	75	55	3.9	12.75	No	"overhang" of scour hole prevented impingement	No	No	Subaerial	4	3	Poor Test - Narrow hole (jet deflection), stones at 75 min	Poor Test - Not Useable
TCH-01-14	135	53	0.4	21.89	No	No	No	No	Subaerial	3.5	3	Good Test - flat surface/minimal scour occurred	Good Test
TCH-01-15	130	53.5	1.2	21.77	No	No	No	No	Subaerial	4.5	4	Good Test	Good Test
TCH-01-16	135	53	0.4	32.67	No	No	No	NO	Subaerial	5	4	Good Test	Good Test
TCH-01-17	135	57	0.9	28.75	No	No	No	No	Subaerial	5	4	Good Test - weird hole ~ 2 cm away from impingement but no effect on test	Good Test

TCH-01-18	125	59	1.3	32.15	No	No	No	minor root presence, no impact	Subaerial	7.5	6	Good test but there was 3-4 mm of deeper scour off centre of the MP	Good Test
TCH-01-21	135	54	3.65	15.81	No	NO	No	No	Subaerial	6.5	5.5	Good test - some stones fell into hole upon removal of jet but mp was clear whole test	Good Test
TCH-01-22	135	58	1.15	27.47	No	NO	small amount present, no impact on MP - abrasion?	No	Subaerial	6	5	Good test	Good Test
TCH-01-23	120	49.5	3.6	17.42	No	No	No	No	Subaerial	4.5	3	Good Test -Narrow hole	Good Test
TCH-01-24	145	52	1.35	30.68	No	No	small amount present, no impact on MP - abrasion?	No	Subaerial	8	7.5	Good Test	Good Test
TCH-01-25	130	53	1.3	30.22	No	No	Np	No	Subaerial	9	8	Good Test	Good Test
TCH-01-26	180	52	3.2	24.07	No	No	No	NO	Subaerial	5	4	Good test- narrowish hole	Good Test
TCH-01-27	130	58	4.2	17.2	some minor preexisting desiccation cracks	No	small amount present, no impact on MP - abrasion?	No	subaerial	11	9	Good test	Good Test
TCH-01-31	19	59.5	5.7	9.7	some "crumbling	No	No	minor root presence - no impact	Subaerial	10.5	8.5	Moderate test- short duration	Type 1 Only
TCH-01-32	135	61	4.65	5.14	No	No	sand/stones present but did not impede MP, they ended up in scour hole upon removal of JT	No	Subaerial	9	8.5	Good Test	Good Test

254

TCH-01-33	130	52.5	5.6	4.51	minor preexisting fractures, but its representative of material	No	No	No	Subaerial	9.5	8.5	Good Test	Good Test
TCH-01-34	120	62	5.1	3.33	minor preexisting fractures, but its representative of material	No	No	No	Subaerial	8.5	7.5	Good test - minor abrasion caused by sand?	Good Test
TCH-01-35	100	70	3.8	4.1	No	No	NO	NO	Subaerial	11	8.5	Good Test	Good Test
TCH-02-11	40	73	2.1	18.02	No	yes, stopped at 40 min	No	No	Submerged	9	8	Moderate test - block fell into hole at 50 mins short duration	Type 1 Only
TCH-02-12	45	78	3.8	12.14	No	NO	NO	NO	subaerial	12	9	Moderate test- max scour reached after 45 mins - short duration	Type 1 Only
DCB-01-01	75	57	5.95	12.12	some minor fracturing near edge	No	No	No	Submerged	9	7.5	Lots of block erosion. MP was clear the whole time	Good Test
DCB-01-02	136	76	1.1	7.15	some minor fracturing near edge	No	No	No	Submerged	7.5	6	Good Test- block separation noted within test surface	Good Test
DCB-01-03	130	67	0.35	11.11	some slight "plate-like" crumbling	No	No	No	Submerged	8	7	Good Test- block separation noted within test surface	Good Test
DCB-01-04	130	64.5	2	4.28	minor preexisting fractures, but its representative of material	No	No	No	submerged	6	5.5	good test - block separation, mp was clear the whole time, but upon removal of jet, block fell in	Good Test
DCB-01-05	130	75	1.65	3.65	No	No	No	No	submerged	4	3	Good test -block separation noted mp was clear the whole time, but upon removal of jet, block fell in	Good Test
DCB-01-06	27	71.5	0.15	5.73	minor fracturing right by ring - did not impact test	No	No	No	submerged	N/A	N/A	Moderate Test - Short test generator ran out of oil	Type 1 Only
DCB-03-01	120	81	0.15	8.44	No	No	No	No	Submerged	N/a	n/a	Moderate Test - Right at Tc/not exceeded	Tc Not exceeded
DCB-03-02	150	81	0.4	12.68	No	No	No	No	submerged	N/A	N/A	Good Test	Good Test

DCB-02-11	135	83	0.55	9.62	No	No	No	No	submerged	1.5	1.5	Poor test - only erosion occurred directly at measuring point - (maybe influenced by staff gauge?)	Poor Test - Not Useable
DCB-02-12	140	79	0.8	20.9	No	No	NO	NO	subaerial	N/A	N/A	Good test - flat plate like block separation	Good Test
DCB-02-13	121	75	1.45	20.41	No	No	No	No	subaerial	N/A	N/A	Good test	Good Test
DCB-02-14	120	81.5	1	16.99	No	No	No	No	subaerial	N/A	N/A	Good test - flat plate like block separation	Good Test
DCB-02-21	90	77	1.85	17.46	No	No	No	No	subaerial	N/A	N/A	good test - deepest part of hole was maybe 2-3 mm deeper than MP	Good Test
DCB-02-22	120	79	1.95	12.47	No	No	NO	NO	Subaerial	N/A	N/A	Good test - last measurement indicated additional block separation was occurring but test was stopped	Good Test
WCM-01-01	65	75	1.2	5.97	No	No	No	No	Submerged	6	5	Block fell into hole at 80 mins stopping test	Good Test
WCM-01-02	120	80	0.45	6.33	Minor fracturing near edge of test surface	No	No	No	Submerged	N/A	N/A	good test - lots of block erosion around MP but it was clear the whole time	Good Test
WCM-01-03	120	72	0.75	8.89	Minor fracturing off centre of MP	No	No	No	Submerged	N/A	N/A	Poor Test - this test describes a block that separated but was trapped under the impinging jet	Poor Test - Not Useable
WCM-02-01	120	75.5	0.2	4.68	slight fracturing but representative of material	No	No	No	Submerged	N/A	N/A	Good test - at end of test, the test surface was fractured but no block separation had occurred	Good Test
WCM-02-02	65	81	0.7	5.21	no	yes	no	surficial algae gently removed	submerged	N/A	N/A	Good test but was testing a block that was trapped under the jet	Good Test
WCM-02-03	11	76	3.05	11.53	No	not until test stopped	No	surficial algae gently removed	submerged	6.5	6	Moderate Test - Short test at max pressure	Type 1 Only
WCM-02-04	100	69.5	0.8	15.87	No	No	No	surficial algae gently removed	submerged	7	6.5	Good test - lots of block separation but MP was clear the whole test	Good Test

WCM-01-11	24	70	2.3	9.33	minor crumbling near edge of test surface	not until test stopped	No	No	Subaerial	N/A	N/A	Moderate Test - Tons of block erosion- block fell into hole at 30 mins and jet apparatus could not be replaced accurately	Type 1 Only
WCM-01-12	24	60	3.8	8.84	slight crumbling near edge of test surface	not until test stopped	No	No	Subaerial	N/A		Moderate Test -Tons of block erosion- block fell into hole at 30 mins and jet apparatus could not be replaced accurately	Type 1 Only
WCM-01-13	120	51.5	0.25	17.47	minor fracturing off centre	No	No	No	Subaerial	N/A	N/A	some slight fracturing on ring insertion but off centre of MP and did not impact test - good test	Good Test
WCM-01-14	120	82	0.2	10.83	No	No	No	No	Subaerial	N/A	N/A	Good test- not much erosion occurred	Good Test
WCM-01-21	35	72	4.45	5.32	No	not until test stopped	No	No	Subaerial	11	8.5	Moderate Test - staff gauge max reached after 35 min	Type 1 Only
WCM-01-22	40	74	4.25	3.6	No	No	No	minor root presence around edge of scour hole	subaerial	8	7	Moderate Test	Type 1 Only
WCM-01-23	50	76.5	2.45	3.95	No	not until test stopped	No	minor root presence	subaerial	8.5	6	Moderate Test - block fell in at 65 mins	Type 1 Only
WCM-01-24	120	78.5	0.25	5.5	No	No	No	NO	Subaerial	N/A	N/A	Good test	Good Test
WCM-01-25	100	59.5	4.4	3.37	minor fracturing	No	No	minor root presence	subaerial	8	7	Good test - block fell in at 120	Good Test
GRL21-01-01	35	50	5	12.71665242	No	No	No	No	Submerged	9	9	Moderate Test - Short duration, Some till pebbles fell in upon JET removal but did not influence test progression - maybe influenced by alluvial contact weathering	Poor (type1 usable)
GRL21-01-11	140	52	3.9	15.89823867	No	No	Some pebbles present but no armouring (slight abrasion?)	No	Subaerial	9	8.5	Good Test	Good Test

257

GRL21-01-12	130	48.5	4.2	13.38741855	No	No (2 stones off centre - no impact)	No (some abrasion?)	No	Subaerial	10	8	Good Test	Good Test
GRL21-01-21	90	39	1.85	18.23753056	No	No	No	No	Subaerial	7	5	Good Test	Good Test
GRL21-01-22	63	50	3.4	15.81617702	No	No	No (some sand and pebbles, Abrasion?)	No	Subaerial	10	8	Good Test	Good Test
GRL21-01-23	60	61	4.15	17.64202902	No	Stopped at 60 because of stone	No (abrasion?)	No	Subaerial	10	9	Good Test, till pebbles fell in upon JET removal but were not present during test and did not influence test progression	Good Test
GRL21-01-24	95	49.5	3.6	15.45768936	No	Stopped at 95 cus of stone	No	No	Subaerial	8	7	Good Test, some sand and minor abrasion noted	Good Test
GRL21-01-25	125	46	1.25	24.35834113	No	No	No	No	Subaerial	9	8	Good Test	Good Test
GRL21-01-26	70	48.5	1.05	27.55253156	No	No	No	No	Subaerial	N/A	N/A	Good Test	Good Test
GRL21-01-31	9	55	2.35	23.23209794	No	Yes, stopped at 11	Yes, Stopped at 11	No	Subaerial	N/A	N/A	poor Test - useful for Type 1, lots of till pebbles/blocks present afterwards, but short	Poor (type1 usable)
GRL21-01-32	130	46	2.3	18.49974279	No	No	No	No	Subaerial	N/A	N/A	Good Test	Good Test
CCT-01-01	55	46	0.4	15.09621724	no	Yes, big stone right in middle of jet impingement	no	no	submerged	9	8	Poor - not useable from stone effect on impingement	Poor
CCT-01-02	140	55	1.85	13.75904218	no	no	minor pebble presence but no impact	no	submerged	8	7	good test	Good Test
CCT-01-03	130	55	0.95	18.27137643	no	no	minor pebble presence but no impact	no	submerged	7	6	good test	Good Test

258

Appendix E: Test Segmentation Results

Segmentation Technique Comparison

Test	Total Scour Depth (cm)	Visual identification of type 1		Max Norm Residual identification of type 1		Gill Technique		Method Deemed Representative
		Time of Type 1 Region (min)	Depth of Type 1 Region (cm)	Time of Type 1 Region (min)	Depth of Type 1 Region (cm)	Time of Type 1 Region (min)	Depth of Type 1 Region (cm)	
MCE-01-01	4.20	1.00	0.25	40.00	0.95	1.00	0.25	VA+GM
MCE-01-02	2.90	0.75	0.25	75.00	1.55	0.75	0.25	VA+GM
MCE-01-03	1.85	3.00	0.30	9.00	0.50	0.75	0.15	VA
MCE-02-01	1.75	2.00	0.40	3.00	0.45	0.75	0.20	VA
MCE-01-11	2.20	0.25	0.10	30.00	0.50	1.50	0.15	VA
MCE-01-12	0.30	3.00	0.10	3.00	0.10	3.00	0.10	All
MCE-02-11	5.30	4.00	1.00	30.00	1.45	2.00	0.65	VA
MCE-02-12	5.70	24.00	2.70	14.00	1.10	0.50	0.15	VA
MCE-03-11	1.50	3.00	0.55	3.00	0.55	0.50	0.30	VA+MNR
MCE-03-12	5.35	1.50	0.90	1.50	0.90	1.50	0.90	All
MCE-03-13	1.50	3.00	0.30	40.00	0.60	3.00	0.30	VA+GM
MCE-03-14	2.70	1.50	0.10	50.00	0.75	85.00	2.45	VA
MCE-03-21	5.40	8.00	2.40	8.00	2.40	0.50	0.40	All
MCE-03-22	4.00	0.75	2.00	1.50	2.10	0.75	2.00	VA+GM
GRL-01-01	0.90	1.50	0.20	9.00	0.35	1.50	0.20	VA+GM
GRL-01-02	1.10	1.00	0.20	7.00	0.35	1.00	0.20	VA+GM
GRL-01-04	0.35	0.25	0.05	5.00	0.16	2.00	0.10	VA
GRL-01-05	1.25	0.00	0.00	65.00	0.45	4.00	0.10	VA
GRL-01-06	1.25	0.25	0.05	24.00	0.15	2.00	0.10	VA
GRL-04-01	2.30	1.00	0.25	40.00	0.85	0.50	0.20	VA
GR-04-02	3.15	0.25	0.15	100.00	2.95	3.00	0.40	VA
GRL-01-11	2.40	0.50	0.25	14.00	0.50	0.50	0.25	VA+GM
GRL-01-12	0.45	1.50	0.10	1.50	0.10	1.50	0.10	VA+GM
GRL-01-13	0.85	0.75	0.55	0.75	0.55	0.50	0.50	VA+MNR
GRL-05-11	6.50	0.00	0.00	12.00	0.85	6.00	0.70	VA
GRL-05-12	0.30	0.75	0.05	0.75	0.05	50.00	0.10	VA+MNR
GRL-01-21	0.35	0.75	0.15	0.75	0.15	0.75	0.15	All
GRL-02-11	0.55	1.00	0.10	7.00	0.15	1.00	0.10	VA+GM
GRL-02-21	0.20	1.50	0.05	9.00	0.10	9.00	0.10	VA
GRL-03-11	4.25	1.50	0.55	1.50	0.55	0.50	0.40	All
GRL-03-21	0.30	0.75	0.15	0.75	0.15	0.75	0.15	All
GRL-03-22	0.60	0.75	0.10	0.75	0.10	0.75	0.10	All
GRL-01-31	1.10	7.00	0.65	11.00	0.80	0.50	0.10	VA
GRL-02-31	1.30	0.50	0.05	80.00	0.65	9.00	0.10	VA

ETC-01-03	0.85	1.00	0.20	5.00	0.30	1.00	0.20	VA+GM
ETC-02-01	2.60	2.00	0.20	2.00	0.20	1.50	0.15	VA+MNR
ETC-01-11	0.45	1.50	0.10	14.00	0.25	1.50	0.10	VA+GM
ETC-01-13	1.85	0.75	0.10	80.00	0.45	0.75	0.10	VA+GM
ETC-02-11	1.55	1.50	0.20	50.00	0.90	1.00	0.15	VA
ETC-02-12	1.90	2.00	0.25	2.00	0.25	0.50	0.10	VA+MNR
WCN-01-01	2.05	0.50	0.35	0.50	0.35	0.50	0.35	All
WCN-01-02	0.30	0.25	0.10	3.00	0.15	3.00	0.15	VA
WCN-01-03	1.50	14.00	1.10	14.00	1.10	0.50	0.20	VA+MNR
WCN-01-11	3.30	4.00	1.50	4.00	1.45	1.00	1.00	VA+MNR
WCN-01-12	0.50	11.50	0.40	0.25	0.05	1.50	0.10	VA
WCN-01-13	0.75	3.00	0.15	7.00	0.20	1.50	0.10	VA
WCN-02-21	2.70	7.00	1.70	7.00	1.70	1.00	0.45	VA+MNR
WCN-02-23	2.50	2.00	1.60	2.00	1.60	2.00	1.60	All
FC-01-01	4.20	4.00	2.70	0.75	2.30	0.50	2.20	VA
FC-01-02	1.00	0.50	0.10	64.00	0.45	0.50	0.10	VA+GM
FC-01-03	0.65	4.00	0.35	4.00	0.35	0.75	0.20	VA+MNR
FC-03-01	5.30	9.00	4.00	9.00	4.00	0.50	0.75	VA+MNR
FC-03-02	0.70	1.00	0.20	1.00	0.20	0.50	0.15	VA+MNR
FC-03-03	0.50	2.00	0.20	4.00	0.25	0.50	0.10	VA
FC-01-11	1.55	4.00	0.55	4.00	0.55	0.75	0.30	VA+MNR
FC-01-12	1.50	5.00	0.70	5.00	0.70	0.50	0.35	VA+MNR
FC-02-11	0.95	4.00	0.25	4.00	0.25	0.50	0.10	VA+MNR
FC-02-12	1.05	1.00	0.25	1.00	0.25	0.50	0.20	VA+MNR
FC-02-13	2.50	1.00	1.70	1.00	1.70	0.50	1.60	VA+MNR
FC-03-11	0.95	1.00	0.10	11.50	0.20	1.00	0.10	VA+GM
FC-03-12	1.40	4.00	0.35	9.00	0.45	2.00	0.25	VA
FC-03-13	1.65	1.50	0.30	4.00	0.40	1.00	0.25	VA
FC-02-21	3.25	1.00	0.10	29.00	0.60	1.00	0.10	VA+GM
FC-02-22	4.70	16.50	2.05	11.50	0.70	0.50	0.10	VA
FC-02-23	0.55	5.00	0.30	5.00	0.30	1.50	0.20	VA+MNR
FC-02-24	1.40	3.00	0.20	69.00	0.65	2.00	0.15	VA
FC-02-25	2.25	9.00	1.05	7.00	0.35	0.75	0.15	VA
FC-02-26	2.50	1.00	0.25	49.00	1.10	1.00	0.25	VA+GM
FC-03-21	2.95	15.00	1.70	6.00	1.20	1.00	0.20	VA
FC-03-22	5.40	2.00	2.95	2.00	2.95	2.00	2.95	All
FC-03-23	1.45	9.00	0.55	7.00	0.25	19.00	1.15	VA
HC-02-03	1.10	1.00	0.45	3.00	0.50	1.00	0.45	VA+GM
HC-03-01	0.25	1.50	0.10	1.50	0.10	1.50	0.10	All
HC-03-02	0.45	0.00	0.00	11.50	0.10	11.50	0.10	VA
HC-03-03	0.80	0.00	0.00	114.00	0.35	5.00	0.10	VA

260

HC-01-12	2.10	12.00	1.50	21.00	1.85	3.00	0.70	VA
HC-01-13	0.85	1.50	0.15	6.00	0.30	0.75	0.10	VA
HC-01-14	0.40	1.50	0.10	9.00	0.20	1.50	0.10	VA+GM
HC-02-11	2.50	1.00	0.75	1.00	0.75	0.75	0.70	VA+MNR
HC-02-13	3.00	5.00	1.65	9.00	1.95	0.75	1.00	VA
HC-03-11	4.20	3.00	2.30	3.00	2.30	0.50	1.25	VA+MNR
HC-03-12	5.30	6.00	3.00	6.00	3.00	1.50	1.75	VA+MNR
HC-03-13	4.80	4.00	2.70	0.75	2.30	0.50	2.20	VA
HC-01-21_IP	0.90	1.50	0.35	2.00	0.40	1.50	0.35	VA+GM
HC-01-22	3.50	0.75	1.80	0.75	1.80	0.50	1.70	VA+MNR
HC-01-23	4.65	2.00	2.10	2.00	2.10	0.50	1.65	VA+MNR
HC-02-22	4.95	3.00	3.50	2.00	0.35	3.00	3.50	VA+GM
HC-01-31	2.55	2.00	1.75	2.00	1.75	0.50	0.95	VA+MNR
HC-01-32	1.70	5.00	1.00	9.00	1.20	0.50	0.40	VA
HC-01-33	0.65	1.00	0.35	2.00	0.40	0.50	0.25	VA
LNC-01-01_IP	1.85	0.50	1.10	0.50	1.10	0.50	1.10	All
LNC-01-03	4.15	5.00	0.80	17.50	1.30	0.75	0.30	VA
LNC-01-04	5.40	1.00	0.65	0.75	0.60	0.75	0.60	MNR+GM
LNC-01-05	5.70	1.00	1.85	2.00	2.10	1.00	1.85	VA+GM
LNC-01-07	5.30	4.00	1.90	4.50	2.00	3.00	1.60	VA
LNC-01-08	0.75	1.00	0.25	1.00	0.25	1.00	0.25	All
LNC-01-28	1.65	2.00	0.45	3.00	0.50	0.50	0.30	VA
LNC-01-29	0.90	0.75	0.10	11.50	0.35	0.75	0.10	VA+GM
LNC-01-210	1.05	0.75	0.20	0.75	0.20	0.75	0.20	All
LNC-02-02_IP	3.10	6.00	1.90	7.00	2.00	0.50	0.25	VA
LNC-02-04	2.00	2.00	0.90	4.50	1.05	0.75	0.60	VA
LNC-02-05_IP	4.20	2.50	1.10	3.50	1.30	0.75	0.60	VA
LNC-03-21	3.80	17.00	3.30	15.00	2.10	20.00	3.50	VA
LNC-03-31	2.50	2.00	1.15	2.00	1.15	0.50	1.00	VA+MNR
LNC-04-01	1.50	0.50	0.55	0.50	0.55	0.50	0.55	All
LNC-04-02	1.70	0.25	0.10	19.00	0.85	2.00	0.15	VA
LNC-04-03	0.35	0.75	0.20	0.75	0.20	0.75	0.20	All
lnc-04-04	1.60	3.00	1.40	0.50	0.65	1.00	0.70	VA
GT-01-04	6.25	5.00	3.10	1.00	2.25	0.50	1.65	VA
GT-01-05	0.80	0.75	0.30	3.00	0.35	0.50	0.25	VA
GT-01-06	0.70	1.50	0.50	3.00	0.55	1.00	0.45	VA
GT-01-09	3.50	8.00	2.00	8.00	2.00	8.00	2.00	All
GT-01-010	4.05	0.75	0.15	30.00	0.95	0.75	0.15	VA+GM
GT-01-011	1.70	2.00	0.95	2.00	0.95	0.50	0.65	VA+MNR
GT-01-012	3.55	10.00	1.60	10.00	1.60	0.50	0.30	VA+MNR
GT-01-013	4.40	1.00	1.45	1.00	1.45	0.50	1.05	VA+MNR

GT-01-11	3.65	1.50	1.60	2.00	1.70	1.50	1.60	VA+GM
GT-01-12	4.55	3.00	3.40	3.00	3.40	0.50	1.50	VA+MNR
GT-01-13	2.70	1.50	1.50	2.00	1.55	1.00	1.40	VA
GT-01-15	1.80	1.00	0.25	3.00	0.35	0.75	0.20	VA
GT-01-16	0.55	4.00	0.30	4.00	0.30	0.50	0.15	VA+MNR
NMB-01-01	4.55	2.00	2.30	2.00	2.30	0.50	1.35	VA+MNR
NMB-01-02	3.50	9.00	1.90	9.00	1.90	2.00	1.00	VA+MNR
NBM-01-03	2.80	0.50	0.40	30.00	0.80	0.50	0.40	VA+GM
NMB-01-04	1.85	1.00	1.05	1.00	1.05	1.00	1.05	All
NMB-02-01	2.15	1.00	0.40	1.00	0.40	0.50	0.35	VA+MNR
NMB-02-02	1.25	0.75	0.40	2.00	0.45	0.75	0.40	VA+GM
NMB-02-11	0.90	5.00	0.45	6.00	0.50	1.00	0.10	VA
NMB-02-13	2.60	2.00	1.20	2.00	1.20	0.75	0.90	VA+MNR
NMB-02-14	1.35	0.50	0.05	9.00	0.25	3.00	0.10	VA
NMB-03-11	0.95	1.50	0.25	4.00	0.30	0.75	0.20	VA
NMB-03-12	1.85	0.50	0.20	75.00	1.75	0.50	0.20	VA+GM
NMB-03-13	1.70	19.00	1.20	19.00	1.20	1.00	0.30	VA+MNR
NMB-04-11	0.40	0.25	0.20	0.25	0.20	19.00	0.25	VA+MNR
NMB-04-12	0.55	3.00	0.25	3.00	0.25	0.75	0.15	VA+MNR
NMB-04-13	3.40	1.00	0.50	75.00	1.50	0.50	0.35	VA
NTL-01-01	0.35	3.00	0.25	3.00	0.25	0.75	0.25	VA+MNR
NTL-01-02	0.80	24.00	0.55	0.00	0.00	4.00	0.10	VA
NTL-01-03	0.25	1.00	0.05	1.00	0.05	9.00	0.10	VA+MNR
NTL-01-04	0.30	2.00	0.10	2.00	0.10	2.00	0.10	All
NTL-01-05	0.40	3.00	0.10	3.00	0.10	3.00	0.10	All
NTL-01-06	1.20	0.75	0.10	30.00	0.40	0.75	0.10	VA+GM
NTL-01-07	0.45	3.00	0.20	3.00	0.20	0.75	0.10	VA+MNR
NTL-01-11	1.60	1.00	0.05	30.00	0.65	2.00	0.10	VA
NTL-01-13	4.55	19.00	2.75	14.00	1.30	0.75	0.30	VA
NTL-01-14	0.30	0.25	0.05	11.50	0.15	5.00	0.10	VA
NTL-01-15	2.45	14.00	1.10	14.00	1.10	3.00	0.15	VA+MNR
NTL-02-01	0.85	2.00	0.10	9.00	0.25	2.00	0.10	VA+GM
NTL-02-02	3.25	4.00	1.10	4.00	1.10	1.00	0.80	VA+MNR
NTL-02-03	1.80	2.00	0.50	2.00	0.50	1.00	0.40	VA+MNR
NTL-02-11	2.50	0.00	0.00	30.00	1.45	1.00	0.10	VA
NTL-02-12	0.30	1.00	0.05	7.00	0.10	7.00	0.10	VA
NT:-02-13	0.55	5.00	0.20	9.00	0.25	1.50	0.10	VA
NTL-02-14	0.75	4.00	0.20	9.00	0.30	1.50	0.15	VA
NTL-02-21	4.20	14.50	2.95	14.50	2.95	14.50	2.95	All
NTL-02-22	5.15	10.00	3.30	0.50	1.50	0.50	1.50	VA
NTL-02-23	5.35	24.00	4.25	0.75	2.15	0.50	1.85	VA

TCH-01-01	2.55	24.00	1.90	19.00	1.30	0.50	0.30	VA
TCH-01-02	1.55	4.00	0.50	9.00	0.65	0.50	0.20	VA
TCH-01-11	0.35	1.50	0.15	5.00	0.20	1.50	0.15	VA+GM
TCH-01-12	1.10	2.00	0.50	4.00	0.60	2.00	0.50	VA+GM
TCH-01-14	0.40	1.50	0.20	1.50	0.20	1.00	0.15	VA+MNR
TCH-01-15	1.20	9.00	0.75	9.00	0.75	0.50	0.25	VA+MNR
TCH-01-16	0.40	5.00	0.25	9.00	0.30	0.75	0.10	VA
TCH-01-17	0.90	4.00	0.40	4.00	0.40	0.50	0.20	VA+MNR
TCH-01-18	1.30	4.00	0.50	4.00	0.50	0.50	0.25	VA+MNR
TCH-01-21	3.65	3.00	1.00	3.00	1.00	0.50	0.25	VA+MNR
TCH-01-22	1.15	2.00	0.50	3.00	0.55	0.50	0.25	VA
TCH-01-23	3.60	2.00	3.25	0.75	3.05	0.50	2.85	VA
TCH-01-24	1.35	19.00	0.90	19.00	0.90	0.75	0.15	VA+MNR
TCH-01-25	1.30	14.00	0.90	16.50	0.95	0.75	0.10	VA
TCH-01-26	3.20	9.00	1.75	4.00	0.15	9.00	1.75	VA+GM
TCH-01-27	4.20	2.00	2.10	2.00	2.10	0.75	1.35	VA+MNR
TCH-01-32	4.65	3.00	2.30	3.00	2.30	0.50	1.40	VA+MNR
TCH-01-33	5.60	4.00	1.30	4.00	1.30	3.00	1.05	VA+MNR
TCH-01-34	5.10	5.00	2.00	5.00	2.00	0.50	0.80	VA+MNR
TCH-01-35	3.80	3.00	2.25	0.75	1.65	0.75	1.65	VA
TCH-02-11	2.10	1.50	1.10	1.00	0.10	1.50	1.10	VA+GM
TCH-02-12	3.80	12.50	2.90	4.00	0.60	8.00	2.30	VA
DCB-01-01	5.95	0.25	0.10	19.00	0.60	0.75	0.15	VA
DCB-01-02	1.10	0.75	0.65	0.75	0.65	0.50	0.60	VA+MNR
DCB-01-03	0.35	0.50	0.20	0.50	0.20	0.50	0.20	All
DCB-01-04	2.00	2.00	0.60	3.00	0.65	1.50	0.55	VA
DCB-01-05	1.65	3.00	0.65	7.00	0.85	3.00	0.65	VA+GM
DCB-02-12	0.80	1.00	0.10	11.50	0.30	1.00	0.10	VA+GM
DCB-02-13	1.45	0.25	0.10	50.00	0.60	1.00	0.15	VA
DCB-02-14	1.00	19.00	0.65	0.50	0.20	0.50	0.20	VA
DCB-02-21	1.85	0.25	0.20	14.00	1.30	1.00	0.30	VA
DCB-02-22	1.95	2.00	0.20	120.00	1.95	2.00	0.20	VA+GM
ETC-01-02	0.20	3.00	0.15	1.00	0.10	1.00	0.10	MNR+GM
WCN-02-22	0.25	2.00	0.15	9.00	0.20	0.50	0.10	VA
HC-02-01	0.20	3.00	0.10	3.00	0.10	3.00	0.10	All
HC-02-02	0.15	0.50	0.10	0.50	0.10	0.50	0.10	All
NMB-01-12	0.20	0.75	0.10	0.75	0.10	0.75	0.10	All
TCH-01-31	5.70	0.50	3.05	0.50	3.05	0.50	3.05	All
DCB-01-06	0.15	0.25	0.05	0.25	0.05	4.00	0.10	VA+MNR
DCB-03-01	0.15	0.75	0.10	0.75	0.10	0.75	0.10	All
DCB-03-02	0.40	1.00	0.10	7.00	0.15	1.00	0.10	VA+GM

WCM-01-01	1.20	0.75	0.75	1.50	0.80	0.50	0.70	VA
WCM-01-02	0.45	1.00	0.20	1.00	0.20	1.00	0.20	All
WCM-02-01	0.20	1.50	0.15	1.50	0.15	0.75	0.10	VA+MNR
WCM-02-02	0.70	1.00	0.50	1.50	0.55	1.00	0.50	VA+GM
WCM-02-03	3.05	5.00	2.80	4.00	1.25	0.50	0.60	VA
WCM-02-04	0.80	1.00	0.60	1.50	0.65	0.75	0.55	VA
WCM-01-11	2.30	7.00	1.70	4.00	0.20	9.00	2.15	VA
WCM-01-12	3.80	7.00	3.55	2.00	1.10	3.00	2.40	VA
WCM-01-13	0.25	2.00	0.10	2.00	0.10	2.00	0.10	All
WCM-01-14	0.20	4.00	0.10	4.00	0.10	4.00	0.10	All
WCM-01-21	4.45	9.00	2.90	2.00	0.15	9.00	2.90	VA+GM
WCM-01-22	4.25	7.00	2.35	7.00	2.35	7.00	2.35	VA+GM
WCM-01-23	2.45	11.50	2.20	9.00	1.55	2.00	0.35	VA
WCM-01-24	0.25	1.50	0.10	5.00	0.15	1.50	0.10	VA+GM
WCM-01-25	4.40	3.00	2.30	3.00	2.30	0.50	0.95	VA+MNR

Appendix F: Type 2 Region Erodibility Parameters

Type 2 Erodibility Parameters

test	TcBM	KdBM	TcSD	KdSD	TcLR	KdLR
MCE-01-01	1.122677	0.201343	11.33434	0.397863	11.20196	0.038174
MCE-01-02	1.781298	0.157758	12.36996	0.442336	11.6915	0.042198
MCE-01-03	5.69484	0.155086	12.67111	0.402368	11.8192	0.048724
MCE-02-01	4.732988	0.222734	9.850346	1.026094	10.18263	0.132746
MCE-01-11	2.165771	0.343014	1.549114	0.314328	3.150845	0.037822
MCE-01-12	13.91977	0.077688	17.53323	0.603891	16.99506	0.040856
MCE-02-11	0.568919	0.657706	8.630634	0.998586	8.527674	0.053013
MCE-02-12	0.470628	0.498162	6.006691	1.337873	5.935299	0.134519
MCE-03-11	6.383083	0.238352	13.03076	0.812509	12.70799	0.073606
MCE-03-12	0.344655	0.38508	3.280731	0.496395	7.657269	0.066145
MCE-03-13	4.611043	0.117032	15.31985	0.299098	12.00945	0.022786
MCE-03-14	1.048499	0.152686	17.3589	0.302442	17.15558	0.026772
MCE-03-21	2.288587	0.233602	8.225677	0.509328	5.008375	0.036821
MCE-03-22	3.750063	0.618821	6.094374	1.25745	7.216253	0.352643
GRL-01-01	7.221349	0.209926	10.22974	0.637827	10.9487	0.178099
GRL-01-02	10.00365	0.173807	16.12779	0.756956	16.60416	0.113744
GRL-01-04	21.66489	0.106706	26.53227	1.263274	26.75097	0.227813
GRL-01-05	9.369764	0.100683	17.93689	0.27816	17.27388	0.030294
GRL-01-06	9.319769	0.166338	17.59625	0.422228	12.284	0.025286
GRL-04-01	6.07273	0.166922	18.13914	0.403579	19.78627	0.062772
GR-04-02	1.286819	0.143557	12.45388	0.240806	12.7731	0.029308
GRL-01-11	6.106496	0.090582	18.23309	0.20795	12.15988	0.015862
GRL-01-12	18.78476	0.04613	27.04584	0.309245	27.11074	0.034888
GRL-01-13	17.06982	0.061489	19.51787	0.108695	21.44539	0.036103
GRL-05-11	0.004231	0.338859	8.385828	0.566267	3.683756	0.044715
GRL-05-12	13.62025	0.016747	24.59917	0.075256	24.30571	0.009232
GRL-01-21	18.9447	0.123612	23.1844	1.156264	23.17116	0.118309
GRL-02-11	15.85702	0.058633	22.90346	0.246554	23.11325	0.030429
GRL-02-21	21.28675	0.081631	23.83739	0.856899	23.95538	0.174281
GRL-03-11	1.43104	0.236675	15.67433	0.709576	12.59834	0.048875
GRL-03-21	19.768	0.14961	21.87327	2.890536	21.86797	0.286717
GRL-03-22	14.61461	0.046931	21.83658	0.097329	21.73135	0.010125

GRL-01-31	15.21565	0.14135	19.70103	1.544589	19.90665	0.312372
GRL-02-31	4.483298	0.070686	20.58401	0.239519	20.3339	0.020118
ETC-01-03	11.85801	0.154142	16.64255	0.710253	17.05328	0.13179
ETC-02-01	2.823094	0.154343	11.42521	0.354314	11.84337	0.037956
ETC-01-11	17.70706	0.092866	22.3609	0.78666	22.56223	0.157632
ETC-01-13	4.818885	0.100497	12.57131	0.254356	12.42016	0.027905
ETC-02-11	11.09835	0.178916	22.96132	0.417224	21.37991	0.047898
ETC-02-12	4.854933	0.116875	17.32418	0.345011	15.59518	0.028448
WCN-01-01	3.308294	0.310744	10.15693	1.205369	10.2327	0.124831
WCN-01-02	17.69861	0.124507	19.63976	1.144537	19.77571	0.400126
WCN-01-03	11.76255	0.086435	17.47582	0.337855	14.20077	0.01655
WCN-01-11	3.197092	0.185467	13.83355	0.524316	13.66584	0.037572
WCN-01-12	19.11234	0.094973	30.95005	1.342801	29.83669	0.096972
WCN-01-13	13.51396	0.087616	19.46248	0.241995	9.842442	0.008369
WCN-02-21	7.803098	0.202257	16.8483	1.589457	16.21247	0.09211
WCN-02-22	27.34315	0.058839	29.61875	0.584647	29.69587	0.173454
WCN-02-23	11.58843	0.196352	19.92743	1.580709	19.94205	0.178275
FC-01-01	2.832649	0.697275	4.732169	1.420296	5.643951	0.31086
FC-01-02	6.48834	0.210855	10.62605	0.513238	10.97113	0.083414
FC-01-03	8.198289	0.166816	11.20812	1.231598	11.20286	0.134264
FC-03-01	3.326614	0.489894	8.27165	3.794205	8.20287	0.429345
FC-03-02	6.681592	0.302894	9.815911	2.683244	9.830301	0.326714
FC-03-03	8.797209	0.474953	10.64052	4.083625	10.82311	1.275169
FC-01-11	1.768796	0.361781	5.540738	1.744395	5.626893	0.217083
FC-01-12	2.56381	0.370081	0.47997	0.20775	4.059527	0.091015
FC-02-11	2.960039	0.357675	5.279308	1.515942	5.360816	0.191322
FC-02-12	4.124006	0.328276	7.142667	1.412682	7.210102	0.18521
FC-02-13	5.702321	0.319211	9.604817	2.268155	9.679692	0.319645
FC-03-11	5.573581	0.514687	7.82703	1.836853	7.587378	0.135719
FC-03-12	5.62733	0.268009	1.189884	0.144064	9.542672	0.135985
FC-03-13	3.666015	0.318279	8.260092	1.412421	7.90238	0.165341
FC-02-21	1.107364	0.317956	6.037085	0.496522	8.829673	0.052038
FC-02-22	0.742962	0.327826	3.327186	0.419366	4.383532	0.047813
FC-02-23	17.25902	0.073687	22.33123	0.643281	22.47947	0.101382
FC-02-24	7.974053	0.116	16.61486	0.247009	16.41367	0.034879
FC-02-25	5.186766	0.155046	15.40609	0.676829	15.5772	0.076689

FC-02-26	4.356003	0.27558	12.3297	0.552442	12.79474	0.074549
FC-03-21	2.872666	0.324977	6.271891	0.752017	7.23355	0.127669
FC-03-22	2.100593	1.171209	2.617224	1.32431	4.87147	0.364504
FC-03-23	6.017777	0.366047	7.606607	4.095495	7.653868	0.649451
HC-02-03	18.22141	0.051114	19.40128	0.054568	30.63401	0.033789
HC-03-01	13.92833	0.14278	15.34044	3.918843	15.37994	0.572601
HC-03-02	13.49018	0.096382	14.03071	0.104583	18.40346	0.057103
HC-03-03	13.71639	0.083552	19.36962	0.166151	15.63999	0.018048
HC-01-12	1.890122	1.385711	2.596894	14.35191	2.626389	2.482342
HC-01-13	2.596291	0.825493	3.974052	5.136466	4.058612	0.815358
HC-01-14	5.661134	0.38026	6.804377	4.115129	6.815762	0.613658
HC-02-11	2.245342	0.372219	6.757996	1.073257	5.200446	0.074708
HC-02-13	3.506584	0.710558	4.936666	1.398075	5.948328	0.741814
HC-03-11	1.598063	0.651548	4.798262	1.884984	5.393709	0.294075
HC-03-12	0.757344	0.859943	4.270093	3.52159	3.993353	0.291198
HC-03-13	1.439026	1.156502	3.231575	2.975898	3.513089	0.475884
HC-01-21_IP	3.685617	1.000079	5.652695	9.577056	5.697522	1.267272
HC-01-22	2.033427	0.697655	5.288316	2.672232	5.545954	0.399314
HC-01-23	1.134578	0.641616	3.943835	1.202811	4.140461	0.134531
HC-02-22	0.742893	1.286369	3.082583	8.31026	2.834717	0.58816
HC-01-31	3.099523	0.595399	5.148511	4.431717	5.280892	0.871159
HC-01-32	4.048454	0.372083	6.800072	2.301415	7.056549	0.52535
HC-01-33	6.154338	0.371669	7.456827	2.819289	7.568371	0.941984
LNC-01-01_IP	3.160592	1.382346	4.832518	16.00734	4.909856	2.487496
LNC-01-03	0.053626	1.003191	3.32538	2.726128	1.143768	0.241011
LNC-01-04	0.169359	2.324347	2.03635	8.161062	1.763275	0.727993
LNC-01-05	0.376002	2.759229	1.869576	10.37713	1.901678	1.267147
LNC-01-07	0.516137	1.903843	0.817883	2.163194	2.061868	0.524875
LNC-01-08	2.463374	1.300007	3.508113	13.29272	3.47667	1.303285
LNC-01-28	2.204842	0.483955	4.375629	1.272221	4.878565	0.223087
LNC-01-29	3.570287	0.334385	6.607685	1.295628	6.99268	0.23962
LNC-01-210	2.376248	0.311957	5.13076	0.958128	4.686411	0.083878
LNC-02-02_IP	1.907451	0.854023	3.965622	4.952114	4.124663	0.827673
LNC-02-04	1.934813	0.846815	3.425005	2.993586	3.715634	0.73021
LNC-02-05_IP	0.65556	0.920673	2.794715	1.470602	3.34126	0.246972
LNC-03-21	6.278569	0.581384	7.755527	5.531123	7.900082	2.056982

LNC-03-31	3.536667	0.263764	8.624286	0.930972	9.280082	0.151144
LNC-04-01	1.255061	0.417263	4.189546	1.034287	4.140054	0.165777
LNC-04-02	1.139374	0.841014	4.561699	5.469947	3.60562	0.260809
LNC-04-03	8.474003	0.277965	9.684676	5.138697	9.570754	0.502076
lnc-04-04	5.746329	0.597719	6.456382	10.53168	6.467375	1.43181
GT-01-04	0.623594	2.922368	1.702128	5.270146	2.329481	1.143539
GT-01-05	4.213519	0.338889	5.762891	2.094255	5.797126	0.386587
GT-01-06	5.206763	0.658395	5.72676	4.761241	5.785183	4.302952
GT-01-09	1.061129	1.154134	2.716383	6.261399	2.792609	0.86546
GT-01-010	0.213573	1.609151	1.187737	2.000375	2.482201	0.232422
GT-01-011	2.017841	0.863789	3.370368	6.339843	3.439702	1.186312
GT-01-012	0.453913	1.425493	1.766663	3.399615	0.563415	0.151258
GT-01-013	0.386751	2.270261	2.314734	10.8821	2.162663	0.878593
GT-01-11	1.465321	0.739524	5.234209	2.182636	2.40555	0.163429
GT-01-12	1.683085	0.744585	3.934028	5.871195	3.949833	0.786708
GT-01-13	2.779094	0.663791	3.96754	1.311685	4.700908	0.608418
GT-01-15	1.568074	0.709555	3.24216	1.493038	3.835052	0.260755
GT-01-16	3.481483	0.257704	5.003173	2.52371	4.989754	0.267948
NMB-01-01	1.591343	0.543996	5.467012	1.355978	6.445446	0.254308
NMB-01-02	1.36411	0.780541	3.142627	1.693477	3.105041	0.146444
NBM-01-03	0.473599	1.189021	2.079932	2.225871	2.65623	0.290448
NMB-01-04	2.13104	1.509925	3.098163	14.41282	3.16166	2.794524
NMB-01-12	4.045534	1.000247	4.230294	18.06231	4.238869	4.597571
NMB-02-01	2.907633	0.373332	9.838864	1.561187	7.572033	0.097684
NMB-02-02	2.331877	0.841111	3.731246	3.623986	3.63966	0.420366
NMB-02-11	5.723874	0.550021	7.123667	4.862549	7.212617	1.01461
NMB-02-13	1.724662	0.54727	7.115132	2.719761	4.525081	0.117388
NMB-02-14	4.014411	0.241694	8.268835	0.623432	8.467802	0.095482
NMB-03-11	4.201156	0.385211	6.170397	1.725071	6.449276	0.464462
NMB-03-12	2.25107	0.341049	5.722122	0.595439	4.5027	0.047399
NMB-03-13	4.491235	0.214468	6.796194	0.583582	7.182534	0.090642
NMB-04-11	8.804359	0.082073	12.39715	0.890454	12.25725	0.061956
NMB-04-12	11.07883	0.062834	16.72491	0.37805	16.75456	0.041322
NMB-04-13	4.747318	0.178507	14.78181	0.251351	10.15152	0.024794
NTL-01-01	6.895513	0.353179	7.291014	4.308616	7.301571	0.890421
NTL-01-02	6.733226	0.227467	8.75255	2.666289	8.722061	0.250547

NTL-01-03	11.92548	0.120641	14.34771	1.265096	14.37015	0.15154
NTL-01-04	15.36413	0.159104	17.52245	2.414662	17.52622	0.284557
NTL-01-05	13.24027	0.096123	17.3845	0.661114	17.51917	0.08921
NTL-01-06	4.911932	0.155136	12.37236	0.425728	6.234204	0.017184
NTL-01-07	16.71491	0.095769	20.6831	1.09521	20.78425	0.154277
NTL-01-11	5.281066	0.222296	13.14704	0.699052	13.68667	0.080712
NTL-01-13	1.951974	0.296042	9.778409	0.97842	9.570059	0.089577
NTL-01-14	21.19461	0.062862	25.98307	0.408993	26.30269	0.102474
NTL-01-15	4.181097	0.161391	12.28328	0.446599	12.13674	0.041271
NTL-02-01	10.56062	0.149723	15.11604	0.42411	16.50036	0.152455
NTL-02-02	1.89303	0.276912	10.8889	0.96883	6.665888	0.047904
NTL-02-03	6.581872	0.206261	12.27399	0.524506	13.47513	0.093311
NTL-02-11	2.764591	0.366791	12.17355	1.632566	12.47399	0.189844
NTL-02-12	18.7438	0.059527	23.85595	0.355578	24.12263	0.061402
NT:-02-13	24.07268	0.050232	34.04532	0.284898	34.50067	0.077899
NTL-02-14	15.44925	0.0688	27.06493	0.494392	27.30013	0.066506
NTL-02-21	7.269022	0.137565	15.58171	0.356069	15.39697	0.030468
NTL-02-22	3.116524	0.239854	12.85357	0.953349	13.22391	0.106417
NTL-02-23	6.192443	0.243175	12.32134	1.133097	12.86692	0.19913
TCH-01-01	2.698813	0.532845	4.854936	3.973995	4.834137	0.379697
TCH-01-02	3.158622	0.526737	4.665684	1.242838	4.607184	0.224957
TCH-01-11	13.17804	0.111738	15.73954	1.066727	15.83611	0.232749
TCH-01-12	19.10109	0.076372	28.19162	0.383633	29.28006	0.133446
TCH-01-14	17.66872	0.089529	21.88304	1.232933	21.95042	0.157278
TCH-01-15	14.13789	0.08998	21.77212	0.722187	21.96604	0.104699
TCH-01-16	25.51285	0.069651	32.67014	1.023813	32.80686	0.220315
TCH-01-17	15.03369	0.051366	28.06083	0.309578	28.13694	0.032868
TCH-01-18	13.9361	0.051077	29.79992	0.163318	26.90806	0.013269
TCH-01-21	1.88784	0.249648	14.47312	0.812751	12.92362	0.065003
TCH-01-22	17.73027	0.089352	27.05058	0.403097	28.22264	0.091642
TCH-01-23	13.3726	0.160556	17.52248	2.0457	17.52579	0.232477
TCH-01-24	18.19708	0.048064	29.01388	0.183464	29.88615	0.026768
TCH-01-25	20.77551	0.061559	29.30137	0.270615	30.42129	0.057485
TCH-01-26	8.185473	0.096038	24.21378	0.583704	25.29224	0.094672
TCH-01-27	5.78962	0.19099	14.17077	0.406312	16.7341	0.065572
TCH-01-32	1.480557	0.794681	4.539946	2.164499	4.931438	0.288711

269

TCH-01-33	0.425878	0.886572	4.179179	1.465932	4.130895	0.104037
TCH-01-34	0.59038	1.286797	3.231727	4.201773	3.467872	0.546237
TCH-01-35	1.770478	1.576305	4.095111	13.15429	4.145755	1.595791
DCB-01-01	0.3193	0.617983	11.23726	0.714138	11.1032	0.039124
DCB-01-02	5.588114	0.422155	7.15208	3.344926	7.26118	0.725282
DCB-01-03	9.485549	0.149772	11.10364	2.037373	11.07994	0.268433
DCB-01-04	1.889738	0.697711	2.42037	0.794748	3.450985	0.155523
DCB-01-05	2.257561	0.862597	3.517644	3.001036	3.745077	0.828014
DCB-03-02	9.866765	0.118415	12.51315	0.688644	12.7343	0.128728
DCB-02-12	13.16517	0.09871	19.48115	0.286415	21.11347	0.108609
DCB-02-13	10.87256	0.164096	18.91712	0.381227	20.07702	0.066517
DCB-02-14	13.04628	0.19162	17.0218	2.02098	17.12881	0.260829
DCB-02-21	6.869038	0.376249	17.54975	2.364562	17.52532	0.254014
DCB-02-22	6.26353	0.222155	11.56146	0.246716	11.42179	0.026039
WCM-01-01	4.737865	0.81401	5.768837	2.596724	5.848359	0.658561
WCM-01-02	5.30222	0.363419	6.376165	5.06927	6.410615	0.701143
WCM-02-01	4.647504	1.516514	4.678344	3.483132	4.678344	0.348313
WCM-02-02	4.820567	1.440543	5.206146	12.67123	5.242676	6.89564
WCM-02-04	14.35163	0.42874	15.86569	7.1645	16.00745	3.16352
WCM-01-13	14.4566	0.08035	17.45188	0.828557	17.52757	0.130322
WCM-01-14	10.06137	0.210014	10.83115	2.737954	10.84574	0.440985
WCM-01-24	5.017733	0.459884	5.500594	5.061158	5.522901	1.316795
WCM-01-25	0.794912	1.698126	3.395705	11.81654	3.369677	1.233448
GRL21-01-01	N/A	N/A	N/A	N/A	N/A	N/A
GRL21-01-11	4.349623	0.189455	12.51722	0.413066	13.93396	0.054821
GRL21-01-12	7.325546	0.156881	12.41014	0.488662	12.26209	0.047923
GRL21-01-21	5.65997	0.130068	10.90653	0.19937	13.46317	0.029725
GRL21-01-22	11.79856	0.536698	15.81618	3.933729	16.0977	1.059649
GRL21-01-23	7.567752	1.552434	17.51473	3.680317	17.32253	0.429171
GRL21-01-24	4.65481	0.196322	14.32928	0.613959	14.15833	0.05737
GRL21-01-25	17.78534	0.165589	20.0038	0.203654	25.74891	0.298092
GRL21-01-26	17.7815	0.159442	27.71272	1.269301	27.72823	0.137999
GRL21-01-31	N/A	N/A	N/A	N/A	N/A	N/A
GRL21-01-32	12.45824	0.250915	18.5492	2.036197	18.3957	0.278796

Appendix G: Confinement Effect within the mini-JET Apparatus

To provide stronger comparisons of the current research to previous studies, the influence of jet nozzle diameter to jet reservoir ratios between the original jet and the mini-jet was investigated. Consistent samples were prepared in a laboratory setting and tested in triplicate batches representing three different jet nozzle-to-jet reservoir ratios: mini-jet confinement, original jet confinement and unconfined.

Maryhill till was retrieved from Maple Hills Creek from Waterloo, Ontario and used for all laboratory tests. With some modifications, the soil samples were prepared following the general methodology detailed in Al-Madhhachi et al. (2013a). Samples were oven-dried for 24 hours at a temperature of 105 degrees Celsius and subsequently crushed by hand with a mortar and pestle. To remove pebbles and gravels present within the till, the geologic media was passed through a 1.4 mm sieve with any coarser grain fractions being discarded. Sufficient material to prepare three standard proctor molds was then hand-mixed to a desired moisture content and stored for a minimum of 24 hours in a sealed Ziploc bag to ensure an even distribution of water content throughout the prepared sample. After 24 hours, samples were hand-mixed again and aggregates larger than 4.75mm formed during the addition of water to the samples were manually pulverized before sample compaction occurred. Samples were subject to different levels of compaction to test the effect of confinement under different pressure settings.

Sample Group 1 and Sample Group 2 were prepared at the lowest level of compaction by following the ASTM Standard Proctor compaction methodology. Samples were compacted in three different lifts in a standard mold (101.6 mm Dia. x 116.4 mm height) using the Standard Proctor hammer at 25 blows per layer. The standard proctor hammer had a 30.5 cm drop height, 50.8 mm diameter and a weight of 2.49 kg. The ASTM Standard D698A (2006) specifies 25 blows per layer with the standard proctor hammer resulting in a compaction effort of 600 kN-m/m^3.

Sample Group 3 and sample Group 4 were prepared using an identical methodology as Sample Groups 1 and 2 except 50 blows per layer were applied. After compaction, the top of the soil sample was trimmed using a straight steel edge.

Sample Groups 5 through 9 were compacted using the same methodology as sample Groups 1 and 2 and subsequently subjected to additional consolidation using a 100-kilonewton MTS Criterion Model

45 electromagnetic press (*Figure G1a*). To maintain consistency between sample groups, the force of consolidation was incrementally increased based on a pre-determined schedule until the desired load was achieved. The position of the actuator on the electromagnetic press was manually adjusted to maintain the applied load according to the schedule and was kept within +/-0.5 kN of the target load. The samples were subject to maximum loads between 65 to 90 kN across the 0.1 m diameter actuator head for maximum consolidation forces ranging between approximately 8280 to 11464 kPa. Assuming a 0.917 $\frac{kg}{m^3}$ density of ice, this corresponds to compressive gravitational forces similar to glacial ice sheets in the range of 0.9 to 1.3km thick acting on underlying soils (ignoring shear forces imposed by flowing glaciers). The total duration of each compression procedure was 160 min, with the duration of the maximum load being applied ranging between 15 to 20 minutes.

After completion of each consolidation procedure using the electromagnetic press, samples commonly experienced a reduction in sample height (approximately 1 cm below the top of the standard proctor mold as shown in *Figure G1b*). To apply the jet test to each of these samples, and to avoid heterogeneities arising from the trimming of the samples during the Standard Proctor procedure, the sample was inverted, and the JET was performed on the bottom of the sample which remained visually consistent and flush with the mold (*Figure G1c*).

Figure G1: *a) sample consolidation using EM press. b) reduction in sample height after consolidation. c) bottom of prepared sample which was used as test surface*

For Sample Groups 1 through 4, each sample group (consisting of three samples) was prepared, and tested on the same day while maintaining a constant moisture content (as measured by sample mass). In the cases of sample Groups 5 through 9, each set of triplicate samples was prepared on three sequential days with jet tests being performed on the same days as sample preparation. In each case, moisture contents were held constant between days as measured by sample mass and small amounts of water were added into the sealed sample bag as required to compensate for any moisture loss. As summarized in *Table G1*, the range in the compacted soil masses within each Sample Group is between 0.82% to 4.14% of the average mass of the samples. The small variations in compacted soil masses within each Sample Group were considered negligible to compare differences in levels of confinement within the jet testing apparatus. It should be highlighted that no comparisons were made between different Sample Groups, so any sample deviations beyond those internal to each Sample Group did not influence the experimental outcome. The 9 different sample groups are summarized in *Table G1*.

Table G1: Sample Group Summary

Sample Group Number	Sample ID	Method of Compaction	Moisture Content	Range of compacted soil masses (g) (Maximum % difference)
1	CCT12-H02	Standard Proctor Compaction	12%	1985.2 – 2014.4 (1.46%)
2	CCT12-H03	Standard Proctor Compaction	12%	1948.7 - 1997.2 (2.45%)
3	CCT12-H04	Standard Proctor Compaction (modified to 50 blows/layer)	12%	2000.0 – 2084.5 (4.14%)
4	CCT12-H05	Standard Proctor Compaction (modified to 50 blows/layer)	12%	2124.5 – 2179.4 (2.55%)
5	CCT12-HP01L	EM Press (maximum force of 65 kN)	12%	1945.2 – 1970.5 (1.30%)
6	CCT9-HP02L	EM Press (maximum force of 75 kN)	9%	1876.5 – 1918.0 (2.18%)
7	CCT12-HP02M	EM Press (maximum force of 75 kN)	12%	1994.1 – 2025.9 (1.58%)
8	CCT9-HP02M	EM Press (maximum force of 75 kN)	9%	1870.3 – 1898.7 (1.51%)
9	CCT9-HP03H	EM Press (maximum force of 90 kN)	9%	1917.0 – 1932.8 (0.82%)

Average: 2.00%

The various JETs were performed following the same methodology as the field methodology (*Section 3.1.2*) including the same measurement scheme and submergence for 5 minutes prior to test initiation.

In general, the laboratory tests were shorter than the field tests due to the maximum depth of scour being reached quickly.

Tests were performed in a 1.8m diameter by 0.3m deep submergence tank (*Figure G2d*) with one sample in each triplicate group being performed in each experimental setup (i.e. each jet diameter to jet reservoir ratio) listed in *Table G2*. The mini-jet confinement ratio was replicated by placing the Standard Proctor mold containing the prepared soil samples within a plastic mold which supported the foundation ring and jet reservoir (*Figure G2a*). The confinement within the original jet was replicated by placing a vertical PVC pipe around the standard proctor mold (*Figure G2b*) resulting in a nozzle-to-reservoir ratio of 0.021 (the same confinement ratio used in the device by Hanson et al. (1990) to measure the shear stress distributions resulting from an impinging jet).

Table G2: *Nozzle Diameter to Reservoir Diameter Ratios of Experimental Set-ups*

Set up	Jet nozzle diameter	Reservoir diameter	Nozzle diameter to reservoir diameter ratio
MiniJet Confinement (MJC)	3.175 mm	12.5 cm	0.0254
Original Jet Confinement (OJC)	3.175 mm	15.24cm	0.0210
Unconfined (UC)	3.175 mm	1.8m	0.0018

In the OJC experimental set-up, a plastic insert was placed flush around the top of the standard proctor mold to prevent secondary flow paths from developing between the standard proctor mold and the confinement reservoir (*Figure G2b*). The mini-jet nozzle was then centred over the soil sample by placing the mini-jet apparatus on three bolts protruding from the confinement reservoir. Importantly, this set-up did not include an enclosed top to the confining device with a gap between the wall of the confining reservoir and the jet apparatus which is representative of the device used by Hanson et al. (1990). An unconfined setup was replicated by suspending the jet apparatus between three threaded rods (*Figure G2c* and *Figure G2d*); resulting in the only confining component being the walls of the 1.8 m submergence tank. Any influence from the threaded rods was assumed to be negligible.

Best efforts were made to keep the initial nozzle heights similar between tests to isolate the effects of the confining reservoir. However, for Sample Groups 1 to 3, the unconfined set-up had a higher initial nozzle height compared to the mini-jet confinement and original jet confinement set-ups. The

temperature of water was monitored during each test to ensure that it did not substantially deviate during a test or between tests. All water used during laboratory tests was provided by the Region of Waterloo water distribution network and was assumed to be constant in water chemistry across all tests. Similar to field tests, aspect ratios of scour holes were measured upon test completion where it was applicable. The three confinement set-ups are demonstrated in *Figure G2* along with an unconfined test occurring within the submergence tank.
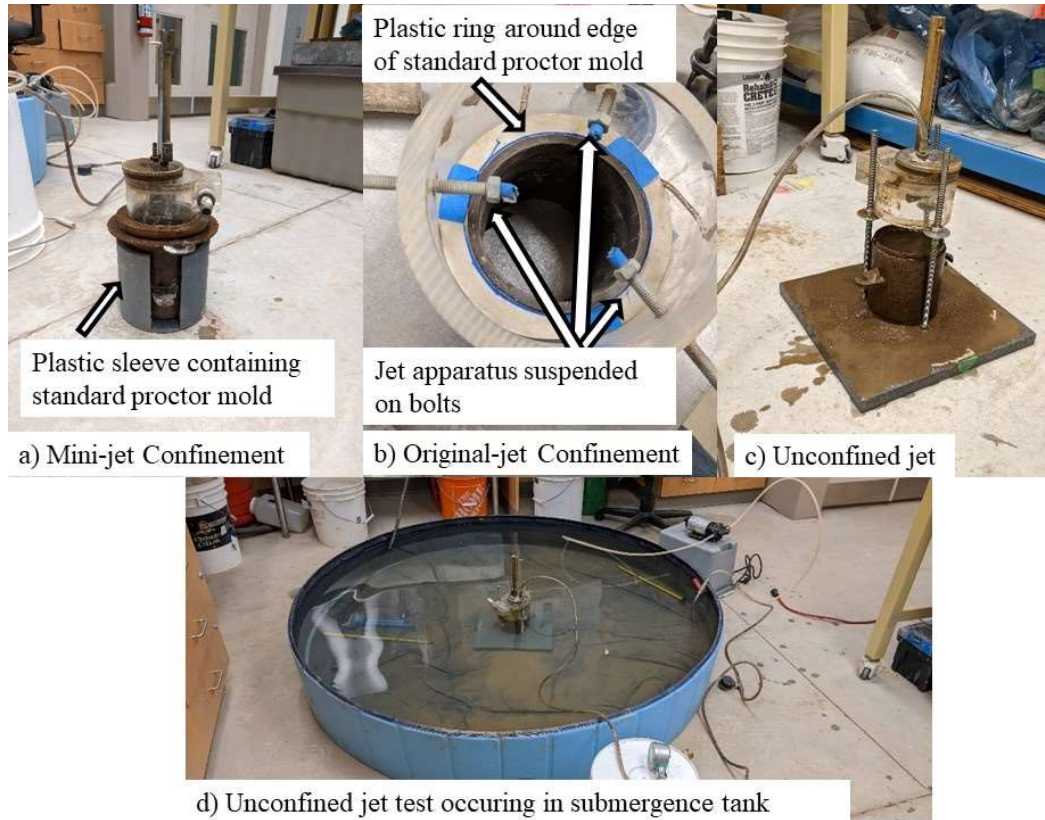
Figure G2: JET apparatus set-up for a) mini-jet confinement, b) original jet confinement, c) unconfined mini-jet, d) unconfined mini-jet within submergence tank

The results of the laboratory investigation were analyzed to determine if any differences in test progression or erosion rates were observed between the experimental confinement set-ups. If the effect of confinement significantly alters the stress imposed upon the sample during a JET, then the experimental results will indicate

$$Erosion_{unconfined} < Erosion_{OriginalJET} < Erosion_{miniJET}$$

for a given nozzle height and pressure head. With the assumption that each sample in a sample group is equivalent if the mini-JET is analyzed using the JET solution techniques (e.g. BM or LR), the mini-JET confinement would obtain the highest K_d and lowest τ_c and the unconfined set-up would obtain the highest τ_c and lowest K_d. Only BM and LR were employed in this analysis because of the frequency of SD failures (*Appendix H*) in the analysis of the laboratory results.

It was observed during the laboratory investigations that the boundary effect caused by the steel standard proctor mold in which the samples were prepared may have had some influence on the test progression. First, while the actuator head of the EMP used to prepare the samples and the inner diameter of the steel mold only differed by 2mm, that may have led to a ring along the outside of the sample which was subject to less consolidative pressures than the rest of the sample. The same occurrence can be attributed to the samples prepared using the standard proctor method with the thickness of the hammer wall preventing the hammer from dropping along the edge of the mold, however, the disparity in compressive and consolidative forces would be much more apparent at the larger forces imposed by the EMP. Additionally, most of the tests in the laboratory set-up were observed to have flat test surfaces within the steel mold at test termination. This resulted in secondary confinement from the steel walls of the mold becoming more apparent as the test progressed and likely overriding the primary confinement effect controlled for in the experimental set-up. This secondary confinement was non-existent at test initiation and became more prominent as the test progressed. To compensate for this, a secondary method of analysis was employed that compared the scour depth measurements between experimental set-ups at the 5-minute, 9-minute and 14-minute marks and an additional comparison with the depth of scour at test termination. The earlier measurements offer a comparison between tests before the secondary confinement is believed to have had any substantial contributions to the test progression. The comparison of terminal measurements provides a view of the full test duration but avoids uncertainties that may be introduced by the JET solution techniques.

The progression of the scour holes from the laboratory jet tests performed on samples prepared in triplicate is demonstrated below in *Figure G3*. If there were strong indications that the confinement offered by the submergence tank is a contributing factor to the shear stress imposed upon the test material, then the experimental setup reflecting the highest level of confinement (MJC) would develop deeper scour holes more quickly, and the experimental setup reflecting the lowest level of

276

confinement (UC) would develop shallower scour holes at a slower rate. The results indicate that the MJC setup results in the deepest scour hole 2/9 times and the UC setup results in the shallowest scour hole 1/9 times, however, the depth of the scour holes in the UC setup may be skewed in the first three trials due to the sample starting further away from the jet nozzle. Interestingly, in this circumstance it would be expected that this would result in even slower rates of erosion (due to more energy dissipation before contacting the test material), however, this is not reflected in the rates of erosion in the tests. It was also observed during the tests and is demonstrated in *Figure G3* that the erosion rates throughout the tests generally did not plateau as the distance from the nozzle increased. This relatively linear progression of scour hole depth with time, regardless of the estimated shear stress imposed upon the surface is not what is expected based on jet hydraulics. This phenomenon may be related to a consistent observation of a thin layer (noted to range between 1-4mm in depth) of saturated and soft material present at the surface of the test specimen at test completion. This indicates that the erosion rates may be representative of how fast the wetting front is advancing through the material and subsequently reducing the material's resistance to erosion rather than testing the resistance to erosion of the underlying material representative of the prepared sample.
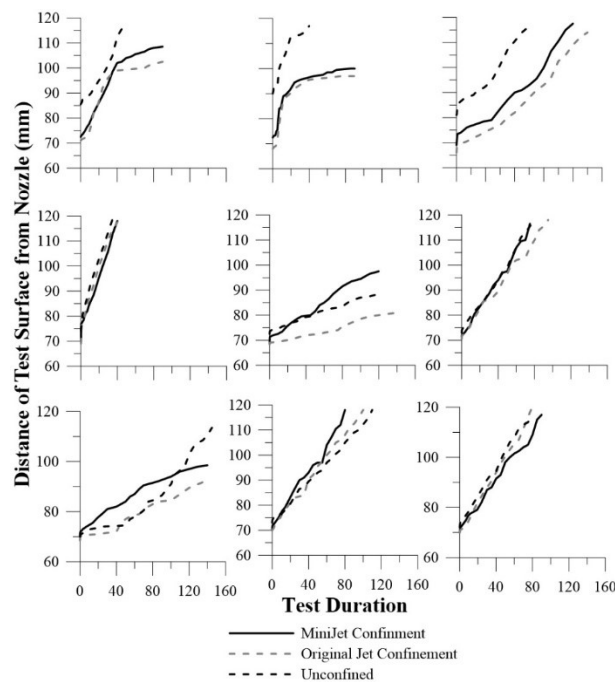
Figure G3: *Scour hole Development for Laboratory JETs at Different Confinement Levels*

277

The scour holes that were observed during these laboratory experiments were atypical (*Figure G4*). They generally presented as flat surfaces or in some instances slightly convex surfaces with the middle of the test surface slightly higher than the edge of the samples. CCT12-HP02-UC and CCT12-HP02-OJC both developed the typical concave scour hole shapes after progressing approximately 2.5cm into the steel mold.

CCT12-HP02-UC Pre-test | CCT12-HP02-UC Post-Test (concave scour hole)

CCT9-HP03-UC Pre-test | CCT9-HP03 Post-test (convex test surface)

CCT9-HP02-MJC2 Pre-test | CCT9-HP02-MJC2 Post-Test (Flat Test Surface)

Figure G4: *Example Scour Hole Shapes from Laboratory Tests*

To investigate whether the tests representing the various levels of confinement have statistically different scour depths at various times throughout the test, the three levels of confinement with populations composed of scour depth measurements from the 9 laboratory tests (n=9) were compared using the non-parametric Friedman test. Scour depths were compared at time intervals of 5 minutes, 9 minutes and 14 minutes to compare portions of the tests where the potential influence from the secondary of the steel mold would be at a minimum. Scour depths were also compared at the full test lengths. The null hypothesis of the Friedman test failed to be rejected at the 90% confidence level for the 4 time intervals investigated indicating that there is no statistical difference in scour depths between the levels of confinement at those points of the test.
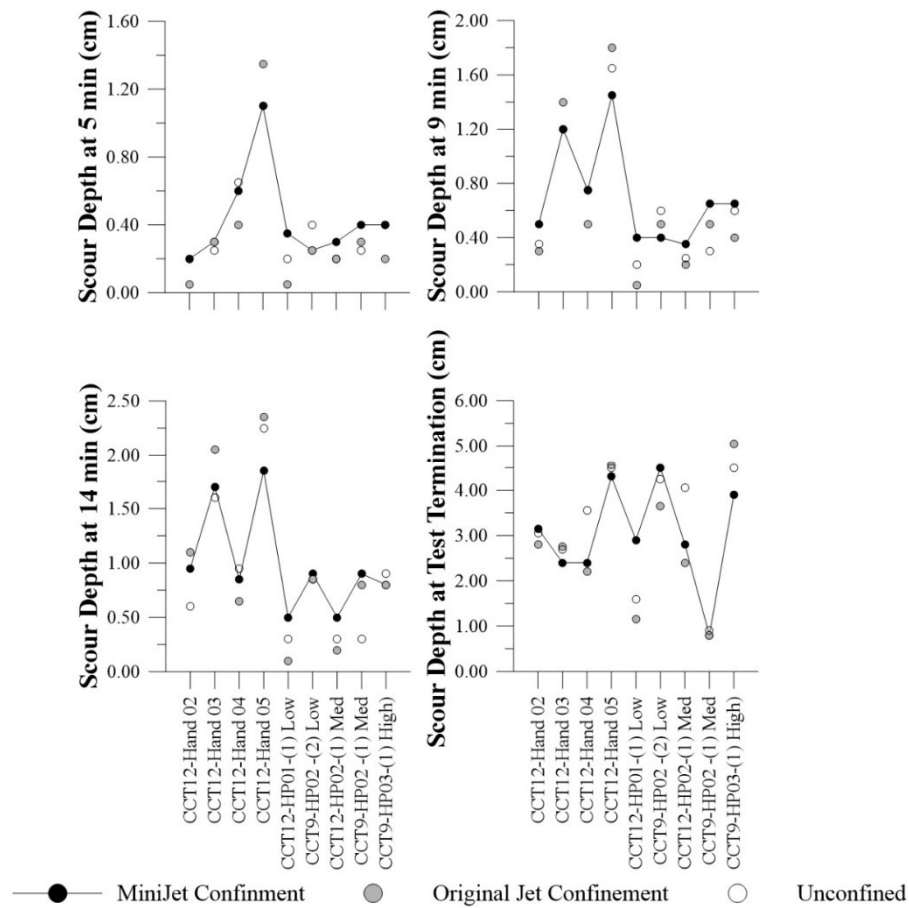
Figure G5: *Scour Depth Comparisons between Levels of Confinement at Fixed Test Durations*

One limitation of this approach is that it does not account for the fact that it would be expected that the influence of shear stress imposed upon the test material would be more notable at the highest

279

pressure head settings the JETs are run at. Qualitatively reviewing *Figure G5*, it is observed that at 5-minute and 9-minute durations the MJC level of confinement has the highest scour depths for the three tests run at the highest pressure heads (CCT12-HP02-(1) Med, CCT9-HP02-(1) Med and CCT9-HP03-(1) High) which indicates that at the higher pressure heads some confinement effect may become more important. However, this qualitative observation is convoluted by the observation that there is not an observable difference between the OJC and UC levels of confinement at these pressures.

The 9 laboratory JETs were also analyzed using LR and BM. SD was excluded due to the high level of failures associated with the test population, arising from the lack of plateauing previously discussed. If the level of confinement is influencing the shear stress imposed upon the samples this would be reflected in lower τ_c values and higher K_d values for tests representing higher levels of confinement. For this analysis, when negative values of τ_{cLR} were estimated they were included in the analysis because although they are not representative of a physically realistic scenario, they are representative of the linear regression of erosion rates and applied shear stresses during the test and do not alter the relative ranking of the estimated critical shear stresses. The relative rankings of the estimated critical shear stresses and erodibility coefficients for the different levels of confinement are demonstrated in *Table G3* and *Table G4* with 1 indicating the highest value of the variable compared to the other levels of confinement for the same test and 3 indicating the lowest value for the same test.

Table G3: Rankings of confinement Levels based on their Estimated τ_c

	τ_{cBM} Rank			τ_{cLR} Rank		
Test	MJC	OJC	UC	MJC	OJC	UC
CCT12-Hand 02	2	3	1	2	1	3
CCT12-Hand 03	2	3	1	1	2	3
CCT12-Hand 04	3	2	1	2	3	1
CCT12-Hand 05	1	3	2	1	2	3
CCT12-HP01-(1) Low	3	1	2	3	1	2
CCT9-HP02 -(2) Low	1	2	3	3	1	2
CCT12-HP02-(1) Med	2	1	3	2	1	3
CCT9-HP02 -(1) Med	2	3	1	2	3	1
CCT9-HP03-(1) High)	2	3	1	2	3	1

Table G4: *Rankings of confinement Levels based on their Estimated K_d*

Test	K_{dBM} Rank MJC	OJC	UC	K_{dLR} Rank MJC	OJC	UC
CCT12-Hand 02	2	3	1	2	1	3
CCT12-Hand 03	3	2	1	2	3	1
CCT12-Hand 04	2	3	1	2	3	1
CCT12-Hand 05	3	2	1	1	2	3
CCT12-HP01-(1) Low	1	3	2	1	3	2
CCT9-HP02 -(2) Low	2	3	1	3	1	2
CCT12-HP02-(1) Med	2	3	1	2	1	3
CCT9-HP02 -(1) Med	1	2	3	1	3	2
CCT9-HP03-(1) High)	3	2	1	2	3	1

Friedman tests were performed on the $\tau_{cBM}, \tau_{cLR}, K_{dBM}$ and K_{dLR} to assess whether there are observable differences in the erodibility parameters between the levels of confinement. At the 90% confidence level, there were no observable differences between τ_{cBM}, τ_{cLR}, or K_{dLR} populations. The K_{dBM} populations rejected the null hypothesis of the Friedman Test and by performing follow-up Wilcoxon Signed-Rank Test on pairs of the populations it was identified at the 95% confidence level that UC has a higher K_{dBM} than OJC and at the 90% confidence level that UC has a higher K_{dBM} than MJC. The null hypothesis of the Wilcoxon Signed-Rank Test failed to be rejected when comparing MJC and OJC indicating no differences between those populations. The only statistically significant result of UC having a higher K_{dBM} than the other levels of confinement is contrary to what would be expected if the level of confinement was influencing the test results.

As a secondary comparison of the effect of the different levels of confinement within the Original Jet and the mini-jet, field data collected at Fletchers Creek in Mississauga with the mini-jet during this investigation is compared to data collected by Khan (2006) during an independent investigation using the original jet. Both investigations occurred at the same reach of Fletchers Creek and both occurred within the summer months. To ensure a proper comparison of the two datasets, the mini-jet tests were analyzed using BM to match the analytic method used by Khan and Kostachuck (2011). The two data sets are displayed in *Figure G6*. Comparing the means of the K_d of the two samples using a Mann-Whitney test fails to reject the null hypothesis that the samples have the same mean at the 90% confidence level. Comparing the means of the τ_c of the two samples using a Mann-Whitney test fails to reject the null hypothesis that the samples have the same mean at the 90% confidence level. These

results indicate that the means of both of the erodibility parameters are statistically indistinguishable at the 90% confidence level between the original jet and mini-jet results at Fletchers Creek.
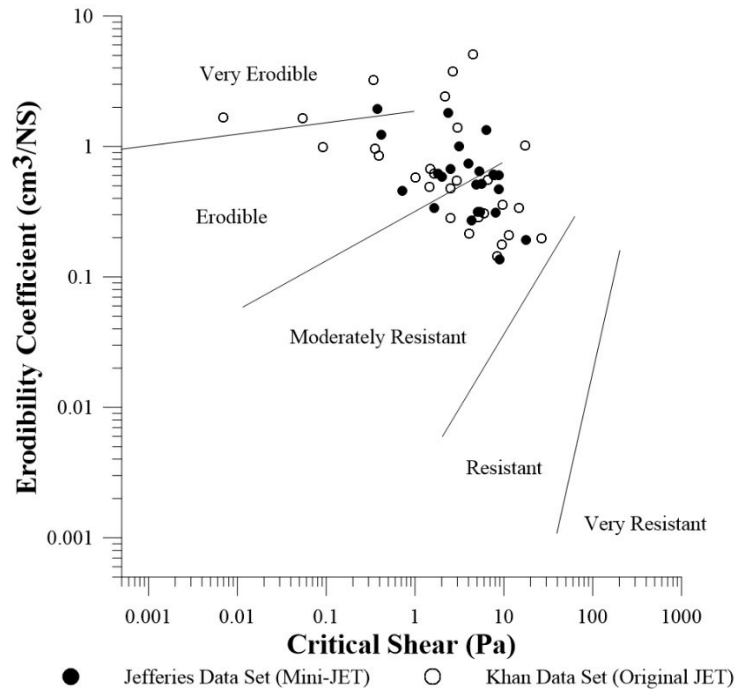
Figure G6: *Comparison of Original Jet and Mini-Jet data from Fletchers Creek*

Discussion

While the results of the laboratory experiment do not indicate any substantial deviation in applied shear stress as the level of confinement within the JET reservoir changes, some observations made during the study indicate that other external factors may have imposed limitations on the experimental setup. The atypical scour hole shapes observed during the tests are an indication that the test conditions may be influenced by two potential limitations.

First, the material preparation methods may have limited the ability to apply the same consolidation loads along a thin edge (~1mm in width) of the sample. This may have resulted in material more prone to erosion at the outer edge of the sample compared to the centre of the sample causing more erosion to occur at locations away from the maximum shear stress imposed by the impinging hydraulic jet. Further, the boundary conditions between the steel mold containing the specimen and the prepared soil sample may result in turbulent micro-hydraulic conditions locally increasing the shear stress imposed upon the sample. This could arise from imperfections of the soil sample at the

boundary creating a rougher surface than the sample interior, or from a change in surface roughness between the steel mold and soil sample altering the flow conditions at their interface. Cosette (2016) reported potential boundary influences from molds on samples retrieved from the field and tested using the JET methodology, however, the planar progression of scour observed in this investigation was not previously reported. This could be an indication that the atypical results of the scour hole are a manifestation of the sample preparation methodology and not a result of the boundary impacts on hydraulics within the steel mold. Alternatively, the boundary between the mold and sample may also create a preferential seepage pathway for water to enter the sample locally increasing the pore pressure and reducing the material's resistance to erosion at the outer edge of the sample more than the more tightly packed centre of the sample.

A second observation made during the experiment was the presence of a 1-4 mm layer of softer, saturated material at the test surface. This layer seemed to be less resistant to erosion than the underlying material which was more representative of the prepared specimen. The presence of this material may be related to the lack of plateauing within the scour depth versus time curves of the laboratory JETs which is similarly observed in the example comparative plots of original and mini-jet data presented by Al-Madhachi et al. (2013a). Instead of subjecting a homogenous material to continually decreasing stresses, the test may have been measuring how fast the wetting front propagated through the material, subsequently preparing a surficial layer of material to be eroded at stresses lower than the critical shear stress representative of the underlying sample material. However, this lack of plateauing is not consistently observed across JETs of remolded material, with the scour depth versus time curves presented by Khanal et al . (2016a) showing a more pronounced plateau in the datasets.

Despite these experimental limitations, there remains no evidence that altering the level of confinement within the JET reservoir alters the rates of erosion or the shear stresses imposed upon the material. Even at the beginning of the tests where the experimental limitations are at their lowest influence, and the applied shear stresses are highest (and the differences are expected to be greatest) there is no consistent, detectable difference in how much erosion is occurring between the levels of confinement. Further, a comparison between independent studies of Original JET and mini-JET data at Fletchers Creek, Mississauga, Ontario does not indicate any statistical differences in the estimated median erodibility parameters of the Blaisdell Method.

Based on these results, it is not recommended to apply any correction factor to mini-JET data when comparing between Original-JET and mini-JET results in the field. This is counter to the observations and recommendations of Simon et al. (2010) and Al-madhachi et al. (2013a), which presented results of laboratory and field investigations indicating similar K_d values between the Original JET and mini-JET, but lower estimated critical shear stresses (estimated from the Blaisdell method) for the mini-JET. The current investigation controlled for the primary experimental influence during the Al-Madhachi et al. (2013a) investigation which was reported as different ratios of the JET nozzle sizes to the depths of lifts during sample preparation. The analysis also considered the results of independent field investigations at the same site with both original and mini-JET data. The inability to obtain results indicating a difference in estimated critical shear stresses or differences in applied shear between the original and mini-JET devices introduces sufficient uncertainty to refrain from applying a correction to mini-JET data until further research can confirm an appropriate method to ensure proper comparisons between the data sets of the two devices. Nor do the results of this investigation support the proposed correction by Ghaneeizad et al. (2015), suggesting that the applied shear stress within the original jet reservoir is 2.4 times greater than the typically used values for jet impingement within an unconfined environment. Additionally, with the goal of this investigation to obtain in-situ datasets representative of field conditions, it is reasonable to conclude that other areas of uncertainty within the JET procedure are more important to control for and focus research efforts upon rather than the effect of confinement within the JET reservoir. These contributing factors include standardizing test duration, accounting for material heterogeneity and weathering, and standardizing the solution technique. All of which can demonstrably alter the estimated erodibility parameters to a greater extent than the effect of confinement within the JET reservoir.

Appendix H: Correcting SD and LR Failures

SD was noted by Wahl (2016) to occasionally result in critical shear estimates of zero, which do not coincide with the observations during testing. This same phenomenon was observed in this investigation when analyzing the Type 2 region of JETs with the SD solution technique. When this type of SD failure occurs, it is accompanied by a correspondingly lower estimate of the erodibility parameter than anticipated. Further, there are several other anomalous instances where $\tau_{cSD} \neq 0$ but $\tau_{cSD} < \tau_{cBM}$ and $K_{dSD} < K_{dBM}$; this is counter to the consistent trend of SD having higher estimates of both erodibility parameters compared to BM (*Figure H1a*). In these anomalous instances, the erodibility parameter estimates provided by SD do not align with results from similar tests demonstrating similar scour development in the same material reducing the confidence in their representativeness. Further, alterations to the input scenarios of these anomalous tests frequently result in SD failure ($\tau_{cSD} = 0$); these tests were deemed to be on the "brink of failure".
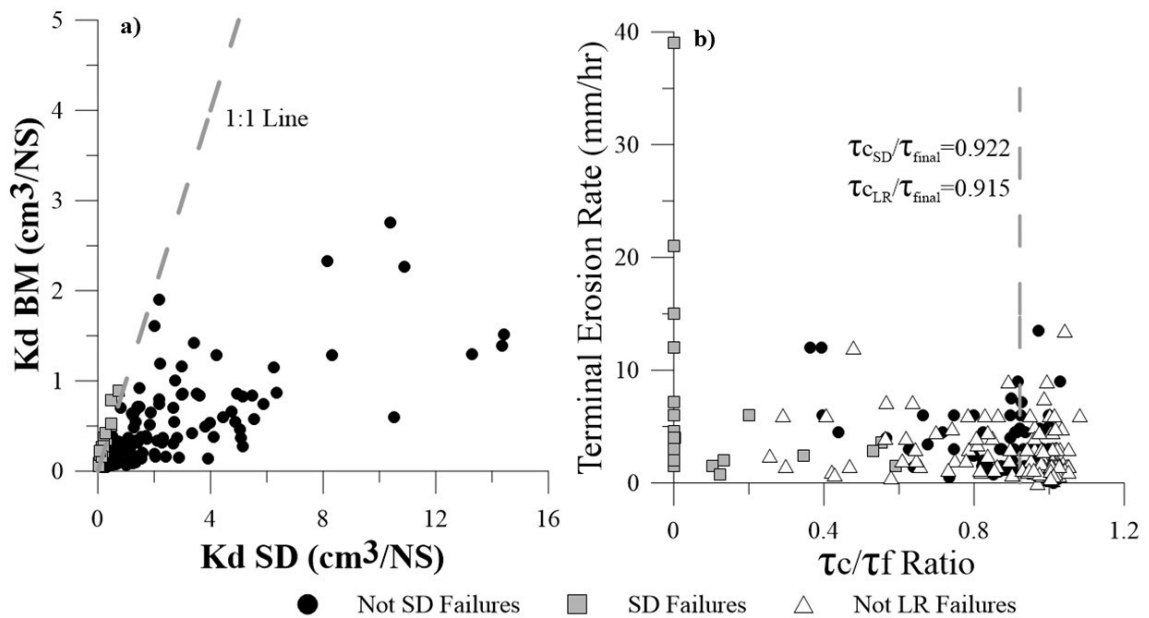
Figure H1: *Basis for Proposed Correction Methods for SD and LR Failures. a) demonstrates the rationale for the K_d based correction and b) demonstrates the rationale for the τ_C based correction*

LR also provides unrealistic erodibility parameters in the form of a negative τ_{cLR} or a negative K_{dLR}; which are recognized as extraneous non-real results based upon the applied model technique. Where

these conditions were observed, the frequency of SD and LR failures are recorded for each input scenario with and without-segmentation and two proposed methods to overcome SD failures and one method to overcome LR failures are offered below.

K_d based correction (Method 1)

The first method of correction for SD leverages the consistent trend of $K_{dSD} > K_{dBM}$. As demonstrated in *Figure H1a*, this relationship does not hold true when SD fails. The objective of the Excel® GRG (Generalized Reduced Gradient) non-linear solver routine within SD methodology (Daly et al., 2013) is to minimize $\sum_{i=1}^{n}(E_{predicted} - E_{measured})^2$ where $E_{pridcted}$ is the erosion predicted by *Equation 1* at a trialled set of erodibility parameters (K_d, τ_c), $E_{measured}$ is the erosion measured during the JET and n is the number of measurements taken during the JET. The routine continuously trials sets of erodibility parameters until the minimization objective has been optimized. SD methodology is subject to the constraint that $E_{pridcted_i} < E_{predicted_{i+1}}$. The K_d based method of correction proposed here adds an additional constraint upon the K_d values that are be trialled during the Excel® GRG non-linear solver routine such that $\frac{K_{dSD}}{K_{dBM}} \geq 1$ This constrains the grey squares in *Figure H1a* to fall on or to the right of the 1:1 line. No constraints are proposed to be applied directly to the τ_C variable in this correction method, however, given that τ_C and K_d are solved for simultaneously within SD the additional constraint upon K_{dSD} will also affect the estimation of τ_{CSD}.

τ_C based correction (Method 2)

This method of correction for both SD and LR is based on the proximity of τ_c estimates provided by SD and LR to the terminal shear stress imposed upon the material at the end of the test. As demonstrated in *Figure H1b*, τ_{cSD} and τ_{cLR} are observed to frequently yield results near the terminal shear stress imposed at the end of the JET (i.e. $\tau_{CSD}/\tau_{cfinal} \approx 1.0$) where τ_{cfinal} is the shear stress applied at the termination of the JET. The mean ratio of τ_{CSD}/τ_{cfinal} in tests where SD failure does not occur is $\tau_{CSD}/\tau_{cfinal} \approx 0.92$. The τ_c based method of correction proposed here forces $\tau_{cSD} = 0.92\tau_{cfinal}$ and as a result it is then removed as a variable during the Excel® GRG non-linear solver routine. With τ_{cSD} now fixed and no longer a variable within the SD solution technique, the Excel® GRG non-linear solver routine can proceed to minimize $\sum_{i=1}^{n}(E_{predicted} - E_{measured})^2$ subject to

the constraint $E_{pridcted_i} < E_{predicted_{i+1}}$ by varying only K_{dSD} instead of both K_{dSD} and τ_{cSD} simultaneously.

Demonstrated within *Figure H1b*, $\tau_{CLR}/\tau_{cfinal} \approx 0.92$. When the τ_c based method of correction proposed here is applied to the LR solution technique the critical shear stress is forced to $\tau_{cLR} = 0.92\tau_{cfinal}$. This is equivalent to fixing the x-intercept of the linear regression. Now with the τ_{cLR} already determined, the LR solution technique can proceed to minimize $\sum_{i=1}^{n}(ER_{predicted} - ER_{measured})^2$ (where $ER_{measured}$ is the erosion rate observed for a τ_o applied during the JET and $ER_{predicted}$ is the erosion rate predicted by the linear regression of τ_o and observed erosion rates) by altering only K_{dLR} (the slope of the regression line) rather than both K_{dLR} and τ_{cSD}.

Frequency of Occurrence

The frequency of failures was tracked to determine if they became more or less frequent with different input scenarios or if their frequency was exaggerated or ameliorated by the segmentation of tests. The results of tracking their frequency of occurrences are demonstrated below in *Figure H2*. There does not appear to be any relation between test duration and SD failure with the highest frequency of occurrence with and without segmentation occurring at 80-minute test duration. Segmentation of the test results in an increase in SD failures in both test duration input scenarios and measurement frequency input scenarios compared to looking at the full data set. With segmentation, there appears to be some relationship between measurement frequency and failure rate with more coarse measurement frequencies having lower failure rates and measurement schemes with rapid measurements having higher failure rates compared to their non-rapid counterparts, however, this observation is not reflected without segmentation.

LR failure rate appears to have a relationship with test duration with more failures occurring during shorter tests. This is a stronger relationship with segmentation with only the 45minute test duration not fitting the trend. It is also apparent that the inclusion of rapid measurements results in lower failure rates for LR. For both test duration scenarios and measurement frequency, the segmentation of tests increases the occurrence of failure in the LR methodology.
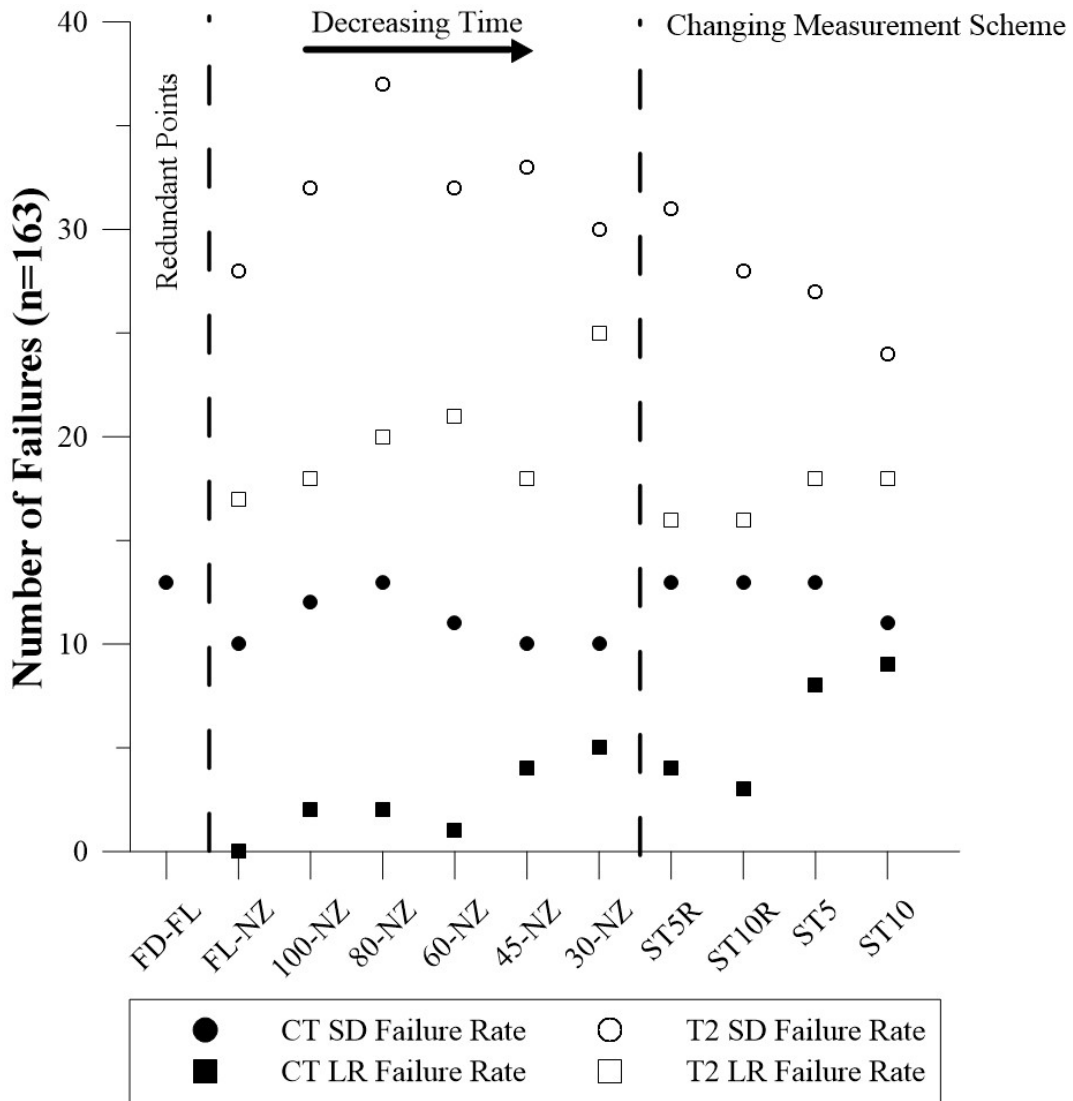
Figure H2: *Frequency of Failures of SD and LR with Input Scenario*

Correction Results

Figure *G3* shows the results of the proposed correction methods in comparison to the SD solution technique where failure does not occur and the BM solution technique. Correction method 1, where K_{dSD} is forced to be greater than K_{dBM}, plots within the population of BM results. Indeed, investigating each test that is corrected using this method shows that forcing K_{dSD} to be greater than or equal to K_{dBM} is equivalent to forcing K_{dSD} to be equal to K_{dBM}. This agrees with intuition; in

288

these instances, the solver routine is optimized by having a low K_{dSD} and adding in the additional constraint simply changes the lower limit that can be obtained in the solver routine.
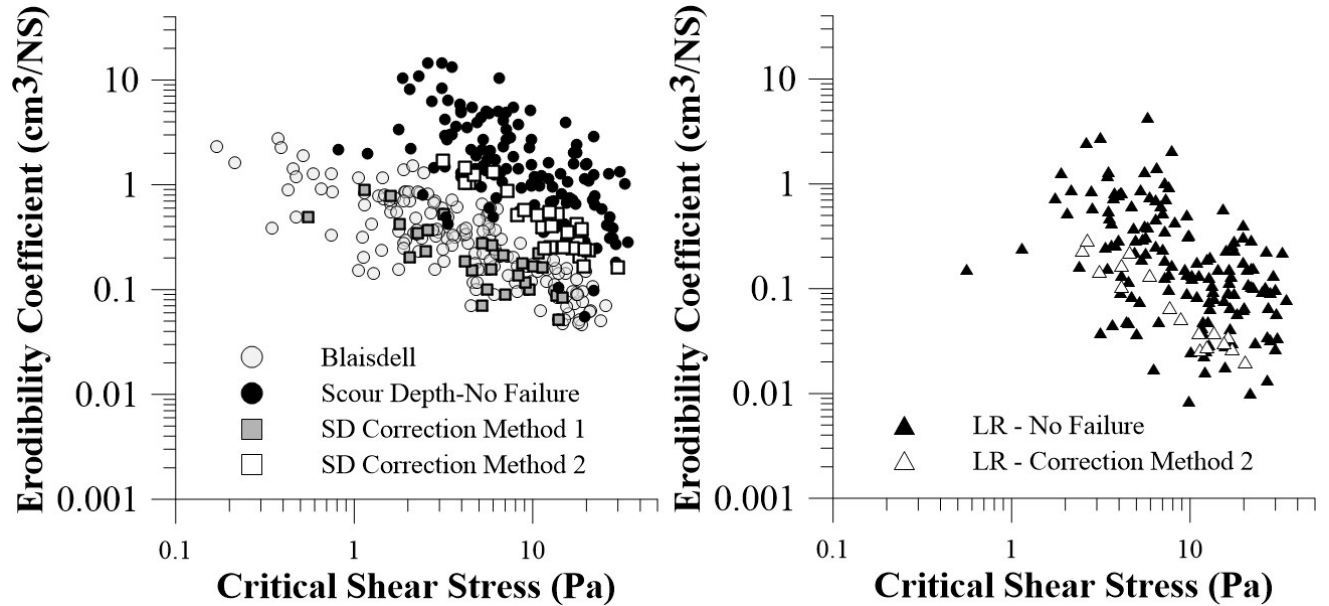
Figure G3: *Results of Proposed Correction Methods for LR and SD*

The second correction method shows a greater alignment with the SD population where no failure occurs. However, the corrected tests plot on the lower limits of the non-failure population. The same result is observed when it is applied to LR. This indicates that the corrected tests tend to have a lower K_d and lower τ_c but are still within the bounds of what is to be expected to be estimated by their respective methods of analysis.

Discussion

The frequency of failure rates for both SD and LR increases with segmentation of the tests. This is perhaps attributed to the removal of higher erosion rates at the beginning of tests and the application of the highest shear stresses which forces a stronger positive relationship between erosion rates and shear stress application compared to the remainder of the test. SD failures do not appear to have any relation to the test duration, however, LR failures increase as test durations decrease. This trend is strengthened after segmentation occurs. This most likely arises from the tail end of tests with lower applied shear stresses and the importance of lower erosion rates in forcing the linear regression to have a positive slope (K_d) and a positive x-intercept (τ_c) compared to more scatter during the middle portions of the tests. After segmentation, the high erosion rates and applied shear stresses which assist

in obtaining a positive slope and x-intercept during regression are removed, increasing the importance of the region of lower erosion rates and lower applied shear stresses at the end of the test. By reducing the test duration this portion is removed leading to a regression being based upon the more variable middle test portion and an increase in failures of the LR solution technique.

Method 1 of correcting for SD failure does not produce reliable results and from *Figure G3* it is clear from a visual assessment that the results of the correction show a greater affinity for the population of tests from BM than the population of tests from SD.

Given the generally consistent low erosion rates experienced at the end of JETs, it is reasonable to expect the critical shear stress to be proximal to the final applied shear during the test. When Method 2 is applied to SD and LR failures, it produces results that generally align with the populations of LR and SD that did not fail. The results of the corrected LR and SD tests fall within the range of results of the tests with no failures with a slight visual bias to lower predicted K_d values. The only site with a sufficient population of LR failures to justify a comparison between LR erodibility parameters estimated through Correction Method 2 and tests which did not fail is MCE; here a Mann-Whitney test is not able to identify any differences in the median estimate of K_d or τ_c at the 95% confidence level between tests corrected with Method 2 and tests which did not fail. This indicates that the level of variability inherently present at a site outweighs any additional variability caused by correcting LR tests using this method. Three sites had sufficient tests corrected for SD failure to compare the erodibility coefficients estimated through Correction Method 2 and tests that did not have an SD Failure: MCE, GRL and FC. The only erodibility parameter that is found to have a significantly different median at the 95% confidence level is K_{dSD} at the FC site. Compared to GRL and MCE, FC has a slightly higher median K_{dSD} value which may indicate that a bias towards lower corrected K_{dSD} values is more pronounced at sites with higher K_{dSD} estimates. Alternatively, this could be a representation of the tests themselves and not the method of correction. Tests with lower erodibility may be more prone to these failures, so a direct comparison assuming equal characteristics of the populations is not necessarily appropriate. More research is required to assess how persistent any apparent bias is in the corrected K_{dSD} values, and how that influences the characterization of a site. Until a more detailed investigation can be performed, these results provide sufficient evidence to support using Correction Method 2 to obtain reasonable and realistic erodibility parameters when presented with the unrealistic and unrepresentative values obtained when the SD and LR solution techniques fail.

Appendix I: Scour Depth vs Time Plots

DCB-01-01	
Without Segmentation	With Segmentation
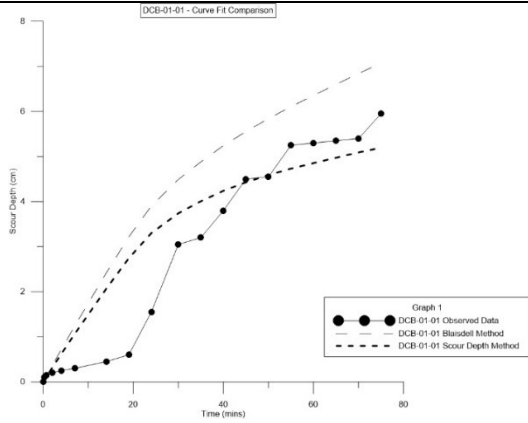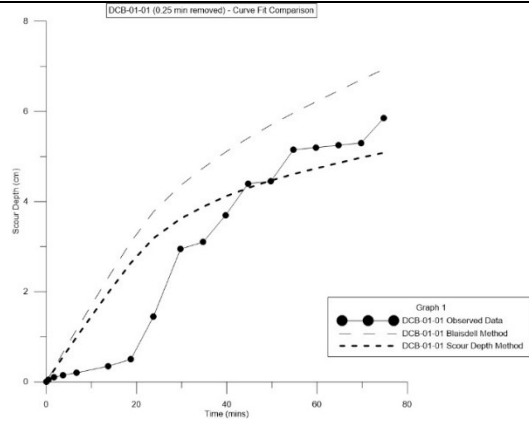
DCB-01-02	
Without Segmentation	With Segmentation
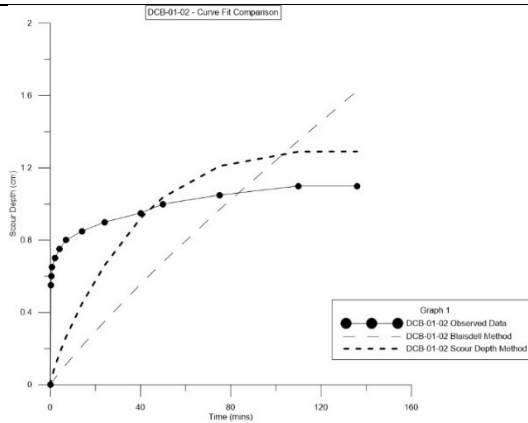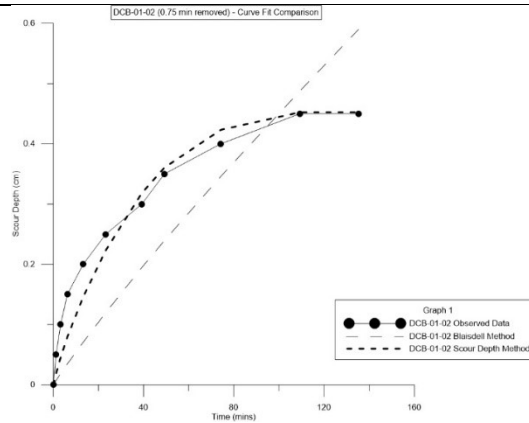
DCB-01-03	
Without Segmentation	With Segmentation
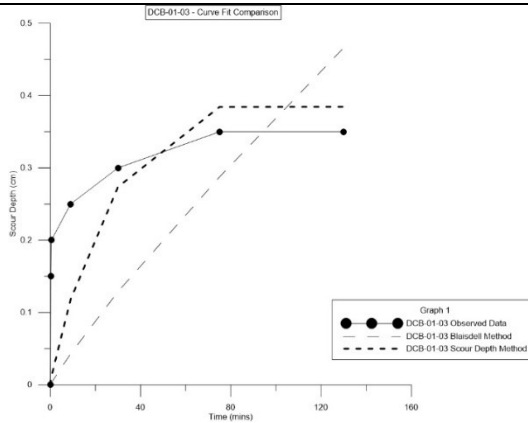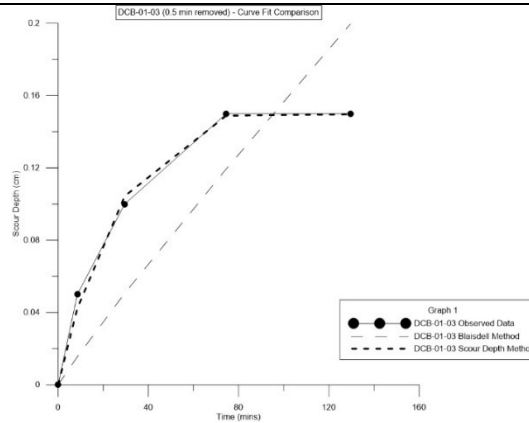
DCB-01-04
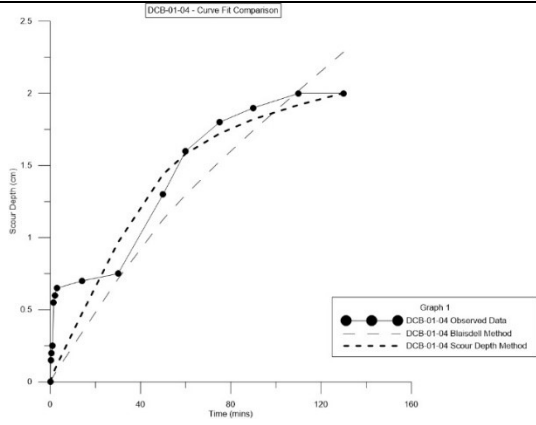
Without Segmentation	With Segmentation
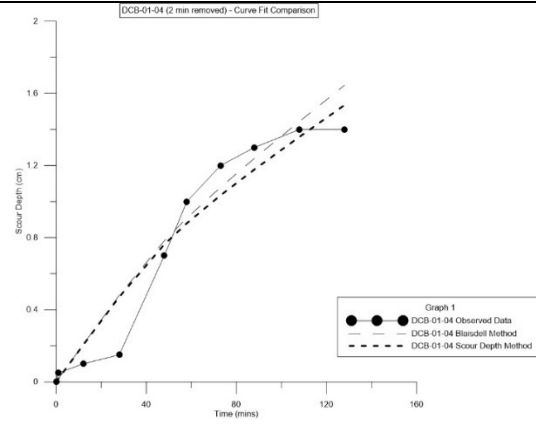
DCB-01-05
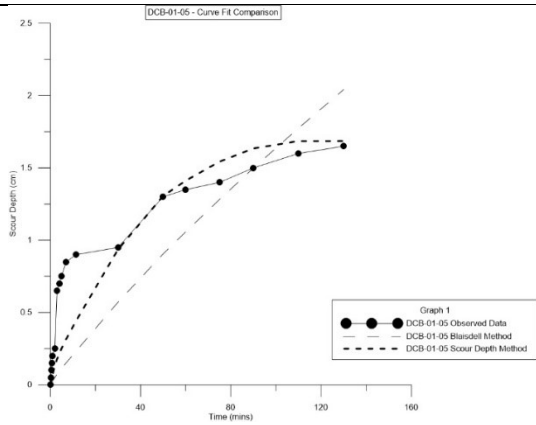
Without Segmentation	With Segmentation
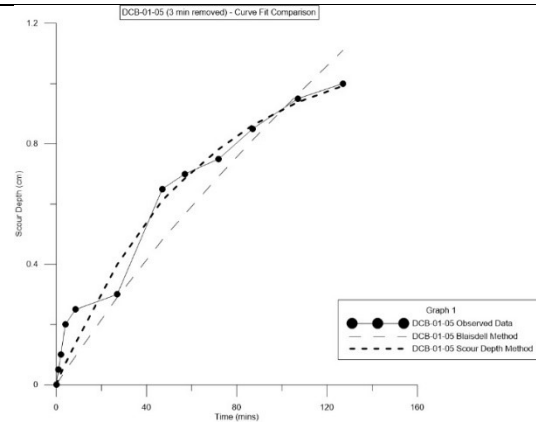
DCB-02-12
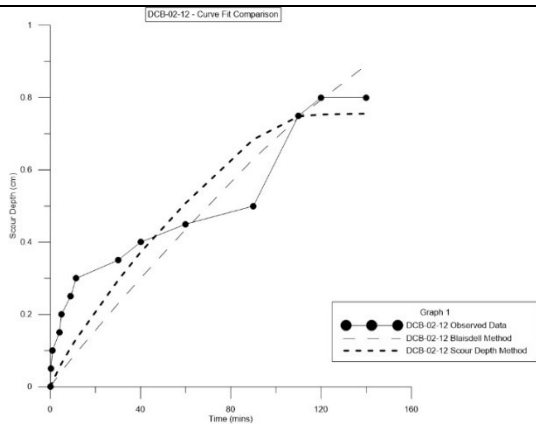
Without Segmentation	With Segmentation
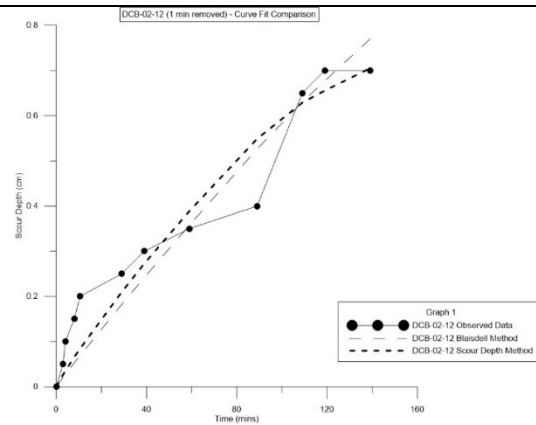
DCB-02-13	
Without Segmentation	With Segmentation
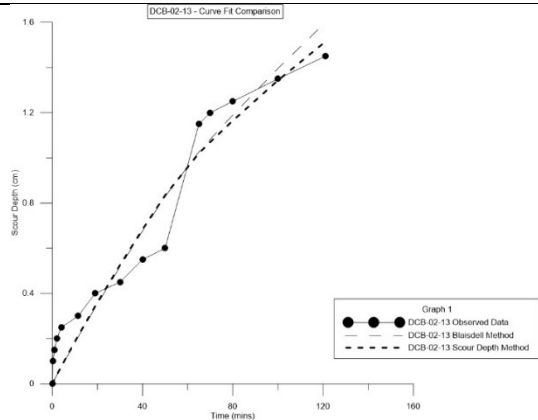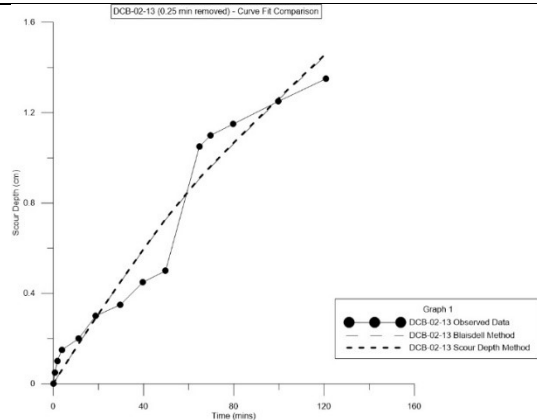
DCB-02-14	
Without Segmentation	With Segmentation
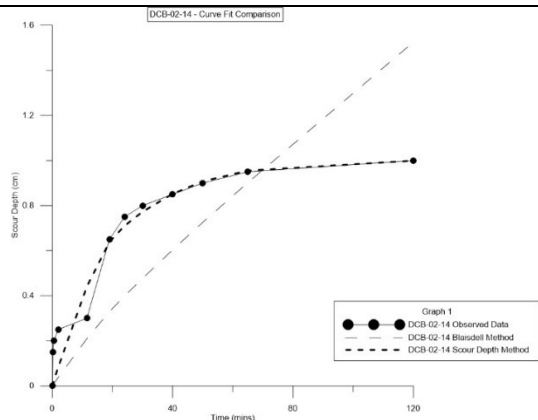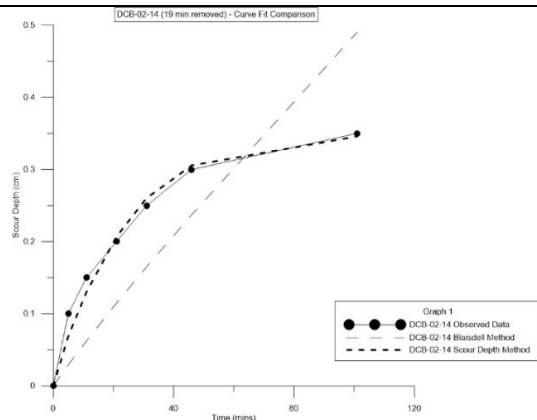
DCB-02-21	
Without Segmentation	With Segmentation

294
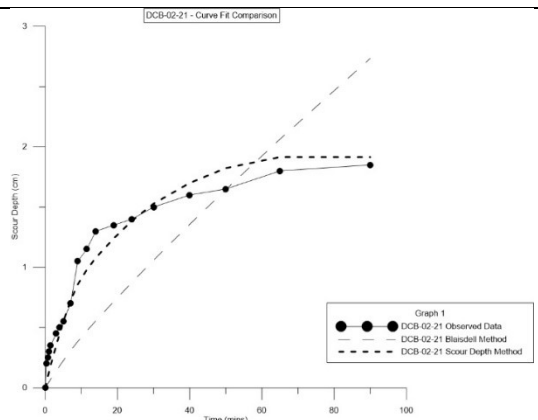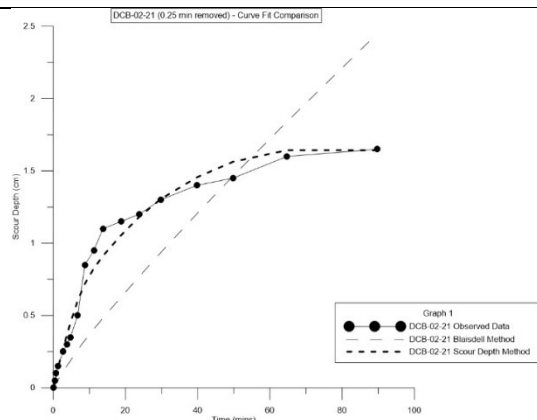
DCB-02-22	
Without Segmentation	With Segmentation
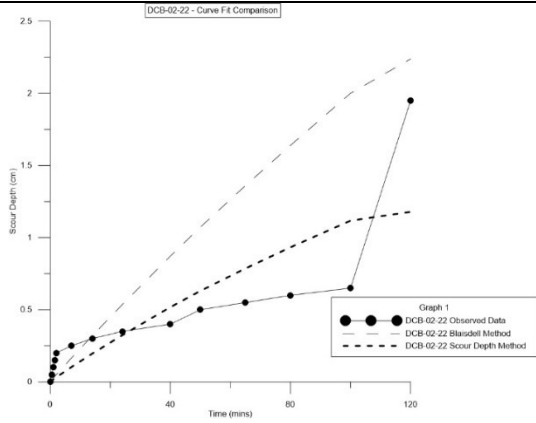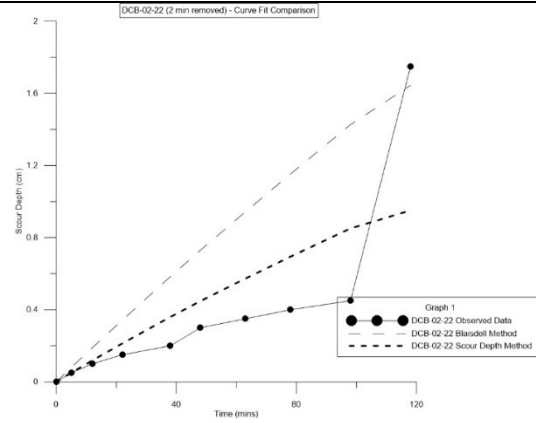
DCB-03-01	
Without Segmentation	With Segmentation
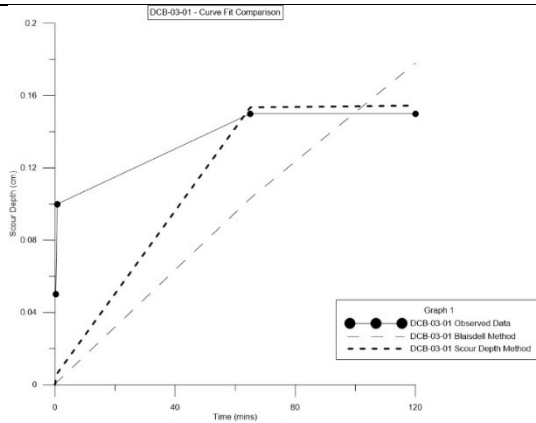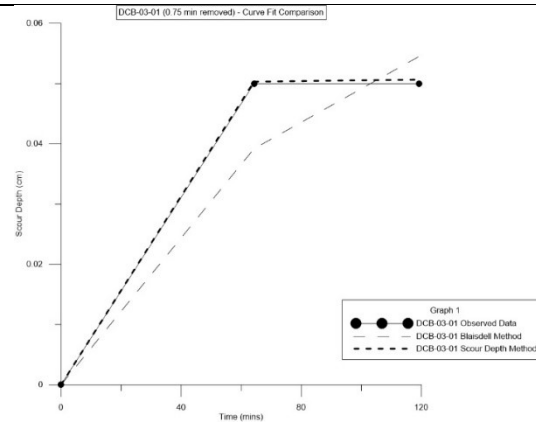
DCB-03-02	
Without Segmentation	With Segmentation
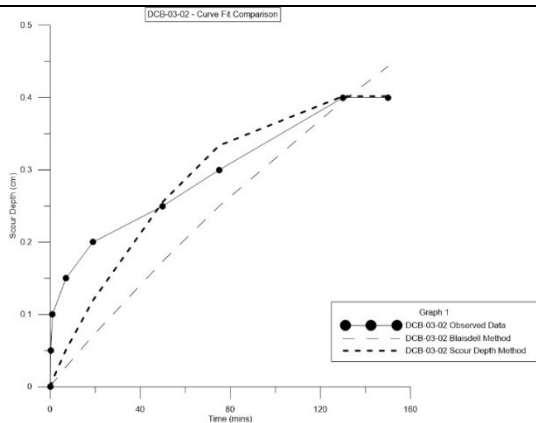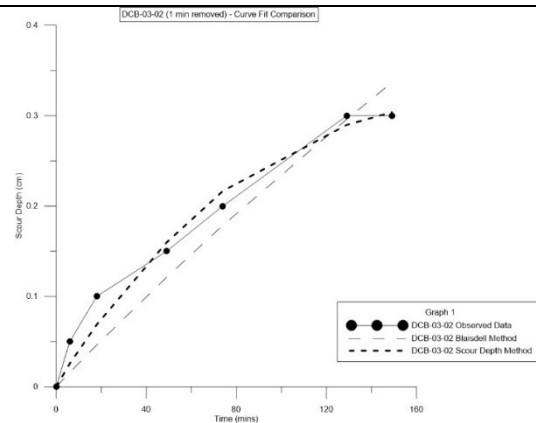
ETC-01-02
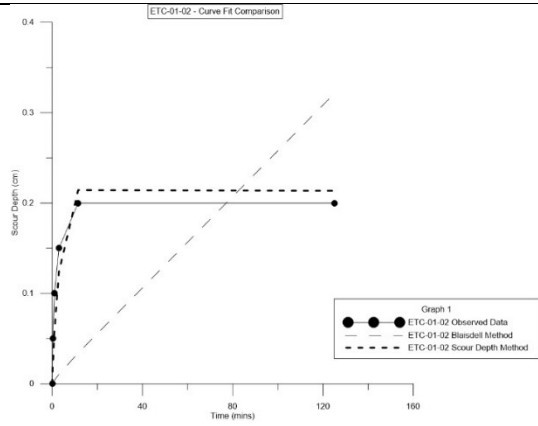
Without Segmentation	With Segmentation
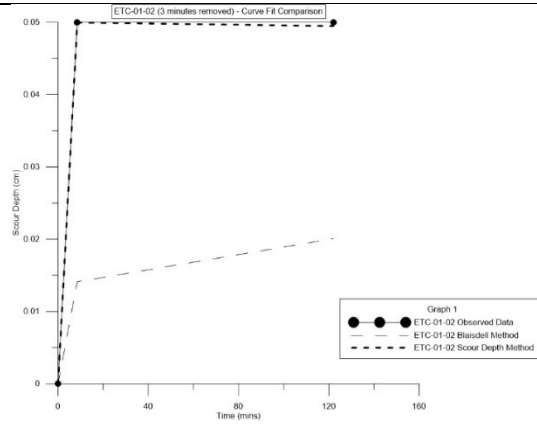
ETC-01-03
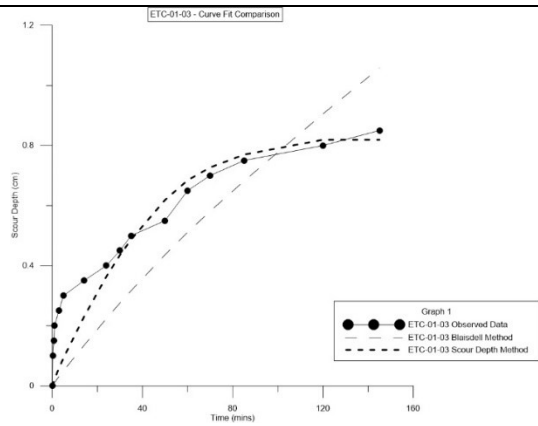
Without Segmentation	With Segmentation
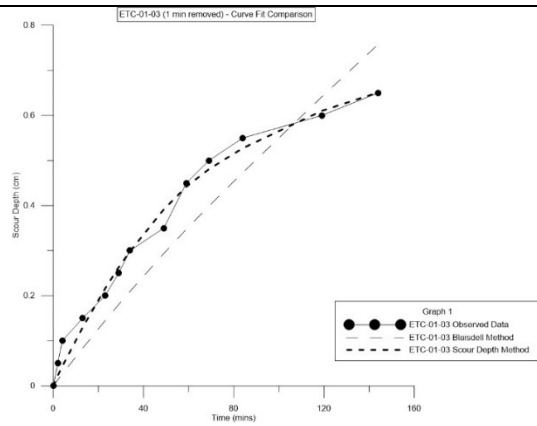
ETC-01-11

Without Segmentation	With Segmentation

296
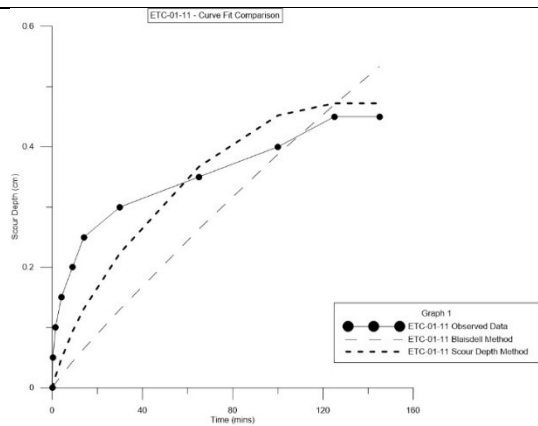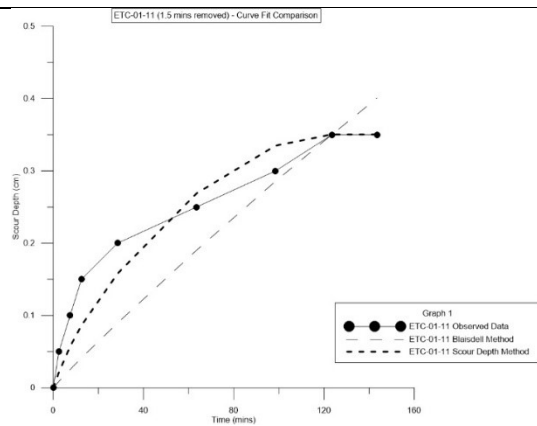
ETC-01-13
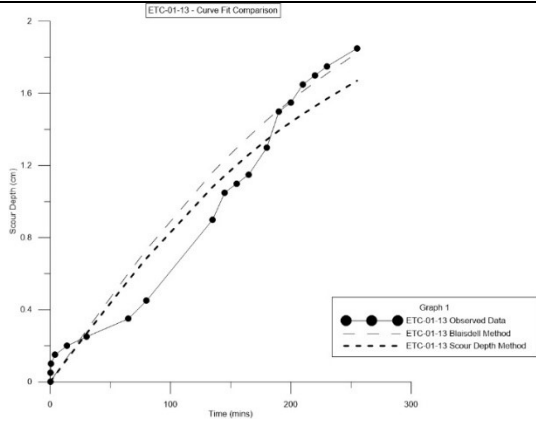
Without Segmentation	With Segmentation
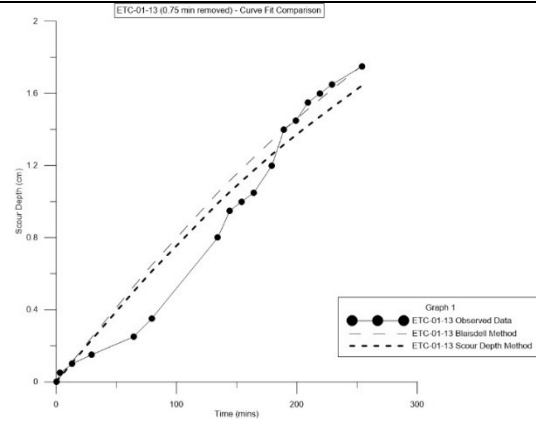
ETC-02-01
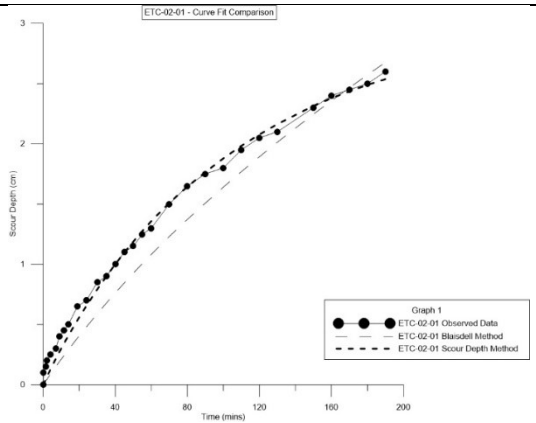
Without Segmentation	With Segmentation
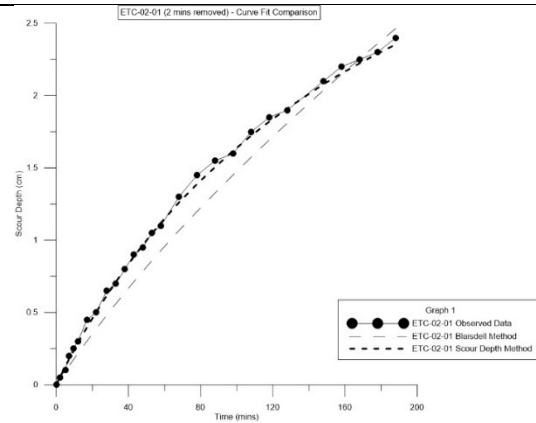
ETC-02-11
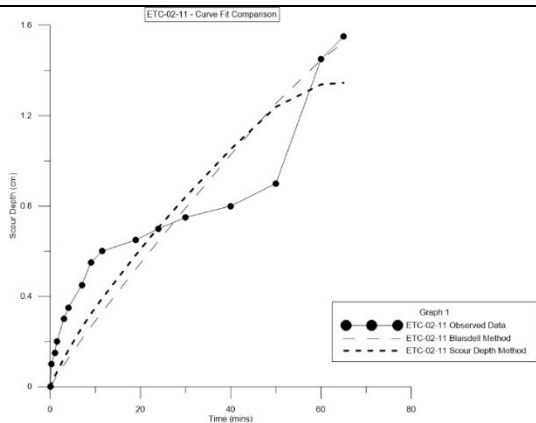
Without Segmentation	With Segmentation
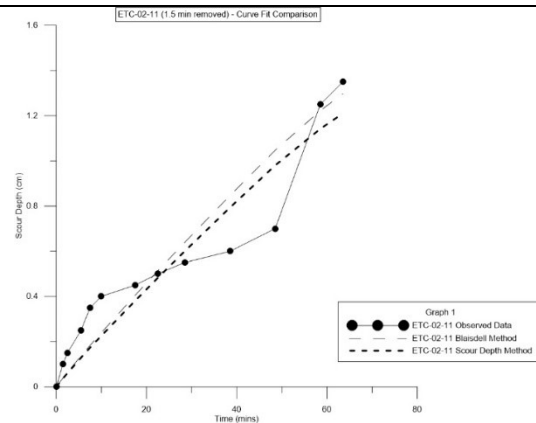
ETC-02-12
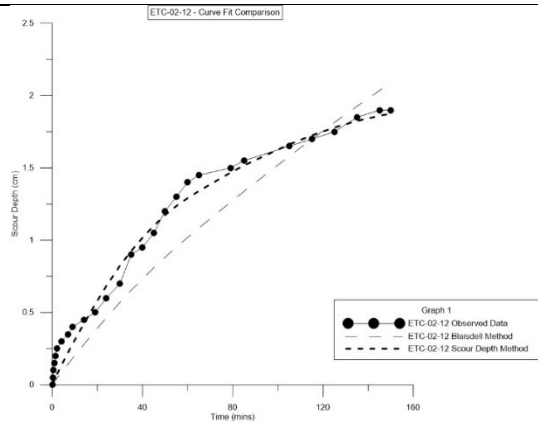
Without Segmentation	With Segmentation
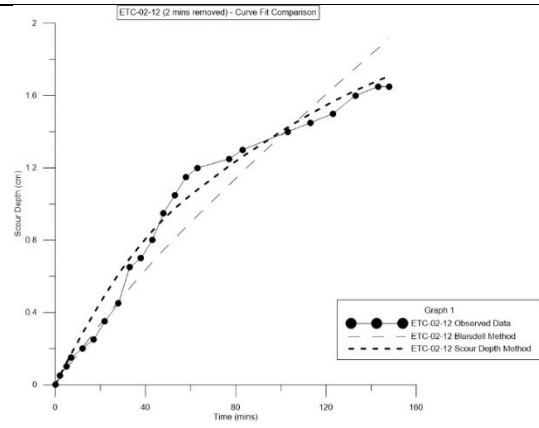
FC-01-01
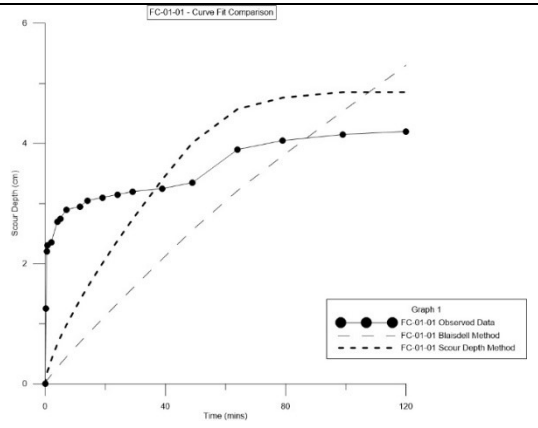
Without Segmentation	With Segmentation
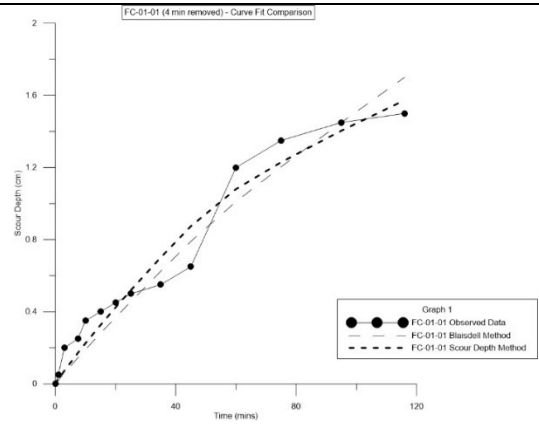
FC-01-02
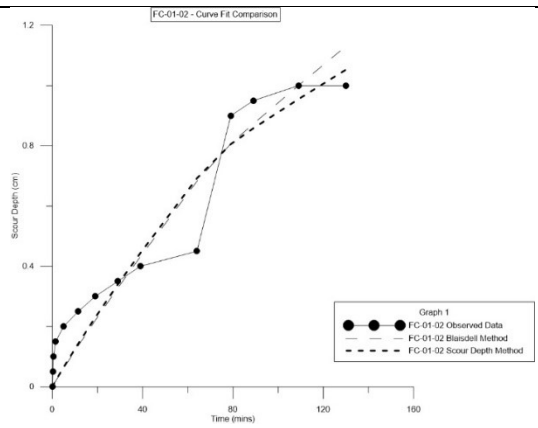
Without Segmentation	With Segmentation
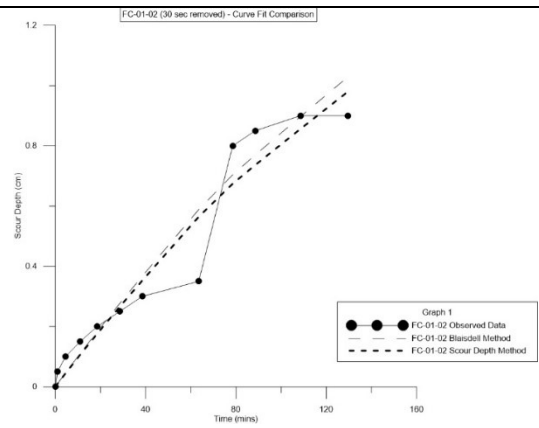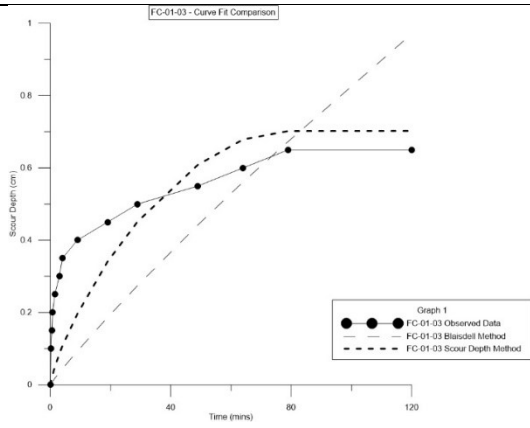
FC-01-03	
Without Segmentation	With Segmentation
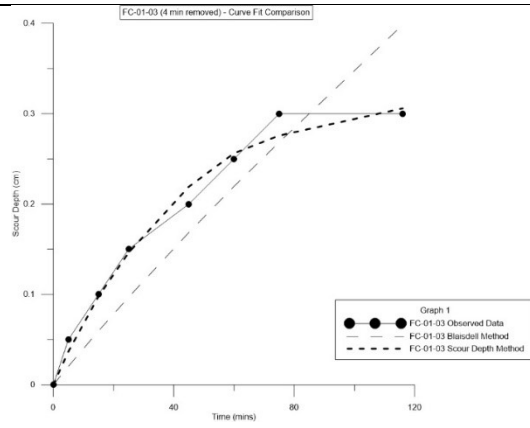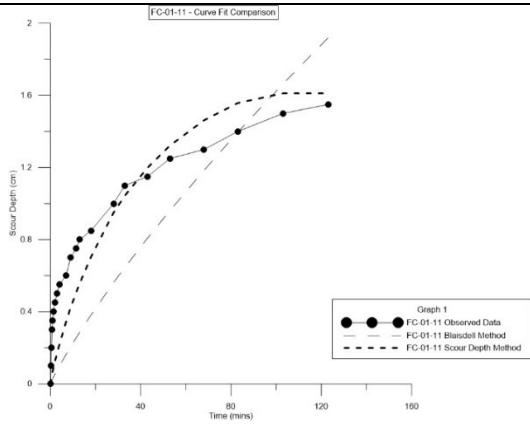
FC-01-11	
Without Segmentation	With Segmentation
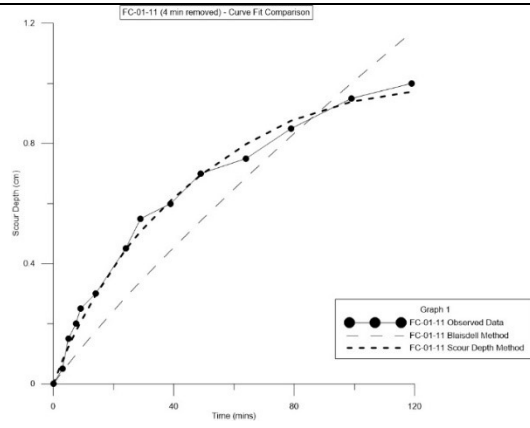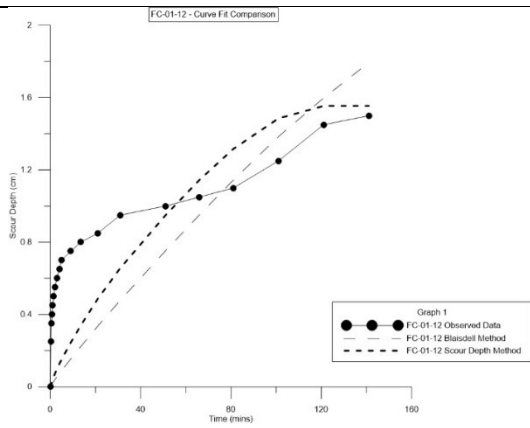
FC-01-12	
Without Segmentation	With Segmentation
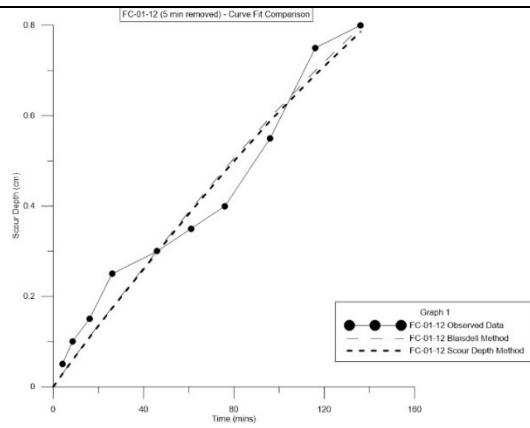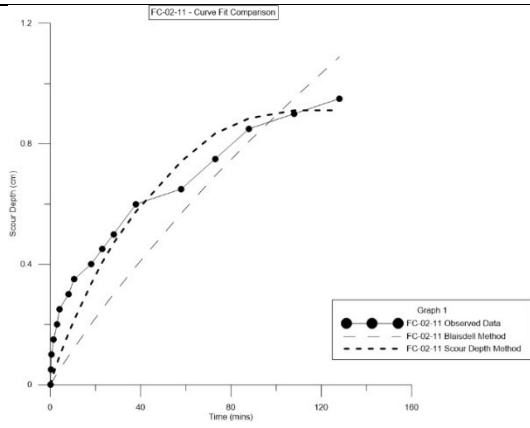
FC-02-11	
Without Segmentation	With Segmentation
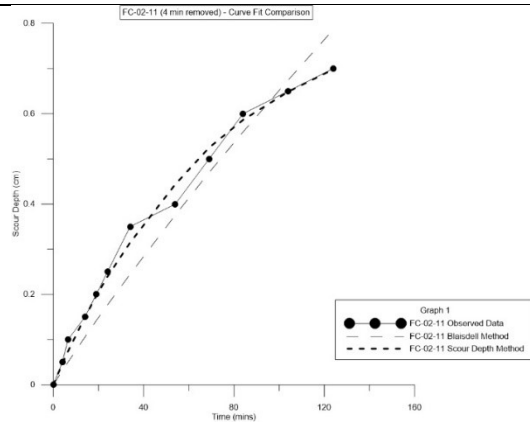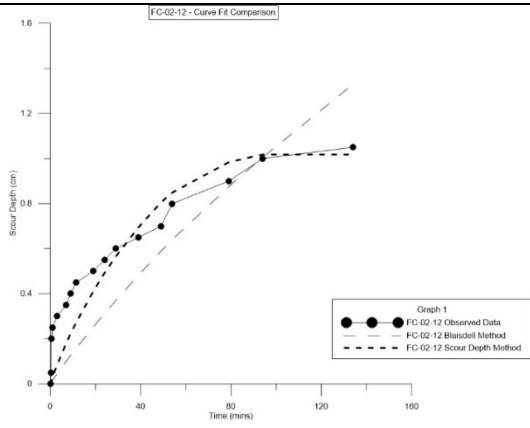
FC-02-12	
Without Segmentation	With Segmentation
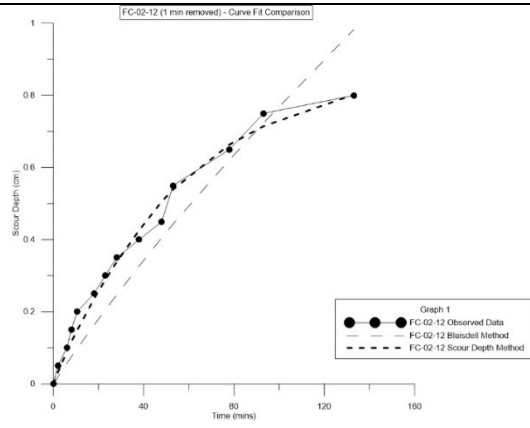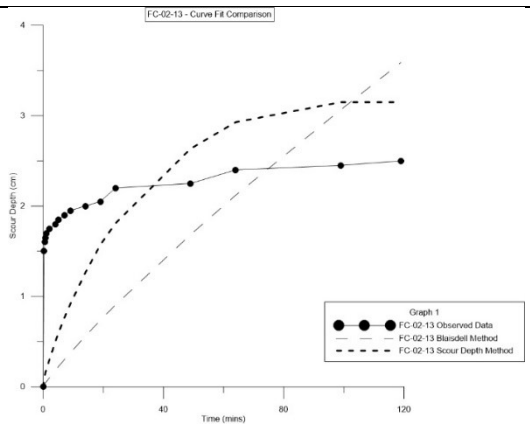
FC-02-13	
Without Segmentation	With Segmentation
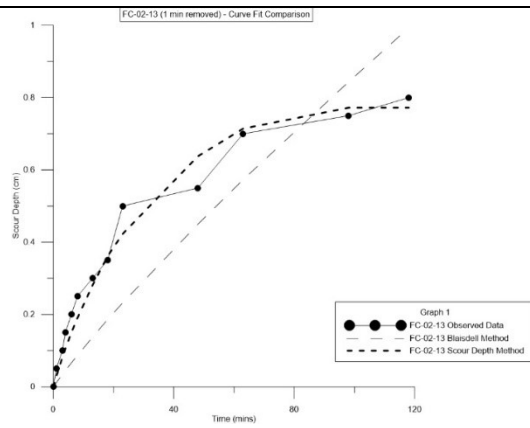
FC-02-21	
Without Segmentation	With Segmentation
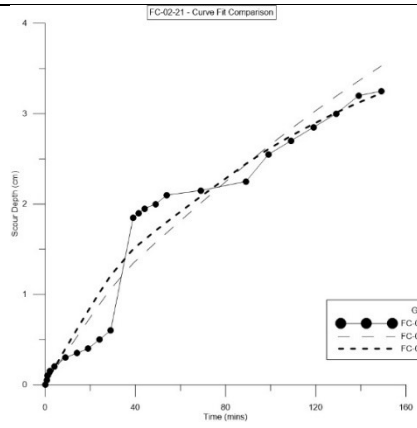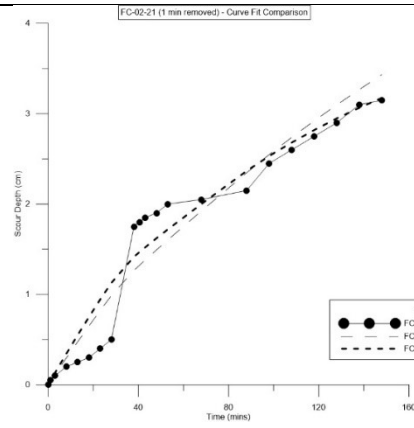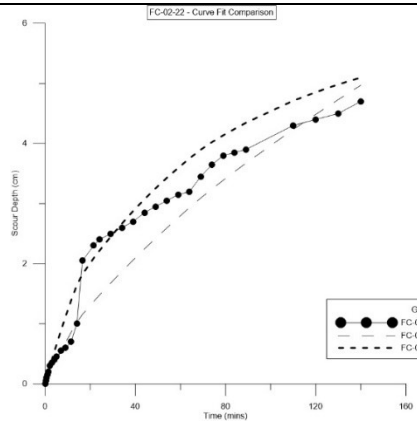
FC-02-22	
Without Segmentation	With Segmentation
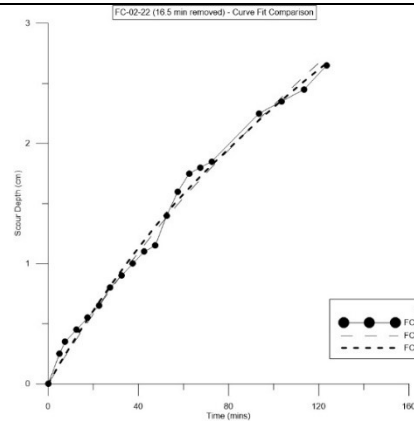
FC-02-23	
Without Segmentation	With Segmentation
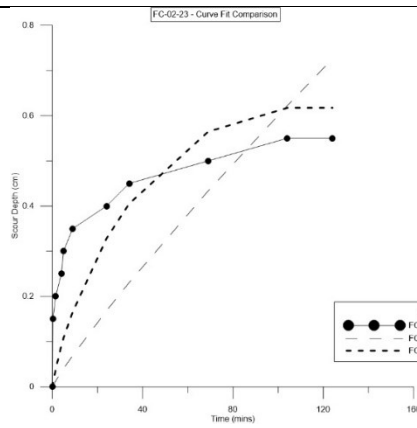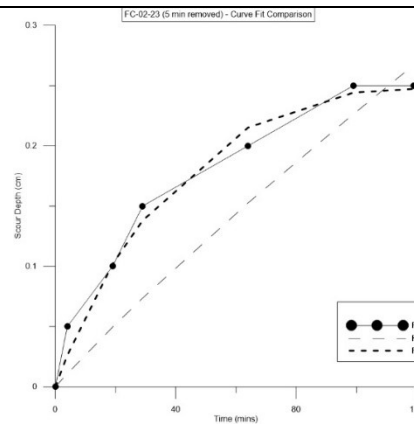
FC-02-24
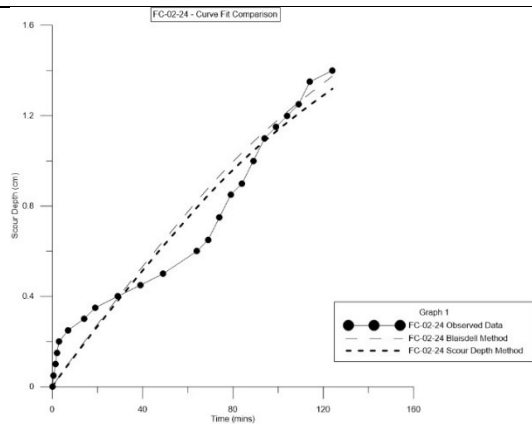
Without Segmentation	With Segmentation
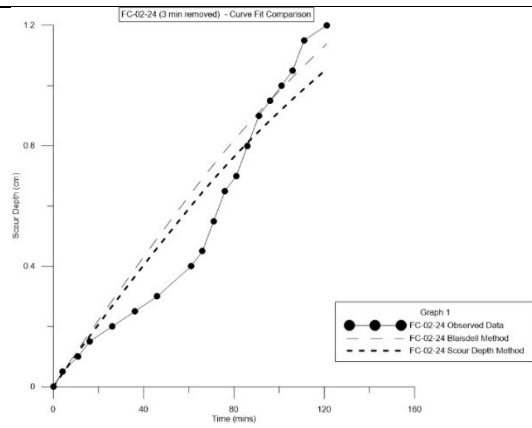
FC-02-25
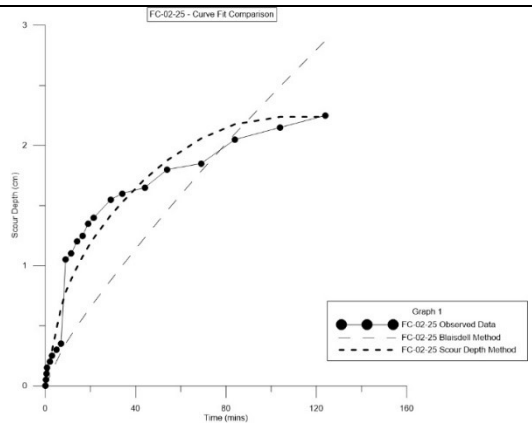
Without Segmentation	With Segmentation
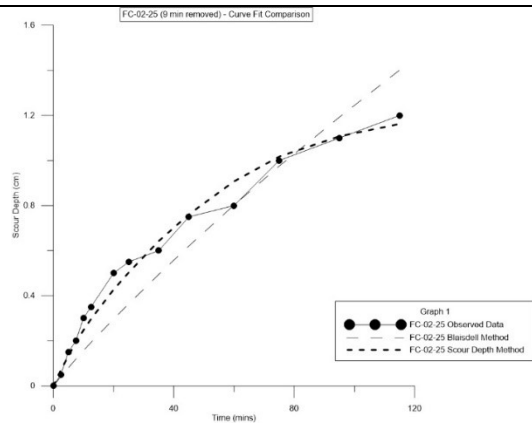
FC-02-26

Without Segmentation	With Segmentation

302
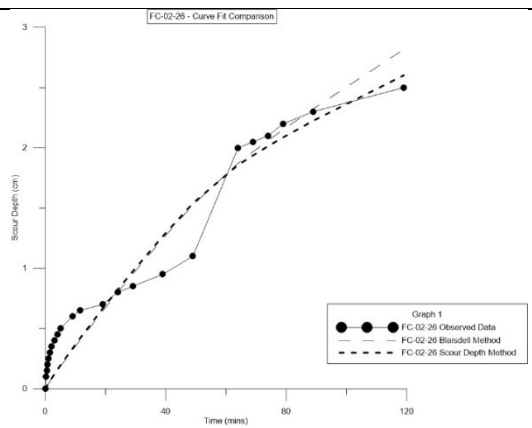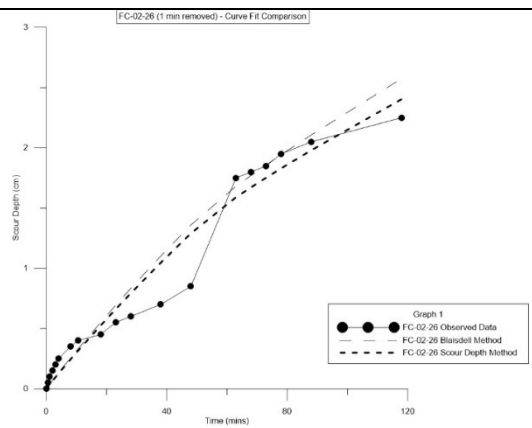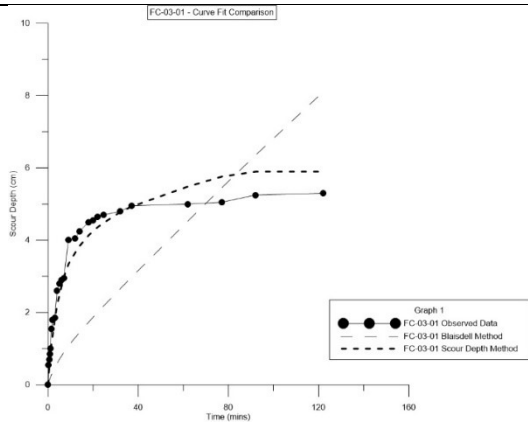
FC-03-01	
Without Segmentation	With Segmentation
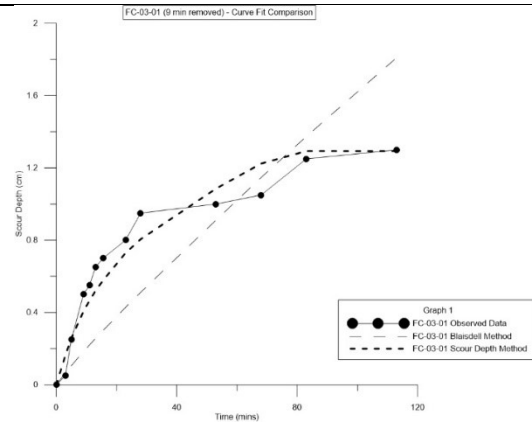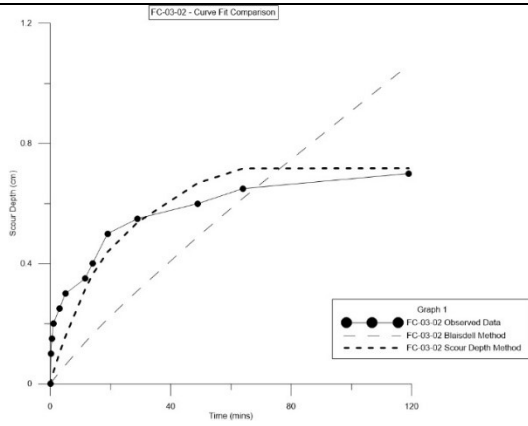
FC-03-02	
Without Segmentation	With Segmentation
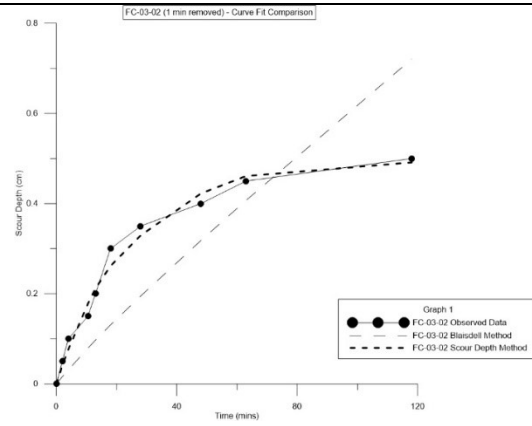
FC-03-03	
Without Segmentation	With Segmentation

303
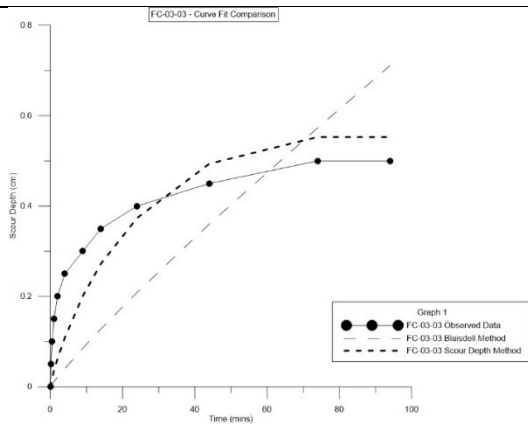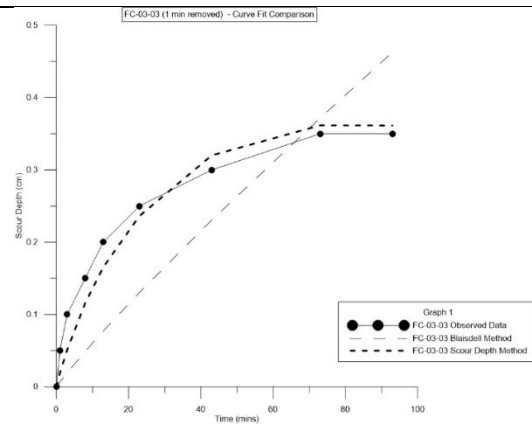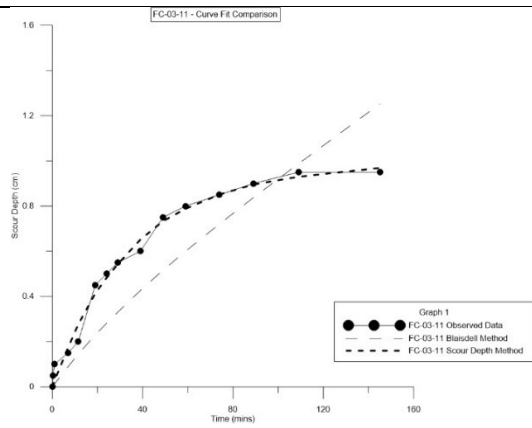
FC-03-11	
Without Segmentation	With Segmentation
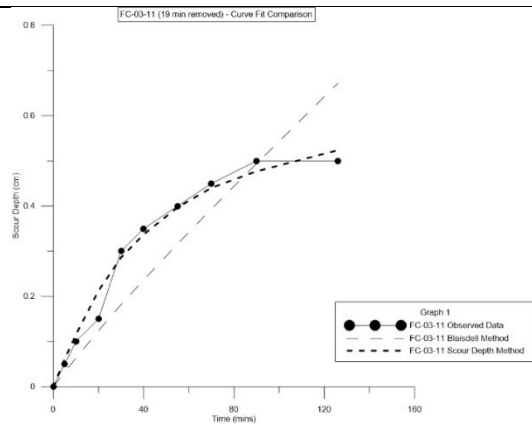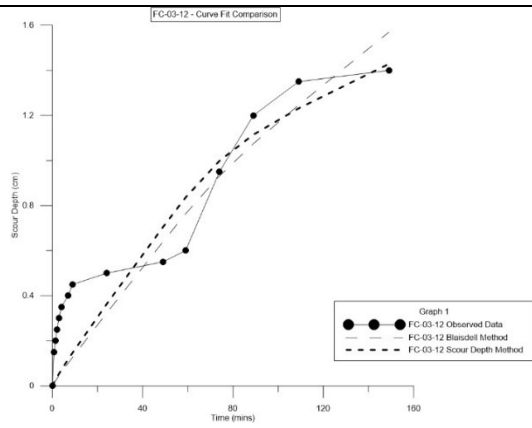
FC-03-12	
Without Segmentation	With Segmentation
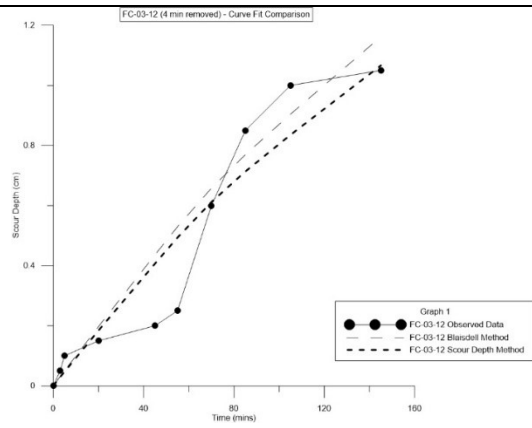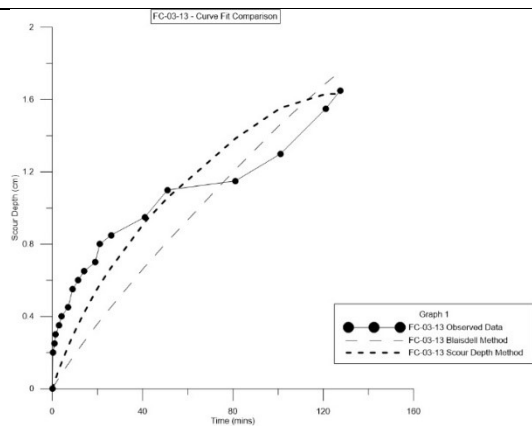
FC-03-13	
Without Segmentation	With Segmentation
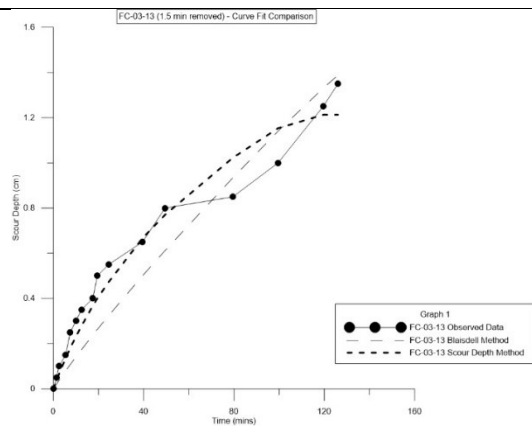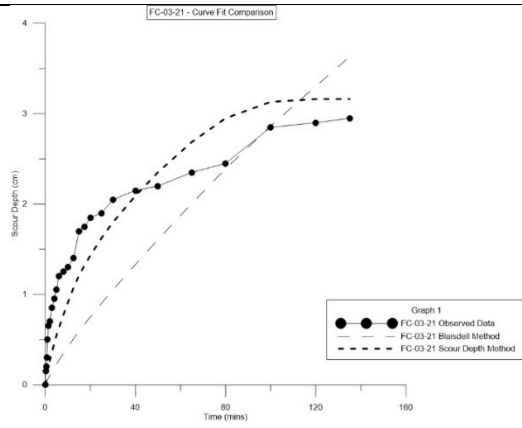
FC-03-21	
Without Segmentation	With Segmentation
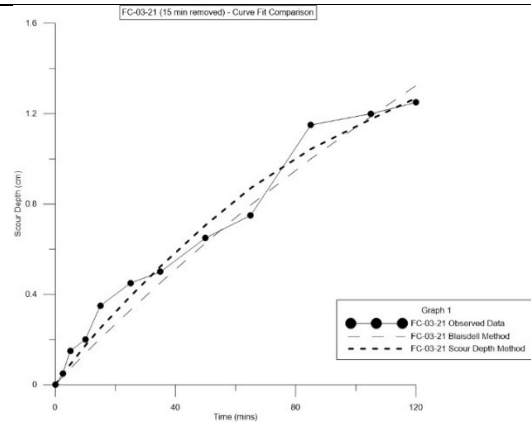
FC-03-22	
Without Segmentation	With Segmentation
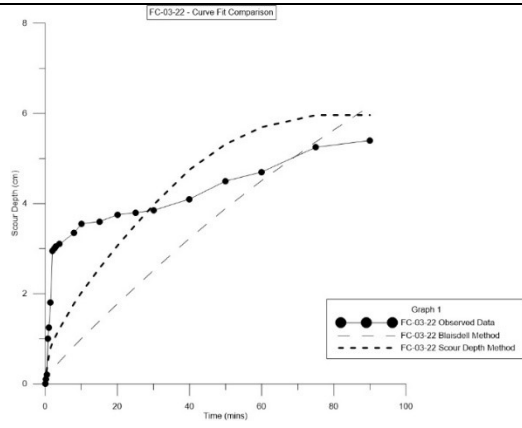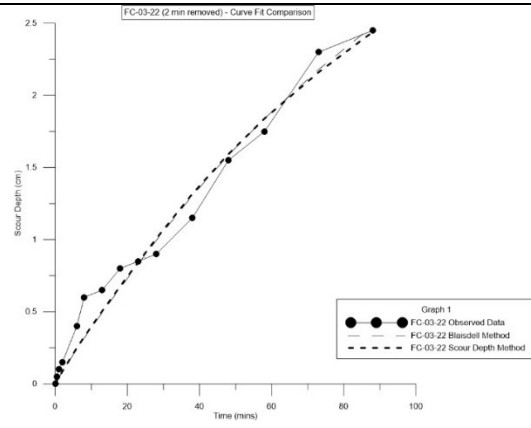
FC-03-23	
Without Segmentation	With Segmentation
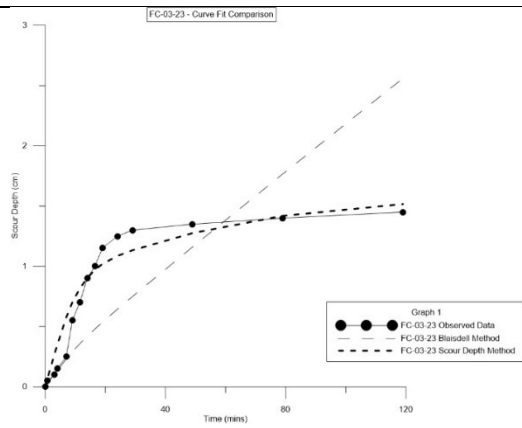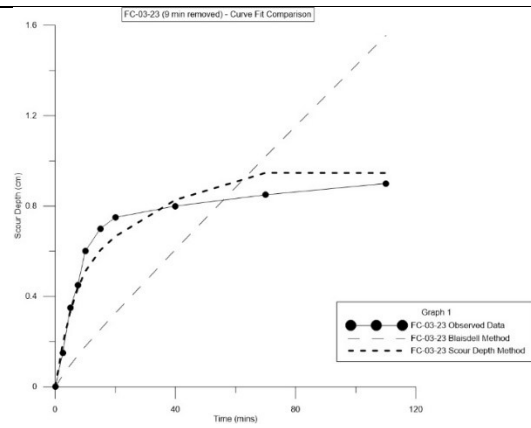
GRL-01-01	
Without Segmentation	With Segmentation
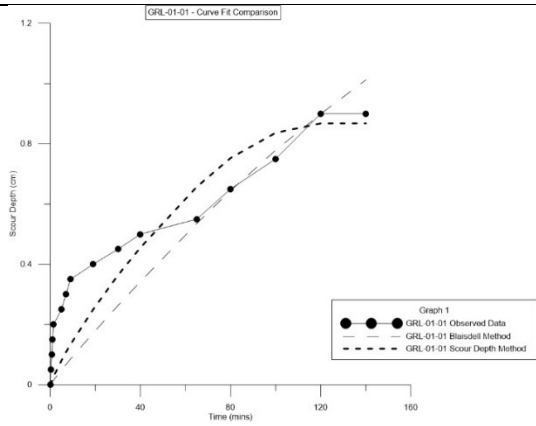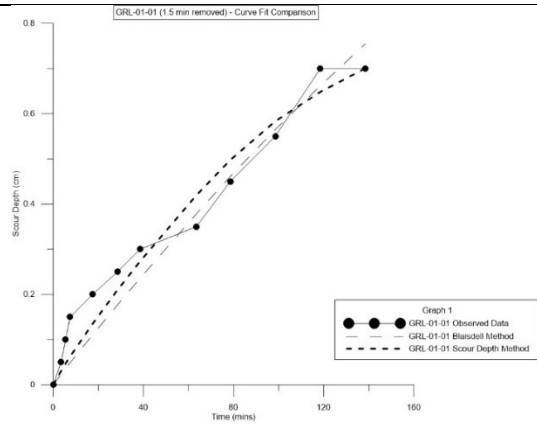
GRL-01-02	
Without Segmentation	With Segmentation
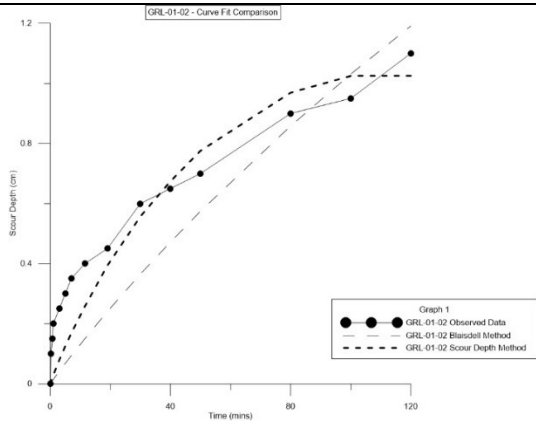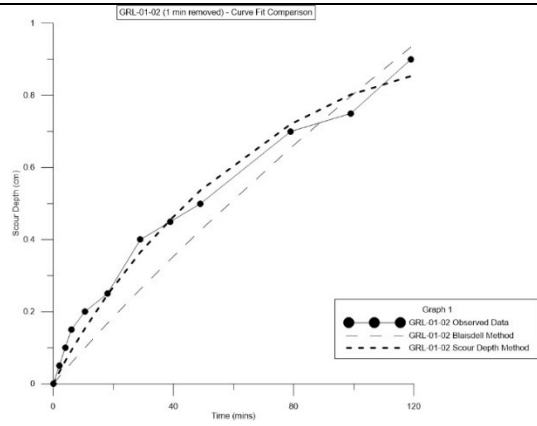
GRL-01-03	
Without Segmentation	With Segmentation
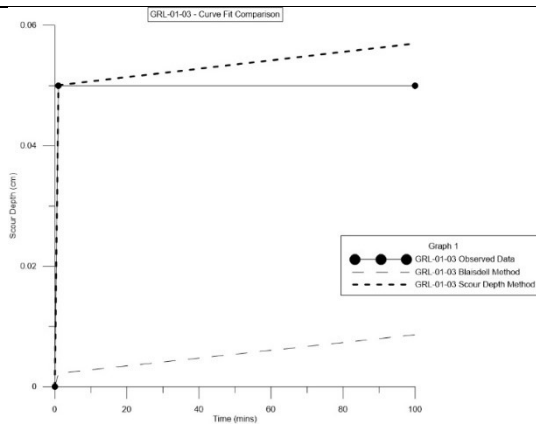
GRL-01-04	
Without Segmentation	With Segmentation
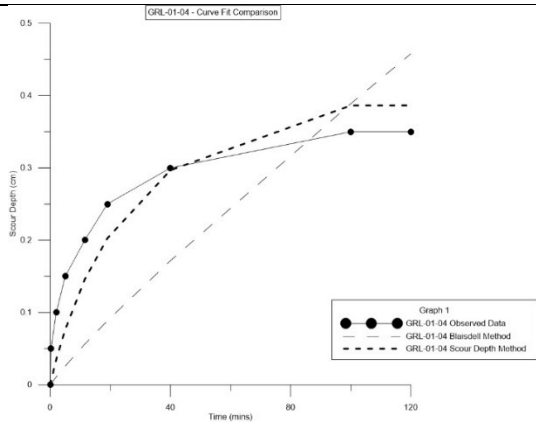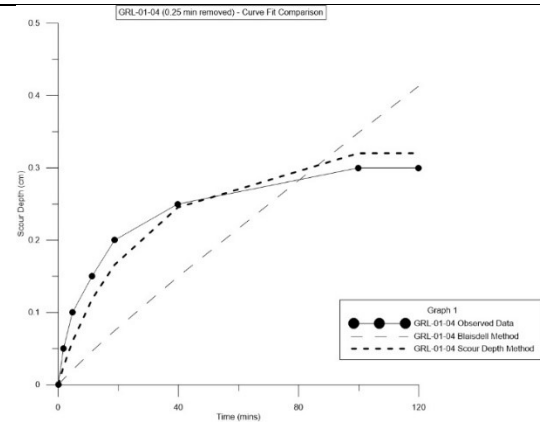
GRL-01-05	
Without Segmentation	With Segmentation
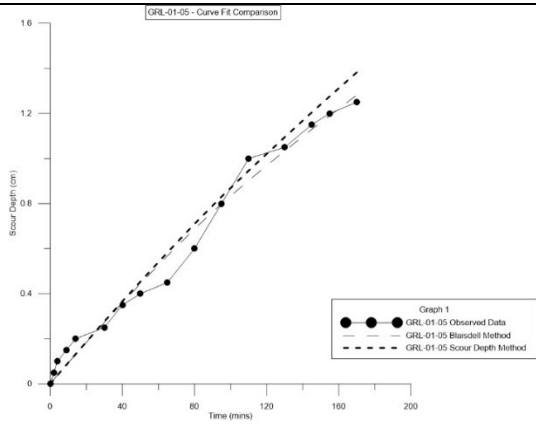
GRL-01-06	
Without Segmentation	With Segmentation
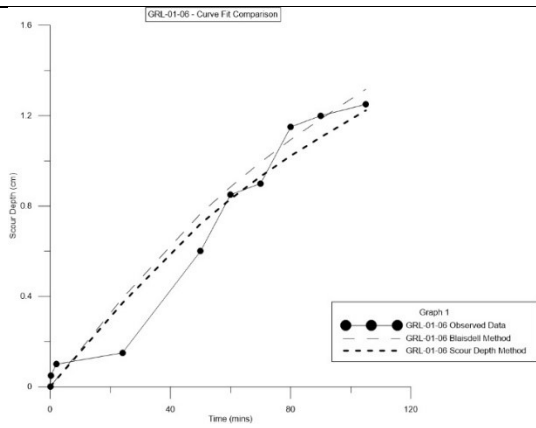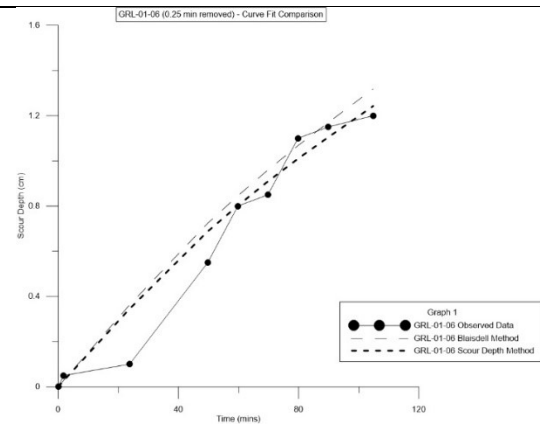
GRL-01-11	
Without Segmentation	With Segmentation
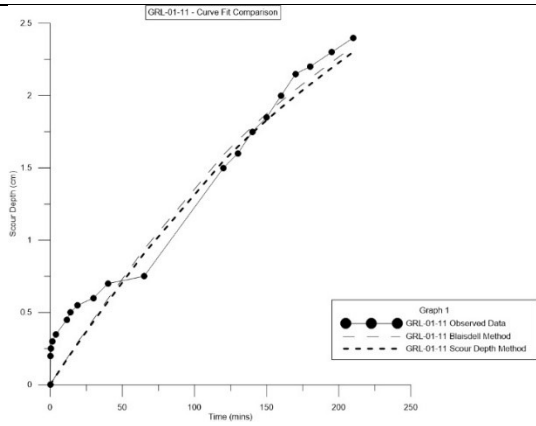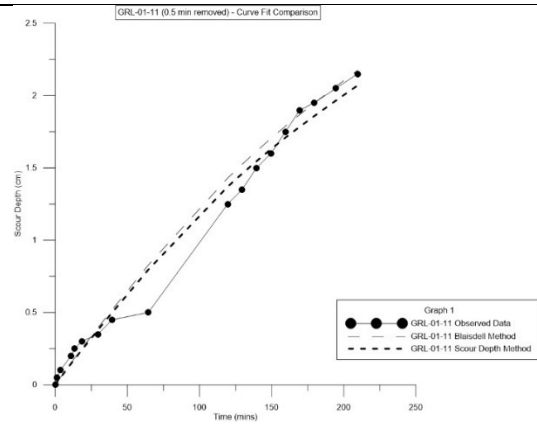
GRL-01-12	
Without Segmentation	With Segmentation
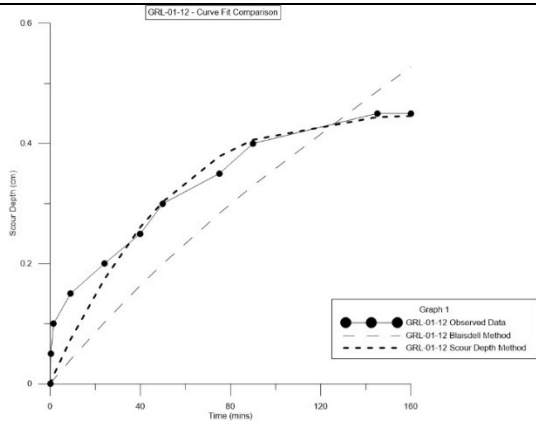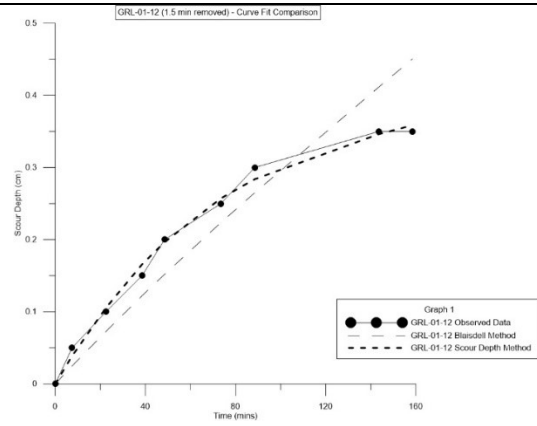
GRL-01-13	
Without Segmentation	With Segmentation
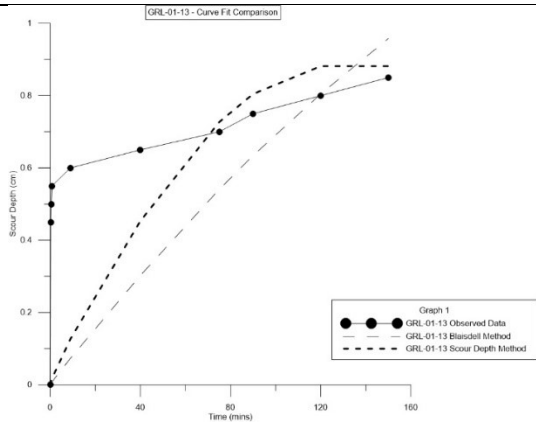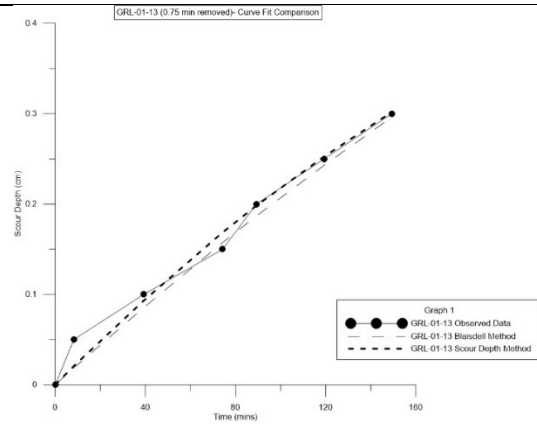
GRL-01-21	
Without Segmentation	With Segmentation
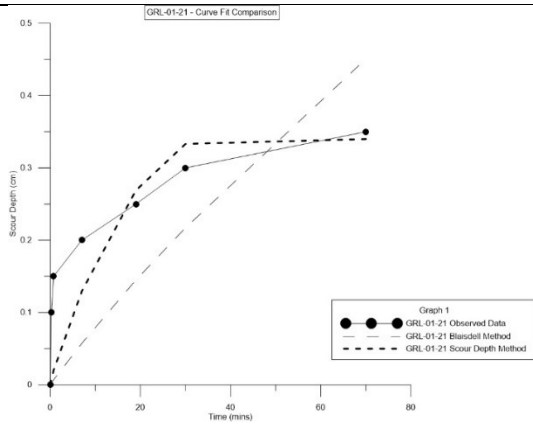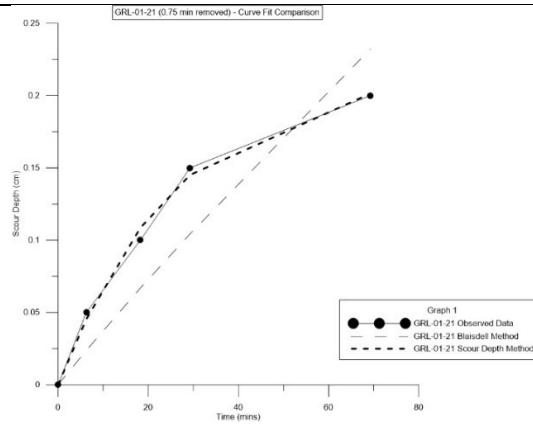
GRL-01-31	
Without Segmentation	With Segmentation
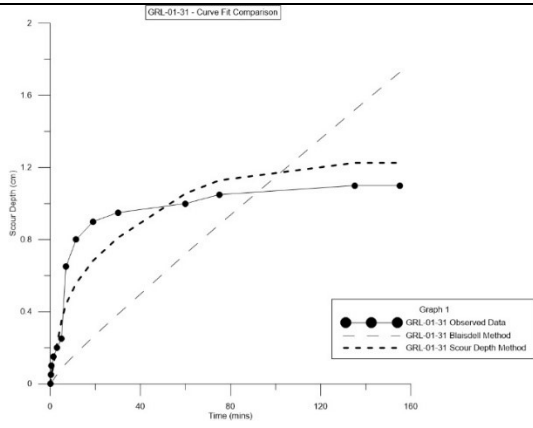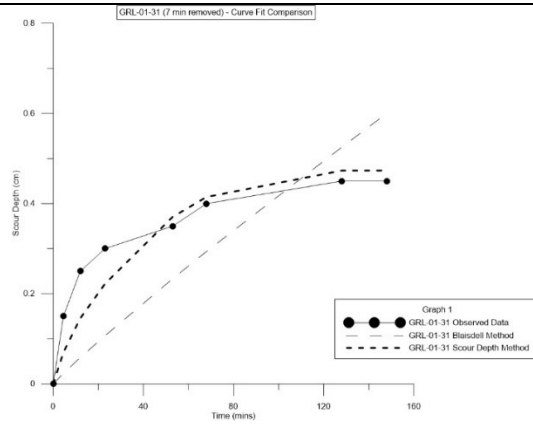
GRL-02-11	
Without Segmentation	With Segmentation

309
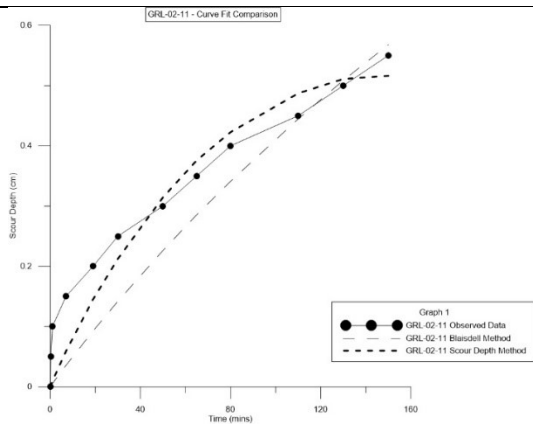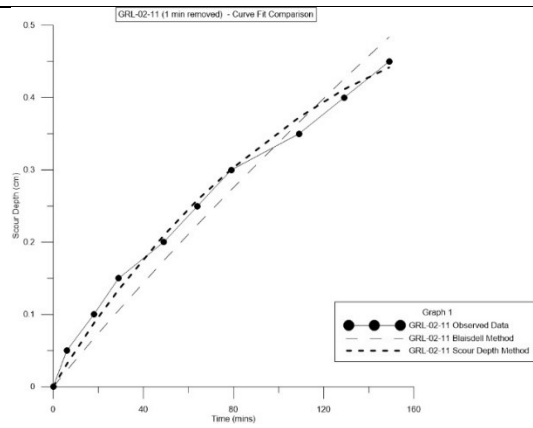
GRL-02-21	
Without Segmentation	With Segmentation
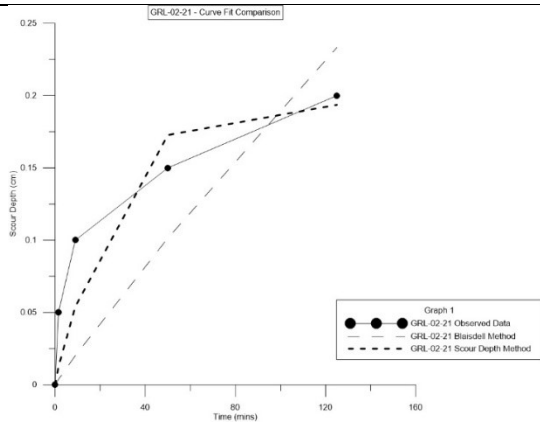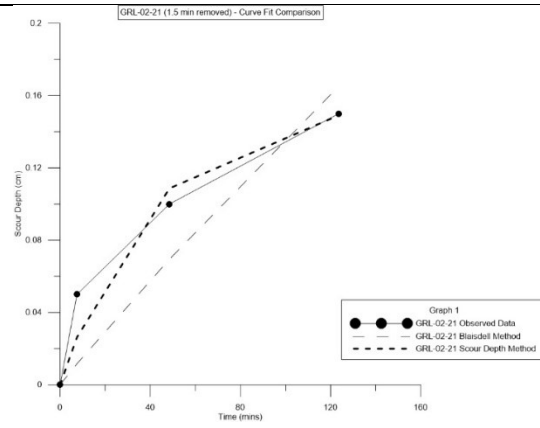
GRL-02-31	
Without Segmentation	With Segmentation
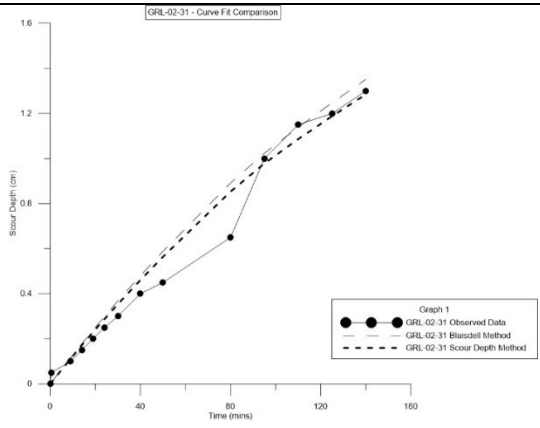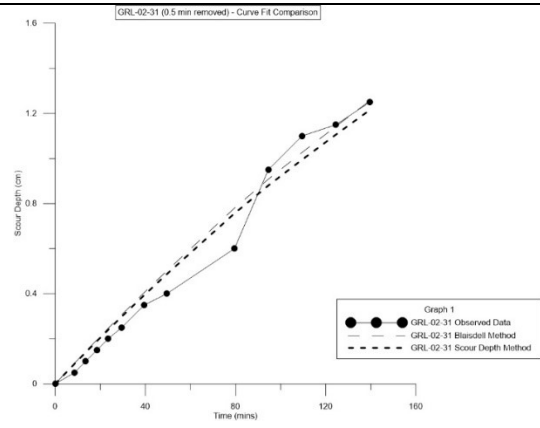
GRL-03-11	
Without Segmentation	With Segmentation

310
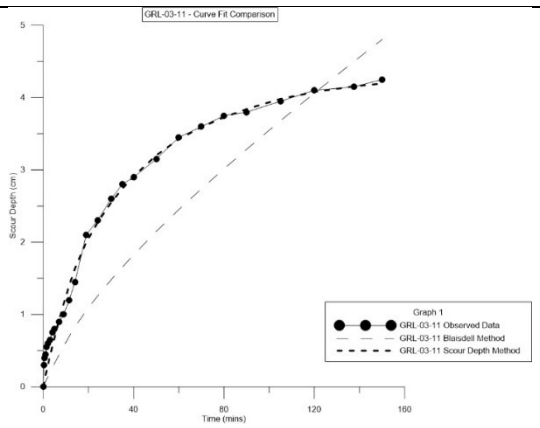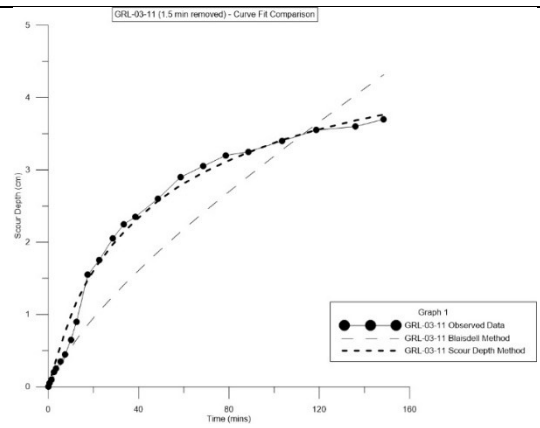
GRL-03-21	
Without Segmentation	With Segmentation
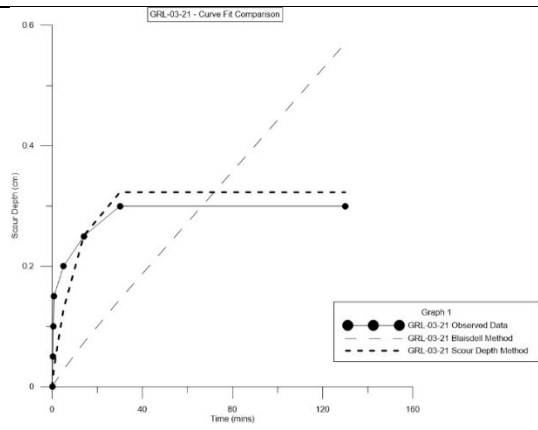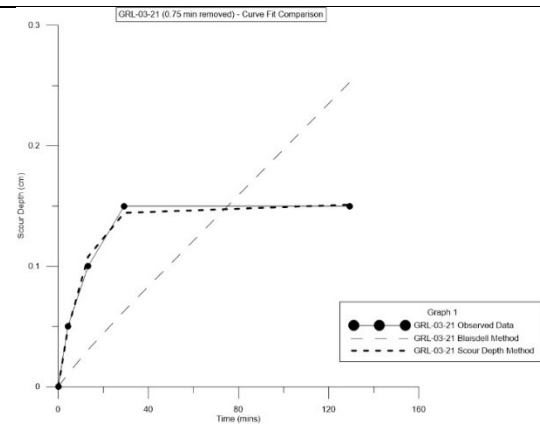
GRL-03-22	
Without Segmentation	With Segmentation
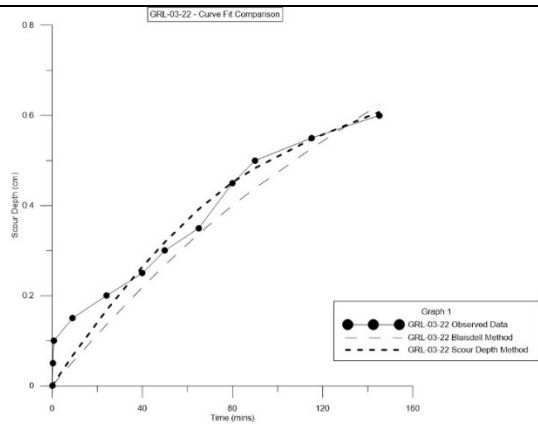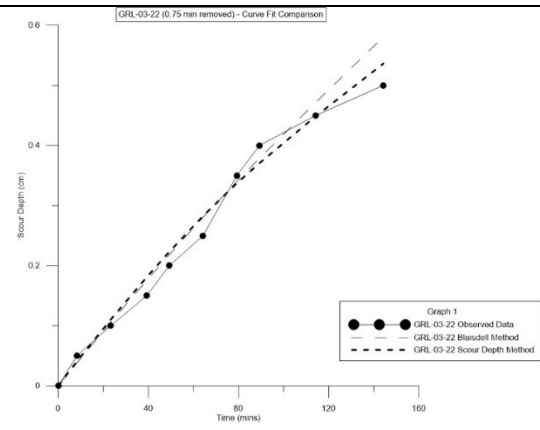
GRL-04-01	
Without Segmentation	With Segmentation
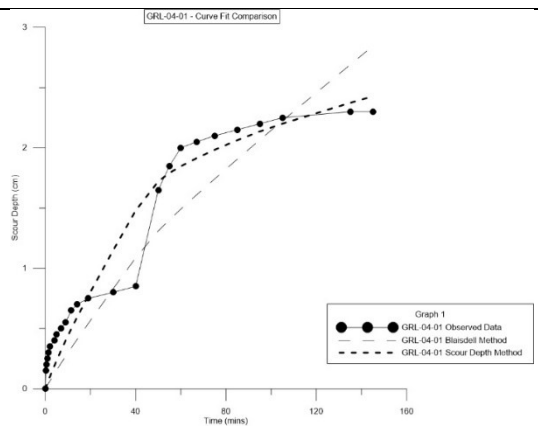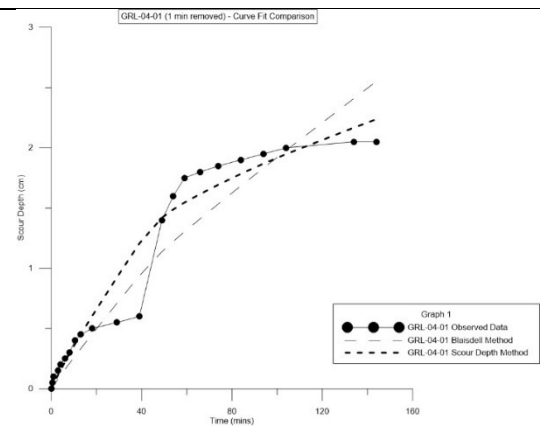
GRL-04-02	
Without Segmentation	With Segmentation
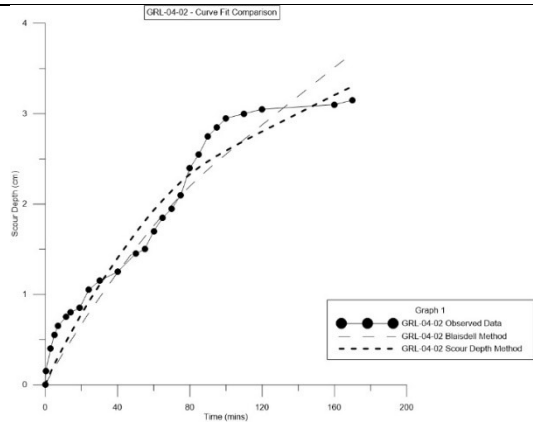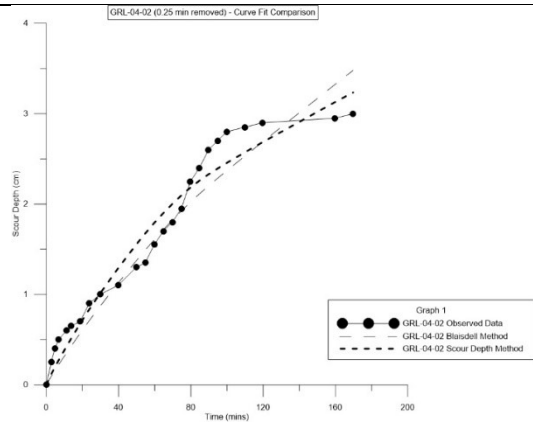
GRL-05-11	
Without Segmentation	With Segmentation
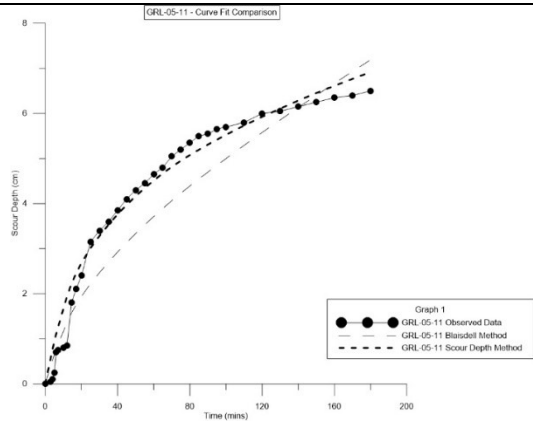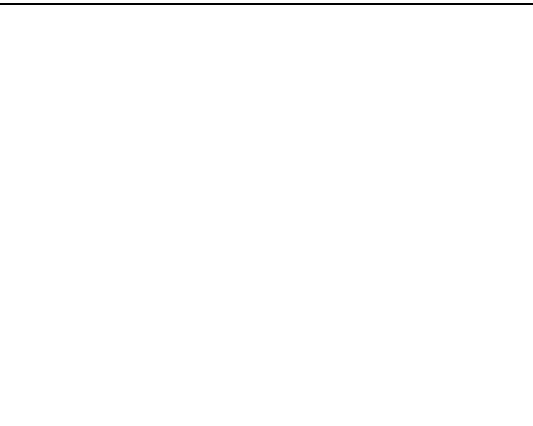
GRL-05-12	
Without Segmentation	With Segmentation
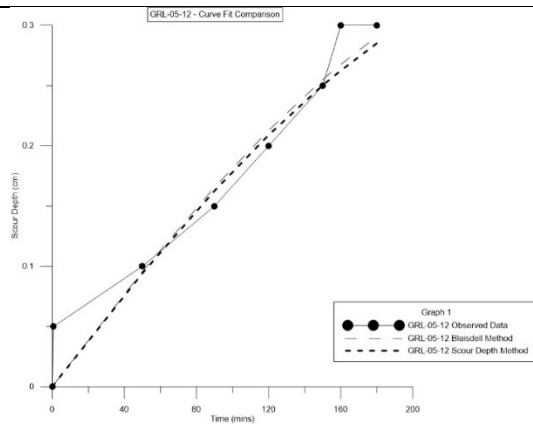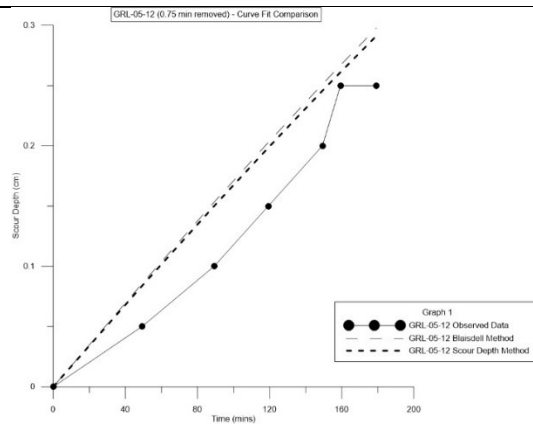
GRL21-01-01	
Without Segmentation	With Segmentation
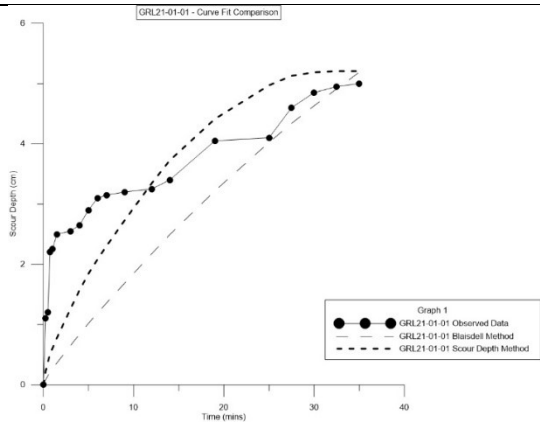
GRL21-01-11	
Without Segmentation	With Segmentation
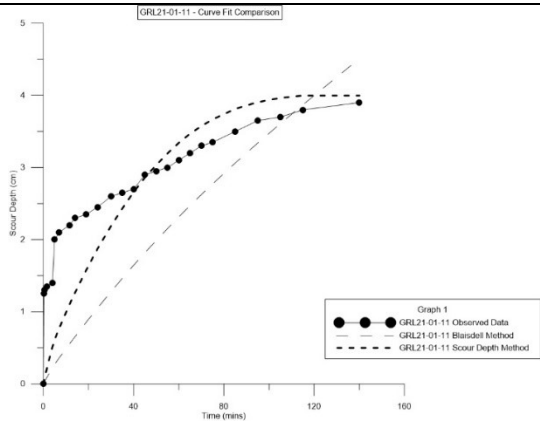
GRL21-01-12	
Without Segmentation	With Segmentation
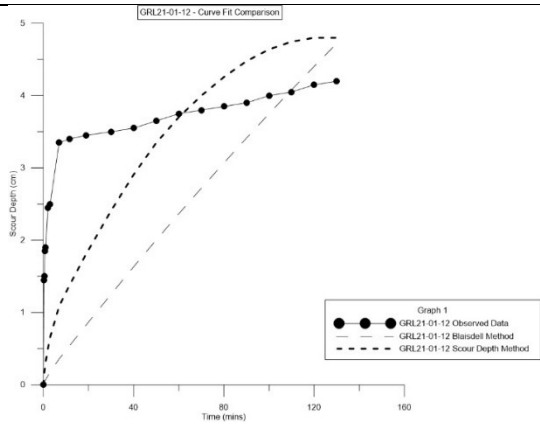
GRL21-01-21	
Without Segmentation	With Segmentation
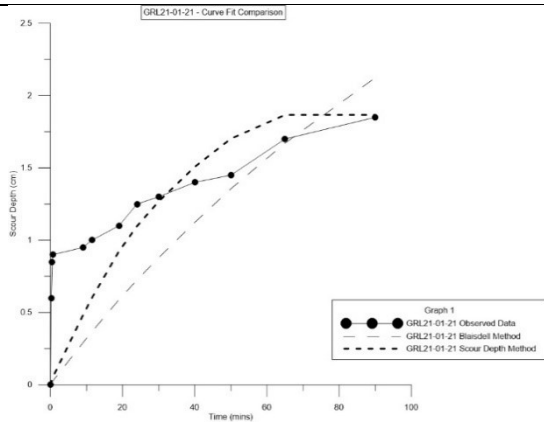
GRL21-01-22	
Without Segmentation	With Segmentation
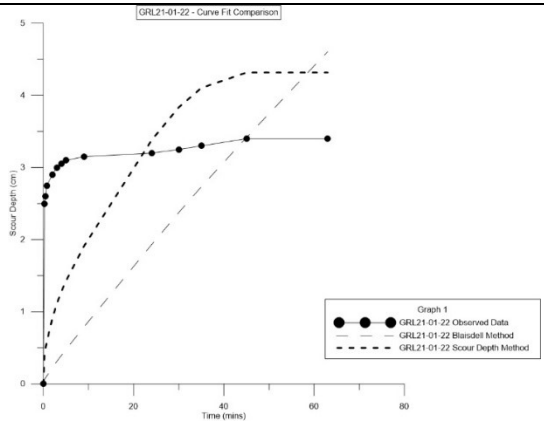
GRL21-01-23	
Without Segmentation	With Segmentation
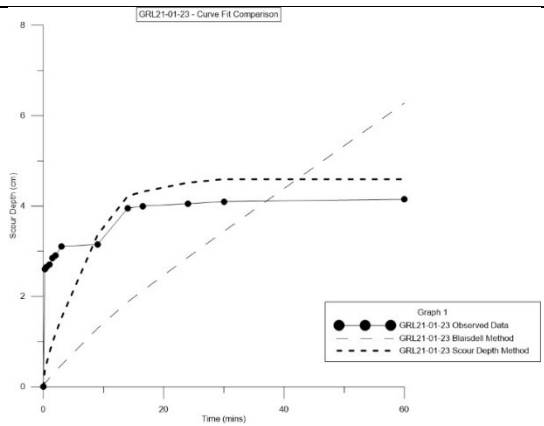
GRL21-01-24	
Without Segmentation	With Segmentation
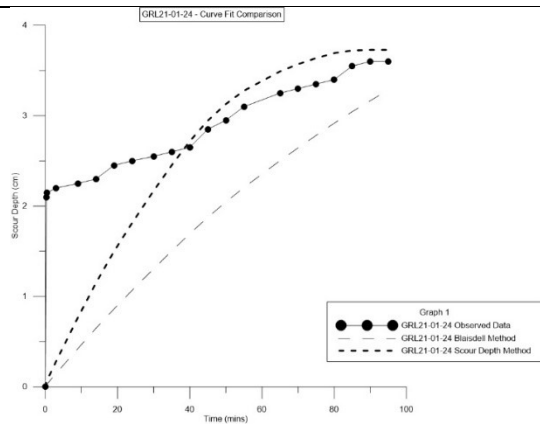
GRL21-01-26	
Without Segmentation	With Segmentation
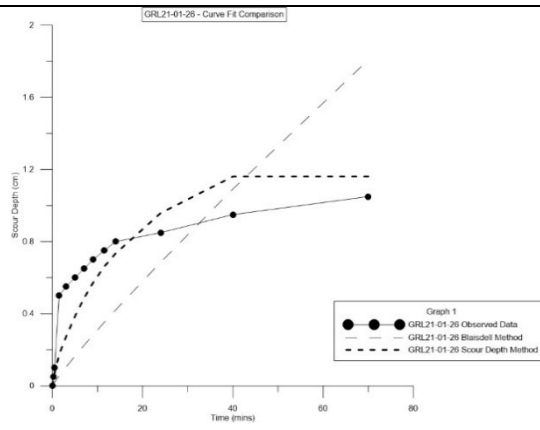
GRL21-01-31	
Without Segmentation	With Segmentation

GRL21-01-32
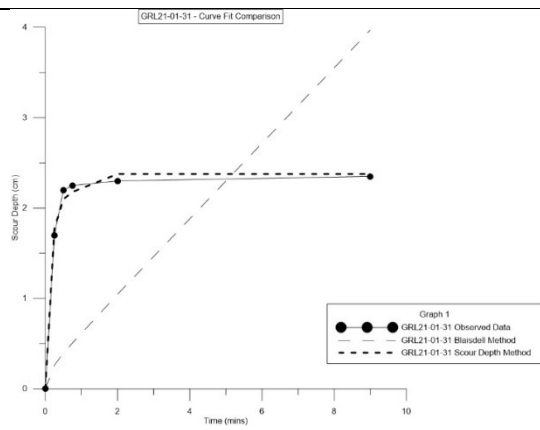
Without Segmentation	With Segmentation
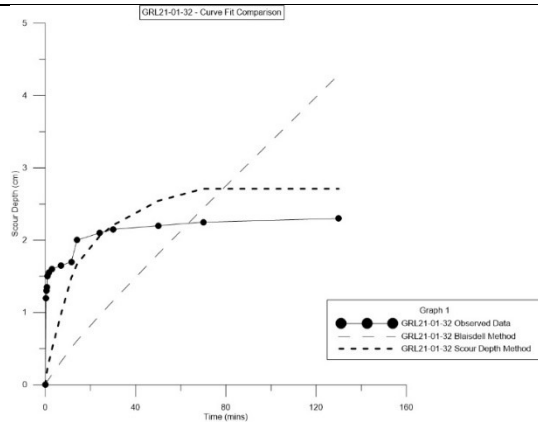
GT-01-04

Without Segmentation	With Segmentation
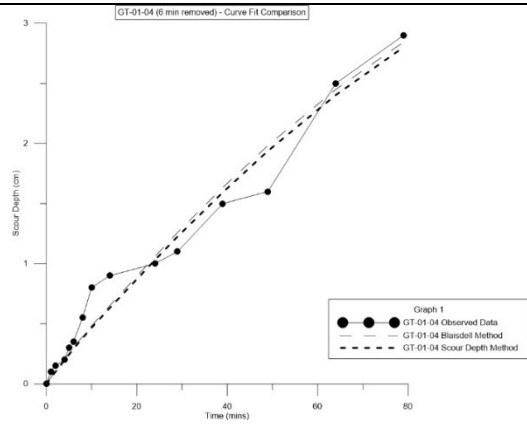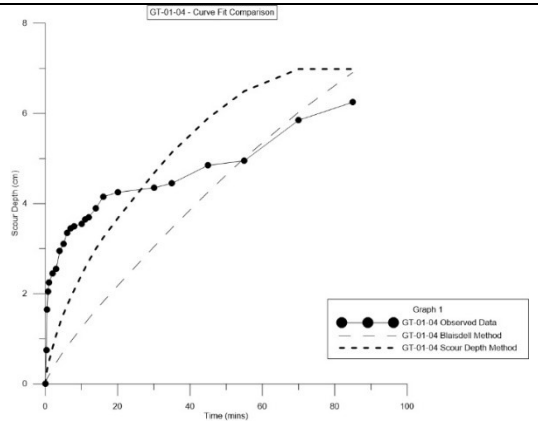
GT-01-05

Without Segmentation	With Segmentation

316
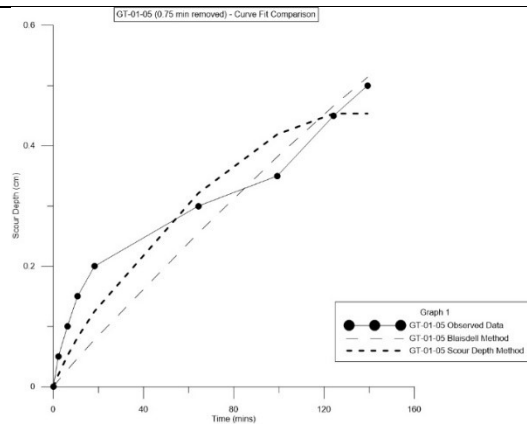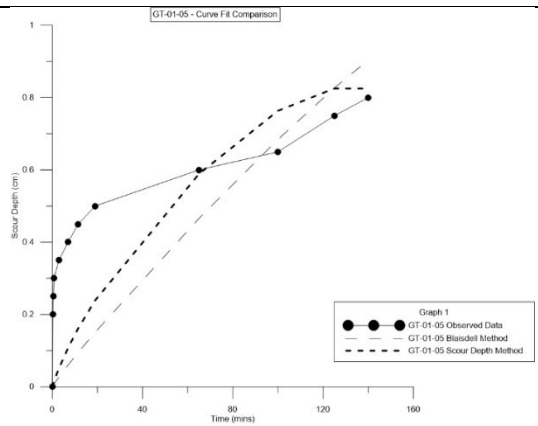
GT-01-06	
Without Segmentation	With Segmentation
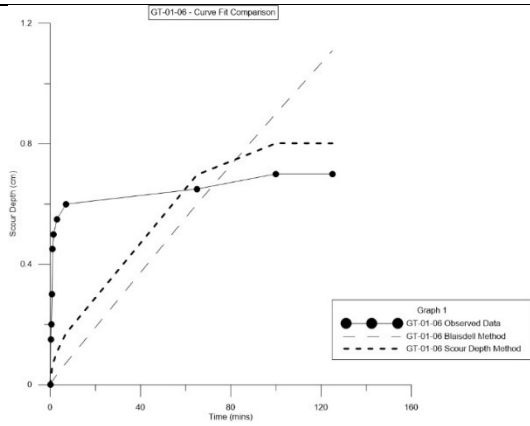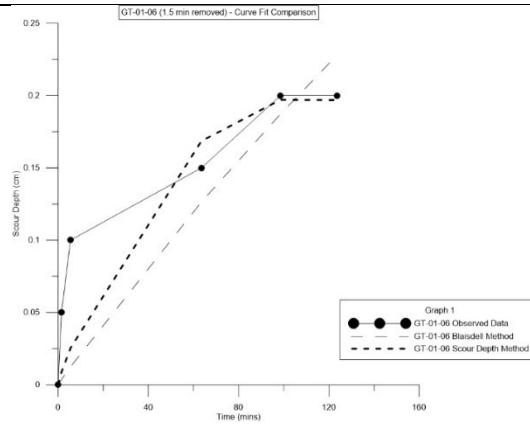
GT-01-09	
Without Segmentation	With Segmentation
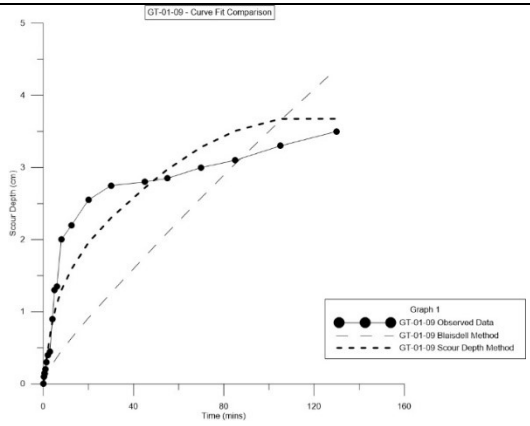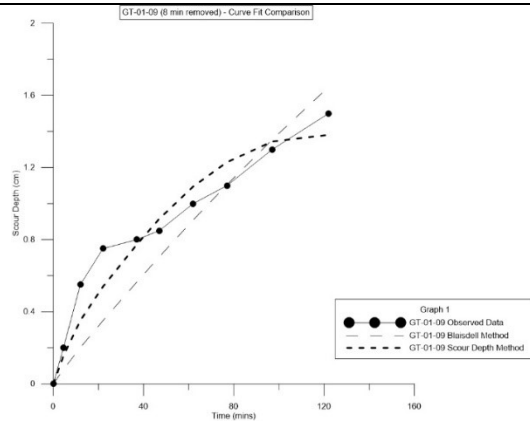
GT-01-010	
Without Segmentation	With Segmentation
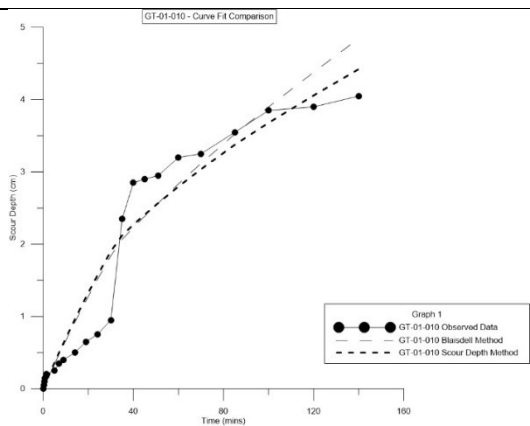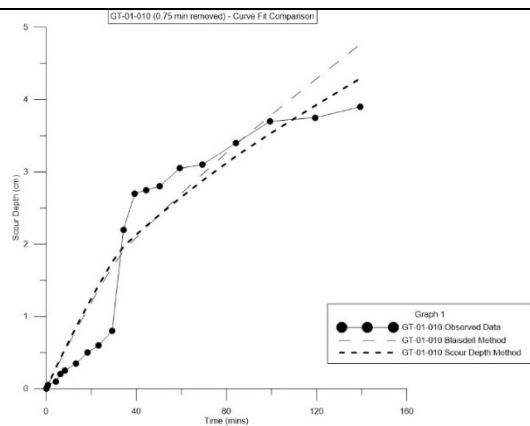
GT-01-011	
Without Segmentation	With Segmentation
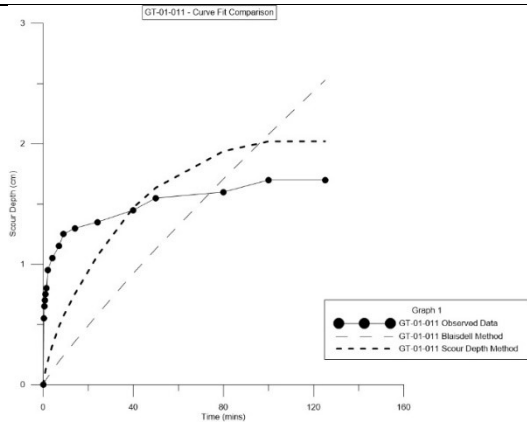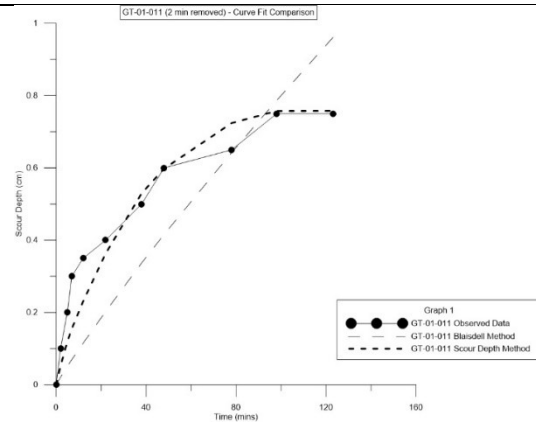
GT-01-11	
Without Segmentation	With Segmentation
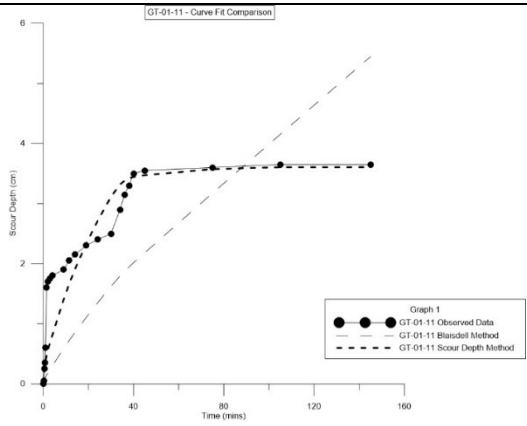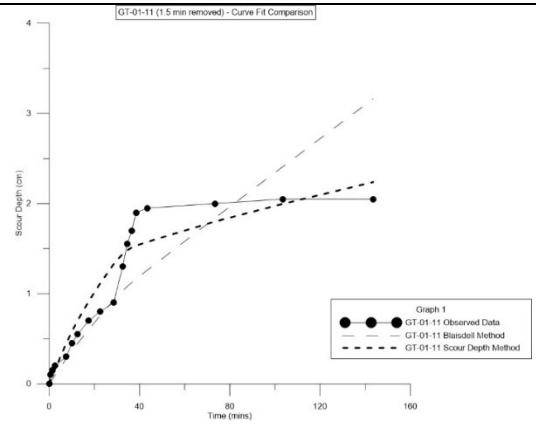
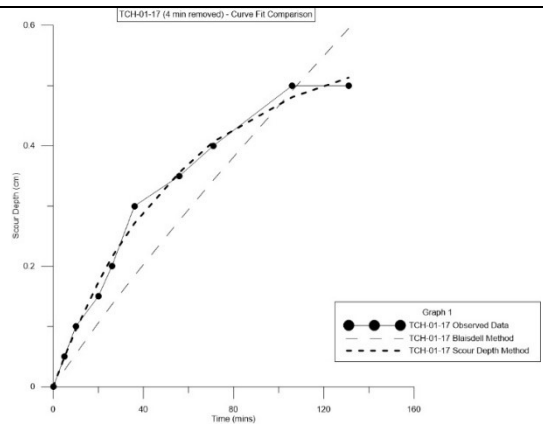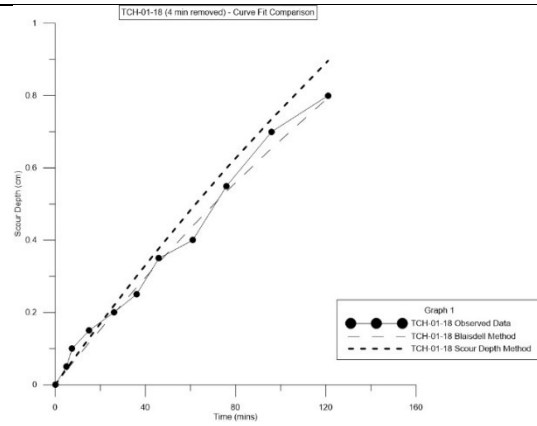| GT-01-012	
Without Segmentation	With Segmentation
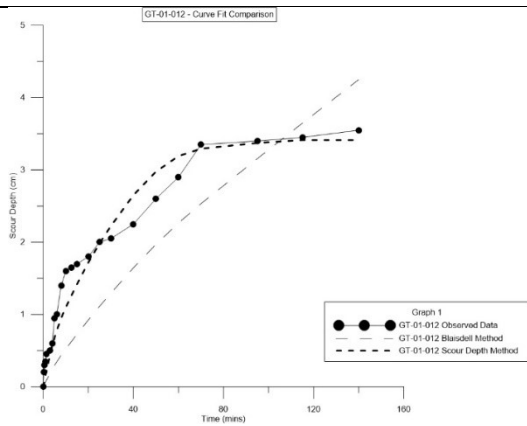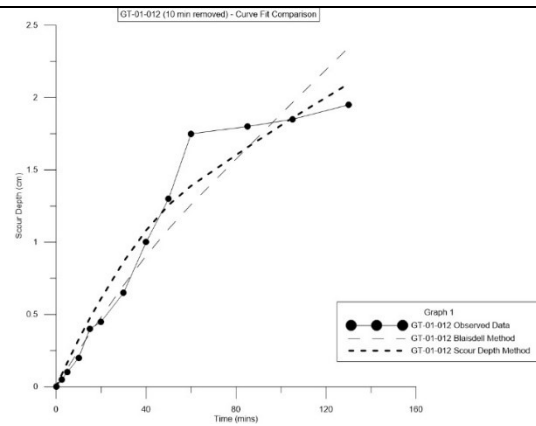
GT-01-12
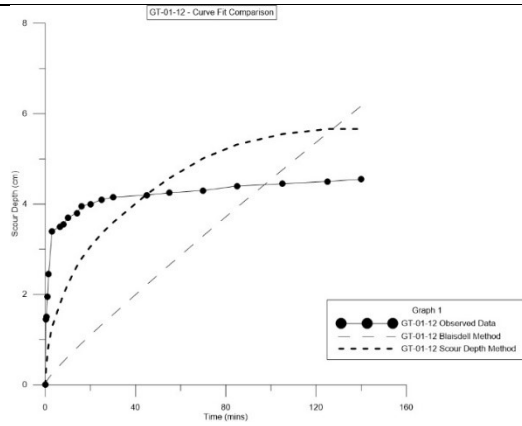
Without Segmentation	With Segmentation
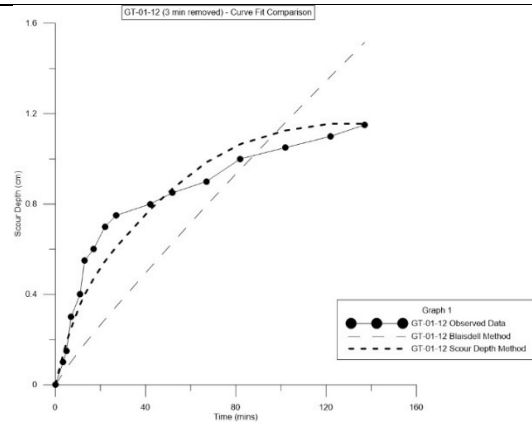
GT-01-013
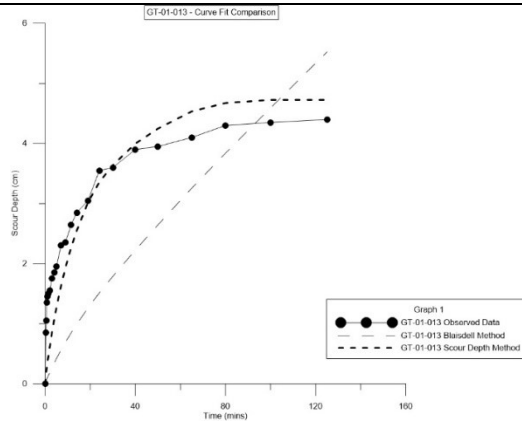
Without Segmentation	With Segmentation
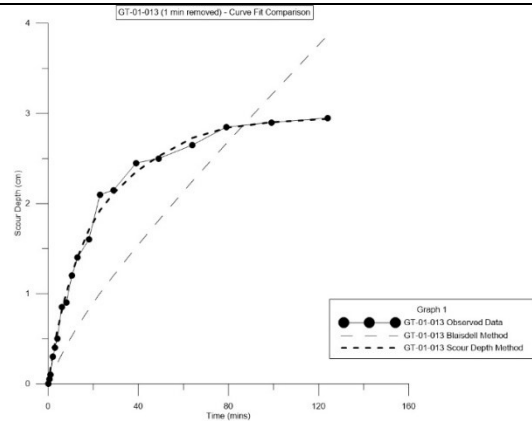
GT-01-13
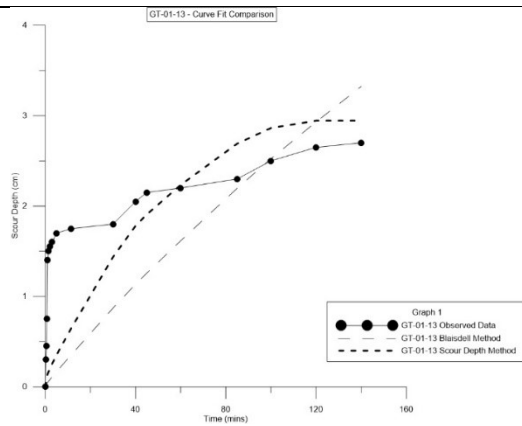
Without Segmentation	With Segmentation
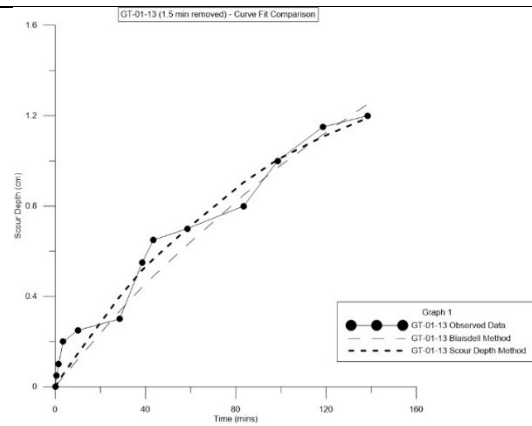
GT-01-15
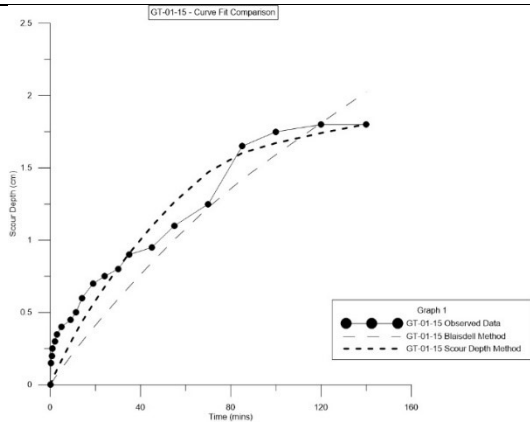
Without Segmentation	With Segmentation
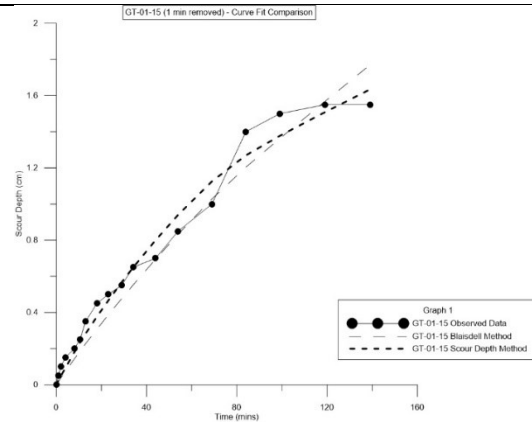
GT-01-16
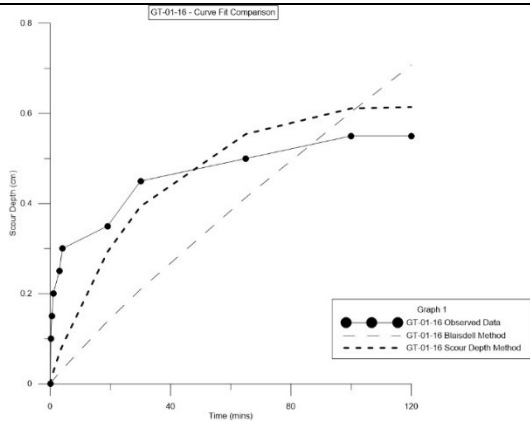
Without Segmentation	With Segmentation
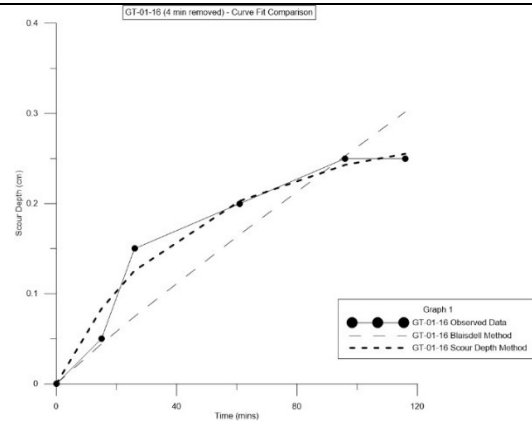
HC-01-12
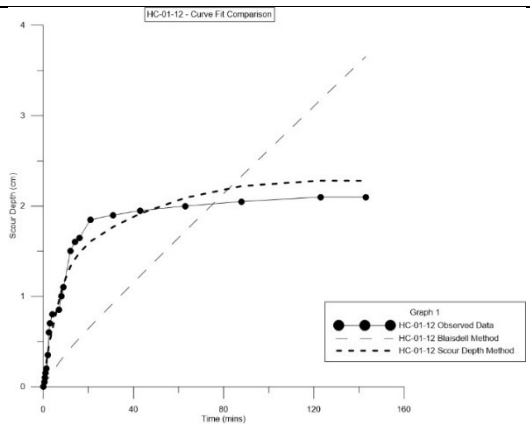
Without Segmentation	With Segmentation
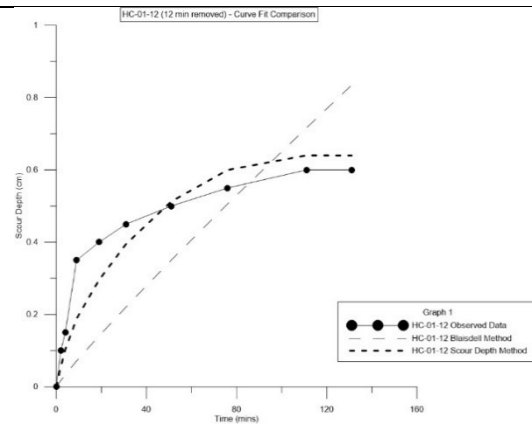
HC-01-13
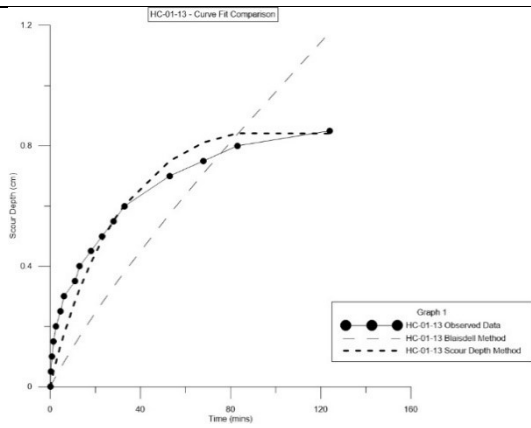
Without Segmentation	With Segmentation
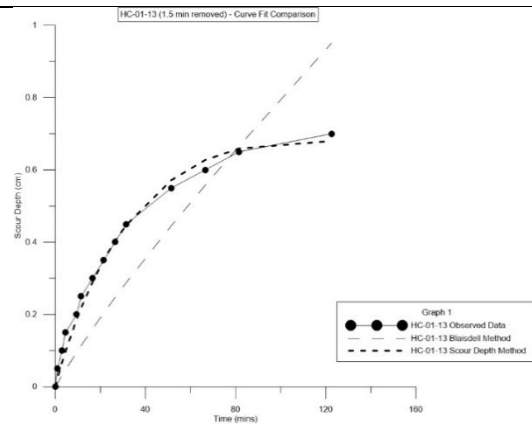
HC-01-14
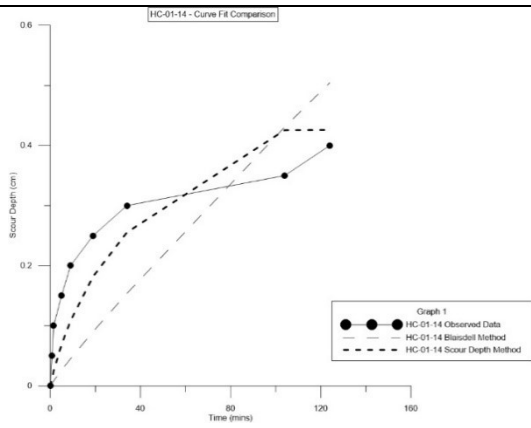
Without Segmentation	With Segmentation
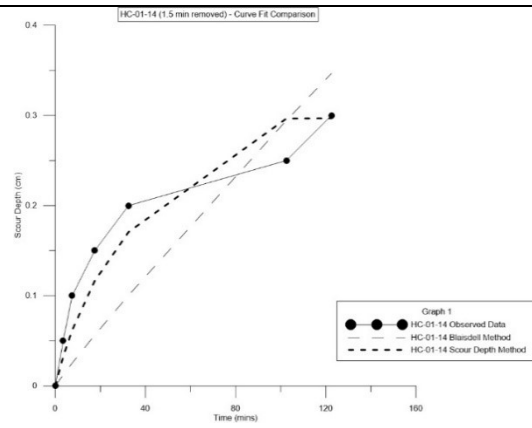
HC-01-21_IP
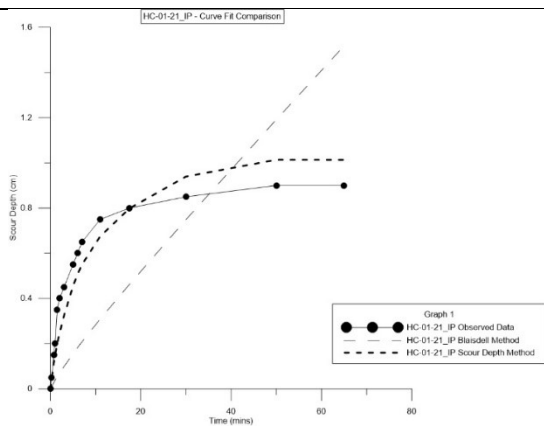
Without Segmentation	With Segmentation
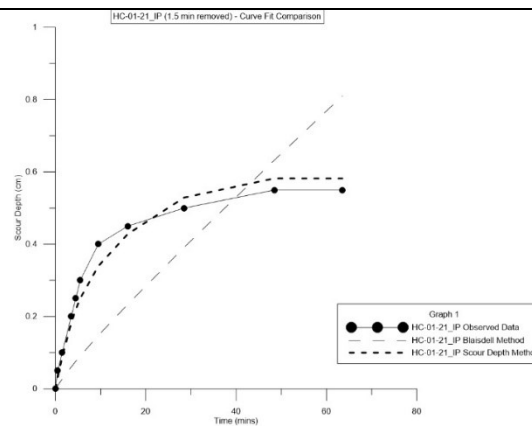
HC-01-22	
Without Segmentation	With Segmentation
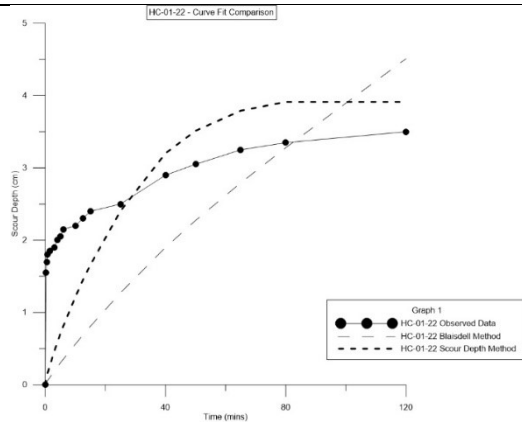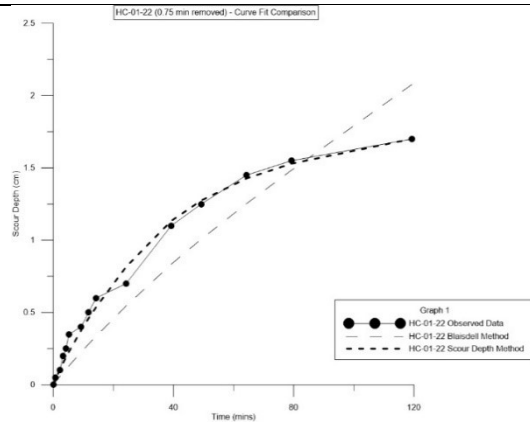
HC-01-23	
Without Segmentation	With Segmentation
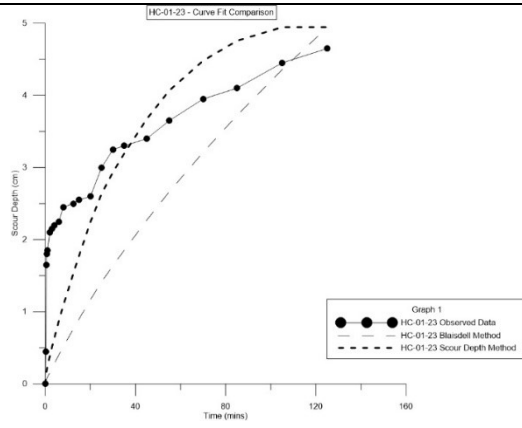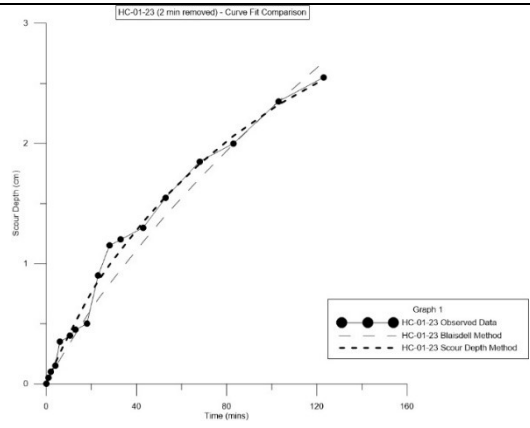
HC-01-31	
Without Segmentation	With Segmentation
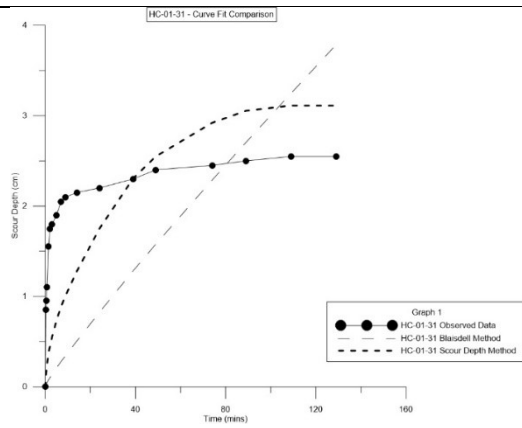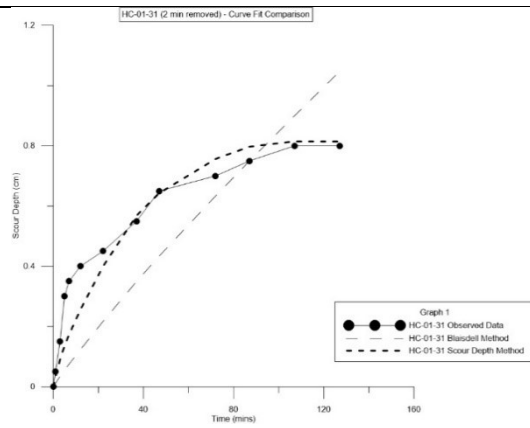
HC-01-32	
Without Segmentation	With Segmentation
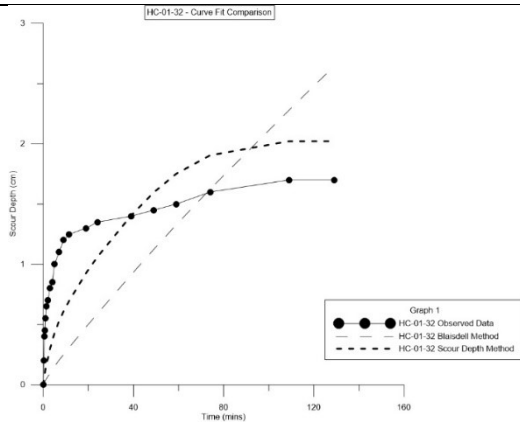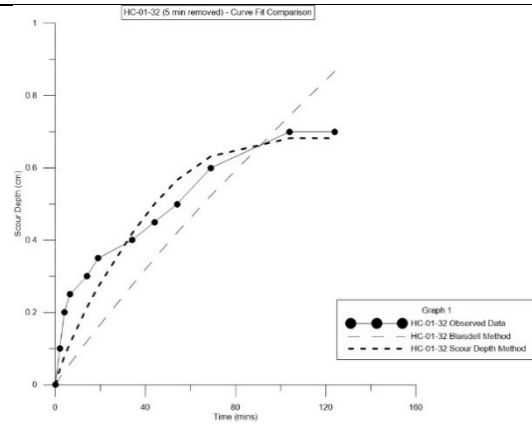
HC-01-33	
Without Segmentation	With Segmentation
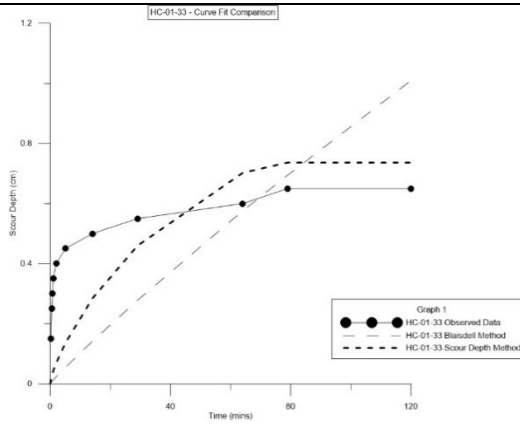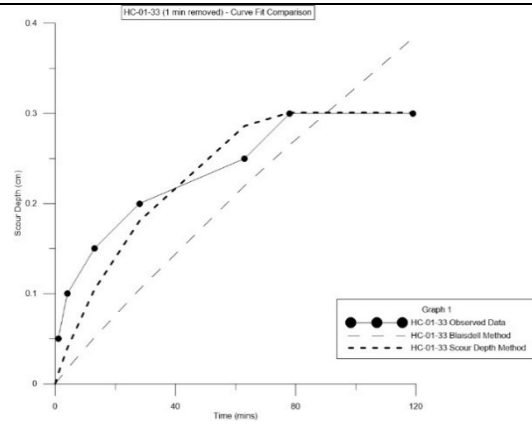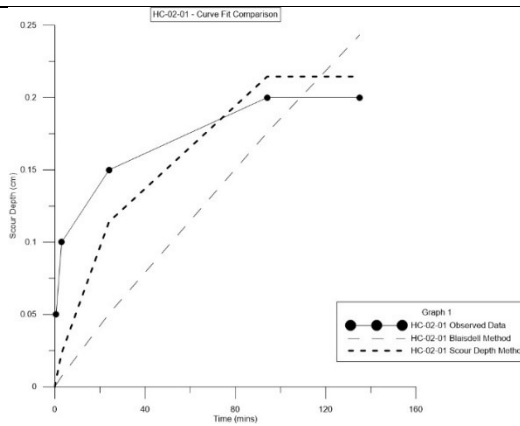
HC-02-01	
Without Segmentation	With Segmentation
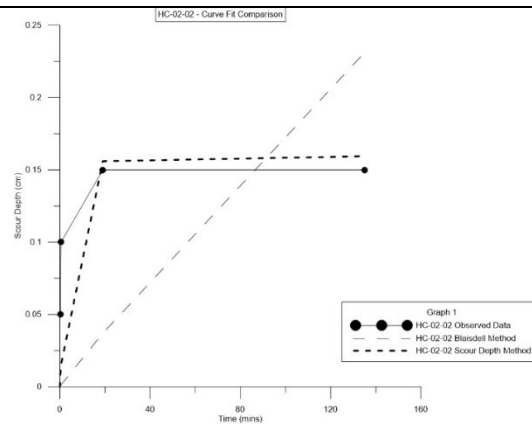
HC-02-03	
Without Segmentation	With Segmentation
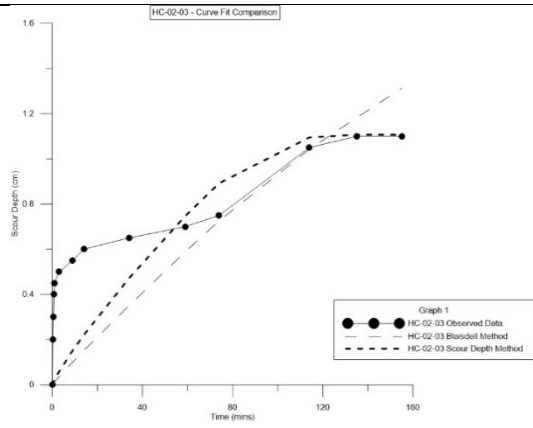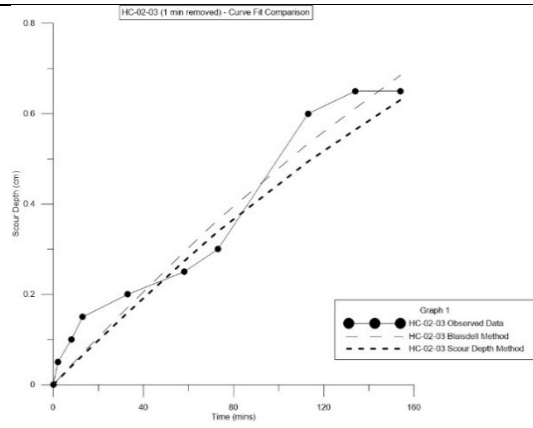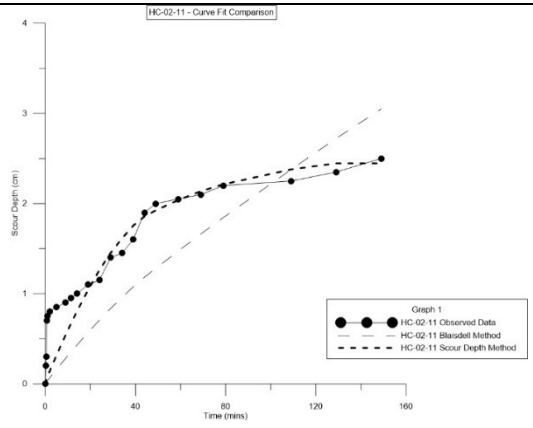
HC-02-11	
Without Segmentation	With Segmentation
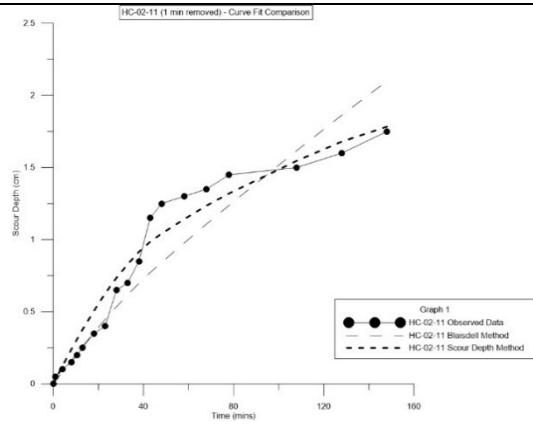
HC-02-13	
Without Segmentation	With Segmentation

324
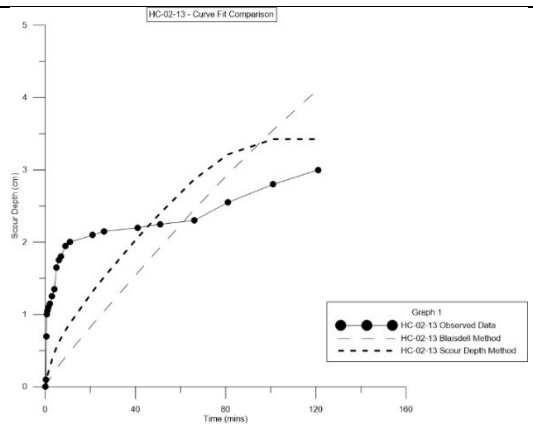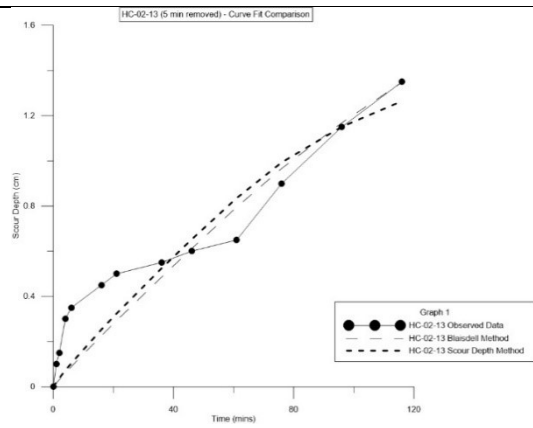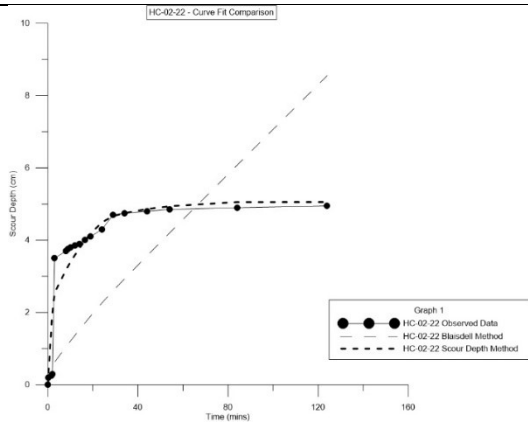
HC-02-22	
Without Segmentation	With Segmentation
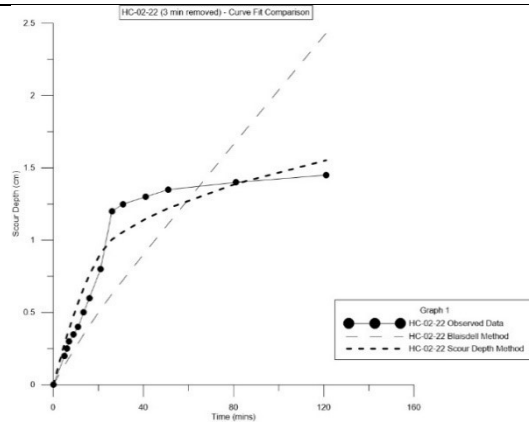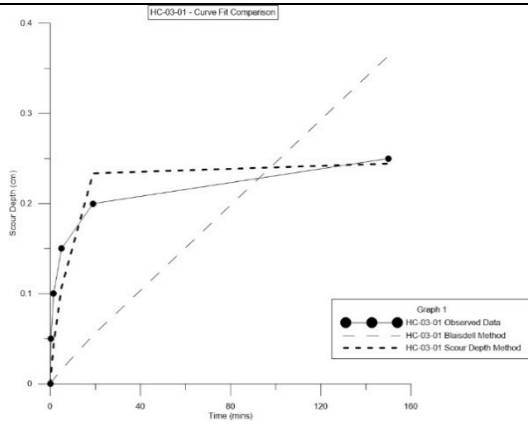
HC-03-01	
Without Segmentation	With Segmentation
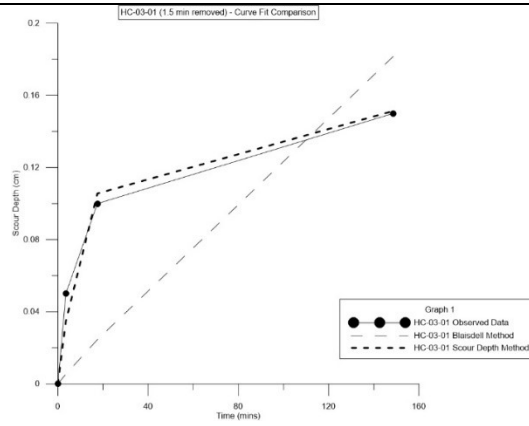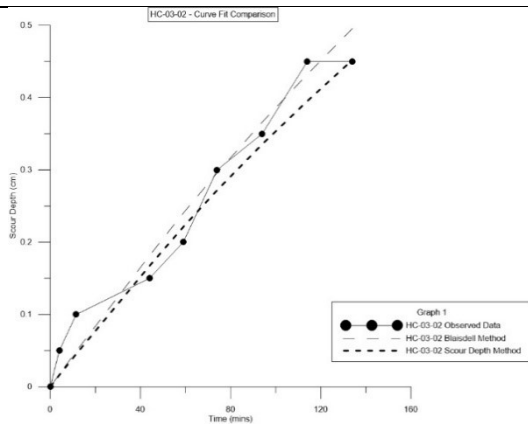
HC-03-02	
Without Segmentation	With Segmentation

HC-03-03
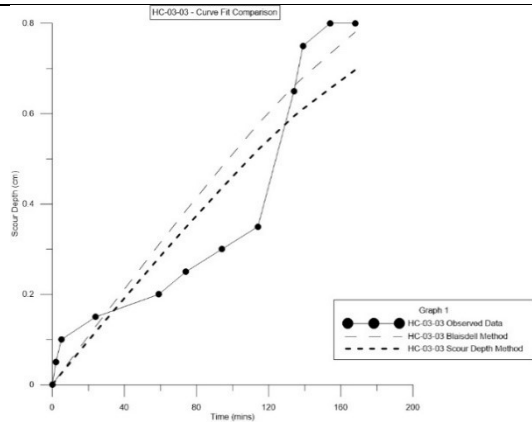
Without Segmentation	With Segmentation

HC-03-11
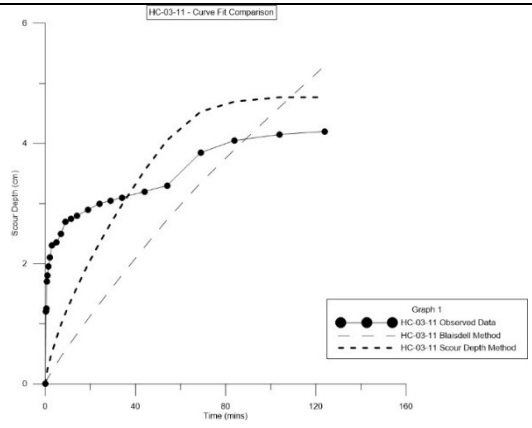
Without Segmentation	With Segmentation
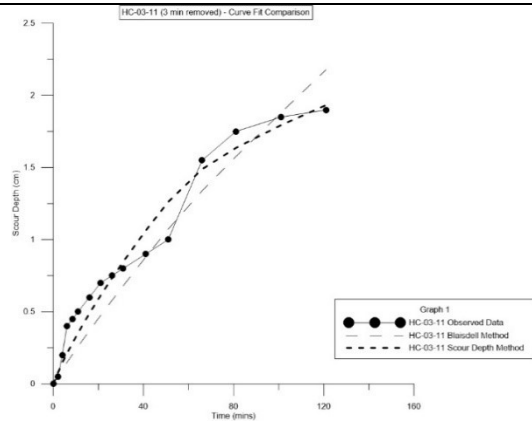
HC-03-12
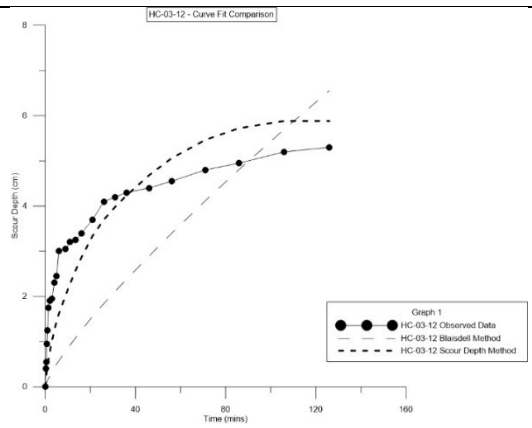
Without Segmentation	With Segmentation
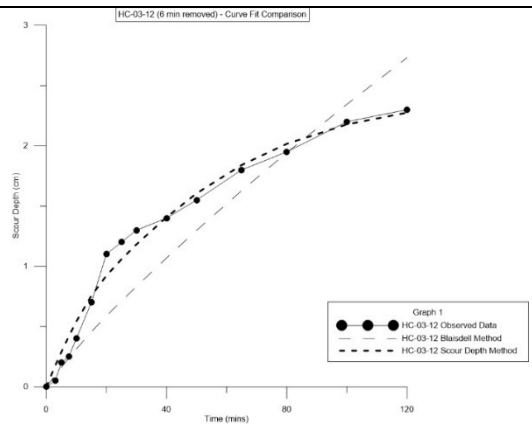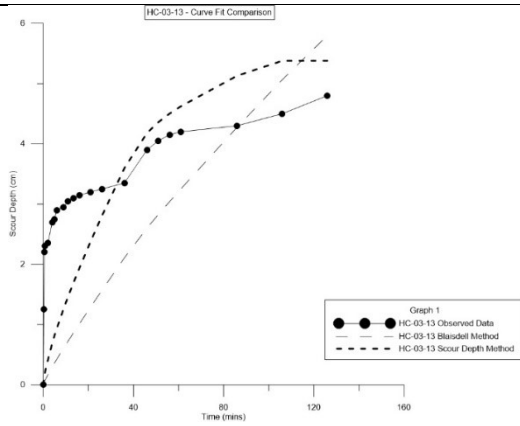
HC-03-13	
Without Segmentation	With Segmentation
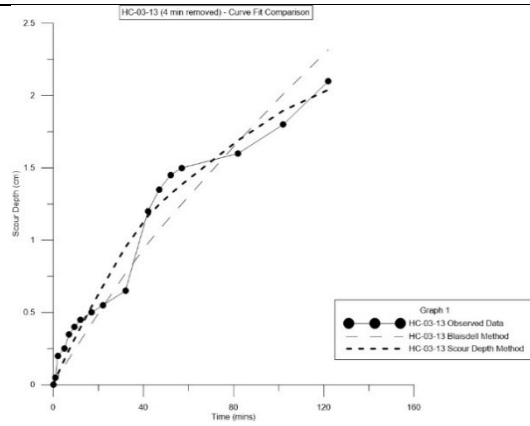
LNC-01-01	
Without Segmentation	With Segmentation
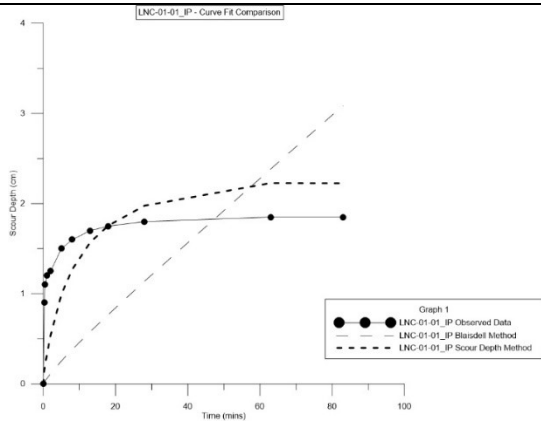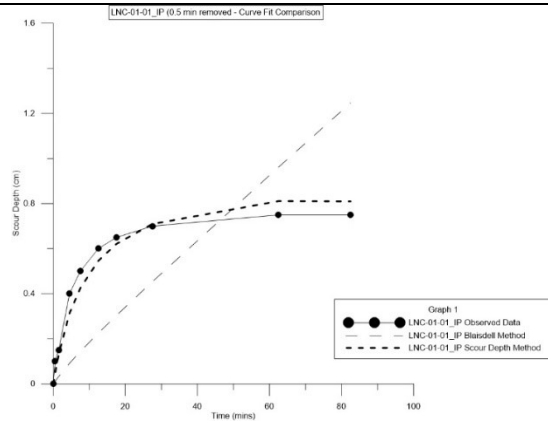
LNC-01-03	
Without Segmentation	With Segmentation
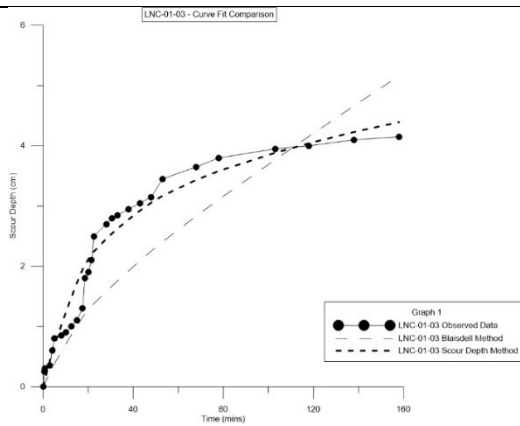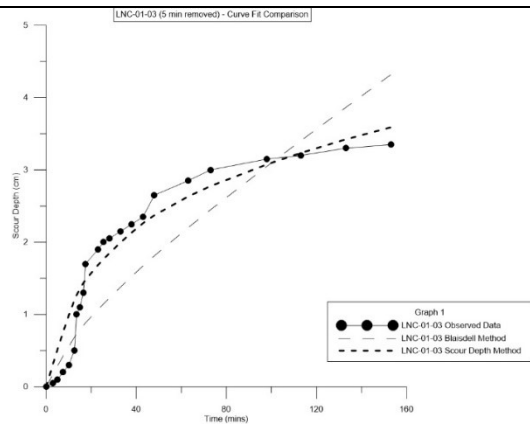
LNC-01-04	
Without Segmentation	With Segmentation
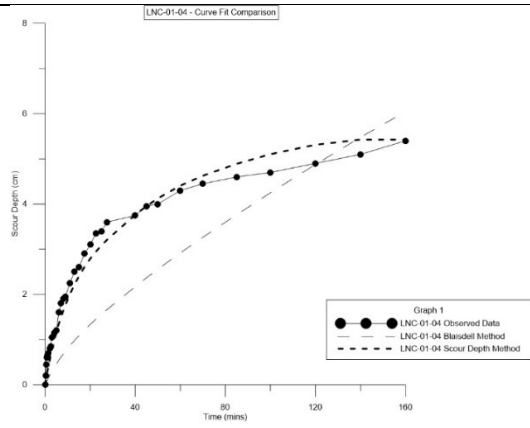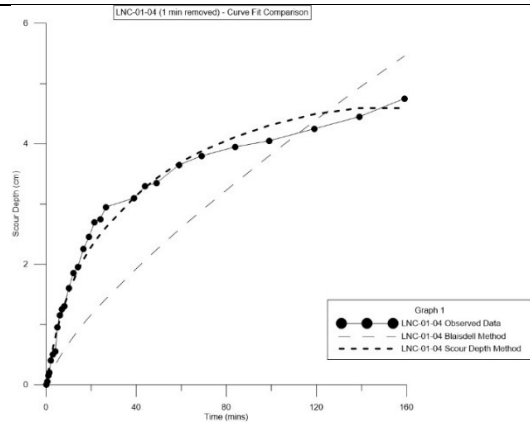
LNC-01-05	
Without Segmentation	With Segmentation
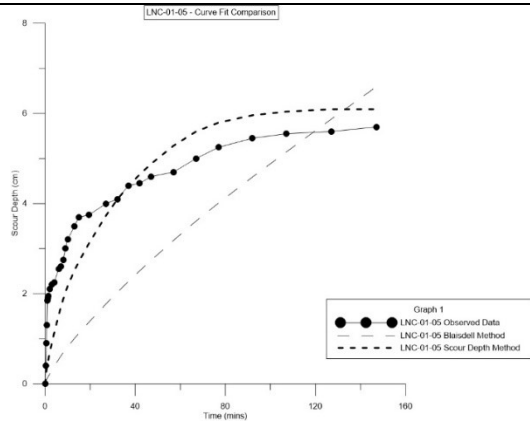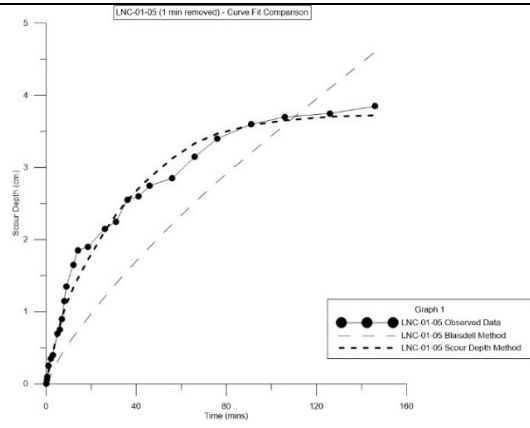
LNC-01-07	
Without Segmentation	With Segmentation

328
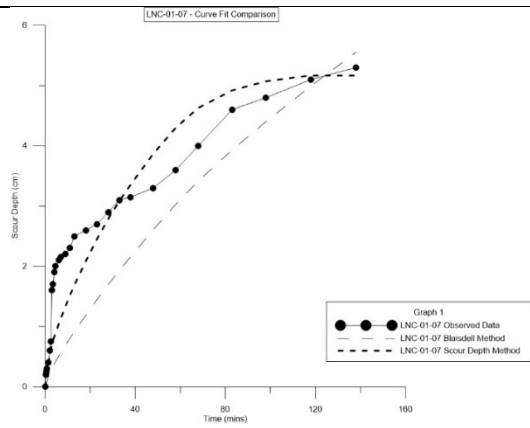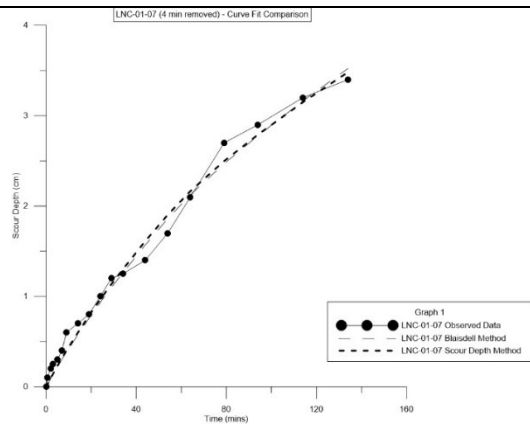
LNC-01-08	
Without Segmentation	With Segmentation
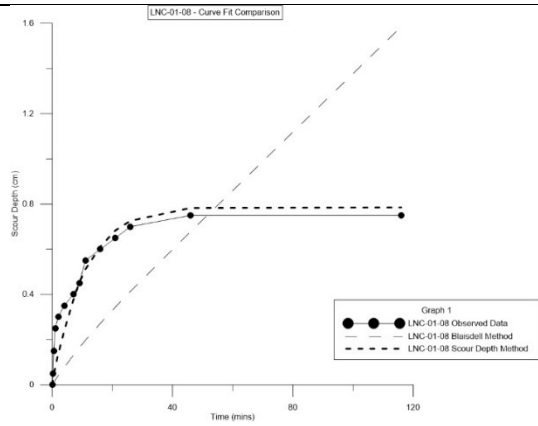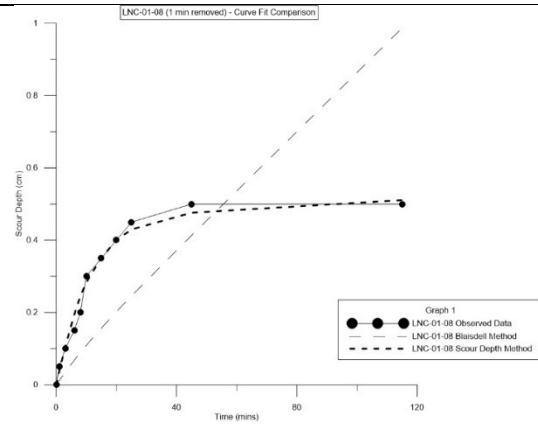
LNC-01-28	
Without Segmentation	With Segmentation
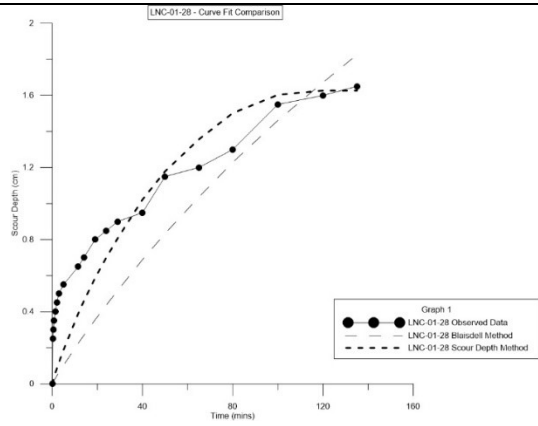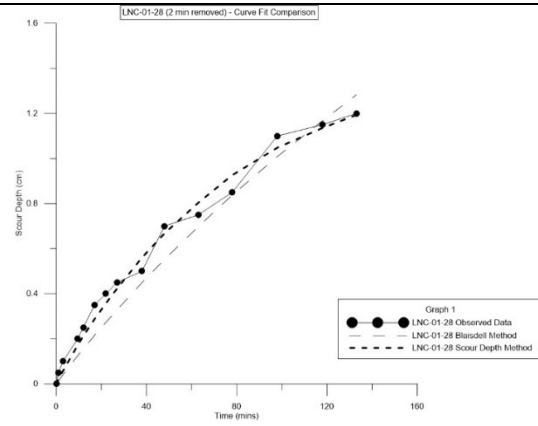
LNC-01-29	
Without Segmentation	With Segmentation
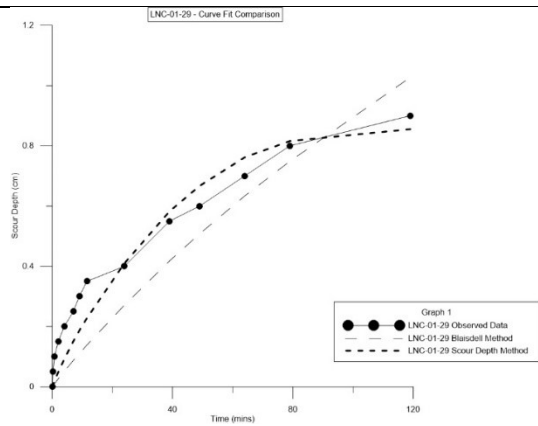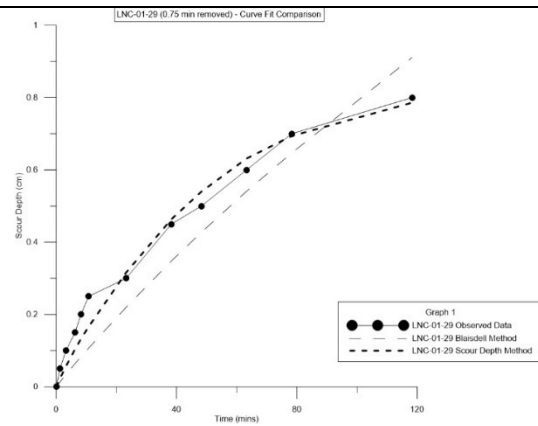
LNC-01-210	
Without Segmentation	With Segmentation
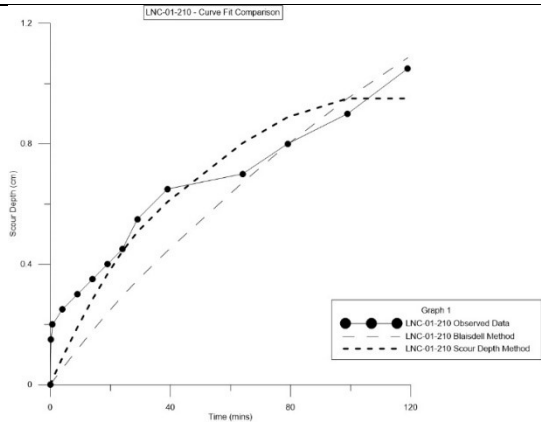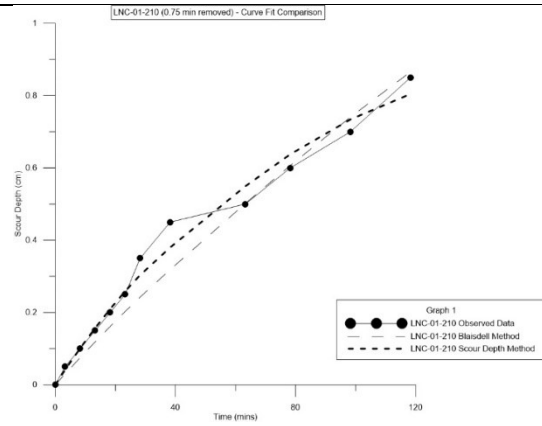
LNC-02-02	
Without Segmentation	With Segmentation
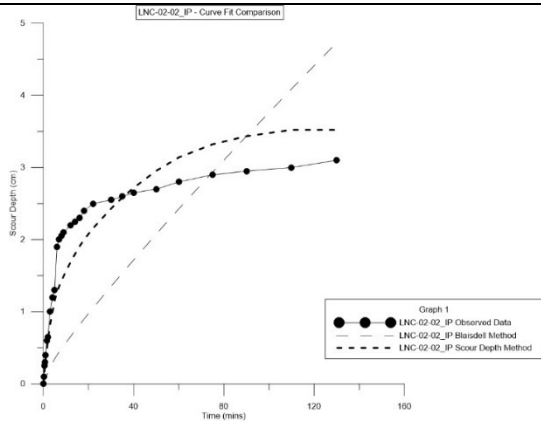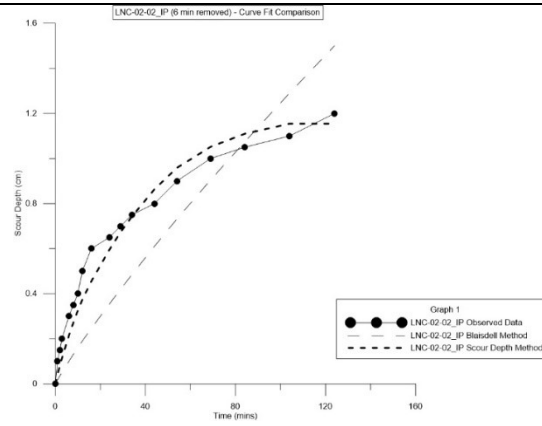
LNC-02-04	
Without Segmentation	With Segmentation
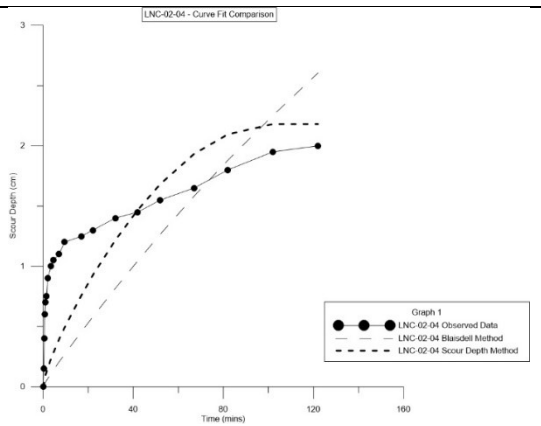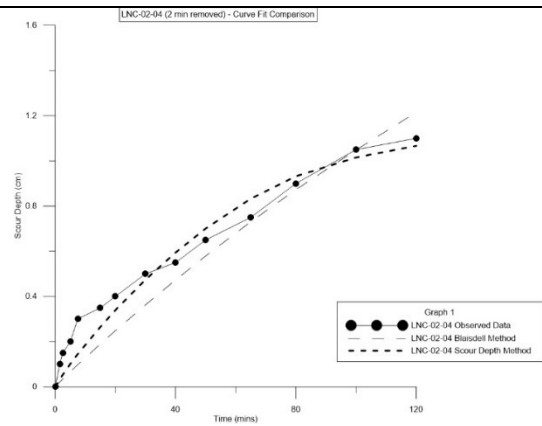
	LNC-02-05	
Without Segmentation		With Segmentation
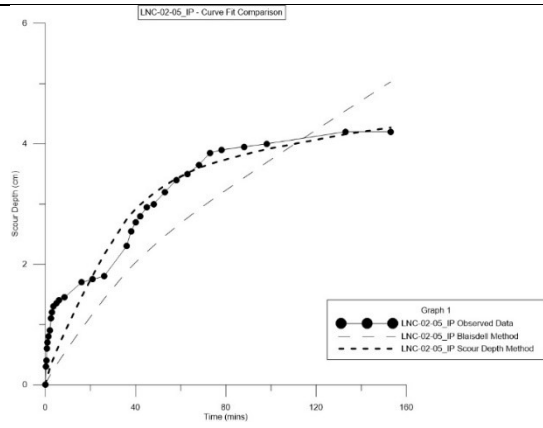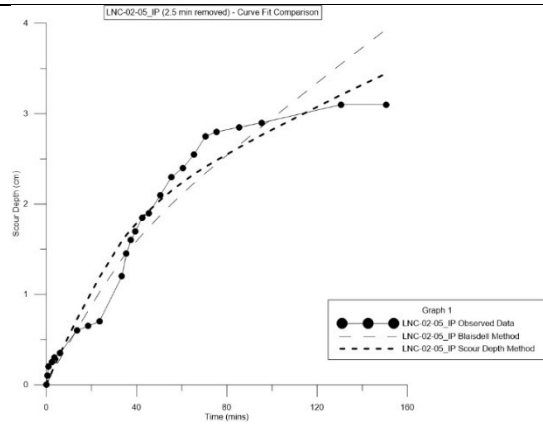
	LNC-03-21	
Without Segmentation		With Segmentation
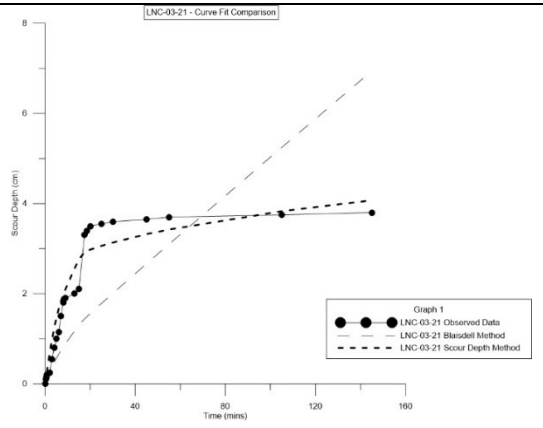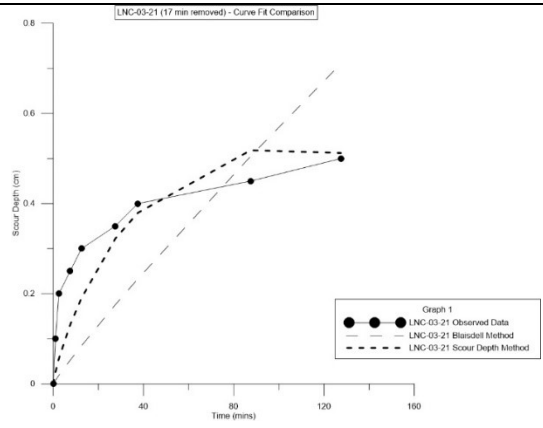
	LNC-03-31	
Without Segmentation		With Segmentation

331
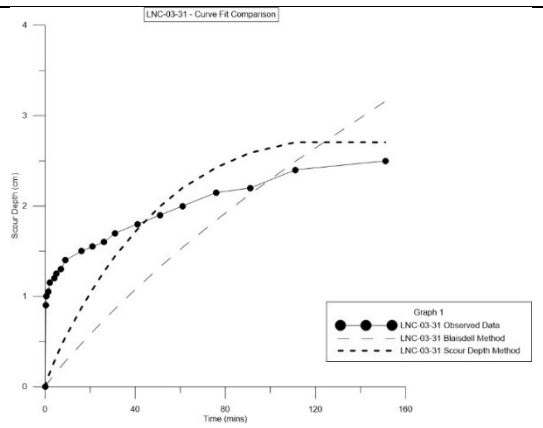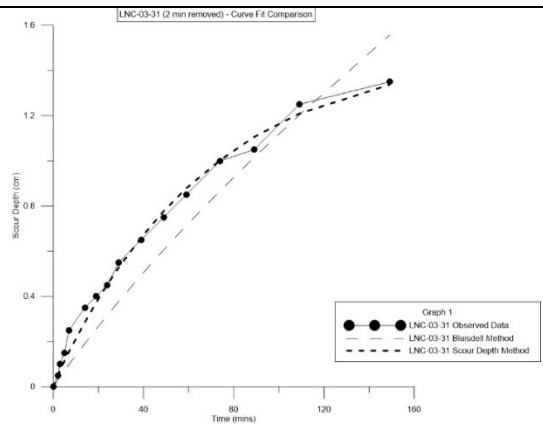
LNC-04-01	
Without Segmentation	With Segmentation
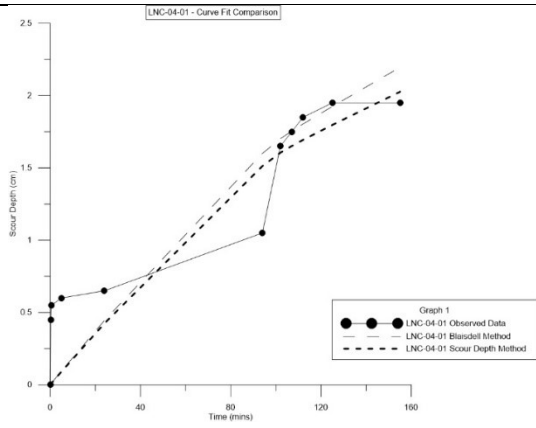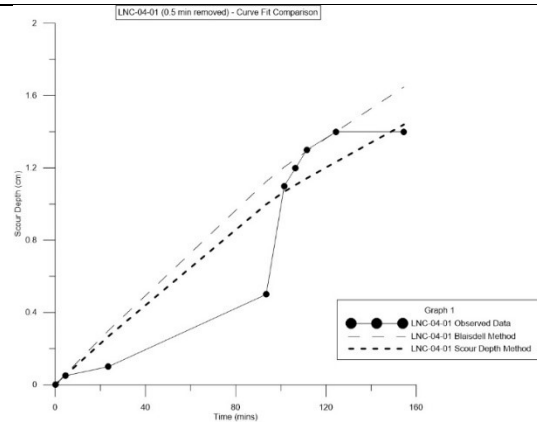
LNC-04-02	
Without Segmentation	With Segmentation
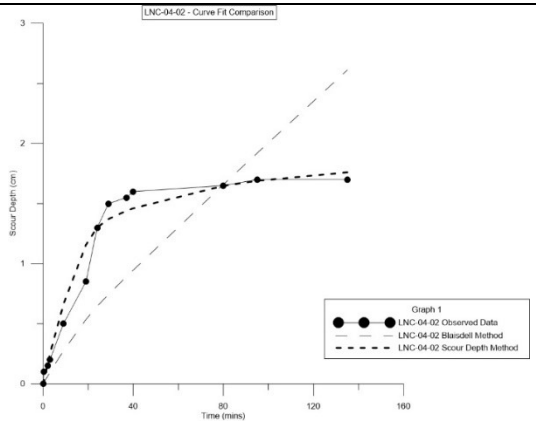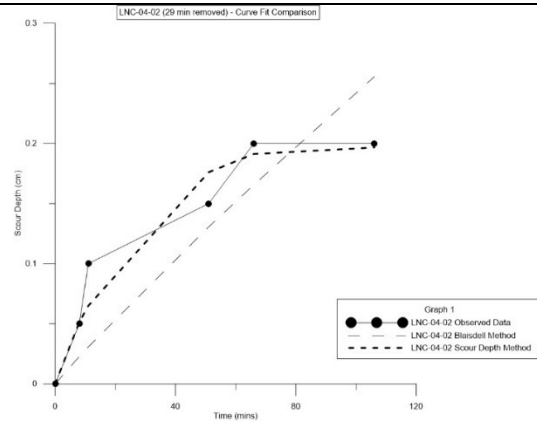
LNC-04-03	
Without Segmentation	With Segmentation
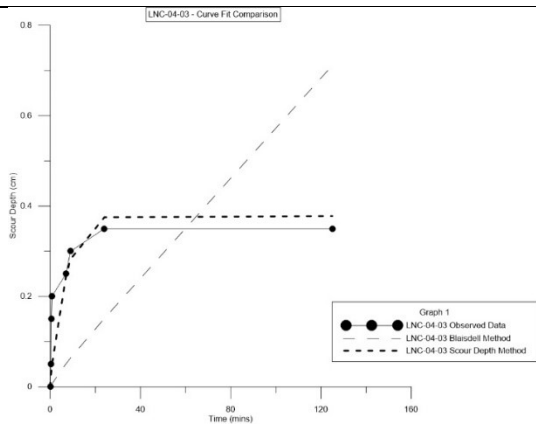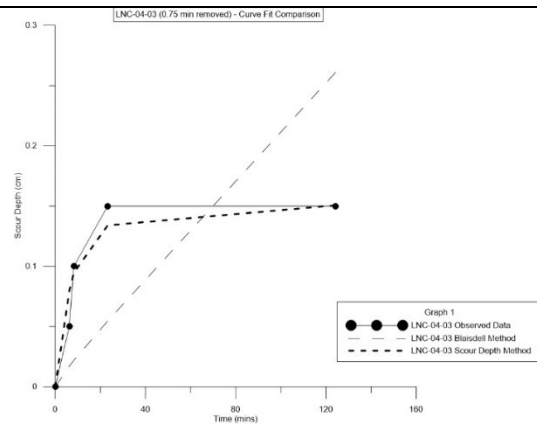
LNC-04-04
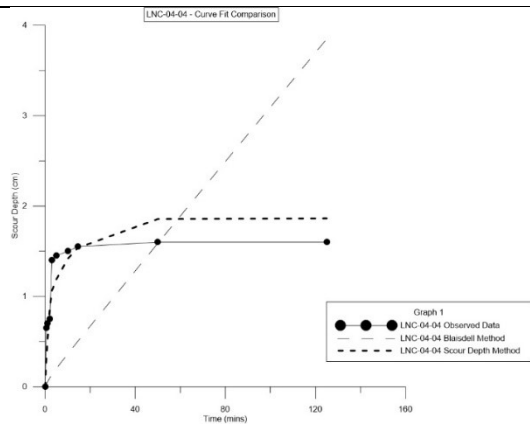
Without Segmentation	With Segmentation
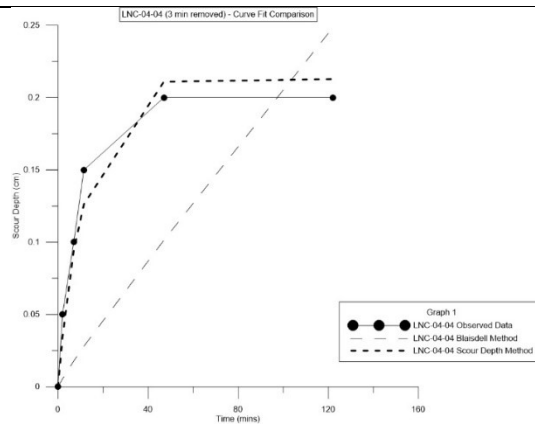
MCE-01-01
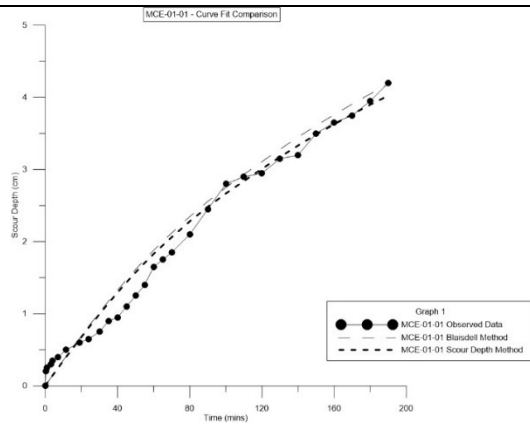
Without Segmentation	With Segmentation
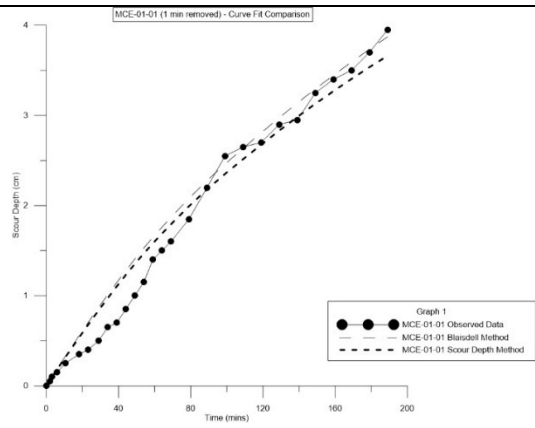
MCE-01-02
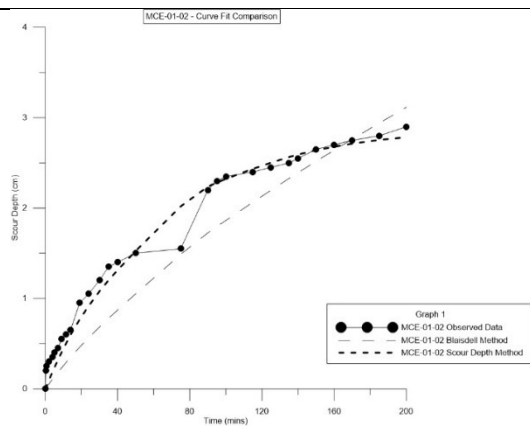
Without Segmentation	With Segmentation
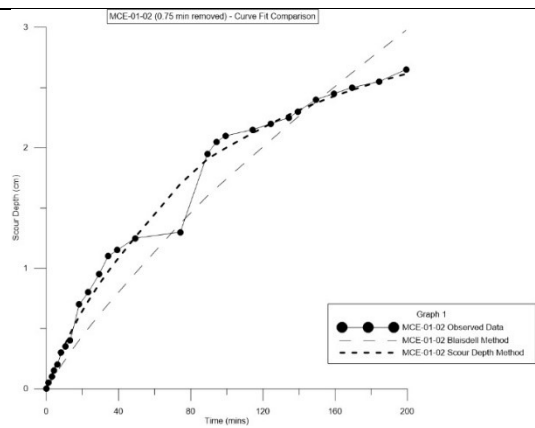
MCE-01-03	
Without Segmentation	With Segmentation
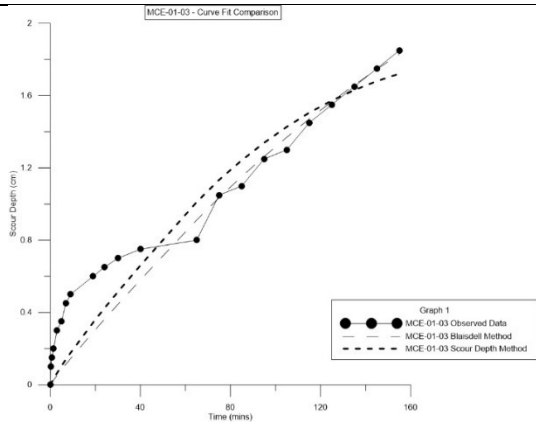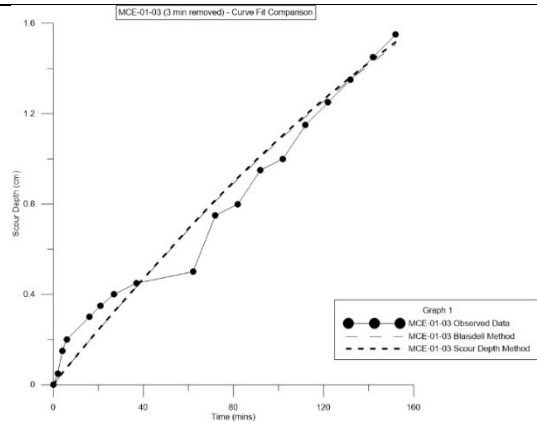
MCE-01-11	
Without Segmentation	With Segmentation

MCE-01-12	
Without Segmentation	With Segmentation

334
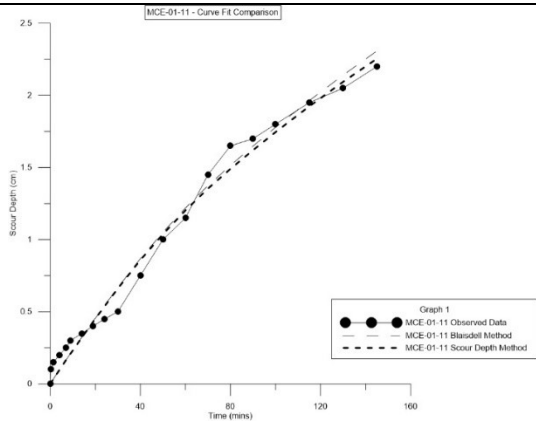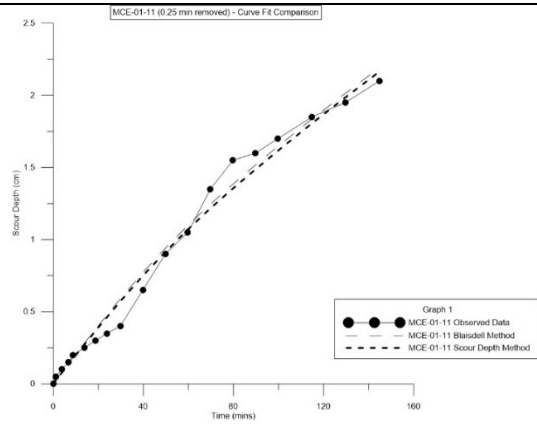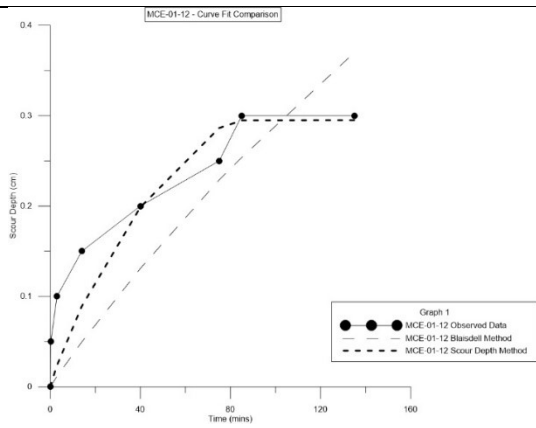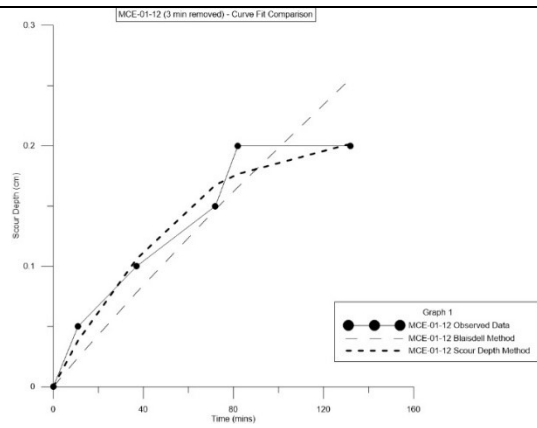
MCE-02-01
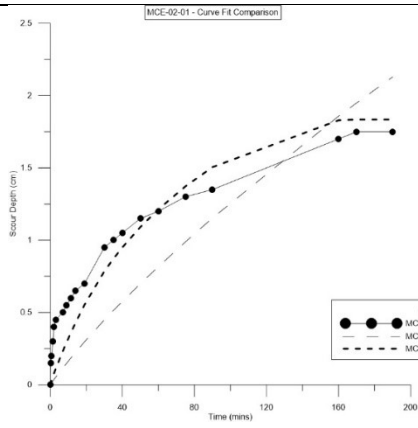
Without Segmentation	With Segmentation
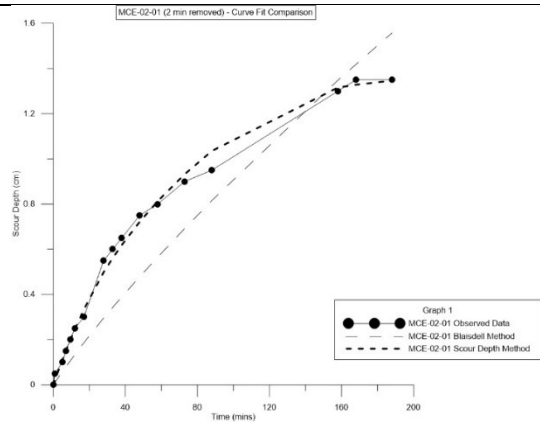
MCE-02-11

Without Segmentation	With Segmentation
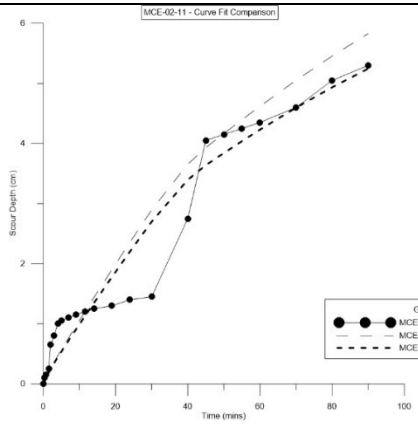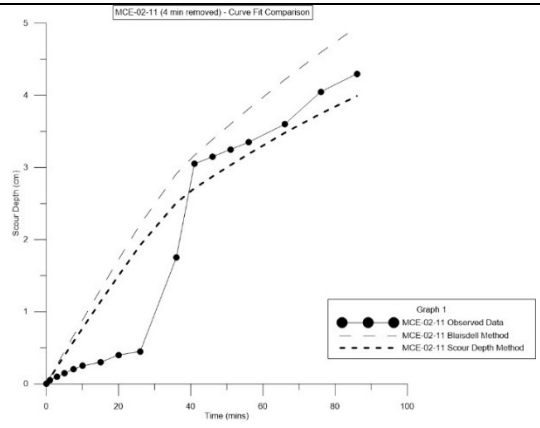
MCE-01-12
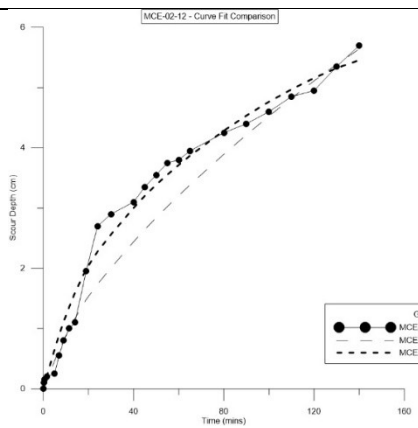
Without Segmentation	With Segmentation
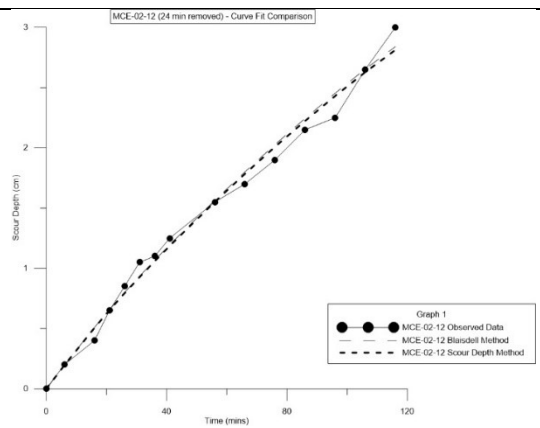
MCE-03-11
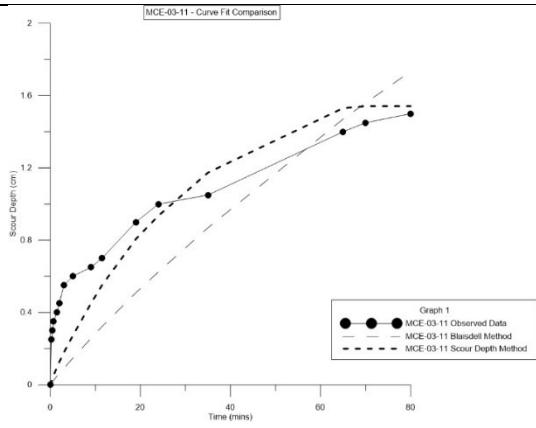
Without Segmentation	With Segmentation
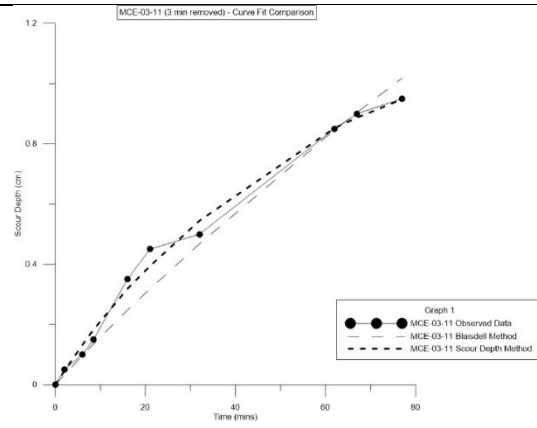
MCE-03-12

Without Segmentation	With Segmentation
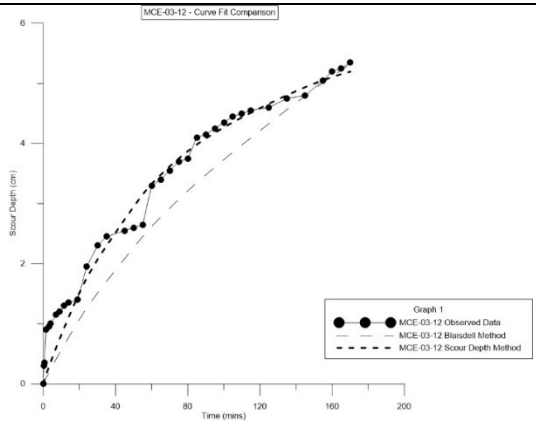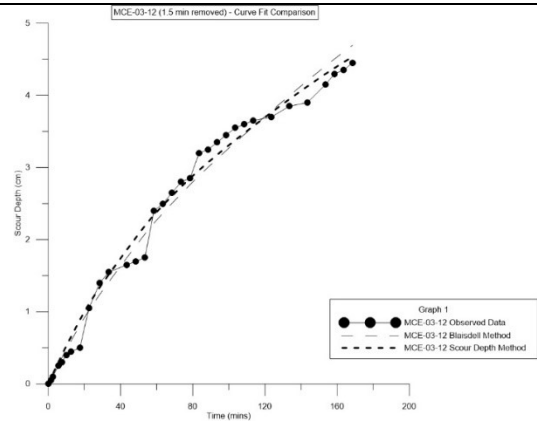
MCE-03-13
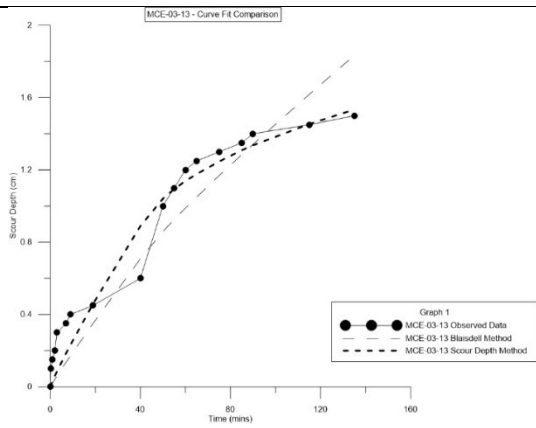
Without Segmentation	With Segmentation
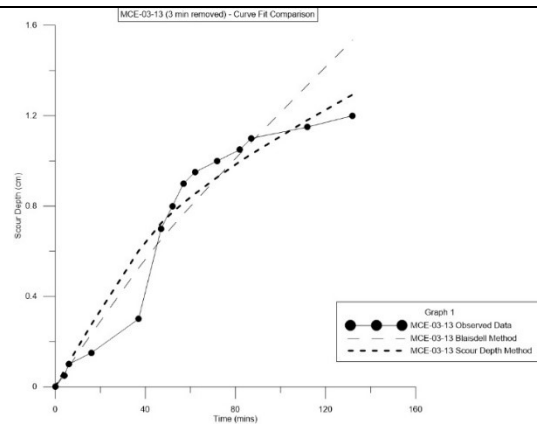
MCE-03-14
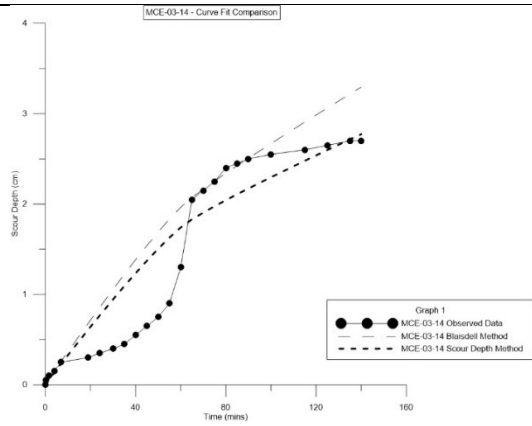
Without Segmentation	With Segmentation
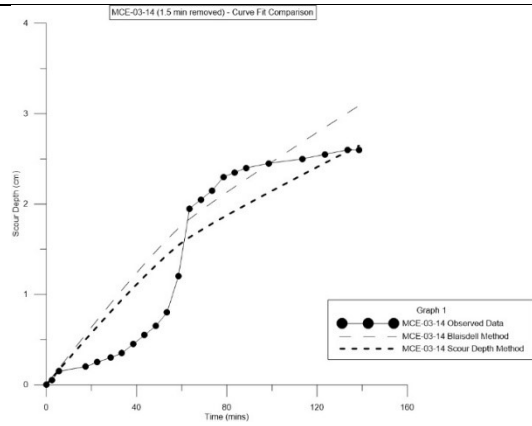
MCE-03-21

Without Segmentation	With Segmentation
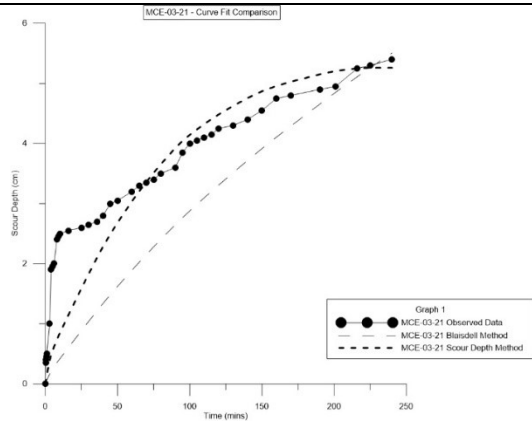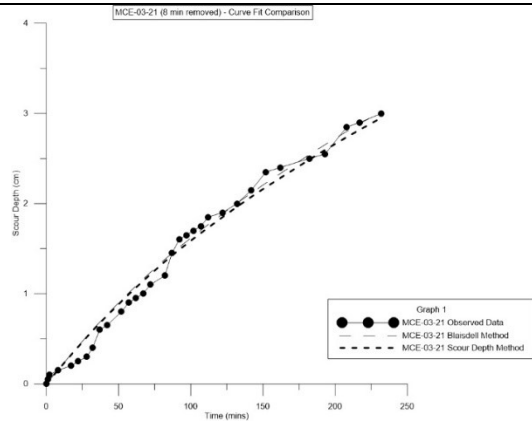
MCE-03-13
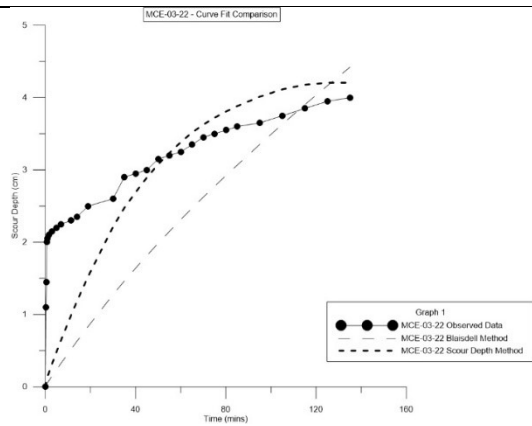
Without Segmentation	With Segmentation
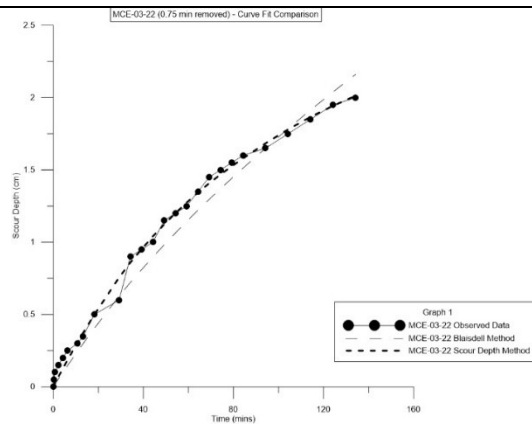
NMB-01-01
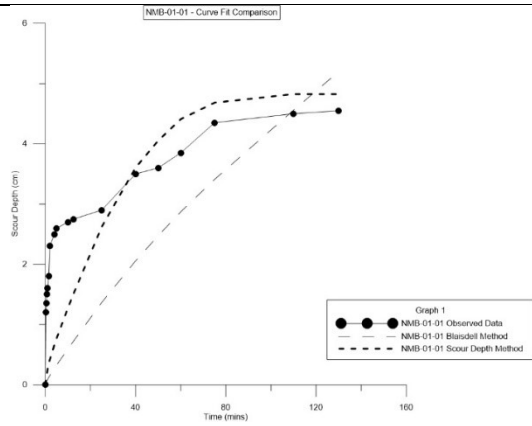
Without Segmentation	With Segmentation
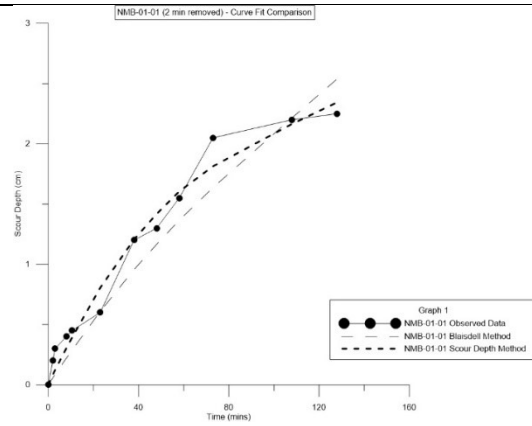
NMB-01-02
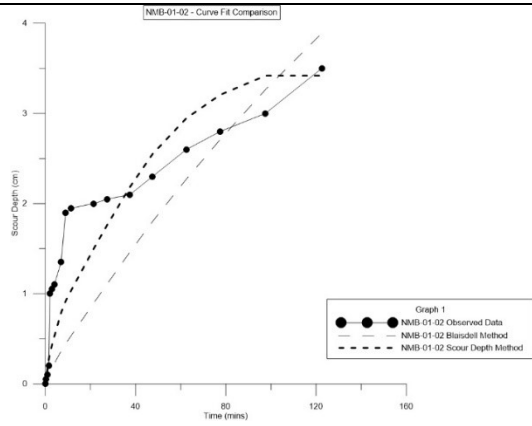
Without Segmentation	With Segmentation
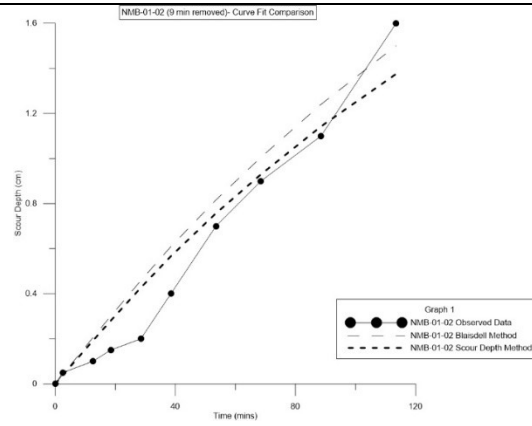
NMB-01-03

Without Segmentation	With Segmentation

338
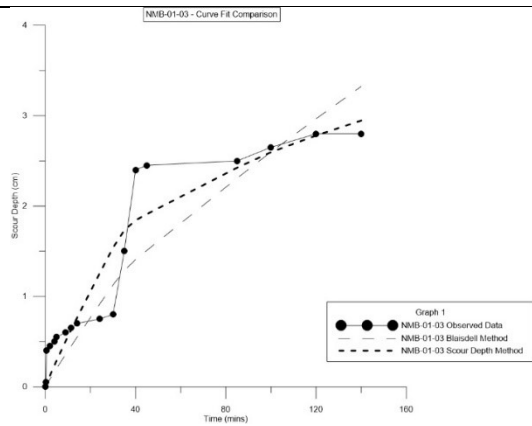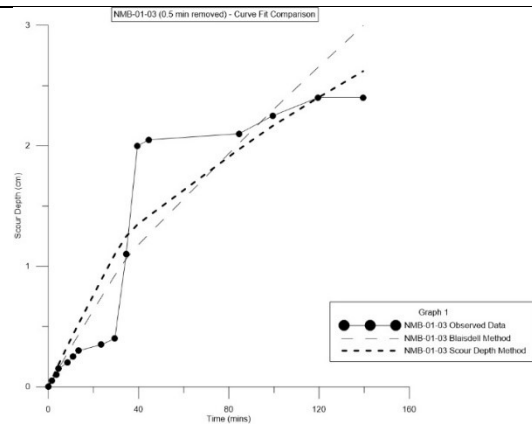
NMB-01-04	
Without Segmentation	With Segmentation
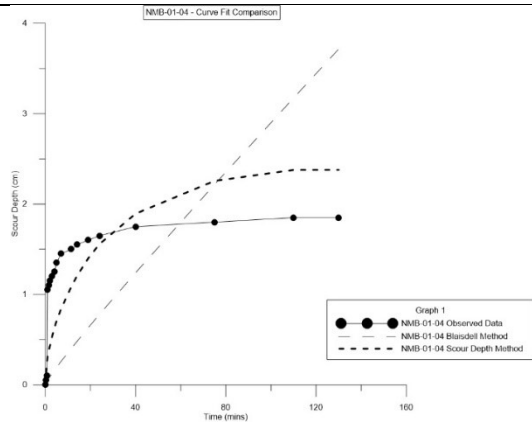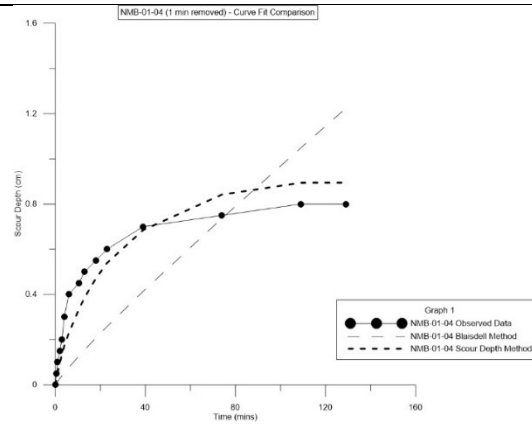
NMB-01-12	
Without Segmentation	With Segmentation
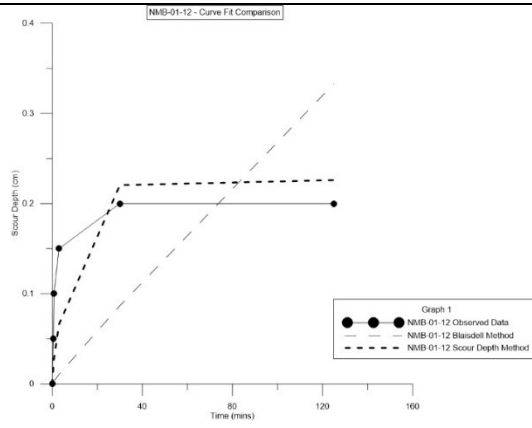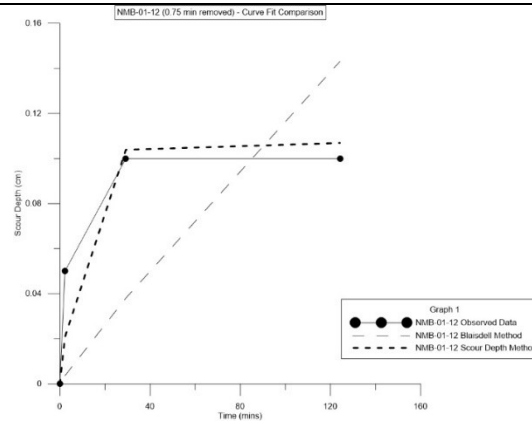
NMB-02-01	
Without Segmentation	With Segmentation

339
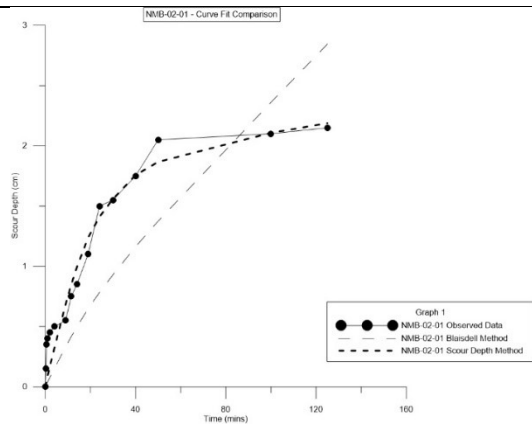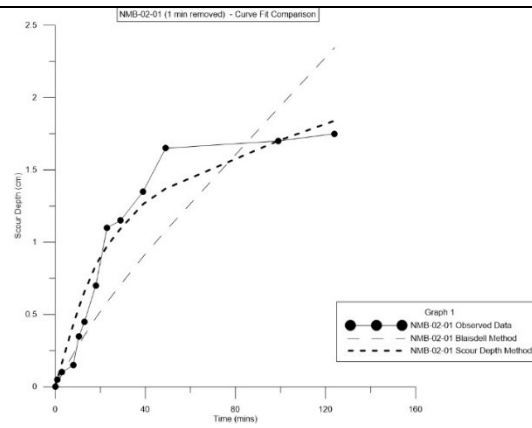
NMB-02-02
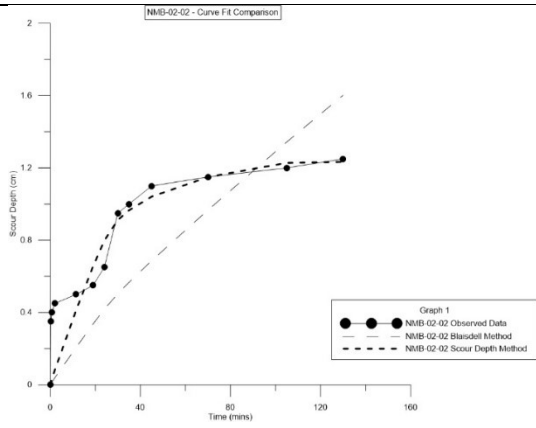
Without Segmentation	With Segmentation
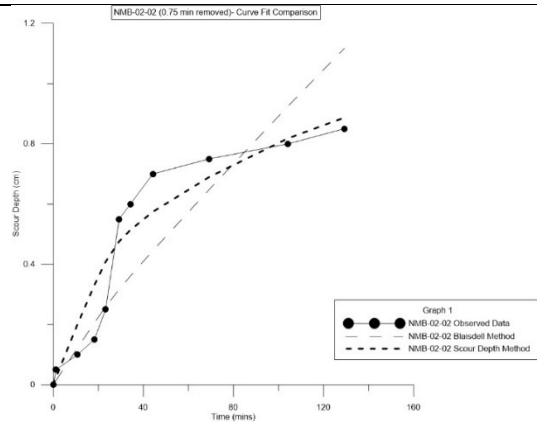
NMB-02-11
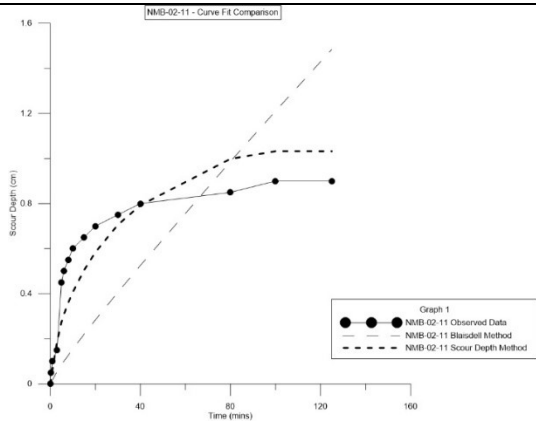
Without Segmentation	With Segmentation
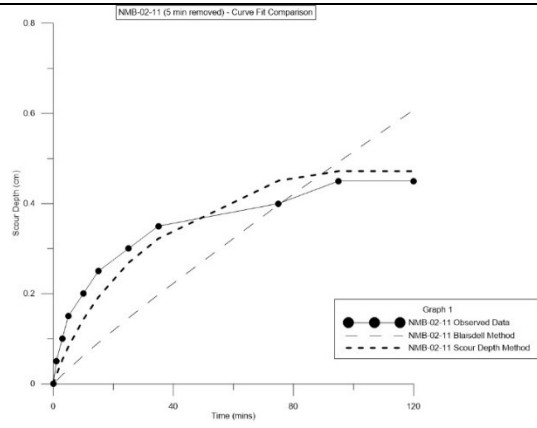
NMB-02-13

Without Segmentation	With Segmentation

340
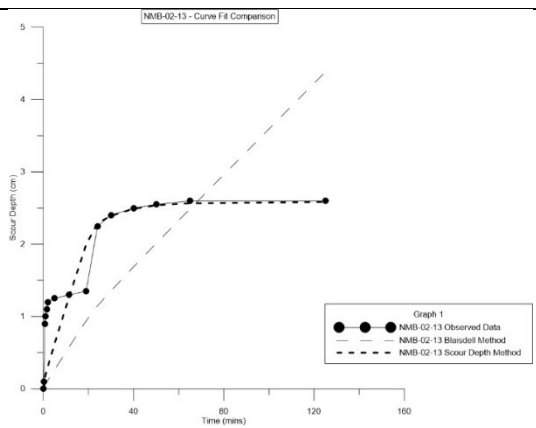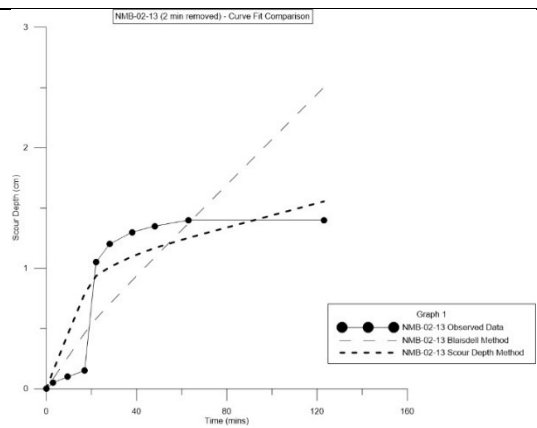
NMB-02-14
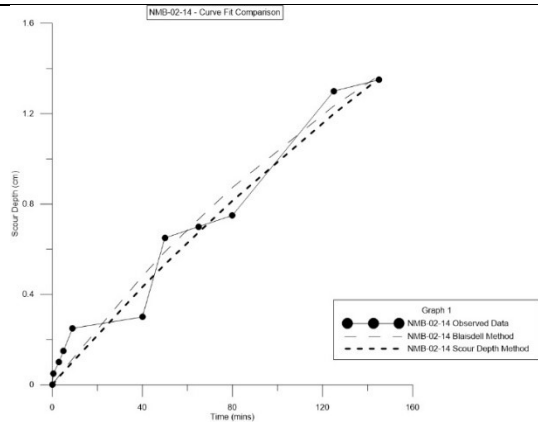
Without Segmentation	With Segmentation
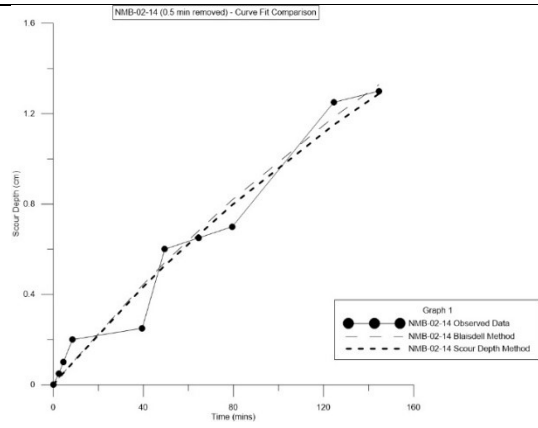
NMB-03-11
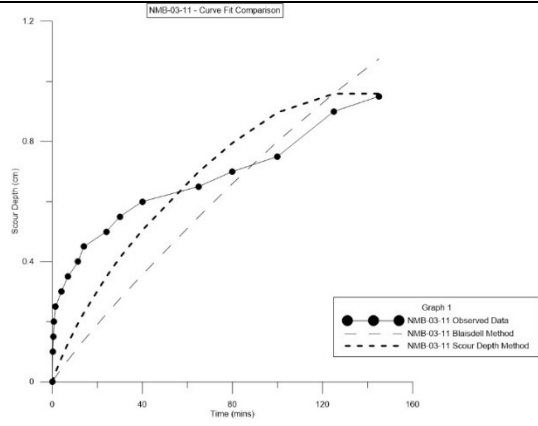
Without Segmentation	With Segmentation
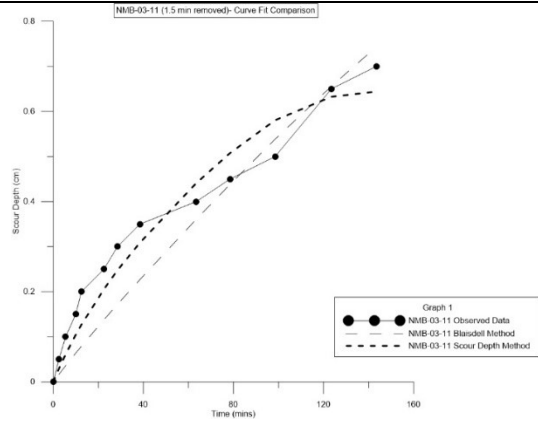
NMB-03-12
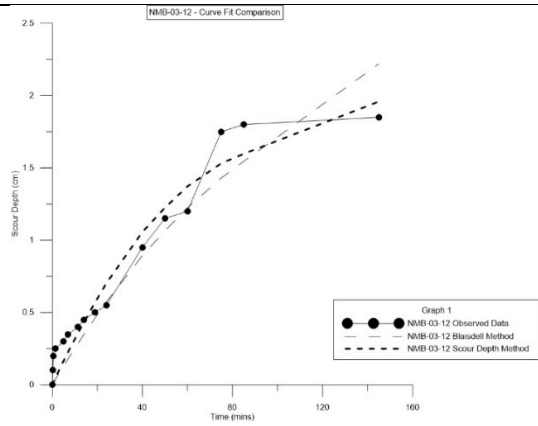
Without Segmentation	With Segmentation
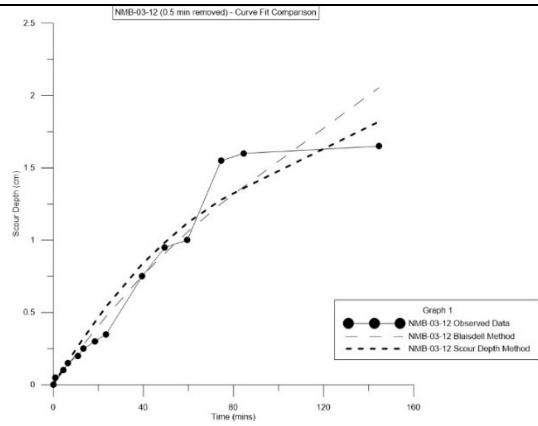
NMB-03-13
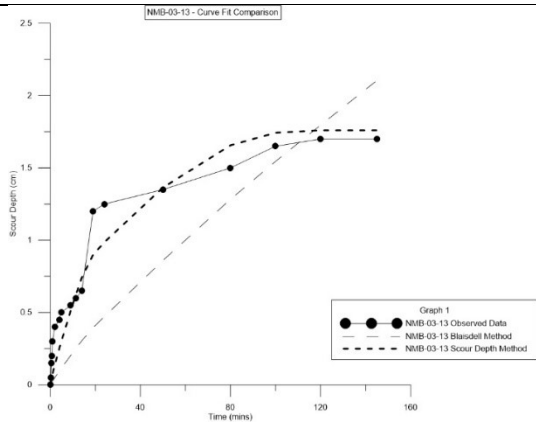
Without Segmentation	With Segmentation
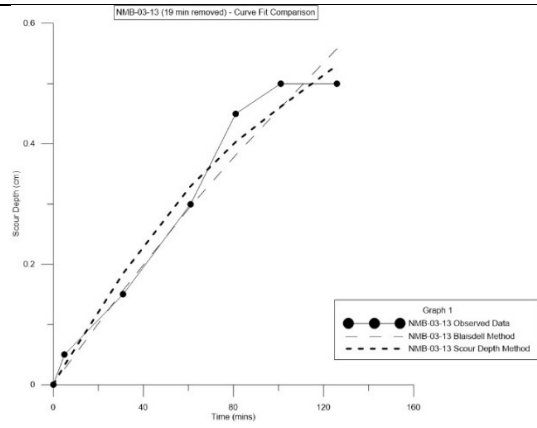
NMB-04-11
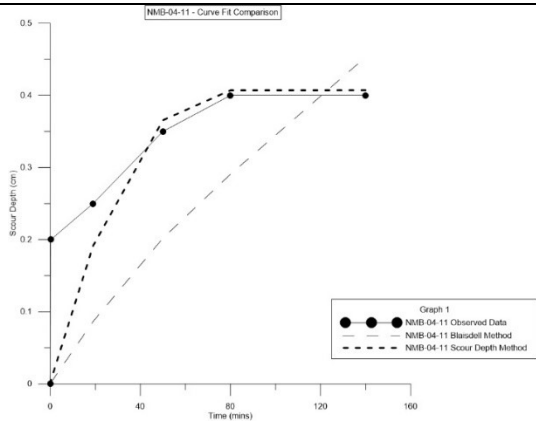
Without Segmentation	With Segmentation
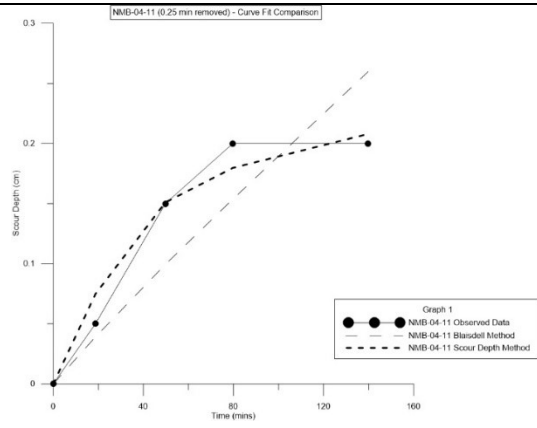
NMB-04-12

Without Segmentation	With Segmentation

342
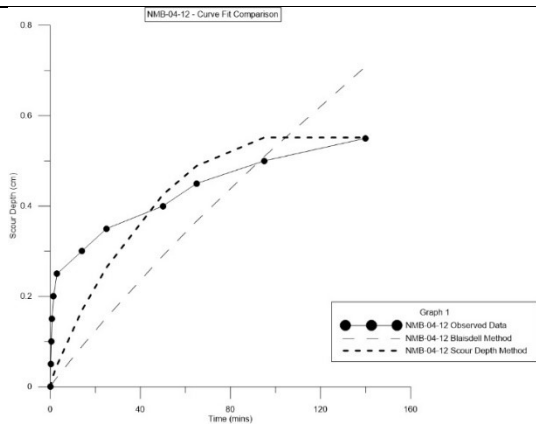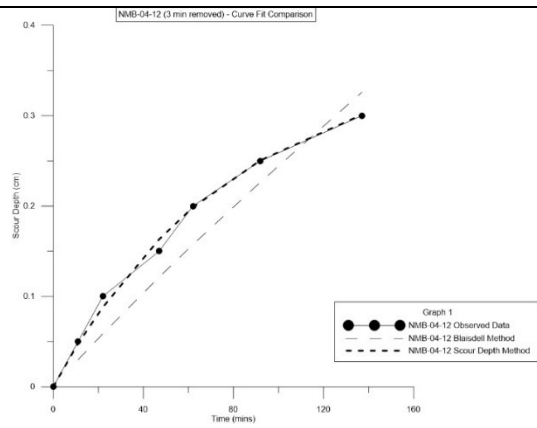
NMB-04-13
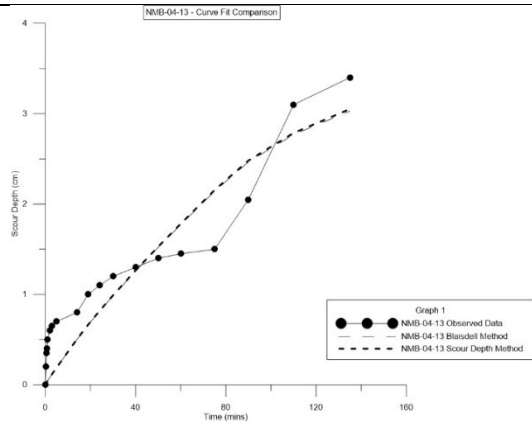
Without Segmentation	With Segmentation
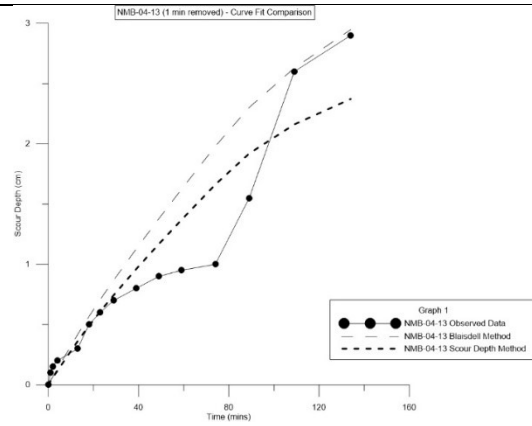
NTL-01-01
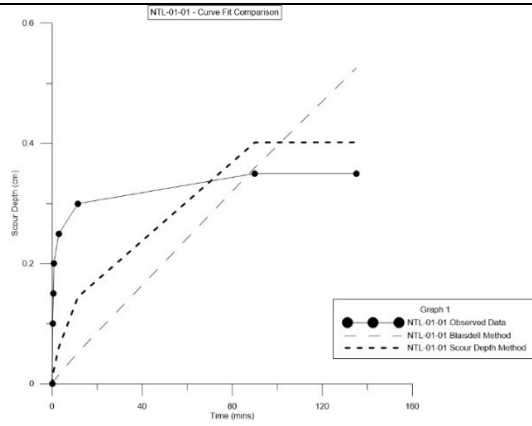
Without Segmentation	With Segmentation
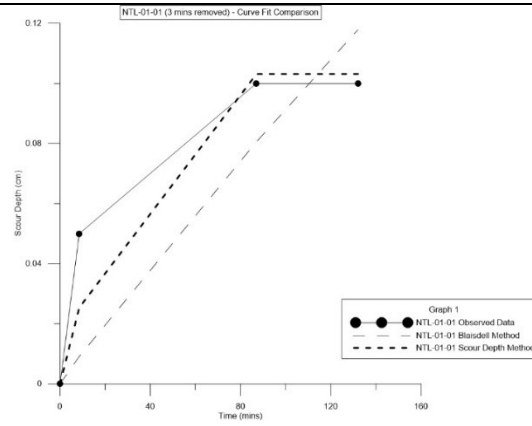
NTL-01-02
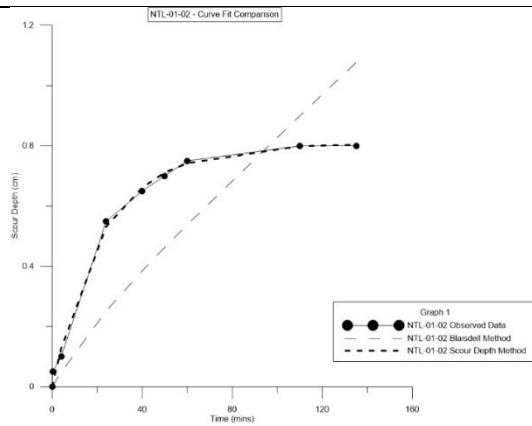
Without Segmentation	With Segmentation
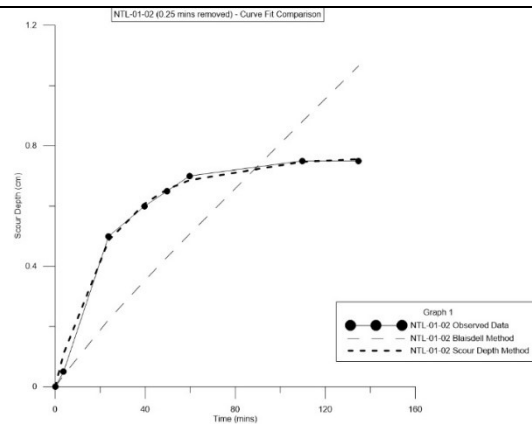
NTL-01-03	
Without Segmentation	With Segmentation
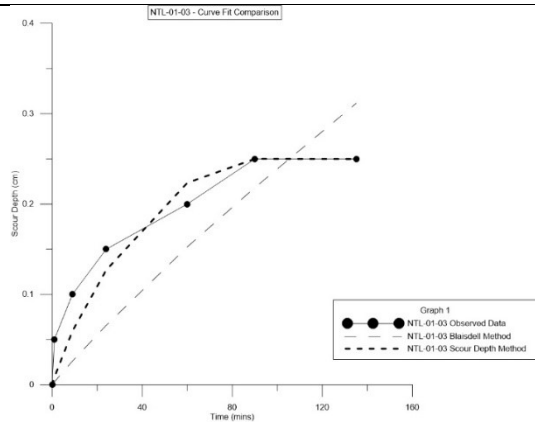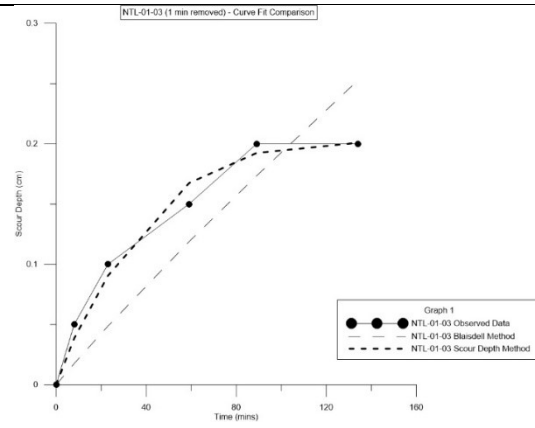
NTL-01-04	
Without Segmentation	With Segmentation
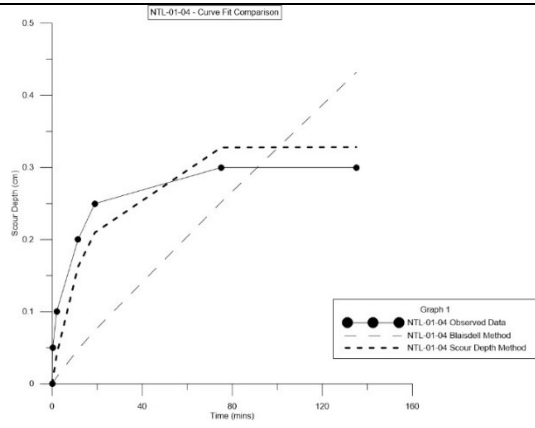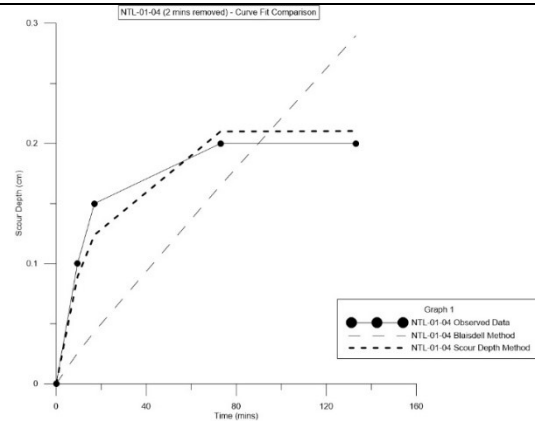
NTL-01-05	
Without Segmentation	With Segmentation
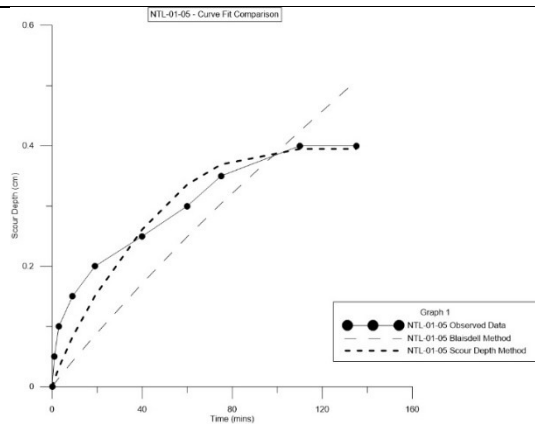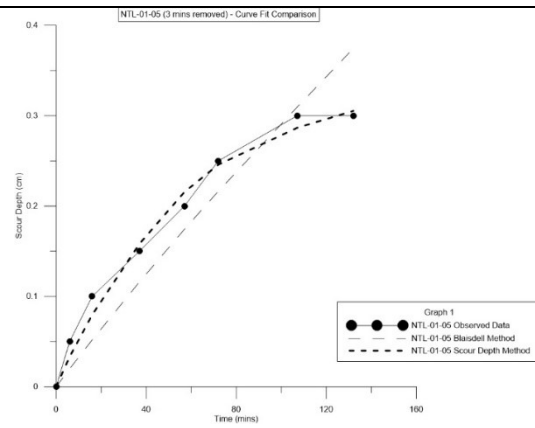
NTL-01-06	
Without Segmentation	With Segmentation
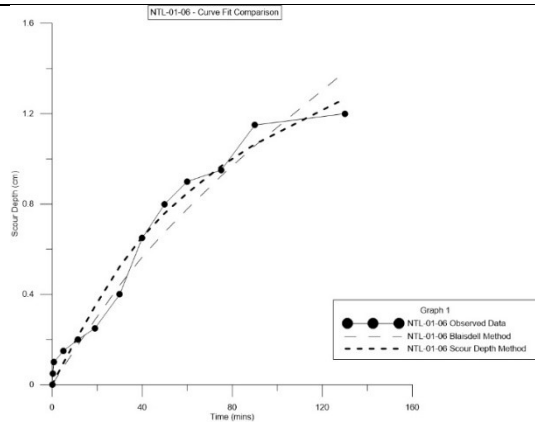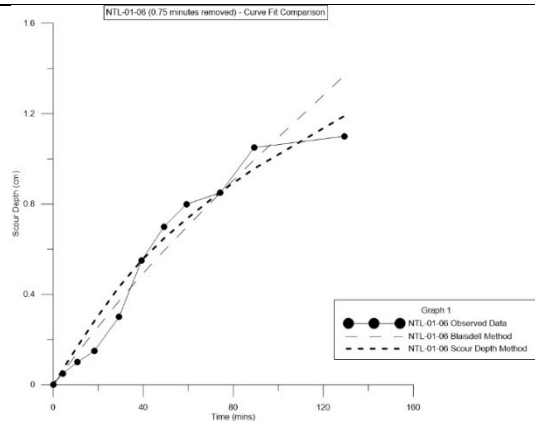
NTL-01-07	
Without Segmentation	With Segmentation
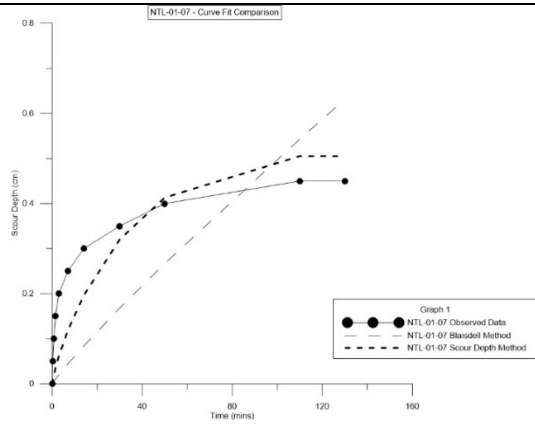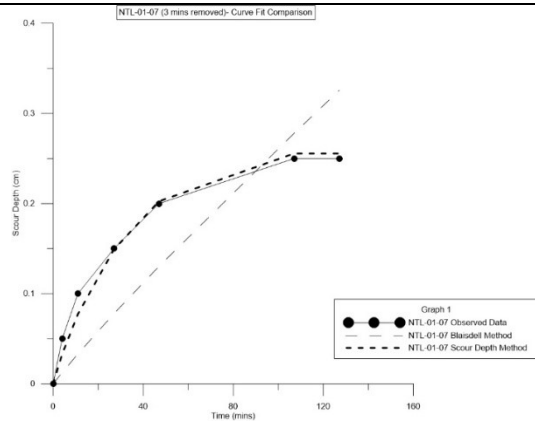
NTL-01-11	
Without Segmentation	With Segmentation
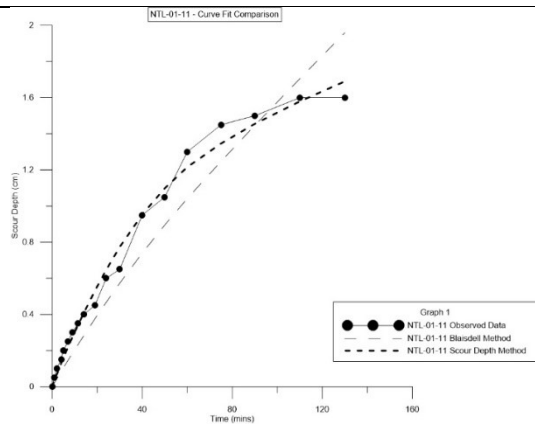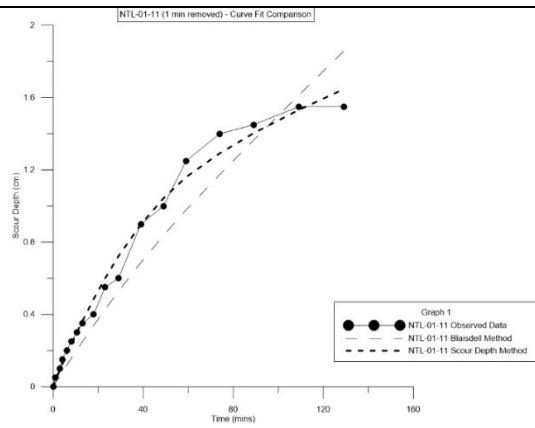
NTL-01-13
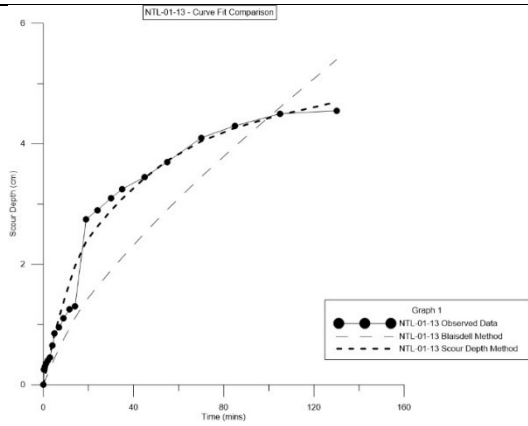
Without Segmentation	With Segmentation
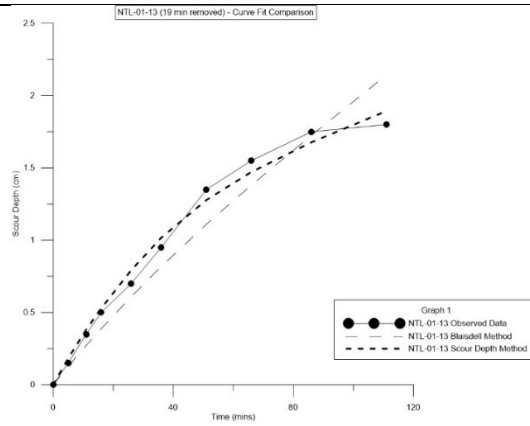
NTL-01-14
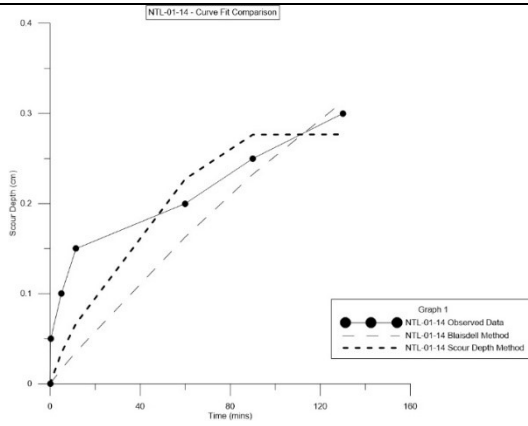
Without Segmentation	With Segmentation
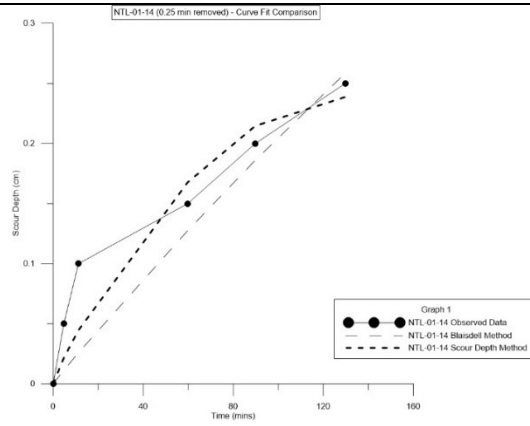
NTL-01-15

Without Segmentation	With Segmentation

346
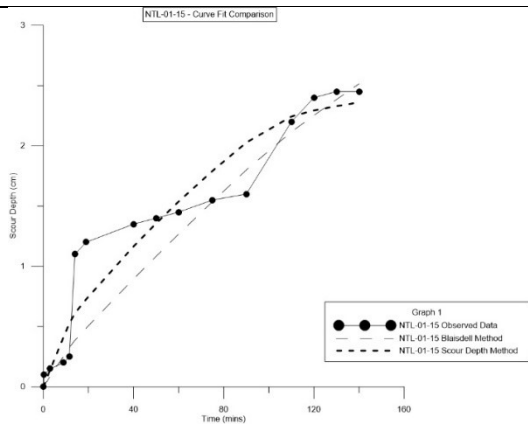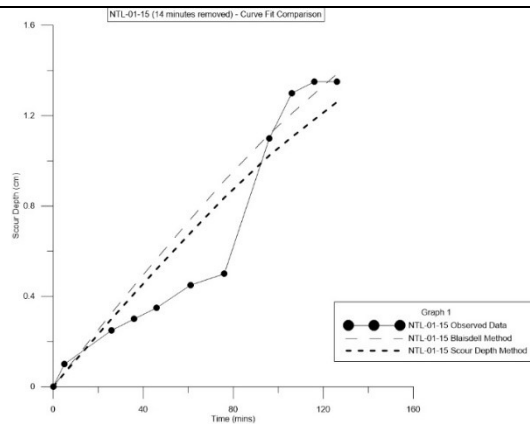
NTL-02-01	
Without Segmentation	With Segmentation
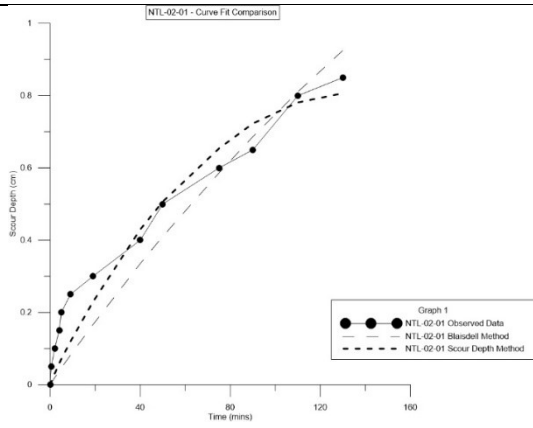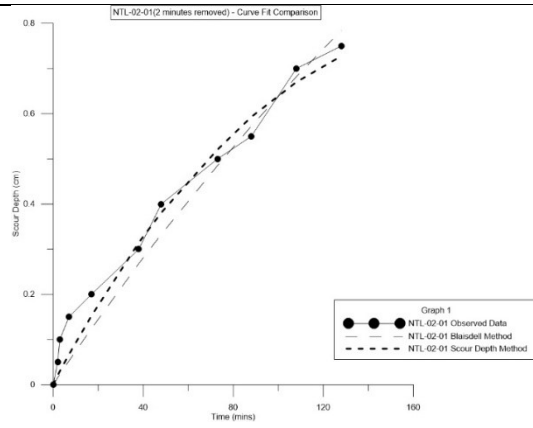
NTL-02-02	
Without Segmentation	With Segmentation
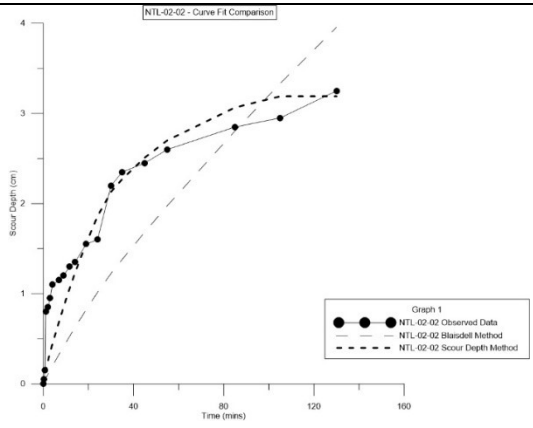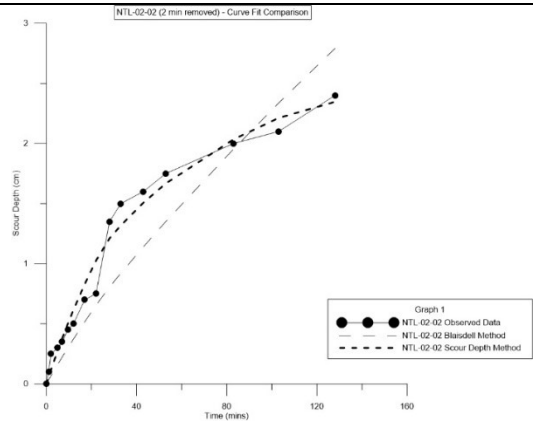
NTL-02-03	
Without Segmentation	With Segmentation
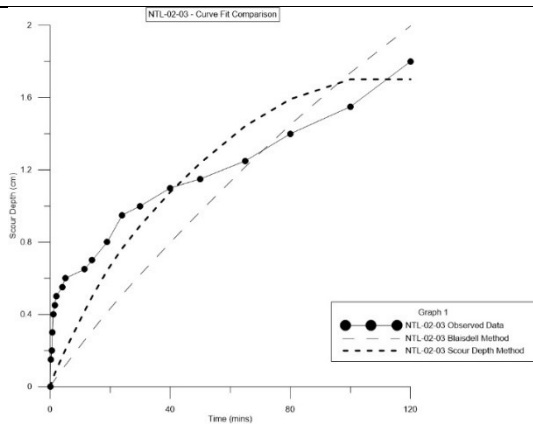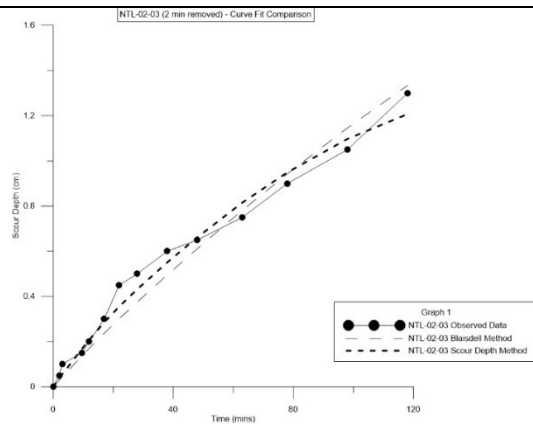
NTL-02-11
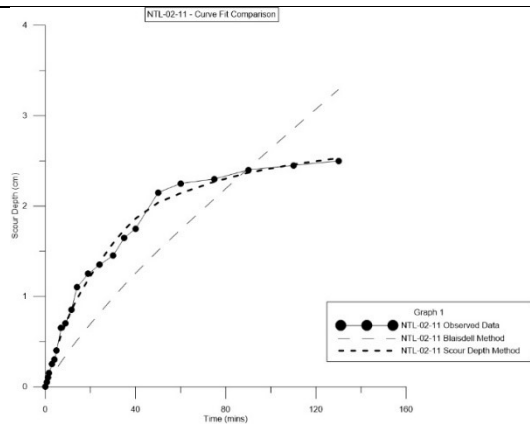
Without Segmentation	With Segmentation
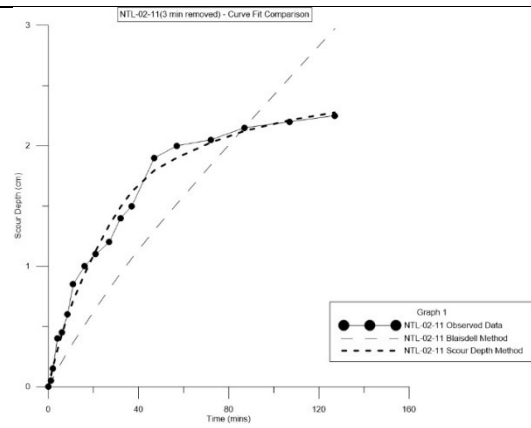
NTL-02-12
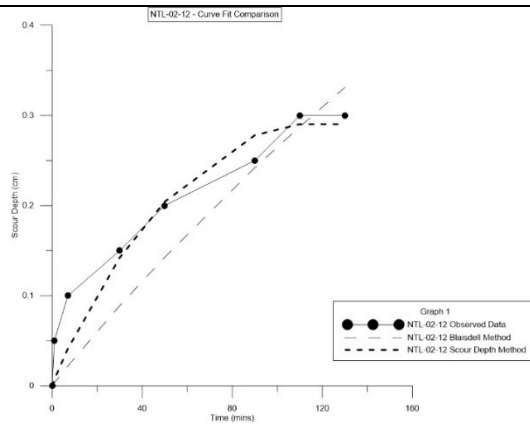
Without Segmentation	With Segmentation
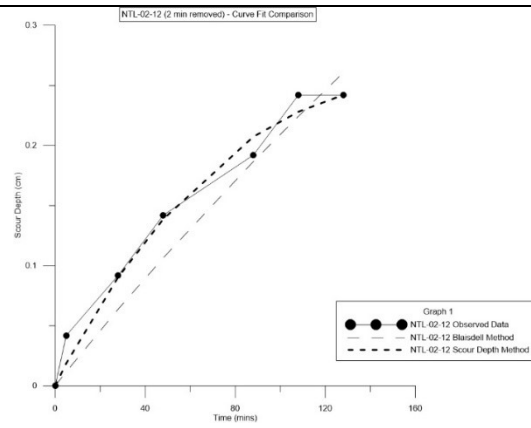
NTL-02-13

Without Segmentation	With Segmentation

348
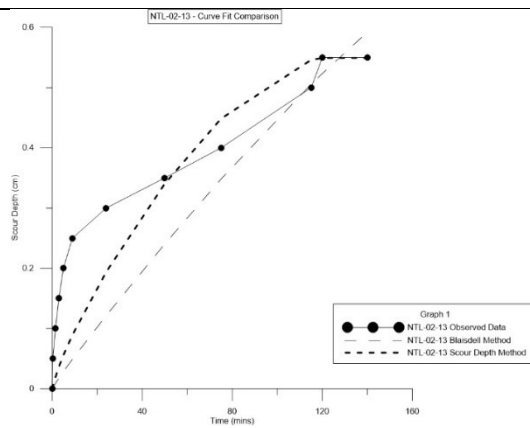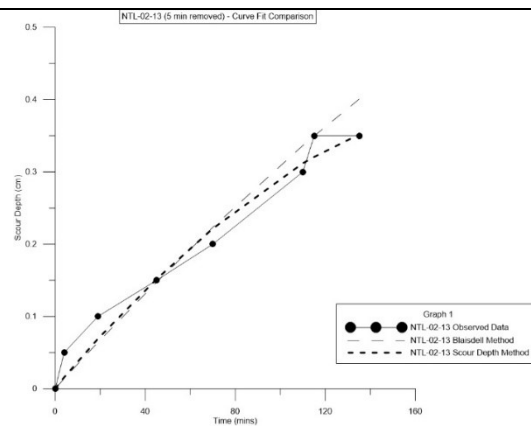
NTL-02-14
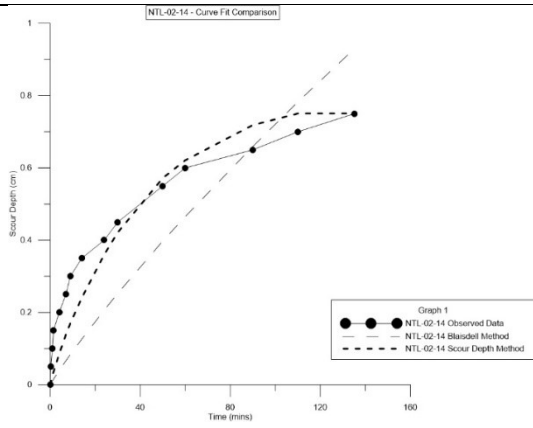
Without Segmentation	With Segmentation
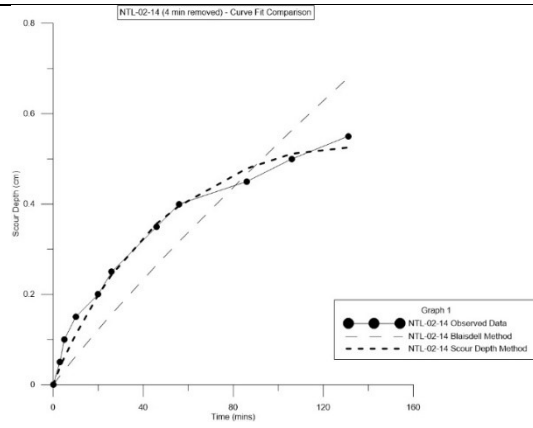
NTL-02-21
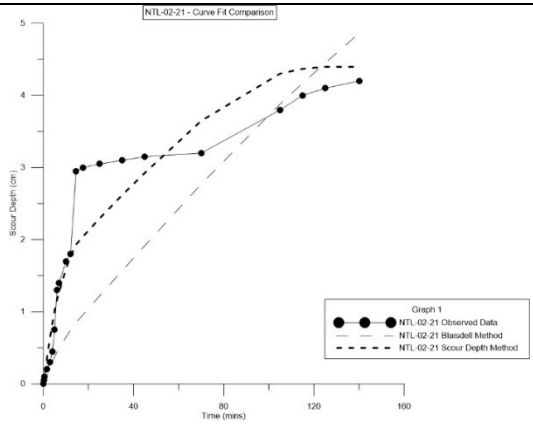
Without Segmentation	With Segmentation
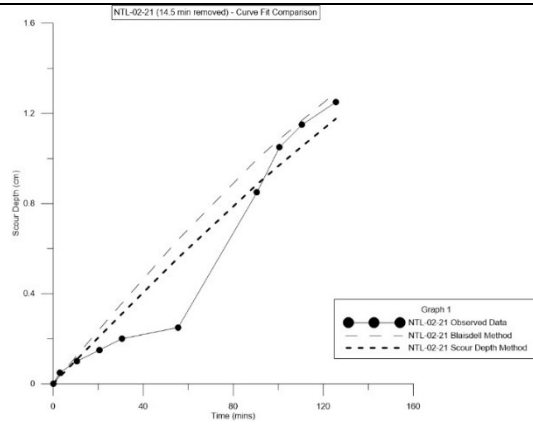
NTL-02-22

Without Segmentation	With Segmentation

349
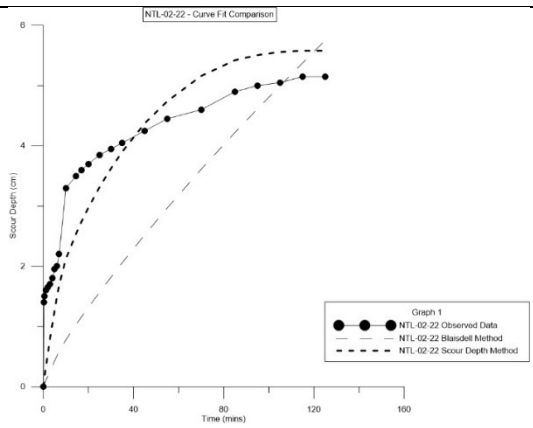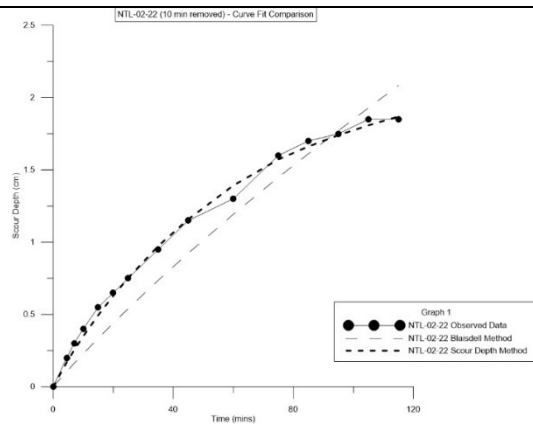
NTL-02-23
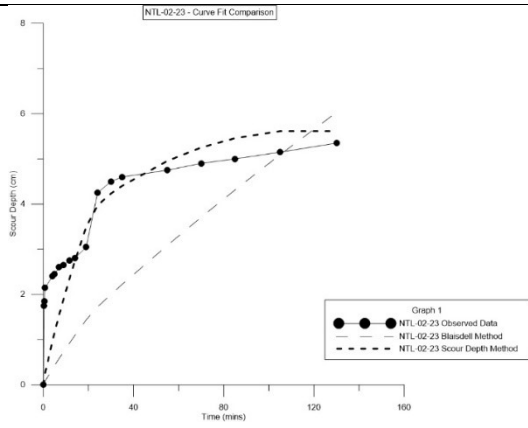
Without Segmentation	With Segmentation
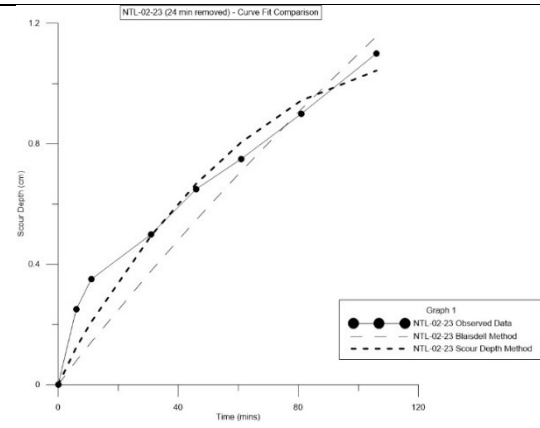
TCH-01-01
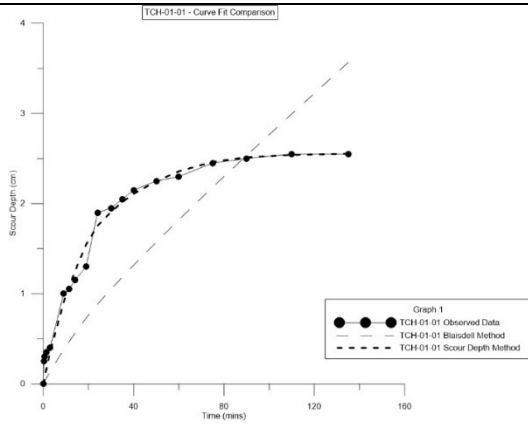
Without Segmentation	With Segmentation
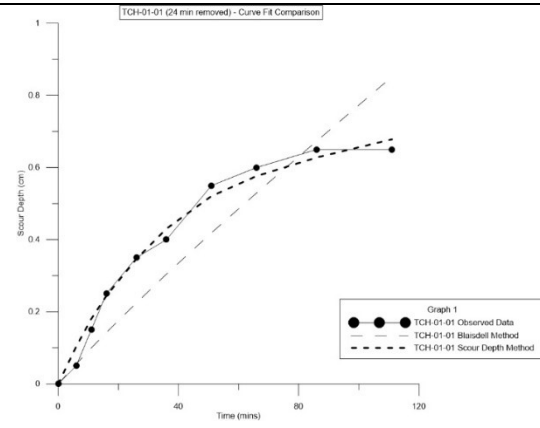
TCH-01-02

Without Segmentation	With Segmentation

350
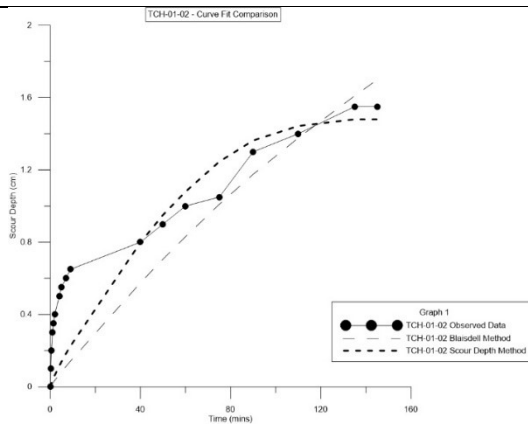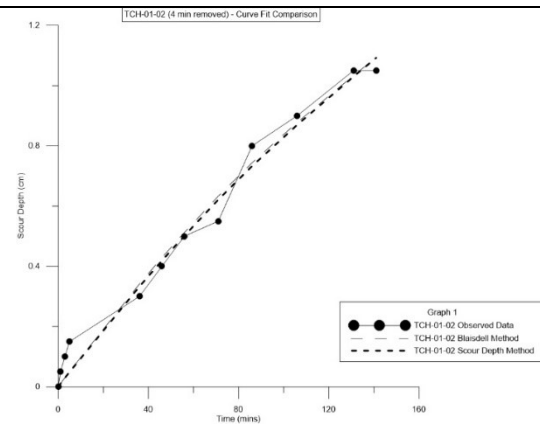
TCH-01-11	
Without Segmentation	With Segmentation
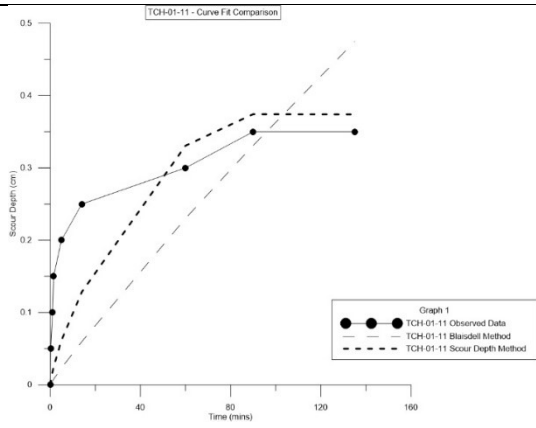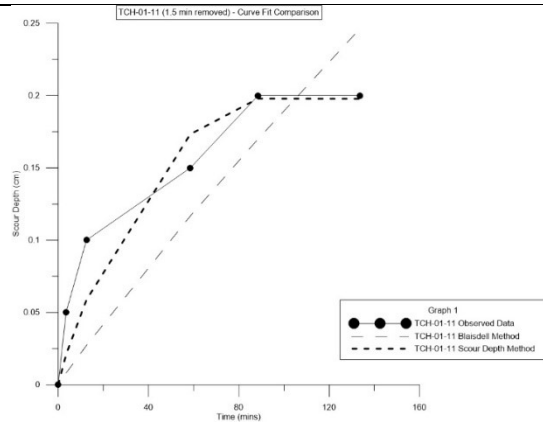
TCH-01-12	
Without Segmentation	With Segmentation
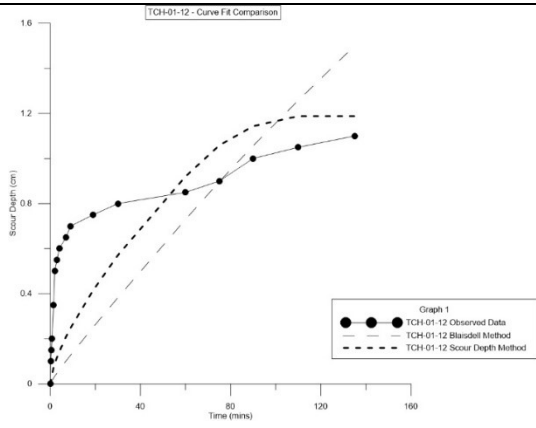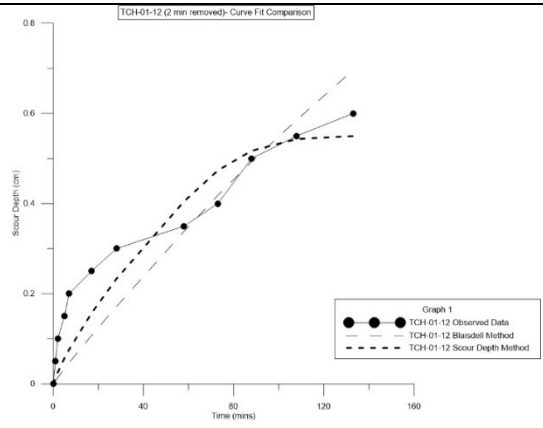
TCH-01-14	
Without Segmentation	With Segmentation
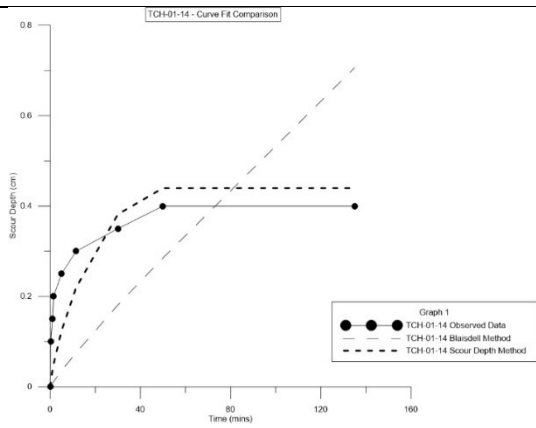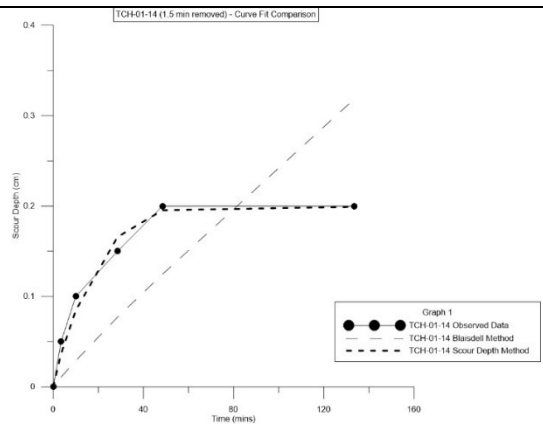
	TCH-01-15	
Without Segmentation		With Segmentation
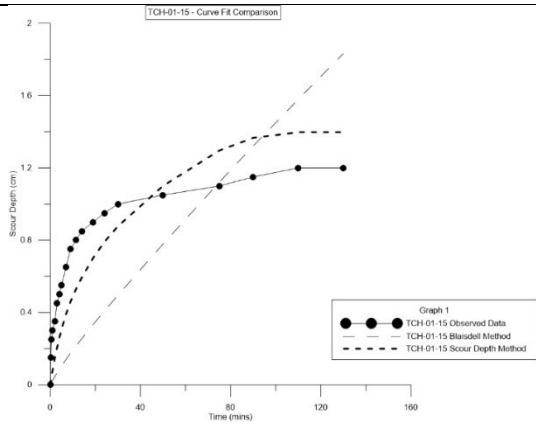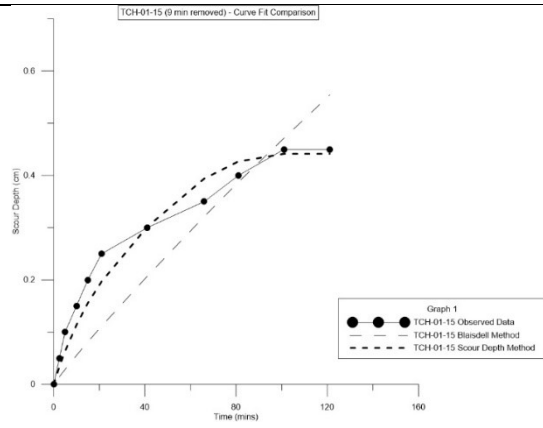
	TCH-01-16	
Without Segmentation		With Segmentation
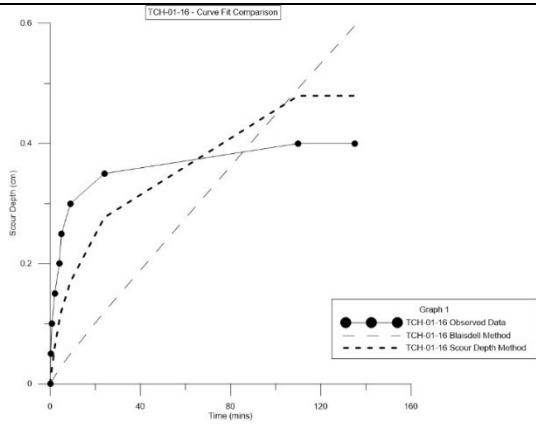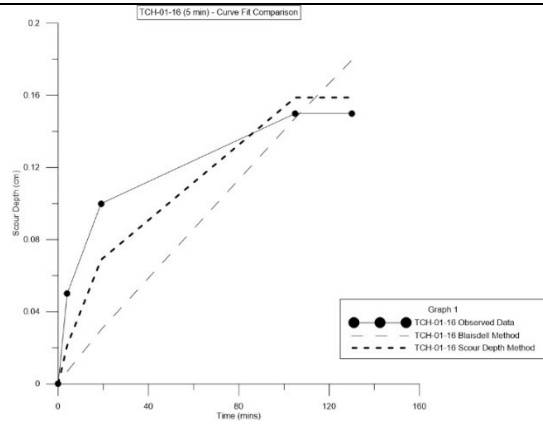
	TCH-01-17	
Without Segmentation		With Segmentation
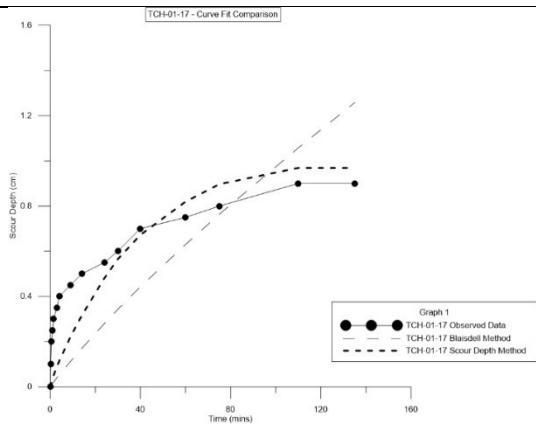
TCH-01-18
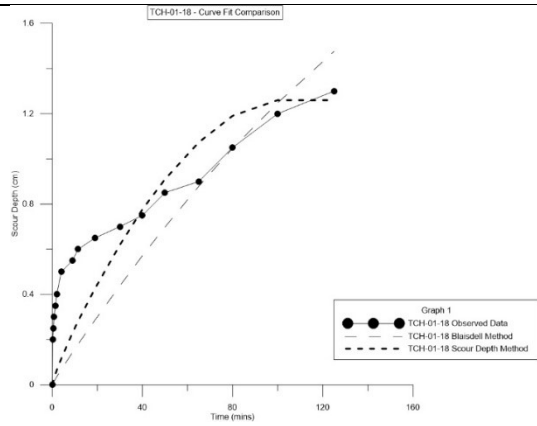
Without Segmentation	With Segmentation

TCH-01-21
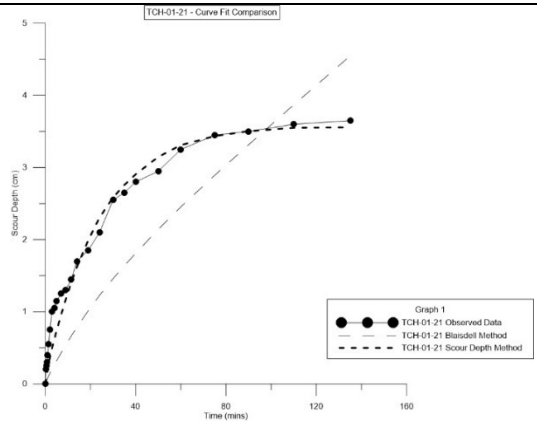
Without Segmentation	With Segmentation
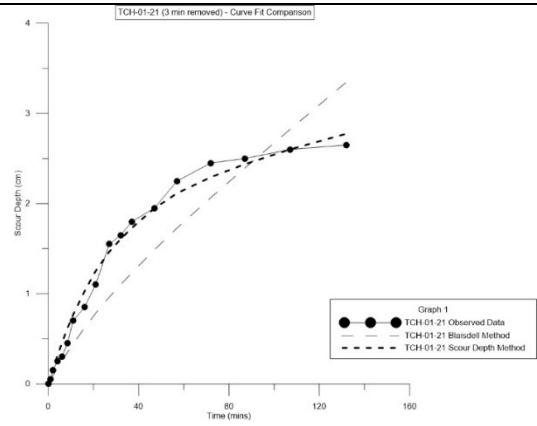
TCH-01-22
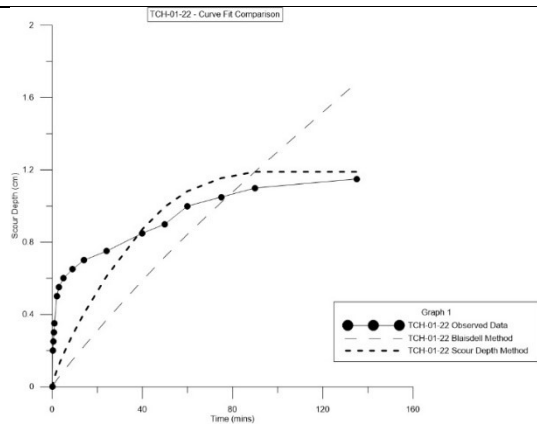
Without Segmentation	With Segmentation
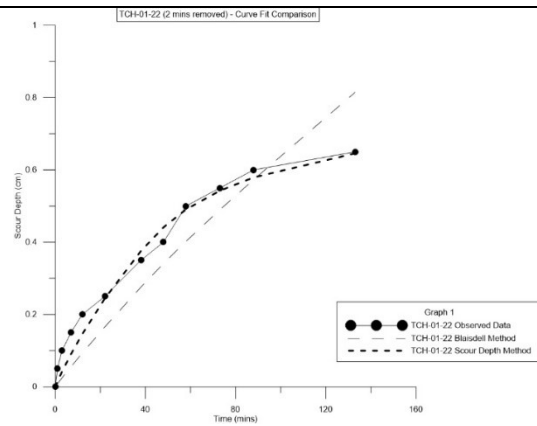
TCH-01-23
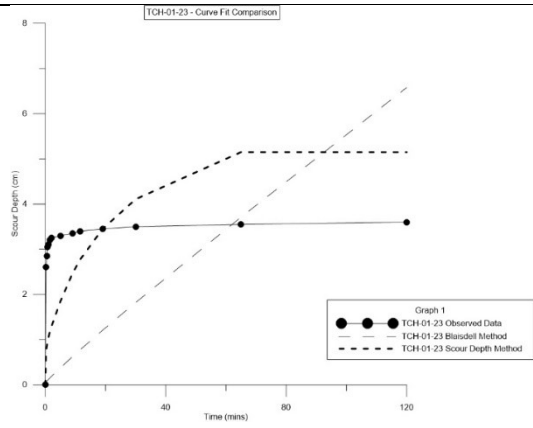
Without Segmentation	With Segmentation
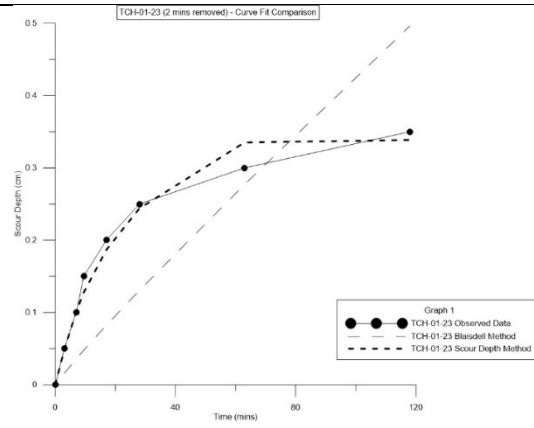
TCH-01-24
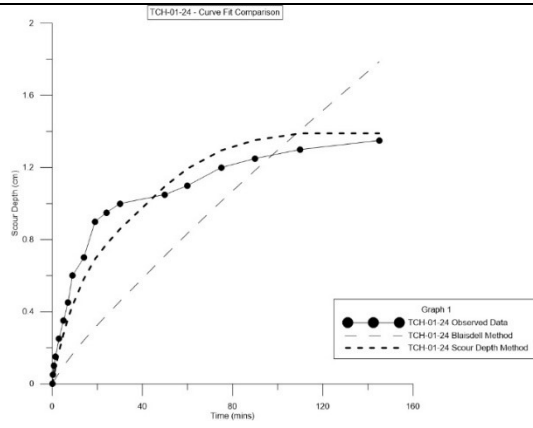
Without Segmentation	With Segmentation
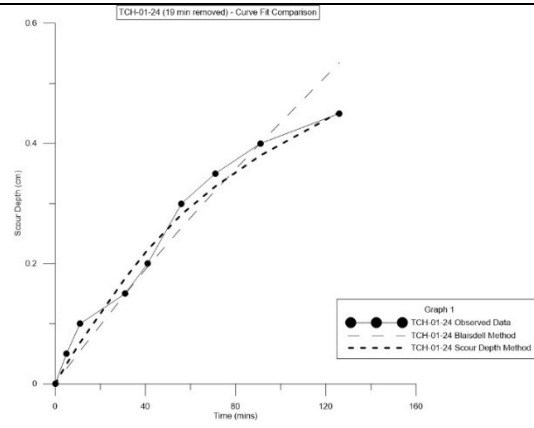
TCH-01-25

Without Segmentation	With Segmentation

354
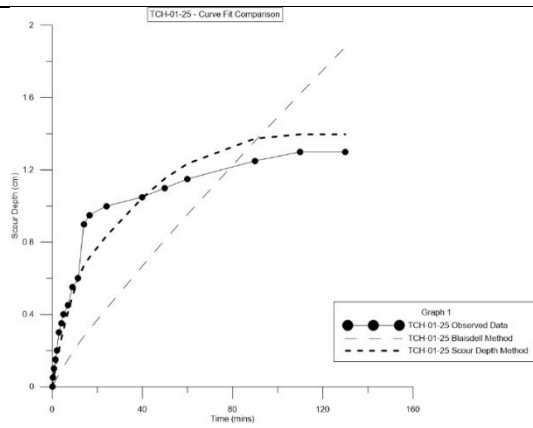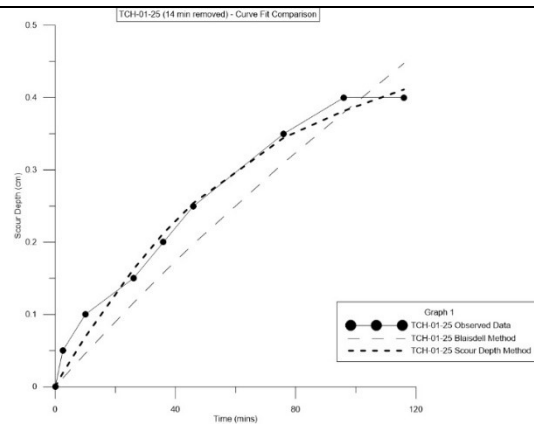
TCH-01-26	
Without Segmentation	With Segmentation
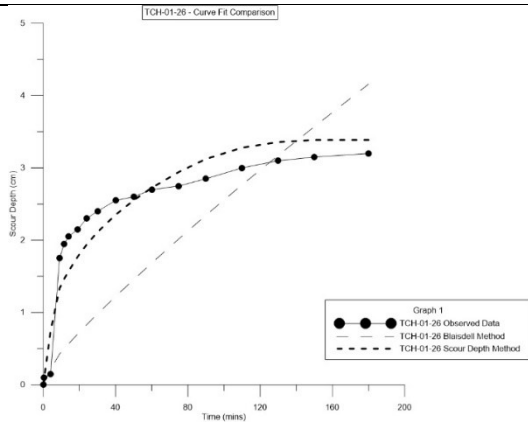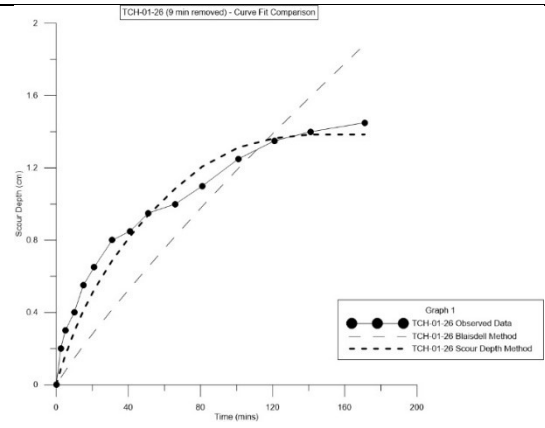
TCH-01-27	
Without Segmentation	With Segmentation
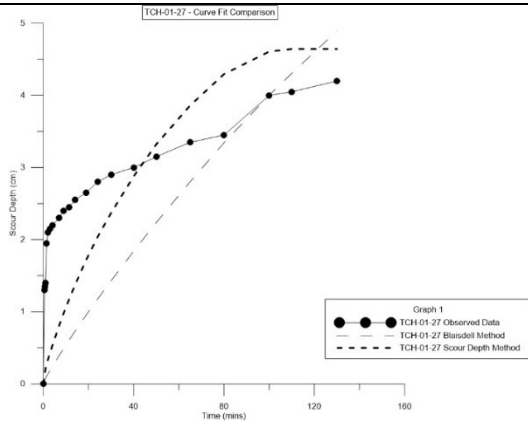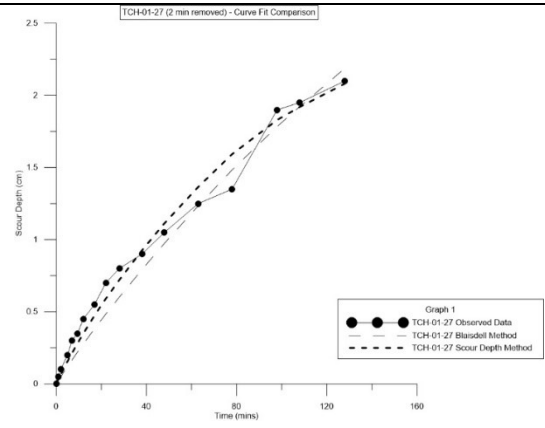
TCH-01-31	
Without Segmentation	With Segmentation
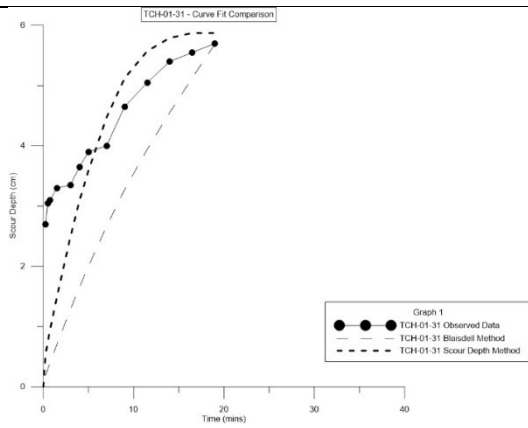
TCH-01-32
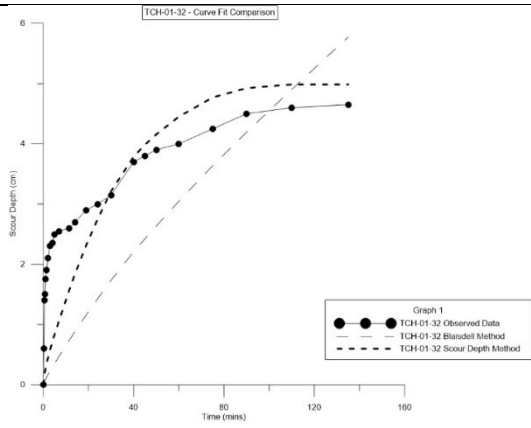
Without Segmentation	With Segmentation
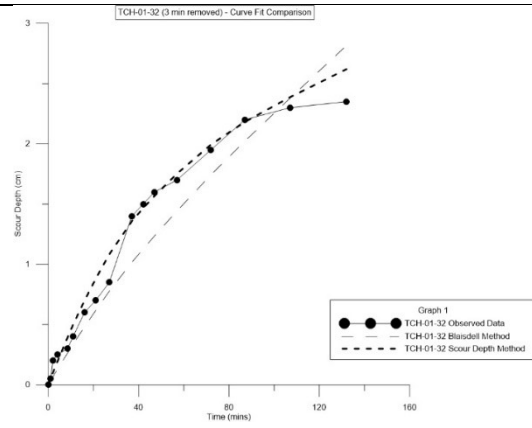
TCH-01-33
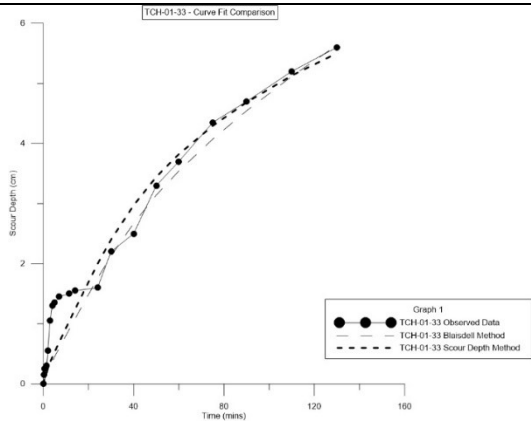
Without Segmentation	With Segmentation
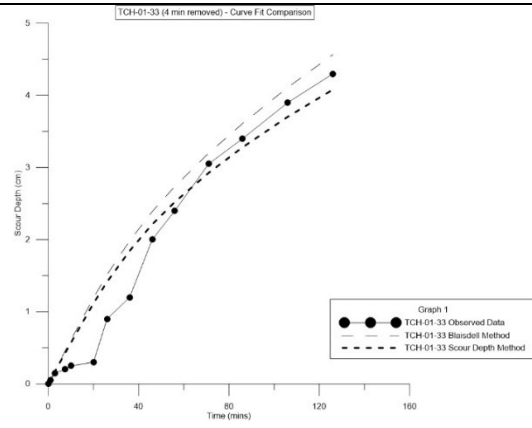
TCH-01-34

Without Segmentation	With Segmentation

356
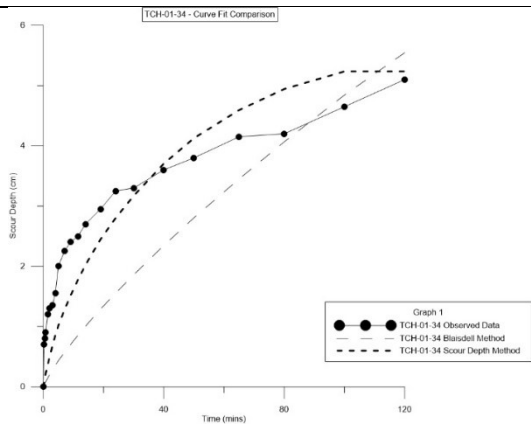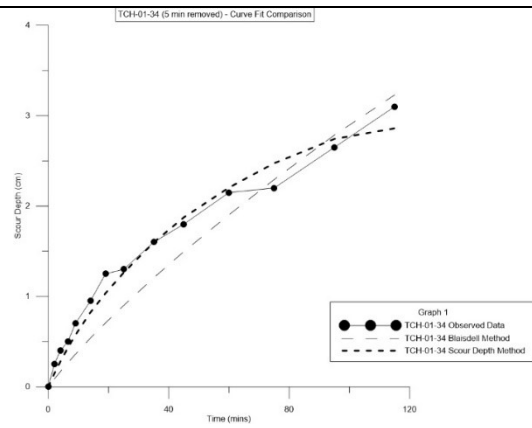
TCH-01-35	
Without Segmentation	With Segmentation
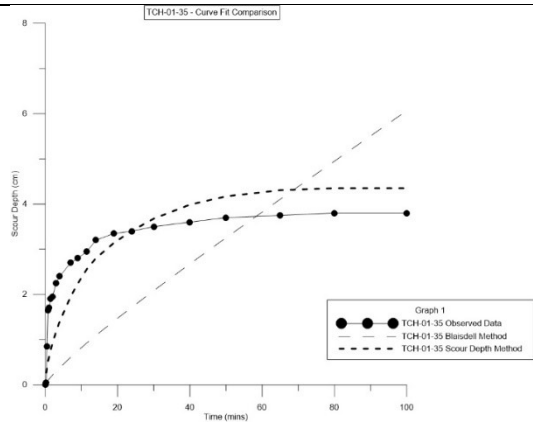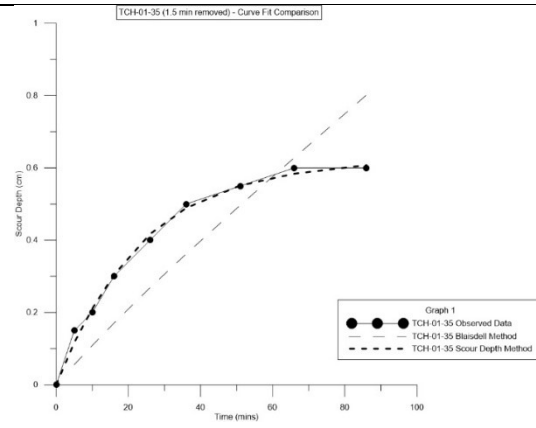
WCM-01-01	
Without Segmentation	With Segmentation
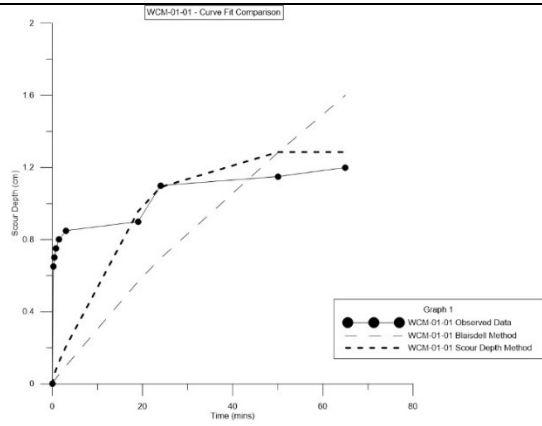
WCM-01-02	
Without Segmentation	With Segmentation
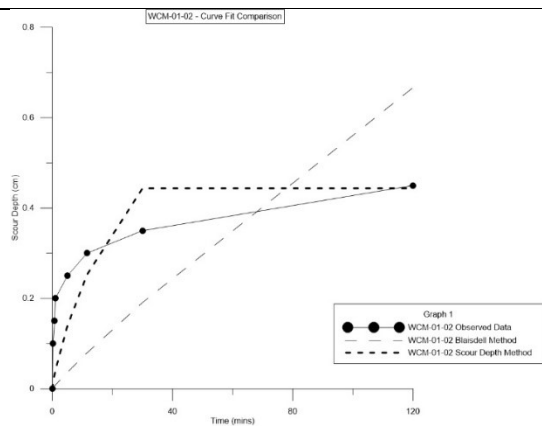
WCM-01-11	
Without Segmentation	With Segmentation
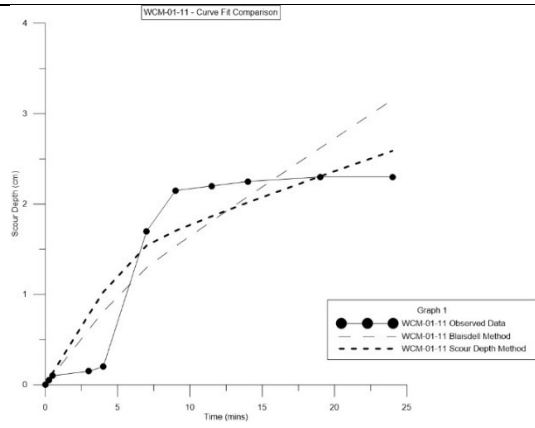
WCM-01-12	
Without Segmentation	With Segmentation
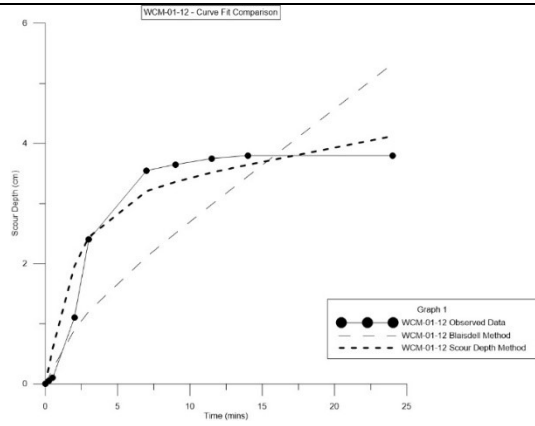
WCM-01-13	
Without Segmentation	With Segmentation

358
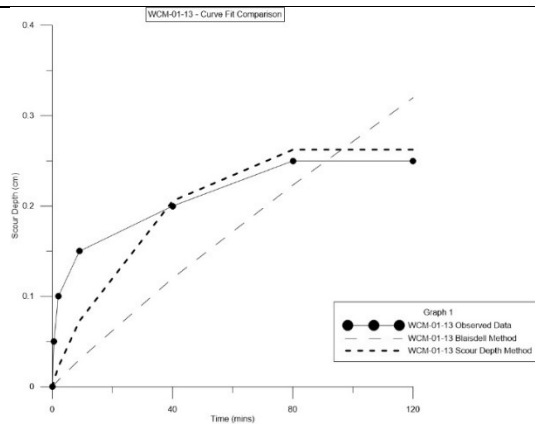
WCM-01-14	
Without Segmentation	With Segmentation
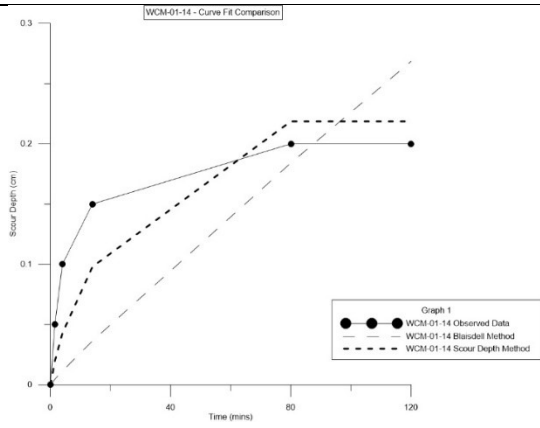
WCM-01-21	
Without Segmentation	With Segmentation
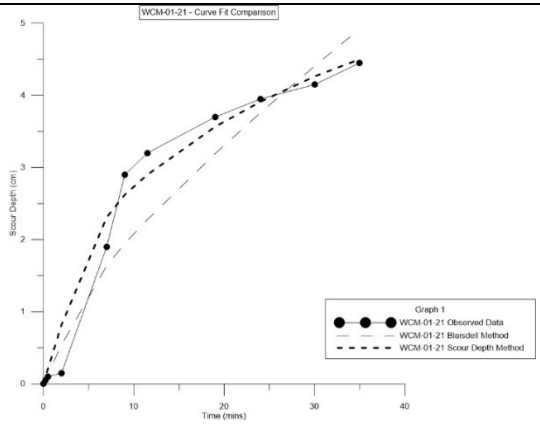
WCM-01-22	
Without Segmentation	With Segmentation
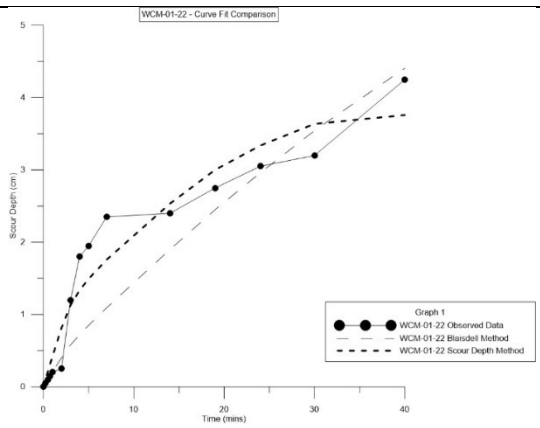
WCM-01-23	
Without Segmentation	With Segmentation
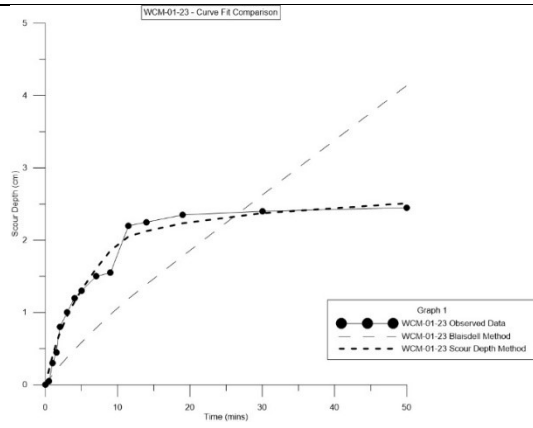
WCM-01-24	
Without Segmentation	With Segmentation
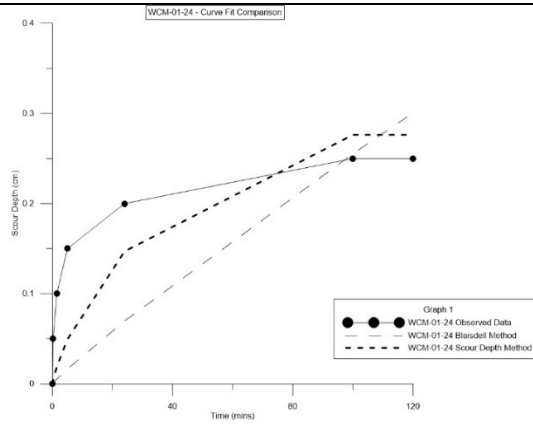
WCM-01-25	
Without Segmentation	With Segmentation
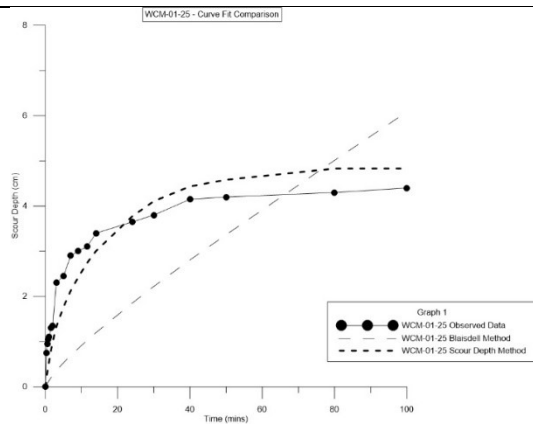
WCM-02-01	
Without Segmentation	With Segmentation
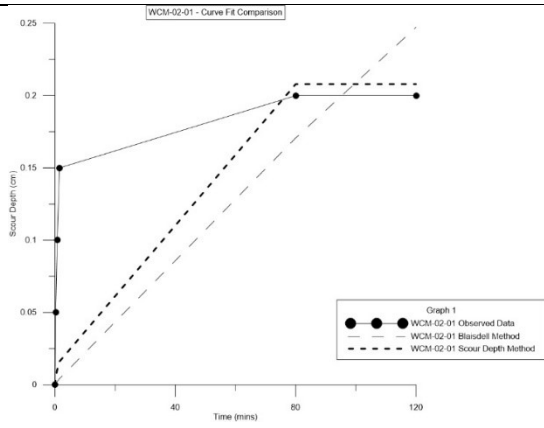
WCM-02-02	
Without Segmentation	With Segmentation
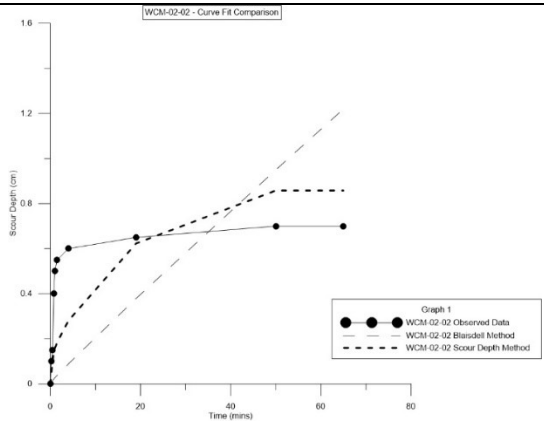
WCM-02-03	
Without Segmentation	With Segmentation
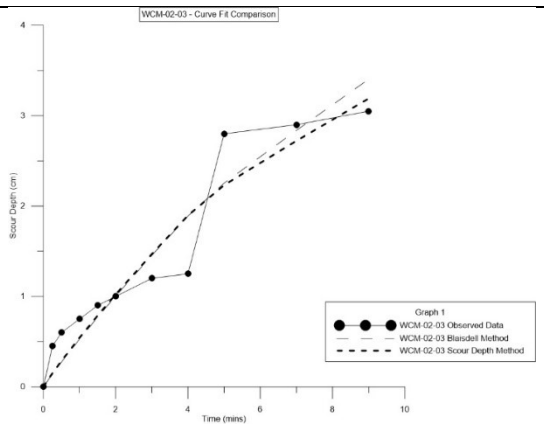
WCM-02-04	
Without Segmentation	With Segmentation
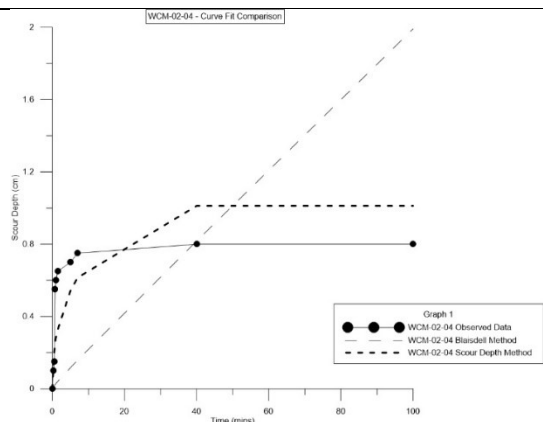
WCN-01-01	
Without Segmentation	With Segmentation
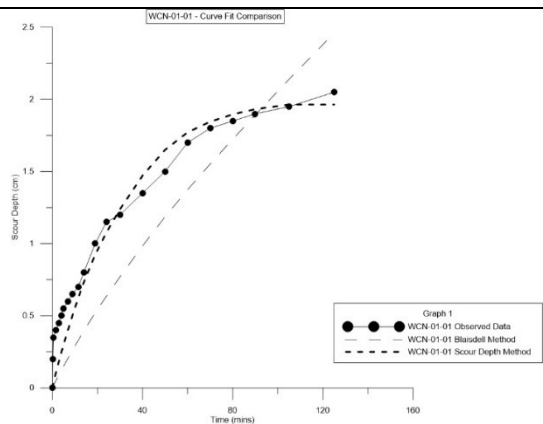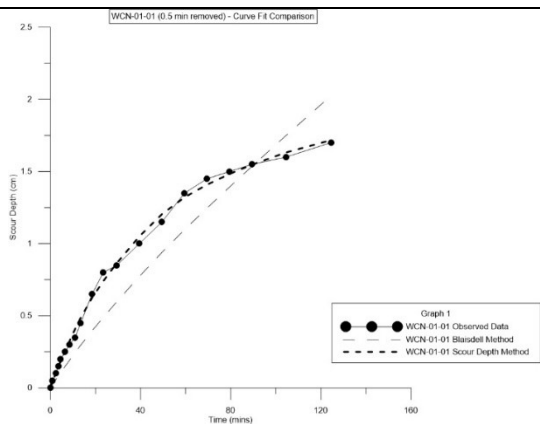
WCN-01-02	
Without Segmentation	With Segmentation
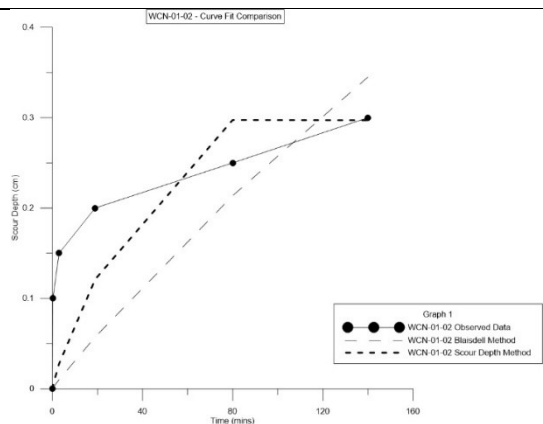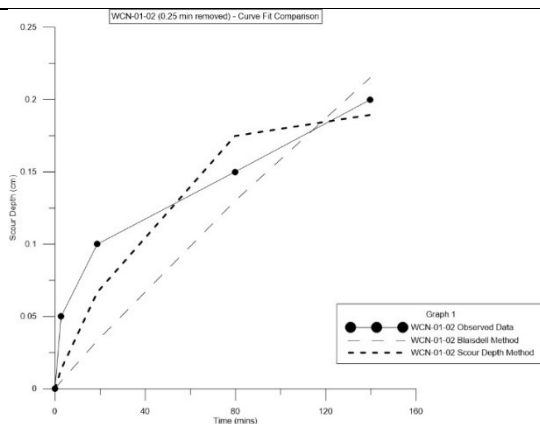
WCN-01-03	
Without Segmentation	With Segmentation
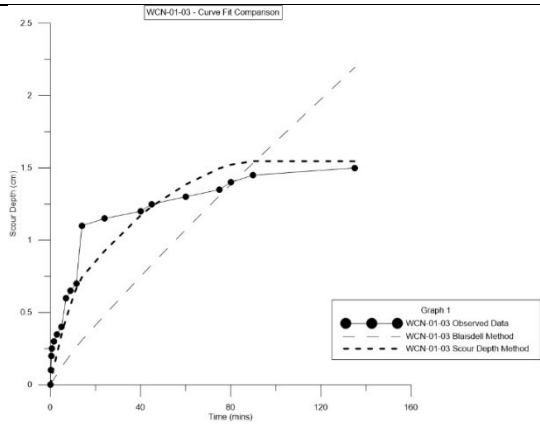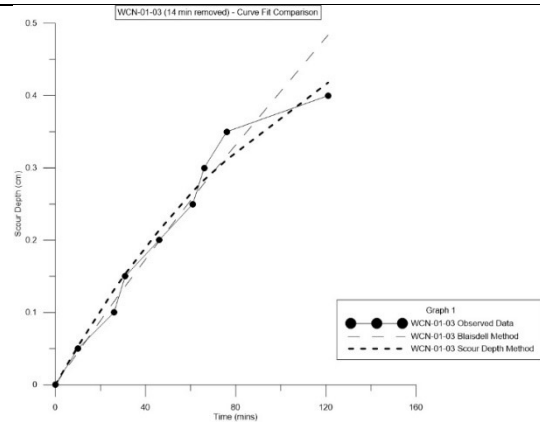
WCN-01-11	
Without Segmentation	With Segmentation
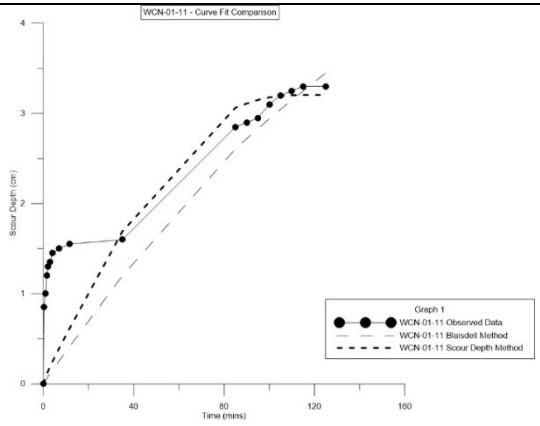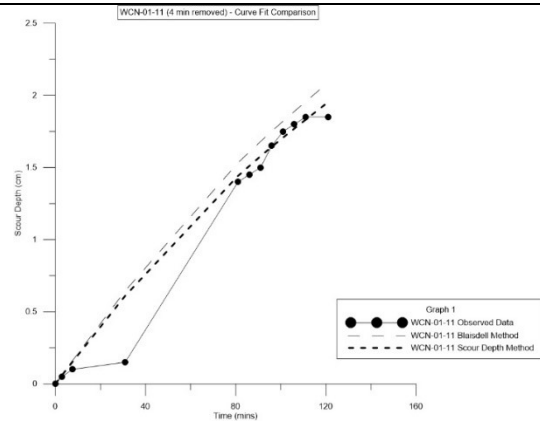
WCN-01-12	
Without Segmentation	With Segmentation
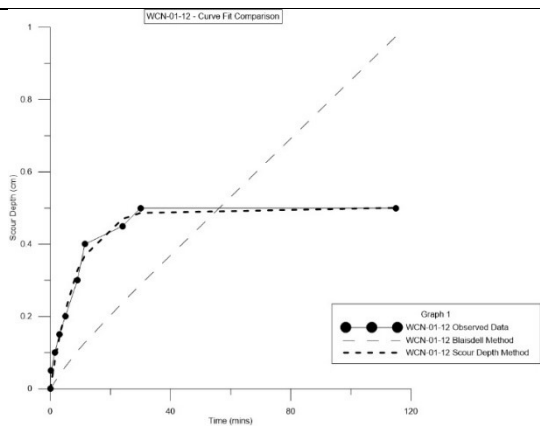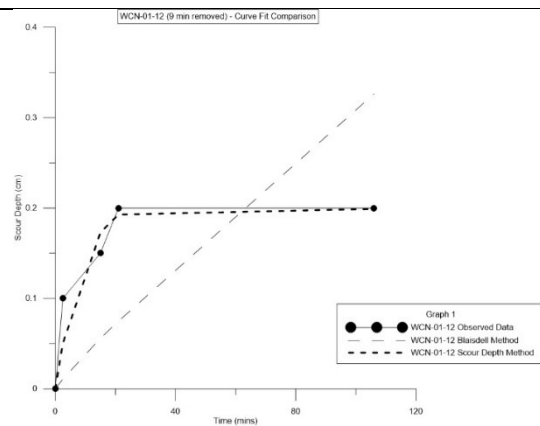
	WCN-01-13	
	Without Segmentation	With Segmentation
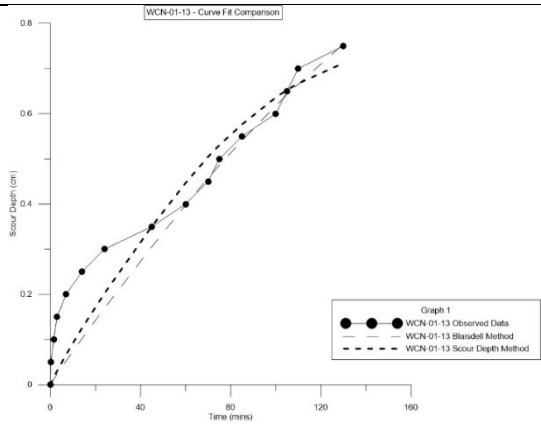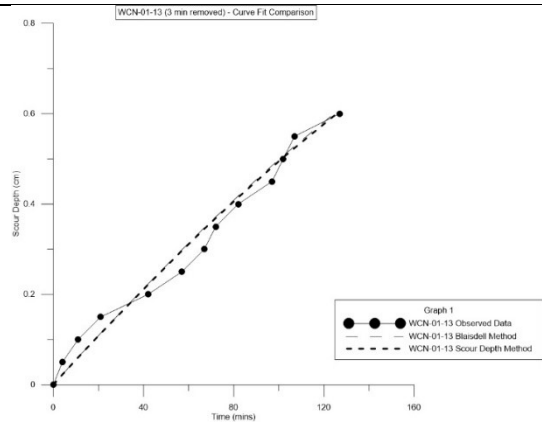
	WCN-02-21	
	Without Segmentation	With Segmentation
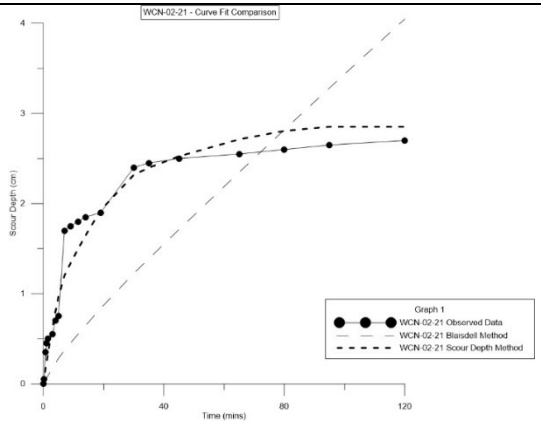
	WCN-02-22	
	Without Segmentation	With Segmentation

WCN-02-23	
Without Segmentation	With Segmentation